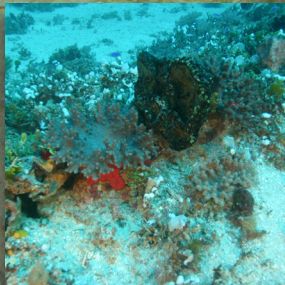


Seabed Biodiversity on the Continental Shelf of the Great Barrier Reef World Heritage Area



- Roland Pitcher
- Peter Doherty • Peter Arnold
- John Hooper • Neil Gribble

FINAL REPORT to the
Cooperative Research Centre
for the Great Barrier Reef World Heritage Area
JULY 2007



National Library of Australia Cataloguing-in-Publication entry:

Pitcher, C. R. (Clifford Roland).
Seabed biodiversity on the continental shelf of the Great
Barrier Reef World Heritage Area.

Bibliography.
Includes index.
ISBN 978-1-921232-87-9 (pbk.).
ISBN 978-1-921232-88-6 (web).

1. Marine biodiversity - Queensland - Great Barrier Reef.
2. Marine biodiversity - Research - Queensland - Great
Barrier Reef. 3. Great Barrier Reef (Qld.) - Environmental
aspects. I. CRC Reef Research Centre. II. Title.

333.95616

Citation:

Pitcher, C.R., Doherty, P., Arnold, P., Hooper, J., Gribble, N., Bartlett, C., Browne, M., Campbell, N., Cannard, T., Cappo, M., Carini, G., Chalmers, S., Cheers, S., Chetwynd, D., Colefax, A., Coles, R., Cook, S., Davie, P., De'ath, G., Devereux, D., Done, B., Donovan, T., Ehrke, B., Ellis, N., Ericson, G., Fellegara, I., Forcey, K., Furey, M., Gledhill, D., Good, N., Gordon, S., Haywood, M., Hendriks, P., Jacobsen, I., Johnson, J., Jones, M., Kinninmoth, S., Kistle, S., Last, P., Leite, A., Marks, S., McLeod, I., Oczkowicz, S., Robinson, M., Rose, C., Seabright, D., Sheils, J., Sherlock, M., Skelton, P., Smith, D., Smith, G., Speare, P., Stowar, M., Strickland, C., Van der Geest, C., Venables, W., Walsh, C., Wassenberg, T., Welna, A., Yearsley, G. (2007). Seabed Biodiversity on the Continental Shelf of the Great Barrier Reef World Heritage Area. AIMS/CSIRO/QM/QDPI CRC Reef Research Task Final Report. 320 pp.

Published: July 2007 by CSIRO Marine and Atmospheric Research

© Australian Institute of Marine Science, CSIRO Marine and Atmospheric Research, Queensland Museum, Queensland Department of Primary Industries, CRC Reef Research Centre, Fisheries Research and Development Corporation, and the National Oceans Office, 2007.

This work is copyright. Except as permitted under the Copyright Act 1968 (Cth), no part of this publication may be reproduced by any process, electronic or otherwise, without the specific written permission of the copyright owners. Neither may information be stored electronically in any form whatsoever without such permission.

DISCLAIMER

The authors have taken all reasonable steps to ensure that the information contents in this publication are accurate at the time of publication. Readers should ensure that they make appropriate inquiries to determine whether new information is available on the particular subject matter.

July 2007

Seabed Biodiversity on the Continental Shelf of the Great Barrier Reef World Heritage Area

CRC-REEF Task Number: C1.1.2

FRDC Project Number: 2003/021

NOO Contract Number: 2004/015

Roland Pitcher², Peter Doherty¹, Peter Arnold³, John Hooper³, Neil Gribble⁴, Chris Bartlett³, Matthew Browne², Norm Campbell², Toni Cannard², Mike Cappo¹, Giovannella Carini³, Susan Chalmers⁴, Sue Cheers², Doug Chetwynd², Andrew Colefax³, Rob Coles⁴, Stephen Cook³, Peter Davie³, Glenn De'ath¹, Drew Devereux², Barbara Done³, Tim Donovan¹, Barry Ehrke⁴, Nick Ellis², Gavin Ericson¹, Ida Fellegara³, Karl Forcey², Melodyrose Furey², Dan Gledhill², Norm Good⁴, Scott Gordon², Mick Haywood², Patricia Hendriks³, Ian Jacobsen, Jeff Johnson³, Michelle Jones³, Stuart Kinninmoth¹, Sarah Kistle⁴, Peter Last², Anita Leite³, Shona Marks², Ian McLeod², Sybilla Oczkowicz⁴, Melissa Robinson³, Cassandra Rose⁴, Denise Seabright³, Jacque Sheils², Matt Sherlock², Posa Skelton⁴, David H Smith², Greg Smith², Peter Speare¹, Marcus Stowar¹, Colleen Strickland³, Claire Van der Geest⁴, Bill Venables², Cath Walsh⁴, Ted Wassenberg², Andrzej Welna², Gus Yearsley²

¹**Australian Institute of Marine Science**
Cape Ferguson, TOWNSVILLE, Qld. 4810, Australia

²**Commonwealth Scientific & Industrial Research Organisation**
Marine & Atmospheric Research
Mathematics & Information Sciences
233 Middle Street, CLEVELAND, Qld. 4163 Australia

³**Queensland Museum**
MTQ, TOWNSVILLE, Qld. 4810, Australia
South Bank, SOUTH BRISBANE, Qld. 4101, Australia

⁴**Queensland Department of Primary Industries**
Northern Fisheries Centre, Tingara Street, CAIRNS, Qld. 4870, Australia



ISBN 978-1-921232-87-9.

CRC Reef Research Task Final Report

ACKNOWLEDGEMENTS

This document is the final report of the *Great Barrier Reef Seabed Biodiversity Project*, a collaboration between the Australian Institute of Marine Science (AIMS), the Commonwealth Scientific and Industrial Research Organisation (CSIRO), Queensland Department of Primary Industries & Fisheries (QDPI&F), and the Queensland Museum (QM); funded by the CRC Reef Research Centre (CRC-Reef), the Fisheries Research and Development Corporation (FRDC), and the National Oceans Office (NOO) of the Department of Environment and Water Resources. We gratefully acknowledge the support of end-user agencies Great Barrier Reef Marine Park Authority (GBRMPA), QDPI & Fisheries, Queensland Seafood Industry Association (QSIA) and the NOO, and the contributions of the project's Steering Committee members: David Williams (CRC-Reef), Dorothea Huber & Phil Cadwallader (GBRMPA), Brigid Kerrigan & Malcolm Dunning (QDPI&F), Duncan Souter, Barry Ehrke & Martin Hicks (QSIA), Vicki Nelson (NOO) and Vern Veitch (Sunfish). For the provision of physical environmental data, we thank Chris Jenkins (Ocean Sciences Institute – OSI), Lance Bode (James Cook University – JCU), Scott Condie (CSIRO), the GBRMPA, the RAN Hydrographers Office (RAN HO) — and Peter Harris, Andrew Heap, Emma Mathews, Alison Hancock (Geoscience Australia – GA) for processing the sediment samples. We also wish to thank the multi-agency teams and the crews of the *RV Lady Basten* (AIMS) and *FRV Gwendoline May* (QDPI&F) that contributed to the success of the fieldwork; the research agencies AIMS, CSIRO, QM, QDPI&F for providing support to the project; and all the project's team members without whose valuable efforts this project would not have been possible. A large number of other people also helped with aspects of the project and we are grateful for their assistance, including: Tony Reese, Steve Edgar, Mark Tonks, Quinton Dell, Gary Fry, William White, Al Graham, Louise Conboy, Spikey Riddoch, Bob Ward, Bronwyn Holmes, Tom Munro, Hiro Motomura, Mike Sugden, Henok Goitom, Barry Russell, Barry Hutchins, Martin Gomon and Di Bray. Shane Griffiths, John Kirkwood and Piers Dunstan provided valuable comments that improved the document. Louise Bell designed the cover.

This Report is dedicated to the memory of our friend, colleague and expert extraordinaire on “all matters seabed”, Dr Peter William Arnold, Senior Curator Biodiversity, Museum of Tropical Queensland, Townsville (1949-2006)



TABLE OF CONTENTS

| | |
|--|-------|
| ACKNOWLEDGEMENTS | ii |
| TABLE OF CONTENTS | iii |
| FIGURES | v |
| TABLES | xi |
| NON-TECHNICAL SUMMARY | xv |
| 1. INTRODUCTION | 1-1 |
| 1.1. BACKGROUND | 1-1 |
| 1.2. NEED | 1-2 |
| 1.3. OBJECTIVES | 1-3 |
| 2. METHODS | 2-5 |
| 2.1. SAMPLING DESIGN | 2-5 |
| 2.1.1. Physical environmental data (I McLeod & R Pitcher) | 2-5 |
| 2.1.2. Study Area Stratification (N Ellis) | 2-15 |
| 2.1.3. Site Selection | 2-29 |
| 2.2. FIELD SAMPLING | 2-31 |
| 2.2.1. Research Vessels (T Wassenberg & N Gribble) | 2-31 |
| 2.2.2. Towed Video Camera (G Smith, K Forcey, M Haywood) | 2-32 |
| 2.2.3. Baited Remote Underwater Video Stations (M Cappel) | 2-34 |
| 2.2.4. Single-beam Acoustics | 2-35 |
| 2.2.5. Epibenthic Sled (T Wassenberg & M Stowar) | 2-36 |
| 2.2.6. Scientific Trawl (T Wassenberg, D Gledhill & N Gribble) | 2-37 |
| 2.2.7. Sample Processing at Sea (T Wassenberg, M Stowar, C Bartlett) | 2-38 |
| 2.3. LABORATORY PROCESSING AND IDENTIFICATION | 2-43 |
| 2.3.1. Towed Video (T Wassenberg, J Sheils) | 2-43 |
| 2.3.2. BRUVS Video (M Cappel) | 2-46 |
| 2.3.3. Samples Processing (T Hendriks, M Stowar, C Bartlett, T Wassenberg, D Gledhill) | 2-49 |
| 2.4. DATA ANALYSES | 2-53 |
| 2.4.1. BRUVS Species Models, Characterization & Prediction (M Cappel, G De' Ath) | 2-53 |
| 2.4.2. Single Species Biophysical Models and Prediction (M Browne, W Venables) | 2-54 |
| 2.4.3. Species Groups Characterization and Prediction (M Browne) | 2-58 |
| 2.4.4. Site Groups Characterization and Prediction (W Venables) | 2-59 |
| 2.4.5. Video Habitat Characterization and Prediction (W Venables) | 2-64 |
| 2.4.6. Acoustics Discrimination and Classification | 2-68 |
| 2.4.7. Ecological Risk Indicators | 2-75 |
| 2.4.8. Trawl Management Scenario Model (N Ellis, A Welna, R Pitcher) | 2-77 |
| 3. RESULTS | 3-86 |
| 3.1. BRUVS SPECIES MODELS, CHARACTERIZATION & PREDICTION (M Cappel, G De' Ath) | 3-86 |
| 3.1.1. BRUVS Species richness | 3-86 |
| 3.1.2. BRUVS Species presence/absence Biophysical Models and Prediction | 3-87 |
| 3.1.3. BRUVS Site-groups Characterization and Prediction | 3-105 |
| 3.2. SINGLE SPECIES, BIOPHYSICAL MODELS AND PREDICTION | 3-112 |
| 3.2.1. Sled and Trawl samples species richness | 3-113 |
| 3.2.2. Single species models (M Browne & R Pitcher) | 3-116 |
| 3.2.3. Selected single species distribution maps | 3-125 |
| 3.3. SPECIES GROUPS CHARACTERIZATION AND PREDICTION (M Browne & R Pitcher) | 3-133 |
| 3.3.1. Characterization and Prediction Model performance | 3-133 |
| 3.3.2. Selected species group distribution maps | 3-135 |
| 3.4. SITE GROUPS CHARACTERIZATION AND PREDICTIONS (W Venables & R Pitcher) | 3-138 |
| 3.4.1. Decision tree results | 3-138 |
| 3.4.2. Species affinity groups | 3-141 |
| 3.4.3. Description of site-group assemblages | 3-142 |
| 3.5. VIDEO HABITAT CHARACTERIZATION AND PREDICTION | 3-145 |
| 3.5.1. Seabed substratum | 3-145 |
| 3.5.2. Seabed biological habitat | 3-145 |
| 3.5.3. Statistical characterization and prediction (W Venables & R Pitcher) | 3-151 |
| 3.6. ACOUSTICS DISCRIMINATION AND CLASSIFICATION | 3-155 |
| 3.6.1. Wavelet Packet-Based Techniques Applied to Data in the Angular Domain (D H Smith) | 3-155 |
| 3.6.2. Canonical Variate Analysis of Acoustic Data (N Campbell & D Devereux) | 3-166 |

| | | |
|--------|--|--------|
| 3.6.3. | Linear Discriminant Analyses of QTC View data (I McLeod) | 3-186 |
| 3.7. | ECOLOGICAL RISK INDICATORS | 3-197 |
| 3.7.1. | Indicators for species-groups biomass..... | 3-198 |
| 3.7.2. | Indicators for individual species biomass..... | 3-202 |
| 3.7.3. | Assemblage indicators..... | 3-238 |
| 3.7.4. | Habitat indicators | 3-239 |
| 3.8. | TRAWL MANAGEMENT SCENARIO MODEL (N Ellis, R Pitcher) | 3-243 |
| 4. | DISCUSSION | 4-250 |
| 4.1. | BRUVS SPECIES MODELS, CHARACTERIZATION & PREDICTION (M Cappel, G De' Ath)..... | 4-251 |
| 4.1.1. | BRUVS Fish species | 4-251 |
| 4.1.2. | BRUVS Fish Assemblages..... | 4-251 |
| 4.2. | SINGLE SPECIES, BIOPHYSICAL MODELS AND PREDICTION | 4-253 |
| 4.3. | SPECIES GROUPS CHARACTERIZATION AND PREDICTION | 4-255 |
| 4.4. | SITE GROUPS CHARACTERIZATION AND PREDICTION | 4-255 |
| 4.5. | VIDEO HABITAT CHARACTERIZATION AND PREDICTION | 4-256 |
| 4.6. | ACOUSTICS DISCRIMINATION AND CLASSIFICATION..... | 4-257 |
| 4.6.1. | Wavelet Packet-Based Techniques Applied to Data in the Angular Domain (D H Smith)..... | 4-257 |
| 4.6.2. | Canonical Variate Analysis of Acoustic Data (N Campbell & D Devereux)..... | 4-258 |
| 4.6.3. | Linear Discriminant Analyses of QTC View data..... | 4-259 |
| 4.6.4. | Acoustics summary | 4-260 |
| 4.7. | ECOLOGICAL RISK INDICATORS | 4-261 |
| 4.8. | TRAWL MANAGEMENT SCENARIO MODEL..... | 4-264 |
| 5. | BENEFITS | 5-266 |
| 6. | FURTHER DEVELOPMENT | 6-267 |
| 7. | ACHIEVEMENT OF OUTCOMES | 7-269 |
| 8. | CONCLUSIONS..... | 8-271 |
| 9. | RECOMMENDATIONS | 9-273 |
| 10. | REFERENCES..... | 10-276 |
| 11. | ABBREVIATIONS..... | 11-281 |
| 12. | APPENDIX 1: INTELLECTUAL PROPERTY | 12-282 |
| 13. | APPENDIX 2: STAFF..... | 13-283 |
| 14. | APPENDIX 3: PROJECT STEERING COMMITTEE MEMBERS | 14-285 |
| 15. | APPENDIX 4: SINGLE SPECIES TRAWL EXPOSURE..... | 15-286 |

FIGURES

| | |
|---|------|
| Figure 2-1: DEM of the bathymetry, slope and aspect of the GBR continental shelf, on a 0.01° grid, from various sources including soundings in uncharted areas recorded by the Project; map of modeled seabed current shear stress (RMS N/m ²) (sources, see Section 2.1.1.1 for)..... | 2-9 |
| Figure 2-2: Maps of sediment attributes for the GBR continental shelf: percent mud/sand/gravel grain size fractions and percent carbonate (source, Geoscience Australia. Includes samples collected by the project and processed by GA)..... | 2-10 |
| Figure 2-3: Maps of CARS bottom water physical attributes for the GBR continental shelf: temperature (mean & SD °C), salinity (mean & SD ‰), dissolved oxygen (mean & SD ml/l) (source, see Section 2.1.1.1)..... | 2-11 |
| Figure 2-4: Maps of CARS bottom water nutrient attributes: silicate (mean & SD μM), nitrate (mean & SD μM), and phosphate (mean & SD μM), (source, see section 2.1.1.1)..... | 2-12 |
| Figure 2-5: Maps of SeaWiFS predicted chlorophyll-A (mean & SD mg/m ³), light absorption (attenuation coefficient K) at 490 nm (mean & SD m ⁻¹), benthic irradiance (relative to sea surface at equator estimated from latitude, K490 and Depth), and weighted average annual trawl effort (hrs/0.01° grid) for the GBR continental shelf (sources, see section 2.1.1.1)..... | 2-13 |
| Figure 2-6. Partitioning covariate space in two dimensions: (a) 1,000 points randomly sampled from the square covariate space. (b) a partitioning into 20 clusters using PAM; (c) a preferred partitioning that accounts for the relative importance of the variables; (d) the partitioning in (c) is achieved using PAM on the scaled covariate space..... | 2-16 |
| Figure 2-7. Variable importance computed by (a) cross-validated trees and (b) random forests..... | 2-17 |
| Figure 2-8. Importance measures without reliability ($I_{bio}Q$), with reliability ($I_{bio}QR$), and tuned reliability ($I_{bio}QR$) ^{0.74} to match the shape without reliability. Each version is normalized to sum to 1. The orders of the variables with and without reliability are different..... | 2-20 |
| Figure 2-9. (a) Bivariate normal distribution of 1,000 points. (b) Partitioning into 20 clusters using PAM. Each cluster is labeled by the number of points in the cluster. The more populous clusters tend to be tighter and so more homogeneous..... | 2-23 |
| Figure 2-10. Density of bottom stress estimated by a Gaussian kernel of width 0.01 calculated using biased cross-validation. Also shown is a ‘rug’ of values for 200 randomly selected sites..... | 2-24 |
| Figure 2-11. Number of subclusters vs primary cluster size for 3 different values of the exponent a . The sloping line corresponds to $N_{sub} \propto S$, the curve to $N_{sub} \propto \sqrt{S}$, and the horizontal line to $N_{sub} = \text{constant}$ | 2-24 |
| Figure 2-12. The 200 primary clusters in geographical space. Sixty of the clusters have been separated into six panels in order to make them distinct and assess the degree of fragmentation..... | 2-25 |
| Figure 2-13. Distribution of the most important physical covariates on the full the GBR data (orange). The thin curves are 90% confidence intervals for the density sampled from the clusters. For clarity we show covariates on a log scale for bottom stress, a logit scale for mud and an inverse scale for chlA. Also shown is a rug of 200 sample values (jittered for mud)..... | 2-26 |
| Figure 2-14: Map of the biophysical stratification of the Great Barrier Reef continental shelf. Inset: colour key showing distribution of seabed grids on the first two principal components (which explain 65% of the variation) of the biologically weighted physical covariates; biplot vectors indicate direction and magnitude of the major physical factors..... | 2-29 |
| Figure 2-15: Map of the sites selected for sampling the seabed on the continental shelf in the GBR. * : sites for benthic and trawl sampling; + : sites for benthic sampling only..... | 2-30 |
| Figure 2-16: The 27 m Australian Institute Marine Science research vessel <i>RV Lady Basten</i> | 2-31 |
| Figure 2-17: The 18 m Queensland Department of Primary Industries & Fisheries research trawler <i>FRV Gwendoline May</i> | 2-32 |
| Figure 2-18: The Drop-Cam system being recovered after completion of a 500 m video transect and the surface real-time monitoring, control and data acquisition system..... | 2-33 |
| Figure 2-19: Diagram of single BRUVS frame and housing..... | 2-35 |
| Figure 2-20: Applying camera and bait arm to BRUVS before deployment. Note ballast on frame and 8 mm hauling rope..... | 2-35 |
| Figure 2-21: The epibenthic sled being deployed through the A-frame for a 200 m tow along the seabed; note the weak link at the top of the bridle and retrieve chain leading to the rear of the sled..... | 2-36 |
| Figure 2-22: Sediment pipe dredge, showing sister-clip for attachment behind the sled..... | 2-37 |
| Figure 2-23: Net plan for the eight fathom Florida Flyer net used for scientific trawl sampling and the net suspended from the A-frame on the stern of the <i>Gwendoline May</i> | 2-37 |
| Figure 2-24: Drop chain links and trawl boards..... | 2-38 |
| Figure 2-25: Sorting the catch from the epibenthic sled on the 10 mm square mesh sieve drawer into major taxonomic classes..... | 2-39 |

| | |
|--|------|
| Figure 2-26: Samples of sorted dredge catch organisms with bar code labels ready to be photographed and data recorded in the vessel data base. | 2-40 |
| Figure 2-27: Data and images from each sled site were entered into the vessel database entry form that also included a photo of the entire site sample (left) and of the sample (in this case, of echinoderms). | 2-40 |
| Figure 2-28: A photograph of an entire trawl catch (site photo) showing the diversity of organisms. | 2-41 |
| Figure 2-29: A sample of crustaceans showing the barcode label. The label number, weight and class were entered into a data base at sea. | 2-42 |
| Figure 2-30: Data and images from each trawl site were entered into the vessel database entry form that also contained a photo of the entire catch (left) and of the sample (in this case, of an elasmobranch). | 2-42 |
| Figure 2-31: Data entry screens of the Delphi video analysis software showing the trapezoid overlaid on the paused video image. | 2-44 |
| Figure 2-32: Drop down lists of physical and biological attributes to be used in analyzing the video image.... | 2-45 |
| Figure 2-33: Image reference form in BRUVS2.1.mdb..... | 2-48 |
| Figure 2-34: Reference image for <i>Pristipomoides multidens</i> , with <i>Lutjanus sebae</i> , <i>L. adetii</i> and <i>Epinephelus undulatostratus</i> and <i>E. areolatus</i> in the background..... | 2-48 |
| Figure 2-35: An example of the form used in the laboratory to enter data obtained from the field samples. The sample barcode number is entered and the database retrieves the site details including the sample photograph from onboard the vessel. Individual species or OTU were then entered into genus or species boxes (middle fields) and a pick list of names appears. By selecting the appropriate name the species numbers and weights were then able to be recorded into the bottom RHS field..... | 2-50 |
| Figure 2-36: Identifying and processing invertebrate samples at the Queensland Museum. | 2-50 |
| Figure 2-37: Colour scheme used for species distribution mapping | 2-57 |
| Figure 38: Spans, medoids, deviance and deviance reduction due to partition. (a) shows a group of ten sites using two-dimensional Euclidean distances to represent Bray-Curtis distances. (b) shows the span of the group from an arbitrary reference site. (c) shows the minimum span, which defines the medoid; the sum of squared distances from the medoid is then the deviance of the group. (d) shows a partition of the original group into two subgroups, and the spans defining the deviance component of each. The partition is achieved by a split on the x-coordinate. The reduction in deviance achieved by partition is then $32.83 - 14.28 = 18.55$ | 2-61 |
| Figure 2-39: An acoustic data sample from site 1505, with indicated depth of 23.97 m, shown in the original distance/time domain, and after transformation to the angular domain. | 2-68 |
| Figure 2-40: Measured depth and pressure signals derived from the drop camera and sonar transducer for site 1505, highlighting the segment of matched sonar data for which the calculated delay result is 0.502 minutes. | 2-69 |
| Figure 2-41: Three dimensional plot of the first three Local Discriminant Basis coordinates for data representing (sand, no biohabitat) and (sand, seagrass) seabed types, generated with Daubechies 2 wavelet filter coefficients, showing visible separation between the two classes..... | 2-70 |
| Figure 2-42. Total effort in the study area for the period 1993–2005. Also shown is the projected mean effort for 4 scenarios..... | 2-79 |
| Figure 2-43. Pitcher <i>et al.</i> (2004) models (<i>points</i>) and fitted Schaefer model response (<i>lines</i>) for 0 to 10 initial trawl tows for two OTUs: (<i>left</i>) <i>Ianthella flabelliformis</i> and (<i>right</i>) <i>Junceella juncea</i> . The vertical scale is biomass relative to initial unimpacted biomass. The horizontal scale is years since impact..... | 2-81 |
| Figure 2-44. Models obtained from sled video observations for 18 OTUs (Pitcher <i>et al.</i> 2004). The vertical (<i>b</i>) axis represents biomass relative to initial unimpacted biomass, <i>t</i> is time since trawl impact (ranging from 0 to 5 years), and <i>i</i> is the number of trawl tows (ranging from 0 to 10). | 2-82 |
| Figure 2-45. Recovery and depletion parameter estimates using sled (<i>green</i>) and ROV (<i>blue</i>) measurements. Where both sled and ROV measurements are available the points are joined by a dashed line. Also shown (<i>red triangles</i>) are the values from Poiner <i>et al.</i> (1998) and Hill <i>et al.</i> (2002) (not all labeled)..... | 2-83 |
| Figure 3-1: Patterns of species prevalence and richness at BRUVS stations. | 3-86 |
| Figure 3-2: Species richness from BRUVS data by location in the GBRMP. | 3-87 |
| Figure 3-3: "Heatmap" showing relationships amongst and between the top 20 predictors and 25 species responses (presence/absence). The dendrogram along the side of the heatmap shows which species are similar in having a relationship with a set of predictor variables. It does not imply these species have the same relationship. The dendrogram along the top shows which explanatory variables cluster together, and the coloured bars along the top show the percentage of the variation in the explanatory variables explained by a particular variable. Red indicates higher influence. The "redness" of the individual cells in the figure show the relative influence of the particular explanatory variable on the presence/absence of the particular species, and the heaviness of the blue line shows the degree and shape of the relationship. | 3-90 |
| Figure 3-4: Species occurrence as a function of location across the shelf. Plots are ranked in descending order of relative influence of the predictor variable for the species. The "rugs" on the X axes are 10 percentiles in the distribution of the predictor variable. The Yaxes (log-odds) are Log(base 2) (1-Probability of occurrence) and the plots are centred on the mean of Y. | 3-91 |
| Figure 3-5: Species occurrence as a function of mud content of the sediments. Details as for Figure 3-4. | 3-92 |

| | |
|---|-------|
| Figure 3-6: Species occurrence as a function of carbonate content of the sediments. Details as for Figure 3-4.3-93 | |
| Figure 3-7: Species occurrence as a function of gravel content of the sediments. Details as for Figure 3-4. | 3-94 |
| Figure 3-8: Species occurrence as a function of average seawater temperature. Details as for Figure 3-4..... | 3-95 |
| Figure 3-9: Species occurrence as a function of average salinity. Details as for Figure 3-4..... | 3-96 |
| Figure 3-10: Species occurrence as a function of trawl effort index. Details as for Figure 3-4..... | 3-97 |
| Figure 3-11 Predicted occurrence of 3 species of <i>Nemipterus</i> recorded by BRUVS. Circles represent observed abundance (untransformed) and influential covariates are listed in the inset panels. “%XVar” describes the percentage of the variation in the presence/absence of the species accounted for by the gbm model. “yes” is (1-%prediction error). | 3-99 |
| Figure 3-12 Predicted occurrence of small benthic microcarnivores in the genera <i>Pentapodus</i> , <i>Lethrinus</i> and <i>Upeneus</i> . Conventions as for Figure 3-11..... | 3-100 |
| Figure 3-13 Predicted occurrence of small carangids in the genera <i>Alepes</i> , <i>Decapterus</i> , <i>Selaroides</i> and <i>Seriolina</i> . Conventions as for Figure 3-11..... | 3-101 |
| Figure 3-14 Predicted occurrence of predators in the genera <i>Scomberomorus</i> , <i>Echeneis</i> , <i>Saurida</i> and <i>Parapercis</i> . Conventions as for Figure 3-11..... | 3-102 |
| Figure 3-15 Predicted occurrence of demersal omnivores and predators in the genera <i>Abalistes</i> , <i>Lagocephalus</i> , <i>Paramonacanthus</i> and <i>Gymnothorax</i> . Conventions as for Figure 3-11..... | 3-103 |
| Figure 3-16 Predicted occurrence of the large predatory carangids in the genera <i>Carangoides</i> and <i>Gnathanodon</i> . Conventions as for Figure 3-11..... | 3-104 |
| Figure 3-17 Predicted occurrence of the large benthic macrocarnivore <i>Choerodon venustus</i> . Conventions as for Figure 3-11..... | 3-105 |
| Figure 3-18: Multivariate regression tree analysis defining abundance (transformed by 4th root) of vertebrate assemblages (top 25 species) in terms of location across and along the GBRMP (366 sites). The terminal nodes represent 12 assemblages (see Table 3-4 for definitions of nodes), corresponding with different regions of the GBRMP, and the higher level nodes represent the 11 assemblages at higher spatial scales. The indicator species are shown with the DLI value for nodes where maxima in DLI occurred..... | 3-106 |
| Figure 3-19 Predicted distribution of 12 fish assemblages (terminal nodes from Table 3-4) as defined by the explanatory variables “across” and “along” the shelf. | 3-108 |
| Figure 3-20 Multivariate regression tree analysis defining abundance (transformed by 4th root) of vertebrate assemblages (top 25 species) in terms of the top 20 environmental covariates in the GBRMP (366 sites). The terminal nodes represent 12 assemblages (see Table 3-5 for definitions of nodes), corresponding with various levels of mud, sand, gravel and silica and different regions of the GBRMP. The indicator species are shown with the DLI value for nodes where maxima in DLI occurred. | 3-109 |
| Figure 3-21 Predicted distribution of 12 fish assemblages (terminal nodes from Table 3-5) as defined by the top 20 explanatory environmental variables and location. | 3-111 |
| Figure 3-22: Patterns of prevalence and richness of 4,723 species at 1,190 Sled stations..... | 3-114 |
| Figure 3-23: Patterns of prevalence and richness of 3,510 species at 457 Trawl stations..... | 3-114 |
| Figure 3-24: Species richness from epibenthic Sled data by location in the GBRMP..... | 3-115 |
| Figure 3-25: Species richness from research Trawl data by location in the GBRMP..... | 3-115 |
| Figure 3-26: Example of a single species distribution map, for the Platycephalid fish, <i>Elates ransonnetii</i> | 3-116 |
| Figure 3-27: ROC curve for presence-absence estimation of <i>Actinopterygii: Elates ransonnetii</i> . As noted in the previous figure, this ROC has an AUC of 0.97..... | 3-118 |
| Figure 3-28: Scatter plot of the weighted versus unweighted AUCs for all species. | 3-119 |
| Figure 3-29: Frequency distributions of species biomass distribution model performance diagnostics for the presence model weighted AUC (P_AUCW) and for the biomass model relative deviance explained (Deviance ratio). The median is indicated by the dashed vertical lines. | 3-120 |
| Figure 3-30: Relationship between species biomass distribution model performance diagnostics for presence model weighted AUC (P_AUCW) and for biomass model Deviance ratio. The medians are indicated by the dashed lines. Symbol colour indicates frequency: least frequent=dark blue to most frequent=red..... | 3-120 |
| Figure 3-31: Model distribution maps of selected species with higher performing diagnostics. | 3-122 |
| Figure 3-32: Model distribution maps of selected species with among the poorest performing diagnostics. ... | 3-123 |
| Figure 3-33: Model distribution maps of selected species with median performing diagnostics..... | 3-124 |
| Figure 3-34: Model distribution maps of selected species with positive and negative affinities for mud..... | 3-126 |
| Figure 3-35: Model distribution maps of selected species with positive and negative affinities for benthic irradiance..... | 3-127 |
| Figure 3-36: Model distribution maps of selected species with positive and negative affinities for seabed current stress..... | 3-128 |
| Figure 3-37: Model distribution maps of selected species with affinities for shallow and deep bathymetry... .. | 3-129 |
| Figure 3-38: Model distribution maps of selected species within genera having contrasting distributions. | 3-130 |
| Figure 3-39: Model distribution maps of selected species within genera having contrasting distributions. | 3-131 |
| Figure 3-40: Model distribution maps of selected species within genera having contrasting distributions. | 3-132 |
| Figure 3-41: Cluster dendrogram of the single species estimates illustrating the hierarchical cluster structure determined by Ward’s method. | 3-133 |

| | |
|--|-------|
| Figure 3-42: Aggregated biomass map and model for an example species-group (“7”). The top 10 of 22 species is tabulated with cumulative biomass..... | 3-134 |
| Figure 3-43: Model distribution maps of selected species groups. | 3-136 |
| Figure 3-44: Model distribution maps of selected species groups. | 3-137 |
| Figure 3-45: Recursive decision tree partitioning the sites into 16 groups, corresponding to the terminal nodes. The labels indicate the split variable and threshold for the group corresponding to the left hand branch in each case. The distances used were Bray-Curtis dissimilarities on $1/8^{\text{th}}$ root transforms of the predicted site species biomass data. | 3-138 |
| Figure 3-46: Dendrogram of biological similarities between the medoids of the site groups, as defined by the tree | |
| Figure 3-45, based on hierarchical clustering of Bray-Curtis dissimilarities using Ward's method..... | 3-139 |
| Figure 3-47: Map of predicted distributions of 16 seabed assemblages (site groups clusters)..... | 3-140 |
| Figure 3-48: Dendrogram for species, defining clusterings based on inter-species distances that reflect affinities between species and site-groups. The red line shows a cut-off that defines the 12 groups used in this analysis. The dendrogram was constructed using Ward's method. | 3-141 |
| Figure 3-49: Plot of relative biomass of 12 species affinity groups (labeled A–L) across the 16 site-group assemblages mapped in Figure 3-47. | 3-142 |
| Figure 3-50: Map of the distribution of seabed substratum types summarized as percent of transect length observed by towed video camera. | 3-146 |
| Figure 3-51: Map of the distribution of broad biological seabed habitat types summarized as percent of transect length observed by towed video camera. | 3-146 |
| Figure 3-52: Photos of some example habitat types observed by towed video camera. | 3-147 |
| Figure 3-53: Map of the distribution and cover of conspicuous genera and other morpho-types of algae. | 3-148 |
| Figure 3-54: Map of the distribution and cover of morpho-types of seagrasses. | 3-148 |
| Figure 3-55: Map of the distribution and cover of conspicuous genera & other morpho-types of sponges..... | 3-149 |
| Figure 3-56: Map of the distribution and cover of conspicuous genera & other morpho-types of gorgonians..... | 3-149 |
| Figure 3-57: Map of the distribution and cover of conspicuous genera & other morpho-types of alcyonarian soft-corals. | 3-150 |
| Figure 3-58: Map of the distribution and cover of morpho-types of bryozoans..... | 3-150 |
| Figure 3-59: Map of the distribution and cover of morpho-types of hard corals. | 3-151 |
| Figure 3-60: Recursive partitioning of sites based on the grouped vessel biological cover proportions, the Manhattan (Bray-Curtis) distance metric and the medoid partitioning algorithm..... | 3-152 |
| Figure 3-61: Mean profiles (centroids) of 9 site groups as defined by the recursive partitioning algorithm. ... | 3-153 |
| Figure 3-62: Map of predictions of group membership to the GBR grid. The groups are those from the medoid algorithm with grouped vessel biological data and Manhattan distances shown in (Figure 3-60). | 3-154 |
| Figure 3-63: Results for a single two-class classification experiment for sand substratum with no biohabitat and sand substratum with seagrass, calculated with a Tree classifier. Training data is from sites 1701 and 2441 and test data is from sites 1580 and 2083..... | 3-156 |
| Figure 3-64: Classification results across 54 different test sets for training data from sites 1701 and 2441, calculated with a Tree classifier. Circles and squares indicate test sets containing no contributions in common with the training set. | 3-157 |
| Figure 3-65: Mis-classification results from Figure 5 plotted against absolute depth difference between the sand components of the training and test sets, showing a distinct depth divide near 15 m separating the good and poor results. | 3-158 |
| Figure 3-66: Tree classification results for (sand, no biohabitat) and (sand, seagrass) seabed types across 54 test sets with training data from sites 2005 and 2441. | 3-159 |
| Figure 3-67: Results of a single two-class classification experiment for (sand, sponge garden dense) and (sand, seagrass) seabed types, generated with a Tree classifier. Training data is from sites 2580 and 2441 and test data is from sites 2593 and 2084. | 3-160 |
| Figure 3-68: Tree classification results across 15 different test sets for training data from sites 2580 and 2441. Circles indicate test sets containing no contribution in common with the training set. Seagrass is well classified across the full test set range, while sponge garden undergoes larger variation to be the dominant error source for those test sets with high mis-classification rates | 3-160 |
| Figure 3-69: Results for a single classification experiment on three seabed classes comprising (sand, no biohabitat), (sand, sponge garden dense) and (sand, seagrass), calculated via Linear Discriminant Analysis. Training data is from sites 1701, 2009 and 2441, and test data is from sites 1580, 2593 and 2083..... | 3-161 |
| Figure 3-70: Additional classification results for the three classes (sand, no biohabitat), (sand, sponge garden dense) and (sand, seagrass), showing maximum confusion matrix diagonal elements against training/test depth departure, for test sets containing contributions from all available sites. | 3-162 |
| Figure 3-71: Results for a single classification experiment on four seabed classes, with training data taken from sites 2191, 1701, 2009 and 2441, and test data from sites 2447, 1580, 2593 and 2083, calculated via a Tree classifier. | 3-163 |
| Figure 3-72: Computed four-class classification results for additional test sets, displayed as maximum confusion matrix diagonal elements for each of the four seabed classes. | 3-164 |

| | |
|---|-------|
| Figure 3-73: Confusion matrix diagonals and overall mis-classification rates for a 5-class classification experiment on selected substrata without biohabitat, generated with Linear Discriminant Analysis. Training data is supplied from sites 1828, 1701, 2458, 2407 and 2163, with test data from sites 2315, 1580, 2750, 1897 and 1940. | 3-166 |
| Figure 3-74: (a) Plot of the original pelagic data against sample time for a shallow sandy site (depth = 12 m); and (b) plot of depth-normalised data against sample number for the same site. | 3-167 |
| Figure 3-75: (a) Plot of the original pelagic data against sample time for a deep sandy site (depth = 87 m); and (b) plot of depth-normalised data against sample number for the same site. | 3-167 |
| Figure 3-76: Plot of the depth-normalised pelagic data against sample number for sand sites for a range of depths: (a) 12 m; (b) 20 m; (c) 50 m; and (d) 87.5 m. | 3-167 |
| Figure 3-77: (a) Plot of the original pelagic data against sample time for a sand/algae group; and (b) plot of the corresponding bottom data for the same group. | 3-168 |
| Figure 3-78: Plot of the depth-normalised pelagic data against sample number for (a) a shallow sandy site (depth = 12 m); and (b) a deep sandy site (depth = 70 m). | 3-168 |
| Figure 3-79: (a) Plot of the response averaged over sample numbers 110 – 112 against depth for all groups of >100 contiguous pings for all classes; and (b) plot of the difference in response for sample numbers 110 – 112 against depth for the same data. | 3-169 |
| Figure 3-80: Plot of the response averaged over sample numbers 110 – 112 against depth for (a) class 617 (sand) and (b) class 217 (coarse sand). | 3-169 |
| Figure 3-81: Plots of the depth-normalised pelagic data against sample number for sand sites for depths ranging from 12 m (a) to 85 m in (h). | 3-170 |
| Figure 3-82: Plot of the response for the peak-aligned data against 100/depth for (a) sand class 617 for sample number 113; (b) sand class 617 for sample number 115; (c) silt class 817 for sample number 113; (d) silt class 817 for sample number 115; (e) mud class 917 for sample number 113; and (f) mud class 917 for sample number 115. | 3-171 |
| Figure 3-83: Plot of the group means for the first two canonical variates for the canonical variate analysis of the 4519 groups from 117 classes, without regard to the class labels, for (a) the peak-aligned and depth-adjusted data; and (b) the peak-aligned, row-corrected and depth-adjusted data. | 3-173 |
| Figure 3-84: Plot of the first canonical vector for the canonical variate analysis of the 4519 groups from 117 classes, without regard to the class labels, for the peak-aligned and depth-adjusted data. | 3-174 |
| Figure 3-85: Plot of the canonical vectors for the canonical variate analysis of the 4519 groups, for (a) the peak-aligned and depth-adjusted data; and (b) the peak-aligned, row-corrected and depth-adjusted data. | 3-174 |
| Figure 3-86: Plot of (a) the second canonical vector for the canonical variate analysis of the 4519 groups for the peak-aligned and depth-adjusted data; and (b) the first canonical vector the peak-aligned, row-corrected and depth-adjusted data. | 3-174 |
| Figure 3-87: Plot of (a) the third canonical vector for the canonical variate analysis of the 4519 groups for the peak-aligned and depth-adjusted data; and (b) the second canonical vector the peak-aligned, row-corrected and depth-adjusted data. | 3-174 |
| Figure 3-88: Plot of the group means for the first two canonical variates for the canonical variate analysis of the 4519 groups from 117 classes, without regard to the class labels, for the peak-aligned, row-corrected and depth-adjusted data for (a) sand class 617; (b) seagrass class 621; (c) silt class 817; (d) mud class 917. | 3-175 |
| Figure 3-89: Plot of the group means for the first two canonical variates for the canonical variate analysis of the 4519 groups which result from contrasts between class 617 vs classes 618 and 621, and class 618 vs class 621, for the peak-aligned, row-corrected and depth-adjusted data for (a) all groups for all classes; (b) sand class 617; (c) sponge class 618; and (d) seagrass class 621. | 3-176 |
| Figure 3-90: Plot of the group means for the first canonical variate for the canonical variate analysis of the 4519 groups for the peak-aligned, row-corrected and depth-adjusted data (a) against depth; and (b) against 1/depth. | 3-177 |
| Figure 3-91: Plot of the group means for the first canonical variate for the canonical variate analysis of the 4519 groups which result from contrasts between class 617 vs classes 618 and 621, and class 618 vs class 621, for the peak-aligned, row-corrected and depth-adjusted data (a) against depth; and (b) against 1/depth. | 3-177 |
| Figure 3-92: Plot of the group means for the first canonical variate for the canonical variate analysis of the 4519 groups which result from contrasts between class 617 vs classes 618 and 621, and class 618 vs class 621, for the peak-aligned, row-corrected and depth-adjusted data against depth for (a) all groups for all classes; (b) sand class 617; (c) sponge class 618; and (d) seagrass class 621. | 3-178 |
| Figure 3-93: Plot of the group means for the first canonical variate for the canonical variate analysis of the 4519 groups which result from contrasts between class 617 vs classes 618 and 621, and class 618 vs class 621, for the peak-aligned, row-corrected and depth-adjusted data against 1/depth for (a) all groups for all classes; (b) sand class 617; (c) sponge class 618; and (d) seagrass class 621. | 3-179 |
| Figure 3-94: Plot of the group means for the first two canonical variates for the canonical variate analysis of the 3358 groups in the larger CV1-CV2 cluster for the peak-aligned, row-corrected and depth-adjusted data for (a) all groups; (b) sand class 617; (c) seagrass class 621; and (d) mud class 917. | 3-180 |

| | |
|---|-------|
| Figure 3-95: Plot of the group means for the first canonical variate for the canonical variate analysis of the 3358 groups for the peak-aligned, row-corrected and depth-adjusted data against depth..... | 3-180 |
| Figure 3-96: Plot of the group means for the first two canonical variates for the canonical variate analysis of the 1161 groups in the smaller CV1-CV2 cluster for the peak-aligned, row-corrected and depth-adjusted data for (a) all groups; (b) sand class 617; and (c) mud class 917 | 3-181 |
| Figure 3-97: Plot of the group means for the first canonical variate for the canonical variate analysis of the 1161 groups for the peak-aligned, row-corrected and depth-adjusted data against depth..... | 3-182 |
| Figure 3-98: Plots of (a) the canonical variate scores and (b) the group means for the first two canonical variates for a canonical variate analysis of the depth-normalised data for 42 groups from sites 1631 and 2552, without regard to the class labels. | 3-182 |
| Figure 3-99: Plots of the depth-normalised pelagic data against sample number for group means for (a) 12 groups for the seagrass site 1631 (class 621); and (b) 30 groups for the sand site 2552 (class 617). | 3-183 |
| Figure 3-100: Plots of (a) the canonical variate scores and (b) the group means for the first two canonical variates for a canonical variate analysis of the depth-normalised data for 56 groups from sites 1631, 2552 and 2224, without regard to the class labels. | 3-183 |
| Figure 3-101: Plots of the depth-normalised pelagic data against sample number for group means for (a) 30 groups for class 617 (sand) from site 2552, and (b) 14 groups for class 617 (sand) from site 2224. | 3-184 |
| Figure 3-102: Plots of the echo responses for the depth-normalised pelagic data against sample number for profiles 48 – 50 for group 53 (from the sand site 2552 - class 617). | 3-184 |
| Figure 3-103: Plots of (a) the canonical variate scores and (b) the group means for the first two canonical variates for a canonical variate analysis of the depth-normalised data for 61 groups from sites 1631, 2552, 2224 and 2441, without regard to the class labels. | 3-185 |
| Figure 3-104: Plots of the depth-normalised pelagic data against sample number for group means for (a) 12 groups for class 621 (seagrass) from site 1631, (b) 5 groups for class 621 (seagrass) from site 2441. | 3-185 |
| Figure 3-105: Plots of the depth-normalised pelagic data against sample number for group means for (a) 14 groups for class 617 (sand) from site 2224 and (b) the group for class 617 from site 1580 superimposed on the groups from site 2224. | 3-185 |
| Figure 3-106: Distribution maps of the most exposed species groups (a) exposed over 50 %, (b) – (d) exposed by 25-50%. | 3-200 |
| Figure 3-107: Distribution maps of the most exposed species groups: (a) and (b) exposed by 25-50%; and species groups with negative trawl effort coefficients and possible population decreases in abundance as a result of trawling of >5%; (c) -5.3% and (d) -6% respectively. | 3-201 |
| Figure 3-108: Model distribution maps of selected species with higher trawl exposure indicators. | 3-209 |
| Figure 3-109: Model distribution maps of selected species with higher trawl exposure indicators. | 3-210 |
| Figure 3-110: Model distribution maps of selected species with higher trawl exposure indicators. | 3-211 |
| Figure 3-111: Model distribution maps of selected species with higher trawl exposure indicators. | 3-212 |
| Figure 3-112: Model distribution maps of selected species with higher trawl exposure indicators. | 3-213 |
| Figure 3-113: Model distribution maps of selected species with higher trawl exposure indicators. | 3-214 |
| Figure 3-114: Model distribution maps of selected species with higher trawl exposure indicators. | 3-215 |
| Figure 3-115: Model distribution maps of selected species with higher trawl exposure indicators. | 3-216 |
| Figure 3-116: Model distribution maps of selected species with larger negative trawl coefficients. | 3-220 |
| Figure 3-117: Model distribution maps of selected species with larger negative trawl coefficients. | 3-221 |
| Figure 3-118: Model distribution maps of selected species with larger positive trawl coefficients. | 3-225 |
| Figure 3-119: Model distribution maps of selected species with multiple trawl coefficients. | 3-227 |
| Figure 3-120: Plot of estimated percentage of population caught against mean RSA recovery rank. Species at greatest potential risk should plot towards the upper left quadrant. The top ranking species are labeled with the first three letters of their genus and species name (see Table 3-57). | 3-229 |
| Figure 3-121: Model distribution maps of selected species with higher relative risk identified from exposure and SRA recovery attributes. | 3-231 |
| Figure 3-122: Model distribution maps of selected species with higher relative risk identified from exposure and SRA recovery attributes. | 3-232 |
| Figure 3-123: Model distribution maps of selected species with highest sustainability risk indicators. | 3-237 |
| Figure 3-124. Total annual effort averaged over 20 replicate simulations for the 7 scenarios. | 3-243 |
| Figure 3-125. Average and standard deviations over 20 replicates for scenarios SQ2001 (<i>blue</i>) and CL/BB2001+P+RAP+BB2005 (<i>green</i>) of (a) effort and (b) relative biomass. | 3-244 |
| Figure 3-126. Relative biomass histories for all scenarios for two widely different vulnerability types: (<i>left</i>) a highly resilient taxon (r, d) = (0.7, 0.1); (<i>right</i>) a highly vulnerable taxon (r, d) = (0.1, 0.44). | 3-244 |
| Figure 3-127. Average density of genus- and higher-level taxa in 2025 under each scenario. | 3-245 |
| Figure 3-128. Average density of individual species in 2025 under each scenario. | 3-246 |
| Figure 3-129. Time histories since 1990 of mean density 20 individual species under all scenarios. | 3-248 |
| Figure 3-130. Time histories since 1990 of mean density of 18 genus- and higher-level taxa under all scenarios. | 3-248 |

TABLES

| | |
|--|-------|
| Table 2-1. Correlation matrix of physical environmental covariates. Non-significant correlations are greyed; larger positive and negative correlations >0.05 are highlighted..... | 2-14 |
| Table 2-2. Calculation of adjusted importance I_{adj} : d_{err} is error distance in degrees, I_{bio} is the random forests biotic importance, reliability is $R = (d_{err})^{-1/2}$, and $I_{adj} = (I_{bio}QR)^{0.74}$ | 2-19 |
| Table 2-3. Variable loadings for the first 7 principal components. Absolute loadings greater than 0.5 are highlighted in yellow, and absolute loadings between 0.3 and 0.5 are highlighted in green. The variables are ordered by adjusted importance. Relative variance is the fraction of the total variance explained by the principal component..... | 2-21 |
| Table 2-4. Voyages completed by the <i>Lady Basten</i> with scheduled duration, numbers of sites sampled by towed camera, epibenthic sled and BRUVS..... | 2-31 |
| Table 2-5: Voyages completed by the <i>Gwendoline May</i> with scheduled duration, numbers of scientific trawl sites sampled, sites with hookups and those too rough to trawl..... | 2-32 |
| Table 2-6: Substratum and Biological habitat types and animal events types entered in real time to annotate the video transect. Numbers in parentheses show index values used in acoustics sections..... | 2-34 |
| Table 2-7: Designated preservation methods on board the vessel and destinations for further processing (MTQ-TVL = Museum of Tropical Queensland; QMSB-BRS = Queensland Museum South Brisbane; CMR-CV = CSIRO Cleveland, QDPI-TVL = Queensland Department of Primary Industries Townsville)..... | 2-39 |
| Table 2-8: The taxonomic groups into which samples were sorted onboard and their specific requirements for preservation on board the vessel and destinations for further processing were provided..... | 2-42 |
| Table 2-9: Sediment and group biological cover classes for analysed video tow data. Note that sediment classes up to large pebble could be further classified as rippled or in waves and cobble as waves..... | 2-64 |
| Table 2-10. Habitat Events re-coding table showing mapping from the original BioHabitat code to Habitat_Code2..... | 2-74 |
| Table 2-11. Habitat Events re-coding table showing mapping from the original BioHabitat code to Habitat_Code3..... | 2-74 |
| Table 2-12. Substratum Events re-coding table showing mapping from the original Substratum code to Substratum_Code2..... | 2-75 |
| Table 2-13. Substratum Events re-coding table showing mapping from the original Substratum code to Substratum_Code3..... | 2-75 |
| Table 2-14. Effort (boat days) in various regions of the East Coast Trawl Fishery, 2001–2005..... | 2-78 |
| Table 2-15. Parameters c_i , c_r , c_t , c_{it} and c_{it} for the ROV recovery data from Pitcher <i>et al.</i> (2004); and corresponding estimates r and d fit by non-linear least squares. *For <i>Subergorgia suberosa</i> and <i>Solenocaulon</i> the value $r = 0.22$ was used..... | 2-80 |
| Table 2-16. Parameters c_i , c_r , c_t , c_{it} and c_{it} for the sled recovery data from Pitcher <i>et al.</i> (2004); and corresponding estimates r and d fit by non-linear least squares..... | 2-81 |
| Table 2-17. Parameters r and d for coarse taxonomic groupings; d comes from Poiner <i>et al.</i> (1998) and r from Hill <i>et al.</i> (2002)..... | 2-83 |
| Table 2-18. Relationship between modeled OTU and the source OTU for providing r and d at 3 levels of taxonomic resolution: A) species, B) genus, and C) coarse (family or higher). The 3 rd column indicates whether a GLM model exists for the OTU..... | 2-85 |
| Table 3-1: Twenty-five most predictable species (y) using best 20 explanatory variables. "yres" = (1 - %prediction error). "%Var" is the percentage of the variation in presence/absence of the species explained by the best gbmmv model, for production of biophysical maps..... | 3-88 |
| Table 3-2: Top 20 explanatory variables (x) sorted by descending order of "xres" = (% of [1-% prediction error] for each x). "xvar" is the mean percentage of the variation in the responses (species occurrence) explained by each of the explanatory variables in the best gbmmv model, for production of biophysical maps..... | 3-88 |
| Table 3-3: Matrix of percentage of the variability in occurrence of 25 species responses explained by the top 20 explanatory variables..... | 3-89 |
| Table 3-4: Hierarchy of nodes in the multivariate tree using location along and across the shelf to represent the location of species assemblages. The number of BRUVS stations and of species with maxima in DLI values are listed for each node. Terminal nodes are in bold font..... | 3-107 |
| Table 3-5 Hierarchy of nodes in the multivariate tree using spatial and environmental covariates to represent the location of species assemblages. The number of species with maxima in DLI values are listed for each node. Terminal nodes are in bold font..... | 3-110 |
| Table 3-6: Number of OTUs by Phyla sampled by the epibenthic sled and research trawl, and in the merged dataset..... | 3-112 |
| Table 3-7: Overall total and mean sampling rates (g per Ha) for the major Phyla sampled by the epibenthic Sled and research Trawl, indicating overall composition and relative catchability. Ratio shows the trawl sampling rate relative to the sled..... | 3-113 |
| Table 3-8. List of species comprising species group 7..... | 3-135 |

| | |
|--|-------|
| Table 3-9: A sample confusion matrix for the two-class case of sand and seagrass. | 3-155 |
| Table 3-10: Sites with at least 1,000 consecutive samples of (sand, no biohabitat) seabed type | 3-155 |
| Table 3-11: Sites with at least 1,000 consecutive samples of (sand, seagrass) seabed type..... | 3-156 |
| Table 3-12: Sites with 1,000 consecutive samples of (sand, sponge garden dense) seabed type (6,18). | 3-159 |
| Table 3-13: The calculated confusion matrix at feature dimension 50 from Figure 3-69. | 3-161 |
| Table 3-14: Sites with 1,000 consecutive samples of (sand, bioturbated) seabed type (6,5). | 3-163 |
| Table 3-15: The calculated confusion matrix at feature dimension 40 from Figure 3-71. | 3-163 |
| Table 3-16: Sites with 1,000 consecutive samples of (coarse sand, no biohabitat) seabed type (2,17). | 3-165 |
| Table 3-17: Sites with 1,000 consecutive samples of (sand waves/dunes, no biohabitat) seabed type (7,17). | 3-165 |
| Table 3-18: Sites with 1,000 consecutive samples of (silt, no biohabitat) seabed type (8,17). | 3-165 |
| Table 3-19: Sites with 1,000 consecutive samples of (soft mud, no biohabitat) seabed type (9,17). | 3-165 |
| Table 3-20: The calculated confusion matrix at feature dimension 40 from Figure 3-73. | 3-166 |
| Table 3-21: Intercept, slope and r^2 values for regressions of the response at various sample numbers for the peak-aligned depth-normalised pelagic data on 1/depth. | 3-172 |
| Table 3-22. Sub1_Hab2: Observed (Row Totals) counts and percentage contribution, Observed versus Predicted Diagonal counts and percentages. | 3-187 |
| Table 3-23. Sub2_Hab2: Observed (Row Totals) counts and percentage contribution, Observed versus Predicted Diagonal counts and percentages. | 3-188 |
| Table 3-24. Habitat_Code2: Confusion matrix of total counts observed vs. predicted..... | 3-189 |
| Table 3-25. Habitat_Code2: Confusion matrix of percentage contribution as a percentage of row totals..... | 3-189 |
| Table 3-26. Habitat_Code2: Confusion matrix of percentage contribution as a percentage of totals..... | 3-190 |
| Table 3-27. Habitat_Code3: Confusion matrix of total counts observed vs. predicted..... | 3-190 |
| Table 3-28. Habitat_Code3: Confusion matrix of percentage contribution as a percentage of row totals..... | 3-191 |
| Table 3-29. Habitat_Code3: Confusion matrix of percentage contribution as a percentage of totals..... | 3-191 |
| Table 3-30. Substratum_Code1: Confusion matrix of total counts observed vs. predicted..... | 3-192 |
| Table 3-31. Substratum_Code1: Confusion matrix of percentage contribution as a percentage of row totals. | 3-192 |
| Table 3-32. Substratum_Code1: Confusion matrix of percentage contribution as a percentage of totals..... | 3-192 |
| Table 3-33. Substratum_Code2: Confusion matrix of total counts observed vs. predicted..... | 3-193 |
| Table 3-34. Substratum_Code2: Confusion matrix of percentage contribution as a percentage of row totals. | 3-193 |
| Table 3-35. Substratum_Code2: Confusion matrix of percentage contribution as a percentage of totals..... | 3-193 |
| Table 3-36. Substratum_Code3: Confusion matrix of total counts observed vs. predicted..... | 3-194 |
| Table 3-37. Substratum_Code3: Confusion matrix of percentage contribution as a percentage of row totals. | 3-194 |
| Table 3-38. Substratum_Code3: Confusion matrix of percentage contribution as a percentage of total..... | 3-194 |
| Table 3-39. Substratum_Code3 Depth Partitioned: Confusion matrix of total counts observed vs. predicted..... | 3-195 |
| Table 3-40. Substratum_Code3 Depth Partitioned: Confusion matrix of percentage of rows..... | 3-195 |
| Table 3-41. Substratum_Code3 Depth Partitioned: Confusion matrix of percentage of total..... | 3-195 |
| Table 3-42. Summary of LDA classification performance of QTC View data. | 3-196 |
| Table 3-43: Total area and percentage of the study area on the continental shelf of the GBRMP in various management zones considered for estimating ecological risk indicators. | 3-197 |
| Table 3-44: Total area of the study area on the continental shelf of the GBRMP exposed to various levels of trawl effort, measured by VMS in 2005, considered for estimating ecological risk indicators. The total effective area trawled and total area swept are also estimated. | 3-197 |
| Table 3-45: Ecological Risk Indicators with respect to trawling for estimated Biomass (tonnes) of correlated species groups: by GBRMP Zoning indicating percent of biomass available; by areas not trawled/trawled indicating percent biomass potentially exposed; by trawl intensity (ann_hrs/0.01° cell) indicating percent biomass directly exposed to effort. | 3-199 |
| Table 3-46: Ecological Risk Indicators with respect to trawling for estimated Biomass (kg) of species in group#29: biomass available in General Use zone; biomass potentially exposed in trawled cells; and biomass directly exposed to trawl effort. Pale orange: >25% biomass exposed; dark orange: >50% biomass exposed; red: >50% biomass exposed..... | 3-204 |
| Table 3-47: Ecological Risk Indicators with respect to trawling for estimated Biomass (kg) of species in group#9: biomass available in General Use zone; biomass potentially exposed in trawled cells; and biomass directly exposed to trawl effort. Pale orange: >25% biomass exposed; dark orange: >50% biomass exposed; red: >50% biomass exposed..... | 3-204 |
| Table 3-48: Ecological Risk Indicators with respect to trawling for estimated Biomass (kg) of species in group#22: biomass available in General Use zone; biomass potentially exposed in trawled cells; and biomass directly exposed to trawl effort. Pale orange: >25% biomass exposed; dark orange: >50% biomass exposed; red: >50% biomass exposed..... | 3-205 |
| Table 3-49: Ecological Risk Indicators with respect to trawling for estimated Biomass (kg) of species in group#14: biomass available in General Use zone; biomass potentially exposed in trawled cells; and biomass directly exposed to trawl effort. Pale orange: >25% biomass exposed; dark orange: >50% biomass exposed; red: >50% biomass exposed..... | 3-205 |

| | |
|--|--------|
| Table 3-50: Ecological Risk Indicators with respect to trawling for estimated Biomass (kg) of species in group#13: biomass available in General Use zone; biomass potentially exposed in trawled cells; and biomass directly exposed to trawl effort. Pale orange: >25% biomass exposed; dark orange: >50% biomass exposed; red: >50% biomass exposed..... | 3-206 |
| Table 3-51: Ecological Risk Indicators with respect to trawling for estimated Biomass (kg) of species in group#33: biomass available in General Use zone; biomass potentially exposed in trawled cells; and biomass directly exposed to trawl effort. Pale orange: >25% biomass exposed; dark orange: >50% biomass exposed; red: >50% biomass exposed..... | 3-206 |
| Table 3-52: Ecological Risk Indicators with respect to trawling for estimated Biomass (kg) of species in group#27: biomass available in General Use zone; biomass potentially exposed in trawled cells; and biomass directly exposed to trawl effort. Pale orange: >25% biomass exposed; dark orange: >50% biomass exposed; red: >50% biomass exposed..... | 3-206 |
| Table 3-53: Ecological Risk Indicators with respect to trawling for estimated Biomass (kg) of top ranking species in groups with low total exposure (<25%): biomass available in General Use zone; biomass potentially exposed in trawled cells; and biomass directly exposed to trawl effort. Pale orange: >25% biomass exposed; dark orange: >50% biomass exposed; red: >50% biomass exposed. | 3-207 |
| Table 3-54: Results for the Trawl Effort covariate: species with negative coefficients for presence (P) or biomass (B), coefficients with $p>0.05$ are greyed, the magnitude of the coefficient in terms of overall % change in abundance is also indicated. The group membership, total estimated biomass (kg), % available, % exposed and effort exposed % are as above. | 3-218 |
| Table 3-55: Results for the Trawl Effort covariate: species with positive coefficients for presence (P) or biomass (B), coefficients with $p>0.05$ are greyed, the magnitude of the coefficient in terms of overall % change in abundance is also indicated. The group membership, total estimated biomass (kg), % available, %exposed and effort exposed are as above. | 3-223 |
| Table 3-56: Results for the Trawl Effort covariate: species with an additional term involving the Trawl Effort covariate, as well as coefficients for presence (P) or biomass (B), coefficients with $p>0.05$ are grayed, the magnitude of the coefficient in terms of overall % change in abundance is also indicated. The group membership, total estimated biomass (kg), % available, % exposed and effort exposed are as above. | 3-226 |
| Table 3-57: Summary of species exposure estimates for the top 280 of 840 species ranked by percent biomass exposed to trawl effort intensity, showing estimated relative catchability from various sources and indicative uncertainty, possible BRD effect for bycatch fish, leading to an estimate of potential percentage of population caught annually. Recovery attributes from SRA and natural mortality estimates (M) are tabulated where available. Where M was available, a sustainability indicator — estimate proportion Caught/M — is also tabulated. Column * relates to indicator uncertainty due to catchability (see explanation in text, page 3-230). | 3-233 |
| Table 3-58: Ecological Risk Indicators with respect to trawling for estimated area (km ²) of predicted distributed of species assemblages (site clusters): by GBRMP Zoning indicating percent of area available; by area not trawled/trawled indicating percent area potentially exposed; by trawl intensity (ann_hrs/0.01° cell) indicating percent area exposed to effort. | 3-241 |
| Table 3-59: Ecological Risk Indicators with respect to trawling for estimated area (km ²) of predicted distributed of video habitat clusters: by GBRMP Zoning indicating percent of area available; by area not trawled/trawled indicating percent area potentially exposed; by trawl intensity (ann_hrs/0.01° cell) indicating percent area directly exposed to effort. | 3-241 |
| Table 3-60. Species with greatest affinity (top 40) for site-group assemblages identified in Section 3.4, with the highest levels of trawl exposure. | 3-242 |
| Table 3-61. Lowest historical (pre-2001) percentage relative biomass and final relative biomass in 2025 under scenarios SQ2001 and SQ2006 for (<i>left</i>) species- and genus-level taxa and (<i>right</i>) coarse-level taxa. ... | 3-246 |
| Table 9-1. Top 20 ranked species for four different indicators. (a) Percent of biomass directly exposed to effort (red = >75%, orange = >50%). (b) Estimated percent of biomass caught per annum (red = >75%, orange = >50%, pale = >25%). (c) highest relative risk ranked species from plotting 'Recovery' rank from 'SRA' against estimated catch from b (no reference points are possible). (d) Sustainability indicator: estimated catch b / natural mortality rate (red = exceeds limit reference point 1.0, orange = exceeds conservative reference point 0.8, pale = exceeds conservative reference point 0.6). (e) Highest ranked species from assemblage exposure and species affinities for assemblages (no reference points). | 9-275 |
| Table 15-1: Summary of species exposure estimates for all 840 modelled species, ranked in descending order by percent of biomass exposed to trawl effort intensity; showing also species group membership, total estimated biomass, percent of biomass available in General Use zone, percent of biomass potentially exposed in trawled cells. Pale orange: >25% biomass exposed; dark orange: >50% biomass exposed; red: >50% biomass exposed. | 15-286 |

NON-TECHNICAL SUMMARY

PROJECT:

CRC-REEF C1.1.2: Seabed Biodiversity on the Continental Shelf of the Great Barrier Reef World Heritage Area (GBRWHA)

FRDC 2003/021: Mapping Bycatch & Seabed Benthos Assemblages in the GBR Region for Environmental Risk Assessment & Sustainable Management of the Queensland East Coast Trawl Fishery (QECTF).

NOO 2004/15: Assessment of the performance of acoustic remote sensing for Seabed Mapping and as a surrogate for biodiversity on the continental shelf of the GBR

PRINCIPAL INVESTIGATORS:

Dr C. Roland Pitcher, CSIRO, Task Leader

Dr Peter Doherty, AIMS

Dr Neil Gribble, QDPI-F

Drs Peter Arnold & John Hooper, QM

ADDRESS:

| | | | |
|----------------------------------|---------------------------------|---------------------------------|---|
| CSIRO | AIMS | QDPI-F/NFC | Qld Museum |
| PO Box 120, Cleveland, Q.4164 | PMB 3 Townsville MC, Q. 4810 | PO Box 5396, Cairns, Q. 4870 | PO Box 3300, South Brisbane, Q. 4101 |
| Ph: 07 3826 7200 | 07 4753 4211 | 07 4035 0100 | 07 3840 7722 |
| Fax: 07 3826 7222 | 07 4772 5852 | 07 4035 1401 | 07 3846 1226 |
| roland.pitcher@csiro.au | p.doherty@aims.gov.au | neil.gribble@dpi.qld.gov.au | john.hooper@qm.qld.gov.au |

OBJECTIVES:

The overall objective was to address key issues identified by the GBRMPA, QDPI&F, QSIA and their advisory committees, in relation to biodiversity assessment and provision of information for future Marine Park planning needs, and environmental sustainability assessments of the Qld East Coast Trawl Fishery with respect to effects on bycatch, benthic assemblages and seabed habitat, to support ecologically-based management of the fishery. Specifically:

1. Develop comprehensive inventories & maps of the distribution and abundance of seabed habitats & assemblages, as a benchmark of their current status, and provide these to GBR Marine Park and Fisheries managers and stakeholders for future planning, management and status reporting, with the outcome of management strategies effective in minimising fishery effects on seabed habitats & assemblages, and achievement of Management Plan targets.
2. Analyse bio-physical relationships and assess the utility of environmental correlates for spatial prediction of assemblages of biodiversity.
3. Provide information for refining the non-reef bio-regions defined for the continental shelf by the Representative Areas Program (RAP) process
4. Develop attributes (e.g. biomass, species richness, rarity, uniqueness, condition, potential vulnerability to impact etc.) for bio-assemblages defined by this project, and for RAP bio-regions, for future planning, management and World Heritage Area (WHA) reporting.
5. Provide recommendations for monitoring trends in the status of bio-assemblages and highly protected area (HPAs) selected by the RAP process.
6. Develop & provide maps of the distribution of vulnerable seabed habitats and assemblages to fishery managers and stakeholders, with the outcome of management strategies effective in

minimising fishery effects, achievement of Management Plan targets and for future planning needs.

7. For both bycatch & benthos, develop quantitative indicators of exposure to & effects of trawling, and sustainability risk indicators, as required for the environmental Strategic Assessment of the Queensland East Coast Trawl Fishery (QECTF).
8. Provide critical input to a dynamic model of indicators for the status of seabed assemblages and conduct ecological assessments of recent and proposed management changes using an MSE approach, and enable capability for evaluation of future options.
9. Contribute to quantifying the large-scale effects of trawling on bycatch species and benthos assemblages by analysing their abundance across the range of trawl intensities within and outside trawl grounds, while accounting for habitat variability.
10. Develop transferable scientific methods and tools to facilitate regional marine management planning nationally, including: knowledge of bio-physical relationships between assemblages and the physical environment (surrogates), cost-effective survey designs & techniques (including development & performance assessment of non-invasive remote tools video & single-beam acoustics for mapping seabed and as surrogates for patterns in seabed assemblages), spatial-statistical classification & prediction methods, and sustainability risk indicators for seabed species, assemblages and communities.

NON-TECHNICAL SUMMARY:

The Great Barrier Reef is a unique World Heritage Area of national and international significance. As a multiple use Marine Park, activities such as fishing and tourism occur along with conservation goals. Managers need information on habitats and biodiversity distribution and risks to ensure these activities are conducted sustainably. However, while the coral reefs have been relatively well studied, less was known about the deeper seabed in the region. From 2003 to 2006, the GBR Seabed Biodiversity Project has mapped habitats and their associated biodiversity across the length and breadth of the 210,000 km² shelf in the Marine Park to provide information that will help managers with conservation planning and to assess whether fisheries are ecologically sustainable, as required by environmental protection legislation (e.g. EPBC Act 1999).

Holistic information on the biodiversity of the seabed was acquired by visiting almost 1,400 sites, representing a full range of known environments, during 10 month-long voyages on two vessels and deploying several types of devices such as: towed video and digital cameras, baited remote underwater video stations (BRUVS), a digital echo-sounder, an epibenthic sled and a research trawl to collect samples for more detailed data about plants, invertebrates and fishes on the seabed. Data were collected and processed from >600 km of towed video and almost 100,000 photos, 1150 BRUVS videos, ~140 GB of digital echograms, and from sorting and identification of ~14,000 benthic samples, ~4,000 seabed fish samples, and ~1,200 sediment samples.

The project has analysed this information and produced all of the outputs as originally proposed; these included:

- Images and videos of seabed habitat types and fishes, including more than 150 substratum and biological habitat component types; and >300 fishes, sharks, rays and sea snakes attracted to BRUVS.
- An inventory of more than 5,300 species of benthos, bycatch and fishes, with catalogued museum voucher specimens, many of which were new species, and a database of more than 140,000 records of species distribution and abundance on the seabed.
- Identification of the key environmental variables likely to be important in structuring seabed distributions, including: sediment grain size and carbonate composition, benthic irradiance, current stress, bathymetry, bottom water physical attributes, nutrients and turbidity — and predictive models of bio-physical relationships between seabed species, their assemblages and the physical environment.
- Maps of the distribution and abundance of ~850 seabed species throughout the GBR shelf region.
- Estimates of the likely extent of past effects of trawling on benthos and bycatch over the entire shelf of the GBR region, which indicated that trawl effort had a significant effect on the biomass of

6.5% of 850 species mapped; with negative biomass change of -1% to -36% for 4.5% of these species and positive biomass change of +1% to +96% for 2% of these species.

- Estimates of exposure to trawl effort showed that about 70% of the 850 species mapped had low or very low exposure, and at the other extreme, about 33 species had high to very high exposure to trawl effort — of these species, after taking relative catch rates into account, five had high estimates of proportion caught annually and 28 were intermediate. The remainder (>800 species) had low or very low estimates of proportion caught annually.

- Indicators based on qualitative recovery ranks showed that about 15 species stood out as being at higher relative risk with respect to trawling. An additional, quantitative absolute sustainability indicator showed that three species (*Fistularia petimba*, *Brachirus muelleri*, *Trixiptichthys weberi*) exceeded a limit reference point (analogous to maximum sustainable yield, MSY), one species (*Pomadasy maculatus*) exceeded a first conservative reference point ($\equiv 0.8 \times \text{MSY}$) and two others (*Psettodes erumei*, *Sillago berrus*) exceeded a second conservative reference point ($\equiv 0.6 \times \text{MSY}$) — another 10 species were also listed due to uncertainty in parameters, though they were below the sustainability reference points.

- Evaluations of the environmental performance of several recent management interventions showed that generalized depletion trends up until the late 1990s have all been arrested and reversed — the 2001 buyback of fishing licences and subsequent penalties made the biggest positive contributions with the 2004 rezoning of the marine park making a small positive contribution for some species.

- Methods and tools for regional marine planning, including: representative survey design and techniques, spatial-statistical classification and prediction methods, and biodiversity and bycatch species risk assessment methods.

A key output from the project is the identification, by means of the trawl exposure and sustainability indicators, of species at risk or potentially at risk from trawling. Different species were highlighted by different indicators, though there was some overlap. The most quantitative indicator was directly related to sustainability, with biologically based reference points — while three species appeared to be at risk and another three species exceeded conservative reference points (as listed above), there was uncertainty that requires a more precautionary response. Hence, the top ranked 50 species, across all indicators developed, were listed herein and recommended to be considered for stakeholder consultation regarding future action. Options may include clarification of the identified uncertainties, monitoring of species at risk, management interventions that reduce risk or combinations of these actions.

It is also recommended that long-term monitoring of trends in ecological condition of identified key seabed habitats and constituent species be implemented to assess responses to regional pressures, including climate change. Candidate habitats should include those that have been demonstrated to be particularly species rich such as vegetated areas and epibenthic gardens. The seabed may be vulnerable to climate change, as climate change modelling has indicated that the thermocline is likely to deepen and upwellings to become weaker and less frequent, with potential consequences for productive habitat dependent on nutrients from such sources. Such a possibility should be investigated.

Further work is needed to address the uncertainties in the risk assessments that arise from uncertainties in estimates of catchability and natural mortality rates. Currently, the uncertainty is such that several additional species could exceed the reference points and many species with unknown mortality might be of concern. It is also possible that clarification of these uncertainties may show that species currently thought to be at risk or potentially at risk may be demonstrated to be of no sustainability concern. Thus, it is recommended that further studies of catchabilities and natural mortality rates be conducted to address this key uncertainty for affected species. Such results are likely to have wide application in risk assessments being conducted in multiple jurisdictions.

Many fisheries in Australia are conducting qualitative approaches to Ecological Risk Assessments. The results of the quantitative sustainability indicators applied here raise concerns about the reliability of the qualitative approaches, which have not been benchmarked because of the lack of a suitable test bed. Such a test bed is now available with the Seabed Biodiversity dataset and an assessment of the performance of the qualitative methods is recommended. The Seabed dataset also provides an opportunity to develop condition and trend and vulnerability indicators for seabed communities and ecosystems that are needed to meet the increasing requirement for ecosystem-based management approaches.

The results of the Seabed Biodiversity Project have been adopted for marine park zoning assessment by a follow on project supported by the Reef and Rainforest Research Centre and involving collaboration with marine park managers. This project has contributed to ongoing marine park planning with respect to meeting WHA obligations.

Another project supported by the CERF National Marine Biodiversity Hub will use the unique Seabed Biodiversity dataset in comparisons with other datasets to test the inter-regional utility of physical variables and cross-taxonomic patterns as surrogates for application in marine planning at a national scale.

Other further opportunities include: sorting and identification of remaining samples that could not be completed within the scope of the project, taxonomic work to properly identify the more difficult specimens, and quantification of visible species from the available towed camera video and digital photos to fill significant gaps in areas too rough for sampling and currently lacking species information. These activities would provide full utilization of the samples and deliver additional value, with expected benefits for greater understanding of the seabed ecosystem, fishery sustainability, zoning assessment and ongoing marine park planning.

Outcomes Achieved

Preliminary outputs have been presented to management and stakeholder committees during the course of the project and team members contributed to management/industry activities such as bycatch risk assessments, assessments of trawl plan targets and marine park monitoring strategies. The final results for each objective have become available only near the end of the project and, with delivery of the final outputs and planned uptake activities, the anticipated outcomes may now be achieved. Progress against expected industry, management and stakeholder outcomes has included:

- Reports and presentations to various audiences and multimedia information available via a website have contributed to raising the level of stakeholder knowledge of the status of the region's ecosystems, facilitating understanding of reasonable use, development and implementation of regional ecosystem management plans to achieve sustainable and acceptable multiple use. Further activities are planned to disseminate and adopt the outputs of the project among managers, stakeholders and scientists. Further development of the website would be valuable.
- Contributions by team members to management/industry assessments of the current Trawl Plan targets and bycatch risk assessments. The 40% bycatch and 25% benthos reductions were considered largely with respect to reductions in trawl effort; the outputs from this project have now provided an assessment of their likely sustainability.
- Ecological risk/sustainability indicators and biological reference points, developed with management and industry involvement, and evaluations of recent management changes showing positive implications for the environment, have contributed to meeting an Environmental Assessment condition on the wildlife trade operation (WTO) for this fishery and, with management response, can be expected to facilitate meeting of environmental sustainability objectives under Commonwealth legislation.
- Indicators of the level of impact under the current management arrangements and biological reference points that will contribute to planned revisions of the Trawl Management Plan.
- Capability to evaluate future alternative management strategies needed to meet environmental sustainability legislation, by estimating outcomes for the environment and for the fishery in a MSE context.

KEYWORDS: Great Barrier Reef, seabed, biodiversity, habitat, trawl, epibenthic sled, video, BRUVS, acoustics, benthos, bycatch, fish, distribution, abundance, biophysical relationships, surrogates, statistical models, classification, prediction, mapping, effects of trawling, ecological risk assessment, sustainability indicators, biological reference points, management strategy evaluation, effort reduction, zoning, survey design, stratification.

1. INTRODUCTION

1.1. BACKGROUND

The Key Result Areas of the CRC Reef Program C "Maintaining Ecosystem Quality" and Project C1 "Conserving Biodiversity" included "...to know the status and trends of marine ecosystems within the GBRWHA..." and "...contribute to regional marine planning...". This project has delivered to these KRAs and the outputs will benefit the GBRMPA by assisting evaluation of the marine park zoning and future planning needs for managing human uses, to optimise trade-offs in a multiple-use environment to meet its goals of conserving habitat and species diversity, and to meet Australia's international obligations for reporting and monitoring the status of values in the WHA.

The goals of the Queensland Trawl Management Plan included achieving environmental sustainability with respect to the Queensland East Coast Trawl Fishery (QECTF), as a response to stakeholder and community concerns about effects of trawling. The CSIRO/QDPI Effects of Trawling Study (Poiner *et al.*, 1998; GBRMPA & FRDC 93/096) clearly showed that the cumulative effects of repeated trawling could be substantial, though the impacts differ greatly for different types of organisms and for different habitats. The overall impacts depend not only on how much life is removed when a trawl passes and how fast the seabed recovers between trawls, but most importantly also on where trawling occurs in relation to where the vulnerable seabed plants and animals live. The most vulnerable types of seabed organisms are those that are easily removed or killed and/or slow to recover — as vulnerability is a function of mortality and recovery rates. That Study concluded that prawn trawling has the potential to be environmentally sustainable, but there remained important assessments that needed to be conducted. The additional information needs for these assessments include:

1. Distribution of trawling effort at scales of 10x10 km and finer (from logbooks and VMS)
2. Recovery rates of fauna after trawling (GBRMPA Trawl Recovery Project & FRDC 97/205 Megabenthos Dynamics)
3. Distribution of seabed fauna and bycatch throughout the GBR (provided by this project)
4. Impacts of trawling on soft-sediment fauna (FRDC 2002/102 Effects of Trawling in the NPF)

This information was critical because the status of vulnerable seabed organisms is greatly affected by their spatial exposure to trawl effort, in addition to impact and recovery rates. The environmental sustainability of the fishery would be greatly facilitated and demonstrable if the distribution of vulnerable seabed life could be taken into account in management of the distribution of trawl effort. The provision of this knowledge of biotic assemblage distributions by this project has overcome a major impediment. These data have now been synthesized by this project, into a Trawl Management Scenario Model to conduct ecological assessments of alternative management strategies (Management Strategy Evaluation, MSE).

The Trawl fishery, like other fisheries, has been required to conduct environmental Strategic Assessments and respond to points raised by the assessors (Department of Environment & Water Resources, DEW) — this project has provided quantification of the broad scale effects of trawling on benthos and bycatch, and developed sustainability risk indicators as key components of the response required for this Strategic Assessment.

The inventories of the distribution and abundance of bycatch species and seabed fauna will also enable development and evaluation of future strategies to minimise impacts and improve the environmental sustainability of the fishery. This will assist managers to respond effectively to industry and community concerns and achieve an informed objective balance between the pressures of exploitation and needs for conservation in a multiple-use environment. The community will have available objective and independent information on the environmental sustainability of trawling.

The benefits of this project's outputs to the Queensland trawl fishery, its managers and the community include a factual biological/ecological basis for objective management decisions and facilitating the assessment of the QECTF Management Plan's stated goals of reducing catch of benthos by 25% and catch of bycatch by 40%. The Project has also developed and delivered operational ESD indicators for use under State and Commonwealth fishery and environmental legislation, including the EPBC Act; and for the national ESD reporting system.

The outputs from this project have national applicability to the implementation of Australia's Oceans Policy, Regional Marine Planning and to the National Work Programs of the National Oceans Office. These outputs have contributed to our understanding of how acoustic remote sensing instruments can be used in approaches to seabed habitat mapping and deliver to priorities identified at the joint NOO/FRDC Habitat Workshop in Melbourne 23-24 September 2002. The large acoustics data-set collected by the project has been extremely valuable for this purpose and can serve as an example for marine assessment for conservation planning and multiple-use management (incl. the National Representative System of marine Protected Areas – NSRMPA) elsewhere.

The objectives of the project have also delivered to the highest 'High Priority' research areas identified by the Biological Diversity Advisory Council as well as the "areas of research of national importance" (Biodiversity Research: Australia's Priorities — a Discussion Paper. Environment Australia, 2000).

1.2. NEED

Information from strategic mapping and analysis of seabed biodiversity was a fundamental need to assess the status and condition of benthic biodiversity in the large and complex ecosystems of the GBR seabed; to establish benchmarks and performance indicators for feedback to management; and to develop sustainability risk indicators and facilitate detection of anthropogenic impact in seabed ecosystems (particularly trawling) among the milieu of natural environmental variability.

With respect to trawling, the CSIRO/QDPI Effects of Trawling Study (Poiner *et al.*, 1998) concluded that if the potentially substantial cumulative environmental effects of trawling are to be managed for sustainability then fundamental information on the distribution and abundance of seabed assemblages and bycatch would be needed. The "Trawl Management Scenario Model" for the QECTF indicated that potential sustainability indicators for Management Strategies Evaluations (MSE) are highly sensitive to current assumptions about the distribution and abundance of species vulnerable to trawling. This project has addressed this important information gap and impediment to management for environmental sustainability by conducting a comprehensive inventory and mapping of seabed assemblages and species caught in bycatch throughout the GBR region, for development of sustainability risk indicators and MSE approaches.

Bycatch sustainability has been a priority issue in the QECTF. This project has addressed the information needs of this issue in two ways: by (1) developing bycatch sustainability risk indicators and (2) quantification of the impacts on populations of bycatch species. To address (1), the project has mapped the distribution and abundance of species caught in bycatch, within and beyond trawl grounds, and estimated the proportion of their populations exposed to trawling by conducting spatial analyses of bycatch species abundance in relation to trawl effort distribution and intensity. For (2) this analysis was developed further, using available data on the catch-rate of bycatch species by the fishery, to estimate the proportion of bycatch populations caught annually, as a risk indicator. The Project has also applied the bycatch vulnerability criteria for life history traits (recovery), which were developed by the NPF Bycatch Sustainability Project (FRDC 96/257), and are now playing a key role in the NPF Bycatch Action Plan. Together, this information has been used to identify those species potentially at risk in the QECTF and has delivered directly to the bycatch reporting requirements for Strategic Assessment and subsequent accreditation outcomes. Similar information has become available for several target and byproduct species, as well as some threatened or potentially threatened species such as syngnathids.

The direct impacts of trawling on seabed benthic assemblages have also been a priority issue in the QECTF. This project has addressed the information needs of this issue by mapping the distributions of seabed assemblages, conducting spatial analyses and developing benthos sustainability indicators similar to that for the bycatch. This has been done by applying the vulnerability algorithms developed for the CSIRO/QDPI Effects of Trawling Study FRDC 93/096 (i.e. the dynamics of per trawl removal rate \times trawl-effort, plus recovery rate information from the GBRMPA follow-on project Seabed Habitat Recovery Dynamics, as well as the FRDC 97/205 Megabenthos Dynamics Project). This information has enabled development of benthos status indicators and evaluation of the environmental performance of different management scenarios (MSE) that may be adopted by the fishery management. Again, these outputs have delivered directly to the reporting requirements for Strategic Assessment and subsequent accreditation outcomes.

Management and Industry considered the outputs from this project essential for the requirement to provide a comprehensive assessment of the sustainability of the fishery. Information from this project will assist stakeholders with their management of the fishery, including: assessment of performance against Trawl Management Plan targets (40% reduction in bycatch and 25% reduction in benthos), response to Strategic Assessment and meeting requirements of the EPBC Act, conduct of ecological risk assessments and development of biologically meaningful reference points, evaluation of the zoning changes in the GBRMP, review of the Trawl Management Plan (2004-06) — and reaching the goal of achieving a sustainable fishery. The Project will deliver results progressively, so that timely outputs will be available for these review processes.

This Project will also deliver information needed for the sustainability of the Queensland Reef Line Fishery. A significant uncertainty regarding the sustainability of this fishery is the unknown area of deeper reef habitat and the populations of demersal fishes therein — this Project has provided estimates for these uncertainties and it is expected that the Effects of Line Fishing Project can capitalise on this information. The Project will also deliver priority research needs relevant to the development of national habitat classification and mapping methods, as identified at the FRDC/NOO Habitat Workshop, 23-24 September 2002.

The challenging broad-scale objectives of this task have been met by multidisciplinary inputs from collaborating specialists from several research providers. This approach will serve as a model for marine conservation planning and multiple-use management (incl. NSRMPA) elsewhere and so is also relevant to the needs of DEW's national objectives and the regional marine planning promoted by Australia's Oceans Policy. In this context, the performance of so-called rapid marine assessment methods, such as acoustic remote sensing, as a surrogate for patterns in seabed biodiversity needed to be formally tested.

1.3. OBJECTIVES

The overall objective is to address key issues identified by the GBRMPA, QDPI&F, QSIA and their advisory committees, in relation to biodiversity assessment and provision of information for future Marine Park planning needs, and environmental sustainability assessments of the Qld East Coast Trawl Fishery with respect to effects on bycatch, benthic assemblages and seabed habitat, to support ecologically-based management of the fishery. Specifically:

1. Develop comprehensive inventories and maps of the distribution and abundance of seabed habitats and assemblages, as a benchmark of their current status, and provide these to GBR Marine Park and Fisheries managers and stakeholders for future planning, management and status reporting, with the outcome of management strategies effective in minimising fishery effects on seabed habitats and assemblages, and achievement of Management Plan targets.
 2. Analyse bio-physical relationships and assess the utility of environmental correlates for spatial prediction of assemblages of biodiversity.
 3. Provide information for refining the non-reef bio-regions defined for the continental shelf by the RAP process
-

4. Develop attributes (e.g. biomass, species richness, rarity, uniqueness, condition, potential vulnerability to impact etc.) for bio-assemblages defined by this project, and for RAP bio-regions, for future planning, management and WHA reporting.
 5. Provide recommendations for monitoring trends in the status of bio-assemblages and HPAs selected by the RAP process.
 6. Develop and provide maps of the distribution of vulnerable seabed habitats and assemblages to fishery managers and stakeholders, with the outcome of management strategies effective in minimising fishery effects, achievement of Management Plan targets and for future planning needs.
 7. For both bycatch and benthos, develop quantitative indicators of exposure to and effects of trawling, and sustainability risk indicators, as required for the environmental Strategic Assessment of the QECTF.
 8. Provide critical input to a dynamic model of indicators for the status of seabed assemblages and conduct ecological assessments of recent and proposed management changes using an MSE approach, and enable capability for evaluation of future options.
 9. Contribute to quantifying the large-scale effects of trawling on bycatch species and benthos assemblages by analysing their abundance across the range of trawl intensities within and outside trawl grounds, while accounting for habitat variability.
 10. Develop transferable scientific methods and tools to facilitate regional marine management planning nationally, including: knowledge of bio-physical relationships between assemblages and the physical environment (surrogates), cost-effective survey designs and techniques (including development and performance assessment of non-invasive remote tools video and single-beam acoustics for mapping seabed and as surrogates for patterns in seabed assemblages), spatial-statistical classification and prediction methods, and sustainability risk indicators for seabed species, assemblages and communities.
-

2. METHODS

This Project characterised the major patterns in the seabed biodiversity and habitats of the Great Barrier Reef, at spatial scales relevant to regional conservation and management needs. The information included seabed species and habitat distribution in inter-reef areas, and physical attributes that may drive patterns within the region.

The approach was to collate and integrate the available biological, habitat, physical and bottom-water data; analyse bio-physical relationships to identify important environmental variables; stratify the GBR seabed based on these variables weighted by their biological importance; design sampling and conduct a series of seabed surveys to obtain representative inclusion of important biological components, major habitat strata, and areas of uncertainty; sort and identify samples and analyse data to produce predictive maps of habitats and biodiversity, which formed the basis of ecological risk assessments for the trawl fishery in the region. Details of these approaches are described below.

2.1. SAMPLING DESIGN

The sampling design was based on a bio-physical stratification of the GBR continental shelf and the analyses were based on the same types of broad-scale bio-physical data (updated where possible). This required collation of available broad coverage bio-physical environmental datasets that were likely to be important in influencing patterns of distribution of biota.

2.1.1. Physical environmental data (I McLeod & R Pitcher)

2.1.1.1. Datasets collated

Phase 1 of the project (Pitcher *et al.* 2002) collated 22 datasets of biological and physical data from internal and external sources. There was some duplication of the data types available among datasets from different sources, in which case the dataset providing the widest reliable coverage was selected. The remaining variables useful for modelling and stratification included 21 physical factors and measures of seasonal variability for eight of these.

The **Effects of Trawling dataset for the Far Northern Section cross-shelf closure** and adjacent areas from CSIRO Marine Research. This dataset was used in the design phase and included:

- Station information (lat/lon, mud/sand/gravel/carbonate, temperature, salinity), 311 sites
- Catch of fish trawl net sampled fish species, 436 taxa from 292 stations
- Catch of prawn trawl net sampled bycatch species, 926 taxa from 269 stations
- Catch of epibenthic sled net sampled benthos species, 1194 taxa from 306 stations
- Combined dataset from all devices (Kg/Ha), accounts for overlapping taxa, 1655 taxa from 311 stations

Bathymetry model grid, as used in RAP, collated from various sources by Adam Lewis, GBRMPA.

- Bathymetry grid, resolution 15 arc-second (~500 m); used in design phase

Bathymetry from RAN Hydrographic Office (HO) and acquired by the project

- Coverage extensive in GBR but not complete
 - Updated with soundings acquired by the project during fieldwork at sea
-

- Used to produce a 36 arc-second resolution DEM for analysis phase

Seabed current-stress from Lance Bode & Lou Mason, JCU/Reef-CRC

- Modelled coverage for the entire GBR region, 1 minute of arc resolution
- RMS stress (Pascals (N/m²)) over period of model run (approximately 6 months)

Seabed sediment composition and related attributes, from Chris Jenkins OSI, Sydney University; used in design phase

- Coverage extensive, but not complete
- Resolution: gridded at 0.01 degree, where samples were available
- % carbonate
- % gravel grainsize fraction, percent
- % sand grainsize fraction, percent
- % mud grainsize fraction, percent
- Characteristic Grain size (phi)

Seabed sediment composition, samples collected by the project and processed by Geoscience Australia (Mathews & Heap 2006); used in analysis phase

- Approximately 1190 samples collected, average 13 km apart throughout the GBR shelf
- % carbonate
- % gravel grainsize fraction, percent
- % sand grainsize fraction, percent
- % mud grainsize fraction, percent
- laser volume fractions
- dataset supplemented by existing data from CSIRO, QDPI seagrass survey, and other sources

CSIRO Atlas of Regional Seas (CARS2000) from Scott Condie & Jeff Dunn, CSIRO Marine Research Hobart (Ridgway *et al.* 2002). A weighted averaging, which takes into account bathymetry and seasonality, of all available measurements of water column properties. Properties were evaluated at the seabed:

- full-coverage of the GBR region at 1/8 degree resolution (~14 km)
- T – temperature – degrees C, mean and standard deviations
- S – salinity – psu, mean and standard deviations
- O₂ – oxygen – ml/l, mean and standard deviations
- Si – silicate – uM, mean and standard deviations
- PO₄ – phosphate – uM, mean and standard deviations
- NO₃ – nitrate – uM, mean and standard deviations

SeaWiFS ocean color satellite data from Scott Condie & Jeff Dunn, CSIRO Marine & Atmospheric Research Hobart. The data provided are chlorophyll concentration and turbidity, averaged over 36 months, based on SeaWiFS Calibration and Validation algorithms:

- full-coverage of the GBR region, with 0.01° resolution ~(1.11 km)
- Chlorophyll-a (mg/m³) concentration, mean and standard deviations
- K490 diffuse attenuation coefficient at wavelength 490nm, m⁻¹, mean and standard deviations
- relative benthic irradiance calculated, based on K490, latitude and depth.

Queensland east coast trawl effort data from QDPI&F. The data are a combination of full-coverage 30-minute grid resolution logbook effort data and higher resolution voluntary data, mapped at 6-minute resolution, and vessel monitoring system (VMS) data processed by Norm Good QDPI&F.

- full-coverage of the GBR region,

- logbook effort (boat-days) at 6 minute (0.1°) resolution (~11.1 km) for 1996–2001
- VMS effort (hours) at (0.1°) resolution for 2002
- a weighted average of the above 1996–2002 data was used for design phase
- logbook data 1996–2001 and VMS data 2001–2005 updated for analysis phase

Old State permanent spatial Trawl Closure Areas, from QDPI&F.

- State permanent spatial Trawl Closure boundaries
- updated in 2006 for analysis phase

GBRMPA Spatial Information, from GBRMPA,

- GBR Marine Park Zoning
- RAP Bioregions (Reef and Non-Reef)
- Topographic coverages (Water, Shoal, Reef, Cay, Foreshore, Mangrove, Land)
- 2004 RAP Rezoning.

2.1.1.2. Data Processing:

After accounting for redundancy among the collated data, there were 21 covariates (+8 measures of variability in the CARS and SeaWiFS attributes) for stratification of the GBR non-reef region and for developing bio-physical models of biodiversity. These datasets were checked and imported into an ArcInfo GIS.

The covariates were constrained to the continental shelf by establishing a base study area bounded by the GBRWHA excluding those areas deeper than 80 m but including areas deeper than 80 m across the mouth of the Capricorn Trough, and excluding those areas shallower than 7 m near the coast, or shallower than 12 m if topographically identified as shoal, or topographically identified as reef.

A 36-arc-second grid (0.01 decimal degree, ~1.11 km) was generated for this area. Each grid cell was assigned a unique identifier that was the key to this dataset. As the collated data were of various spatial resolutions, we resampled those data to the 36-arc-second grid framework by a discrete thin plate spline technique (Wahba, 1990) using the TOPOGRID module in ArcInfo, to provide a consistent set of full-coverage covariates for the Project. As some covariates were not available for every grid cell, a “reliability indicator” was calculated that represented the distance to the nearest source data.

The GBR wide coverage of all of the collated covariates was thematically mapped using a colour range appropriate to the individual covariate distribution. These were presented as a landscape map of the study area divided up into two areas: north and south (see Section 2.1.1.3).

The full coverage interpolated physical data for each grid cell were exported out of ArcInfo for statistical analysis. This physical data set was also geographically matched to the location of each sampling station in the Effects of Trawling dataset and the GBR Seabed Biodiversity. These were also exported from the ArcInfo GIS into a database suitable to provide physical covariates matching biological sample data for statistical analyses of bio-physical relationships.

2.1.1.3. Maps of Physical Covariate Data

The Great Barrier Reef has a complex physical seabed environment. The major physical environmental factors that appear to influence the distribution and abundance of seabed habitats and assemblages in the GBR include: sediment grain size (particularly the amount of mud); force of water currents (benthic stress); chlorophyll and/or turbidity, hence benthic irradiance; and to a lesser extent depth and some nutrients (Pitcher *et al.* 2002). The complex multi-dimensional physical environment of the GBR has been analysed and used to stratify the region for sampling (Section 2.1.2). The most

common environments (>50% of the seabed) are mostly carbonate sands (Figure 2-2) away from the coast.

Benthic stress (Figure 2-1) is one of the strongest bio-physical forces and corresponds to the red areas in the map. The red inshore areas of Broad Sound and Shoalwater Bay have the largest tidal range in the GBR and are accompanied by extreme currents that scour the seabed re-suspend sediments and leave behind only gravel and larger particle sizes (Figure 2-2). The red offshore areas show where these strong tidal currents surge through the narrow channels of the reef matrix, scouring the seabed to gravel and rock substratum. High tidal current areas also occur in Torres Strait in the far northern GBR and in some other areas such as Whitsunday Passage. The scoured sediments typically are deposited in ripples, waves and dunes on the fringes of these red areas (Figure 2-2). At the opposite extreme are muddy seabeds (Figure 2-2).

Inshore areas along much of the length of the GBR are muddy or silty (Figure 2-2), and comprised of terrestrial sediments (low carbonate). Typically, with distance across the shelf, the substratum becomes sandier or even coarser (Figure 2-2), and comprised of biogenic carbonate (of biological origin). In offshore areas, coralline outcrops, reefs and shoals may occur in deep areas between emergent coral reefs. The Capricorn Channel, a wide area of GBR lagoon, has a very silty and muddy seabed. The south-eastern entrance to this channel is the deepest area on the GBR shelf, at 100-130 m.

The Capricorn Region, the southernmost part of the GBR, is typically sandy right across the shelf. It lies at the northern end of the Great Sandy Region, just beyond Fraser Island, the source of large quantities of terrestrial sand.

Many inshore areas are also very turbid and/or have high levels of chlorophyll (Figure 2-5). These inshore areas also tend to be very muddy (Figure 2-2). Along the outer margins of the inshore turbid/muddy areas, the water is clear enough to allow sufficient light for photosynthesis to reach the seabed (Figure 2-5). The deeper areas in clear waters near the outer edge of the continental shelf may at times be influenced by nutrients upwelled from below the ocean thermocline (Figure 2-4).

Many of the physical environmental covariates are correlated (Table 2-1). In particular, SeaWiFS light attenuation coefficient (K490) and Chlorophyll-a are very strongly correlated, and most of the CARS bottom-water parameters are also highly correlated. The sediment fractions (% mud, sand, gravel) are complementary, so are negatively correlated. Bathymetry is highly correlated with a large number of other covariates. These correlations among covariates make interpretation of analysis results difficult — when significant relationships between biota and any covariates were identified, not only does correlation not imply causality, but further other correlated covariates may be important.

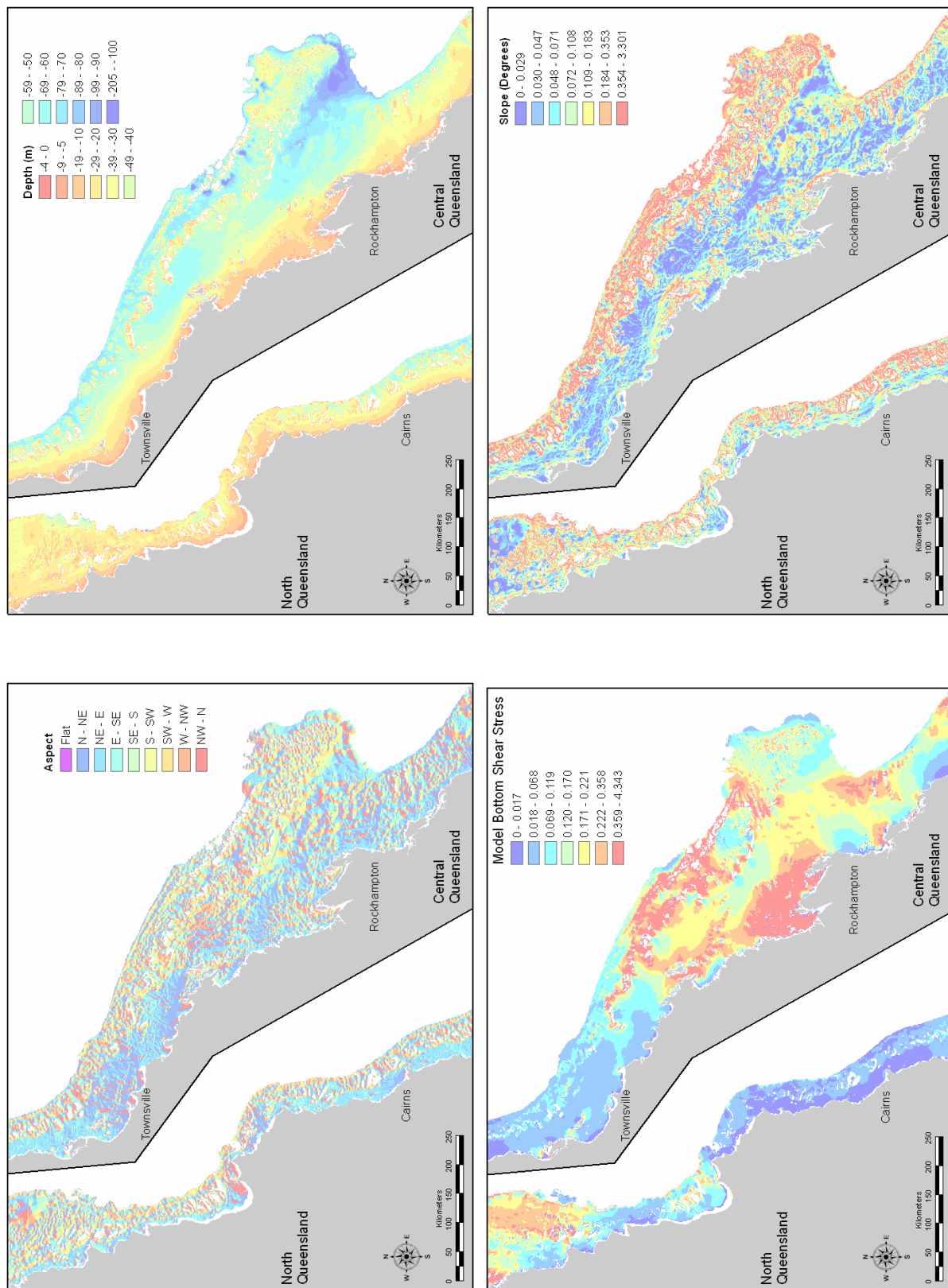


Figure 2-1: DEM of the bathymetry, slope and aspect of the GBR continental shelf, on a 0.01° grid, from various sources including soundings in uncharted areas recorded by the Project; map of modeled seabed current shear stress (RMS N/m²) (sources, see Section 2.1.1.1 for).

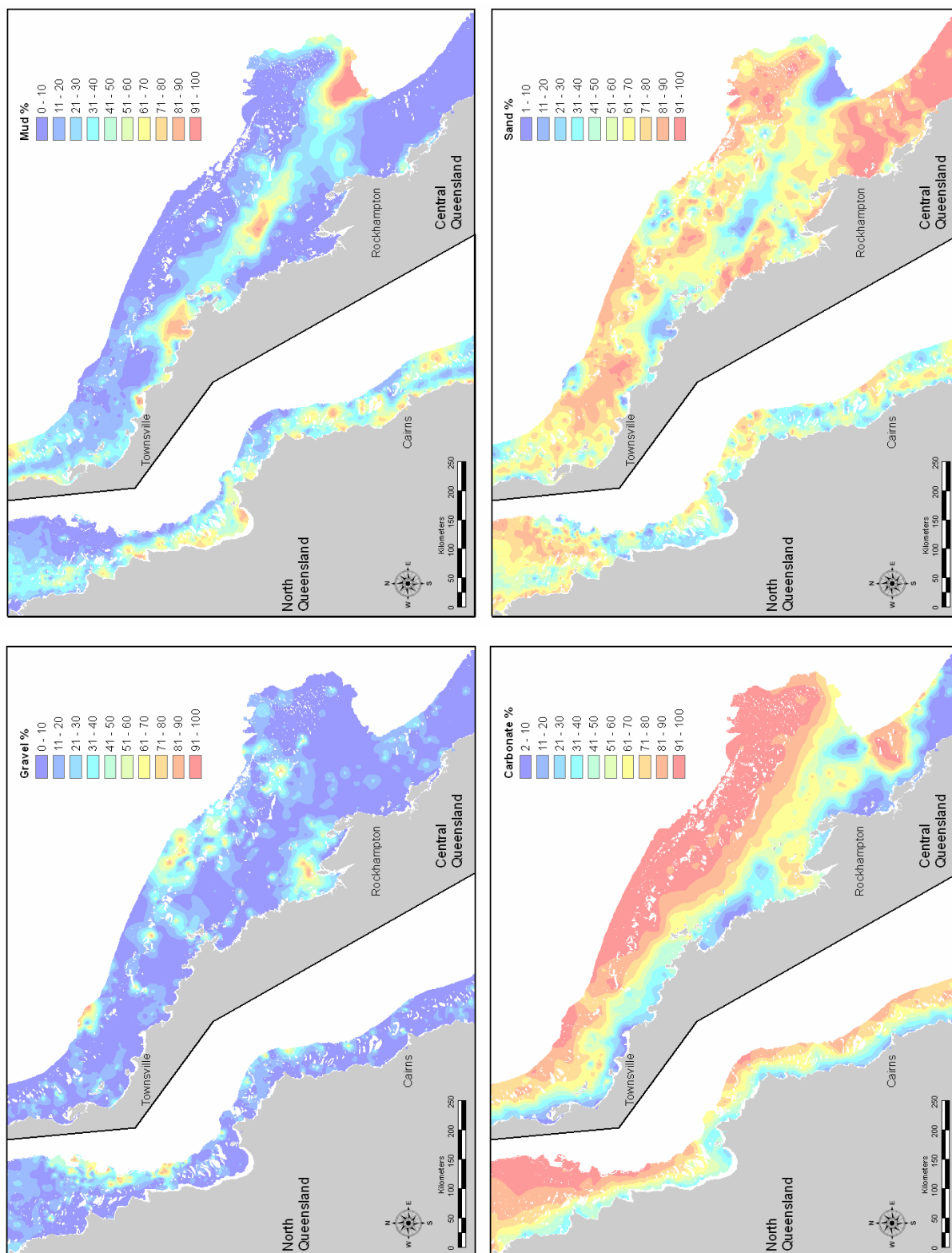


Figure 2-2: Maps of sediment attributes for the GBR continental shelf: percent mud/sand/gravel grain size fractions and percent carbonate (source, Geoscience Australia. Includes samples collected by the project and processed by GA).

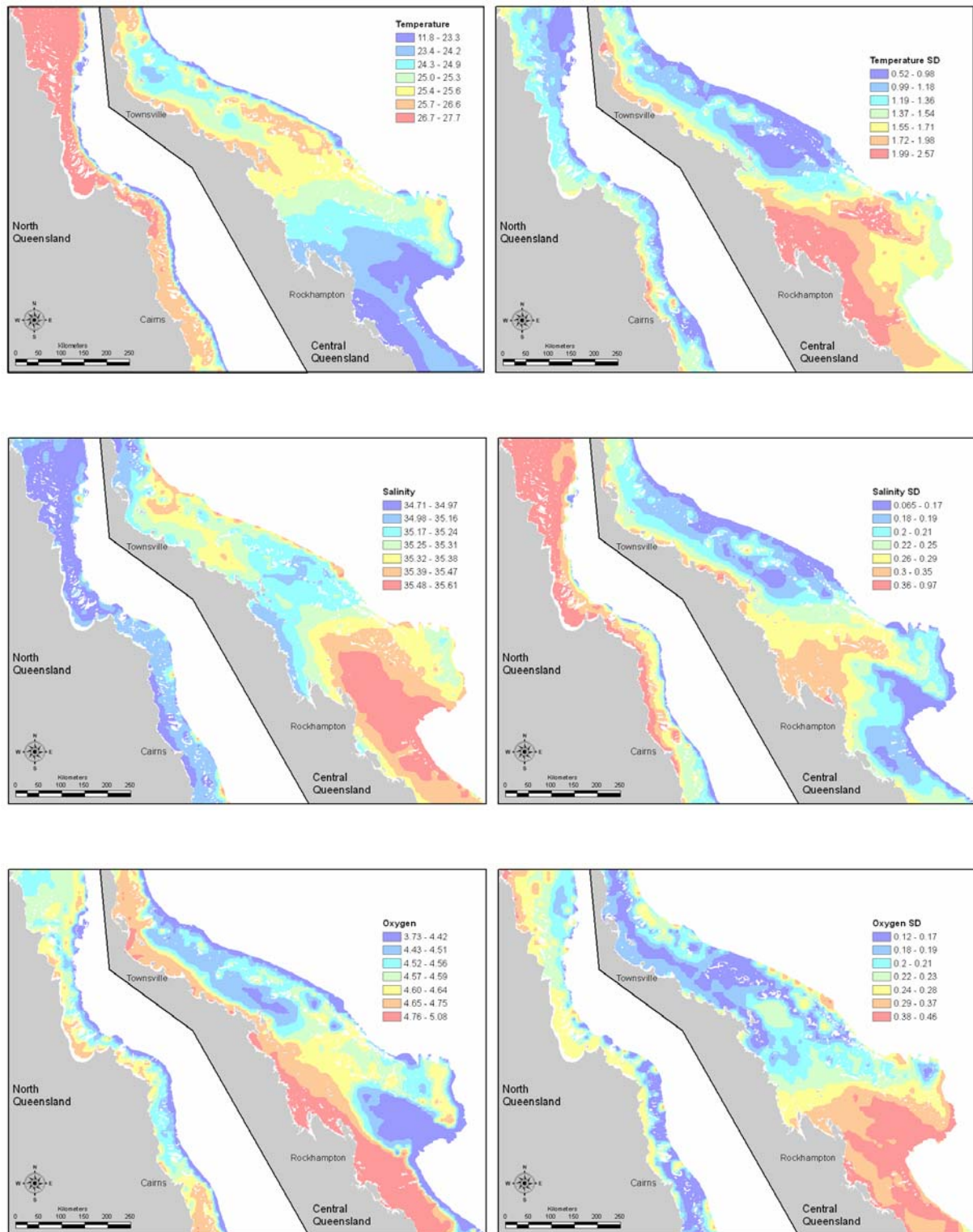


Figure 2-3: Maps of CARS bottom water physical attributes for the GBR continental shelf: temperature (mean & SD °C), salinity (mean & SD ‰), dissolved oxygen (mean & SD ml/l) (source, see Section 2.1.1.1).

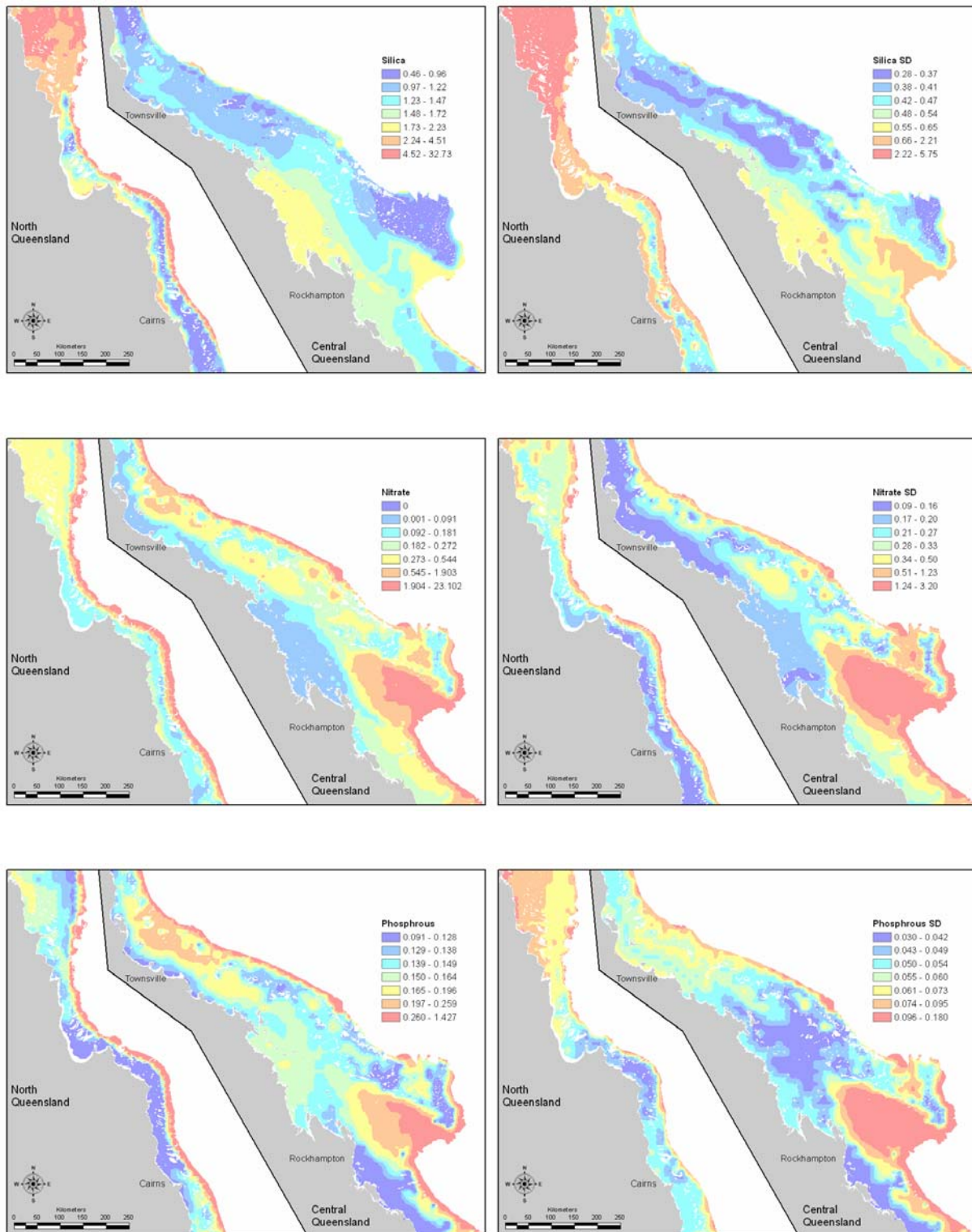


Figure 2-4: Maps of CARS bottom water nutrient attributes: silicate (mean & SD μM), nitrate (mean & SD μM), and phosphate (mean & SD μM), (source, see section 2.1.1.1).

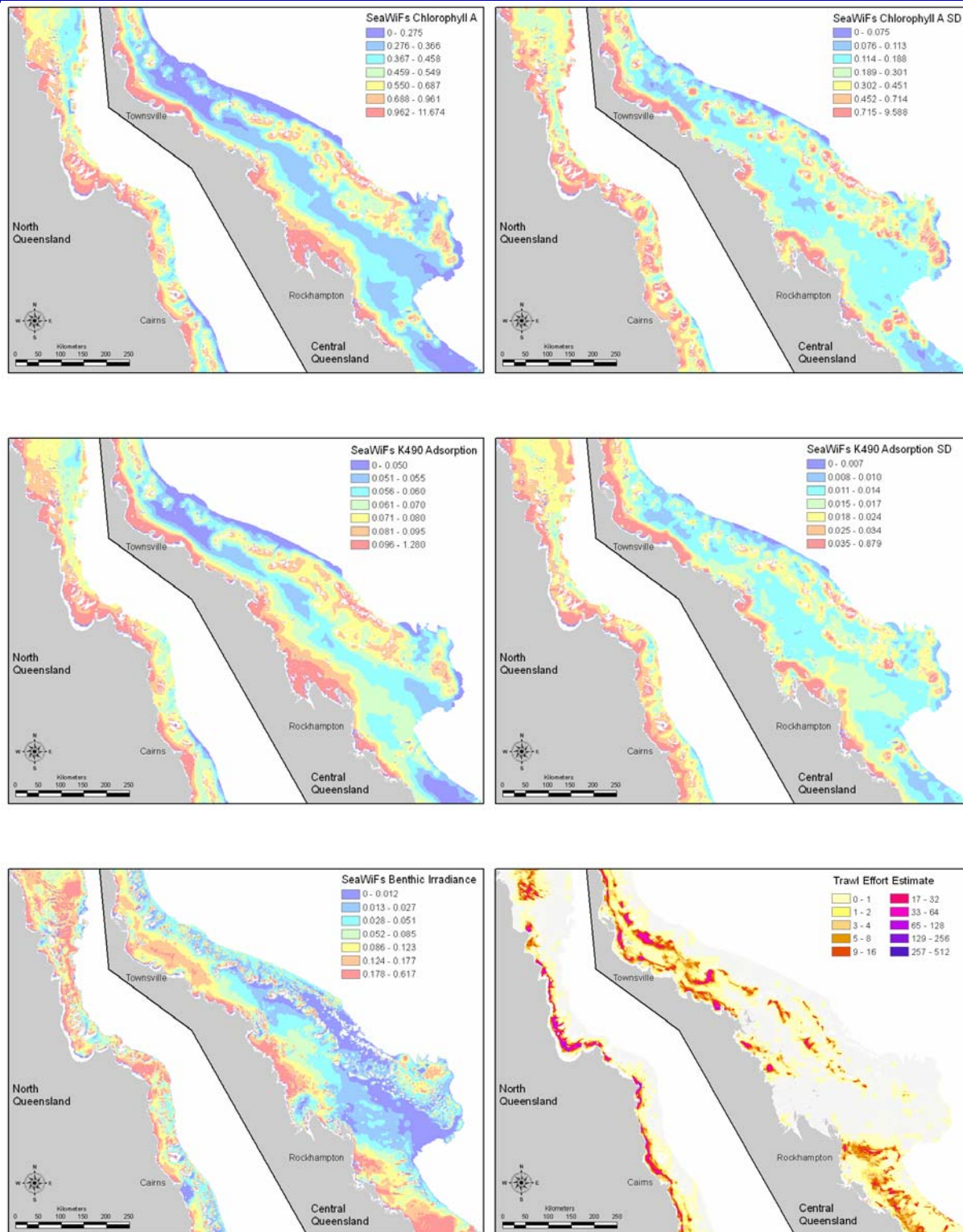


Figure 2-5. Maps of SeaWiFS predicted chlorophyll-A (mean & SD mg/m³), light absorption (attenuation coefficient K) at 490 nm (mean & SD m⁻¹), benthic irradiance (relative to sea surface at equator estimated from latitude, K490 and Depth), and weighted average annual trawl effort (hrs/0.01° grid) for the GBR continental shelf (sources, see section 2.1.1.1).

Table 2-1. Correlation matrix of physical environmental covariates. Non-significant correlations are greyed; larger **positive** and **negative** correlations >0.05 are highlighted.

| Variable | Bathy | Aspect | Slope | B Stress | Crbnt | Gravel | Sand | Mud | NO ₃ Av | NO ₃ sd | O ₂ Av | O ₂ sd | PO ₄ Av | PO ₄ sd | Si Av | Si sd | S Av | S sd | T Av | T sd | Chla Av | Chla sd | K ₄₉₀ Av | K ₄₉₀ sd | Ben Irr | Trwl Eff | Topo | | |
|---------------------|---------------|--------|--------|--------------|--------|--------|---------------|--------|--------------------|--------------------|-------------------|-------------------|--------------------|--------------------|--------------|---------------|---------------|--------------|--------|--------|--------------|--------------|---------------------|---------------------|---------|----------|-------|--|--|
| Bathy | 1.000 | | | | | | | | | | | | | | | | | | | | | | | | | | | | |
| Aspect | -0.125 | 1.000 | | | | | | | | | | | | | | | | | | | | | | | | | | | |
| Slope | -0.201 | 0.084 | 1.000 | | | | | | | | | | | | | | | | | | | | | | | | | | |
| B Stress | 0.075 | 0.123 | 0.123 | 1.000 | | | | | | | | | | | | | | | | | | | | | | | | | |
| Crbnt | -0.479 | 0.239 | 0.309 | 0.158 | 1.000 | | | | | | | | | | | | | | | | | | | | | | | | |
| Gravel | 0.059 | 0.086 | 0.156 | 0.522 | 0.330 | 1.000 | | | | | | | | | | | | | | | | | | | | | | | |
| Sand | -0.033 | 0.048 | 0.024 | -0.031 | 0.003 | -0.302 | 1.000 | | | | | | | | | | | | | | | | | | | | | | |
| Mud | -0.009 | -0.106 | -0.133 | -0.335 | -0.234 | -0.411 | -0.745 | 1.000 | | | | | | | | | | | | | | | | | | | | | |
| NO ₃ Av | -0.271 | 0.054 | 0.212 | -0.146 | 0.217 | 0.103 | -0.155 | 0.077 | 1.000 | | | | | | | | | | | | | | | | | | | | |
| NO ₃ Sd | -0.617 | 0.068 | 0.135 | -0.125 | 0.177 | -0.075 | -0.102 | 0.150 | 0.667 | 1.000 | | | | | | | | | | | | | | | | | | | |
| O ₂ Av | 0.590 | -0.074 | -0.224 | 0.205 | -0.419 | 0.015 | 0.215 | -0.216 | -0.682 | -0.725 | 1.000 | | | | | | | | | | | | | | | | | | |
| O ₂ Sd | -0.247 | 0.022 | -0.114 | 0.017 | -0.205 | -0.131 | 0.113 | -0.016 | 0.050 | 0.559 | -0.023 | 1.000 | | | | | | | | | | | | | | | | | |
| PO ₄ Av | -0.300 | 0.051 | 0.213 | -0.142 | 0.230 | 0.110 | -0.127 | 0.044 | 0.984 | 0.658 | -0.698 | 0.022 | 1.000 | | | | | | | | | | | | | | | | |
| PO ₄ Sd | -0.540 | 0.044 | 0.086 | -0.154 | 0.125 | -0.128 | -0.106 | 0.191 | 0.506 | 0.925 | -0.702 | 0.585 | 0.512 | 1.000 | | | | | | | | | | | | | | | |
| Si Av | 0.139 | 0.068 | 0.071 | -0.074 | 0.139 | 0.128 | -0.109 | 0.015 | 0.754 | 0.271 | -0.317 | -0.095 | 0.727 | 0.182 | 1.000 | | | | | | | | | | | | | | |
| Si Sd | 0.260 | 0.062 | -0.008 | -0.090 | 0.134 | 0.029 | -0.095 | 0.071 | 0.312 | 0.076 | -0.163 | -0.039 | 0.276 | 0.197 | 0.681 | 1.000 | | | | | | | | | | | | | |
| S Av | -0.541 | 0.008 | -0.004 | 0.110 | 0.032 | -0.036 | 0.273 | -0.236 | 0.012 | 0.424 | -0.080 | 0.530 | 0.062 | 0.339 | -0.335 | -0.594 | 1.000 | | | | | | | | | | | | |
| S Sd | 0.547 | -0.023 | -0.193 | 0.021 | -0.227 | -0.023 | -0.183 | 0.191 | -0.315 | -0.353 | 0.303 | 0.008 | -0.360 | -0.177 | 0.131 | 0.556 | -0.570 | 1.000 | | | | | | | | | | | |
| T Av | 0.387 | -0.012 | -0.128 | -0.012 | -0.046 | -0.099 | -0.078 | 0.144 | -0.755 | -0.661 | 0.388 | -0.363 | -0.776 | -0.457 | -0.368 | 0.167 | -0.556 | 0.618 | 1.000 | | | | | | | | | | |
| T Sd | 0.234 | -0.067 | -0.231 | 0.303 | -0.428 | 0.076 | 0.062 | -0.113 | -0.342 | -0.074 | 0.554 | 0.467 | -0.351 | -0.077 | -0.291 | -0.305 | 0.385 | 0.176 | -0.107 | 1.000 | | | | | | | | | |
| Chla Av | 0.513 | -0.111 | -0.133 | 0.192 | -0.362 | 0.105 | -0.268 | 0.183 | -0.198 | -0.289 | 0.339 | -0.040 | -0.233 | -0.246 | -0.036 | 0.017 | -0.314 | 0.396 | 0.224 | 0.340 | 1.000 | | | | | | | | |
| Chla Sd | 0.381 | -0.090 | -0.057 | -0.017 | -0.236 | -0.008 | -0.232 | 0.227 | -0.087 | -0.209 | 0.204 | -0.073 | -0.139 | -0.186 | 0.024 | 0.033 | -0.288 | 0.322 | 0.224 | 0.069 | 0.597 | 1.000 | | | | | | | |
| K ₄₉₀ Av | 0.412 | -0.112 | -0.115 | 0.098 | -0.332 | 0.034 | -0.218 | 0.185 | -0.170 | -0.237 | 0.251 | -0.051 | -0.201 | -0.204 | -0.044 | 0.025 | -0.304 | 0.340 | 0.209 | 0.264 | 0.920 | 0.397 | 1.000 | | | | | | |
| K ₄₉₀ Sd | 0.318 | -0.107 | -0.097 | -0.042 | -0.231 | -0.051 | -0.212 | 0.239 | -0.100 | -0.158 | 0.170 | -0.009 | -0.143 | -0.127 | -0.001 | 0.015 | -0.221 | 0.316 | 0.205 | 0.075 | 0.547 | 0.891 | 0.377 | 1.000 | | | | | |
| Ben Irr | 0.609 | -0.037 | -0.121 | -0.159 | -0.318 | -0.093 | 0.102 | -0.032 | -0.104 | -0.290 | 0.272 | -0.110 | -0.122 | -0.223 | 0.108 | 0.229 | -0.316 | 0.283 | 0.211 | 0.003 | -0.049 | 0.025 | -0.088 | 0.019 | 1.000 | | | | |
| Trwl Eff | 0.214 | -0.095 | -0.129 | -0.130 | -0.206 | -0.116 | -0.127 | 0.203 | -0.112 | -0.148 | 0.102 | -0.009 | -0.130 | -0.098 | -0.047 | 0.042 | -0.202 | 0.200 | 0.186 | 0.005 | 0.104 | 0.071 | 0.112 | 0.094 | 0.123 | 1.000 | | | |
| Topo | 0.138 | 0.096 | 0.150 | 0.007 | 0.175 | 0.074 | 0.035 | -0.085 | 0.056 | -0.041 | -0.054 | -0.123 | 0.049 | -0.012 | 0.135 | 0.224 | -0.184 | 0.042 | 0.088 | -0.166 | -0.060 | -0.034 | -0.050 | -0.037 | 0.195 | -0.061 | 1.000 | | |

2.1.2. Study Area Stratification (N Ellis)

The sampling for seabed biodiversity mapping in the Great Barrier Reef required an optimal strategy for the selection of survey sites. The primary purpose of the survey is to obtain data on the spatial distribution of benthic biota, so that subsequent bio-physical modelling can make use of the physical environment covariates to interpolate and map. Given that the number of sites that can be sampled is limited, it was obviously important to place the samples in a way that would yield as much information as possible. This required that the environment space, or multi-dimensional covariate space, rather than the 2-dimensional space must be sampled representatively and the approach to achieve this is stratification. Further, the stratification must be relevant to the benthic biotic, so it must be informed by measures of the biological importance of each covariate. This approach will optimally ensure that the biodiversity and physical attributes of as many different habitats types as possible, given the available resources, would be characterised. The physical variables collated as part of this project, which were known in advance of the survey, were used to guide the stratification. Biological information will be taken into account by weighting the physical variables based on their relative importance in bio-physical relationships — variables of greater influence on biological patterns having a larger weighting and influence in the stratification.

From an earlier study (Pitcher *et al.*, 2002) we have measures of the “importance” of these covariates with respect to correlations with the abundance of many benthic species in a detailed survey of an 8,000 km² area of the far northern GBR. Conceptually, important variables are those for which benthic composition changes significantly along a gradient of the variable. The survey should be designed to ensure that such important variables are sampled finely, so that the expected benthic diversity is reliably captured. That is, we should stratify our design with respect to the important variables.

Further, the sampling strategy should also consider the spatial resolution required for management utility. A scale of several 10s km was considered appropriate for broad scale characterisation. The implications of the spatial auto-correlation distance (the similarity of locations decreases with distance, such that on average sites ~10 km apart are uncorrelated; Pitcher *et al.*, 2002) and considerations of the benefit-cost of logistics (at maximum 1 site per hour) also indicate a sampling density of approximately 10 km average separation. In this approach, approximately 200 primary strata with similar physical characteristics were identified from importance weighted physical covariates of more than 170,000 0.01° grid cells covering the shelf area of the GBR. The size (area) of strata will vary depending on the number of grid cells having particular similar physical characteristics. About 10 ‘Replicate’ sampling sites were assigned to each primary stratum by an importance weighted process.

The potential survey area in the GBR, after excluding reefs and other areas that were too shallow, included 171,560 cells of size 0.01° (~1.11 km), each cell being a candidate sample site. Given the spatial autocorrelation distances, the average distance between sites should not exceed about 0.1° (~11.1 km) indicating that about 1,400–1,600 of these cells should be sampled. A margin was added to this lower limit, thus the design provided for 1450 sites. At the centre of each 0.01 degree cell, the values of 28 physical variables were collated or interpolated and represent the GBR region as a cloud of 171,560 points within a 28-dimensional physical-variable space. Ultimately, this space was to be partitioned into 1450 relatively homogeneous regions (or *strata*), such that the expected benthic biodiversity would be homogeneous within each stratum but heterogeneous among strata. A sampling site would then be selected from each stratum to produce a set of 1450 sites. This section describes the methods for achieving this partitioning or stratification of physical-variable space.

2.1.2.1. Principles of Partitioning

The basic principle behind the partitioning can be illustrated with the following simple two-dimensional example. Consider two physical variables x and y for which we have values at 1,000 sites, and suppose that these sites sample the covariate space roughly uniformly (Figure 2-6(a)). We wish to partition the covariate space into 20 strata. If the two variables were equally important, then the partitioning in Figure 2-6(b) would be adequate, since the strata are roughly the same width in x and y .

This partitioning was achieved using the “partitioning around medoids” (PAM) algorithm (Kaufman and Rousseeuw, 1990) (see below).

However, suppose the x variable is known to be 4 times more important than the y variable. Then we would prefer a partitioning more like that in Figure 2-6(c), where the strata are roughly 4 times narrower in the x direction than in the y . This is very simply achieved by first scaling the x variable 4-fold and then applying PAM to the scaled covariates, as in Figure 2-6(d).

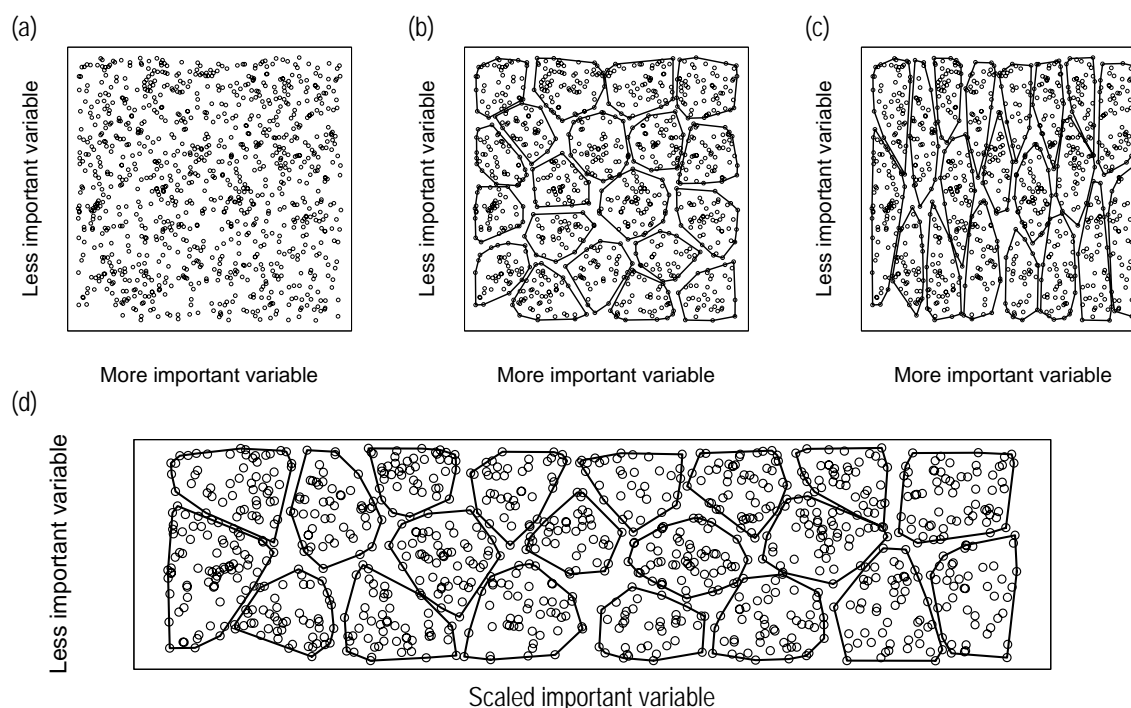


Figure 2-6. Partitioning covariate space in two dimensions: (a) 1,000 points randomly sampled from the square covariate space. (b) a partitioning into 20 clusters using PAM; (c) a preferred partitioning that accounts for the relative importance of the variables; (d) the partitioning in (c) is achieved using PAM on the scaled covariate space.

The partitioning of the GBR grid cells was an analogous procedure in 28 dimensions. Each variable was scaled so that its ‘range’ was proportional to its importance. However, unlike in the example, the physical variables were not uniformly distributed across their range and may have extreme outlying values. To guard against the distorting influence of such values, the ‘range’ was taken as that of the middle 95 percentiles. The term “*I95R*” is used here for this range, in acknowledgment of the inter-quartile range, *IQR*, of which this is a generalization. Formally,

$$I95R(v) = v_{(97.5\%)} - v_{(2.5\%)},$$

where $v_{(i\%)}$ is the i -th percentile of variable v .

2.1.2.2. Variable Importance

The collated physical variables were quantified on various disparate measurement scales that were unlikely to have any direct relevance to their biological importance. To scale the variables appropriately to inform the stratification, it was necessary to derive an importance value for each variable. The primary component was the biotic importance, but it was also necessary to include a study area adjustment and a reliability adjustment. The biotic importance quantifies the link between the biota and the physical variables and was developed from the detailed species data in the Effects of Trawling dataset. The study area adjustment was a refinement to the biotic importance to account for potential differences in the range of the physical variables between the Effects of Trawling study area in the far northern GBR and the entire GBR shelf to be sampled by the Seabed Biodiversity Project.

The reliability adjustment was a further refinement to reduce the influence of variables that are spatially poorly resolved. These are described in detail below.

2.1.2.2.1 Biotic importance I_{bio}

In a previous study, Pitcher *et al.* (2002) performed univariate analyses of 30 benthic statistical assemblages (comprising ~800 species) and 90 single species analyses on 306 sites of the Effects of Trawling dataset using the same suite of physical covariates as explanatory variables. They derived tree models for abundance, logistic regression models for presence/absence data and lognormal regression models for abundance conditional on presence. Their method used model selection to arrive at parsimonious models with some explanatory power and lead to the derivation of a measure of importance for each variable. For each species the relative amount of variation explained by each variable was computed, i.e. the contribution of the variable to the overall R^2 . The average of this quantity over all species was defined to be the importance for that variable.

Clearly, the actual dependence of biota on the physical variables is multivariate and highly complex. Moreover, the explanatory power of the physical variables was often low, averaging about 30%. Nevertheless, this definition of importance captured the broad pattern over a fairly diverse range of biota. Also it allowed for variation in explanatory power, since species that had low R^2 contributed less to the importance.

The three types of models considered by Pitcher *et al.* (2002) were in broad agreement over the ranking of the variables. However, as the tree model approach was most readily cross-validated, these results are reproduced here; the importances are shown in Figure 2-7(a).

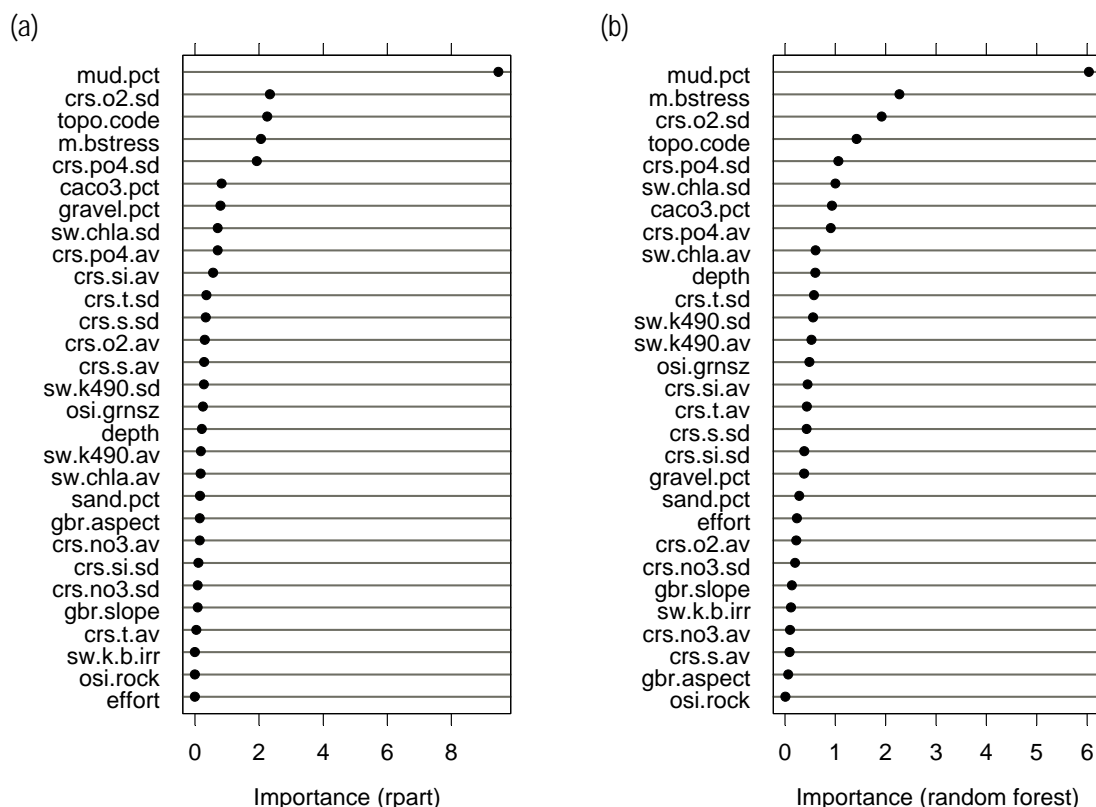


Figure 2-7. Variable importance computed by (a) cross-validated trees and (b) random forests.

An alternative but similar approach called random forests (Breiman, 2001) was also considered. In this procedure a bootstrap sample (with replacement) of all 306 sites was taken and a full tree model is fit without pruning. The method for selecting the splitting variable at each node differs from standard trees, where all variables are considered for splitting. In contrast, for random forests, a reduced set of

m candidate variables, chosen at random, are considered for splitting and the candidate with the best split is selected as usual. This bootstrap procedure is repeated 500 times to produce a ‘forest’ of tree models. Predictions can be made from the forest by taking the average prediction from the individual trees. For each sample, roughly 37% of sites are not selected. These ‘out-of-bag’ sites provide a test data set for estimating (without bias) the prediction error of the forest as a whole. As m increases two effects occur: the prediction error of individual trees improves, and the correlation among trees increases. The first acts to reduce overall prediction error but the second acts to increase it. There is therefore an optimal value for m , which Breiman has shown to be close to the square root of the total number of variables. Given that 28 covariates were available for the GBR, $m = 5$ was chosen.

The out-of-bag sites also provide a means of defining importance. The importance of variable v is the percent rise in the out-of-bag mean sum-of-squared errors when the values of v are randomly permuted. This is a relative measure that can be averaged over species. The results are shown in Figure 2-7(b).

The results for random forests were qualitatively similar to those for the tree models with slight adjustments to the rankings. The decay in importance with ranking was somewhat smoother for the random forests. Also, because of the use of random candidate variables, the random forests procedure tended to overcome the potential of some variables to dominate other closely correlated variables in the fitting; each variable gets a ‘fair go’. Thus, the random forest importances were considered more robust and were used in the stratification approach.

2.1.2.2.2 Study area adjustment Q

The raw importance values from the Effects of Trawling study area needed to be adjusted to take into account that the full GBR study area is different. Some variables, such as bottom stress, have a larger range elsewhere in the GBR than in the far northern GBR survey area. Such variables may therefore have more importance in the GBR as a whole. Thus, importances were rescaled in proportion to the ratio of $I95R$ between the smaller and larger regions; the scale factor Q (see Table 2-2).

The derived importances were also checked by comparisons with analyses of biotic data from the QDPI Deepwater Seagrass Survey (Pitcher *et al.* 2002). It was not possible to perform an importance analysis for the Seagrass dataset in the same way as for the northern GBR study, because it largely consisted of generalized habitat characterisation or biotic Class level presence/absence data. However, a guide to relative covariate importance was available from F -values from stepwise discriminant analysis on clusters defined from the Seagrass dataset. The selected variables were in broad agreement with the adjusted importances here.

2.1.2.2.3 Reliability adjustment R

The third consideration was that the physical variables had widely differing reliability that needed to be taken into account when using the calculated importance. All the physical variables were available on the design grid of 0.01° cells. However, most variables were interpolated onto this grid based on sample data at a coarser resolution. Therefore, an error distance d_{err} was defined to quantify this spatial imprecision (see Table 2-2).

The CARS data were interpolated from a rather limited number of CTD casts; the worst case was for phosphate, the average density of casts with this attribute was approximately 1 in 1,400 km^2 , corresponding to an average distance d_{err} of 0.36 degrees between casts. For the effort data, which came from logbooks reporting effort at 6-minute resolution, d_{err} was set to be the average distance from the design grid cell to the centre of the 6-minute effort cell. For the OSI data, d_{err} was set to be the average distance to a sample point from each design grid cell. The SeaWiFS data in their raw form were already specified at the same scale as the design grid; in this case d_{err} was set to be the average distance to the grid cell centre within a grid cell.

The ratio of largest to smallest d_{err} was about 270 (refer Table 2-2). It was considered that rescaling over such a large range would be too severe an adjustment and would effectively eliminate the CARS

variables from influencing the stratification. Thus, the square root of d_{err} was taken and its reciprocal was defined as the reliability scaling factor R .

Table 2-2. Calculation of adjusted importance I_{adj} : d_{err} is error distance in degrees, I_{bio} is the random forests biotic importance, reliability is $R = (d_{\text{err}})^{-1/2}$, and $I_{\text{adj}} = (I_{\text{bio}}QR)^{0.74}$.

| Variable | Distance $d_{\text{err}}(^{\circ})$ | Biotic imp. I_{bio} | <i>I95R</i> ratio Q | Reliability R | Adjusted imp. I_{adj} |
|------------|--|---------------------------------|--------------------------|--------------------|-----------------------------------|
| m.bstress | 0.008 | 2.3 | 2.3 | 11.5 | 20.8 |
| osi.mud | 0.017 | 6.0 | 1.1 | 7.7 | 18.5 |
| sw.chla.av | 0.004 | 0.6 | 3.4 | 16.0 | 13.4 |
| sw.chla.sd | 0.004 | 1.0 | 1.8 | 16.0 | 12.0 |
| sw.k490.av | 0.004 | 0.5 | 3.0 | 16.0 | 10.9 |
| sw.k490.sd | 0.004 | 0.6 | 2.1 | 16.0 | 8.8 |
| crs.po4.av | 0.359 | 0.9 | 8.1 | 1.7 | 6.4 |
| crs.po4.sd | 0.359 | 1.1 | 4.1 | 1.7 | 4.4 |
| crs.o2.sd | 0.224 | 1.9 | 1.7 | 2.1 | 4.2 |
| topo.code | 0.010 | 1.4 | 0.4 | 10.0 | 3.9 |
| gbr.bathy | 0.098 | 0.6 | 2.6 | 3.2 | 3.3 |
| osi.crbnt | 0.102 | 0.9 | 1.6 | 3.1 | 3.2 |
| crs.no3.sd | 0.198 | 0.2 | 7.4 | 2.2 | 2.5 |
| osi.gravel | 0.039 | 0.4 | 1.5 | 5.0 | 2.2 |
| crs.t.sd | 0.179 | 0.6 | 2.1 | 2.4 | 2.2 |
| osi.grnsz | 0.040 | 0.5 | 1.1 | 5.0 | 2.1 |
| crs.no3.av | 0.198 | 0.1 | 10.8 | 2.2 | 2.0 |
| crs.si.sd | 0.198 | 0.4 | 2.2 | 2.2 | 1.6 |
| osi.sand | 0.039 | 0.3 | 1.2 | 5.1 | 1.5 |
| crs.si.av | 0.198 | 0.4 | 1.7 | 2.2 | 1.5 |
| gbr.slope | 0.098 | 0.1 | 3.3 | 3.2 | 1.3 |
| crs.t.av | 0.179 | 0.4 | 1.3 | 2.4 | 1.2 |
| effort | 0.039 | 0.2 | 0.9 | 5.1 | 1.1 |
| crs.s.av | 0.179 | 0.1 | 4.2 | 2.4 | 0.9 |
| crs.s.sd | 0.179 | 0.4 | 0.9 | 2.4 | 0.9 |
| crs.o2.av | 0.224 | 0.2 | 1.7 | 2.1 | 0.9 |
| sw.k.b.irr | 0.051 | 0.1 | 0.9 | 4.4 | 0.6 |

2.1.2.2.4 Adjusted biotic importance I_{adj}

To incorporate reliability, initially the product $I_{\text{bio}}QR$ was considered and compared with the study area-adjusted importance $I_{\text{bio}}Q$. First, the two adjusted importances were normalized to sum to 1 and sorted in descending importance, as in Figure 2-8. The reliability-adjusted importance has much stronger contrast between low-ranked and high-ranked variables, a distortion which was considered unacceptable. Therefore, the reliability-adjusted importance was ‘tuned’ by raising to a power γ . The value of γ was chosen to make the tuned importance match the study area-adjusted importance as closely as possible: $\gamma = 0.74$ gave the minimum sum-of-square differences (compare the blue and green lines in Figure 3):

$$I_{\text{adj}} = (I_{\text{bio}}QR)^{0.74}.$$

Finally, for each physical variable v , the scaled version v_{scaled} that was used in the stratification was defined thus:

$$v_{\text{scaled}} = [v \div I95R(v)] \times I_{\text{adj}}(v)$$

This scaling ensures the *I95R*’s of the scaled variables are proportional to the adjusted importances.

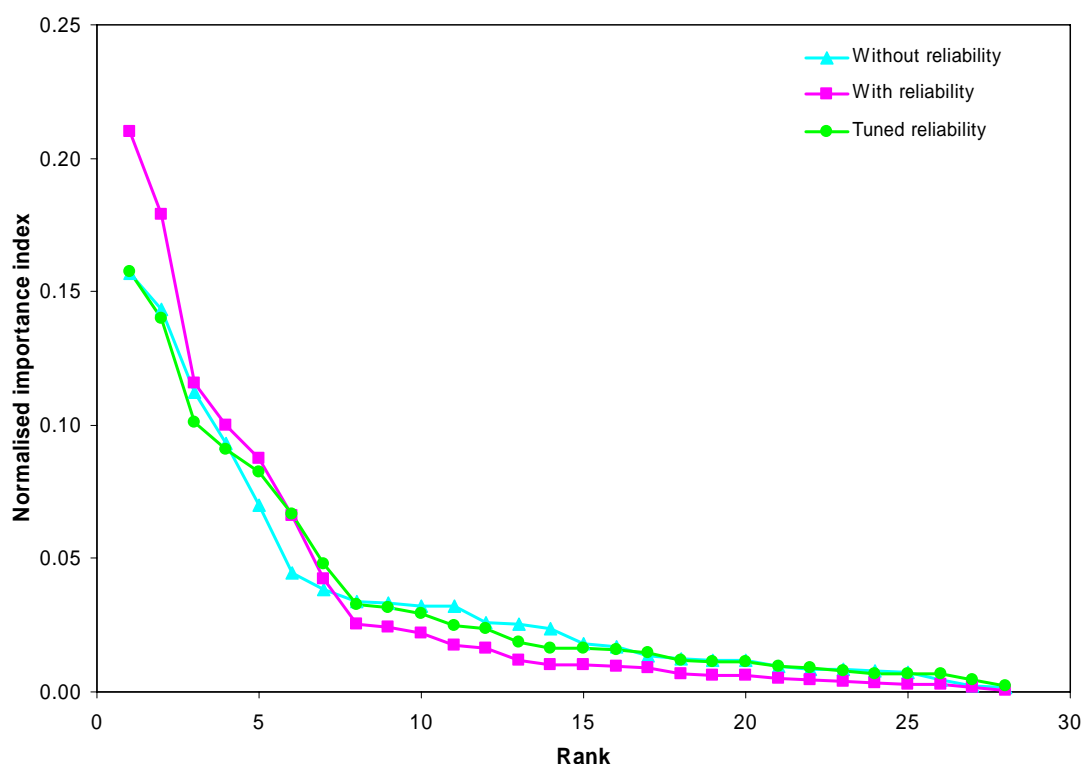


Figure 2-8. Importance measures **without reliability** ($I_{\text{bio}Q}$), **with reliability** ($I_{\text{bio}QR}$), and **tuned reliability** ($I_{\text{bio}QR}^{0.74}$) to match the shape without reliability. Each version is normalized to sum to 1. The orders of the variables with and without reliability are different.

2.1.2.3. The Clustering Process

Having achieved a biologically informed scaling of the physical variables, the next step was partitioning. However, before proceeding, it was necessary to reduce the dataset for computational manageability and to provide an orthogonal coordinate space for clustering.

There was a certain degree of redundancy among the physical variables (see correlation matrix Table 2-1). For instance, some variables (phosphate, silicate, chlorophyll A, K490) had a high correlation between their average value and standard deviation. There was strong correlation among all SeaWiFS chlorophyll A and K490 measurements, and there were also some negative correlations, e.g. between temperature and silicate standard deviations. Hence, there was an opportunity to apply data reduction techniques to make the data set more manageable and, importantly, orthogonal prior to clustering.

2.1.2.3.1 Data reduction

Singular value decomposition (SVD) was used to separate the data into principal components, from which we retained the most important components accounting for 99% of the variance in the data. This was contained in the first 14 components, and in fact the first 7 components contained 95% of the variance. SVD decomposed the $171,560 \times 28$ data matrix X of scaled physical variables into a product of matrices UDV^T , where U was the $171,560 \times 28$ score matrix, D was the 28×28 diagonal matrix of singular values, and V was the 28×28 orthogonal loadings matrix. To project the data into a smaller dimensional space, but retain the relative distances of the data, a new data set was defined as UD^* where D^* (28×18) consists of the first 18 columns of D . This data is equivalent to rotating the scaled data by V (i.e. XV) and projecting into the 18-dimensional subspace spanned by the first 18 columns.

The effect of this transformation was observed by examining the variable loadings V . The rows of V correspond to the original variables and the columns to the principal components. Large values (on the scale 0 to 1) indicate alignment of the variable with the principal component. The important variables

should be expected to have high loadings on the first few principal components, and the less important variables to have higher loadings on the later principal components.

The loadings on the first seven principal components are shown in Table 2-3. Principal component 1 was mainly associated with mud and various SeaWiFS measurements, whereas the second and third components were associated with bottom stress and mud. Because the 3 most important SeaWiFS variables are highly correlated with one another, they have similar loadings. The 4th component introduced contrasts between the SeaWiFS means and standard deviations, the 5th introduced phosphate and oxygen, and the 6th contrasted the standard deviations of chlorophyll A and K490. Other variables were also loaded to a lesser extent.

Table 2-3. Variable loadings for the first 7 principal components. Absolute loadings greater than 0.5 are highlighted in yellow, and absolute loadings between 0.3 and 0.5 are highlighted in green. The variables are ordered by adjusted importance. Relative variance is the fraction of the total variance explained by the principal component.

| Variable | Principal Component | | | | | | |
|-----------------------|---------------------|-------|-------|-------|-------|-------|-------|
| | 1 | 2 | 3 | 4 | 5 | 6 | 7 |
| m.bstress | -0.07 | -0.80 | -0.55 | 0.23 | -0.03 | 0.01 | -0.01 |
| osi.mud | -0.55 | 0.51 | -0.65 | 0.07 | -0.03 | -0.03 | 0.01 |
| sw.chla.av | -0.42 | -0.22 | 0.14 | -0.46 | -0.09 | -0.05 | 0.04 |
| sw.chla.sd | -0.45 | -0.10 | 0.37 | 0.42 | 0.00 | -0.54 | 0.39 |
| sw.k490.av | -0.36 | -0.18 | 0.10 | -0.60 | -0.09 | 0.03 | -0.11 |
| sw.k490.sd | -0.42 | -0.06 | 0.32 | 0.42 | -0.01 | 0.62 | -0.40 |
| crs.po4.av | 0.07 | 0.03 | 0.02 | 0.07 | -0.73 | -0.22 | -0.33 |
| crs.po4.sd | 0.04 | 0.02 | 0.00 | 0.04 | -0.43 | 0.11 | 0.15 |
| crs.o2.sd | 0.02 | -0.01 | 0.00 | -0.01 | -0.31 | 0.38 | 0.59 |
| topo.code | 0.00 | -0.01 | 0.01 | 0.01 | 0.02 | -0.08 | -0.15 |
| gbr.bathy | -0.07 | -0.01 | 0.02 | -0.04 | 0.18 | -0.01 | -0.02 |
| osi.crbnt | 0.03 | -0.01 | 0.00 | 0.05 | -0.01 | -0.23 | -0.26 |
| crs.no3.sd | 0.03 | 0.01 | 0.00 | 0.02 | -0.26 | 0.07 | 0.10 |
| osi.gravel | 0.02 | -0.02 | 0.02 | 0.01 | 0.02 | -0.08 | -0.13 |
| crs.t.sd | -0.01 | -0.02 | -0.01 | -0.04 | -0.01 | 0.14 | 0.20 |
| osi.grnsz | -0.04 | 0.03 | -0.03 | -0.01 | -0.03 | 0.05 | 0.07 |
| crs.no3.av | 0.02 | 0.01 | 0.01 | 0.03 | -0.23 | -0.08 | -0.09 |
| crs.si.sd | -0.01 | 0.00 | 0.00 | 0.01 | -0.03 | -0.03 | -0.06 |
| osi.sand | 0.02 | -0.01 | 0.02 | -0.01 | 0.01 | 0.04 | 0.08 |
| crs.si.av | 0.00 | 0.00 | 0.00 | 0.01 | -0.09 | -0.06 | -0.11 |
| gbr.slope | 0.00 | -0.01 | 0.00 | 0.02 | -0.01 | -0.07 | -0.05 |
| crs.t.av | -0.01 | 0.00 | -0.01 | 0.00 | 0.05 | 0.02 | 0.00 |
| effort | -0.01 | 0.01 | 0.00 | -0.01 | 0.02 | 0.02 | 0.01 |
| crs.s.av | 0.01 | 0.00 | 0.00 | 0.00 | -0.03 | 0.06 | 0.08 |
| crs.s.sd | -0.02 | 0.00 | 0.00 | -0.01 | 0.03 | 0.01 | 0.00 |
| crs.o2.av | 0.00 | -0.01 | 0.00 | -0.01 | 0.05 | 0.03 | 0.05 |
| sw.k.b.irr | 0.00 | 0.00 | 0.00 | 0.00 | 0.02 | 0.00 | 0.00 |
| gbr.aspect | 0.00 | 0.00 | 0.00 | 0.00 | 0.00 | -0.01 | 0.00 |
| Relative variance (%) | 35.1 | 31.6 | 16.7 | 6.0 | 3.3 | 2.1 | 1.6 |

2.1.2.3.2 Including geographic constraints

Another important consideration was whether spatial position should be included in the stratification. In the absence of covariate information, it would be usual to stratify entirely on geographical position, making each stratum simply connected. On the other hand, if we ignore geography completely, and base the stratification only on physical covariates, then the strata will tend to be fragmented in geographical space. This would not necessarily be a bad thing. However, if the fragments become very small then the quality of the stratification may become degraded by spatial uncertainty in the covariates themselves.

Instead of using latitude and longitude as geographical coordinates, *along* and *across* were used, which are covariates tailored to the shape of the GBRMP region (see section 2.4.1), one varying from

0 to 1 along the coastline and the other going from 0 on the coast to 1 at the outer edge of the reef. To assess the relative scaling to apply to these, we ran a simple linear fit of all the covariates to *along* and *across*, and found the average absolute value of the coefficients; they were 1.17 and 1.21 respectively. We therefore used the two covariates in equal scaling.

After studying the degree of fragmentation of clustering under various scalings of *along* and *across*, we decided that the *I95R* of *along* should equal 0.25 times the *I95R* of the first principal component of the rotated data. The scaled spatial variables were included as extra dimensions in the clustering, and their effect was generally to prevent the clusters becoming too highly fragmented in space.

2.1.2.3.3 The PAM and CLARA algorithms

The clustering algorithm “partitioning around medoids” (PAM) of Kaufman and Rousseeuw (1990), which is implemented in Splus, was used to cluster the physical dataset. The PAM algorithm is a robust alternative to the k-means algorithm. It uses a distance matrix and the number of clusters must be specified. Whereas K-means minimizes distances to the average for the cluster, in PAM, each cluster contains a *medoid* that is the cluster member whose summed distance to all other cluster members is a minimum. The medoid is a kind of generalized median for multiple dimensions; it is to this that the algorithm owes its robustness. The algorithm works by searching for clusters that minimize the total distance to cluster medoids.

PAM is not immediately useable for large data sets, because the size of the distance matrix becomes unmanageable. Therefore Kaufman and Rousseeuw’s CLARA algorithm, which is an implementation of PAM for large data sets, was applied. This works by first selecting a random subset of the data, then applying PAM to generate a clustering, and finally assigning the remainder of the data to the nearest cluster in the subset. The procedure is repeated many times to give several candidate clusterings, from which the candidate that minimizes the total distance to cluster medoids is chosen. The algorithm can be tuned by adjusting the subset size and the number of repeats, both of which should be as large as practicable.

Further, a weighted version of CLARA was developed specifically for this project. In this implementation, each initial subset was selected with non-uniform probabilities or weights, which enabled the clustering to be influenced to some extent to seek rarer physical environment strata, as explained below.

2.1.2.3.4 Two-stage partitioning

The partitioning was performed in two stages. In stage 1, we generated an initial coarse partitioning of the entire data set into 200 ‘primary clusters’, or primary strata. Then in stage 2, each primary cluster in turn was partitioned, generating a total of 1450 subclusters.

The initial reason for having two stages was computational efficiency. For k clusters and n observations, the computation time is of order kn^2 ; but if \sqrt{k} primary clusters was computed first, and then \sqrt{k} subclusters (on average), the computation time can be reduced to the order $\sqrt{k}n^2$. In fact stage 1 is the most computationally intensive stage, taking of order \sqrt{k} times longer than stage 2. Even for 200 primary clusters, which was rather larger than $\sqrt{1450}$, the computational saving was substantial. This was an important consideration when developing a method, particularly where many subsets of the data must be run.

However, the main reason for using a two-stage method was that it allowed more control over the partitioning. This was because at stage 2, it becomes possible to choose the number of subclusters within each primary cluster, subject to a total of 1450. In particular, it was possible to raise the level sampling effort into uncommon and rarer areas in covariate space, which may be potentially more interesting in terms of biota, at some expense to common areas.

2.1.2.3.5 Choosing the number of subclusters

After stage 1, there were 200 primary clusters of various sizes ranging from 2 to 7680 cells. Then it was important to determine how to optimally distribute the 1450 subclusters among the 200 primary clusters.

In order to answer this question, initially the following hypothesis was adopted: clusters with large numbers of cell members tend to be more homogeneous and represent commonness, compared with small clusters. Support for this hypothesis can be seen in Figure 2-9 for a synthetic bivariate normal data set. The larger clusters (in terms of numbers of cells) near the middle have smaller bivariate space (i.e. are more homogeneous), whereas the more heterogeneous clusters around the fringes tend to have fewer points (i.e. are smaller clusters).

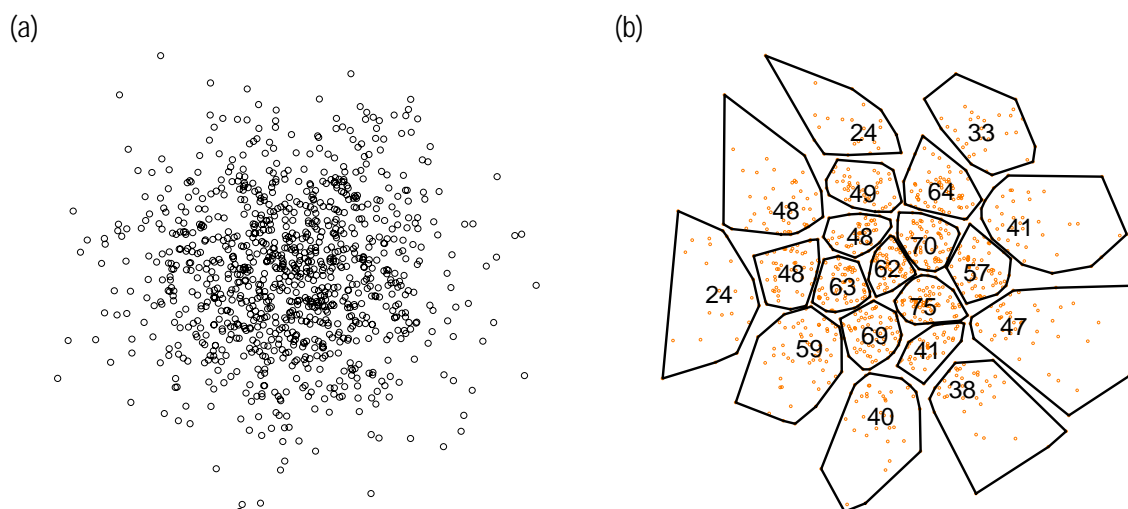


Figure 2-9. (a) Bivariate normal distribution of 1,000 points. (b) Partitioning into 20 clusters using PAM. Each cluster is labeled by the number of points in the cluster. The more populous clusters tend to be tighter and so more homogeneous.

Therefore the stratification strategy should be such that the density of sampling should be lower for larger primary clusters, i.e. the number of subclusters N_{sub} depends sub-linearly on the primary cluster size S . This issue also arises in the context of species-area curves, where the number of species increases with area sampled, but less than linearly. In fact, for species-area curves a square-root relationship is sometimes used. Following this principle, the initial approach could be $N_{\text{sub}} \propto \sqrt{S}$.

This approach would attempt to bias the sampling away from common sites towards rarer, perhaps more ‘interesting’, sites so that they also can be sampled adequately. Nevertheless, the square-root approach provides a somewhat crude approximation to the amount of ‘interest’ in a primary cluster, relating it simply to the size of the primary cluster, without regard to its contents. A better approach would be to quantify the interest as a sum over the interest in individual sites. For this, it was necessary to define the interest at a site.

The more common sites are those lying in high-density areas of covariate space. Since common sites will be well sampled in any case, it was reasonable to define ‘interest’ as some inverse power of density. However, computing the density in more than 2 dimensions is difficult; instead the one-dimensional density of each physical variable was considered separately. Suppose d_{vi} is the density of variable v at site i , normalized so that the total density over all sites is 1. Then we define the interest w_i at site i as the variable importance-weighted sum,

$$w_i = \sum_{v=1}^{28} I_{\text{adj}}(v) d_{vi}^{-a},$$

where $a > 0$ is a parameter to be chosen. Then define the interest of a primary cluster as the total interest over sites within the primary cluster, and choose the number of subclusters to be proportional to this quantity. That is, for the k^{th} primary cluster $C(k)$:

$$N_{\text{sub}}(k) \propto \sum_{i \in C(k)} w_i .$$

The density is estimated from the 171,560 values using a Gaussian kernel whose width is calculated by biased cross-validation (Scott, 1992). As an example, Figure 2-10 shows the true density (total area = 1) for bottom stress. The bulk of the distribution lies below 0.5; whereas previous experience has demonstrated that sites above 0.7 were of particular interest for epibenthic fauna (Pitcher *et al.* 2002).

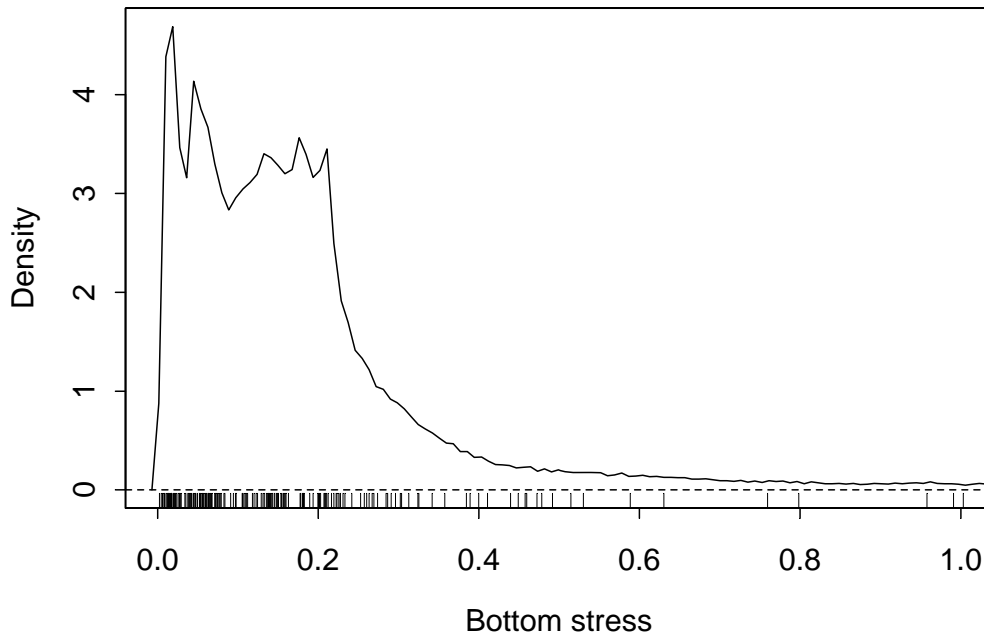


Figure 2-10. Density of bottom stress estimated by a Gaussian kernel of width 0.01 calculated using biased cross-validation. Also shown is a ‘rug’ of values for 200 randomly selected sites.

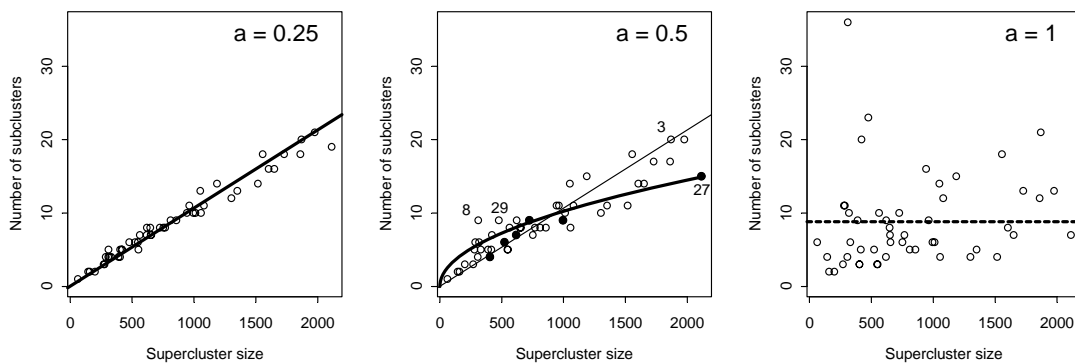


Figure 2-11. Number of subclusters vs primary cluster size for 3 different values of the exponent a . The sloping line corresponds to $N_{\text{sub}} \propto S$, the curve to $N_{\text{sub}} \propto \sqrt{S}$, and the horizontal line to $N_{\text{sub}} = \text{constant}$.

Figure 2-11 shows the relationship between number of subclusters and primary cluster size for $a = (0.25, 0.5, 1)$. For the case $a = 0.25$, the relationship was almost linear; this was barely distinguishable from the case $a = 0$, in which all sites had equal interest. At the other extreme, case $a = 1$ flattened the relationship, making number of subclusters nearly independent of primary cluster size and too sensitive to individual high-interest sites within a primary cluster. The intermediate case $a = 0.5$ was close to the square-root proposal discussed earlier and provided the required increased sampling of rarer sites without unacceptable under-sampling of common sites. This value for a was used as it provided an improved stratification adjustment compared with the initial square-root proposal.

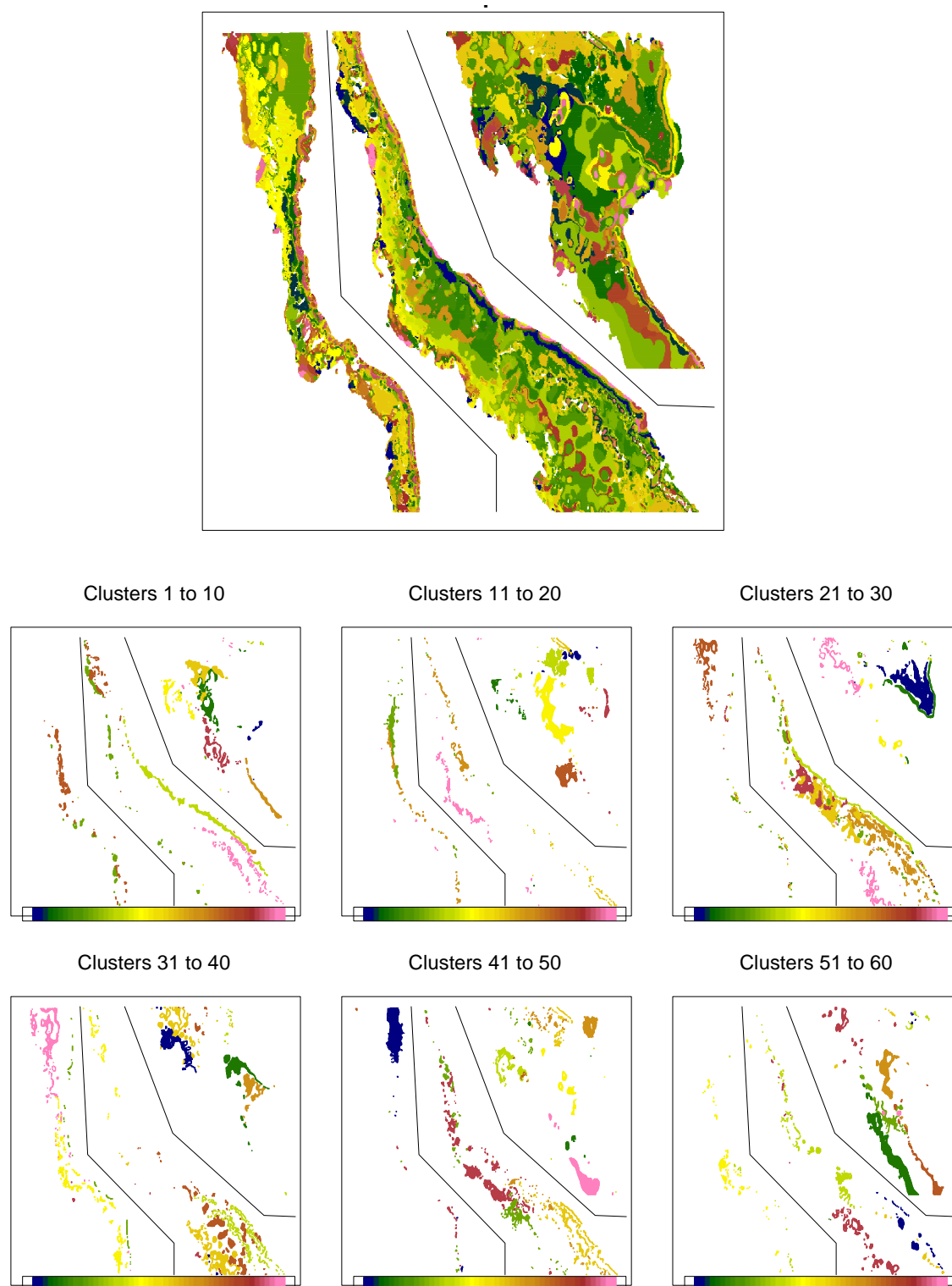


Figure 2-12. The 200 primary clusters in geographical space. Sixty of the clusters have been separated into six panels in order to make them distinct and assess the degree of fragmentation.

There was a concern that, at the primary clustering stage, rarer sites might be missed in the CLARA random subset selection stage since rare sites would be unlikely to be selected in a small random subset and, as a consequence, the primary clusters could be too large and homogeneous. Such primary clusters, being comprised largely of common sites, would have fewer subclusters, and so there would be less chance of isolating the rarer sites into their own subclusters. Two steps were taken to reduce this risk. Firstly, we computed more primary clusters than was computationally optimal (i.e. $200 > \sqrt{1450}$). Thus, primary clusters would be smaller, allowing for better detection of heterogeneity within

a primary cluster. Secondly, a weighted version of CLARA was developed; with site interest w_i as the weighting. Thus, rarer sites were more likely to have a chance at being chosen in the random sample of the algorithm, and therefore more likely to seed a separate primary cluster.

Figure 2-12 shows maps of the resulting 200 primary clusters after the first stage of clustering. Because the clustering was in covariate space, there was no guarantee that the clusters would be simply connected in geographical space, even though latitude and longitude were included as covariates. Indeed some clusters were quite fragmented. Despite their geographical separation, these clusters' sites have similar physical characteristics. In the other hand, some clusters are fairly spatially contiguous. Part of the reason for this is that the covariate values in these regions are based on spatial interpolation from sparse data points, and so the covariates vary smoothly in space. The primary clusters were further partitioned into subclusters as described above.

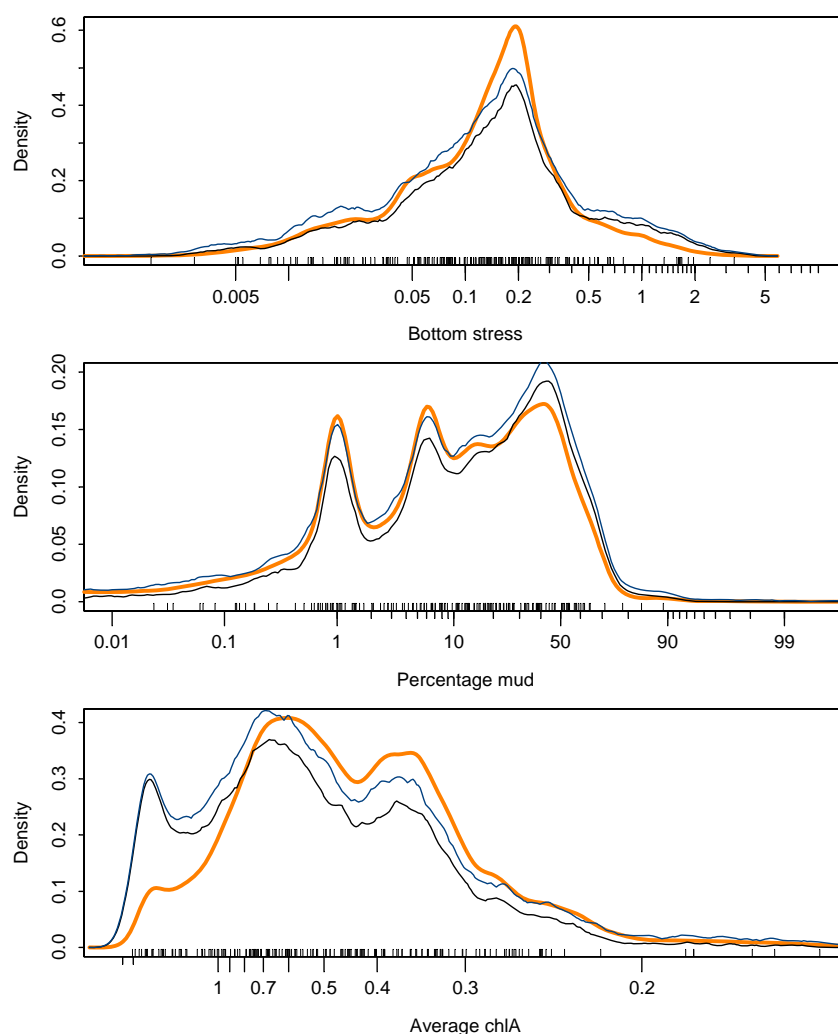


Figure 2-13. Distribution of the most important physical covariates on the full the GBR data (orange). The thin curves are 90% confidence intervals for the density sampled from the clusters. For clarity we show covariates on a log scale for bottom stress, a logit scale for mud and an inverse scale for chlA. Also shown is a rug of 200 sample values (jittered for mud).

2.1.2.3.6 Assessing the resulting stratification

There is no unequivocally optimal approach to survey design. For instance, in the two-dimensional example of Figure 2-6, we could have used the k-means algorithm instead of PAM, and the resulting partitioning, which would have been different, would nevertheless have been a quite reasonable alternative. Although there is no single ‘right answer’, it is nevertheless necessary to establish that the resulting partitioning is reasonable. There are several ways to assess the stratification.

First, the strata were mapped. We have already partially shown this in Figure 2-12. However, a map of all 1450 substrata would be rather overwhelming and very difficult to interpret. Alternatively the locations of the substratum medoids could be plotted, since each medoid was in some sense the most typical representative of the stratum. In fact, the choice of medoids as actual survey sites would be a quite reasonable candidate sampling strategy and could be called “medoid sampling”. This would provide acceptable general coverage of the entire the GBR region. However, the sampling would be finer in some areas where environmental gradients were steeper and coarser in broader more homogeneous areas. This was consistent with expectations and a desirable property of the stratification, which was being sought.

The second way to assess the stratification was to examine the expected distribution of the physical covariates at the sample sites. Again, the medoid sampling can be used as a representative sampling. Figure 2-13 shows the density of bottom stress, percentage mud and average chlA over the stratum medoids compared to over all 171,560 sites. Transformed scales have been used, on which the distributions were roughly symmetrical, to make the comparison clearer. For completely random sampling, the density would be similar to that over the full data set. But in the medoid sampling, there was relatively less sampling in the high density (common) areas, and more sampling in the tails (rarer areas), which was the objective of the stratification. For example, in the case of bottom stress, more sampling is put into sites with values above 0.5, at the expense of the more common sites with values in the range 0.1–0.3.

The representativeness of the medoid sampling can be checked by comparing its density with densities arising from many random samplings of the stratification. Figure 2-13 also shows confidence intervals for the density, which were obtained from the 5th and 95th percentiles of the pointwise densities of 20 random samples. Although there were small biases, overall the medoid-sampling density was fairly representative of the range of possible densities arising from stratified sampling.

2.1.2.3.7 Defining trawl substrata

The above has described how 1450 substrata were defined from which benthic sampling sites may be chosen. However, about one third of these same sites (595) were to be selected for trawl sampling and it was necessary to identify which would be the most representative. Although one method would be to simply choose the 595 sites at random, an approach that took advantage of the existing stratification was preferred, to ensure that the selection was as representative as possible. The approach taken was to go back to the primary clusters and recompute the number of subclusters required per primary cluster to give a total of 595, using the same methodology as before. On average the number of trawl subclusters was about 0.41 (595/1450) the number of original subclusters. For instance, primary cluster 92, which had 20 original strata, had 8 trawl strata. It was not feasible to try to cluster the sites into trawl subclusters, because there was no way to prevent the original strata straddling several trawl strata. Instead, it was necessary to cluster the sites such that all sites in an original stratum remain together.

The simplest way to do this was to cluster the stratum medoids. It was appropriate to use the medoid to represent its stratum as a whole because the medoid lies centrally within the stratum in co-variate space. Since there were at most 44 medoids to cluster, the calculation was computationally simple. For example, in primary cluster 92, substrata 1, 3, 4, 8, 11, 14 and 17 were amalgamated into one trawl cluster, substrata 2, 9 and 16 into a second, and substrata 6, 7, 12, 13 and 18 into a third, while the other 5 trawl clusters coincided with the original substrata.

After the medoids were clustered, each medoid’s trawl substratum number was assigned to all other cells in its substratum. Thus, each cell now belongs to both a substratum and a trawl substratum. Thus for any selection of 1450 benthic survey sites, the trawl sites could be selected from these by choosing one from each trawl stratum, either at random or by other objective.

2.1.2.4. Mapping the Stratification

The biologically informed stratification developed in this section is a physical characterisation of the GBR seabed that can be considered an *a priori* surrogate for patterns in seabed biodiversity

assemblages, to be tested and improved by the sampling to be conducted by the Project. A method of representing this complex multi-variate data in a single map was sought.

2.1.2.4.1 The Colour Key

The objective was to produce a map of the GBR with similar colours representing similar physical environments, which might be expected to have similar benthic biotic assemblages. The colour mapping should encompass as much information as possible in a reduced form — this was achieved by deriving a colour key from the first and second principal components of the biological importance weighted covariate data used in the stratification. A biplot of the principal components and physical variable vectors would provide a key to the environmental characteristics of the map. Particular directions in the biplot that corresponded to important covariates should be coloured in an intuitive manner. Red was used to denote high bottom stress and green to denote high average chlorophyll A (which correlated with K490). Blue corresponded with depth. High density areas of the biplot (common areas) should have a neutral colour such as grey.

A further desirable property of the colour key was that it should cover the data space compactly, to avoid large areas of the key having no data and wasting part of the colour space. The colour key should therefore be shaped to conform to the distribution of the data in principal components (PC-) space. This was done by mapping a circular colour disk to a simply connected region enclosing the data. In order to do this, it was necessary to first define a boundary of the data in PC-space. One way to do this was to find the convex hull; however, for the GBR data, this included voids in which no data existed. Instead, a more compact boundary was found by computing a two-dimensional kernel density function and delineating a contour of sufficiently low density. The boundary is partly concave.

Having defined a boundary, there were two alternative methods for mapping the colour disk to the region inside the outer density contour boundary: polynomial mapping and conformal mapping. The polynomial mapping was found to be more flexible but because of the partly concave shape there was not always a one-to-one mapping between PC-space and colour space, and it was non-trivial to invert from PC-space to colour.

2.1.2.4.2 Conformal Mapping

The conformal mapping method originates from complex number theory. A mapping from the colour disk to a simply connected polygon is expressible as a complex integral, whose parameters must be estimated by a non-linear algorithm. Trefethen (1980) provided a FORTRAN program to compute this integral. An interface to this code was developed that runs in R. Conformal mappings have certain benefits (such as local preservation of angles) but most importantly they are guaranteed to map the interior of the colour disk to the interior of the polygon (i.e. the mapping will not stray outside the boundary).

As with the polynomial method, the point in PC-space that the centre of the disk was mapped to was specified. The matching of points on the edge of the disk with vertices of the polygon was done by the non-linear algorithm. In order to match intuitive colours to the desired directions in PC space, it was necessary to impose a further transformation on the colour disk, which amounted to an angular stretch and shift. This was done using a periodic piecewise linear function of the angle. To complete the physical characterisation map, each grid cell must have a colour associated with it. Hence, the colour key mapping must be inverted, so that points in PC-space become mapped to points in colour space. This inverse mapping is available in FORTRAN code (Trefethen, 1980).

The resulting physical characterisation map of the GBR is shown in Figure 2-14. High bottom stress areas were coloured red, high Chlorophyll/K490 areas green, and the mud direction was coloured cyan. Sites coloured cyan have high levels of mud. Deeper areas tend to be blue.

The colouring of a map to highlight different covariates can be highly effective at illustrating similar and different physical environments, especially when the colour space has been fully utilized. The two colour mapping techniques investigated each had advantages and disadvantages. The main

disadvantage of the polynomial method was discussed above. On the other hand, the conformal mapping method tended to cover jutting-out parts of the PC-space from fairly small regions in colour space (e.g. the red area of the key in Figure 2-14). This would be a significant disadvantage if such an area were densely populated with data.

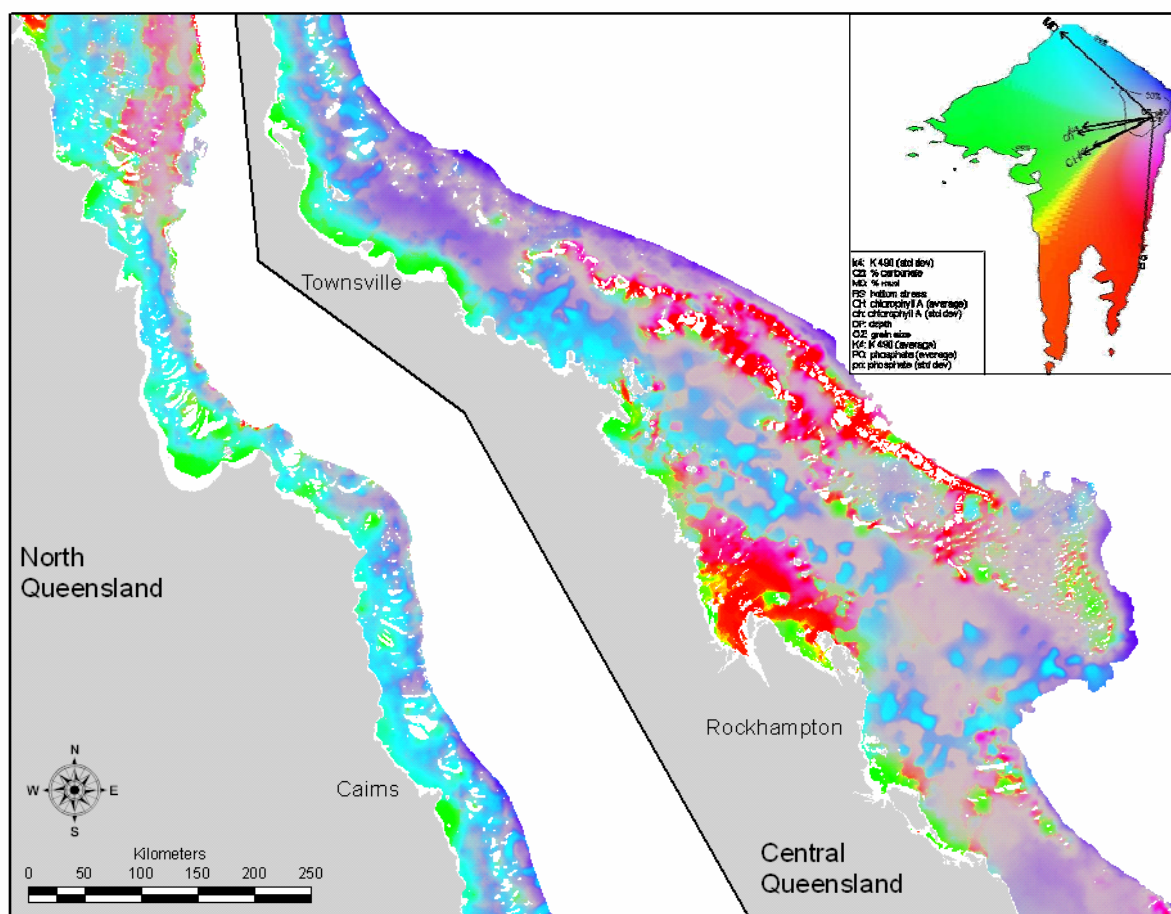


Figure 2-14: Map of the biophysical stratification of the Great Barrier Reef continental shelf. Inset: colour key showing distribution of seabed grids on the first two principal components (which explain 65% of the variation) of the biologically weighted physical covariates; biplot vectors indicate direction and magnitude of the major physical factors.

2.1.3. Site Selection

In the previous section, the idea of medoid sampling was used to illustrate the stratification. Medoid sampling could be an acceptable method of selecting sites that would deliver the “most typical” cell, with respect to physical covariates, within each of the sub-strata. A random selection of sites from within each of the sub-strata would also be an acceptable method. However, random selection has a relatively high risk of selecting some cells too close together and too far apart, creating clumps and voids in the coverage of the survey area, when a representative coverage that also takes account of the spatial autocorrelation distance was desired. Noting also that strata were often fragmented into patches of varying numbers of cells, including single cells, there was also a high risk of selecting isolated cells as sites — these would be less likely to be representative of their stratum due to errors in the covariates. A site selection method that avoided these issues as much as possible was sought.

Initially, a weighted random selection was used, with weights dependent on the spatial geometry of the patch(es) of cells within each stratum that cells belonged to. Cells with fewer neighbours of the same stratum and on the edges of patches (i.e. geographically close to a different stratum) were given less weight, whereas sites in the middle of patches were given more weight. This strategy was intended to

reduce the possibility of a site being unrepresentative of its stratum due to errors in the covariates and to avoid selecting adjacent sites. Examination of several weighted random selection options indicated quite a number of adjacent cells being selected and a number of excessively large voids between selected sites. Consequently, a method that more stringently avoided selection of adjacent cells and voids was preferred.

The method finally used did not include any deliberate random jittering of site selection. For each of the ~1450 benthic sub-strata, first all those cells that had the maximum number of neighbours and were the maximum distance from the edge of patches were selected. For many of the sub-strata, several cells met these criteria and to exclude duplicates, the cell with the minimum medoid distance was selected. In about one-sixth of cases, the actual medoid cell was selected. This strategy maximized the co-variate representativeness and spatial regularity of the selection, within the desired constraint of the stratification, and minimized the likelihood of clumps and voids, and adjacent, edge and isolated cells.

As described in the previous section, fewer sites could be sampled by trawl methods, so the ~1450 benthic medoids were clustered to provide 600 most representative options. Of these, 236 were a one to one match with their benthic strata, so no further selection was needed. However, in 364 cases, a trawl site had to be selected from typically 2-7 benthic site options (up to 19 in an extreme case). In these cases, the benthic site chosen to be sampled by trawl also was, to maintain spatial coverage, that which belonged to the largest patch in its cluster.

The sites selected are mapped in Figure 2-15. Note that sites are more sparsely distributed in broader more homogeneous areas, allowing a higher density of sites where environmental gradients are steeper. This site selection process provided a good compromise between coverage of the range of biologically important physical environments in the GBR and evenness of spatial coverage, given the limited number of sites that could be sampled and the inadequacies of the data available for the stratification. Such coverage could not be achieved with regular grid sampling or completely randomised sampling.

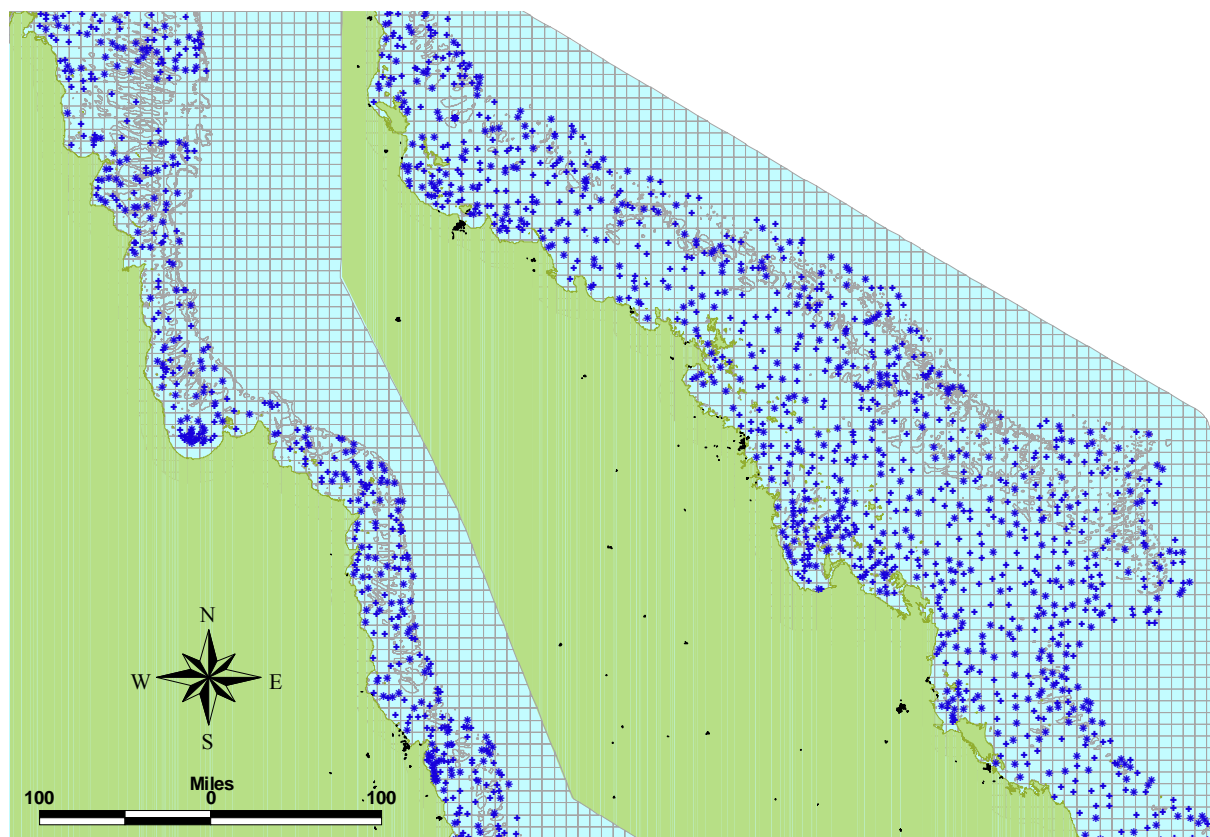


Figure 2-15: Map of the sites selected for sampling the seabed on the continental shelf in the GBR. * : sites for benthic and trawl sampling; + : sites for benthic sampling only.

2.2. FIELD SAMPLING

2.2.1. Research Vessels (T Wassenberg & N Gribble)

Two research vessels were used during the seabed mapping project: the Australian Institute of Marine Science research vessel *RV Lady Basten* (Figure 2-16) and the Queensland Department of Primary Industries and Fisheries research trawler *FRV Gwendoline May* (Figure 2-17).

The *RV Lady Basten* operates from AIMS in Townsville. It generally sails with a crew of seven, Master, Mate, Engineers, deck crew and Cook and can accommodate up to seven scientific staff. Its operational area is up to 2,500 nautical miles from port. The vessel is 27.4 metres in length and has a wet and dry laboratory and can deploy numerous instruments through the stern A-frame.



Figure 2-16: The 27 m Australian Institute Marine Science research vessel *RV Lady Basten*

Six voyages were conducted on the *RV Lady Basten* between September 2003 and November 2005 (Table 2-4). Multiple operations on this vessel continued over 24 hr each day while at sea with the crew and scientific staff working 12 hr shifts.

Table 2-4. Voyages completed by the *Lady Basten* with scheduled duration, numbers of sites sampled by towed camera, epibenthic sled and BRUVS.

| Voyage | Start date | End date | Days | # Camera | # Sled | # BRUVS |
|--------------|------------|----------|------------|-------------|-------------|------------|
| LB_01 | 17-09-03 | 12-10-03 | 26 | 263 | 215 | 89 |
| LB_02 | 22-11-03 | 08-12-03 | 17 | 121 | 137 | 39 |
| LB_03 | 25-04-04 | 30-05-04 | 36 | 124 | 206 | 62 |
| LB_04 | 07-09-04 | 10-10-04 | 34 | 266 | 241 | 81 |
| LB_05 | 10-01-05 | 11-02-05 | 33 | 212 | 181 | 56 |
| LB_06 | 26-10-05 | 30-11-05 | 36 | 233 | 214 | 74 |
| Total | | | 182 | 1219 | 1194 | 401 |

The *Gwendoline May* operates from the QDPI&F Northern Fisheries Centre in Cairns. It sails with a crew of three, Master, Mate and Cook and can accommodate up to five scientific staff. Its operational area is up to 200 nautical miles from the coast, and from New Guinea to Southport. The vessel is 18

metres in length and can operate a single trawl over the stern or quad gear from the booms. It has a Kortz nozzle fitted to increase trawl efficiency and reduce fuel costs. The electronics allows 3D mapping of the seabed and the radar and radios are state of the art.



Figure 2-17: The 18 m Queensland Department of Primary Industries & Fisheries research trawler *FRV Gwendoline May*.

Four primary voyages were conducted on the *FRV Gwendoline May* between November 2003 and December 2005, with several additional days sampled during a subsequent QDPI monitoring survey (Table 2-5), all under the command of a former commercial fisher with substantial experience in the region. Scientific trawl sampling operations on this vessel were conducted at night time.

Table 2-5: Voyages completed by the *Gwendoline May* with scheduled duration, numbers of scientific trawl sites sampled, sites with hookups and those too rough to trawl.

| Voyage | Start date | End date | Days | Sampled | Hook-ups | Too rough |
|---------------|------------|----------|------------|------------|-----------|-----------|
| GM_01 | 17-11-03 | 16-12-03 | 30 | 133 | 6 | 18 |
| GM_02 | 12-04-04 | 02-05-04 | 21 | 103 | 3 | 5 |
| GM_03 | 20-09-04 | 20-10-04 | 30 | 107 | 5 | 27 |
| GM_04 | 09-11-05 | 15-12-05 | 37 | 112 | 1 | 40 |
| GM_05 | 03-03-06 | 04-03-06 | 3 | 6 | | |
| TOTALS | | | 121 | 461 | 15 | 90 |

2.2.2. Towed Video Camera (G Smith, K Forcey, M Haywood)

An underwater video camera system (Drop-Cam, Figure 2-18) was towed just above the seabed at each site wherever possible, for a distance of ~500 m, to characterise habitats and visible biota. The Drop-Cam system consisted of cameras, frame, fibre-optic towing cable, cable winch, hydraulic crane, CTD instrument, Control and data logging computers, video recorders and display monitors.

Video and still cameras, and a CTD instrument, were mounted within a galvanised steel frame. The video cameras were twin 3-chip Panasonic E300 digital video cameras fitted with 2.8 mm Fujinon lens. The video field of view was illuminated with 2 × 500 and 2 × 250 W lights. A Canon 20D 8.2 mega pixel digital still camera fitted with a 4 GB memory card, Canon EF 17 – 40 mm auto focus lens

and two Speedlite 550EX strobes recorded still photographs of the seabed every 5 s during the camera transects. Twin lasers, spaced 28.5 cm apart, were fitted in front of the field of view of the cameras — when visible on the seabed, these enabled scaling of seabed objects. All cameras, lights and strobes were housed in custom built housings rated to 3,000 m.

The CTD was a Seabird SBE 19plus Seacat Profiler fitted with sensors for conductivity, temperature, pressure, oxygen, chlorophyll, turbidity and light (PAR). Data from the sensors was recorded at 0.25 s intervals and logged onto a computer database on board. Data from a PAR sensor fitted to the vessel was also recorded and logged to enable comparison between surface and underwater light levels.

Also mounted in the frame were two pressure housings; one for the power supply and the other for a computing system for data and video collection. Apart from the digital still images, all data and video were sent from the Drop-Cam to the vessel via an optic fibre link, in real time during the transect; the digital still images were downloaded at the end of each transect.

Data and video were converted to fibre optic media through a Focal 903 multiplexer and sent to the demultiplexer surface unit in the vessel via a single optical fibre. At the demultiplexer the signals were separated into data and video. Control of the Drop-Cam system (cameras, lights, lasers, CTD) and all processing and logging of data was done using in-house custom software on Pentium PCs, with the video recorded onto Panasonic DVC-Pro digital tapes.

The general procedure upon arrival at each site was as follows. The video camera was deployed and lowered to within approximately 0.5 m of the seabed. The CTD was set to switch on upon contact with seawater and recorded data throughout the deployment, transect and recovery. The vessel was then driven at approximately 1.5 knots, towing the camera frame for a distance of 500 m. Position and distance towed was recorded by differential GPS every 0.1 s. Video was displayed in real time on a monitor in the vessel laboratory, enabling scientific staff to raise and lower the camera, with remote joystick control of the winch, in order to maintain altitude above the seabed during the transect (Figure 2-18).

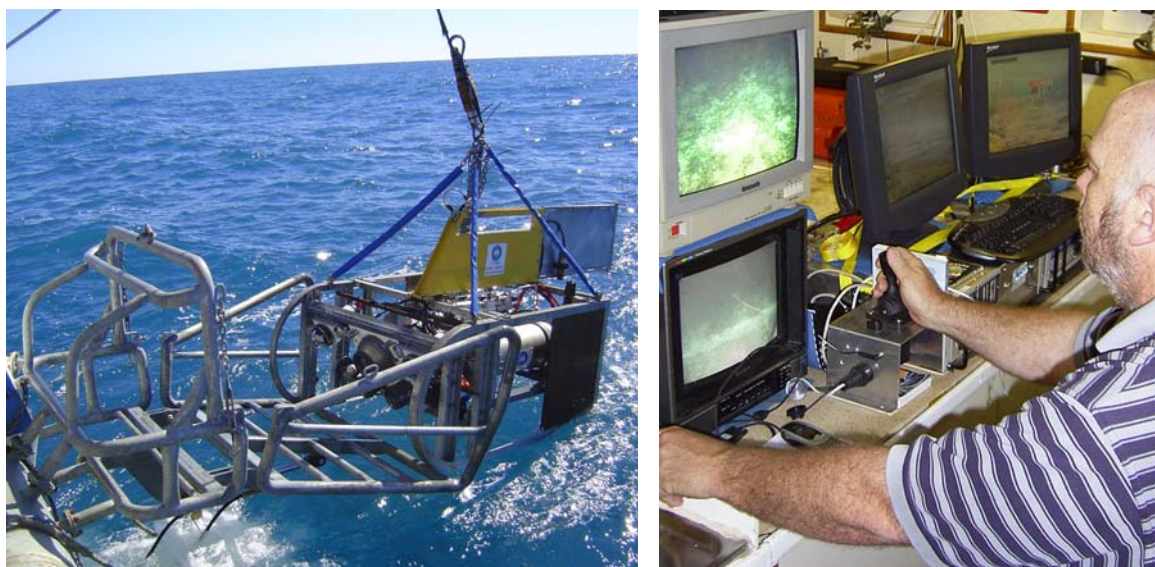


Figure 2-18: The Drop-Cam system being recovered after completion of a 500 m video transect and the surface real-time monitoring, control and data acquisition system.

2.2.2.1. Tasks, Events and Navigation Data Logging

Custom software modules acquired navigation, video and Drop-Cam data on several computers. Independent modules acquired and logged date/time and position data from differential GPS, depth data from the vessel echo sounder and heading data from the vessel gyrocompass on a navigation computer and shared these data onto a local area network. A custom map module also ran on the navigation computer to plot site waypoint and vessel position and constantly checked current position

against the designated site waypoint list and also shared these data onto the network to ensure all modules indexed logged data against the correct site number and date/time. A second computer ran modules for Drop-Cam system control and data (depth, pitch, roll, altitude) acquisition/logging, CTD data acquisition/logging and surface PAR data acquisition/logging. A third computer ran modules for control and data acquisition/logging of the DVC-Pro video tape recorders (VTRs). A fourth computer ran the Tasks control and logging module and events logging module. The Tasks module was manually operated, with touch screens for recording start and end operations for Drop-Cam transects, epibenthic sled tows and BRUVS drops. Each task record included task type logged with site number, date/time, position, and depth data as shared onto the network by other modules. The Tasks module also measured transect and tow lengths, and the touch of the Drop-Cam start task initiated recording of video by the VTRs and data logging by all other modules.

The events module was also manually operated — a scientific staff member used a modified keyboard to enter a real-time summary of the seabed substratum type, biological habitats and conspicuous individual animals. A lookup table transcribed keyboard scan codes into the seabed types listed in Table 2-6, which were logged and prefixed with date/time, position, and depth data for each seabed event recorded. Note that the position recorded was that of the GPS antenna on the vessel, whilst the observed event being recorded could be ~25 m (about 30 seconds) behind that because the camera was being towed from the stern.

Table 2-6: Substratum and Biological habitat types and animal events types entered in real time to annotate the video transect. Numbers in parentheses show index values used in acoustics sections.

| Substratum | Biological habitat | Animal events |
|-------------------------|--------------------------------|---------------------|
| Soft Mud (9) | Bioturbated (5) | Anemone |
| Silt (Sandy-Mud) (8) | Bivalve Shell Beds (6) | Ascidian |
| Sand (6) | Alcyonarians: Sparse (3) | Bryozoan |
| Coarse Sand (2) | Medium (2) | Commercial Fish |
| Sand Waves / Dunes (7) | Dense (1) | Crab |
| Rubble (5-50 mm) (5) | Whip Garden: Sparse (25) | Crinoid |
| Stones (50-250 mm) (10) | Medium (26) | Gastropod |
| Rocks (> 250 mm) (4) | Dense (24) | Holothurian |
| Bedrock / Reef (1) | Gorgonian Garden: Sparse (11) | Hydroid |
| | Medium (10) | Non Commercial Fish |
| | Dense (9) | Sea Pen |
| | Sponge Garden: Sparse (20) | Solitary Coral |
| | Medium (19) | Starfish |
| | Dense (18) | Urchin |
| | Hard Coral Garden: Sparse (15) | |
| | Medium (14) | |
| | Dense (13) | |
| | Live Reef Corals (16) | |
| | Flora: (8) | |
| | Seagrass (21) | |
| | Algae: (4) | |
| | Caulerpa (7) | |
| | Halimeda (12) | |
| | No BioHabitat (17) | |

2.2.3. Baited Remote Underwater Video Stations (M Cappelletti)

A fleet of Baited Remote Underwater Video Stations (BRUVS) were deployed about 350-400 metres apart with the prevailing wind to bracket the coordinate of each sampling site. Each replicate was considered to be sampling independently from the others at this separation (Cappelletti *et al.* 2004). At each site, a stereo-video BRUVS was deployed first, followed by three or four BRUVS with single cameras. Footage from the stereo-video was included for a small number of sites to make up the minimum number of three replicates in the BRUVS data. The BRUVS consisted of a galvanized

trestle-shaped frame enclosing a simple camera housing made from PVC pipe with acrylic front and rear ports (Figure 2-19). Sony™ Mini-DV HandiCams (models TRV18E, TRV19E) with wide-angle lens adapters (0.6X) were used in the housings. Exposure was set to “Auto”, focus was set to “Infinity/manual” and “Standard Play” mode was selected to provide at least 45 minutes of filming at the seabed. Detachable bait arms (20 mm plastic conduit) had a 350 mm plastic mesh canister containing one kilogram of crushed oily sardines (*Sardinops* or *Sardinella* spp) as bait (Figure 2-19, Figure 2-20). BRUVS were deployed with 8 mm polypropylene ropes and polystyrene surface floats bearing a marker flag, and were retrieved with a hydraulic pot-hauler wheel. A scope length of 2 times water depth was used on the ropes.

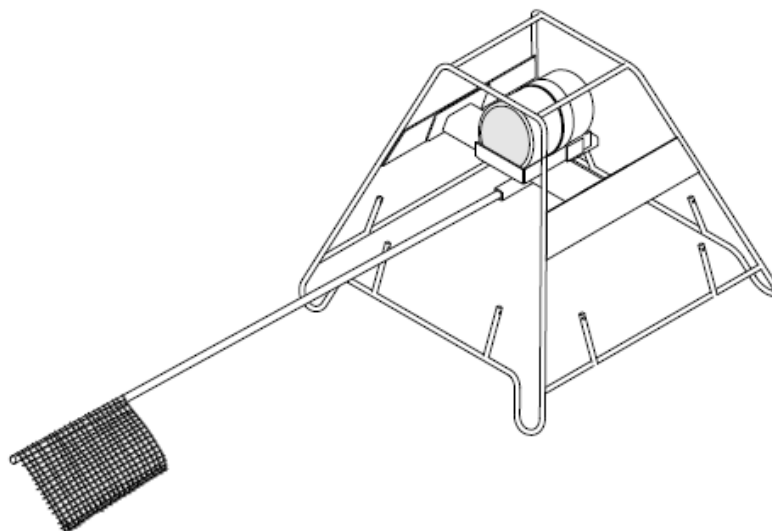


Figure 2-19: Diagram of single BRUVS frame and housing.

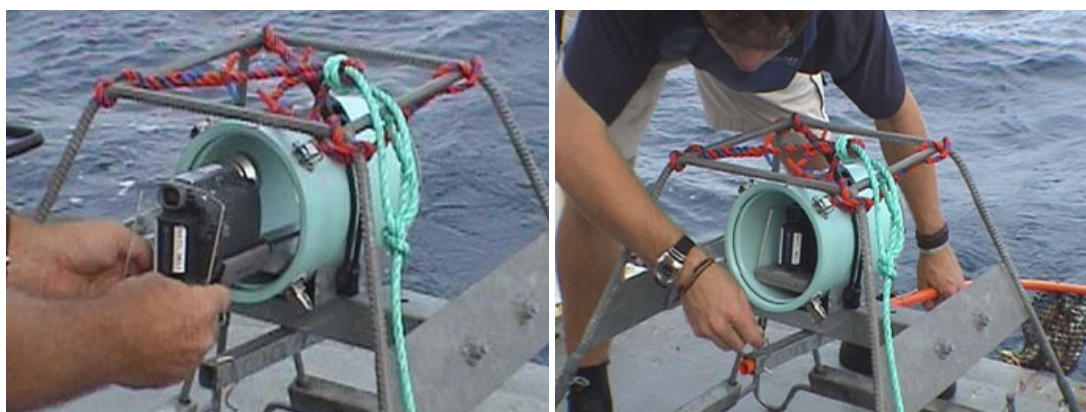


Figure 2-20: Applying camera and bait arm to BRUVS before deployment. Note ballast on frame and 8 mm hauling rope.

2.2.4. Single-beam Acoustics

Single-beam acoustic remote sensing of the seabed was conducted as continuously as possible on board the *RV Lady Basten*, using a Simrad EY500 120 kHz digital echo-sounder with a hull mounted Simrad 120-25 transducer (10° beam angle). Each ping was sampled in two blocks: (1) low resolution: 700 samples from the surface to (usually) beyond the 2nd echo (the depth was monitored and the range setting adjusted (100, 150, or 250 m) to ensure the second echo was captured, thus sampling rate varied with range ~15-35 cm), and (2) high resolution: 500 samples from 5 m above bottom to 10 m below bottom (a constant sampling rate of 3 cm). Data were logged in Simrad format files, each 5Mb (Simrad EY500 Operating Manual). The majority of the data were acquired at the same pulse length

(0.3 ms), but when range setting was 250 m (when depth 75-125 m) a longer pulse was used (1.0 ms), necessitating separate post-analysis. Depths averaged about 40 m (range about 6-120 m).

A Quester Tangent Corporation QTC View Series IV signal processor was also connected to the EY500 transducer, and the QTC proprietary 166 feature data were acquired and logged to QTC CAL files using the QTC CAPS version 3.15 software.

Seabed ‘ground-truth’ data were collected in real-time by entry of substratum and biological habitat during remote video camera tows (see Section 2.2.2), at about 1,200 sites. The towed camera (and so the real time coded habitat category data) trailed about 25 m behind the echo-sounder, and this lag back (estimated separately for each tow) was taken into account before relating ground-truth data to acoustics pings (see Section 2.4.6).

In total, more than 20,000 km of vessel track digital acoustic data were logged from six voyages all over the GBR shelf between 2003 and 2005.

2.2.5. Epibenthic Sled (T Wassenberg & M Stowar)

An epibenthic sled was deployed through the A-frame over the stern of the *Lady Basten*. The sled (Figure 2-21) was 1.0 m long, 1.5 m wide between the skids and 0.5 m high and weighed about 250 kg. The sides were closed with steel plate and the top and bottom panels were 20 mm square steel mesh. A heavy duty net (25 mm stretched mesh, 48 ply) was attached to the rear of the frame. Chafing mats of old nets were attached beneath the codend to minimise the damage to the net codend due to dragging on the seabed. The sled was attached to the main winch warp by two lengths of chain (1.5 m long) and a weak link (2 tonne – connected by chain to the rear of the frame) set to release the front of the frame in the event of a hook-up on the seabed that permitted the frame to flip over and be retrieved backwards. The sled was deployed using the ship’s deck winch whilst the ship maintained a constant bearing and speed of ~2 knots. A winch cable to water depth ratio of 3:1 was used and the towed distance of 200 m measured by onboard differential GPS from the ships position when the full amount of cable had been paid out.

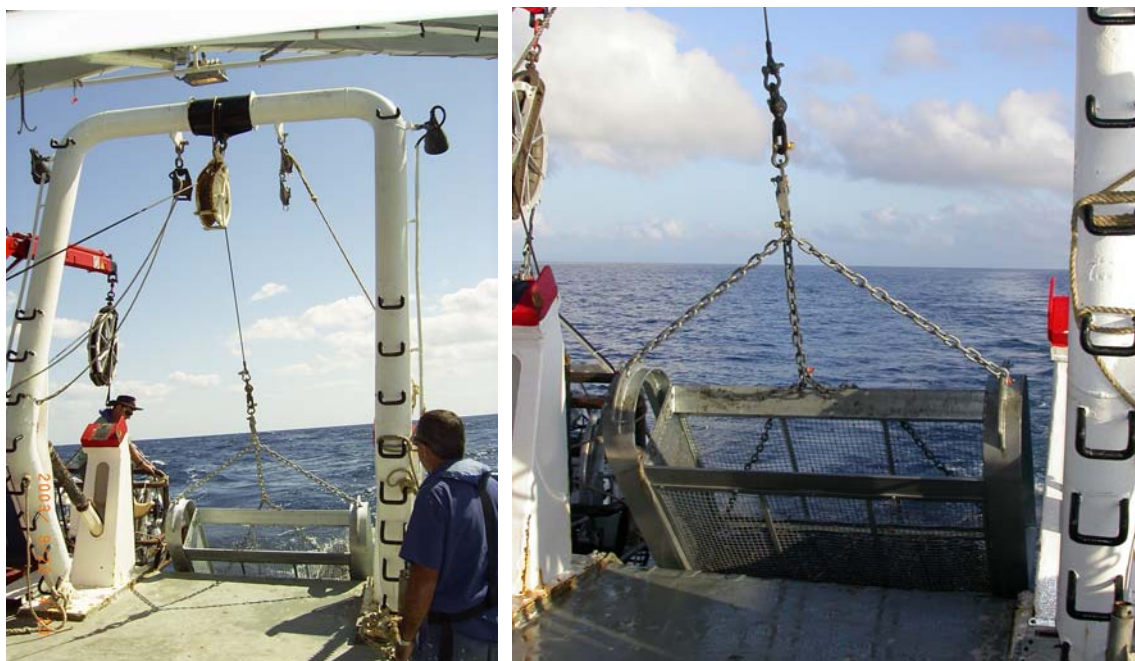


Figure 2-21: The epibenthic sled being deployed through the A-frame for a 200 m tow along the seabed; note the weak link at the top of the bridle and retrieve chain leading to the rear of the sled.

In order to collect sediment samples at the same time as the sled was deployed, a pipe dredge (Figure 2-22) was suspended from each rear corner of the sled frame by ~1 m length of chain. The pipe was 0.6 m long and 90 mm internal diameter. Of the sediment collected at each site, 500 ml was placed into a plastic bag, labelled and retained at 4°C for particle size analysis by Geoscience Australia and a further 500 ml sample was washed in a 1 mm square mesh sieve. The retained portion after sieving was placed into a cloth bag and preserved in a 10% solution of Formalin containing Rose Bengal to stain biological material in the sediment sample.



Figure 2-22: Sediment pipe dredge, showing sister-clip for attachment behind the sled

2.2.6. Scientific Trawl (T Wassenberg, D Gledhill & N Gribble)

A single high-flying Florida Flyer net having a head rope length of 8 fathoms and stretched mesh size of 50 mm of 400D/27 ply was towed over the stern (Figure 2-23) of the *Gwendoline May*. Drop chains were 5 × 8 mm stainless steel links attached to a 10 mm stainless steel link ground chain and twin No. 3 Bison boards with “high-riser” extensions to the board area (approximately the spreading power of a Pollards’ No 4 Bison board) plus extra weights attached giving a total weight 153 kg, were used to spread the net (Figure 2-24).

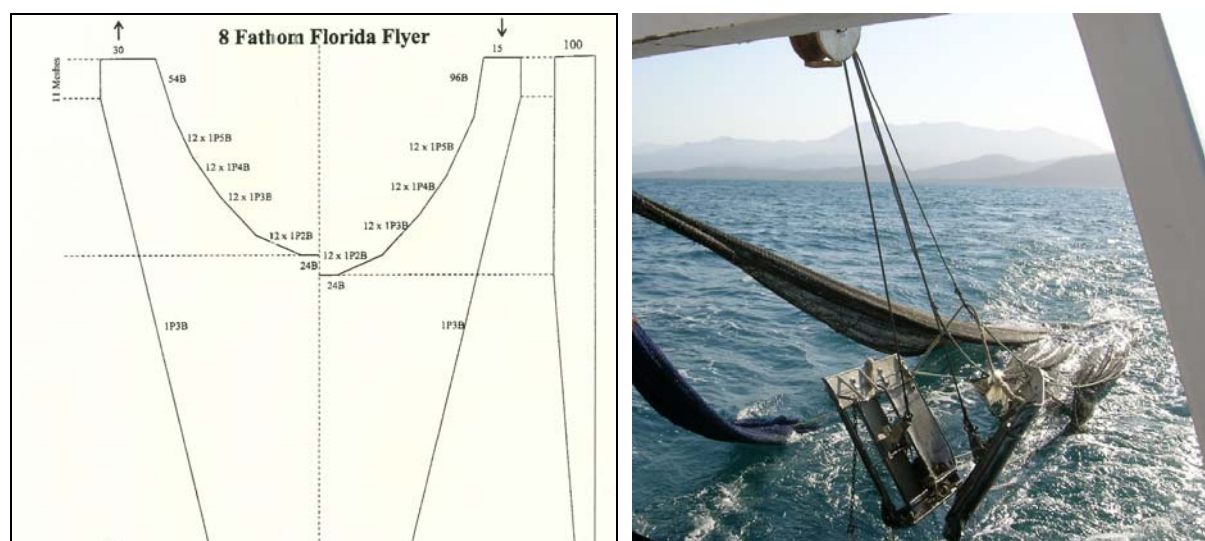


Figure 2-23: Net plan for the eight fathom Florida Flyer net used for scientific trawl sampling and the net suspended from the A-frame on the stern of the *Gwendoline May*.

At the sites that were able to be trawled, the net was towed in a relatively straight line for a distance of 1 km at a speed of about 2.7 knots. At the end of the tow, the catch was retrieved and emptied onto the sorting tray.

All trawling was conducted from one hour after sunset until dawn, to correspond with the activity of commercial prawn trawlers and also because many mobile seabed species have diurnal behaviour. The start and end points for each trawl were logged electronically using computer logging software with a GPS data connection.

The *Gwendoline May* visited 551 sites; 461 sites were sampled, and 15 were curtailed due to hook-ups and 90 were abandoned because the seabed was too rough and therefore unsuitable for sampling by trawl (Table 2-5).



Figure 2-24: Drop chain links and trawl boards.

2.2.7. Sample Processing at Sea (T Wassenberg, M Stowar, C Bartlett)

2.2.7.1. Epibenthic sled samples

On retrieving the epibenthic sled, the catch was placed into fish baskets. First, a photograph was taken of the entire catch. Large animals (sponges, gorgonians, large holothurians, large starfish etc.) were removed for immediate processing. The remaining sample was then processed entirely or subsampled. In either case, the sample was sorted into rough phylogenetic groups (sponges, crustaceans, algae, ascidians, seagrasses, fishes, echinoderms, molluscs and remaining invertebrates).

The fish baskets were emptied onto a sieve table that had three sieve drawers. The top drawer was 100 mm square mesh, the second had 50 mm square mesh and the lower drawer had 10 mm square mesh. The principle being that the smaller items would fall through to the bottom drawer and the largest items retained at the top (Figure 2-25) but the drawers were interchangeable to suit the content of the catch to be sorted.

If the catch was very large (> 140 L), it was necessary to take a random subsample of the catch. Subsampling was undertaken as a two stage process. Firstly, the entire sample was sorted for larger fauna and flora, as retained by a 'coarse' 100 mm × 100 mm sorting table mesh. Secondly, once the coarse fraction had been entirely sorted, a subsample of approximately 70 L of the fine fraction was sorted over the 10 mm square mesh. The total volume of the fine component was also recorded to enable determination of subsampling factors. The plant and animal samples retained from both coarse and fine fractions were sorted, bagged and recorded separately. Corrections for subsampling factors were made during the data analysis stage.



Figure 2-25: Sorting the catch from the epibenthic sled on the 10 mm square mesh sieve drawer into major taxonomic classes.

Table 2-7: Designated preservation methods on board the vessel and destinations for further processing (MTQ-TVL = Museum of Tropical Queensland; QMSB-BRS = Queensland Museum South Brisbane; CMR-CV = CSIRO Cleveland, QDPI-TVL = Queensland Department of Primary Industries Townsville).

| CLASS | PRESERVATION | DESTINATION |
|--------------------------------------|--------------------------|-------------|
| Annelida: Worms | Formalin 10% | MTQ-TVL |
| Ascidia: Tunicata: | Formalin 10% | MTQ-TVL |
| Biological conglomerates (no Sponge) | Formalin 10% | MTQ-TVL |
| Biological conglomerates (+Sponge) | Frozen | QMSB-BRS |
| Brachiopoda: | Frozen | MTQ-TVL |
| Bryozoa: | Frozen | MTQ-TVL |
| Cnidaria: | Frozen | MTQ-TVL |
| Cnidaria: Anthozoon: Octocorallia | Ethanol 70% | QMSB-BRS |
| Cnidaria: Hydrozoa | Frozen | MTQ-TVL |
| Cnidaria: Zoantharia: Hexacorallia | Frozen | MTQ-TVL |
| Crustacea: | Frozen | CMR-CV |
| Crustacea: Penaeidae | Frozen | CMR-CV |
| Echinodermata: | Ethanol 70% | MTQ-TVL |
| Echinodermata: Crinoidea | Ethanol 100% | MTQ-TVL |
| Echinodermata: Holothuroidea | Frozen | MTQ-TVL |
| Fishes: | Formalin 10% | QMSB-BRS |
| Fishes: Syngnathid | Formalin 10% | QMSB-BRS |
| Mollusca: | Frozen | MTQ-TVL |
| Mollusca: Cephalopoda | Frozen | MTQ-TVL |
| Porifera: | Frozen | QMSB-BRS |
| Marine plants: | Frozen | QDPI-TVL |
| Marine plants: Algae: | Frozen | QDPI-TVL |
| Marine plants: Seagrass: | Frozen | QDPI-TVL |
| Sediment animals 1 mm sieved | Rose-Bengal/Formalin 10% | CMR-CV |
| Sediment for grain size | Cool room. | CMR-CV |

Sorted samples were transferred to an onboard laboratory where each was allocated a water and solvent-proof barcoded label (Figure 2-26). Each sample was then individually photographed, weighed and transferred into a plastic bag. All details including barcode, collection details, taxonomic group, weight, photographs, storage location, subsampling factor (if any) and any relevant comments were entered into a database onboard (Figure 2-27). The individually bagged samples were then preserved onboard according to prescribed preservation techniques (Table 2-7) until later processing at several destination laboratories onshore.



Figure 2-26: Samples of sorted dredge catch organisms with bar code labels ready to be photographed and data recorded in the vessel data base.

 A screenshot of the 'GBR Basten Database' software interface. The window title is 'onboard the Lady Basten'. The interface includes a menu bar (File, Edit, View, Insert, Format, Records, Tools, Window, Help) and a toolbar with buttons for 'Edit Sample Data' and 'Hide Images'. On the left, there are input fields for 'RECORDER' (Marcus Stowar), 'CRUISE_ID' (GBRMap_LB_02_2004), 'VESSEL' (Lady Basten), 'DATE/TIME' (24/11/03 11:12:29 PM), 'COUNT' (12), 'SITE WEIGHT' (0), 'PHOTO_LINK' (C:\Archive\gbr\Vessel\Images\LB\Cr...), and 'COMMENT' (Depth = 48 metres). Below these are buttons for 'Insert Site data into database', 'Add Samples to Site', and 'Edit Site Data'. The main area contains a table with columns: SAMPLE_ID, CLASS, BIN, LAB, PRESERVATION, PHOTO_LINK, and TOTAL. The table lists various sample types like 'SEDIMENT FOR GRAIN SIZE', 'SEDIMENT ANIMALS 1MM SIEVED', 'ECHINODERMATA', 'BRYOZOA', 'MOLLUSCA', 'ASCIDIA: TUNICATA', 'FISHES', 'CRUSTACEA', 'Echinodermata: Crinoidea', and 'PORIFERA'. At the bottom, there are two photo upload sections: 'Site photograph' and 'Sample photograph', each with a corresponding image showing the site sample and a close-up of the sample (echinoderms).

| SAMPLE_ID | CLASS | BIN | LAB | PRESERVATION | PHOTO_LINK | TOTAL |
|-----------|-----------------------------|-----|----------|--------------|----------------------------|-------|
| 002783 | SEDIMENT FOR GRAIN SIZE | 296 | CMR-CV | S | C:\Archive\gbr\Vessel\1100 | |
| 002784 | SEDIMENT ANIMALS 1MM SIEVED | 295 | CMR-CV | R | C:\Archive\gbr\Vessel\220 | |
| 002786 | ECHINODERMATA: | 306 | MTQ-TVLL | V | C:\Archive\gbr\Vessel\750 | |
| 002787 | BRYOZOA: | 305 | MTQ-TVLL | C | C:\Archive\gbr\Vessel\800 | |
| 002788 | MOLLUSCA: | 305 | MTQ-TVLL | C | C:\Archive\gbr\Vessel\360 | |
| 002789 | ASCIDIA: TUNICATA: | 299 | MTQ-TVLL | F | C:\Archive\gbr\Vessel\100 | |
| 002790 | FISHES: | 302 | QMSB-BRS | F | C:\Archive\gbr\Vessel\220 | |
| 002791 | CRUSTACEA: | 293 | CMR-CV | C | C:\Archive\gbr\Vessel\620 | |
| 002792 | Echinodermata: Crinoidea | 297 | MTQ-TVLL | A | C:\Archive\gbr\Vessel\10 | |
| 002793 | PORIFERA: | 307 | QMSB-BRS | C | C:\Archive\gbr\Vessel\1550 | |

Figure 2-27: Data and images from each sled site were entered into the vessel database entry form that also included a photo of the entire site sample (left) and of the sample (in this case, of echinoderms).

2.2.7.2. Scientific trawl samples

The catch from the scientific trawl was spilled into a sorting tray and any large rocks were discarded. The entire catch was photographed to give a site photograph (Figure 2-28). Large animals (elasmobranches, turtles, sea snakes, sponges, large holothurians, large fishes etc.) were removed for immediate processing. The remaining catch was examined for uniformity and species that were readily-recognisable and in tractable numbers were removed and processed immediately. If the catch was very small it was sorted in full.



Figure 2-28: A photograph of an entire trawl catch (site photo) showing the diversity of organisms.

If the catch was very large, a random subsample of the catch was taken by making a slice through the catch. The intent was to retain at least 20% of the catch. A photograph was taken of the subsample and the weight of the remainder that was returned to the sea was also taken. The subsample was then sorted into fish, invertebrates and prawns etc, photographed with a bar code label and put into the respectively labelled boxes in the freezer.

Subsamples were also taken if a large quantity of one species or any obviously abundant/common species was caught. For example: a very large sponge would be weighed but only a smaller portion would be retained for detailed analysis; whereas in the cases of very large catches of Leionathids (Ponyfish) only a few specimens were retained after weighing the total.

After the large, low incidence or rare organisms were removed from the catch and given a unique barcode label, photographed, weighed and either retained or returned to the sea, the remainder of the catch was sorted into rough phylogenetic groups (commercial prawns, non-commercial prawns, other crustaceans, algae, seagrasses, syngnathids, remaining fishes, holothurians, squid and remaining invertebrates — Table 2-8). The sorted material was allocated a barcode label, weighed and photographed (Figure 2-29). Some reference specimens of small fishes were preserved in formalin as these can be damaged during freezing. Other material was packed in plastic bags and placed in cardboard cartons. Seagrasses were stored at ca 3 °C and other groups were frozen at -20 °C.

Data and images from each site were entered into the vessel database while on board (Figure 2-30). The weights entered into the database were the total weight and the retained weight for each sample.



Figure 2-29: A sample of crustaceans showing the barcode label. The label number, weight and class were entered into a data base at sea.

Table 2-8: The taxonomic groups into which samples were sorted onboard and their specific requirements for preservation on board the vessel and destinations for further processing were provided.

| CLASS | PRESERVATION | DESTINATION |
|--------------------------|--------------|-------------|
| Crustacea: | Frozen | CMR-CV |
| Crustacea: Penaeidae | Frozen | QDPI-CNS |
| Invertebrates: | Frozen | QMSB-BRS |
| Fishes: | Frozen | CMR-CV |
| Fishes: Syngnathid | Frozen | CMR-CV |
| Marine plants: | Frozen | QMSB-BRS |
| Marine plants: Algae: | Frozen | QMSB-BRS |
| Marine plants: Seagrass: | Frozen | QMSB-BRS |

GBR Vessel Database

onboard the Gwendoline May

RECORDER : Dan Gledhill

CRUISE_ID : GBRMap_GM_03_2004

VESSEL : Gwendoline May

DATE/TIME : 13/10/04

COUNT : 7

SITE WEIGHT : 0

PHOTO_LINK : C:\Archive\gbr\Vessel\Images\GM\Cr

COMMENT : Depth = 20 metres

SITE_ID 1558 requires 7 samples according to the recorded Site data. You currently have 7 samples, this Site should be complete.

| SAMPLE_ID | CLASS | VESSEL | SITE_ID | BIN | LAB | PRESERVATION |
|-----------|----------------------|--------|---------|-----|---------|--------------|
| 024658 | Shark | 2 | 1558 | 1 | CMR-CV | C |
| 024659 | Shark | 2 | 1558 | 1 | CMR-CV | C |
| 024660 | Crustacea | 2 | 1558 | 1 | CMR-CV | C |
| 024661 | FISHES - Ffreezer: | 2 | 1558 | 1 | CMR-CV | C |
| 024662 | INVERTEBRATES | 2 | 1558 | 1 | CMR-CV | C |
| 024663 | Crustacea: Penaeidae | 2 | 1558 | 2 | DPI-CNS | C |
| 024664 | Crustacea: Penaeidae | 2 | 1558 | 2 | DPI-CNS | C |

Site photograph : [Image of entire catch]

Sample photograph : [Image of elasmobranch sample]

Figure 2-30: Data and images from each trawl site were entered into the vessel database entry form that also contained a photo of the entire catch (left) and of the sample (in this case, of an elasmobranch).

On two voyages digital colour images were taken of many specimens of selected fish species, which were preserved in 10% formalin. Penaeid prawn species and seagrass species were forwarded to QDPI&F in Cairns, while the remaining samples were sent to CSIRO Cleveland for further processing.

2.2.7.3. Vessel Sample Database (D Chetwynd)

The purpose of this database was to efficiently store and retrieve data and images for sites visited and samples collected via either the Scientific Trawl or the Epibenthic Sled. It was designed to be portable, user-friendly and, in the often difficult shift-work conditions at sea, minimise errors by means of prompts and real-time checks. Microsoft Access was used for storage of data in tables and Visual Basic for Applications (VBA) for the software development, in particular data entry Forms as well as Reports and Queries.

All data was stored as unique samples at the site level. Sites were a predetermined position within the GBR region and constituted the highest level for the data storage. The critical importance of a unique sample identification system led to the use of barcode labels and barcode readers which proved successful in minimising errors. A single barcode label was assigned to, and bagged with, each sample. A sample constituted a coarse sorting of the Trawl/Sled into general taxonomic groups for each site. Typically there would be one group per site, such as one sample of sponges for any given site, unless there was subsampling. There could be many samples for each site — there was a 1 to many relationship between the site and the sample (barcode).

Once sorted into groups, each sample was assigned a physical barcode Label, torn from a pre-printed perforated roll. A digital image was taken of each sample with its respective barcode. Each sample was then entered into the database against the current site number. The sample's weight, count and depth were recorded. The image for the sample was then associated to the sample's unique barcode by the database within the database and the image stored within a folder for that particular site. Barcode and site number were saved within the image filename.

In the event of subsampling, the total and retained weight was recorded for that sample. If a large animal was brought onboard it was photographed with a barcode then released alive, and the data and photograph were entered.

Once each sample was logged in the database it was preserved by one of several predetermined methods, such as freezing, formalin or alcohol.

The database allowed users to backtrack through previous sites or samples and check images against the recorded data, with updating procedures available to add/update to any stored data.

On completion of each voyage a copy of the vessel data was sent to Cleveland and both the data and images were extracted for use in the Laboratory sample Database.

2.3. LABORATORY PROCESSING AND IDENTIFICATION

2.3.1. Towed Video (T Wassenberg, J Sheils)

2.3.1.1. Video data processing

The recordings of the seabed towed video transects at each site were transferred from the digital tapes via firewire to removable computer hard drives for storage and archiving. Each site's camera tow was saved as a separate .avi video file, a process which was automated using batch files scripted from VTR time-code data logged in the field. The site identity of each video clip was cross-checked during the video capture process, using the audio data stream from the vessel GPS, which had been recorded onto the audio tracks of the video tape during each camera tow. A decoder box and software translated the audio signal on each recording into GPS data and displayed the date-time and positional information and calculated the appropriate site number for cross reference against the data logged in the field.

The objective of the analysis of the towed video was to characterise the seabed habitat by describing abiotic features and sessile biota, and visually estimating their approximate size and percentage cover. The operators who performed the video analysis underwent training before the process began and continued to consult regularly throughout the video processing to maintain consistency. A procedure manual was developed to facilitate consistent decision making.

Video files were copied from the removable hard drives onto work folders on the video analysis workstation computers, from where copies were deleted once analysed. A custom Delphi software application was used to view the videos and enter the data. The software paused the video at random intervals (in this case, between 10 and 30 seconds), overlaying a trapezoid outline onto the screen to highlight the target quadrat to be scored. The operator then entered data for that video frame before proceeding to the next. The user interface of the software is shown in Figure 2-31 and Figure 2-32. The data entry screen included drop-down lists for the operator to choose from, and consisted of three sections:

1: Large Scale Feature

These were defined as topological features of the seabed that of a scale larger than the target quadrat, for example reef, sand dune or flat seabed. Estimates were made of the vertical scale of these features.

2: Biological

Sessile fauna and flora were classified into categories; for example, different growth forms or (where identifiable) genera of sponges, corals and algae etc. The categories were developed to distinguish between different organisms as much as the resolution of the video would permit. Signs of animal activity such as burrows, mounds, pits and tracks were also recorded here. For each category type, estimates were made of percentage cover, along with estimates of their vertical and horizontal scale.

3: Sediment

The abiotic component of the habitat was classified into broad categories based on the Wentworth scale of sediment classification, modified to suit the level of discrimination possible from video footage. The presence and scale of sand ripples and waves were also recorded here. Habitat components larger than the trapezoid were treated in Large Scale Features.

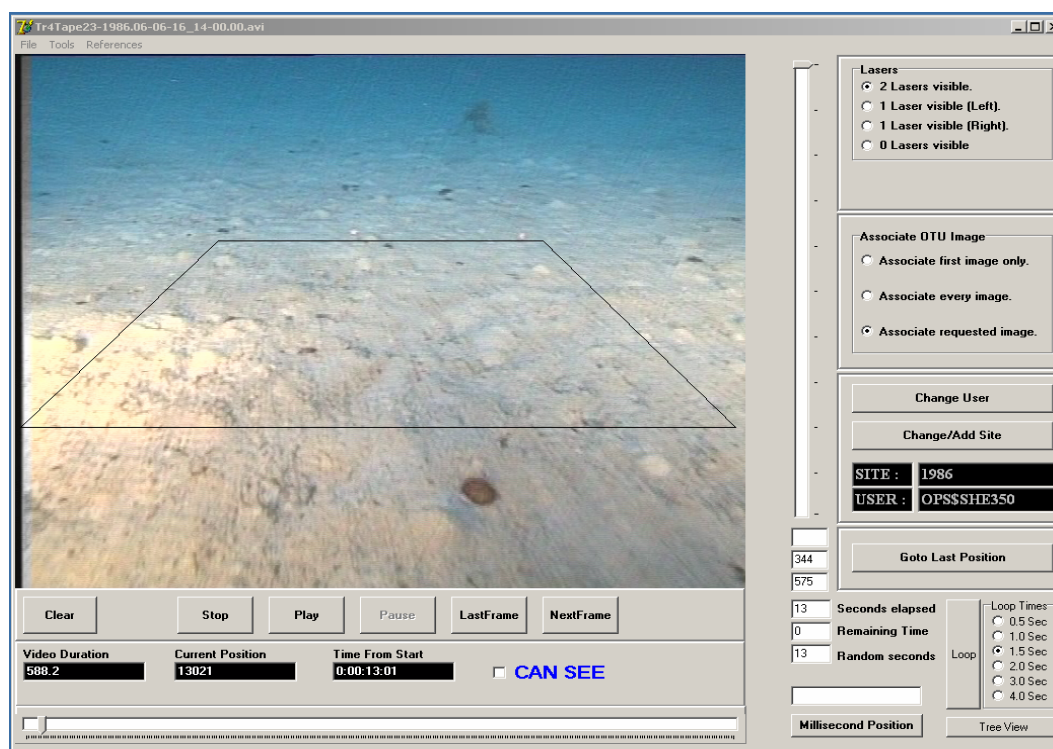


Figure 2-31: Data entry screens of the Delphi video analysis software showing the trapezoid overlaid on the paused video image.

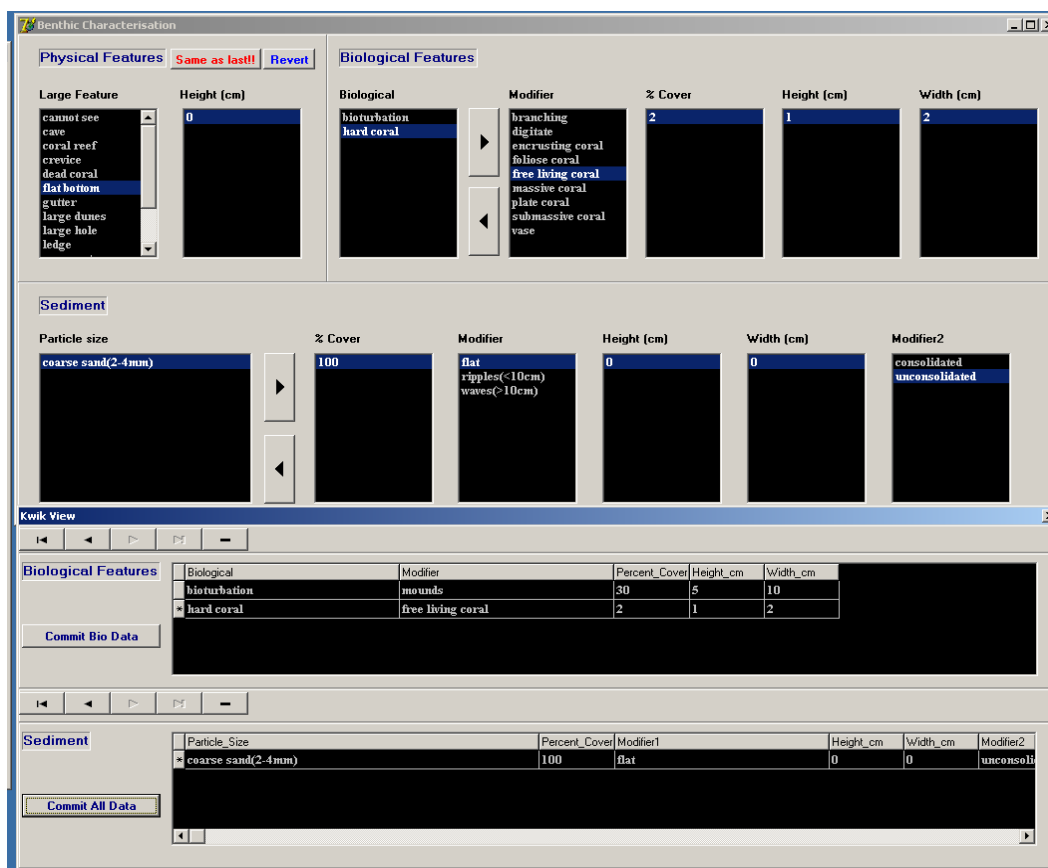


Figure 2-32: Drop down lists of physical and biological attributes to be used in analyzing the video image.

Two lasers aimed at the seabed 28.5 cm apart are visible in the recordings (red dots just in front of the trapezoid), providing a scale for size estimation. Once the operator has made their selections the data was committed to an Oracle database, where it was linked to the site number and millisecond position within the video clip. This allows future retrieval of the image and the record of the exact place in the video archive where the original data entry was made.

2.3.1.2. Laboratory Video Software & Database (D Chetwynd)

The Laboratory processing of the DropCam video used a custom Delphi 7 application which stored data (user selected Benthic information) and images (paused video .bmp) directly to an Oracle database.

Delphi is a Windows Rapid Application Development (RAD) environment that uses Object Oriented Programming, which is effectively a collection of cooperating objects. The video application is form driven (see Section 2.3.1.1) and benthic analysis and images were captured from the video and stored directly into the database.

Viewing the .avi files within the application was controlled by a recognised Active X component 'MoviePro'. This was professionally developed for use within Delphi and other Object Oriented application environments and uses the basic features of Windows Media Player to play, fast-forward, rewind and pause the video, as well as allowing the capture of paused video as a .bmp.

Access from the Video software to the database was provided via the third party tool, Oracle Data Access Components (ODAC). This is a set of VCL native components for Delphi, which supports many Oracle specific features and simplifies developing of client/server applications. Connectivity to the Oracle database works directly through TCP/IP and doesn't require Oracle's software on the client side.

The Oracle database was Oracle Database 10g Enterprise Edition Release 10.2.0.2.0 and is fully supported and backed up as per CSIRO policy.

Data and images were written to the database via a form driven set of Oracle Stored Procedures, called by the Delphi application. Each Database Manipulation Language (DML) call was run within a transaction and any resulting errors forced a ROLLBACK of any insert, updates and deletes within the transaction so the problem could be rectified without affecting any other data. Images (paused video .bmp) are stored in the database itself as a Binary Large Object (BLOB) and therefore are actually stored within the specific row. This ensures any backups encompass the entire dataset, as opposed to the alternative choice of image storing, which stores the image within a predefined directory and the directory address and filename, the pointer, within the database.

2.3.2. BRUVS Video (M Cappo)

Interrogation of each tape was conducted using a custom interface (BRUVS2.1.mdb©, Australian Institute of Marine Science 2006) to manage data from field operations and tape reading, to capture the timing of events and reference images of the seafloor and fish in the field of view. Records were made, for each species, of the time of first sighting, time of first feeding at the bait, the maximum number of fish seen together in any one time on the whole tape (*MaxN*), time at which *MaxN* occurred, and the intraspecific and interspecific behaviour in 8 categories. The use of *MaxN* as an estimator of relative abundance has been reviewed in detail by Cappo *et al.* (2003, 2004).

Species identifications were confirmed by checking the collection of reference images with museum taxonomists [Dr Barry Hutchins (*Paramonacanthus*), Barry Russell (*Pentapodus*)] and with other project staff [Jeff Johnson and Dan Gledhill]. It was decided some taxa were indistinguishable on video footage, so these were pooled at the level of taxa, genus, family or order. These taxa are hitherto referred to as species. The *MaxN* data were then summed for each species over all single BRUVS replicates at a site, and 4th root transformed. Data were analysed at the level of individual sites.

2.3.2.1. BRUVS Video Software & Database

A custom BRUVS tape analysis interface was developed by AIMS staff (Gavin Ericson, Greg Coleman) for this project, and was improved in 8 versions (BRUVS2.1.mdb©, Australian Institute of Marine Science 2006).

One hour of Mini-DV tape footage equates to 12 gigabytes of digital data. Capturing, digitising and compressing the tapes would consume 1.5 hours each. Given 1585 tapes were collected, it was impractical to digitise them.

Instead, we developed a method where the tapes were played in a tapedeck with a jog shuttle control to a 50cm screen. The tapedeck was connected via “firewire” to the BRUVS2.1.mdb, where the video playback was also visible in small windows.

The tape was played to and fro and the timecodes [converted to decimal minutes] of important events were captured via firewire from the tapedeck. When a new fish was seen, drop-down menus in BRUVS2.1.mdb offered selections for family, genus and species. Once species was selected a CAABCODE was generated with the record. When certain “events” buttons were selected, the timecode was grabbed from the tapedeck and stored with the record. The tape deck was paused to allow grabbing of “benthos” and “fish” images, which were named by the software and distributed to folders. If the species was unknown, various buttons allowed the reference imagery to be searched for a match. If the species was new, a dialogue box enabled generation of custom CAABCODES and a description.

2.3.2.1.1 Reading Tapes

The term “fish” in this instance refers to any mobile marine organism, including sharks, rays, sea snakes, sea turtles, squid, cuttlefish, spanner crabs and portunid crabs.

The data gathered from BRUVS tapes and stored in the database concern:

- classification of the habitat in the field of view (topography, sediments, benthos)
- the identity of fish and CAABCODES
- their time of arrival
- their behaviour [8 categories, including feeding on the bait]
- their maturity [adult or juvenile]
- their relative abundance (as *MaxN* = the maximum number visible at one time, or distinguishable at different times as separate individuals – such as much larger and much smaller, male and female)
- the time elapsed before *MaxN* and feeding occurs

The BRUVS2.1mdb adds this data to, and calls up, “operations” data collected at sea when each BRUVS is deployed.

The unique combination of a site and a Camera Number links all records in all tables of the relational database. The main idea of this interface is to easily grab times that events occur in the tape, together with reference images and reference video. Like any reference collection, this allows users to:

- name unknown taxa
- learn identification skills by comparing taxa with existing images
- compile a useful, watermarked, representation of images of species from different locations, aspects, colour phases and sizes/sexes. These can be emailed to international taxonomists for verification of identifications.
- apply “quality assurance” in updates to the parent databases by correct mis-identifications as new information comes to hand
- provide material to help interpret our results with clients.

Tape reading protocols were developed, ensuring tape readers must have:

- captured image(s) for every taxa sighted on every tape, and benthos in the field of view for every tape
- saved the better images as “reference image(s)” for every taxon sighted – all new taxa were accompanied by at least one reference image as they were named. We collected as many shots from different angles, sizes, and colour phases as possible in the “library” (Figure 2-33, Figure 2-34).

The database now contains information on over 39,900 individual animals seen during the Seabed Biodiversity Project, and over 17,000 images for reference by site, with 2,200 of the best reference images in the “reference library”.

These protocols, and the design, operation, and troubleshooting for BRUVS2.1.mdb were fully described in a manual. The software and manual can be obtained with the reference image library, under certain terms and conditions of use, from BRUVS@aims.gov.au.

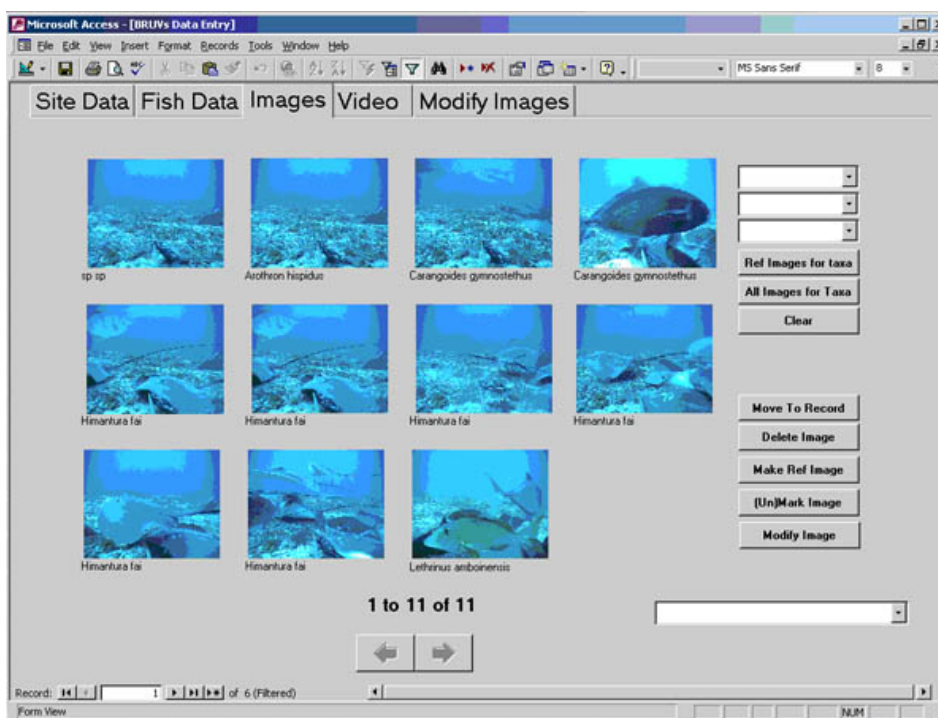


Figure 2-33: Image reference form in BRUVS2.1.mdb



Figure 2-34: Reference image for *Pristipomoides multidentus*, with *Lutjanus sebae*, *L. adetii* and *Epinephelus undulatostratus* and *E. areolatus* in the background.

2.3.3. Laboratory Processing of Samples (T Hendriks, M Stowar, C Bartlett, T Wassenberg, D Gledhill)

Following the field-trips, samples were freighted to several laboratories where detailed sorting, identification, curation and detailed data recording were continued. Comprehensive reference collections of voucher specimens were established and recorded into the database.

- Porifera, octocorals, sled sampled fish and trawl bycatch invertebrates were sorted at the Queensland Museum, South Bank campus (QMSB);
- Molluscs, echinoderms, bryozoans and scleractinians were sorted at the Museum of Tropical Queensland (QM, MTQ campus) by MTQ and Australian Institute of Marine Science (AIMS) staff;
- Crustaceans and trawl sampled fish were sorted at CSIRO Marine and Atmospheric Research, Cleveland;
- Trawl sampled prawns were sorted at Queensland Department of Primary Industries and Fisheries (QDPI&F) in Cairns;
- Sled sampled algae and seagrasses were sorted at Queensland Department of Primary Industries and Fisheries (QDPI&F) in Townsville;
- Particle size and carbonate composition analysis of sediment samples were completed by Geoscience Australia (GA).

By decision of the Project's Steering Committee, annelids, ascidians, crinoids, hydroids and trawl sampled marine plants were not completed within the scope of the project. All other groups have been completed.

For all samples at all agencies, the following processes were completed.

- Each sample was physically separated into groups corresponding to species or species equivalent Operational Taxonomic Unit (OTU);
- Identifications were done to Operational Taxonomic Unit (OTU) level: known species where possible, alpha species otherwise;
- Total counts and weights of each OTU within a sample were recorded;
- Specimen barcodes were assigned to each OTU for database purposes, as well as to facilitate any further studies that may be completed with these specimens.
- Reference material of specimens of all OTUs was retained. Specimens were kept the first time that a new OTU was encountered at any laboratory — a voucher reference. These were preserved and retained at the relevant laboratory.
- Entry of all data into the database (Figure 2-35, Section 2.3.3.3).

2.3.3.1. Queensland Museum

The Queensland Museum, at QMSB and MTQ, was responsible for the taxonomy of many major invertebrate Phyla, including Porifera, Echinodermata, Mollusca, Cnidaria, Ascidacea and Bryozoa (Figure 2-36). All voucher specimens were preserved in ethanol and all other processed specimens were stored either in ethanol, or frozen in freezers located at CSIRO Cleveland.

Identifications of Porifera, Cnidaria and Ascidacea have been especially problematic, as they would normally require extensive preparations before genus/species combinations can be given with a high level of confidence. Time constraints prevented histology from being completed, leaving scope for further research to be completed in the future to allocate species names using histology or other means as necessary.

GBR Laboratory Database

File Edit View Insert Format Records Tools Window Help

Tahoma 8 B I U

OTU

Search Barcode: 020153

Search SBD: All Checked All Unchecked

Description:

Site: 10214316 View Site Photo

Cruise: TSMMap_GM_01_2004

Vessel: Gwendoline May

Grid365: 232

Latitude: -10.21

Longitude: 143.16

Depth: 28.8 metres

Date: 2/01/2004 Hide Sample Photo

Container: 1

Recorder: Ted Wassenberg

Weight g: 1100

Class: INVERTEBRATES

Comment: None

Kingdom Phylum Class Order Family Genus Species Add

Top 10 Taxa

Sample Photo 1 of 1

| Photo | QM_CODE | FAMILY | GENUS | SPECIES | COUNT | WE |
|-------------------------------|------------|-------------|-----------|-----------------|-------|-----|
| <input type="checkbox"/> View | CMR016423 | Bothidae | Bothidae | juv/undent | 1 | 2.5 |
| <input type="checkbox"/> View | SBD2004810 | Portunidae | Charybdis | truncata | 23 | 152 |
| <input type="checkbox"/> View | SBD2004811 | Portunidae | Charybdis | jaubertensis | 1 | 13 |
| <input type="checkbox"/> View | SBD2004812 | Scyllaridae | Scyllarus | demani | 5 | 29 |
| <input type="checkbox"/> View | SBD2004813 | Portunidae | Portunus | rubromarginatus | 7 | 87 |
| <input type="checkbox"/> View | SBD2004814 | Portunidae | Portunus | gracilimanus | 13 | 105 |
| <input type="checkbox"/> View | SBD2004815 | Portunidae | Portunus | tenuipes | 25 | 258 |

Form View NUM

Figure 2-35: An example of the form used in the laboratory to enter data obtained from the field samples. The sample barcode number is entered and the database retrieves the site details including the sample photograph from onboard the vessel. Individual species or OTU were then entered into genus or species boxes (middle fields) and a pick list of names appears. By selecting the appropriate name the species numbers and weights were then able to be recorded into the bottom RHS field.

Sponges were taken to operational taxonomic unit (OTU), with far fewer genus allocations, or even higher taxonomy in some cases due to the difficulty of identification without histology. Some histology has been completed and new species have been found.



Figure 2-36: Identifying and processing invertebrate samples at the Queensland Museum.

Octocoral sclerites could be seen on most specimens using a stereomicroscope, allowing for taxonomic identification to the genus level. Differing specimens were then given an operational taxonomic unit (OTU), rather than species name, in most cases.

Ascidians require treatment when collected to relax the zooids for a short period of time before being fixed in formalin. They are subsequently transferred into ethanol before identification. As these processes could not be followed upon collection at sea, identification became difficult and consequently many samples were not identified.

The first year of the project included the design and implementation of the bar coding system used across the project by different laboratories (QMSB, MTQ, AIMS, QDPI&F and CSIRO). This allowed for a consistent tracking method across all specimens in which duplication of numbers was eliminated. Now that the databases have been combined, this system has proven to be efficient.

The large amount of knowledge and experience gained by staff over the study period facilitated an increase in the sorting rate. This was invaluable as deadlines were fast approaching with a high quantity of material remaining to be sorted. The volume of samples collected for sorting and identification was challenging throughout the project. In response, additional staff resources were applied to the Project by the QM, CSIRO, QDPIF and AIMS. The rate of sorting, identifying, and processing samples into the collections and databases was increased, and has been reviewed regularly, with priorities for the various biotic groups being reviewed by the Steering Committee.

Processes for entry of data into the database were amended to improve efficiency. Originally, all data at QM was initially being hand-written on paper datasets, with data entry only occurring at intervals throughout the sorting process. This created difficulties in OTU allocation and any misprints on the datasheets were difficult to rectify. This process was revised, so that hard copies of datasheets were retained, but the data was entered immediately into the database, as the sorting was being done. This minimised entry times, and any problems could be rectified instantly, rather than revisiting a sample after being re-frozen or preserved and often stored at a different location.

More than 200,000 specimens have been identified in total, which has greatly enhanced the reference collections of the Queensland Museum. This resource is now being used as a basis in taxonomy for other studies of biodiversity and remains a resource for other institutions and researchers who are unlikely to get access to these remote or protected areas in the future.

2.3.3.2. CSIRO (CMAR) and QDPI&F

Trawl-sampled fishes and all crustaceans, except penaeid prawns from the scientific trawl, were sorted and identified at the Cleveland laboratory of CSIRO Marine and Atmospheric Research (CMAR). Samples were stored at -20° C in cardboard cartons, with individual samples double-wrapped in plastic bags to reduce freezer burn and deterioration.

Samples were thawed and sorted to OTU's (Operational Taxonomic Units – roughly equivalent to a species, but potentially not always aligned with currently recognised/named species) and retained on crushed ice during processing to reduce deterioration of colour and body tissues. Each OTU was allocated a registration barcode number and its weight and count for that site's sample were recorded in the laboratory database. Identified fish were re-frozen at -20°C for future work or dissemination to collections, while crustaceans were preserved in 70% ethanol. All but the voucher specimens were forwarded to the Queensland Museum.

To ensure accurate and repeatable identifications of specimen, a reference collection, consisting of a voucher specimen and replicates, was established to represent all OTU's and variants identified. When an OTU was encountered for the first time, the sample was registered and a specimen was allocated as the voucher. The voucher was photographed and given a score to indicate the taxonomist's confidence in the identification, following Williams *et al.* (1996).

Voucher fish were preserved by soaking them in 10% formalin for about a month, prior to transferring them to 70% ethanol for storage. Additional specimens were also preserved to provide replicate

reference material. A tissue sample, for genetic analysis, was removed from some voucher and replicate specimens prior to preservation. Tissues were stored in ethanol. Additional specimens, of virtually all species, ranging from across the geographic range of the study area, were retained (frozen) for the collection of tissue samples at a later date. Sub-collections of frozen and preserved material were sent to the National Fish Collection, CSIRO Hobart, for further examination.

The fresh colour of many fish and crustacean species is a useful diagnostic tool, and for some species colour patterns are the only field characters. A laboratory identification guide was compiled containing images taken onboard and in the laboratory for each OTU and variant. Identification characters were recorded to assist in accurate and consistent identifications. Images and identification characters were also collated in an online database to allow interstate colleagues and visiting international experts to view specimens remotely and thus assist with the identification of taxonomically difficult species.

2.3.3.3. *Laboratory Sample Database (D Chetwynd)*

The Laboratory Database, similar to its Vessel counterpart used MSAccess for storage of data in tables and Visual Basic for Applications (VBA) for the software development, in particular data entry Forms as well as Reports and Queries.

CSIRO, the Queensland Museum Brisbane and Townsville and the QDPI all had networked installations of the Laboratory database local to their laboratory.

The database's main purpose was to log taxonomic specimen information and images against the samples collected in the field. The collected samples, initially sorted on the vessel to a general biotic group level, would be further sorted to a species level or to the nearest taxonomic level possible, given the available resources and or the state of the sample.

A list of Australian Marine species was compiled and stored in the database in taxonomic hierarchy to act as a starting list to build on. Each of these unique entries was given an incrementing ID to denote each Operational Taxonomic Unit (OTU); if and when a new entry was added an incremental value was added as the new ID for the new OTU.

When sorting the samples, a sample was opened and, using the bar code scanner, the barcode label from the sample was read. This triggered a response within the database, which retrieved the site and sample data and images displaying them for the user to verify. The sample was then separated into its various OTU's. For examples, a crustacean sample could have three specimens of different crab species and two specimens of the same species of prawn, therefore 4 OTU's existed within this sample. There was a 1 to many relationship between the sample (barcode) and the OTU's within that sample; for each sample there could be many OTU's.

Once the OTU's were identified the user allocated a separate barcode label to each OTU — this was known as the jar code – and was scanned into the database and the label was placed in the OTU bag or jar. If a digital image of the specimen was required, it was taken at this point with the jar code label within the image.

Once the samples were sorted into OTU's, they were individually added to the database. This was done by selecting the lowest known taxonomic level to each OTU group via the pick lists in the entry forms. If the identified species did not already exist in the precompiled list, then it was added via another entry form for new OTUs, hence making it available.

Once the desired species was selected, the count and weight of specimens were entered against the record, as well as the jar code, read by the barcode scanner. Any images previously taken were stored against the OTU at this point.

Species data can be queried by any of the taxonomic levels, site, sample or even jar code.

2.4. DATA ANALYSES

2.4.1. BRUVS Species Models, Characterization & Prediction (M Cappo, G De'Ath)

A total of 40 environmental and spatial explanatory variables were used in analyses of BRUVS data. These comprised: three spatial variables (depth, “Along”, “Across”); four sediment characteristics (% mud, sand, gravel, carbonate); 20 physico-chemical parameters from the CARS and SeaWiFS dataset, including measures of location (mean) and spread (Std Dev); 12 “harmonics” of polar temporal variables (diurnal, lunar, seasonal); seabed current shear stress and shelf slope; and a trawl effort index.

Distance “along” was set to range from 0 at the southern end to 1 at the far northern end. Distance “across” was 0 on the coast and 1 on the 80 m isobath. The corners of the polygon formed in this way were 142.53°E, -10.69°S and 144.06°E, -10.68°S at the northern end, and 152.49°E, -25.00°S and 152.90°E, -24.22°S at the southern end.

The BRUVS data were analysed in two ways. Firstly each species was treated as a univariate response and, using boosted trees (GBM, Friedman 2001, De’ath 2006), its presence-absence was predicted from the environmental data. Boosted trees are widely regarded as one of the best predictive methodologies, and handle complex data sets and a broad range of loss functions. For the presence-absence data analysed here, the binomial loss function was used. The collection of species was then related to the best environmental predictors. Statistics representing the predictability of each species and the predicting capacity of the environmental measures were then calculated. This produced a “short-list” of 25 species and 20 explanatory variables. The 25 species were the best predicted species that occurred on at least 7% of sites. The 20 explanatory variables were selected as the best predictors of the 25 species. The binomial loss function was used in the boosting.

Secondly, the relative abundances on BRUVS (the sum of *MaxN* for each sampling station) were 4th root transformed and analysed using multivariate regression trees (MRT; De’ath 2002). MRT used sums of squares (Euclidean distance) for splitting. Twenty explanatory variables and twenty-five species responses were short-listed in the same way as described above for the boosted trees. The best-sized tree was selected by five-fold cross-validation.

The tree defines a hierarchy of species communities and their spatial and environmental values that locate them on the GBR. This hierarchical approach can be used with any clustering method (constrained as is the case here with multivariate regression trees, or unconstrained). It also identifies groups of species that co-occur at varying spatial scales to form communities. This contrasts with non-hierarchical methods which derive mutually exclusive clusters at a single spatial scale, thereby lacking high-level (broad spatial scale) structure and ignoring information from highly prevalent species. The homogeneity of the clusters formed by MRT (from 1 through to 13 nodes) was compared with similar numbers of unconstrained cluster groups, using K-means clustering and Euclidean distance.

Indicator values (DLI; Dufrêne and Legendre 1997) were calculated for each species for each node of the tree. For a given species and a given group of sites, the DLI is defined as the product of the mean species abundance occurring in the group divided by the sum of the mean abundances in all other groups (a type of specificity), times the proportion of sites within the group where the species occurs (fidelity), multiplied by 100. DLI takes a maximum value of 100 if the species occurs at all sites in the group and nowhere else, and 0 if it occurs at no sites within a node. Each species was associated with the tree node (assemblage) where its maximum DLI value occurred, and the numbers of indicator species and their values were used to characterize each node of the tree. Species with high DLIs were used as characteristic members of each assemblage, and the spatial extent of the group indicated the region where the species was predominantly found.

2.4.2. Single Species Biophysical Models and Prediction (M Browne, W Venables)

2.4.2.1. Assumptions and Challenges

The distribution of each identified species was considered separately in relation to the available physical variables used as predictors in the study. This approach assumed that the observed geo-spatial distribution of each species may be adequately explained by an underlying physical gradient. Each species would be expected to have its own preferred habitat range and tolerance for various physical parameters, and the spatial variation in physical variables is thought to drive the observed regional scale spatial distributions of the taxa.

From the point of view of biophysical modelling, it is known that sampling in a marine environment is very susceptible to sampling variability. That is, for fixed levels of the biophysical parameters involved, the event of observing a species, and the biomass obtained given that the species was observed, were still liable to be highly variable due to random influences — neither observable nor under the control of the sampling mechanism. Thus, the modelling approach applied needed to be conservative and to anticipate that much random variation will remain unexplained. Technically, the biological response variables may be described as having a zero-inflated log-normal distribution. That is, given that some biomass is observed, the samples are approximately Gaussian on a log-scale, with a mean depending linearly on the physical predictors. However, given that the estimated probability of observing any particular species is typically relatively low (< 10%), the very large number of zeros in any species' site-records strongly suggests a two-phase approach: initially modelling the probability of observing a species at all and conditionally modelling the distribution of the log-biomass given that the species is observed.

2.4.2.2. Model Formulation

The two-stage model used to relate the observed biomass to the underlying physical variables may be described as follows:

- We use a logistic regression model for the chance of observing a species in a sampling event. For any given species, S , the chance of observation is

$$p_s = \Pr(S) = \frac{e^{b^T x}}{1 + e^{b^T x}} \quad \text{or equivalently} \quad \text{logit}(p_s) = b^T x$$

where x is a collection of suitably chosen physical variables for that species and b is the vector of coefficients multiplying them, to be estimated from the data. This first phase model is a standard logistic regression for presence/absence. The first component of x_0 is often a constant predictor (unity) and its coefficient b_0 is called the intercept term.

- The log-biomass of the species given the fact that it has been observed in a sampling event is then modelled as a normal linear regression. In symbols using an evident notation

$$\log B_s | S \sim N(g^T z, s^2) \quad \text{i.e.} \quad E[\log B_s | S] = g^T z, \quad \text{Var}[\log B_s | S] = s^2$$

where again z is a collection of suitably chosen physical predictors for species S and $z_0 = 1$ making g_0 the intercept term.

Note that for the logistic regression stage all site records can be used in the model calibration, but for the second stage only those site records for which there is a non-zero biomass contribute information that can be used in this calibration process. This sometimes limits the modelling strategies possible.

Combining both stages of the model, the estimate of expected biomass at a given sampling site is then

$$\hat{E}[B_s] = \hat{p}_s \exp \hat{E}[\log B_s | S] = \frac{\exp(\hat{b}^T x)}{1 + \exp(\hat{b}^T x)} \exp(\hat{g}^T z)$$

where the circumflex accents denote quantities estimated from sample data. Technically this is the median rather than the mean but since for the lognormal distribution the median is proportional to the mean it produces the same relative picture of biomass distribution.

Approximate standard errors for the quantities involved can be derived by the usual delta method. The formulae are complex, but as the method is entirely standard and can largely be relegated to the computational procedures, we omit them here for simplicity.

2.4.2.3. Explanatory physical variables, covariates, offsets and prediction

In the formulae above, the general-purpose explanatory variable x_j (or z_j) represents any member of the combined set of:

- 28 physical explanatory variables (e.g. *percent_mud*). A full list and description of the physical variables is provided elsewhere (Section 2.1.1).
- 2 spatial variables ('*across*' and '*along*') representing in relative terms the distance between shoreline and outer reef, and between northern- and southern-most points of the GBR.
- Squared terms of physical and spatial variates (e.g. *percent_mud*²)
- Second degree interaction terms between physical or temporal explanatory variables, or both (e.g. *percent_mud* × *benthic_irradiance*)
- Harmonic terms in the temporal covariates: (described specifically below)
- The measurement method used (i.e. modified trawl net / benthic sled) as a factorial predictor,
- A weighted annual average of commercial trawl fishery effort local to the sampling site.

For the purposes of generating predictions on the GBR study region, we were primarily interested in the relationship between the physical variables and observed biomass. It was, however, recognised that other factors were expected to play a role in the observed biomass. For example, many species are known to have a strong diurnal or lunar behavioural cycle, or a seasonal abundance component. Also, when generating estimates on the physical grid for full coverage of the GBR region, it is desirable that the estimated distributions are independent of sampling device, which we term the 'survey type'. These variables are included in the models in order to ensure that these effects do not interfere with estimation of the effect of genuinely physical or spatial predictors. When predictions were later made from these fitted models on to the entire GBR grid, the covariate predictors are set to values that represent the sampling disposition under which the estimated biomass would be largest. This is to promote maximum contrast in the predictions.

The temporal covariates included 'Time of Day', 'Moon Phase', and 'Time of Year' (or 'season'). Since GLMs depend on the explanatory variables through a single linear function, it is appropriate to represent the effect of such temporal predictors through harmonic terms, that is

$$x_a^{(k)}(t) = \sin\left(\frac{2pkt}{T}\right) \quad x_b^{(k)}(t) = \cos\left(\frac{2pkt}{T}\right) \quad k = 1, 2, K$$

where T is the appropriate fundamental period. Including temporal covariates in this way ensures that the predictions will obey the natural periodicity with respect to such predictors.

It has been mentioned that 'survey type', whether the measurement was made with the trawl or sled, was also included as a covariate factor in the analysis. If a species was observed a minimum number of times in both sampling devices, then all data was included in the model, with the 'Survey Type' factor included. However, if a species was observed on very few occasions, or not at all, with either one of the sampling devices, then the usefulness of a model incorporating both devices was limited. In these cases the models were based on data from the most productive sampling device only, obviating the need for a 'Survey Type' covariate in the model.

The area swept by each device at each site was recorded, and although efforts were made to keep this constant, it did vary somewhat. The effect of trawling (or ‘sledding’) over a greater area is to increase the probability of a catch in some monotonic way, and to increase the amount of biomass caught, on average, proportionally. Thus, the recorded swept area on the log scale was included as a candidate predictor for the logistic regression models and as a fixed offset in the biomass models. Predictions were then standardised by setting swept area to 1 Ha.

2.4.2.4. Model construction and variable selection

Each species model included, at a minimum, harmonics in temporal covariates as well as ‘survey type’ and ‘log-swept area’, as explanatory variables (or offset). It has been noted above that potentially included variables included 30 physical or spatial variables, as well as squared terms and interactions between physical explanatory variables ($30 + 30 \times 31/2 = 495$ possible candidate predictors). Not all possible choices, however, are equally reasonable *a priori*. In practice we note that if a physical predictor is important either for the presence/absence or the conditional biomass of a taxon then the linear term will generally make this manifest and the additional contribution to the model due to higher order terms involving these will be much smaller, though often quite useful, of course. We adopted a two-stage variable screening method. At the first stage we allowed selections to occur only on the linear terms. Once these were found, we considered all possible squared and interaction terms involving the identified variables for additional inclusion in the model at the second stage. In this way we ensured that if a second order term was included in the model, its marginal linear terms were also included, which is generally regarded as a desirable feature of empirical statistical modelling.

The physical variables available are by their nature highly collinear (or confounded) and to counteract this we adopted a rigorous variable inclusion policy. Such a policy also has a good chance of ensuring some interpretability for the models as well as predictive effectiveness, although this has to be taken with some caution. The criterion used in these analyses was the ‘Bayesian Information Criteria’ due to Schwarz, 1978, defined as:

$$BIC = -2 \log L + k \log n$$

with $\log L$ denoting the log-likelihood of the optimized model, k the number of estimated parameters used in the model and n being the number of observations. The BIC attempts to balance model performance in the training sample with a penalized measure of model complexity to ensure that the model will capture as much signal and as little noise as possible. The related Akaike Information Criterion (AIC) penalizes complexity by a factor of 2 rather than $\log n$, leading to more complex models which in this context, from our experience seem to sacrifice interpretability for minimal gains in predictive performance.

At each iteration of the stepwise search procedure, a term was added or removed from the working model if the inclusion or removal resulted in the greatest reduction in the BIC criterion. As mentioned earlier, this was done for the linear terms initially, and then for the second degree terms involving those predictors, with the linear terms chosen fixed in the model. This was done independently for the presence/absence and the conditional biomass models for any sampled species.

2.4.2.5. Prediction on the GBR grid

Based on the constructed models, estimates of expected biomass were generated for each species, for each grid location in the GBR study region. This involved interpolation between the sites of the training set and also, as noted, above, a transform back from the log scale to the natural scale. Both of these operations can result in unrealistic estimates and in this case they will be much more likely to be unrealistically large than small. As a heuristic, it was determined that the largest standardised per Ha biomass actually caught for a particular species would be used to determine a ceiling on the largest confident estimate on the grid to be used. Final estimates were truncated at the largest observed standardised catch rate observed in the sample itself. This seems preferable to having unrealistic estimates dominating a graphical presentation.

For plotting purposes, the coefficient of variation ($CV = \text{estimated SD}/\text{estimated mean}$), was then calculated at each grid point. In this case the CV offers a more suitable statistic to represent uncertainty than the SE because it does so in a proportional way. We used models for log biomass, for example, for the same reasons.

2.4.2.6. Graphical presentation of results

Figure 2-37 displays the colouring scheme used to present the species model estimates over the GBR region. Inspection of the table shows that an order 2 'octave' style is used for both the mean biomass estimates and the CV estimates. This method proved effective for illustrating the significant spatial variation over the study area. The other advantage of this approach is that all single-species maps are plotted using the same colour key, facilitating abundance comparisons between species. A rainbow colour scheme is used to differentiate between different mean biomass estimates, whilst colour intensity reduces as the CV increases. Thus, intensity may be taken to indicate the relative certainty of our estimate at each grid point. Finally, a quantized colour scheme (i.e. constant colours within each biomass / CV range) was found improve the readability of the generated maps, without losing any significant information.

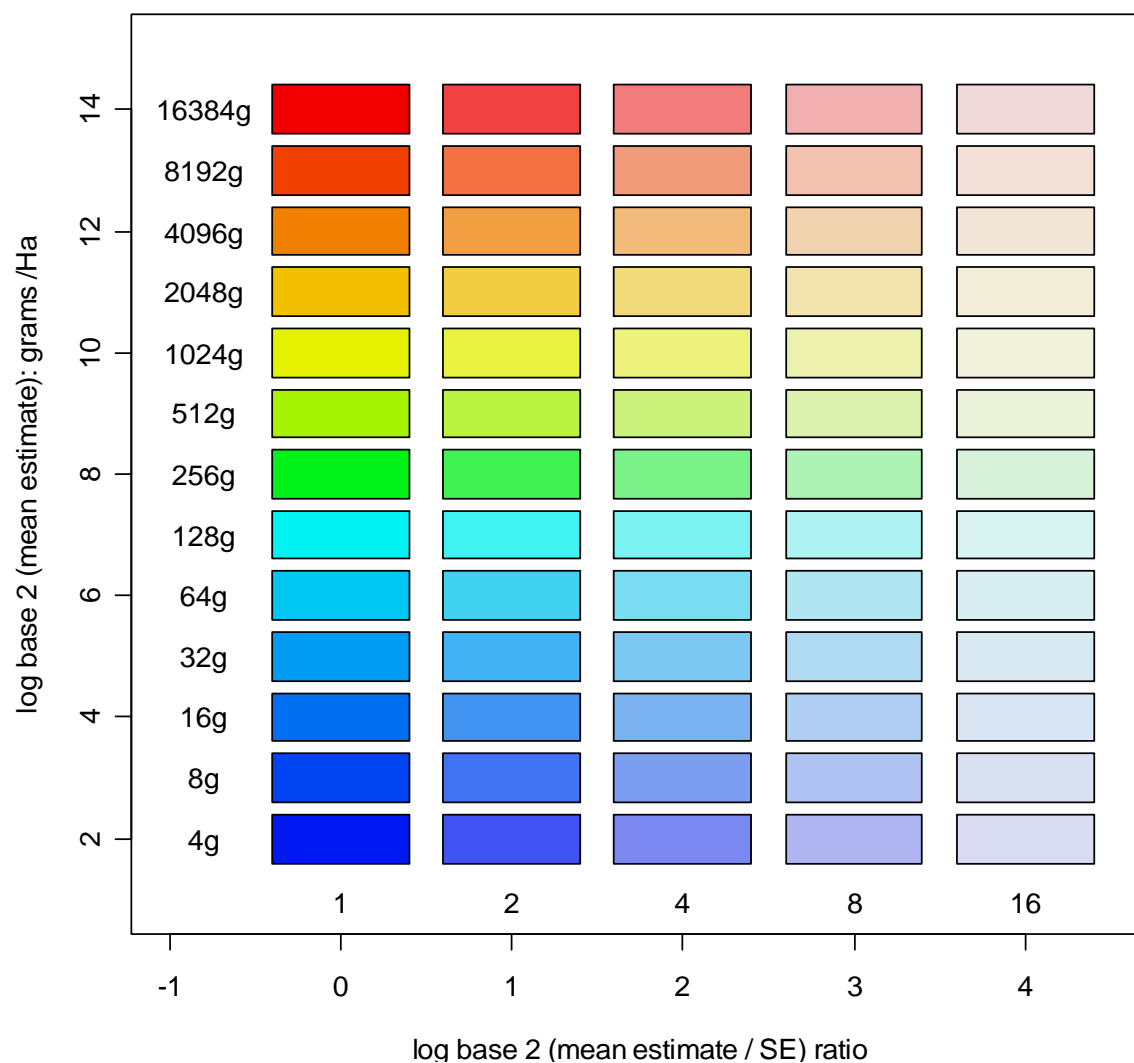


Figure 2-37: Colour scheme used for species distribution mapping

2.4.3. Species Groups Characterization and Prediction (M Browne)

One of the goals of the statistical analyses and modelling was to develop groups of ecologically similar species (at least with regard to their distribution in the physical environment) and to generate predictive models for the biomass of the entire group. We note that the taxonomic hierarchy may not provide a suitable basis for forming groups with this kind of similarity. Clustering here refers to an empirical grouping, hierarchical or otherwise, based on the characteristic distribution of species as observed from the survey effort.

There are several reasons why such a grouping or clustering of species is useful. For example, clustering allows the organisation of species with similar characteristics into common categories. As an exploratory technique it may provide the basis for more targeted analysis for establishing possible ecological dependencies and relationships. Due to the broad scope of the current project, individual modelling and prediction has been carried out for a very large number of distinct species (> 800). Species clustering and aggregated biomass data within groups can be a convenient method for summarising or quantifying the variation in species distributions through a small set of key grouped models. Finally, in cases where distinct and relatively rare species are observed at different sites, but share similar biophysical distributions, aggregation of the separate species into a single group can provide a way to utilise parts of the data set not otherwise available for modelling input.

It should be acknowledged that although clustering methods are well developed with acknowledged utility, to some degree heuristics and arbitrary decisions inevitably play some role, such as, for example, in something as fundamental as the choice of a distance metric. In our view the purposes of clustering have to be always kept in mind, as much biological insight and knowledge has to guide the process at every stage and the results need to be viewed in this light afterwards before a grouping is used.

2.4.3.1. Approach

Most clustering methods work by considering a similarity / dissimilarity matrix which describes 'distances' between objects. Broadly speaking, a clustering algorithm attempts to assign objects to groups so that similar 'objects' (in this case species) are put together in the same groups. The most obvious (and simplest) method for species clustering is to begin with the site / species presence / absence matrix and define species similarity using 'Manhattan' or 'city block' distances calculated between the distribution of species over sampled sites.

The species clustering method that has been adopted here is based on upon estimates at survey sites, as described in section 2.4.2, and thus may be described as *constrained by the physical predictors*. The modelled distributions are used as a species descriptor, rather than using the profile of raw biomass or presence /absence, to describe the similarity between the distribution of species. There are several important considerations that motivated this approach.

There are advantages and disadvantages to this approach. The most obvious disadvantage is that the representation is only as good as the species models were an effective summary of the information in the data itself. This will not always be totally satisfactory, of course. However the advantages include the fact that this allows us to control for factors such as the temporal, sampling method and swept area covariates which are inseparable from the remainder of the information in the raw data itself. It also allows us at least a potential device for counteracting the effects of false negatives, though admittedly, and inevitably, a somewhat speculative one. We note, also, that the data smoothed need not be entirely realistic for the groupings based on it to be effective enough for our subsequent purposes. Once the groups were decided, the subsequent analysis was based on the aggregated data; that is, on real data once again. This provides a useful safeguard in the logical chain of events.

2.4.3.2. Method

There was a total of 840 species (N) that both occurred sufficiently frequently for biophysical modelling, and also led to statistically satisfactory two-stage models by the model construction methods as detailed in the previous sections. Model estimates were generated for the 1644 sites (M) visited by the vessels, controlling for covariate predictions, for the reasons previously outlined.

As a measure of distributional affinities for the species, an $N \times N$ Spearman correlation matrix **C** was created from the model estimates over sites. The correlation was chosen as the base for a similarity measure because it was desired that the clustering criterion be invariant to absolute abundance. Choosing Spearman correlations also makes the estimate robust to outlying values, as are frequently obtained under extrapolation from an empirical model as here. Two species with very different prevalence or mean observed biomass may therefore have high correlations if the standardized pattern of co-variation is similar.

To convert the correlation matrix, **C**, into a dissimilarity matrix **D** to be used for clustering we used the following transformation:

$$D_{ij} = \frac{1 - C_{ij}}{1 + C_{ij}}$$

This guarantees that self-dissimilarities are zero, distances are otherwise non-negative and, since the correlations themselves are between -1 and 1, the dissimilarities are in the range $0 \leq D_{ij} < \frac{1}{2}$. The denominator chosen was motivated by the fact that so defined $\log D_{ij}$ will be approximately normal with equal variance, by a standard result in correlation theory. It also ensures an open-ended upper limit for the dissimilarities themselves. (Fortunately $C_{ij} = -1$ did not occur in practice.)

After extensive experimentation with different methods for clustering species, hierarchical clustering using Ward's method was chosen as a reliable and well established procedure for heuristic clustering. Ward's (1963) method is a clustering procedure seeking to form the partitions P_n, P_{n-1}, \dots, P_1 in a manner that minimizes the approximation error associated with each grouping. At each step in the analysis, the union of every possible cluster pair is considered and the two clusters whose fusion results in minimum increase in the total sum-of-squares are combined. The ANOVA-type approach used by Ward makes this method one of the more principled approaches to clustering.

2.4.4. Site Groups Characterization and Prediction (W Venables)

Another goal of the statistical analysis and modelling was to identify various areas of seabed in the GBR study area in which the mix of biota was as homogeneous as possible and in some way distinct from the mix in other areas. These different, approximately homogeneous, mixtures can be called "assemblages". Any individual assemblage may be expressed in several disjoint geographical regions; there was no requirement that they be spatially contiguous. A further property was that, at the broad scale, these assemblages would be characterised using the available full-coverage physical variables. The biotic data used were the biomasses of identified fauna and flora at sites sampled by the epibenthic sled and research trawl.

A number of strategies are possible to achieve this result. One strategy would involve three separate steps, each with a number of options regarding method:

- First, partition the study sites into clusters based on the biological data alone, then
- Develop models to predict these clusters from the physical variables alone, and
- Use the predictive model to classify the entire GBR region.

The strategy finally adopted essentially combined the above partitioning, modelling and prediction steps into a single procedure, using a tree-modelling method. In outline this procedure was as follows:

- Using the biological information alone, construct a distance matrix between sites,
- Define a deviance measure on any clustering of sites, based on the biological distance matrix,
- Construct a decision tree using the available physical variables; the resulting terminal nodes of the decision tree define the site clusters,
- Use the decision tree to classify the entire GBR study grid and map the result.

The details of this procedure are explained in the following sections.

2.4.4.1. Biological distance matrix

The distance matrix between the sampled sites was based on the species biomass predictions from the individual species modelling, as described in Section 2.4.2. Distance matrices based on real sample biomass data would be preferable. However, more than one third of species had one or more significant temporal cycles (such as season, moon phase and time of day), which strongly affected their sampling-rates but not their abundance, and may have caused the raw data to produce assemblage splits due to arbitrary timing of sampling rather than actual distributions. Use of the predicted values, adjusted for the temporal variables, allowed distances to be based on biomass values for a standardized set of environmental conditions, but optimal with respect to the temporal catchability variables for each species. It was nevertheless acknowledged that the modelled predictions, being smoothed fitted derived data, would not be free of other issues — to minimize these, only predictions to sampled sites were used, rather than predictions (extrapolations) to the full GBR study grid.

The form of the distance matrix was the commonly used Bray-Curtis metric, but a number of possible prior transformations of the predicted biomasses were considered. The final transformation used was the 8th root, which for large biomasses behaves like a ‘weak’ log transformation, but for small biomasses behaves approximately linearly and, unlike $\log(b)$, was not adversely affected by zeros.

Thus, the dissimilarity d between sites i and j was:

$$d_{ij} = \frac{\sum_{k=1}^t |b_{ik}^\alpha - b_{jk}^\alpha|}{\sum_{k=1}^t (b_{ik}^\alpha + b_{jk}^\alpha)}, \text{ where } \alpha = 1/8 \text{ and } t \text{ is the number of taxa.}$$

and b was the biomass of each species k .

2.4.4.2. Deviance measure

Consider any group of g sites, G . These can be represented by points in a plane, where the (Euclidean) distances between them are intended to represent distances from the biological distance matrix. Choosing any site from the group, say S_i , the *span of the group from S_i* was defined to be the sum of squared distances from the reference site, S_i , to all other sites of the group:

$$\text{span}(S_i) = \sum_{k=1}^g d_{ik}^2$$

The *deviance of group G* , say $D(G)$, was then defined as the minimum value of the span, and the reference site from which this minimum was achieved was called the *medoid* of G , say S_M , using the terminology of Kaufmann and Rousseeuw, (1990).

$$D(G) = \min_{S_i \in G} \text{span}(S_i) = \text{span}(S_M)$$

If the group G was partitioned into two subgroups, $G = G_1 \cup G_2$, $G_1 \cap G_2 = \emptyset$, then the deviance of the partition was defined as the sum of the two component deviances:

$$D(G_1, G_2) = D(G_1) + D(G_2)$$

It can be seen that $D(G_1, G_2) \leq D(G)$, since partitioning the group lead to one fewer non-zero distance in the sum defining the deviance, and the remaining distances could be no larger than they were prior to partition. The difference $D(G) - D(G_1, G_2) \geq 0$ was the *reduction in deviance achieved by the partition*. The geometric representation of these notions was illustrated by a simple two-dimensional example in Figure 38 below.

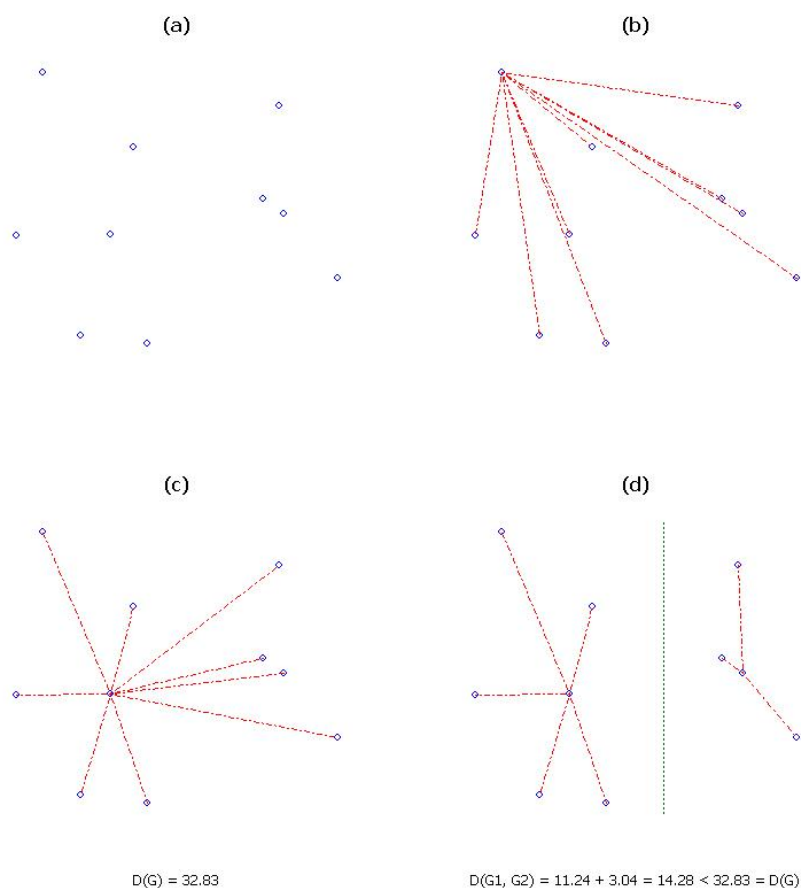


Figure 38: Spans, medoids, deviance and deviance reduction due to partition. (a) shows a group of ten sites using two-dimensional Euclidean distances to represent Bray-Curtis distances. (b) shows the span of the group from an arbitrary reference site. (c) shows the minimum span, which defines the medoid; the sum of squared distances from the medoid is then the deviance of the group. (d) shows a partition of the original group into two subgroups, and the spans defining the deviance component of each. The partition is achieved by a split on the x-coordinate. The reduction in deviance achieved by partition is then $32.83 - 14.28 = 18.55$.

2.4.4.3. Decision tree construction

A decision tree was constructed using the standard technique, described below. The `rpart` package of R (R Development Core Team, 2005), which allows users to define their own deviance and splitting criterion, was used for the computations, with standard defaults selected.

The method was as follows:

- Initially all sites were considered a single cluster, with an initial total deviance.

- Consider any potential predictor variable, X . The sites may be partitioned into two groups by selecting those sites whose values for X are below some threshold, $X \leq a$ as one group and the complementary set, those for which $X > a$, as the other. This was described as a split of the group on variable X at threshold a .
- Partition the group into two clusters by selecting the optimal split variable and the optimal threshold to achieve the greatest possible reduction in deviance of the span of Bray-Curtis distances.
- Apply the same procedure recursively to both clusters, until some stopping criterion has been achieved.
- The stopping criteria were as follows:
 - The group must contain at least 20 sites for further splits to be considered.
 - The group has deviance zero, or
 - A further split of the group would not reduce the deviance by more than 1%.

In this application, the third criterion was typically encountered, the first criterion was achieved only once and the second was never triggered — the outcome of which produced 16 groups. The result was displayed as a decision tree in the usual graphical form.

As a check on the biological similarities between the resulting 16 site groups, as defined by the above tree method that split recursively on physical variables, the following procedure was applied to the biological data only:

- the medoid site of each site-group was identified,
- the Bray-Curtis dissimilarities between the medoids were extracted from the entire distance matrix,
- a hierarchical clustering and dendrogram was computed using Ward's method.

The congruence between the structure of the decision tree and that of the cluster dendrogram was then examined.

2.4.4.4. Classification of the GBR grids

The grids of the entire GBR study region were classified into the 16 groups, based on the decision tree splits of the physical variables, and the resulting pattern of groups was mapped.

In this application, the recursive partitioning algorithm was used for unsupervised learning, which was somewhat unusual. More usually, tree methods are used for supervised learning and the result is used for prediction of some *à priori* defined attribute (classification tree) or quantity (regression tree), i.e. supervised learning. In such cases, the decision tree is normally pruned to some justifiable level of complexity by cross-validation, with the aim of improving the accuracy of prediction for new data.

In the current application, the procedure was used to define the attribute (site groups) itself. Thus, the normal cross-validated pruning process was not available as there is no *à priori* definition of the attribute. Correspondingly, the claims made for the result were simply that it defined a partition of the study sites into groups which were (a) defined by splits in the prediction variables and hence readily extended to the entire GBR study region and (b) as homogeneous as possible within, in the sense of Bray-Curtis distances based on transformed predicted biomasses. There was no “correct” number of site-group assemblages and the resultant number of groups was somewhat arbitrary. While the default criteria were generally accepted guidelines, the 16 groups identified here may be more (or less) than was warranted.

2.4.4.5. Derived species groups and indicators

In addition to defining site-groups assemblages, it was also useful to examine the extent of associations between these site groups and species biomass distributions in a simple and direct way. If a species was strongly associated with one site group and only weakly associated with others, such a species could be described as an indicator species for that site group assemblage. The approach was as follows.

A *site group characteristic distribution* for the k^{th} site group was defined by the vector $\xi^{(k)}$, where the components were defined as:

$$\xi_i^{(k)} = \begin{cases} 1/n_k & \text{for sites } S_i \text{ in site group } k, \text{ which has } n_k \text{ sites, and} \\ 0 & \text{otherwise} \end{cases}$$

Note that $\sum_i \xi_i^{(k)} = 1$ for all k , conforming to the definition of a distribution.

Using the predicted mean biomass for each species, the *species distribution* vector for the m^{th} species was defined as:

$$\eta_i^{(m)} = B_i / \sum_i B_i$$

that is, the predicted biomass, also normalized to add to unity over all study sites.

Further, a quantity termed the *affinity* distance between species and a site-group was defined as:

$$\alpha_{mk} = \frac{2}{\pi} \cos^{-1} \left(\sum_i \sqrt{\eta_i^{(m)} \xi_i^{(k)}} \right),$$

which has values in the range $0 \leq \alpha_{mk} \leq 1$. The quantity was zero only if the species was entirely within the site group and uniformly distributed, and unity if the species distribution was entirely outside the site group. The affinity distance was also a minor variation on the standard Hellinger distance measure between two distributions. It also has a geometric interpretation as the angle between two unit vectors, but heuristically, the affinity measure was an indicator of the preference any species had for any particular site-group.

Then, a distance between species was defined that represented the dissimilarity of their preference patterns for the site-group assemblages. Since the affinities were all measured on the same bounded scale, ordinary Euclidean distances were used:

$$E_{pq}^2 = \sum_k (\alpha_{pk} - \alpha_{qk})^2$$

In turn, this distance matrix was used to generate species clusterings that grouped together species with similar preference patterns for the site-groups. Standard hierarchical clustering, using Ward's method of linkage between groups, was applied. The resulting dendrogram, for all 839 taxa for which prediction models were possible, was cut at the appropriate location — for purposes of this analysis — to define 12 species groups.

While the species affinities provided information that helped characterise the site-group assemblages, it was also useful to investigate the relative density of each species group within each site group as additional characterising information. This computation was done in four stages, namely:

- sum the species biomass predictions within each species group,
- normalize these aggregate biomass distributions, as for single species, to give 12 species group distributions,
- average these species group biomass distributions within each site group, to give “percentage biomass per site” within each site group,
- present the result as a series of bar charts, one for each site group.

The 16 site groups were labelled numerically and the 12 species groups were labelled alphabetically.

2.4.5. Video Habitat Characterization and Prediction (W Venables)

The towed video camera yielded data in two forms. While the vessel was in motion an operator recorded both the substratum type and the biota currently in view in a continuous manner (Section 2.2.2). Also, later, in the laboratory, individual frames from the video record were scored for a substrate and biota in a much more detailed way, though not on a continuous basis but as a sample of about 30 frames from the tow record (Section 2.3.1). This section outlines how the towed video camera data was used to provide some indication of the broad habitat types in the study area.

Table 2-9: Sediment and group biological cover classes for analysed video tow data. Note that sediment classes up to large pebble could be further classified as rippled or in waves and cobble as waves.

| Grouped biological | Sediment |
|----------------------|---------------------------|
| Bioturbation | Mud (0.06 mm) |
| Algae_Caulerpa | Sand (0.06-2.0 mm) |
| Algae_Coralline | Coarse sand (2-4 mm) |
| Algae_Filamentous | Small pebble (4-16 mm) |
| Algae_Halimeda | Large pebble (16-64 mm) |
| Algae_Mixed | Cobble (64-256 mm) |
| Algae_Udotea | Boulder (256-1024 mm) |
| Algae_Ulva | Large boulder (1024 mm+) |
| Seagrass_H.ovalis | Larger than field of view |
| Seagrass_H.spinulosa | |
| Seagrass_strapform | |
| Bryozoan_branching | |
| Bryozoan_encrusting | |
| Hydroid | |
| Sea pen | |
| Soft_Coral | |
| Solenocaulon | |
| Sea_Whip | |
| Gorgonian | |
| Sponge | |
| Solitary_Coral | |
| Hard_Coral | |

2.4.5.1. Features of the data

In all four cases (Vessel or Laboratory, Substratum or Biology) the quantities characterising each site formed a vector of proportions, i.e. they summed to unity. In the case of the Vessel data this was a feature of the recording protocol itself. For the laboratory data, video frames were scored by the laboratory operator on a proportional basis and these were aggregated and re-normalised to give an estimate of the respective covering proportions for the entire transect.

The laboratory data set for the benthic biological cover had 114 different classes. These were determined primarily by a fairly coarse 'feature' type (e.g. algae) with more detail provided by a 'descriptor' (e.g. filamentous). At this level of differentiation the analysis diagnostics indicated little grouping structure in the data, the likely reason being that the finer morphotypical classification did not correspond with the biophysical affinities that were ecologically important. For this reason the biology cover classes were grouped for analysis: the feature/descriptor classes were amalgamated to the feature level except where morphotypes had been observed to be strongly differentiated in the field

(e.g. filamentous mats vs other algae) or where identifiable genera dominated certain habitats (e.g. *Halimeda* or *Caulerpa*). From an observer viewpoint, the resultant groups would appear to represent the more visually dominant habitat components. The cover classes after grouping are shown in Table 2-9.

Some grouping of the vessel biology cover classes was also done for similar reasons. In this case, however, the amalgamation merely grouped ‘sparse’, ‘medium’ and ‘high’ cover classes of several key epibenthic feature types (Table 2-6). No grouping was done for the substratum.

2.4.5.2. Distance metrics

Using data that comes in the form of proportions for clustering is somewhat unusual in ecology and several possible distance metrics were considered. The three that were considered in most detail were:

1. The standard Euclidean metric: $E_{ij}^2 = \sum_{k=1}^K (p_{ik} - p_{jk})^2$
2. The Hellinger distance metric between two probability distributions: $H_{ij}^2 = \sum_{k=1}^K (\sqrt{p_{ik}} - \sqrt{p_{jk}})^2$
3. The Manhattan distance metric, (which for data in the form of proportions is equivalent to the Bray-Curtis metric): $M_{ij} = \sum_{k=1}^K |p_{ik} - p_{jk}|$

These differ in the weight they give to deviations in proportions. The Euclidean metric weights large differences much more than small ones, the Manhattan metric weights all deviations equally and the Hellinger metric is intermediate in the sense that it initially reduces differences before giving higher weight to those which remain large. After clustering, by the methods to be described below, there were noticeable differences between the results, though the same general picture emerged at the higher levels. However the Manhattan metric appeared to best recover the known large scale habitat patterns and this metric has been retained in the results.

2.4.5.3. Clustering methods

The primary aim of this analysis of the video data was to ‘find habitats’. That is, groupings of sites that appeared to have a physical and biological profile that was reasonably consistent within, but as distinct as possible between. These ‘habitats’ must be interpreted as structure at a scale allowed by the data and methods, for management as much as scientific purposes. To be useful for management purposes they must not only be cogent, but they also must be interpolated on to the entire GBR spatial grid. For scientific purposes it is clearly more desirable to have groupings that can be related to the physical variables alone, rather than by physical and spatial variables, as this would suggest that the results to some extent might be interpretable as biological responses and may be transferable outside the study area. The approach taken, however, was to leave the spatial coordinates in the suite of potential predictors and to consider outcomes in which they were not needed. Spatial coordinates were in the form of ‘Along’ and ‘Across’, measured relative to the reef geometry itself. In other analyses, these have been the most flexible and sensitive method for incorporating spatial predictors into the analysis.

Two general clustering strategies were considered:

1. Identify groups using the cover proportions alone and having established the number and content of the groups, develop predictors for them from the physical variables, both to define further the physical characteristics of the ‘habitat’ and to allow some measure of interpolation to the grid.

2. Use methods that partition the data according to the physical variables into groups that are as homogeneous as possible with respect to their cover proportions.

The first strategy was successful in building groups that had a demonstrable cogency, although the number of groups was usually much smaller than either the number of ‘real’ habitats on the GBR, however defined, and frequently probably too broad even for management purposes. The real problem came when trying to develop predictors for them on the basis of the physical variables. No satisfactory prediction outcomes were obtained from application of a variety of possible techniques, including discriminant analysis, classification trees and neural networks.

The second strategy produced the more satisfactory results. Tree-based methods have a number of advantages in this context, in particular:

- They partition the data based on cuts in the predictor variables and so the results are easy to appreciate and may be both practical for management and ecologically informative,
- They intrinsically address the variables selection issue, and
- They simultaneously produce a prediction device to interpolate the results to the GBR grid, (and elsewhere, if somewhat more speculatively).

Trees have a number of disadvantages as well, of course. These include the fact that trees of this kind can be structurally unstable (even if predictively stable), and there is a need for caution in interpreting the structure of the results. Many different tree structures can often lead to virtually equivalent prediction results, particularly when there are strong collinearities in the predictors, as is usually the case.

Multivariate regression trees (De’Ath, 2002) seek to construct a tree predictor for a multivariate response based on a within-group deviance measure that may be described as the sum of the squared Euclidean distances to the group centroid:

$$E_g^2 = \sum_{i \in g} \sum_{j=1}^K (p_{ij} - \bar{p}_j^{(g)})^2$$

where $\bar{p}_j^{(g)}$ is the mean value for group g of the j th proportion. De’Ath’s software is available as a package for the R statistical computing environment. See <http://www.R-project.org>, package ‘mvpart’. This software package can be used for partitioning with the Euclidean metric directly and with the Hellinger metric using square roots of the proportions as the responses. An advantage of this method and software is that it automatically provides cross-validation and hence some guidance on the degree of complexity in the grouping structure warranted by the data. This is because ‘mvpart’ develops a predictor of the proportions, and so the data may be used for cross-validation purposes.

Adapting mvpart to accommodate a general distance metric, and hence evaluation of the Manhattan metric, was well outside the scope of this project. However, an alternative tree strategy, the ‘rpart’ package, was readily adapted for this purpose using its ‘user-written splits’ feature.

This alternative strategy began with the matrix of pairwise distances between sites. Let D_{ij} be the distance between site i and site j . Given a group g , let g^* be the index of, for now, an arbitrary member of the group. The within group deviance was then defined as the sum of squared distances of all members of the group to g^* :

$$E_g^{g^*} = \sum_{i \in g} D_{i g^*}^2$$

To complete the definition, the reference member, g^* , was chosen so as to *minimise* this quantity. The object within the group relative to which this minimum was achieved is sometimes called the ‘medoid’ of the group as opposed to the centroid.

At any stage the partitioning algorithm considered all possible cuts with respect to the predictor variables and, for each, compared the sum of deviances for the two child nodes with that of the parent. A cut was made using the best place within the best predictor, and the process was repeated recursively for each child node. The process stops either when a group was too small for partition

according to a criterion set at the outset (by default 20 sites) or if the improvement in deviance offered by partitioning into child nodes is less than a preset percentage of the deviance of the parent (by default, 1%). In these data, no groups were determined by the group size criterion, implying that the partitioning process was terminated when no further real improvement in group homogeneity could be obtained.

The partitioning algorithm was used directly to find groups in the data, and not to find a predictor for some underlying quantity. The process is technically known as “unsupervised, constrained learning”. However, this method does not perform cross-validation as an objective indicator of the number of groups in the data. While lengthy solutions could be developed, the `mvpart` cross validations were used to give some information on the degree of complexity warranted, given the similarity of the methods.

2.4.5.4. Choice of data source

As noted above, video habitat data was available for both biological structural types as well as substratum, and sourced from real-time entry on the vessel or from more detailed post-analysis in the laboratory. All were evaluated for the purpose of characterising and mapping seabed habitats.

The biological habitat data was seen as the primary output of the video tow, although the substratum data was also investigated as follows:

- Development of predictors for the substratum data provided a reality check on the physical predictors (especially sediment type) used for analysis. This did not reveal any anomalies in the sense that the physical predictors split substratum types as would be expected.
- To check the adequacy of the physical predictors for developing tree models for the biological profile, the substratum variables were included as predictors along with the external physical predictors. Such variables are only known at the observed sites and so cannot be used for predicting to the full coverage GBR grid, but if they were to be chosen ahead of the external predictors it would have suggested that defining useful habitats required either different physical variables from the ones we have available, or that they were required on a finer scale.
- Under the first clustering strategy listed above, partitioning using the substratum variables alone produced groups that were easily predicted by the external variables, perhaps not a surprising result but a reality check nevertheless. Partitioning using the biological proportions alone gave meaningful groups, as noted, but for which no satisfactory predicting device from the external predictors alone could be developed. Combining biological and substratum profiles for inter-site distances produced a somewhat intermediate situation, with only marginally satisfactory predictors possible.

Clustering and predicting sites on the basis of the laboratory biological data was surprising difficult. The reasons were not fully known, but appeared to be related to the relative scales at which the physical variables and the benthic profiles are measured. This was the primary reason that grouping of cover classes was investigated, which did appear to produce some improvement. Partitioning groups with the laboratory biological data led to very few groups, mostly determined by spatial predictors and hence probably linking to a property of the physical environment for which the only surrogates we had in our data set were the spatial ones.

The vessel data, by contrast, was much more amenable to modelling with the external predictors. As will become apparent the number of groups was still smaller than would have been expected if they were to represent all ‘habitats’ that would be commonly recognised in the GBR, suggesting again, that they have potential to form groups at quite a coarse scale, but perhaps useful at least for management purposes.

2.4.6. Acoustics Discrimination and Classification

2.4.6.1. Application of Wavelet Packet-Based Feature Extraction Techniques to Acoustic Data in the Angular Domain (D H Smith)

2.4.6.1.1 Data and data pre-processing

Acoustic data was acquired as described in Section 2.2.4 with ground truth data provided by the underwater DropCam video system (Section 2.2.2) available from about 1,000 sites. The acoustic data constitutes an echo from the seabed, resulting from the transmission and reflection of an acoustic pulse generated by the hull-mounted transducer. In addition to depth, the measured return signal contains information about the seabed, to be determined by applicable data inversion techniques.

Data from the sonar transducer occurs in two forms, surface referenced and bottom referenced, associated with different temporal and spatial measurement intervals and resolution. The former case includes the entire water column while the latter case involves a small interval in the seabed vicinity. In order to partially remove bathymetry effects, the original data is transformed from the time domain into the angular domain (Sternlicht and de Moustier, 2003), prior to feature extraction and classification operations, based on a local tangent (flat seabed) approximation, which ignores the effects of vessel pitch and roll motion. This allows a fixed angular domain, from zero degrees or normal incidence, up to a specified limit determined by the transducer properties, on which all data is compared. Figure 2-39 shows a single data sample, including the bottom and surface referenced values, in their original time/distance domain, and after transformation to the angular domain.

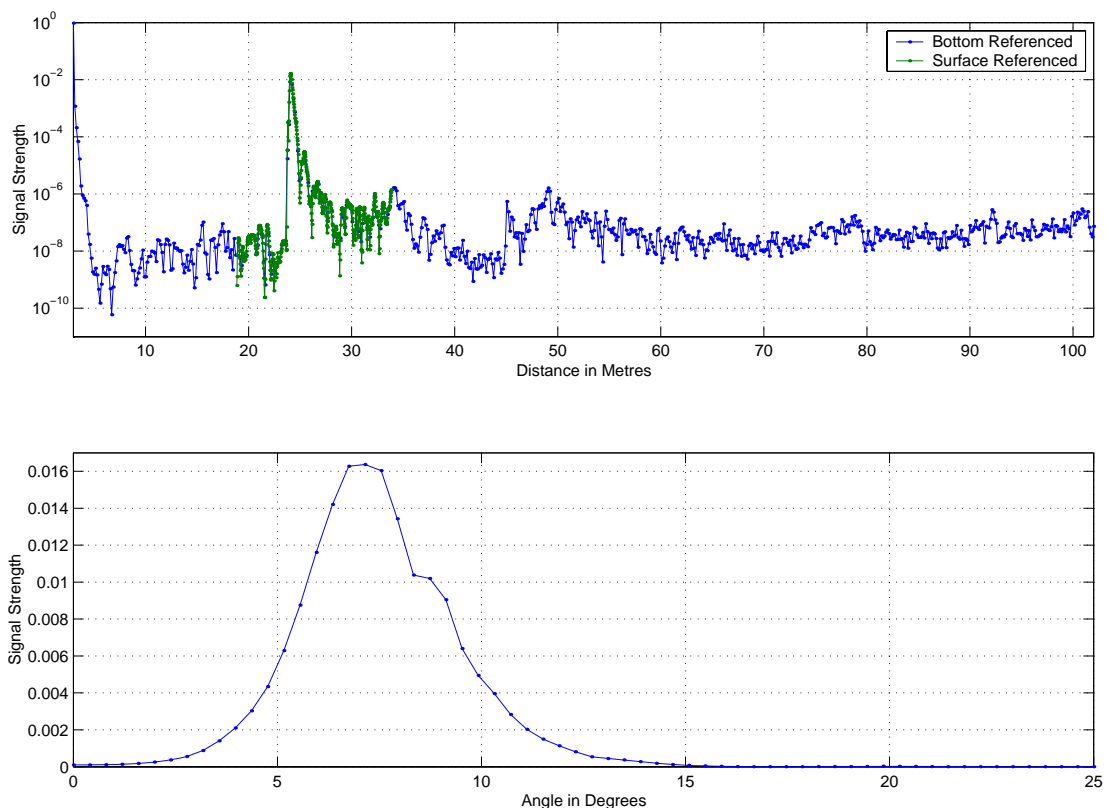


Figure 2-39: An acoustic data sample from site 1505, with indicated depth of 23.97 m, shown in the original distance/time domain, and after transformation to the angular domain.

For each site, the drop camera towed behind the boat recorded video data (Section 2.2.2) for a patch of seabed that was scanned by the sonar transducer roughly half a minute earlier. Calculation of the delay is required in order to match seabed characterisation labels, as input by a keyboard operator viewing the video onboard the vessel (Section 2.2.2.1), with acoustic data for the subsequent application of classification procedures. Figure 2-40 shows a typical pair of signals derived from the echo sounder and drop camera, the latter in this case comprising just under 7.5 minutes of video time, indicating that portion of the echo sounder signal matched to the drop camera signal. Once the delay was calculated for each transect, the seabed habitat classes specified by two attributes, substratum and biohabitat (as detailed in Section 2.2.2.1, Table 2-6) were used to label each matching echo return signal. Application of the matching procedure on the available site data generated an extensive library of single beam acoustic signatures for over 250 different (substratum, biohabitat) combinations.

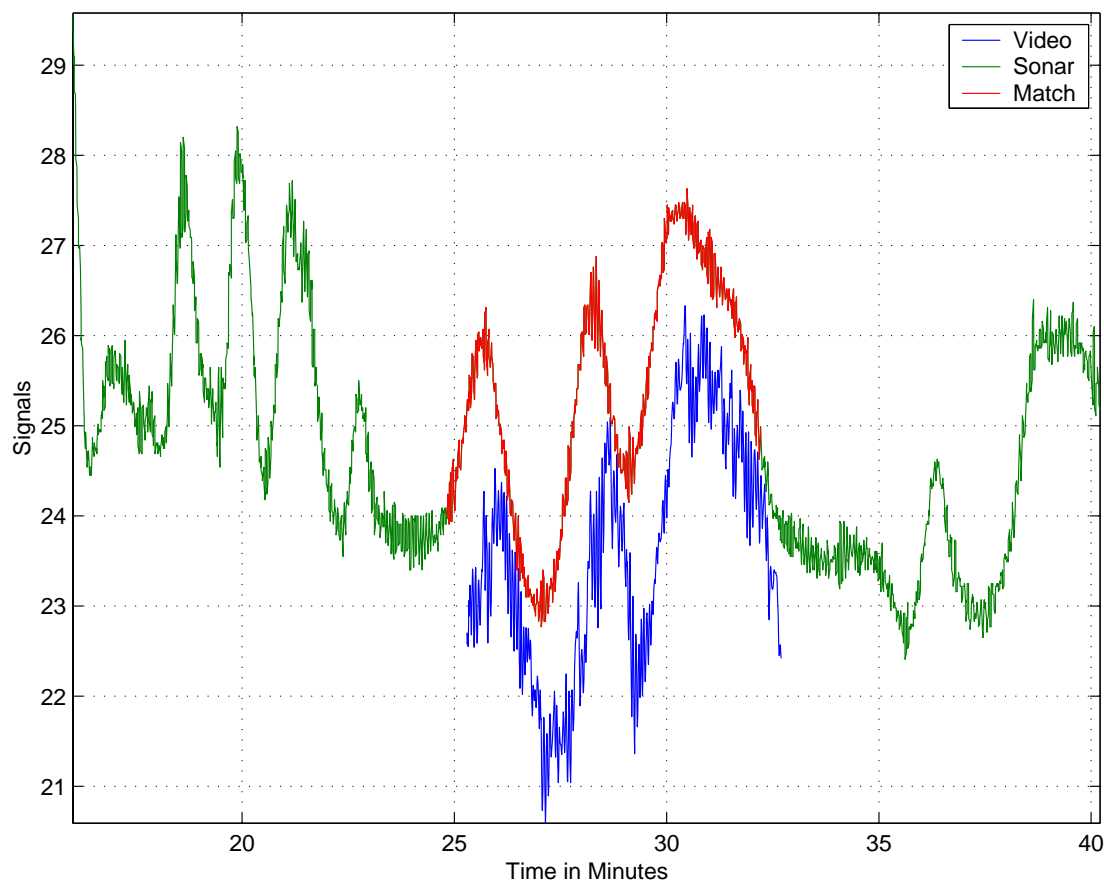


Figure 2-40: Measured depth and pressure signals derived from the drop camera and sonar transducer for site 1505, highlighting the segment of matched sonar data for which the calculated delay result is 0.502 minutes.

2.4.6.1.2 Techniques Applied

Feature extraction and classification are complementary numerical processes aimed at identifying the source of a certain data sample, which in this case constitutes an acoustic echo from the seabed. For supervised classification, training of a particular feature extraction scheme is performed on data of known types from each of several possible seabed classes prior to application on data of unknown type. In this section, feature extraction is performed via a wavelet packet-based technique known as the Local Discriminant Basis (Saito and Coifman, 1995) in conjunction with Daubechies filter coefficients (Cohen *et al.*, 1993). This approach involves selecting a data transform from a very large library of candidate wavelet packet transforms (Jensen and la Cour-Harbo, 2001), in order to provide maximum discrimination between a set of data items representing different classes. A demonstration of this discrimination capacity for the two class case comprising (sand, no biohabitat) and (sand,

seagrass) seabed types is given graphically by the three dimensional plot in Figure 2-41, which displays the first three local discriminant basis coordinates plotted against each other. Distinct clouds have emerged in this “feature space” view, showing a visible separation between classes afforded by the Local Discriminant Basis.

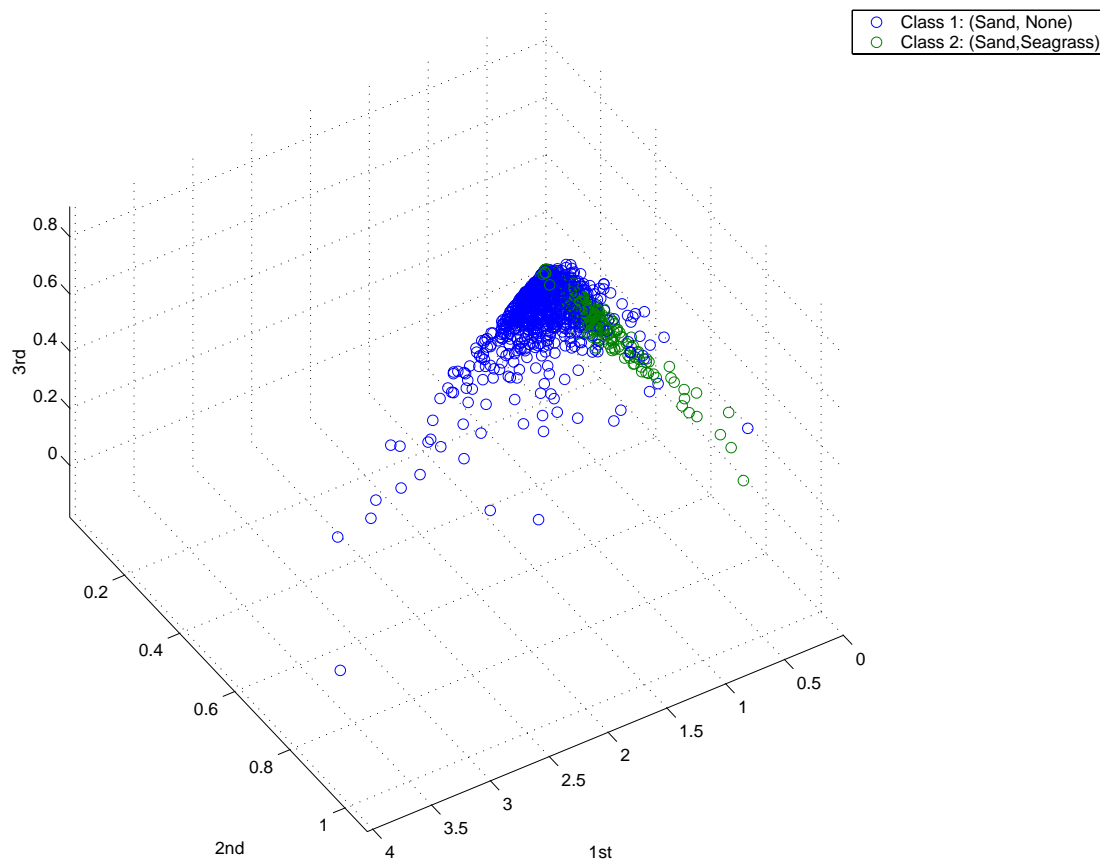


Figure 2-41: Three dimensional plot of the first three Local Discriminant Basis coordinates for data representing (sand, no biohabitat) and (sand, seagrass) seabed types, generated with Daubechies 2 wavelet filter coefficients, showing visible separation between the two classes.

Application of the chosen wavelet packet transform to data in the angular domain returns features which are ranked by discrimination power, providing an automatic truncation facility allowing dimension reduction to seek compact, efficient feature sets. Subsequent classification operations are performed in the transformed domain, or “feature space”, utilising both Tree and Linear Discriminant Analysis classifiers (Duda *et al.* 2001). By providing a relatively small number of significant features to the classifier, the Local Discriminant Basis offers performance enhancement, in comparison to that derived from direct application on the original data. This feature extraction and classification approach constitutes one particular avenue in the performance assessment of single beam acoustic remote sensing technology.

2.4.6.2. Canonical Variate Analysis of Acoustic Data (N Campbell & D Devereux)

This section outlines methods used to analyse the large volume of single-beam sonar echo time-response curve data, collected as described in Section 2.2.4 from a range of seabed habitat cover types, to determine the degree of discrimination between different habitats. The underlying assumption is that different types of seabed exhibit reflected acoustic signals with characteristic shapes. Appropriate mathematical descriptions of these shapes and the use of discrimination-based statistical procedures are used to assess the separability of a range of cover classes. The 700 samples from the surface to

beyond the 2nd echo are here called the pelagic data, and the 500 samples from 5 m above the bottom pick to 10 m below the bottom pick are called the bottom data.

The emphasis initially was on the complete volume of data, to assess the degree to which particular cover types could be consistently and accurately identified over the whole of the GBR. Some analyses of the degree of discrimination among cover classes from sites collected close together in time and hence geographically were also carried out.

The main data analysed here are for all groups of more than 100 contiguous echo responses from the same nominal class as identified from the ground-truth video data labels matched as per Section 2.4.6.1.1. There were 4519 such groups from 117 classes. Because of the sheer volume of data, the individual group means and pooled within-groups covariance matrix were calculated, after appropriate data normalisation.

2.4.6.2.1 Depth Normalisation

Prior to analysis, the acoustic data were depth-normalised to a constant depth so that signatures could be compared over the whole range of the data. This was done by taking the depth pick selection provided by the Simrad EY500 system, $depth_R$, and resampling the echo time series to a constant set of depths. Specifically, the estimated depth in metres for a given sample time is calculated as:

$$depth_t = (t_s - 0.5) \{ (r_e - r_b) / n_s \} + r_b \quad (1)$$

where t_s denotes the sample time; r_b is the beginning range of the echo sounder (that is, the echo sounder is set to commence sampling at the moment when an echo from depth r_b would be received); r_e is the end range of the echo sounder (that is, the echo sounder is set to cease sampling at the moment when an echo from depth r_e would be received); and n_s is the number of samples collected.

The data are resampled by calculating the estimated depths for a range of sample times from 0 to 500, which give a depth of 0 metres at time 0, and a depth of $depth_R$ after 200 sample times, then using (1) to calculate the corresponding sample time on the observed scale, and using nearest neighbour or local smoothing such as bilinear or cubic to calculate the resampled values.

2.4.6.2.2 Data Normalisation

The profiles can be peak-aligned to remove one effect of depth.

Another correction considered is to remove the so-called “size” effect, and focus on differences in shape. This can be done by calculating a row mean (a simple measure of the average area under the curve), and subtracting this mean from all the values across an echo response curve.

Plots of the group means in Section 3.6.2.2 show that there was an obvious effect of depth on the shape of the group means; an attempt to remove this effect is made by regressing the echo response values against $1/depth$.

2.4.6.2.3 Group Discrimination

An obvious approach to examine the discrimination between various seabed cover types is to base the analyses on a number of training groups, each one reasonably homogeneous, and representing a particular cover class. A canonical variate analysis (CVA) can be carried out to examine the degree and nature of the differences between the groups. The means and variances / correlations are calculated for each group. The group means are used to calculate a “between” matrix, B , and the variances / correlations to form a “within” matrix, W . Canonical vectors, c , are then calculated which maximise the ratio of the between-groups to within-groups sums of squares, $f = c^t B c / c^t W c$, for the canonical variate scores, $c^t x$; f is referred to as the canonical root.

The eigen-equation for the canonical variate analysis is $(B - f W) c = 0$; the canonical vectors are scaled so that $c^t W c = n_w$, the within-groups degrees of freedom. That is, the average within-groups variance is one. Successive canonical vectors are chosen so that the corresponding canonical variate scores are uncorrelated with previously-determined sets of scores.

The only assumption made in this approach is that each group of data is reasonably homogeneous (and that the corresponding histograms are roughly symmetric). While each training group is representative of a known cover type, this is not used explicitly in the analysis. In essence, a supervised clustering of the group means is being carried out, with the within covariance matrix providing the metric against which to judge similarities and differences.

A desirable feature of the CVA approach is that it produces linear combinations of the input variables which can then be displayed and analysed in a lower number of dimensions. The analyses can be carried out on the actual echo time response data (after the data have been suitably depth normalised and averaged), or on features derived from the input curves.

2.4.6.2.4 Directed Class Discrimination

An obvious approach to examine the discrimination between various seabed cover classes is to base the analyses on groups from each cover classes. Pool the groups into a super-group for a class, but use the usual within-groups covariance matrix.

2.4.6.2.5 Site Contrast CV Analyses for Depth-Normalised Data

The data analysed here are from sites which were collected close together in time and space, concentrating on potential extremes of cover, such as sand and seagrass, and mud, silt and sand.

The sites included the following:

| Site# | Date | Depth m | Substratum | Biohabitat |
|-------|----------|---------|------------|--------------|
| 1631 | 23/11/03 | ~37 | Sand 100% | Seagrass 98% |
| 2552 | 23/11/03 | ~30 | Sand 100% | Seagrass 0% |
| 2441 | 24/11/03 | ~28 | Sand 100% | Seagrass 98% |
| 1580 | 24/11/03 | ~58 | Sand 100% | Seagrass 0% |
| 2224 | 23/09/04 | ~49 | Sand 100% | Seagrass 0% |

For each site, sequences of contiguous echo responses from the same class were formed as groups, and these groups were then ordered by class.

2.4.6.2.6 Echo Response Curves vs Features

A common approach for the analysis of single-beam echo data is to transform the echo data (after suitable depth normalisation and averaging) to a set of derived parameters or features such as quantiles, amplitudes, power spectrum coefficients and wavelets. A principal component analysis (PCA) is then carried out on these derived parameters, and the first few principal components (PCs) are used in subsequent analyses (ref QTC Manual).

The degree of discrimination provided by the various derived parameters and by the echo time response data was examined for a few groups. The stacked-averages-of-5-pings data that QTC produces as part of its routine processing provide the “raw” data for the data sets discussed in this section. The derived feature parameters are those summarising the echo envelope proposed by Tegowski and colleagues, and 166 parameters capturing the shape and spectral character of the echo produced by QTC. The degree of separation provided by the echo envelope and QTC shape parameters and by the averaged ping time response data are compared.

2.4.6.3. Linear Discriminant Analyses of QTC View data (I McLeod)

As described in Section 2.2.2.1, acoustic data was acquired during a series of cruises. In addition to the raw digital acoustic data collected directly from the EY500 echo sounder, pre-processed data was also recorded from a QTC View IV acoustic processor (Questar Tangent Corporation). This device digitised the acoustic responses from the transducer and processed the wave form. After stacking up five pings envelopes, the QTC processed the raw data and transmitted 166 extracted features to the logging PC, where they were recorded as each observation, interspersed with raw GPS NMEA strings as they were transmitted. Thus, the 166 QTC parameter data string was merged sequentially with the raw GPS strings. Due to system settings, QTC data from areas deeper than 80 m was spurious and data from these areas was excluded from analysis.

In the laboratory, the interspersed data was post-processed into a database record format of GPS date/time/position stamped QTC parameters, which were then joined to the seabed type codes derived from the real-time camera observations of substratum and biological habitat (Events). As noted in Sections 2.2.2 and 2.4.6.1, there was a lag from the QTC data to the habitat code data. As the transducer was mounted to the underside of the hull and facing directly downwards, the acoustic signals processed by the QTC system were reflected by the seabed lying directly under the boat. In contrast, the habitat events data came from the camera sled, which was towed behind the boat but time stamped with the boat's time and position. There was approximately a 30 second delay between the seabed that the acoustics sampled and when that seabed was observed by the towed video and habitat events recorded. The habitat events data was lagged, by a time delay determined separately for each site as described in Section 0, to join it to the QTC data (e.g. we matched events from 10:25:17 with QTC from 10:24:47).

The habitat events data was available only from sites where video transects were conducted, whereas the QTC data was collected ~continuously along the vessel's track — thus, QTC data was also available for tracks between sites. Only a small fraction of the QTC data coincided with where the "ground-truthed" habitat events were available. After completing the merge, there were 141,032 ground-truthed observations in the training set. From the habitat events data we had observations of twenty four classes of biological habitat and nine classes of substratum (Table 2-6). The combination of these two events data classes gave a potential 216 classes, not all of which were represented in the data. The intent was to use the merged data as a training set from which a classifier could be developed, which would be applied to all the along track QTC data to produce a more extensive habitat map predicted from classified acoustic track data.

It was anticipated from the outset that it would not be possible to reliably discriminate all observed combinations and that considerable aggregation of the habitat events classes would be required. Our previous experience had indicated that about 4–5 seabed types might be distinguishable with about 60% success (e.g. Skewes *et al.* 1996; Long *et al.* 1997, McLeod *et al.* 2007). Nevertheless, significant improvement on 4–5 seabed types was expected, due to the greater number and detail of acoustics features extracted in this application.

In a series of analyses, beginning with the most detailed comprising all available classes (24 biohabitat by 9 substratum), classification performance was used to guide aggregation of ecologically similar habitat classes. Several aggregations of the biohabitat and substratum were trialled, including analysing the biological habitats and substratum types separately as well as combined. In each analysis it was necessary to remap the original classes into a new aggregated class schema. These remapping tables are presented below (Table 2-10 to Table 2-13), and the outcomes of selected analyses in section 3.6.3. Further, classification analyses were trialled with and without depth partitioning, as it was clear that the acoustic feature data were not independent of depth.

The statistical method applied was linear discriminant analysis, and classification performance was assessed by cross-validated classification error rates.

Table 2-10. Habitat Events re-coding table showing mapping from the original BioHabitat code to Habitat_Code2.

| Habitat_Code | Habitat_Desc | Habitat_Code2 | Habitat_Des2 |
|--------------|--------------------------|---------------|---------------|
| 0 | No BioHabitat | 0 | No BioHabitat |
| 6 | Bivalve Shell Beds | | |
| 3 | Alcyonarians Sparse | 1 | Sparse garden |
| 11 | Gorgonian Garden Sparse | | |
| 20 | Sponge Garden Sparse | | |
| 25 | Whip Garden Sparse | | |
| 1 | Alcyonarians Dense | 2 | Alcyonarians |
| 2 | Alcyonarians Medium | | |
| 9 | Gorgonian Garden Dense | 3 | Gorgonian |
| 10 | Gorgonian Garden Medium | | |
| 23 | Whip Garden Dense | | |
| 24 | Whip Garden Medium | | |
| 18 | Sponge Garden Dense | 4 | Sponge |
| 19 | Sponge Garden Medium | | |
| 4 | Algae | 5 | Algae |
| 8 | Flora | | |
| 7 | Caulerpa | 6 | Caulerpa |
| 12 | Halimeda | 7 | Halimeda |
| 17 | Seagrass | 8 | Seagrass |
| 5 | Bioturbated | 9 | Bioturbated |
| 13 | Hard Coral Garden Dense | 10 | Coral Dense |
| 16 | Live Reef Corals | | |
| 14 | Hard Coral Garden Medium | 11 | Coral Sparse |
| 15 | Hard Coral Garden Sparse | | |

Table 2-11. Habitat Events re-coding table showing mapping from the original BioHabitat code to Habitat_Code3.

| Habitat_Code | Habitat_Desc | Habitat_Code3 | Habitat_Des3 |
|--------------|--------------------------|---------------|--------------------|
| 0 | No BioHabitat | 0 | No BioHabitat |
| 25 | Whip Garden Sparse | | |
| 1 | Alcyonarians Dense | 1 | Soft – Dense |
| 9 | Gorgonian Garden Dense | | |
| 18 | Sponge Garden Dense | | |
| 2 | Alcyonarians Medium | 2 | Soft - Medium |
| 10 | Gorgonian Garden Medium | | |
| 19 | Sponge Garden Medium | | |
| 23 | Whip Garden Dense | | |
| 3 | Alcyonarians Sparse | 3 | Soft – Sparse |
| 11 | Gorgonian Garden Sparse | | |
| 20 | Sponge Garden Sparse | | |
| 24 | Whip Garden Medium | | |
| 4 | Algae | 4 | Algae and Seagrass |
| 7 | Caulerpa | | |
| 8 | Flora | | |
| 12 | Halimeda | | |
| 17 | Seagrass | | |
| 5 | Bioturbated | 5 | Bioturbated |
| 6 | Bivalve Shell Beds | | |
| 13 | Hard Coral Garden Dense | 6 | Coral - Dense |
| 16 | Live Reef Corals | | |
| 14 | Hard Coral Garden Medium | 7 | Coral – Sparse |
| 15 | Hard Coral Garden Sparse | | |

Table 2-12. Substratum Events re-coding table showing mapping from the original Substratum code to Substratum_Code2

| Substratum_Code | Substratum_Desc | Substratum_Code2 | Substratum_Des2 |
|-----------------|--------------------|------------------|-----------------|
| 1 | Bedrock / Reef | 1 | Reef |
| 2 | Rocks (> 250 Mm) | 2 | Boulders |
| 3 | Stones (50-250 Mm) | 3 | Cobbles |
| 4 | Rubble (5-50 Mm) | 4 | Gravel |
| 5 | Coarse Sand | 5 | Sand |
| 6 | Fine Sand | | |
| 7 | Sand Waves | | |
| 8 | Silt | 6 | Silt |
| 9 | Mud | 7 | Mud |

Table 2-13. Substratum Events re-coding table showing mapping from the original Substratum code to Substratum_Code3.

| Substratum_Code | Substratum_Desc | Substratum_Code3 | Substratum_Des3 |
|-----------------|--------------------|------------------|-----------------|
| 1 | Bedrock / Reef | 1 | Reef |
| 2 | Rocks (> 250 mm) | 2 | Boulders |
| 3 | Stones (50-250 mm) | 3 | Cobbles |
| 4 | Rubble (5-50 mm) | 4 | Gravel |
| 5 | Coarse Sand | 5 | Sand Silt |
| 6 | Fine Sand | | |
| 8 | Silt | | |
| 9 | Mud | 6 | Mud |
| 7 | Sand Waves | 7 | Sand Waves |

2.4.7. Ecological Risk Indicators

A progressive series of indicators of exposure to trawling have been estimated for habitat types, seabed assemblages (predicted sites groups), species-groups and selected individual species. This series includes:

1. estimates of the percentage by area of the distribution of each habitat, assemblage, species-group and individual species, located in areas open to trawling under zoning or other management — without account of the distribution of trawl effort.
2. estimates of the percentage by area of the distribution of each habitat, assemblage, species-group and individual species, located in areas where trawl effort is present — without account of the intensity of trawl effort.
3. estimates of the percentage by area of the distribution of each habitat, assemblage, species-group and individual species, located in areas where trawl effort is present taking account of the intensity of trawl effort.

For species-groups and selected individual species, predicted biomass distributions have been estimated (Sections 2.4.2 and 2.4.3) and biomass related indices can be estimated.

4. estimates of the percentage of biomass of the distribution of each species-group and individual species, located in areas open to trawling under zoning or other management — without account of the distribution of trawl effort.
5. estimates of the percentage of biomass of the distribution of each species-group and individual species, located in areas where trawl effort is present — without account of the intensity of trawl effort.

6. estimates of the percentage of biomass of the distribution of each species-group and individual species, located in areas where trawl effort is present taking account of the intensity of trawl effort.

The intensity of trawl effort was taken into account as a coverage of the study's 0.01 degree grid cells as if trawling were conducted uniformly at that fine scale. Given the typical swept width of gear and speed of trawling for prawns in the region, approximately 8 hours of trawling would be required to have a 1× coverage of a 0.01 degree grid cell. Similarly, 4 hours would have a 0.5× coverage and 16 hours would have a 2× coverage. A given grid cell's contribution to the overall index was the estimated proportion by area or biomass of the respective biological attribute, multiplied by the estimated effort coverage; these estimates for grid cells were summed to provide the overall index for the GBR region. The effort intensity information for each grid cell was provided by spatial processing of the 2005 fishery Vessel Monitoring System (VMS) data by Norm Good, QDPI&F (Gribble *et al.* 2007). The year 2005 was the first full year post the re-zoning of the GBR Marine Park, which came into effect on 1 July 2004.

Exposure to trawl effort may present varying levels of risk for different species depending on how effectively the trawl net catches any given species (catchability), or how much mortality is caused as a result of contact with the net. For example, a species that lives well down in the sediment, or one that moves up into the water column during the night, is unlikely to be directly affected by the pass of a trawl net. On the other hand, a slow moving species that lives less a metre from the seabed may be very effectively caught by a prawn trawl net. For species estimated to have higher levels of exposure, information on relative catchability was sought wherever possible. This study was able to provide relative catch rate information between the research trawl and the epibenthic sled (Section 2.4.2). Wherever the sampling rate of the research trawl was less than the epibenthic sled, the prawn trawl was considered to catch that fraction (0-1) of the population present during a pass of the net. Wherever the trawl had a higher catch rate, the prawn trawl was considered to a relative catch rate of 1. Similar information was available from the GBR Effects of Trawling Study (Poiner *et al.*, 1998), including prawn trawl catch rates relative to those of a fish trawl. Information on the possible impact on species remaining on the seabed was available from the GBR Effects of Trawling Recovery Dynamics Project (Pitcher *et al.*, 2004) and the Northern Prawn Fishery Effects of Trawling Project (Haywood *et al.*, 2005). If evidence was available that could demonstrate that catchability or mortality was <1, this information could reduce the estimated percentage of the biomass of a species exposed in indicator 6 above — i.e. an estimate of the proportion of the total population caught.

Further, the Queensland trawl fishery is required by legislation to have turtle excluder devices (TEDs) and bycatch reduction devices (BRDs) installed in their nets. TEDs are very effective in allowing larger animals such as turtles, rays and sharks to pass out of the trawl net, greatly reducing mortality (Robins-Troeger *et al.* 1995; Robins & McGilvray 1999). BRDs provide escape opportunities for smaller fish and reduce the catch rate of non-target species (bycatch) by varying amounts depending on the species — over all species and different sectors of the industry, the average reduction achieved by BRDs is about 8% (Courtney *et al.* FRDC 2000/170 Report 2006), though greater reductions are possible (Courtney *et al.* 2006). If evidence (from these or other sources, e.g. Brewer *et al.* 1998) was available that demonstrated that TEDs and/or BRDs further reduce catchability or mortality, this information further reduced the estimated percentage of the biomass of a species exposed in indicator 6 above — again, reducing the estimate of the proportion of the total population caught.

Exposure to trawling, leading to estimates of the potential proportion of species populations caught annually is only one axis of vulnerability to trawling. The second axis is the ability of the species to recover from any reductions in population size. A species with a high recovery rate can sustain higher levels of incidental catch than a species with a low recovery rate. Previous ecological risk assessment methods that take this axis into consideration include susceptibility-recovery analysis (SRA) — a qualitative ranking approach (Stobutzki *et al.* 2001, see also Griffiths *et al.* 2006) — and sustainability assessment for fishing effects (SAFE) — a quantitative approach where estimated fishing mortality is compared against reference points of estimated natural mortality (e.g. 0.8M = maximum sustainable mortality) (Brewer *et al.* 2007; Zhou & Griffiths 2007). For species estimated herein to have higher exposure to trawling, information about the recovery axis was obtained, where available, for mean recovery attribute ranks from SRA analyses in northern Australia (e.g. additive ranks of probability of breeding before capture, maximum size, reproductive strategy, hermaphroditism for fishes (Stobutzki *et*

al. 2001) and invertebrates (Hill *et al.* 2002)) and for estimated natural mortality to calculate a sustainability indicator in a manner analogous to the reference points of Zhou & Griffiths (2007). These reference points were based on the Schaffer surplus production model, where for a population at maximum sustainable yield (MSY), fishing mortality (F) is equal to natural mortality (M), that is $F/M=1$. This is regarded as a limit reference point and should not be exceeded. Zhou & Griffiths (2007) consider reviews of exploited species that suggest $F=0.8M$ ($\equiv F/M=0.8$) is a more conservation reference point, and Gulland (1983) suggested a conservative MSY of $0.3MB_0$ in data limited situations, which (as $B_{MSY} = 0.5B_0$) corresponds to $F/M=0.6$. These three reference points are considered in this report. Where exploitation is low, F is approximately equal to exploitation — the estimated proportion of the total population caught — thus, the indicator calculated herein is exploitation divided by natural mortality. Note that this method is only a ‘discrete time’ approximation, it is not an ‘instantaneous time’ stock assessment, and becomes increasingly uncertain with higher levels of exploitation and/or natural mortality (Hilborn & Walters 1992).

A further indicator of potential ecological risk is available from the biophysical modelling (Section 2.4.2). If the trawl effort covariate was selected by the statistical modelling of any species, possibly in addition to other environmental variables such as sediment type, the sign and significance of the coefficient was examined. Further, in order to examine the regional implications of an included trawl effort term, a prediction of the biomass was made with the trawl covariate set to zero throughout the region. This estimate was then contrasted with the biomass prediction for the actual current situation to estimate how much smaller, or larger (in the case of positive effects), the species population may be as a result of incidental trawl catches over the history of the fishery. It is important to note here that many of the physical covariates are correlated and it may not be possible to interpret model coefficients as causal effects. In the case of target species in particular, a positive trawl coefficient could indicate that the effort data — reflecting the searching ability of the fishers — are a good indicator of the sampled distribution, of say commercial prawns, at a scale finer than that of spatial patterns in the physical environmental data, rather than indicating that prawns are more abundant because of trawling.

2.4.8. Trawl Management Scenario Model (N Ellis, A Welna, R Pitcher)

A dynamic model was applied to assess the effects of several major management interventions, which were implemented between the years 2000 and 2006, on benthic fauna — particularly sessile benthic fauna that were the focus of experiments on trawl depletion rates (Poiner *et al.* 1998, Burridge *et al.* 2003) and subsequent recovery (Pitcher *et al.* 2004). The management interventions included two large-scale closures comprising the 2000/2001 low-effort areas closure and the 2004 representative areas program (RAP) re-zoning of the GBR; two effort reductions comprising a major buy-back effective in 2001 and another RAP-associated buy-back effective in 2005; and a progressive penalty system operating between the latter two. The dynamic model applied depletion and recovery parameters estimated from previous experiments and annual trawl effort as provided by industry and management data to estimate the relative status of fauna in model grid cells of 6 minute resolution. The model was run with and without the effects on effort of each management intervention. The relative status estimates were combined with the abundance distributions available from the current project in order to estimate the regional absolute status of these fauna.

2.4.8.1. Specification of the management scenarios

We wanted to test the effect of the management interventions that had been applied over the period 2001–2005. We took as a baseline the ‘status quo’ scenario (SQ2001) from the view-point of the pre-2001 fishery; i.e. we projected from 2001 to 2025 assuming the fishing effort remained at year-2000 levels. We then constructed a sequence of scenarios in which each intervention was included progressively: the 2001 closure (CL2001); the 2001 buyback (BB2001); penalties on trading effort units (P); the 2004 RAP closure (RAP); and the 2005 buyback (BB2005).

Over the period 2001–2005, in reality, some or all of these interventions were in effect simultaneously. We therefore had to make some assumptions about what the separate effects of these interventions were. Table 2-14 shows the total effort in various regions of the East Coast Trawl Fishery for the period 2001–2005. Figure 2-42 shows the total effort in the study area over the period 1993–2005. The reduction in 2001 is evident, followed by a more gradual reduction in subsequent years. The drop in 2005 is attributable to both the 2005 buyback and the continuing penalties. Also, there is some variation due to other (unknown) causes.

Table 2-14. Effort (boat days) in various regions of the East Coast Trawl Fishery, 2001–2005.

| Year | Inside GBRMP | Outside GBRMP | Total | Study Area |
|------|--------------|---------------|--------|------------|
| 2001 | 46,107 | 23,395 | 69,502 | 35,531 |
| 2002 | 47,978 | 19,808 | 67,786 | 35,387 |
| 2003 | 44,753 | 20,363 | 65,116 | 29,465 |
| 2004 | 40,162 | 23,447 | 63,609 | 28,236 |
| 2005 | 34,562 | 21,813 | 58,380 | 24,621 |

In restricting the modelling to the study area, which is a subregion of the GBRMP, we have assumed that management interventions operating at the level of the entire fishery (i.e. effort capping) can be applied proportionally to the study area. This assumption is reasonable given the common trends in the study area, the GBRMP and the rest of the fishery (see Table 2-14). Large-scale relocation of the fleet into or out of the study area caused by influences unrelated to area closures are not accounted for in this analysis.

By modelling the effect of penalties as a constant annual proportional reduction, and the 2005 buyback as a 6% reduction (Andrew Thwaites, QDPI, pers. comm.), we estimated the penalty reduction using a linear model:

$$\log(\text{effort}) = a + b \times (\text{year} - 2001) + \text{buyback}(\text{year}) + \text{error},$$

where

$$\text{buyback}(\text{year}) = \begin{cases} \log(1-0.06) & \text{if year} = 2005 \\ 0 & \text{otherwise.} \end{cases}$$

The error term is a normal variate with mean zero and standard deviation s . The estimate of b was -0.084 , indicating an annual 8% reduction due to penalties, and the estimate of s was 0.043 . This model was then used as the mean projected effort. The coefficient of variation of annual effort was taken to be the same as in the period 1993–2000. Such variation is possible in this fishery because the fleet does not usually fill its allocation; for example in 2005 only 66% of the allocation was used. Figure 2-42 shows the projected mean effort for the 4 effort reduction scenarios. The effort for the CL2001 scenario is the same as for the SQ2001 scenario; the effort for the RAP scenario is the same as for the penalties scenario; and the projected effort (from 2006) for the SQ2006 scenario is the same as for the BB2005 scenario.

2.4.8.2. The trawl depletion-recovery model

The dynamic biomass model is a set of Schaefer-like models operating independently in each 0.1° spatial cell:

$$dB_{sx}/dt = r_s B_{sx}(t) \left(1 - B_{sx}(t)/K_{sx}\right) - d_s E_x(t) B_{sx}(t)$$

where $B_{sx}(t)$ is the biomass at time t of benthic species (or OTU) s in cell x , K_{sx} is the carrying capacity of species s in cell x , $E_x(t)$ is the effort rate at time t in units of swept area per unit time, r_s is the recovery rate of species s , and d_s is the depletion rate per tow of species s . The equation simplifies to:

$$db_{sx}/dt = r_s b_{sx}(t) \left(1 - b_{sx}(t)\right) - d_s E_x(t) b_{sx}(t)$$

$$B_{sx} = K_{sx} b_{sx}$$

where $b_{sx}(t)$ is the *relative* biomass. This has the practical consequence that the biomass distribution can be split into two components, one, b_{sx} , depending only on the vulnerability pair (r_s, d_s) and the other, K_s , depending only on survey data. Each component can then be computed independently and combined later. To provide an initial condition for b_{sx} , we assume the pre-fishery biomass (at time t_0) in each cell was at the carrying capacity, i.e. $b_{sx}(t_0) = 1$.

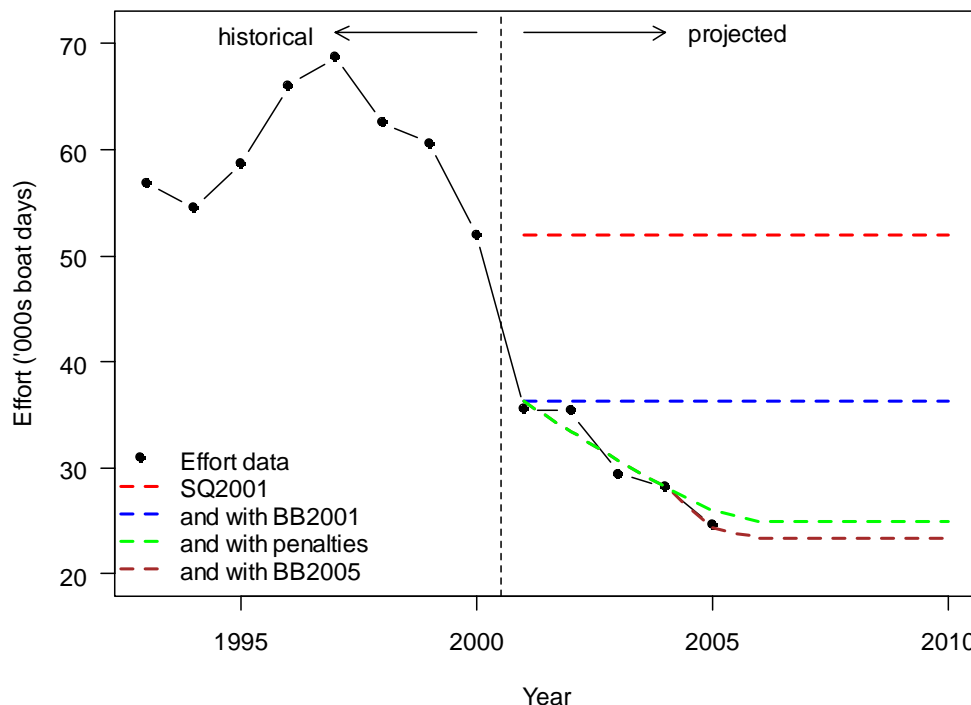


Figure 2-42. Total effort in the study area for the period 1993–2005. Also shown is the projected mean effort for 4 scenarios.

2.4.8.3. Specification of the depletion-recovery parameters

Pitcher *et al.* (2004) obtained parameters describing the depletion and recovery dynamics of a set of benthic taxa following a previous trawl depletion experiment in the Far Northern section of the Great Barrier Reef. They traced over time, using both a video sled and a remotely operated vehicle (ROV), the abundance of several OTUs within differentially impacted transects. Their generalized linear models took the following form:

$$\log(b_{it}) = \log(b_0) + c_i \times i + c_{it} \times i \times t + c_{it^2} \times i \times t^2 + c_{it^3} \times t^3, \quad (1)$$

where i is the number of trawl tows (impact), t is the time in years after impact, b_{it} is the biomass at time t after impact i , and b_0 is the initial biomass. The values for the four model parameters are shown in Table 2-16 and Table 2-15. Figure 2-43 shows the form of these models for a range of times and impacts for the sled-based parameters.

It is evident from (1) and Figure 2-43 that these models do not follow a simple logistic form. In particular, the models are not bound above by an asymptote (e.g. *Alcyonacea*), and the functions can decrease in time after an initial increase (e.g. *Sarcophyton sp.*). In order to allow these species to be modelled by the trawl model, we fit the predicted form of (1) to a logistic

$$b_{it}/b_0 \sim \text{expit}(rt + \text{logit}[(1-d)^i]), \quad (2)$$

where

$$\text{logit}(x) \equiv \log x/(1-x) \quad \text{and} \quad \text{expit}(x) \equiv e^x/(1+e^x)$$

mutual inverses. This form has the property that $b_{i0}/b_0 = (1-d)^i$ and that $b_{it} \rightarrow b_0$ as $t \rightarrow \infty$.

For parameterizing the trawl model, only the initial recovery part of the Pitcher *et al.* model (1) was deemed relevant. We therefore fit this over a range of t from 0 to 5 years and i from 1 to 10 using weighted nonlinear least squares. Parts of the function that were decreasing in time or above the asymptote were down-weighted in the fitting. The weight we used was

$$w_{it} = W(b_{it} < b_0, 1, 0) W(db_{it}/dt > 0, 1, 0.001) i^{-1}$$

where the function $W(x, a, b)$ takes value a if x is true, otherwise b . As an example, Figure 2-44 shows the fits for *Ianthella flabelliformis* and *Junceella juncea*.

Table 2-15. Parameters c_i , c_t , c_{it} and c_{tt} for the ROV recovery data from Pitcher *et al.* (2004); and corresponding estimates r and d fit by non-linear least squares. *For *Subergorgia suberosa* and *Solenocaulon* the value $r = 0.22$ was used.

| Taxa | c_i | c_t | c_{it} | c_{tt} | r | d | used? |
|----------------------------------|---------|----------|----------|----------|-------|-------|-------|
| Alcyonacea | 0.0055 | -0.00237 | 0.00001 | 0.00018 | - | - | - |
| <i>Annella reticulata</i> | -0.0198 | 0.00031 | - | - | 0.57 | 0.417 | yes |
| Asciacea | -0.0196 | 0.00016 | - | - | 0.19 | 0.496 | yes |
| <i>Bebryce</i> sp | -0.0220 | 0.00020 | - | - | 0.22 | 0.447 | yes |
| <i>Ctenocella</i> | 0.0181 | -0.00301 | 0.00004 | - | - | - | - |
| <i>Cymbastella</i> | -0.0050 | -0.00038 | - | - | - | - | - |
| <i>Dichotella</i> sp1 | -0.0068 | -0.00012 | - | - | - | - | - |
| <i>Echinogorgia</i> | -0.0100 | 0.00048 | - | - | 4.17 | 0.712 | yes |
| <i>Ellisella</i> sp | -0.0185 | 0.00022 | - | - | 0.32 | 0.415 | yes |
| <i>Hypodistoma deerratum</i> | -0.0427 | 0.00275 | -0.00004 | - | 0.12 | 0.554 | no |
| <i>Ianthella basta</i> | -0.0117 | 0.00006 | - | - | 0.11 | 0.427 | yes |
| <i>Ianthella flabelliformis</i> | -0.0205 | 0.00019 | - | - | 0.22 | 0.239 | no |
| <i>Iciligorgia</i> sp1 | -0.0107 | 0.00050 | 0.00001 | -0.00011 | 2.12 | 0.692 | yes |
| <i>Junceella juncea</i> | -0.0056 | 0.00006 | - | - | 0.21 | 0.040 | no |
| <i>Junceella</i> sp2 | -0.0072 | -0.00037 | - | - | - | - | - |
| Nepitheidae | -0.0140 | 0.00024 | - | - | 0.58 | 0.164 | no |
| Porifera | -0.0299 | 0.00048 | - | - | 0.62 | 0.310 | no |
| <i>Sarcophyton</i> sp | -0.0291 | 0.00002 | - | - | 0.03 | 0.500 | no |
| Scleractinia | -0.0454 | -0.00177 | - | 0.00020 | -0.41 | 0.484 | no |
| <i>Solenocaulon</i> | -0.0095 | -0.00110 | - | 0.00015 | -0.53 | 0.101 | Yes* |
| <i>Subergorgia</i> sp | -0.0671 | 0.00378 | -0.00005 | - | 1.66 | 0.700 | yes |
| <i>Subergorgia suberosa</i> | -0.0235 | -0.00225 | - | 0.00019 | -0.62 | 0.318 | yes* |
| <i>Turbinaria</i> | -0.0722 | -0.00228 | - | 0.00028 | -0.39 | 0.568 | no |
| <i>Xestospongia testudinaria</i> | -0.0747 | 0.00365 | -0.00005 | - | 0.29 | 0.598 | yes |

The estimated parameters for all fits are shown in Table 2-16 and Table 2-15. When the main temporal effect c_t was negative, it was not usually possible to obtain an estimate for r and d , since the two models were so different. The exceptions were when a positive c_{tt} term counteracted the main effect (e.g. ROV data for *Solenocaulon*). One species, *Junceella* sp2, did not yield any estimates. All other OTUs were estimated by one or the other of the sled and ROV data, and some by both. Figure 2-45 shows all the estimates. Where estimates were available from both sled and ROV we used the sled estimate in preference. For *Subergorgia suberosa* and *Solenocaulon* the estimate of r was unreliable (being negative). We used the median value of all other OTUs having slow recovery, which was 0.22. Except for *Hypodistoma deerratum*, the estimates of d are fairly consistent between the two devices. The estimates of r on the other hand are much more variable. While the two devices observed different though overlapping populations, this is indicative of the precision with which the two parameters can be estimated.

Table 2-16. Parameters c_i , c_s , c_t , c_{it} and c_{tt} for the sled recovery data from Pitcher *et al.* (2004); and corresponding estimates r and d fit by non-linear least squares.

| Taxa | c_i | c_t | c_{it} | c_{tt} | r | d | used? |
|----------------------------------|--------|---------|----------|----------|------|-------|-------|
| Alcyonacea | -0.096 | 0.0143 | -0.00009 | -0.0012 | 1.70 | 0.112 | yes |
| <i>Annella reticulata</i> | -0.130 | -0.0112 | 0.00030 | - | - | - | - |
| <i>Ctenocella</i> | -0.103 | 0.0022 | - | - | 0.69 | 0.115 | yes |
| <i>Cymbastella</i> | -0.413 | 0.0210 | -0.00014 | -0.0026 | 0.75 | 0.369 | yes |
| <i>Dichotella</i> sp1 | -0.080 | 0.0088 | - | -0.0012 | 0.82 | 0.128 | yes |
| <i>Echinogorgia</i> | 0.046 | -0.0015 | - | - | - | - | - |
| <i>Hypodistoma deerratum</i> | -0.078 | 0.0056 | - | - | 2.61 | 0.094 | yes |
| <i>Ianthella flabelliformis</i> | -0.230 | 0.0031 | - | - | 0.38 | 0.211 | yes |
| <i>Junceella juncea</i> | -0.069 | 0.0015 | - | - | 0.64 | 0.078 | yes |
| <i>Junceella</i> sp2 | -0.059 | -0.0020 | - | - | - | - | - |
| Nephtheidae | -0.306 | 0.0058 | - | - | 0.81 | 0.293 | yes |
| Porifera | -0.148 | 0.0027 | - | - | 0.61 | 0.157 | yes |
| <i>Sarcophyton</i> sp | -0.610 | 0.0386 | -0.00050 | - | 3.14 | 0.483 | yes |
| Scleractinia | -0.433 | 0.0294 | -0.00040 | - | 2.96 | 0.390 | yes |
| <i>Solenocaulon</i> | 0.013 | -0.0007 | - | - | - | - | - |
| <i>Subergorgia suberosa</i> | 0.628 | -0.0170 | 0.00038 | -0.0018 | - | - | - |
| <i>Turbinaria</i> | -0.693 | 0.0333 | -0.00029 | -0.0012 | 1.37 | 0.522 | yes |
| <i>Xestospongia testudinaria</i> | -0.096 | -0.0154 | 0.00030 | - | - | - | - |

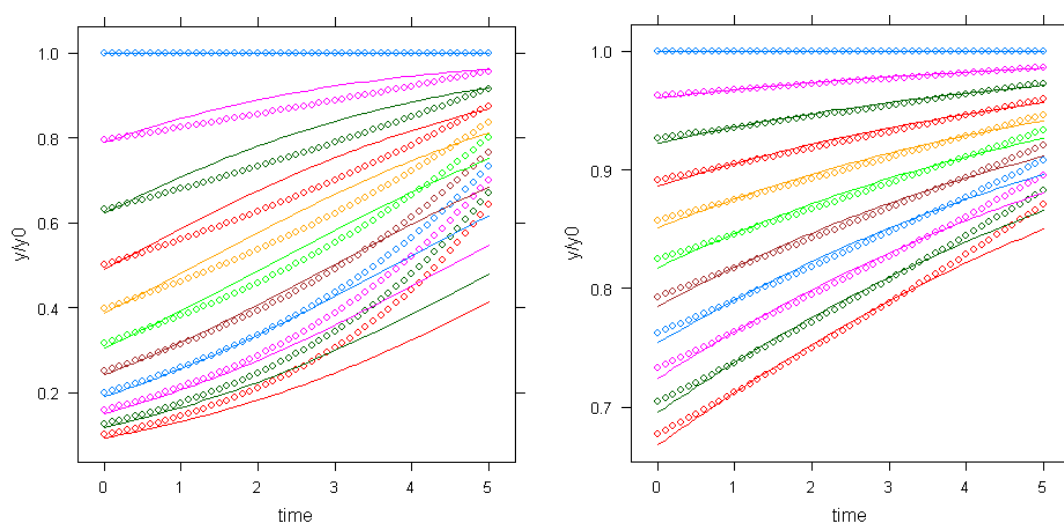


Figure 2-43. Pitcher *et al.* (2004) models (*points*) and fitted Schaefer model response (*lines*) for 0 to 10 initial trawl tows for two OTUs: (*left*) *Ianthella flabelliformis* and (*right*) *Junceella juncea*. The vertical scale is biomass relative to initial unimpacted biomass. The horizontal scale is years since impact.

In addition to the fine taxonomic units from the Pitcher *et al.* (2004) study, we also used the coarser taxonomic groupings reported by Poiner *et al.* (1998) with recovery rates obtained using the categorical method of Hill *et al.* (2002). Table 2-17 summarizes the taxonomic units and their (r , d) values.

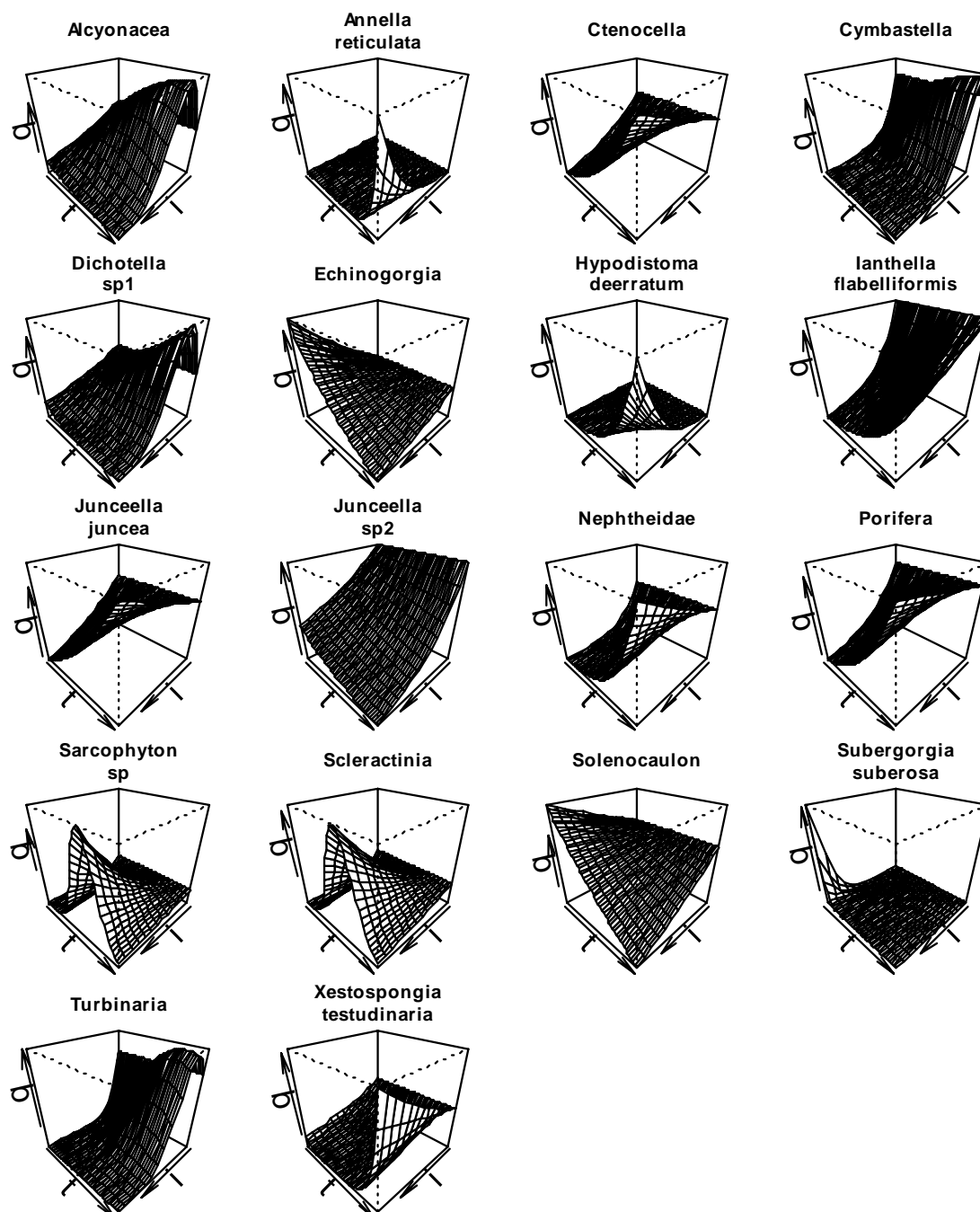


Figure 2-44. Models obtained from sled video observations for 18 OTUs (Pitcher *et al.* 2004). The vertical (b) axis represents biomass relative to initial unimpacted biomass, t is time since trawl impact (ranging from 0 to 5 years), and i is the number of trawl tows (ranging from 0 to 10).

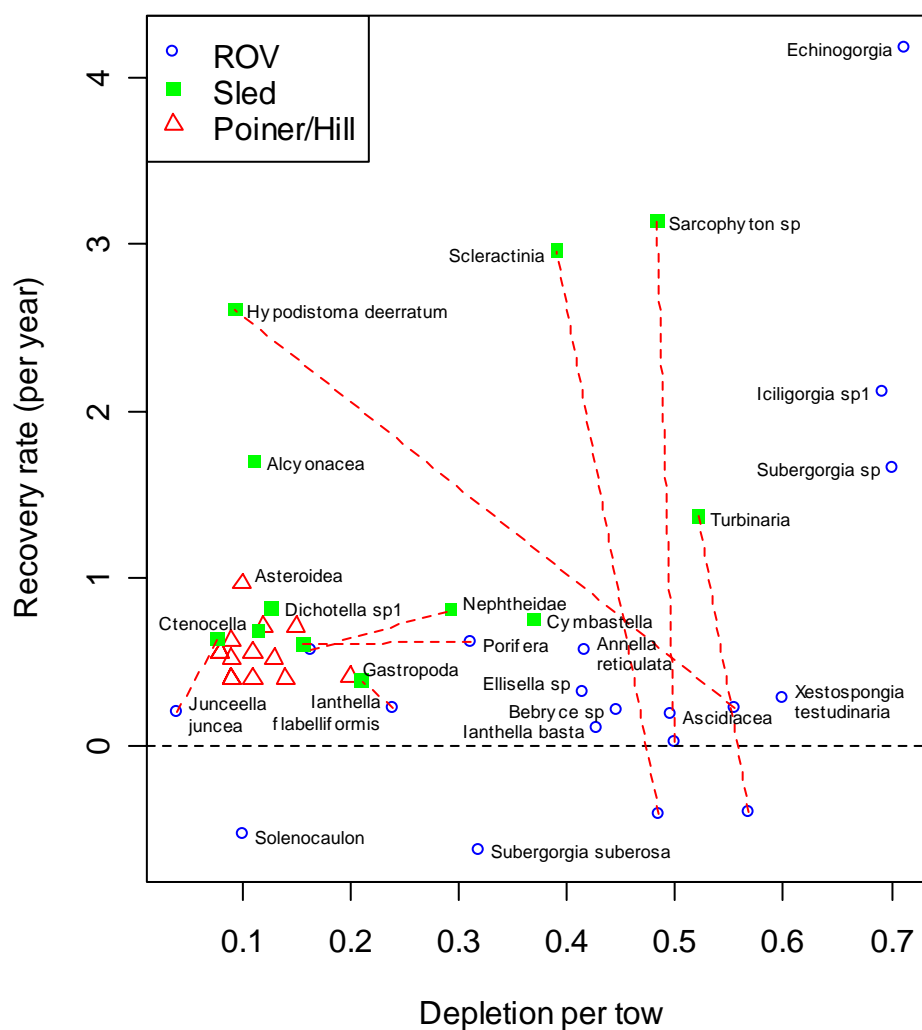


Figure 2-45. Recovery and depletion parameter estimates using sled (*green*) and ROV (*blue*) measurements. Where both sled and ROV measurements are available the points are joined by a dashed line. Also shown (*red triangles*) are the values from Poiner *et al.* (1998) and Hill *et al.* (2002) (not all labeled).

Table 2-17. Parameters r and d for coarse taxonomic groupings; d comes from Poiner *et al.* (1998) and r from Hill *et al.* (2002).

| Taxa | r (year ⁻¹) | d |
|---------------|---------------------------|------|
| Asteroidea | 0.97 | 0.10 |
| Bivalvia | 0.52 | 0.09 |
| Bryozoa | 0.40 | 0.09 |
| Crinoidea | 0.56 | 0.08 |
| Crustacea | 0.52 | 0.13 |
| Echinoidea | 0.40 | 0.14 |
| Gastropoda | 0.41 | 0.20 |
| Gorgonacea | 0.71 | 0.15 |
| Holothuroidea | 0.56 | 0.11 |
| Hydrozoa | 0.56 | 0.08 |
| Ophiuroidea | 0.63 | 0.09 |

2.4.8.4. Specification of the pristine biomass model

In Sections 2.4.2 and 3.2, single-species (or single-OTU) models have been built and density predictions laid on the fine scale spatial grid providing maps. The density predictions are on physical environmental and spatial covariates, under optimal settings of temporal covariates (time of day, time of year, phase of moon). They are also relative to the unknown catchability, which is assumed to be constant.

These models can also be used to predict the *pristine* density over the area of the fishery. This is done by predicting using the optimal covariable settings as before and setting the trawl effort predictor, where selected, to zero. The result is then the predicted density taking into account the physical covariates but in the absence of trawling, i.e. the pristine pre-fishery density. The prediction of pristine density at a trawled site is based on the observed density at sites having similar physical attributes away from trawled areas.

For OTUs having no trawl predictor in their model, the pristine biomass prediction is the same as the current prediction of section 2.4.3. Such OTUs should either have little overlap with trawled areas (for reasons of habitat independently of trawl distribution) or have high resilience to trawling due to high r or low d or both.

Some OTUs had a negative trawl effort coefficient in the linear predictor of either the presence-absence GLM or the biomass GLM. OTUs where these were either statistically significant or of large effect were *Carijoa* sp1, *Dendronephthya* spp, *Echinogorgia* sp3 and sp5, *Euplexaura* sp6, *Iciligorgia* sp1, *Mopsella* sp2 and several Demospongiae taxa. From the list of trawl exposed species in Section 3.7.2, *Alertigorgia orientalis*, *Subergorgia suberosa* and several Demospongiae (including *Ircinia* 1255 and *Ircinia* 2710) were identified.

For several of these species, specific r and d estimates were not available from the recovery study so estimates were used from morphologically and taxonomically related species. The choices are listed in section A2 of Table 2-18. Some taxa were identified only to the genus level. Where possible these were linked to the (r , d) values of the same genus (Table 2-18, section B1); for *Dendronephthya* spp the family Nephtheidae was used.

We also modelled the impact of trawling on coarse taxonomic groupings (family and higher) by summing the available pristine biomass models of all taxa within each grouping, and using the (r , d) values either from Pitcher *et al.* (2004) or from Poiner *et al.* (1998) and Hill *et al.* (2002) (Table 2-18, section C). A GLM model of predicted distribution was not available for all OTUs; MSE results are presented only for those that did.

Table 2-18. Relationship between modeled OTU and the source OTU for providing r and d at 3 levels of taxonomic resolution: A) species, B) genus, and C) coarse (family or higher). The 3rd column indicates whether a GLM model exists for the OTU.

| Taxa | OTU for r and d | model? |
|--|----------------------------------|--------|
| A1. Taxonomy at species level: r and d measured for same species from Pitcher <i>et al.</i> (2004) | | |
| <i>Annella</i> sp2–6 | <i>Annella reticulata</i> | no |
| <i>Bebryce</i> sp1 | <i>Bebryce</i> sp | no |
| <i>Dichotella</i> sp1 | <i>Dichotella</i> sp1 | yes |
| <i>Echinogorgia</i> sp3 | <i>Echinogorgia</i> | yes |
| <i>Echinogorgia</i> sp5 | <i>Echinogorgia</i> | yes |
| <i>Ellisella</i> sp1–3 | <i>Ellisella</i> sp | no |
| <i>lanthella basta</i> | <i>lanthella basta</i> | no |
| <i>lanthella flabelliformis</i> | <i>lanthella flabelliformis</i> | no |
| <i>Iciligorgia</i> sp1 | <i>Iciligorgia</i> sp1 | yes |
| <i>Junceella juncea</i> | <i>Junceella juncea</i> | yes |
| <i>Subergorgia</i> sp1–6 | <i>Subergorgia</i> sp | no |
| <i>Subergorgia suberosa</i> | <i>Subergorgia suberosa</i> | yes |
| <i>Xestospongia testudinaria</i> | <i>Xestospongia testudinaria</i> | no |
| A2. Taxonomy at species level: r and d measured from different species from Pitcher <i>et al.</i> (2004) | | |
| <i>Alertigorgia orientalis</i> | <i>Dichotella</i> sp1 | yes |
| <i>Dichotella gemmacea</i> | <i>Dichotella</i> sp1 | yes |
| <i>Carijoa</i> sp1 | Alcyonacea | yes |
| <i>Euplexaura</i> sp6 | <i>Annella reticulata</i> | yes |
| <i>Hippospongia elastica</i> | <i>Xestospongia testudinaria</i> | yes |
| <i>lanthella quadrangulata</i> | <i>lanthella flabelliformis</i> | yes |
| <i>Ircinia</i> 1255 | <i>Xestospongia testudinaria</i> | yes |
| <i>Ircinia</i> 2710 | <i>Xestospongia testudinaria</i> | yes |
| <i>Ircinia</i> spp | <i>Xestospongia testudinaria</i> | yes |
| <i>Junceella</i> sp2 | <i>Junceella juncea</i> | yes |
| <i>Melithaea</i> sp2 | <i>Annella reticulata</i> | yes |
| <i>Mopsella</i> sp1 | <i>Annella reticulata</i> | yes |
| <i>Mopsella</i> sp2 | <i>Annella reticulata</i> | yes |
| B1. Taxonomy genus level: r and d measured at the same level from Pitcher <i>et al.</i> (2004) | | |
| Ctenocella | Ctenocella | no |
| Cymbastella | Cymbastella | no |
| Echinogorgia | Echinogorgia | yes |
| Solenocaulon | Solenocaulon | yes |
| Turbinaria | Turbinaria | yes |
| B2. Taxonomy genus level: r and d measured at different level from Pitcher <i>et al.</i> (2004) | | |
| <i>Dendronephthya</i> spp | Nephtheidae | yes |
| C1. Taxonomy coarse: r and d measured at the same level from Pitcher <i>et al.</i> (2004) | | |
| Asciacea | Asciacea | yes |
| Porifera | Porifera | yes |
| Alcyonacea | Alcyonacea | yes |
| Nephtheidae | Nephtheidae | yes |
| Scleractinia | Scleractinia | yes |
| C2. Taxonomy coarse: r from Hill <i>et al.</i> (2002) and d from Poiner <i>et al.</i> (1998) measured at the same level | | |
| Asteroidea | Asteroidea | yes |
| Bivalvia | Bivalvia | yes |
| Bryozoa | Bryozoa | yes |
| Crinoidea | Crinoidea | yes |
| Crustacea | Crustacea | yes |
| Echinoidea | Echinoidea | yes |
| Gastropoda | Gastropoda | yes |
| Gorgonacea | Gorgonacea | no |
| Holothuroidea | Holothuroidea | yes |
| Hydrozoa | Hydrozoa | yes |
| Ophiuroidea | Ophiuroidea | yes |

3. RESULTS

3.1. BRUVS SPECIES MODELS, CHARACTERIZATION & PREDICTION (M Cappo, G De'Ath)

The final BRUVS dataset comprised 39,989 individuals from 347 species of fishes, sharks, rays and sea snakes observed at 366 sites. The bony fishes were from 10 orders, dominated by Perciformes (267 species), Tetraodontiformes (27), Anguilliformes (6), Aulopiformes (3), Scorpaeniformes, Clupeiformes, Beryciformes with 2 species, and Siluriformes, Pleuronectiformes and Gasterosteiformes each with a single species. The chondrichthyans were represented by Carcharhiniformes (15 species), Rajiformes (13) and Orectolobiformes (3). There were 5 species of sea snakes from the family Hydrophiidae.

3.1.1. BRUVS Species richness

Most of the 347 species recorded were rare or uncommon, occurring in only a very small percentage of sites surveyed. There was an average of 13.8 ± 6 (s.d.) species per site, ranging from 2 to 43. Ordering of the most diverse sites produced a sigmoid curve (Figure 3-1). Only ~14% of sites had comparatively high species richness (≥ 20 species per site), ~41% had moderate richness (≥ 13 species), and 18% had relatively low richness (≤ 8 species). Just over 90% of the species were recorded in less than 10% of the sites and ~43% were recorded only 1–3 times (Figure 3-1). Only ~5% of the species were moderately prevalent, occurring in $\geq 20\%$ of the sites and, of these, only *Nemipterus furcosus* had a prevalence of $>50\%$. General patterns in species richness by latitude and longitude showed that cross-shelf and long-shore gradients were not simple (Figure 3-2). Higher richness occurred at sites in the outer reef matrix, particularly north of Proserpine (20.4°S), with a “hotspot” off Cape Flattery (15°S) in the far north. Richness in the southern half of the GBRMP was higher around the Capricorn-Bunker (23.5°S) island group, and consistently lower for the coastal bays, the deep mid-shelf waters of the Capricorn trough ($\geq 22.5^\circ\text{S}$), and the inter-reef waters of the outer barrier reefs (Figure 3-2).

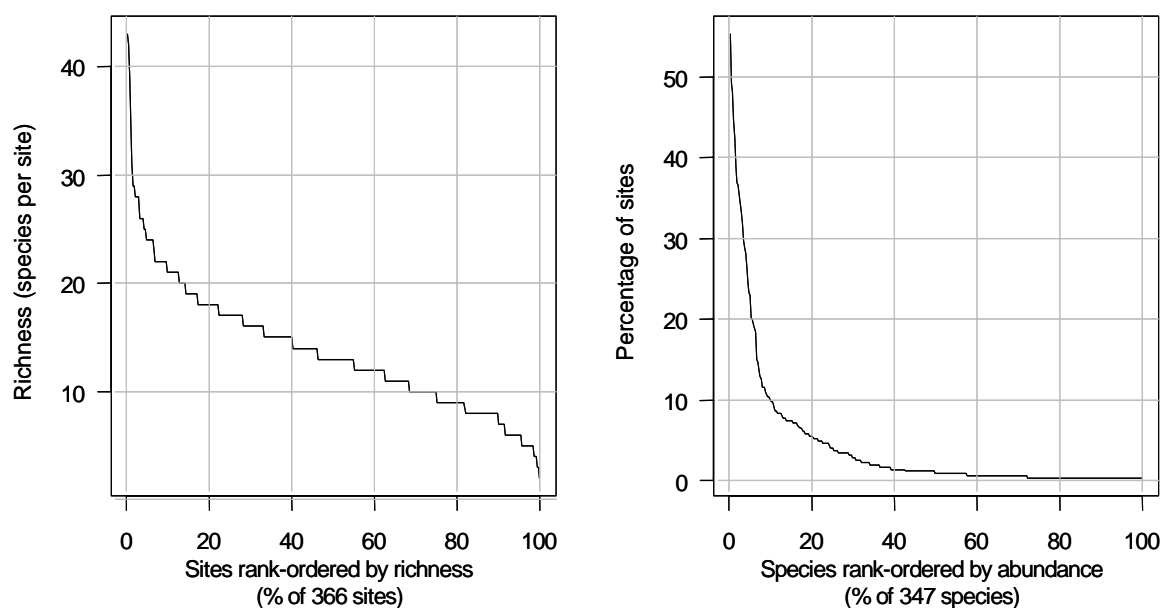


Figure 3-1: Patterns of species prevalence and richness at BRUVS stations.

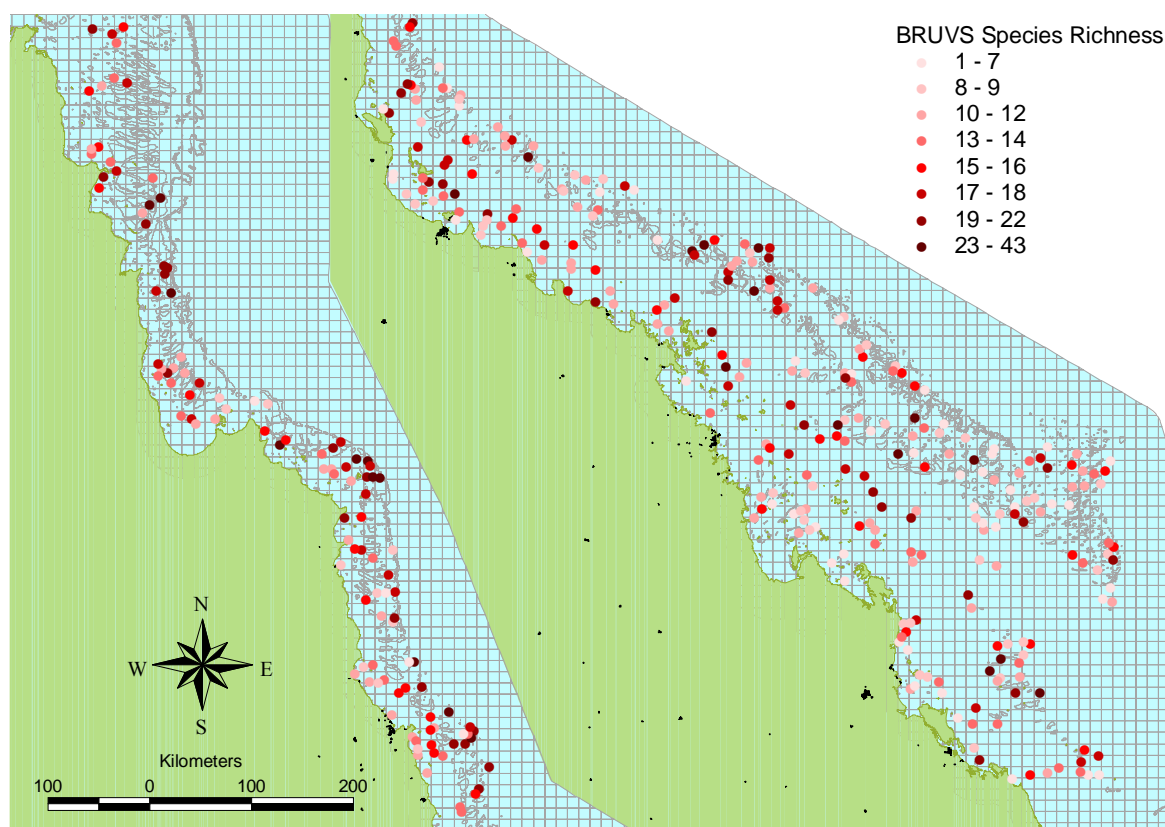


Figure 3-2: Species richness from BRUVS data by location in the GBRMP.

3.1.2. BRUVS Species presence/absence Biophysical Models and Prediction

A number of scenarios were run in univariate models using boosted trees.

First, the top 50 species that occurred on at least 7% ($n=18$) of all BRUVS sites were analysed using (a) all 40 environmental variables, (b) using only spatial (Along, Across, Depth) variables, (c) using only environmental variables, and (d) using all spatial and environmental variables, but dropping “nuisance” temporal harmonics.

It was found that dropping the temporal harmonics had little effect on the models, implying that predictive models would not have to adjust the presence/absence of species by the season, moon phase or time of day of sampling. The top 25 species, with a predictability of $\geq 80\%$, were selected from this analysis. Using “yres” to represent the “predictability” of each of the 25 species ($\text{yres} = (1 - \text{\%prediction error})$), showed “all variables” (mean $\text{yres}=15.15$) not to be different from “all variables, no harmonics” (mean $\text{yres}=15.16$).

The best 20 explanatory spatial and environmental variables (Table 3-2) were analysed with the most predictable 25 species (Table 3-1). Models were produced to apply to the entire sampling grid, in order to make biophysical maps of species occurrence throughout the GBRMP. The mean variance in the species responses explained by these predictive models was 79.3%.

An ideal way to visualize the relationships amongst predictors, amongst species responses, and between response and predictors is to plot them together on a “heatmap” (Figure 3-3). The percentage of the variation in occurrence of each species explained by each predictor is shown in Table 3-1.

Table 3-1: Twenty-five most predictable species (y) using best 20 explanatory variables. "yres" = (1 - %prediction error). "%Var" is the percentage of the variation in presence/absence of the species explained by the best gbmmv model, for production of biophysical maps.

| Species code | Species | yres | %Var |
|--------------|-------------------------------------|-------|-------|
| Sco.quee | <i>Scomberomorus queenslandicus</i> | 19.66 | 79.23 |
| Ser.nigr | <i>Seriolina nigrofasciata</i> | 18.88 | 76.23 |
| Nem.theo | <i>Nemipterus theodorei</i> | 18.76 | 83.33 |
| Nem.furc | <i>Nemipterus furcosus</i> | 17.72 | 72.95 |
| Pen.naga | <i>Pentapodus nagasakiensis</i> | 17.57 | 86.34 |
| Sel.lept | <i>Selaroides leptolepis</i> | 17.52 | 79.23 |
| Pen.para | <i>Pentapodus paradiseus</i> | 17.49 | 77.60 |
| Aba.stel | <i>Abalistes stellatus</i> | 17.4 | 72.95 |
| Sau.grp | <i>Saurida grp</i> | 16.45 | 77.87 |
| Ech.nauc | <i>Echeneis naucrates</i> | 16.25 | 65.85 |
| Nem.hexo | <i>Nemipterus hexodon</i> | 15.73 | 91.80 |
| Lag.scel | <i>Lagocephalus sceleratus</i> | 15.48 | 68.85 |
| Car.coer | <i>Carangoides coeruleopinnatus</i> | 15.2 | 70.22 |
| Dec.russ | <i>Decapterus russelli</i> | 15.05 | 77.32 |
| Let.geni | <i>Lethrinus genivittatus</i> | 14.86 | 77.32 |
| Gym.mino | <i>Gymnothorax minor</i> | 14.31 | 83.33 |
| Car.fulv | <i>Carangoides fulvoguttatus</i> | 14.05 | 72.68 |
| Upe.trag | <i>Upeneus tragula_grp</i> | 13.93 | 78.14 |
| Par.otis | <i>Paramonacanthus otisensis</i> | 13.24 | 87.98 |
| Par.nebu | <i>Parapercis nebulosa_grp</i> | 12.62 | 82.79 |
| Car.gymn | <i>Carangoides gymnostethus</i> | 12.51 | 80.87 |
| Cho.venu | <i>Choerodon venustus</i> | 12.22 | 83.33 |
| Gna.spec | <i>Gnathanodon speciosus</i> | 10.46 | 85.25 |
| Ale.aper | <i>Alepes apercna</i> | 10.29 | 85.52 |
| Nem.pero | <i>Nemipterus peronii</i> | 9.81 | 86.07 |

Table 3-2: Top 20 explanatory variables (x) sorted by descending order of "xres" = (% of [1-% prediction error] for each x). "xvar" is the mean percentage of the variation in the responses (species occurrence) explained by each of the explanatory variables in the best gbmmv model, for production of biophysical maps.

| Explanatory variable | xres | xvar |
|----------------------|------|------|
| across | 1.75 | 8.59 |
| ga.mud | 1.18 | 6.47 |
| ga.crbnt | 1.14 | 5.76 |
| ga.gravel | 0.99 | 5.18 |
| gbr.bathy | 0.88 | 4.34 |
| along | 0.82 | 4.39 |
| m.bstress | 0.74 | 4.05 |
| crs.s.av | 0.71 | 3.64 |
| sw.chla.sd | 0.68 | 3.53 |
| crs.s.sd | 0.67 | 3.28 |
| crs.no3.sd | 0.64 | 3.79 |
| sw.k.b.irr | 0.61 | 3.28 |
| crs.t.av | 0.58 | 3.04 |
| gbr.slope | 0.58 | 3.16 |
| trwl.eff.i | 0.58 | 3.19 |
| crs.o2.av | 0.52 | 2.81 |
| crs.si.sd | 0.52 | 2.94 |
| gbr.aspect | 0.5 | 2.71 |
| crs.si.av | 0.5 | 2.59 |
| ga.sand | 0.49 | 2.58 |

Table 3-3: Matrix of percentage of the variability in occurrence of 25 species responses explained by the top 20 explanatory variables.

| sp.code | across | ga.mud | ga.crbnt | ga.gravel | gbr.bathy | along | m.bstress | crs.s.av | sw.k.b.irr | crs.s.sd | crs.no3.sd | gbr.slope | trwl.eff.i | crs.t.av | ga.sand | gbr.aspect | crs.si.av | crs.o2.av | sw.chla.sd | crs.si.sd |
|----------|--------|--------|----------|-----------|-----------|-------|-----------|----------|------------|----------|------------|-----------|------------|----------|---------|------------|-----------|-----------|------------|-----------|
| Sco.quee | 28.2 | 2.2 | 6.5 | 3.0 | 2.0 | 2.0 | 1.9 | 1.9 | 1.4 | 5.1 | 2.2 | 2.7 | 3.4 | 1.4 | 1.6 | 3.1 | 1.4 | 2.1 | 5.4 | 0.9 |
| Ser.nigr | 16.1 | 2.3 | 6.2 | 3.3 | 8.8 | 4.3 | 1.5 | 3.3 | 3.9 | 3.0 | 1.4 | 1.9 | 0.8 | 2.3 | 1.7 | 1.3 | 1.1 | 3.1 | 7.0 | 4.1 |
| Sel.lept | 24.8 | 2.3 | 6.5 | 2.9 | 3.0 | 4.6 | 2.4 | 1.6 | 0.9 | 8.8 | 3.3 | 1.9 | 1.4 | 5.1 | 1.7 | 1.6 | 1.8 | 1.5 | 0.9 | 1.4 |
| Nem.theo | 6.2 | 5.2 | 4.0 | 6.3 | 14.4 | 5.8 | 1.5 | 10.7 | 2.9 | 2.0 | 1.9 | 2.5 | 0.7 | 0.7 | 2.8 | 1.3 | 3.6 | 2.9 | 4.1 | 3.0 |
| Aba.stel | 3.8 | 2.3 | 6.2 | 9.1 | 8.3 | 1.9 | 0.9 | 4.4 | 1.8 | 5.4 | 1.5 | 4.0 | 5.0 | 1.0 | 2.8 | 1.8 | 2.9 | 1.6 | 5.6 | 1.7 |
| Pen.para | 2.7 | 9.1 | 3.8 | 17.4 | 3.5 | 5.4 | 4.4 | 1.4 | 2.7 | 2.6 | 2.7 | 1.7 | 1.1 | 3.2 | 1.8 | 3.6 | 2.2 | 2.6 | 2.9 | 1.7 |
| Nem.furc | 7.6 | 3.4 | 4.9 | 2.7 | 3.2 | 2.7 | 4.8 | 5.4 | 3.4 | 3.4 | 2.4 | 2.2 | 2.0 | 11.4 | 2.3 | 3.0 | 1.3 | 2.7 | 1.4 | 1.4 |
| Pen.naga | 14.8 | 6.3 | 31.2 | 7.1 | 1.1 | 0.9 | 1.1 | 0.9 | 1.7 | 1.7 | 2.8 | 1.8 | 2.4 | 0.9 | 1.3 | 1.3 | 2.1 | 1.7 | 3.4 | 1.0 |
| Sau.grp | 7.9 | 3.5 | 4.5 | 5.2 | 4.8 | 6.3 | 2.0 | 7.9 | 5.8 | 3.1 | 3.1 | 3.2 | 3.5 | 1.1 | 1.8 | 2.0 | 2.7 | 3.6 | 3.9 | 1.9 |
| Ech.nauc | 4.4 | 2.2 | 3.9 | 5.3 | 1.6 | 1.7 | 2.6 | 2.0 | 4.2 | 2.5 | 3.8 | 4.2 | 3.5 | 3.4 | 4.4 | 2.7 | 2.6 | 2.2 | 5.0 | 2.1 |
| Car.coer | 4.2 | 21.1 | 5.0 | 2.2 | 2.2 | 2.7 | 5.1 | 2.6 | 3.7 | 1.0 | 2.9 | 1.9 | 2.6 | 1.1 | 2.9 | 1.8 | 1.6 | 2.1 | 2.5 | 1.8 |
| Nem.hexo | 20.4 | 30.9 | 4.1 | 2.4 | 2.6 | 1.2 | 4.1 | 4.5 | 1.1 | 2.1 | 1.6 | 3.8 | 5.0 | 1.0 | 1.1 | 0.4 | 2.3 | 0.8 | 1.9 | 0.6 |
| Lag.scel | 1.5 | 2.0 | 3.7 | 3.9 | 2.7 | 10.0 | 5.2 | 1.9 | 3.8 | 1.1 | 4.9 | 1.3 | 4.7 | 4.2 | 1.7 | 3.0 | 6.3 | 2.3 | 2.3 | 3.2 |
| Dec.russ | 5.2 | 6.5 | 5.9 | 2.1 | 7.8 | 3.5 | 5.4 | 5.6 | 2.6 | 7.9 | 2.5 | 4.5 | 1.7 | 1.9 | 2.0 | 2.2 | 2.5 | 2.1 | 5.0 | 1.4 |
| Let.geni | 4.4 | 4.3 | 4.2 | 6.1 | 2.8 | 8.7 | 4.4 | 2.8 | 6.4 | 3.1 | 4.0 | 4.0 | 3.0 | 2.2 | 3.1 | 3.5 | 3.5 | 2.5 | 2.7 | 2.0 |
| Gym.mino | 5.7 | 7.0 | 7.6 | 4.4 | 4.8 | 2.6 | 4.0 | 4.5 | 2.2 | 2.0 | 12.2 | 1.9 | 5.5 | 1.2 | 3.8 | 4.1 | 2.9 | 1.4 | 3.8 | 2.0 |
| Car.fulv | 6.1 | 2.9 | 3.7 | 6.6 | 6.2 | 6.2 | 1.7 | 2.7 | 2.7 | 4.8 | 1.5 | 3.1 | 2.3 | 2.4 | 2.1 | 2.5 | 3.2 | 2.3 | 3.5 | 4.8 |
| Upe.trag | 2.8 | 4.2 | 2.2 | 10.4 | 4.2 | 3.1 | 10.4 | 3.6 | 4.1 | 1.8 | 2.6 | 5.3 | 1.3 | 5.3 | 4.3 | 4.2 | 2.0 | 3.0 | 1.8 | 1.9 |
| Par.otis | 9.4 | 9.7 | 2.9 | 1.7 | 5.3 | 5.5 | 3.1 | 3.6 | 5.0 | 2.8 | 3.3 | 2.8 | 4.0 | 3.5 | 4.3 | 2.5 | 3.1 | 11.9 | 1.1 | 2.9 |
| Par.nebu | 4.8 | 11.5 | 2.0 | 2.8 | 2.3 | 2.1 | 8.4 | 2.6 | 4.8 | 1.7 | 2.8 | 5.2 | 6.1 | 1.9 | 4.4 | 4.2 | 2.7 | 6.1 | 3.5 | 2.6 |
| Car.gymn | 2.8 | 2.2 | 3.9 | 1.6 | 2.5 | 4.3 | 4.3 | 2.8 | 2.3 | 4.3 | 2.1 | 5.1 | 3.2 | 2.5 | 2.5 | 4.7 | 4.7 | 2.8 | 6.0 | 16.2 |
| Cho.venu | 7.0 | 3.7 | 14.2 | 6.8 | 2.1 | 8.4 | 11.4 | 4.3 | 1.9 | 4.7 | 2.9 | 4.5 | 1.5 | 2.0 | 0.9 | 1.4 | 1.9 | 1.1 | 1.8 | 1.5 |
| Gna.spec | 1.8 | 3.2 | 1.8 | 4.8 | 2.7 | 8.6 | 4.1 | 3.7 | 9.9 | 4.7 | 5.5 | 3.4 | 3.4 | 3.8 | 2.9 | 7.4 | 1.6 | 2.1 | 2.0 | 8.0 |
| Ale.aper | 12.0 | 5.6 | 2.2 | 7.7 | 3.5 | 3.9 | 2.9 | 4.1 | 0.9 | 3.8 | 3.3 | 3.4 | 4.1 | 11.9 | 3.4 | 2.3 | 4.1 | 2.3 | 2.2 | 1.7 |
| Nem.pero | 12.3 | 4.9 | 5.9 | 4.0 | 3.2 | 3.1 | 3.4 | 3.9 | 1.4 | 1.3 | 12.9 | 3.1 | 8.3 | 2.8 | 2.0 | 2.8 | 2.2 | 1.8 | 4.9 | 2.3 |

The dendrogram along the side of the heatmap shows which species were similar in having a relationship with a set of predictor variables. It does not imply these species have the same relationship. For example, *Nemipterus hexodon*, *Pentapodus nagasakiensis* and *Scomberomorus queenslandicus* were all highly predictable [orange-red bars on left side of figure] and cluster together in the left-hand dendrogram. However, *N. hexodon* and *P. nagasakiensis* are completely opposite in their response to “Across” and “GA.mud”. The coloured bars along the top show the percentage of the variation in the explanatory variables explained by a particular variable — note that “Across” and “GA.mud” are red. The “redness” of the individual cells in the figure show the relative influence of the particular explanatory variable on the presence/absence of the particular species, and the heaviness of the blue line shows the degree and shape of the relationship.

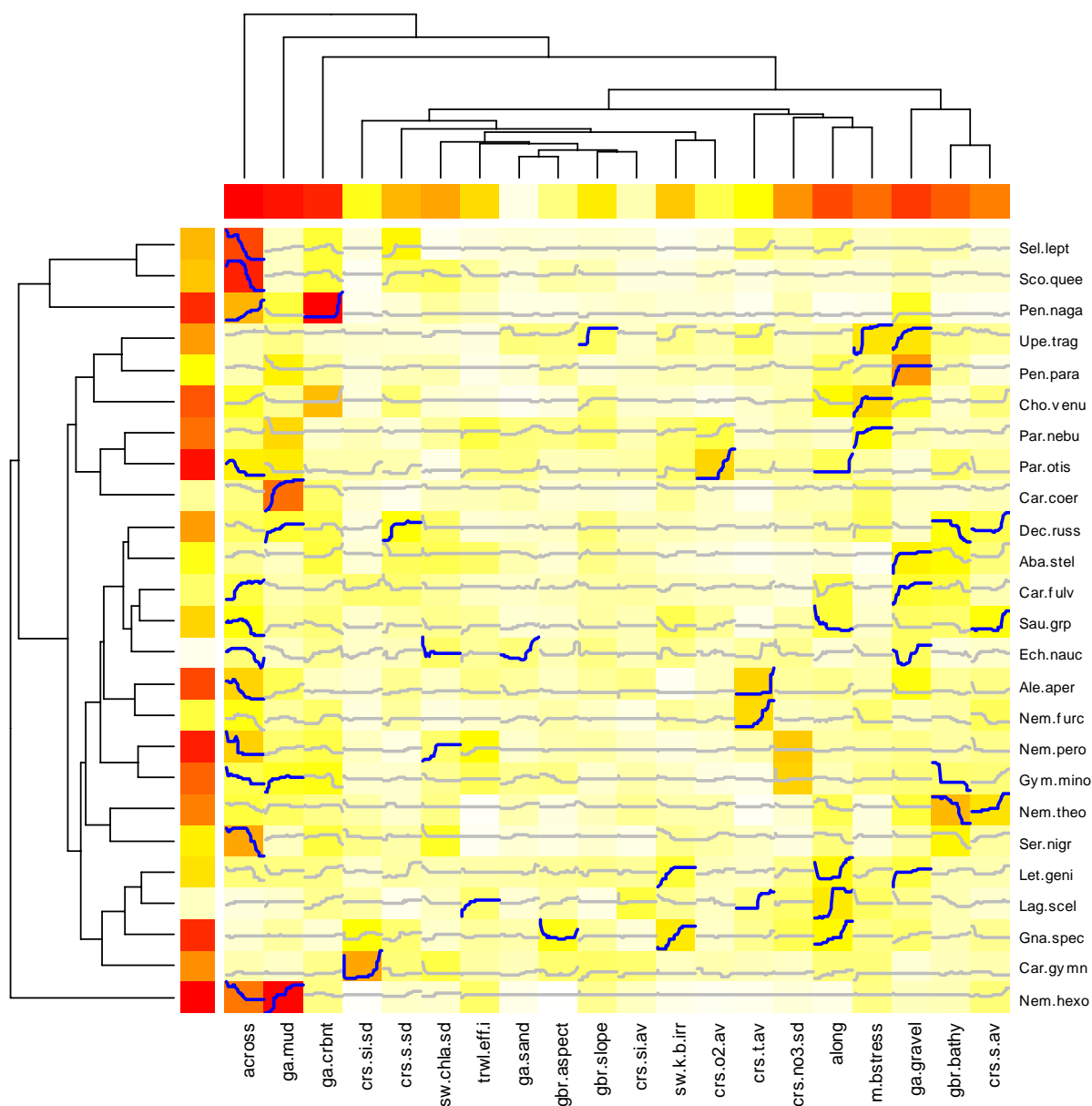


Figure 3-3: "Heatmap" showing relationships amongst and between the top 20 predictors and 25 species responses (presence/absence). The dendrogram along the side of the heatmap shows which species are similar in having a relationship with a set of predictor variables. It does not imply these species have the same relationship. The dendrogram along the top shows which explanatory variables cluster together, and the coloured bars along the top show the percentage of the variation in the explanatory variables explained by a particular variable. Red indicates higher influence. The “redness” of the individual cells in the figure show the relative influence of the particular explanatory variable on the presence/absence of the particular species, and the heaviness of the blue line shows the degree and shape of the relationship.

The relative influence of the predictors and the shape of the relationships between species occurrence and a selection of 7 of the 20 predictors are shown in a series of plots for: position across the shelf (Figure 3-4); content of the sediments in terms of mud (Figure 3-5), carbonate (Figure 3-6), gravel (Figure 3-7); water temperature (Figure 3-8) and salinity (Figure 3-9); and trawl effort (Figure 3-10). The “rugs” on the X axes show the 10 percentiles of the distribution of the predictor variables, and for the trawl index the data is dominated by zero effort in most of the sampling area, with high levels in less than 10 percent of the data. This produces much leverage and complicated shapes in the functional relationships.

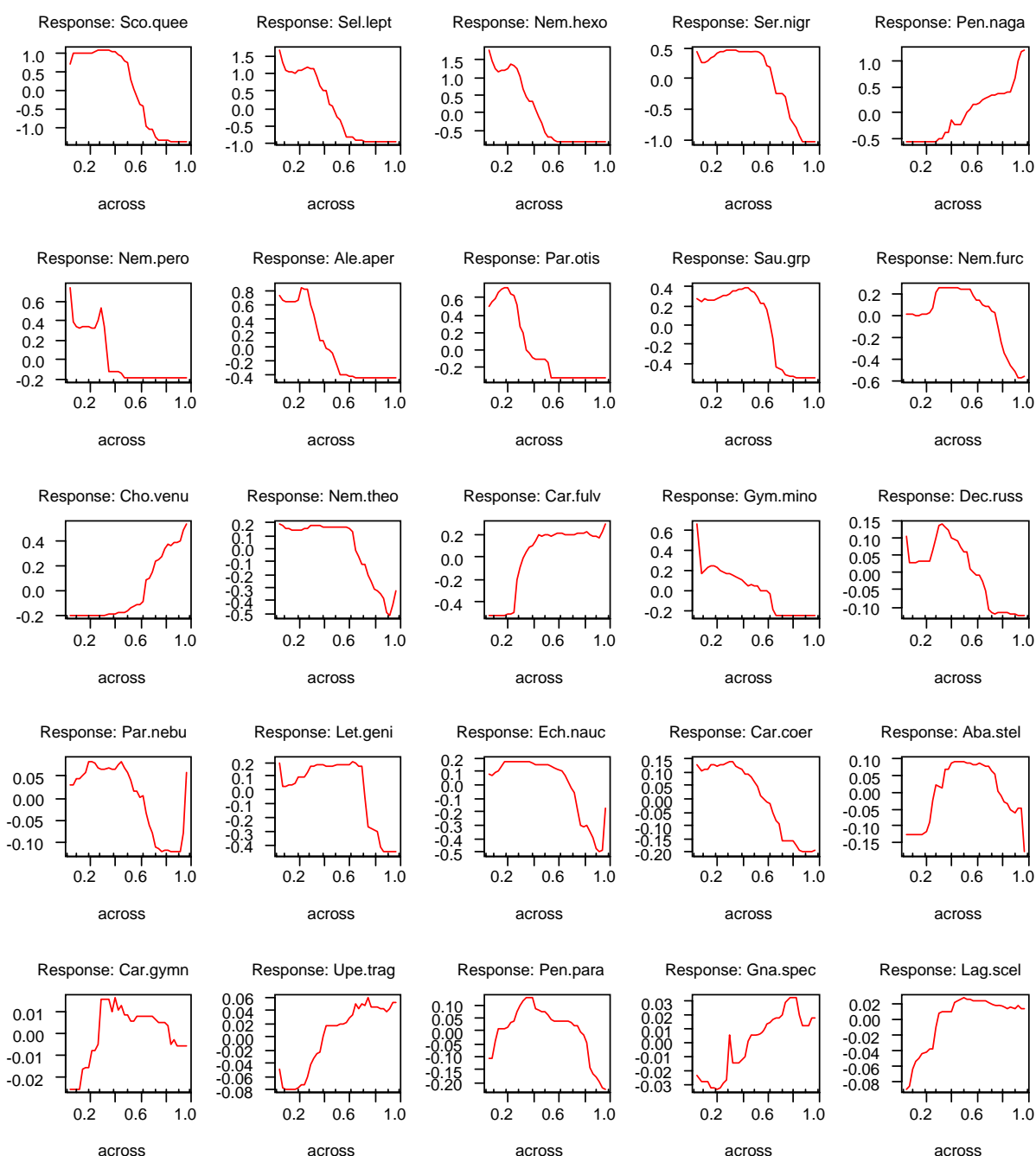


Figure 3-4: Species occurrence as a function of location across the shelf, $f(\text{across})$. Plots are ranked in descending order of relative influence of the predictor variable for the species. The “rugs” on the X axes are 10 percentiles in the distribution of the predictor variable. The Yaxes (log-odds) are $\text{Log}(\text{base } 2)(1 - \text{Probability of occurrence})$ and the plots are centred on the mean of Y.

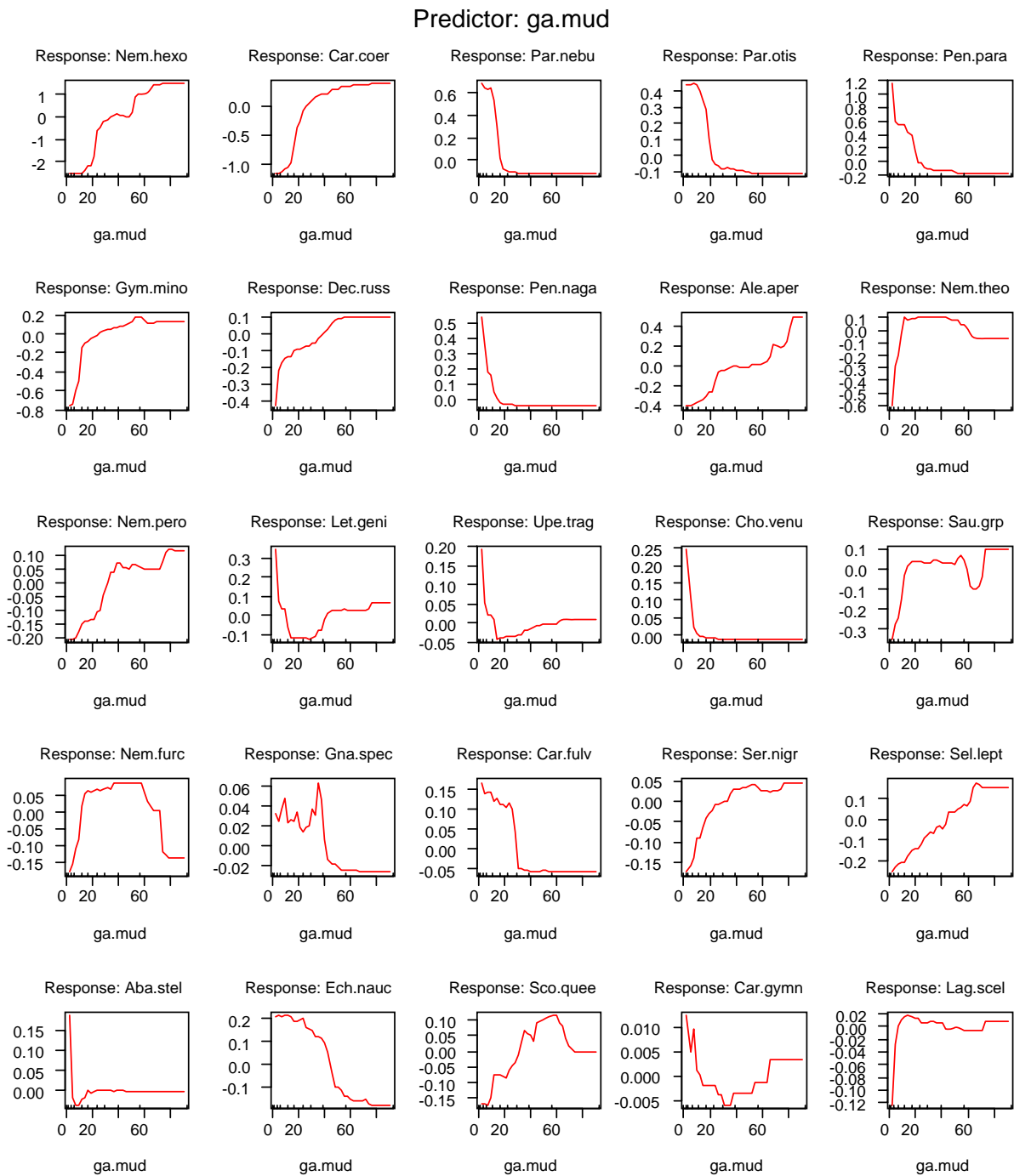


Figure 3-5: Species occurrence as a function of mud content of the sediments, $f(\text{ga.mud})$. Conventions as for Figure 3-4.

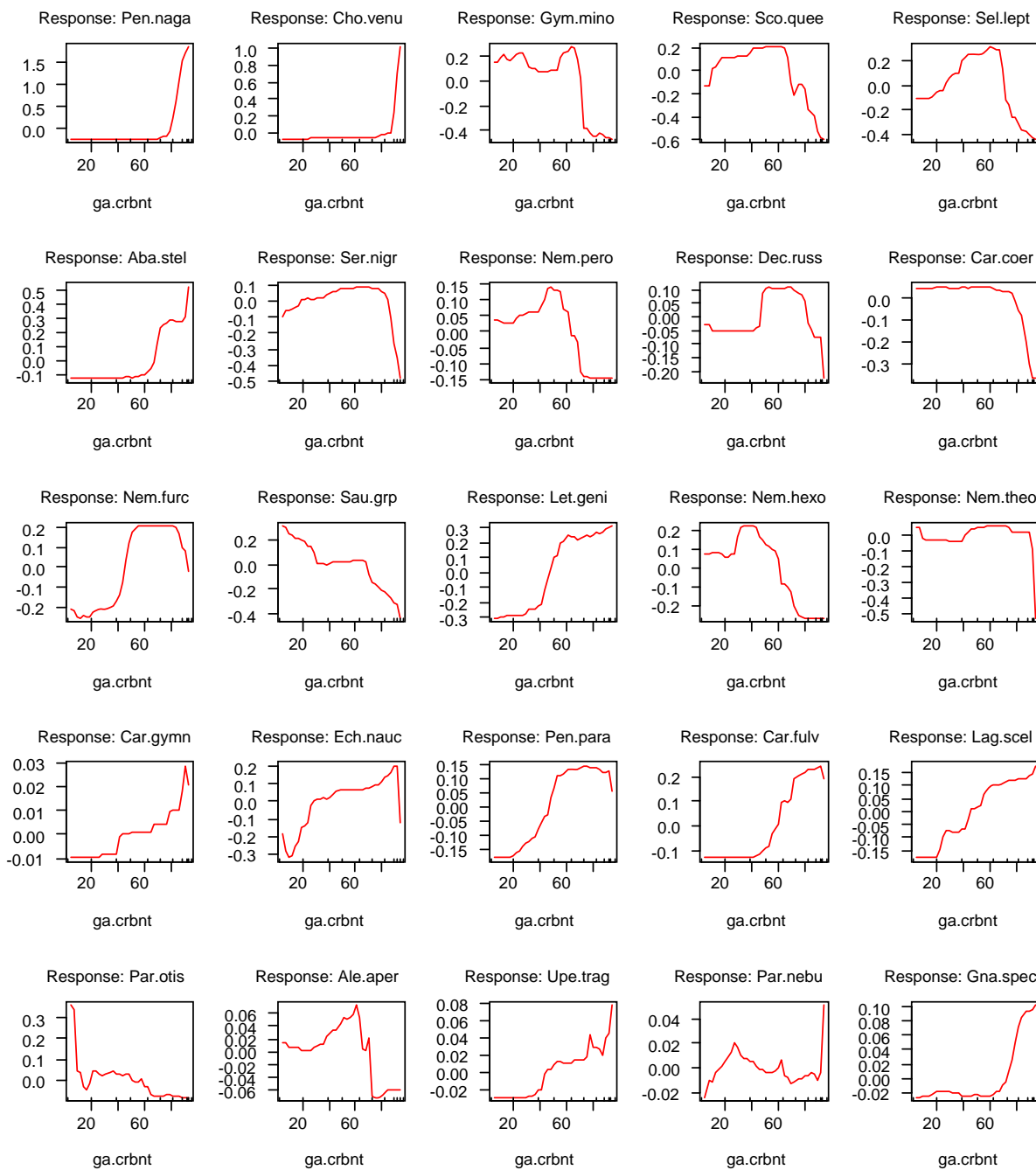


Figure 3-6: Species occurrence as a function of carbonate content of the sediments, $f(\text{ga.crnt})$. Conventions as for Figure 3-4.

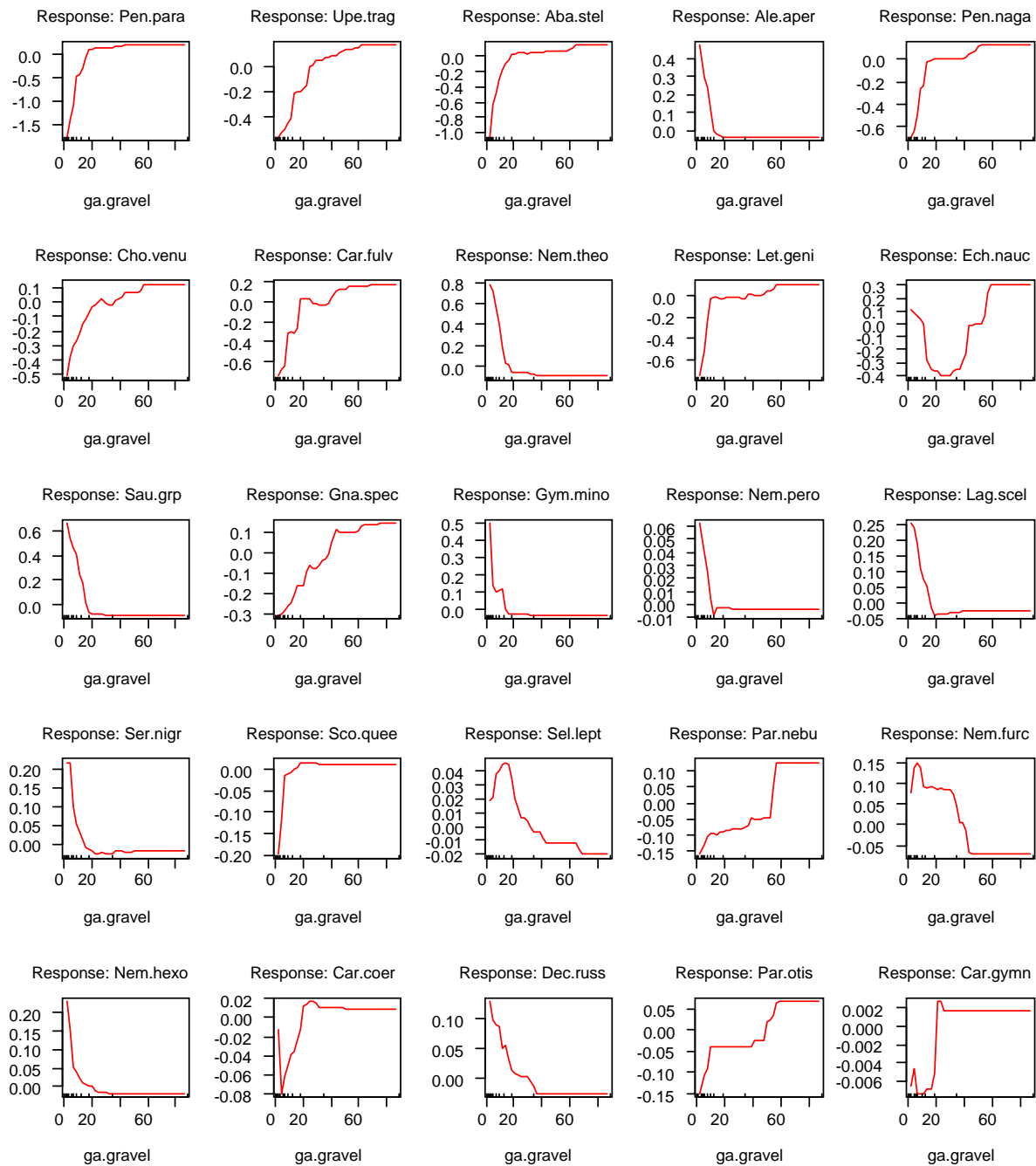


Figure 3-7: Species occurrence as a function of gravel content of the sediments, $f(\text{ga.gravel})$. Conventions as for Figure 3-4.

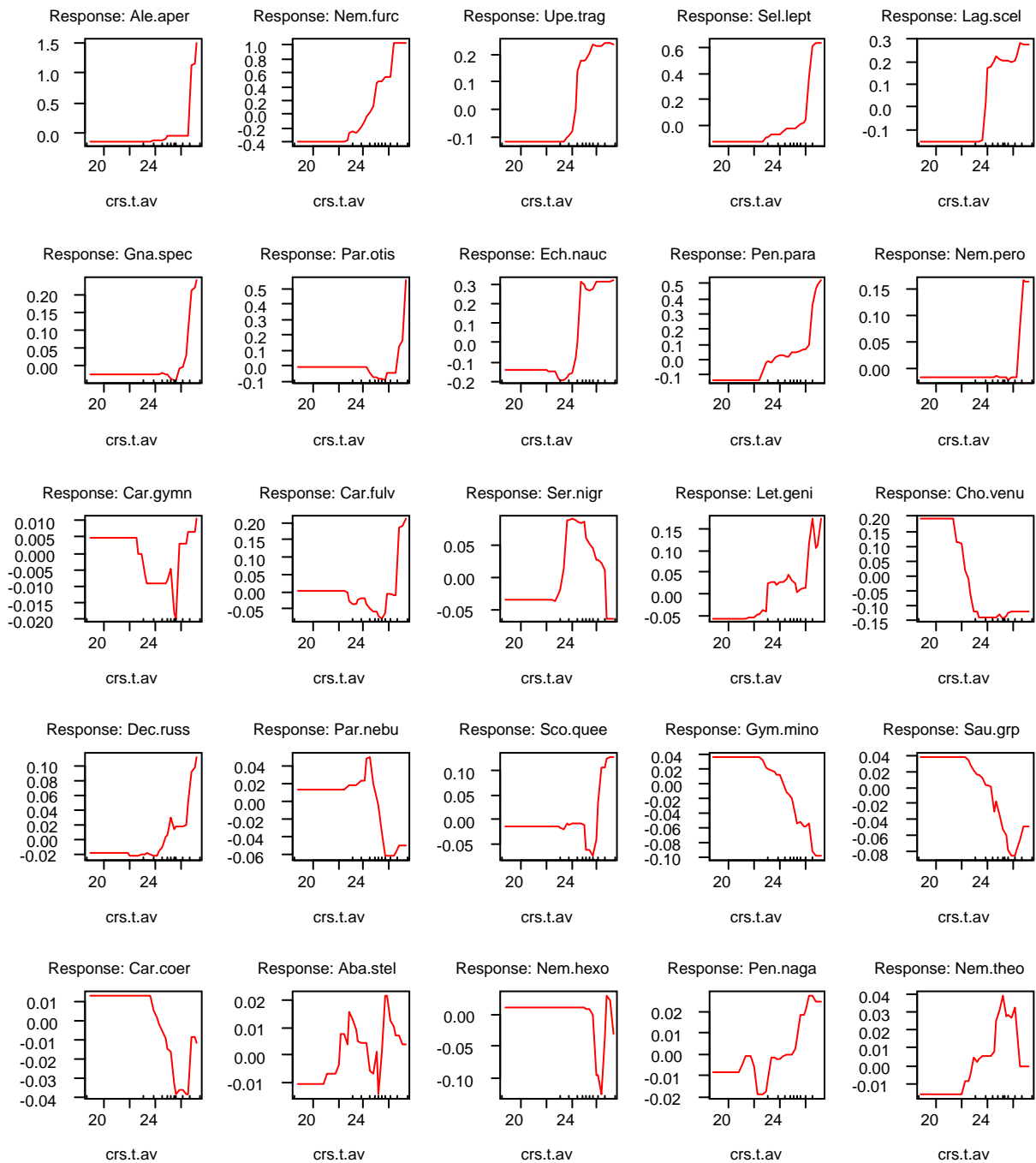


Figure 3-8: Species occurrence as a function of average water temperature, $f(\text{crs.t.av})$. Conventions as for Figure 3-4.

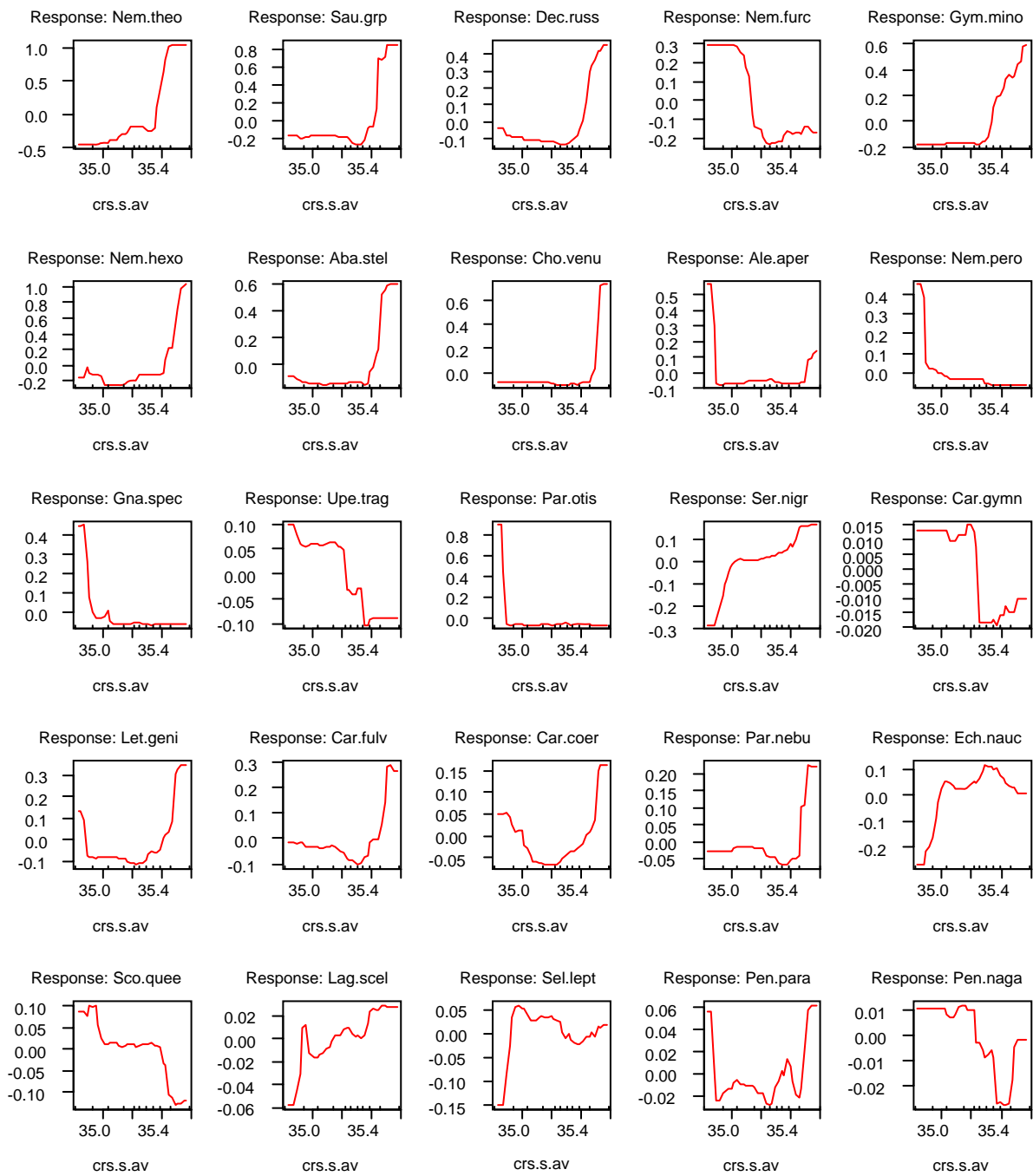


Figure 3-9: Species occurrence as a function of average salinity, $f(\text{crs.s.av})$. Conventions as for Figure 3-4.

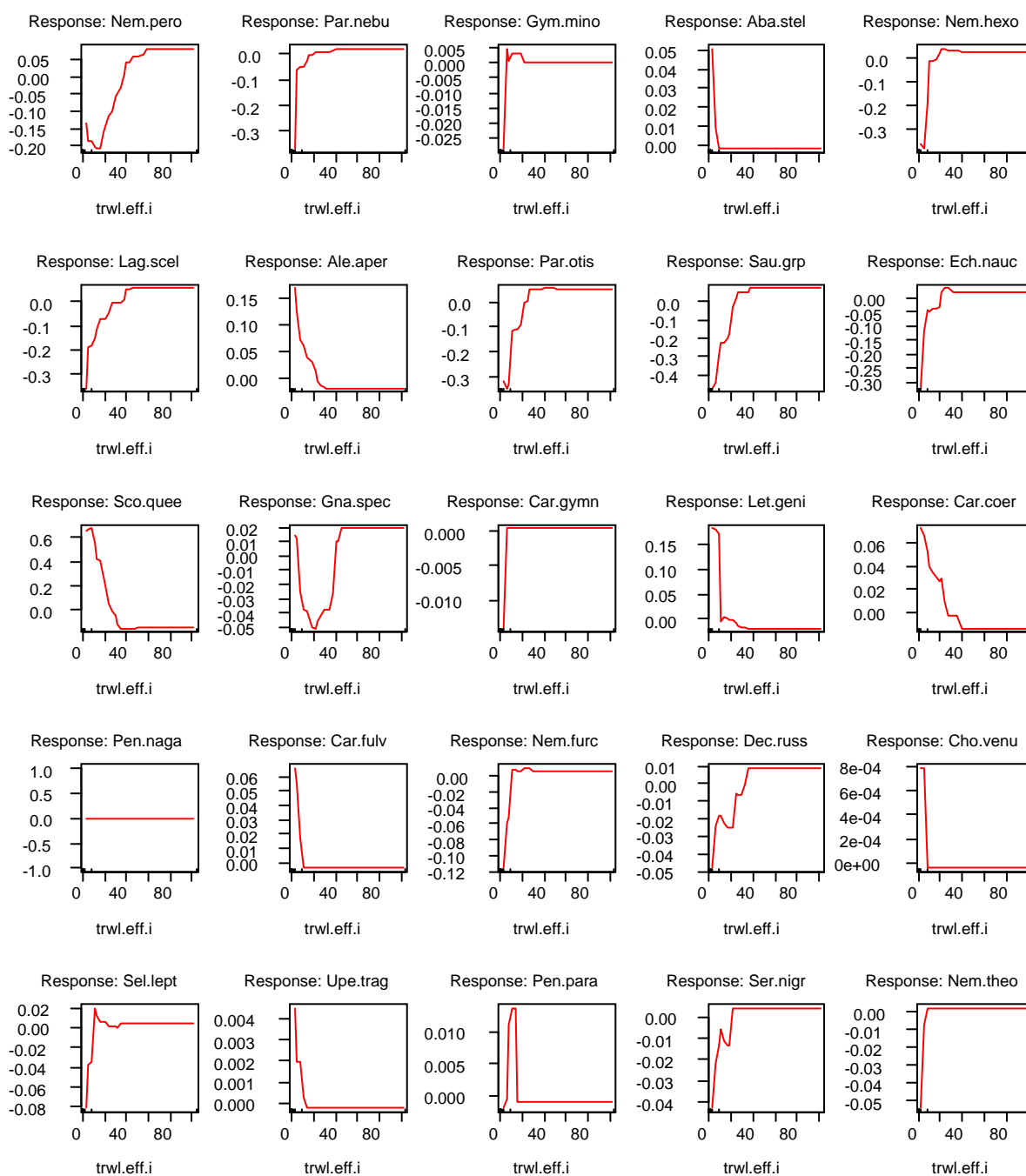


Figure 3-10: Species occurrence as a function of trawl effort index, $f(\text{trwl.eff.i})$. Conventions as for Figure 3-4.

3.1.2.1. BRUVS single species distribution maps

The GBM models produced for the 25 most predictable species seen on BRUVS footage were applied to the overall grid of cells comprising the entire GBRMP, to produce biophysical maps of the occurrence (presence or absence only) of these species. These maps are provided here as six panels of 4 species each, including a measure of reliability of the predictions and a shortlist of the most influential spatial and environmental covariates. Note that the influence of the covariates does not indicate the actual shape of the relationship. For example, high influence of seabed shear stress may influence occurrence of a species positively, negatively, modally or asymptotically. The actual abundance [4th root transformed] recorded at each BRUVS station is featured as scaled circles. This gives some idea of how consistent the predictions are with the actual observations.

In Figure 3-11 the three species in the genus *Nemipterus* are featured. *Nemipterus furcosus* is influenced by seawater temperature and cross-shelf position, and is commonest north of the Palm Islands in lagoonal and inter-reef waters. *Nemipterus peronii* shows only partial concordance with observed concentrations of abundance – the high abundance in Princess Charlotte Bay is not matched by a high probability of occurrence there.

The two small nemipterids, *Pentapodus paradiseus* and *P. nagasakiensis*, are similar in shape, but have different biophysical distribution maps (Figure 3-12). *P. paradiseus* evidently prefers gravelly sediments and is widespread in most habitats across the shelf, except the deeper lagoonal areas. *P. nagasakiensis* was influenced most by high carbonate content of sediments and was found to be prevalent on outer-shelf areas in channels and passes. *Lethrinus genivittatus* was influenced by high light levels at the seabed [perhaps in association with marine plants] and was found in patches throughout the GBRMP. Results from the far north may be less certain due to the lack of sampling off Cape York. Predictions for abundance of *Upeneus tragula* _grp were more prevalent amongst the reef matrix in high current, gravelly areas.

The deep-bodied *Alepes apercna* was predicted to be most common in the far north and also in the area off Mackay (Figure 3-13). Temperature had high influence, but the temperature in these two regions is at opposite extremes. Consistently high occurrence and abundance were predicted and observed for *Decapterus russelli* in the deeper lagoon waters of the Capricorn Channel. This species is both a planktivore and demersal microcarnivore. *Selaroides leptolepis* has a similar habit and diet, but is restricted strongly to inshore waters less than half way across the shelf in the south, although this distribution extends much further offshore north of Cape Flattery. *Seriolina nigrofasciata* is a pelagic, fusiform species seen on BRUVS mainly as a juvenile. Its predicted occurrence was highest in deeper, lagoon waters south of Cape Flattery. It may be both a piscivore and planktivore. It has been seen in the BRUVS field of view settled on the seabed on outstretched pelvic fins.

The Queensland school mackerel, *Scomberomorus queenslandicus*, is an active visual predator that hunts small planktivorous fishes, squid and pelagic crustaceans. Its distribution closely matches that of the potential prey species *Selaroides leptolepis*, being confined to inshore areas in the south and extending further offshore in the north (Figure 3-14). The suckerfish, *Echeneis naucrates*, is reputedly a scavenger associated with large sharks and rays, yet we recorded this species very commonly and in abundance as free-swimming individuals. It is ubiquitous in most habitats, with a “hotspot” of occurrence in the central section off Townsville. The lizardfishes, *Saurida* _grp, were lumped into one taxa and are demersal ambush predators most prevalent in the more saline southern waters of the GBRMP, in the deeper, clearer waters of the lagoon. *Parapercis nebulosa* _grp occurred in the south also with high probability, but more inshore than *Saurida* _grp, influenced by mud content of the sediments. It is also an ambush predator, but moves more frequently than *Saurida* _grp about the BRUVS bait stations.

Deeper waters with high gravel and carbonate were predicted to be the favoured habitat of *Abalistes stellatus*, which extended to the outer shelf, but not nearshore waters (Figure 3-15). The silver toadfish, *Lagocephalus sceleratus*, was most abundant and prevalent across the shelf in the central-northern section between Bowen and Cape Flattery. Highly oxygenated waters and muddy sediments in the southern region were predicted to have the greatest occurrence of the small leatherjacket, *Paramonacanthus otisensis*. Lagoonal sites with high mud content were apparently favoured by the small predatory moray eel, *Gymnathorax minor*.

A variety of carangids were seen on BRUVS footage. One of the most common was the “onion trevally”, *Carangoides coeruleopinnatus*. It was influenced by mud and current, but its inshore habitats north of the Whitsundays were replaced by highest predicted occurrence in the deeper lagoon waters offshore from the macrotidal coast and bays of the southern region (Figure 3-16). *Carangoides fulvoguttatus* and *C. gymnostethus* are much larger predators of fish, crustaceans and molluscs anywhere in the water column and from the seabed. *C. fulvoguttatus* had predicted occurrence in most cross-shelf habitats with the exception of shallow nearshore margins. *C. gymnostethus* had a similar distribution in BRUVS records, but the predictions were very weak on the biophysical map. The golden trevally, *Gnathanodon speciosus*, had patchy distribution of predictions, but consistently higher records in the far north.

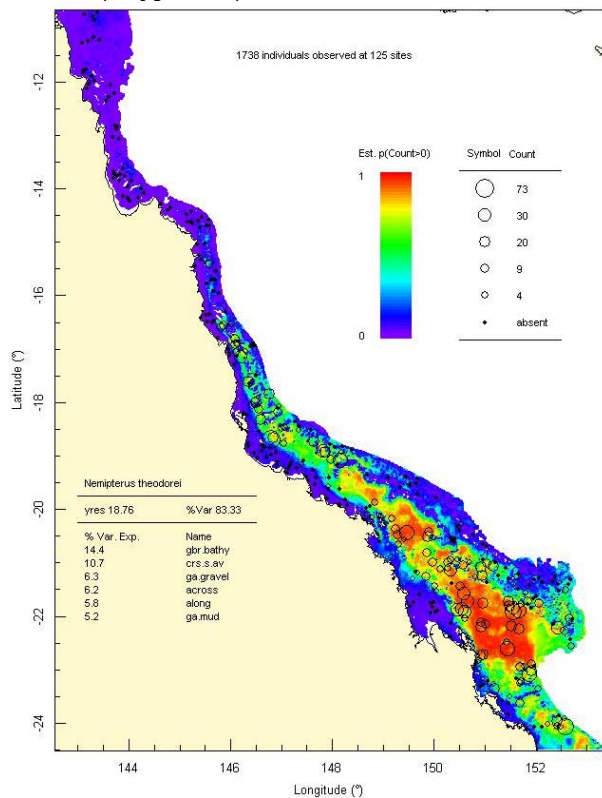
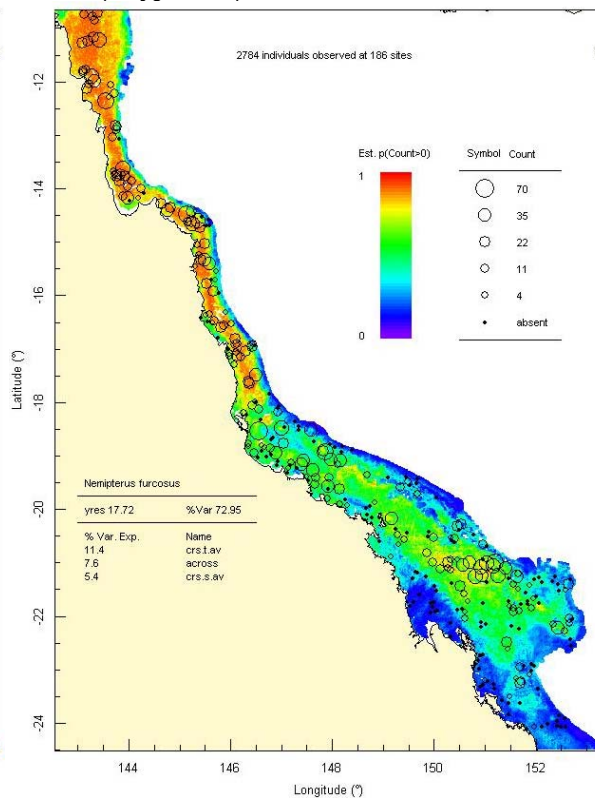
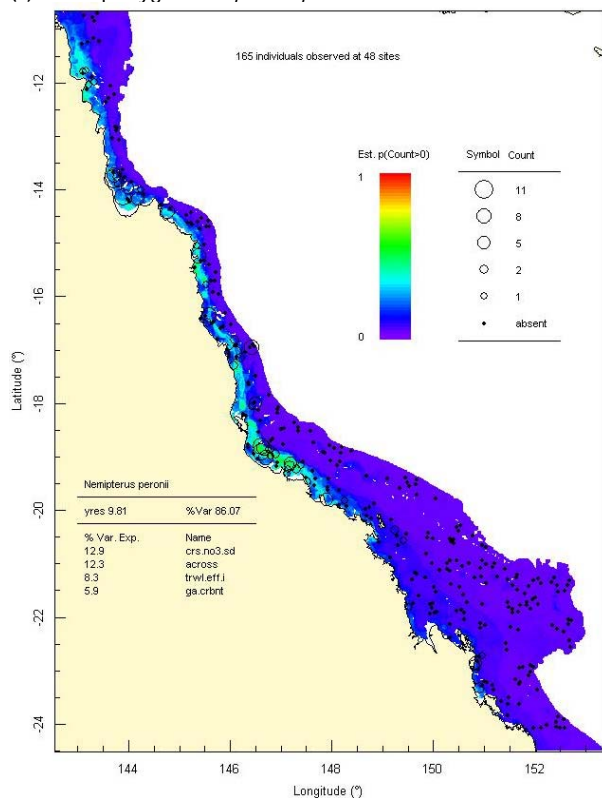
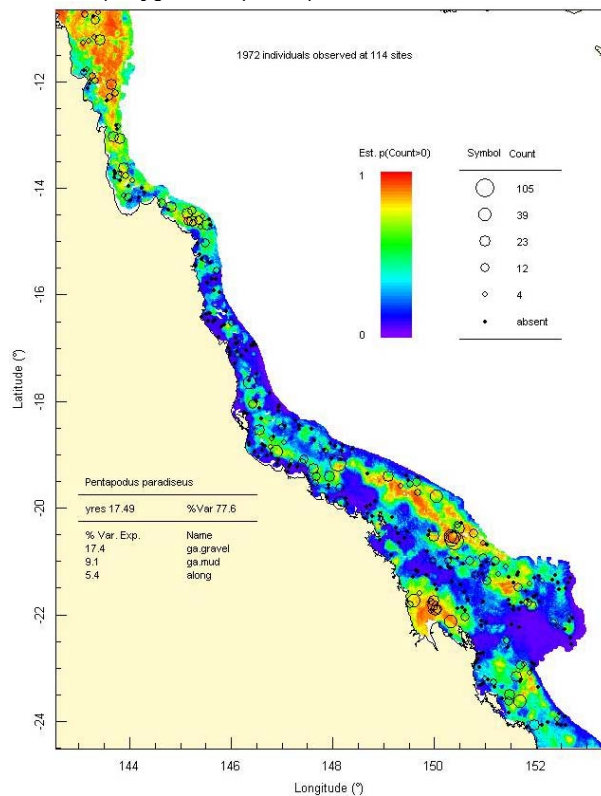
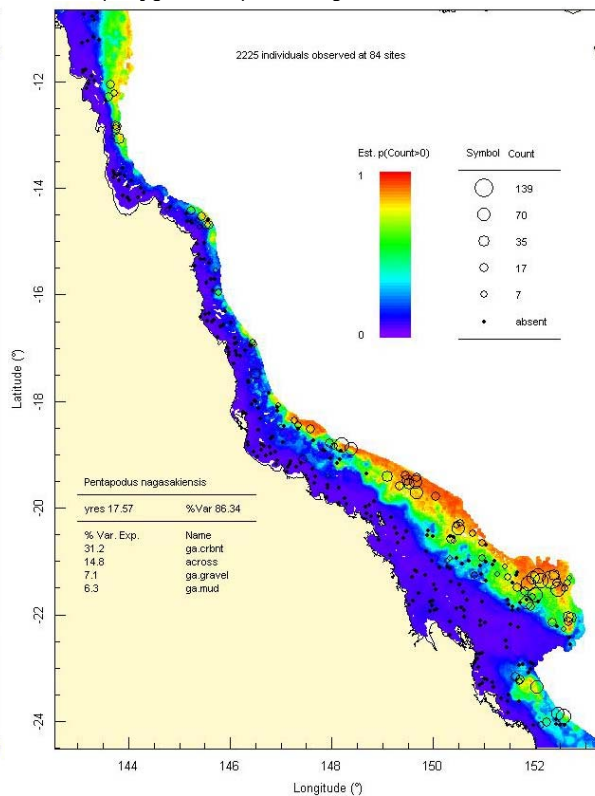
(a) Actinopterygii: *Nemipterus theodorei*(b) Actinopterygii: *Nemipterus furcosus*(c) Actinopterygii: *Nemipterus peronii*

Figure 3-11 Predicted occurrence of 3 species of *Nemipterus* recorded by BRUVS. Circles represent observed abundance (untransformed) and influential covariates are listed in the inset panels. “%XVar” describes the percentage of the variation in the presence/absence of the species accounted for by the gbm model. “yres” is (1-%prediction error).

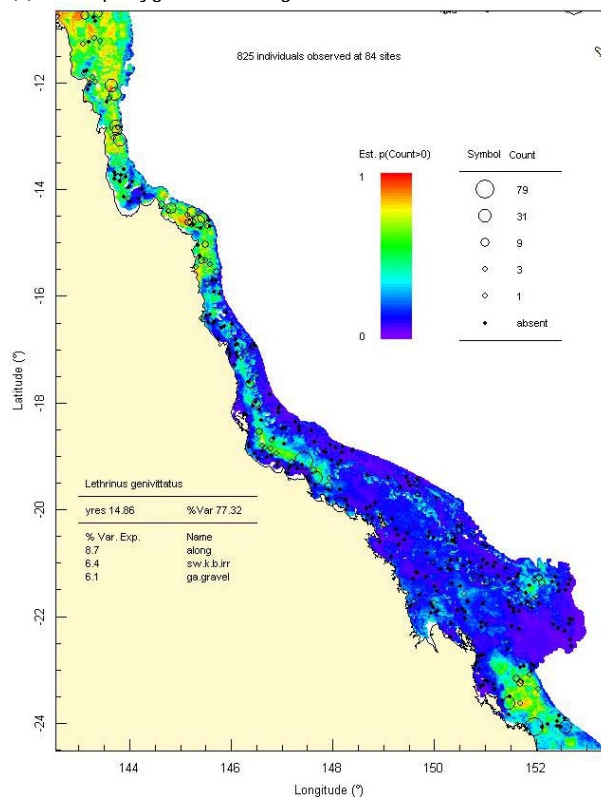
(a) Actinopterygii: *Pentapodus paradiseus*



(b) Actinopterygii: *Pentapodus nagasakiensis*



(c) Actinopterygii: *Lethrinus genivittatus*



(d) Actinopterygii: *Upeneus tragula_grp*

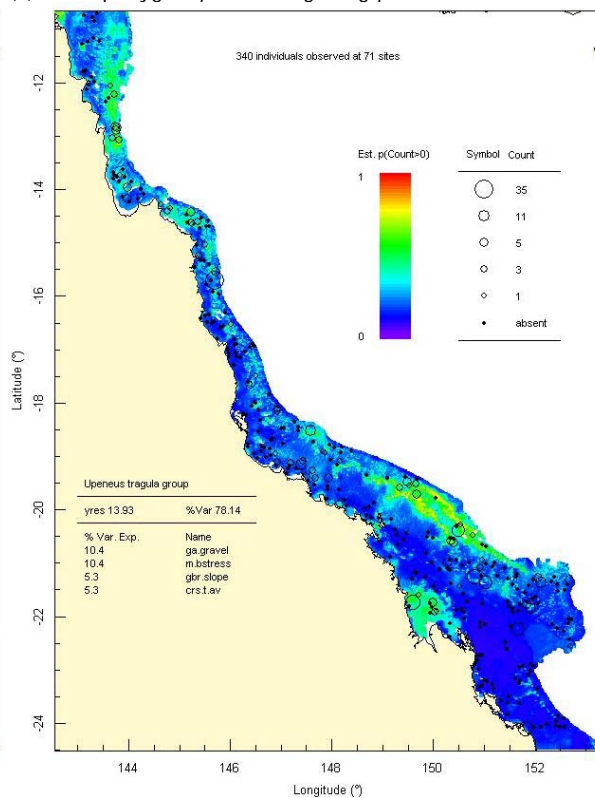


Figure 3-12 Predicted occurrence of small benthic microcarnivores in the genera *Pentapodus*, *Lethrinus* and *Upeneus*. Conventions as for Figure 3-11.

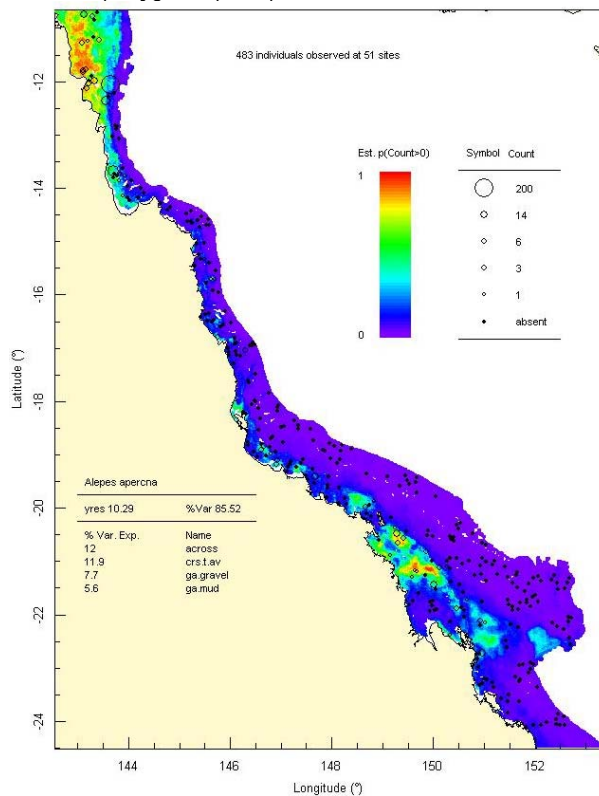
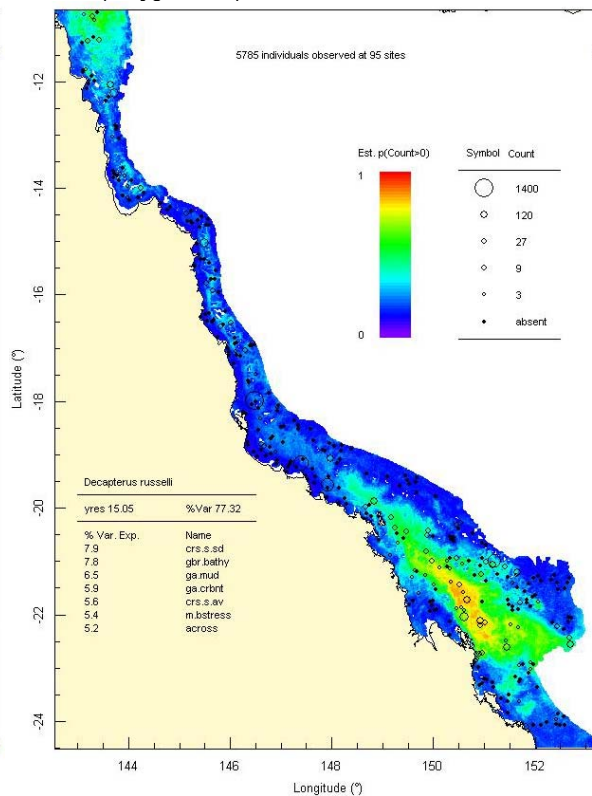
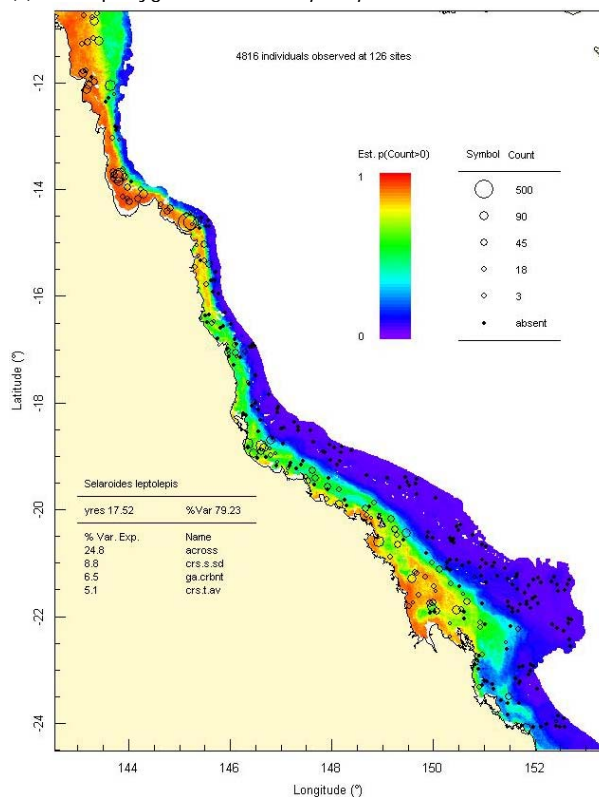
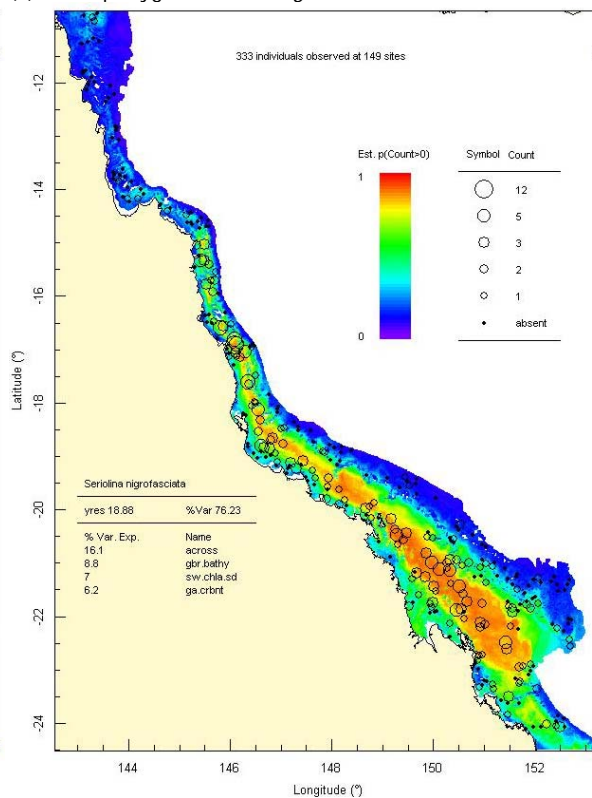
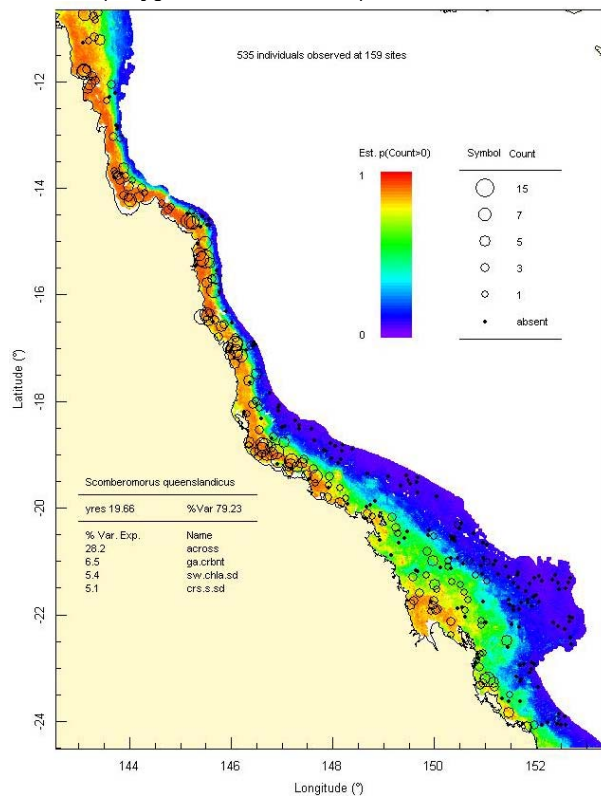
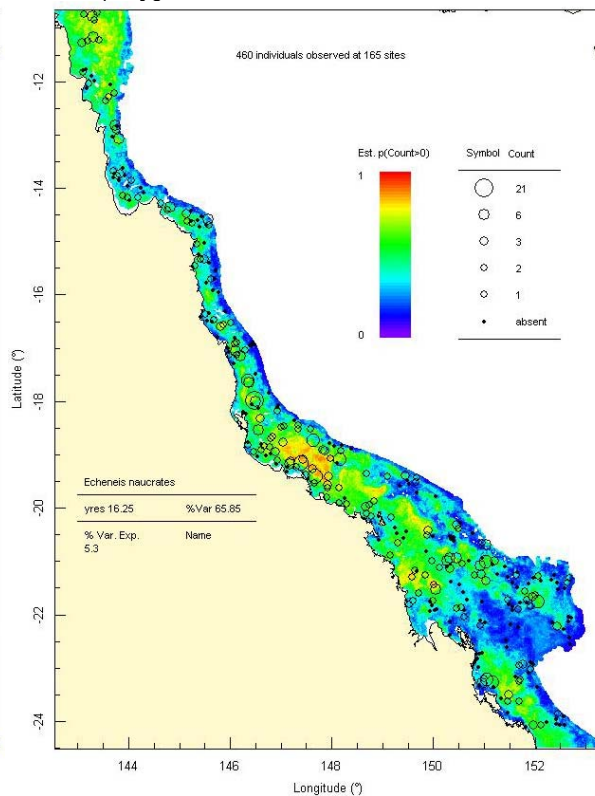
(a) Actinopterygii: *Alepes apercna*(b) Actinopterygii: *Decapterus russelli*(c) Actinopterygii: *Selaroides leptolepis*(d) Actinopterygii: *Seriolina nigrofasciata*

Figure 3-13 Predicted occurrence of small carangids in the genera *Alepes*, *Decapterus*, *Selaroides* and *Seriolina*. Conventions as for Figure 3-11.

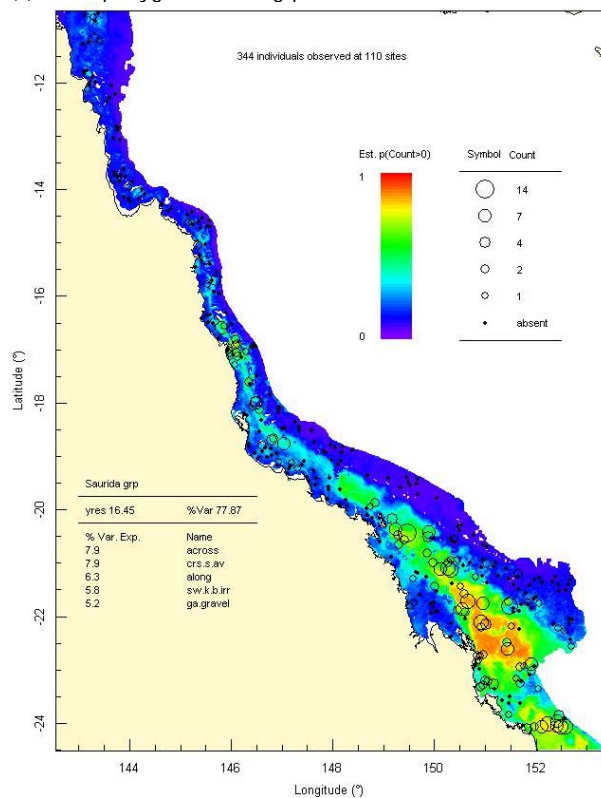
(a) Actinopterygii: *Scomberomorus queenslandicus*



(b) Actinopterygii: *Echeneis naucrates*



(c) Actinopterygii: *Saurida* grp



(d) Actinopterygii: *Parapercis nebulosa* grp

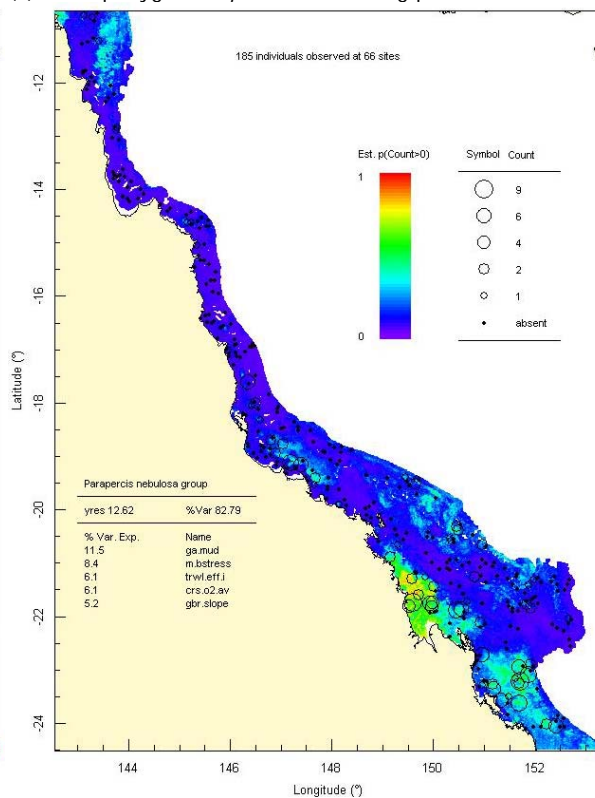
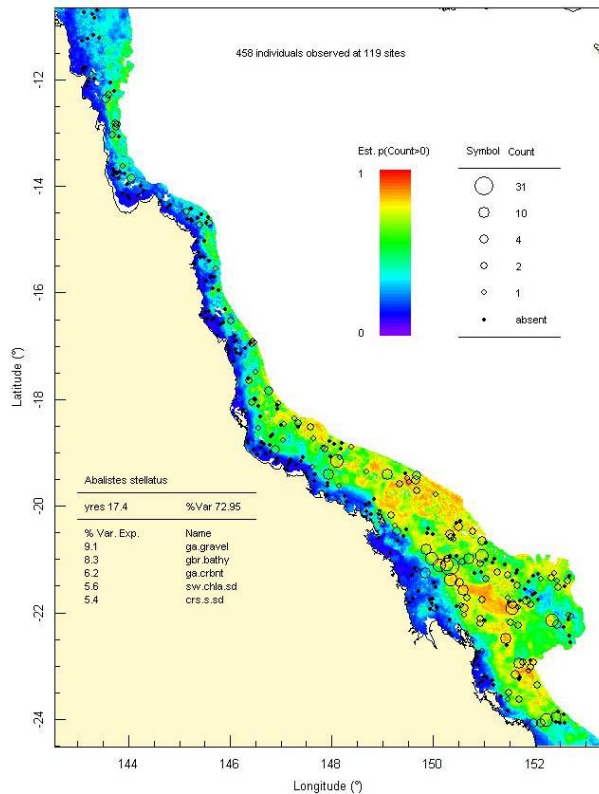
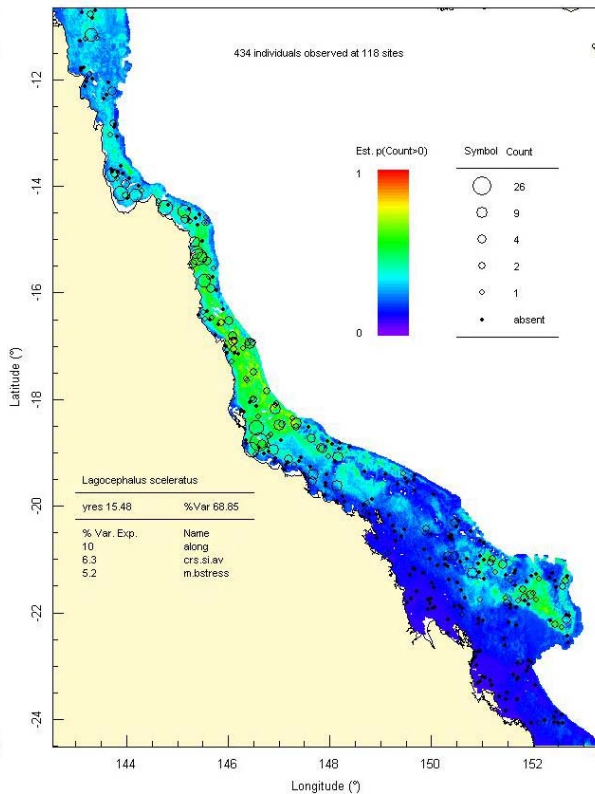


Figure 3-14 Predicted occurrence of predators in the genera *Scomberomorus*, *Echeneis*, *Saurida* and *Parapercis*. Conventions as for Figure 3-11.

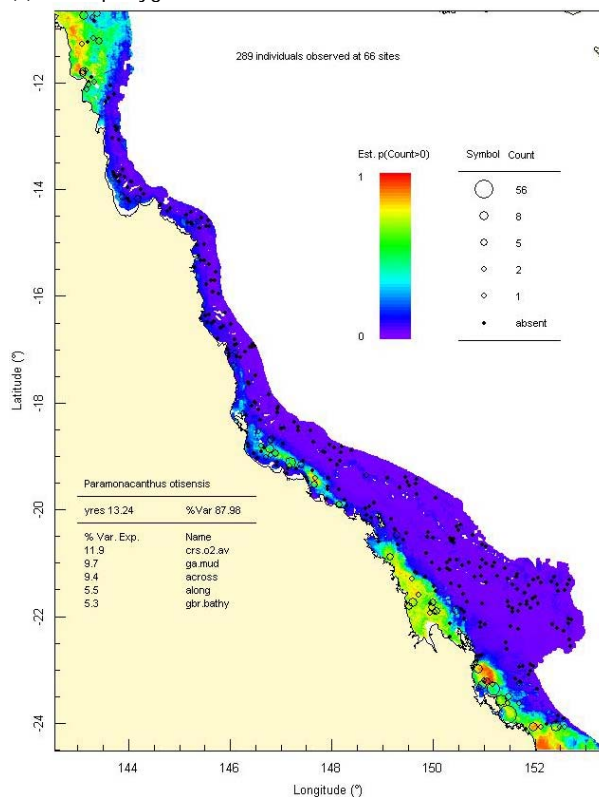
(a) Actinopterygii: *Abalistes stellatus*



(b) Actinopterygii: *Lagocephalus scleratus*



(c) Actinopterygii: *Paramonacanthus otisensis*



(d) Actinopterygii: *Gymnothorax minor*

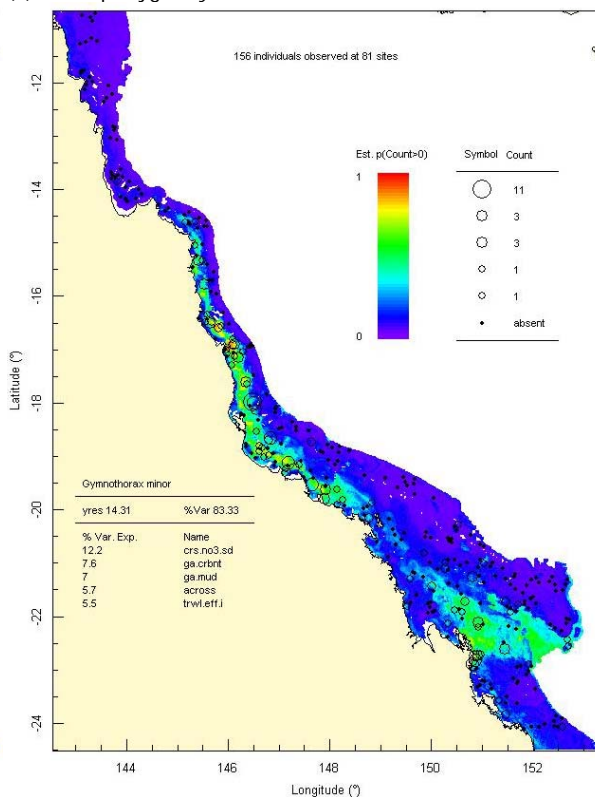


Figure 3-15 Predicted occurrence of demersal omnivores and predators in the genera *Abalistes*, *Lagocephalus*, *Paramonacanthus* and *Gymnothorax*. Conventions as for Figure 3-11.

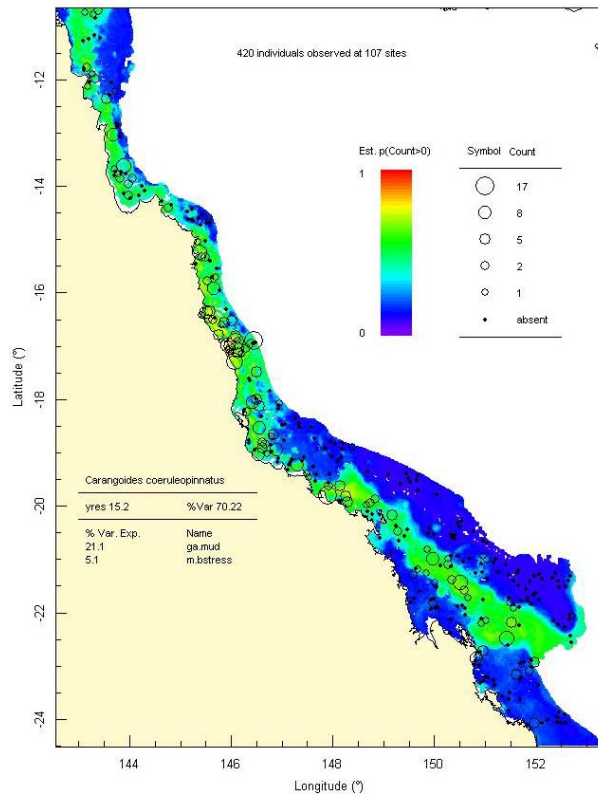
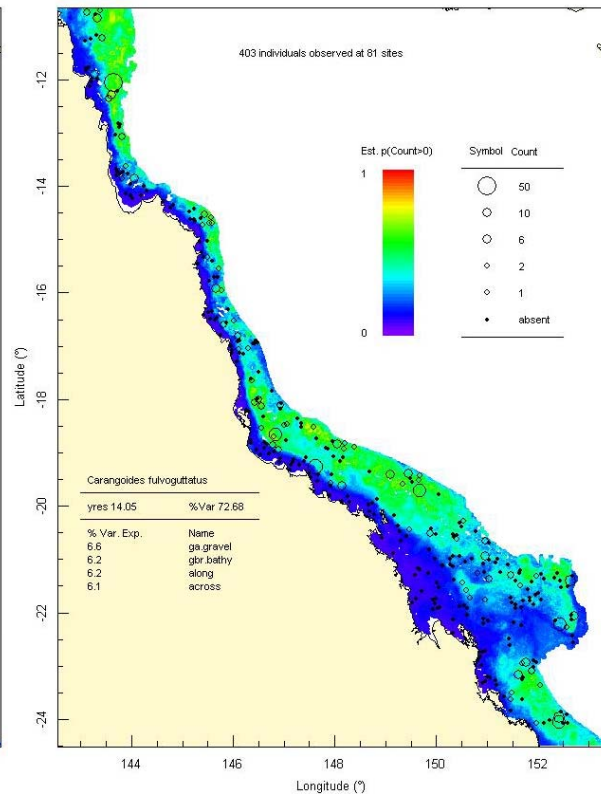
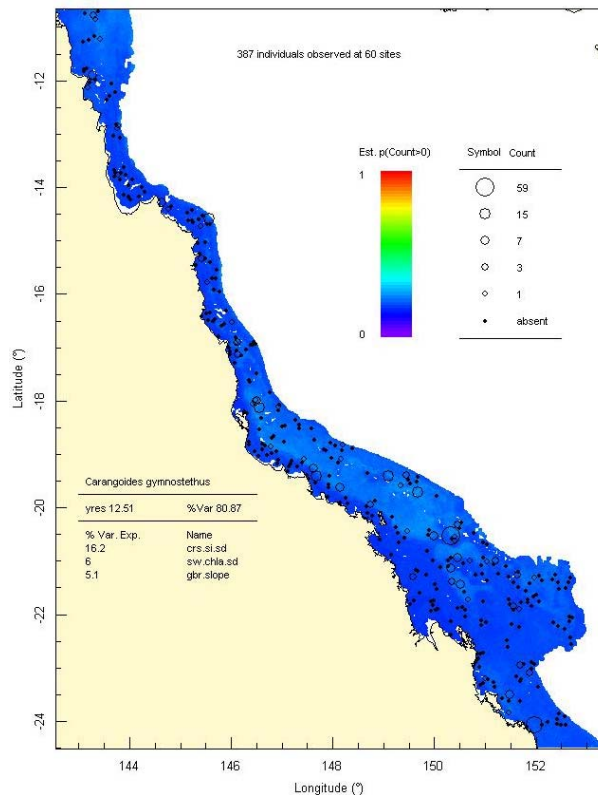
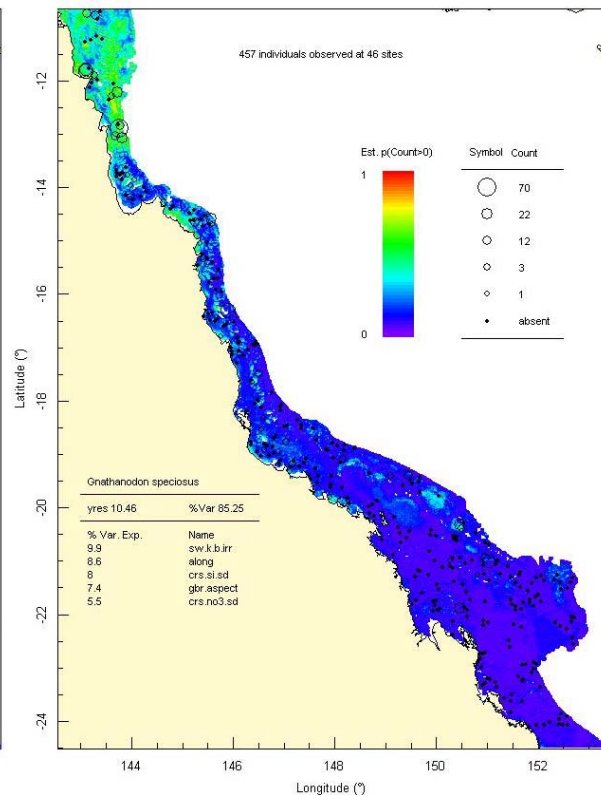
(a) Actinopterygii: *Carangoides coeruleopinnatus*(b) Actinopterygii: *Carangoides fulvoguttatus*(c) Actinopterygii: *Carangoides gymnostethus*(d) Actinopterygii: *Gnathanodon speciosus*

Figure 3-16 Predicted occurrence of the large predatory carangids in the genera *Carangoides* and *Gnathanodon*. Conventions as for Figure 3-11.

High current areas with coarse, gravely sediments and high carbonate produced the highest sightings and predicted occurrence of the Venus Tusk fish, *Choerodon venustus*. This species is known to frequent reef edges and deeper shoals (Figure 3-17).

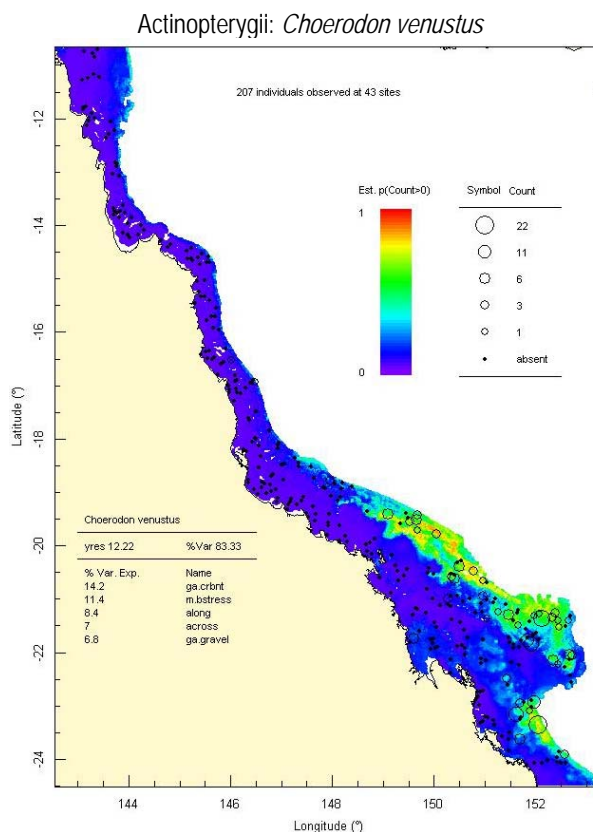


Figure 3-17 Predicted occurrence of the large benthic macrocarnivore *Choerodon venustus*. Conventions as for Figure 3-11.

3.1.3. BRUVS Site-groups Characterization and Prediction

The best 20 predictors and the best 25 responses were selected with the same process described above for the relative abundance (4th root *MaxN*) data obtained from BRUVS. This subset differed slightly in species membership, and was analysed with multivariate trees to allow the definition and biophysical mapping of assemblages in the sampling grid. The aim was to produce maps of assemblages that could be readily interpreted in two dimensions, but reflect also the underlying environmental correlates.

Two scenarios were examined for the top 25 species: a) assemblages defined by only distance along and across the shelf, and b) assemblages defined by all the top 20 environmental covariates.

3.1.3.1. Assemblages defined by location across and along

The top 25 species in the first scenario, and the assemblage groups in which their Dufrene Legendre Indicator (DLI) values were maximised, are shown in Figure 2-26. The best representation of these “spatial only” assemblages for prediction and mapping had 12 terminal nodes that were readily interpreted by distance across and along the shelf, in relation to coastal landmarks at equivalent latitudes (Table 3-4). Six assemblages had no species with DLI maxima, because species comprising these assemblages occurred elsewhere in higher numbers. A large proportion of species were ubiquitous, having maximum DLI in nodes at higher spatial scales. For example, the school mackerel,

Scomberomorus queenslandicus, occurred abundantly in most inshore assemblages along the shelf, so had maximum DLI in the “inshore” node.

A geographical interpretation of the “spatial” assemblages is presented as Figure 3-19, split into the “inshore” and “offshore” groups. Important faunal boundaries can be seen around Bowen and Cape Flattery. Between these break points there are 3 inshore, mid-shelf and outer-shelf groupings evident. This zonation is the “classic” cross-shelf pattern recognised by many authors in previous GBRMP studies. However, north and south of this “central” section the cross-shelf pattern becomes more complex. Offshore in the south, the eastern and western Swains reefs are distinguished from the Pompey's and Whitsunday reefs. Off Bowen, the Gould/Cobham reefs appear to be the western boundary of offshore assemblage “O-Wh”. The adjacent assemblage “O-SRf” is bounded to the west by an extension of Hydrographer’s Passage near the Pompey reefs and to the east by the “TReefs” and Herald’s Prong. Inshore to the south, the macrotidal Whitsunday, Shoalwater Bay and Broad Sound regions have an assemblage separate from the deep Capricorn channel and Curtis Channel stations. The Curtis Channel assemblage is distinct from the Capricorn-Bunker-eastern Swains assemblage. To the north of Cape Flattery both shallow and deep, Cape York and far north, sites can be distinguished in separate assemblages. The narrow channel separating Jewell-Waining reefs from Hicks / Ribbon Reefs consistently appears to be related to this faunal break off Cape Flattery. This is somewhat surprising given the much wider Trinity Opening lies further south.

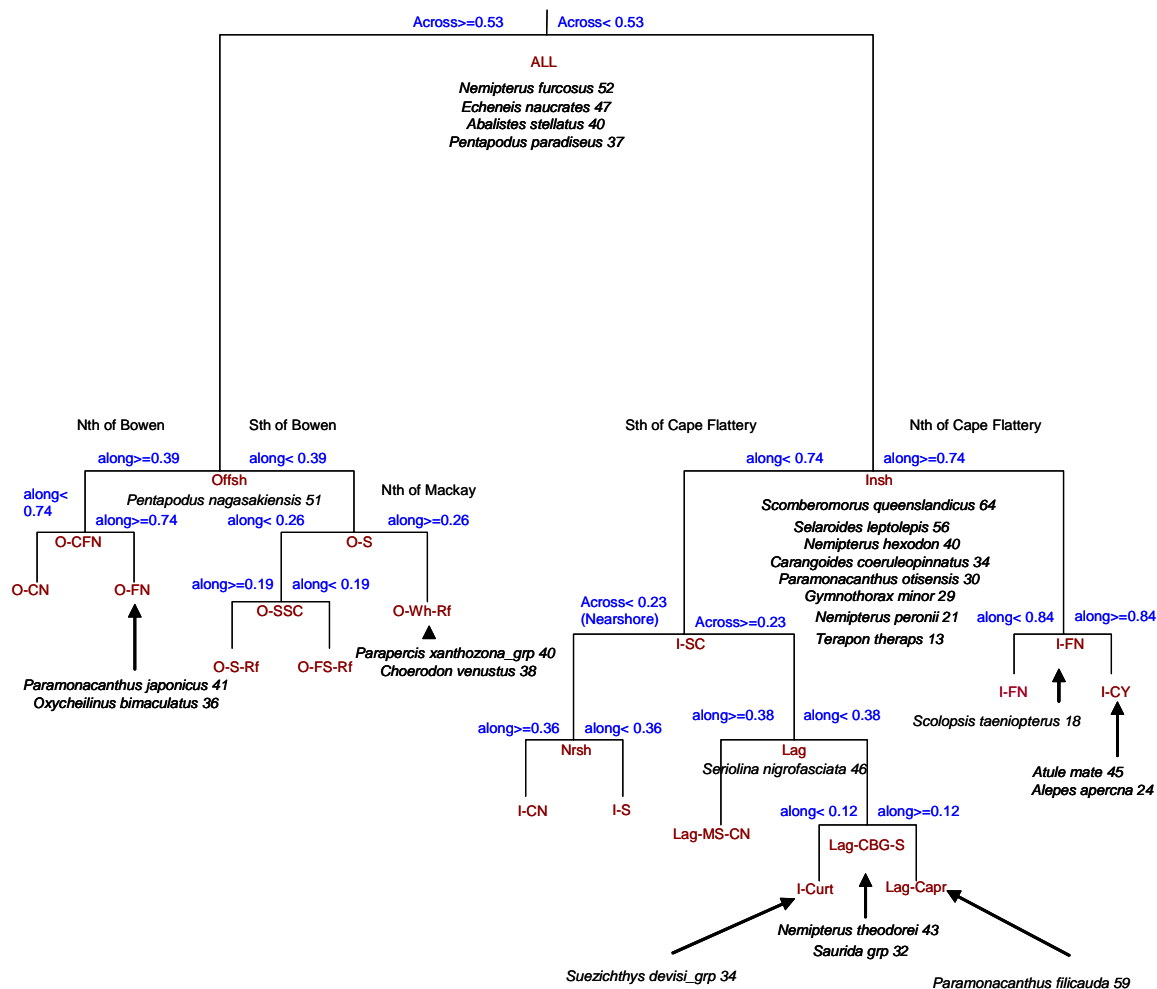


Figure 3-18: Multivariate regression tree analysis defining abundance (transformed by 4th root) of vertebrate assemblages (top 25 species) in terms of location across and along the GBRMP (366 sites). The terminal nodes represent 12 assemblages (see Table 3-4 for definitions of nodes), corresponding with different regions of the GBRMP, and the higher level nodes represent the 11 assemblages at higher spatial scales. The indicator species are shown with the DLI value for nodes where maxima in DLI occurred.

Table 3-4: Hierarchy of nodes in the multivariate tree using location along and across the shelf to represent the location of species assemblages. The number of BRUVS stations and of species with maxima in DLI values are listed for each node. Terminal nodes are in bold font.

| node | abbrvn | split | N sites | Description | Boundary landmarks | DLI |
|------|------------------|--------------------|---------|--|--|-----|
| 1 | All | root | 366 | Entire study area | | 4 |
| 2 | Offsh | across \geq 0.52 | 170 | Offshore | | 1 |
| 4 | O-CFN | along \geq 0.38 | 68 | Offshore, Central to far Northern GBRMP | North of Bowen | |
| 8 | O-CN | along $<$ 0.74 | 53 | Offshore, central-north | between Bowen and Cape Flattery | |
| 9 | O-FN | along \geq 0.74 | 15 | Offshore, far north | between Cape Flattery and Cape Grenville | 2 |
| 5 | O-S | along $<$ 0.38 | 102 | Offshore, Southern | South of Bowen | |
| 10 | O-SSC | along $<$ 0.26 | 71 | Offshore, southern-south-central | South of Mackay | |
| 20 | O-S-Rf | along \geq 0.19 | 20 | Offshore, mid-south, Pompey's and western Swains Reef channels | Mackay to Shaw Island, Whitsundays | |
| 21 | O-FS-Rf | along $<$ 0.19 | 51 | Offshore, eastern Swains channels and Capricorn-Bunker shoals | South of Mackay | |
| 11 | O-Wh | along \geq 0.26 | 31 | Offshore, Whitsunday sector inter-reef | between Bowen and Mackay | 2 |
| 3 | Insh | across $<$ 0.52 | 196 | Inshore | | 8 |
| 6 | I-SC | along $<$ 0.74 | 157 | Inshore, South and Central GBRMP | South of Cape Flattery | |
| 12 | Nrsh | across $<$ 0.23 | 83 | Inshore, nearshore | South of Cape Flattery | |
| 24 | I-CN | along \geq 0.36 | 41 | Inshore, nearshore, central-north section | between Bowen and Cape Flattery | |
| 25 | I-S | along $<$ 0.36 | 42 | Nearshore, south | between Agnes Waters and Bowen | |
| 13 | Lag | across \geq 0.23 | 74 | Inshore, Lagoon | South of Cape Flattery | 1 |
| 26 | Lag-MS-CN | along \geq 0.38 | 37 | Lagoon and mid-shelf, central-north sections | between Bowen and Cape Flattery | |
| 27 | Lag-CBG-S | along $<$ 0.38 | 37 | Inshore, Lagoon | South of Cape Bowling Green | 2 |
| 54 | I-Curt | along $<$ 0.14 | 9 | Curtis Channel | Curtis Channel inshore of Capricorn-Bunker Group | 1 |
| 55 | Lag-Capr | along \geq 0.14 | 28 | Capricorn Channel, lagoon waters | Capricorn Channel to Whitsundays | 1 |
| 7 | I-Nth | along \geq 0.74 | 39 | Inshore, Far North | North of Cape Flattery | |
| 14 | I-FN | along $<$ 0.84 | 21 | Inshore, far north | between Cape Flattery and Cape Sidmouth | 1 |
| 15 | I-CY | along \geq 0.84 | 18 | Inshore, farthest north, Cape York | North of Cape Sidmouth | 2 |

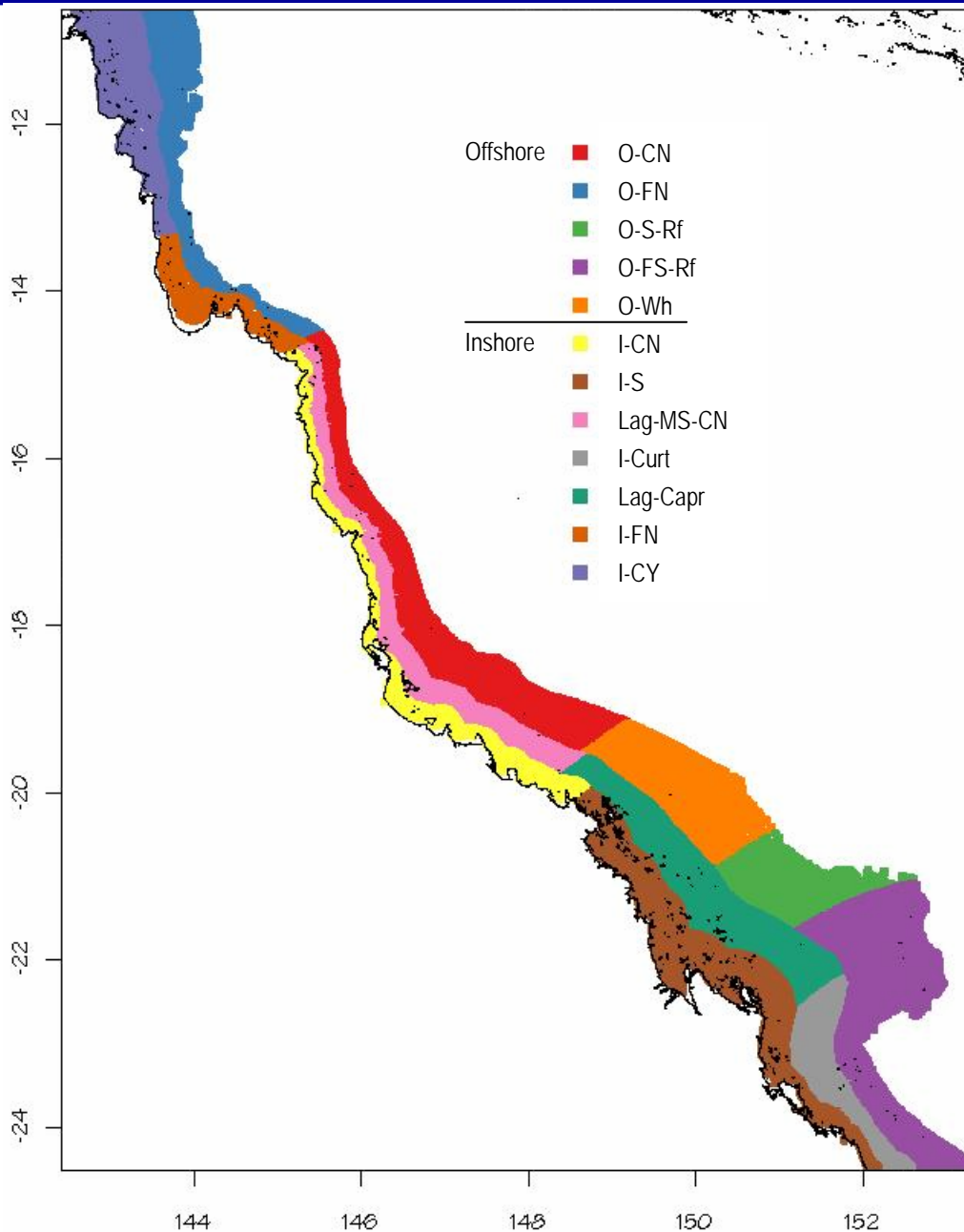


Figure 3-19 Predicted distribution of 12 fish assemblages (terminal nodes from Table 3-4) as defined by the explanatory variables “across” and “along” the shelf.

3.1.3.2. Assemblages defined by influential environmental covariates and location

The second scenario included the top 20 environmental covariates and transformed abundance of the 25 most predictable species. It is notable that only position across and along the shelf, depth, mud, sand and gravel content of the sediments, and silica concentration in the water, predominated in higher nodes of the most parsimonious tree. This tree had 12 nodes also (see Table 3-5 and Figure 3-20).

The location of these 12 fish assemblages is best visualised in inshore and offshore groupings (see Figure 3-21). On the inshore side of the tree, Cape Flattery once again represents a faunal boundary, with shallow assemblages in the far north and off Cape York influenced most by depth, rather than sediment or water column characteristics. The Cape York assemblage had mobile, schooling carangid microcarnivores (*Alepes apercna*, *Atule mate*) with high DLI. Between Cape Flattery and the Palm Islands a widespread assemblage characterised by high mud content of the sediments comprised mid-

shelf regions in the north and lagoonal sites in the south, but there was no evidence from the tree of differences in carbonate levels in the muds of these two regions. Most species in this assemblage were found elsewhere, although the demersal microcarnivore *Scolopsis taeniopterus*, in the family Nemipteridae, had highest DLI there. An assemblage characterised by low mud in the sediments and high silica in the water comprised areas in open, lagoonal waters inside the mid-shelf reefs between about Cardwell and Cape Upstart, and again in the Curtis Channel inside the Capricorn – Bunker group of reefs in the far south.

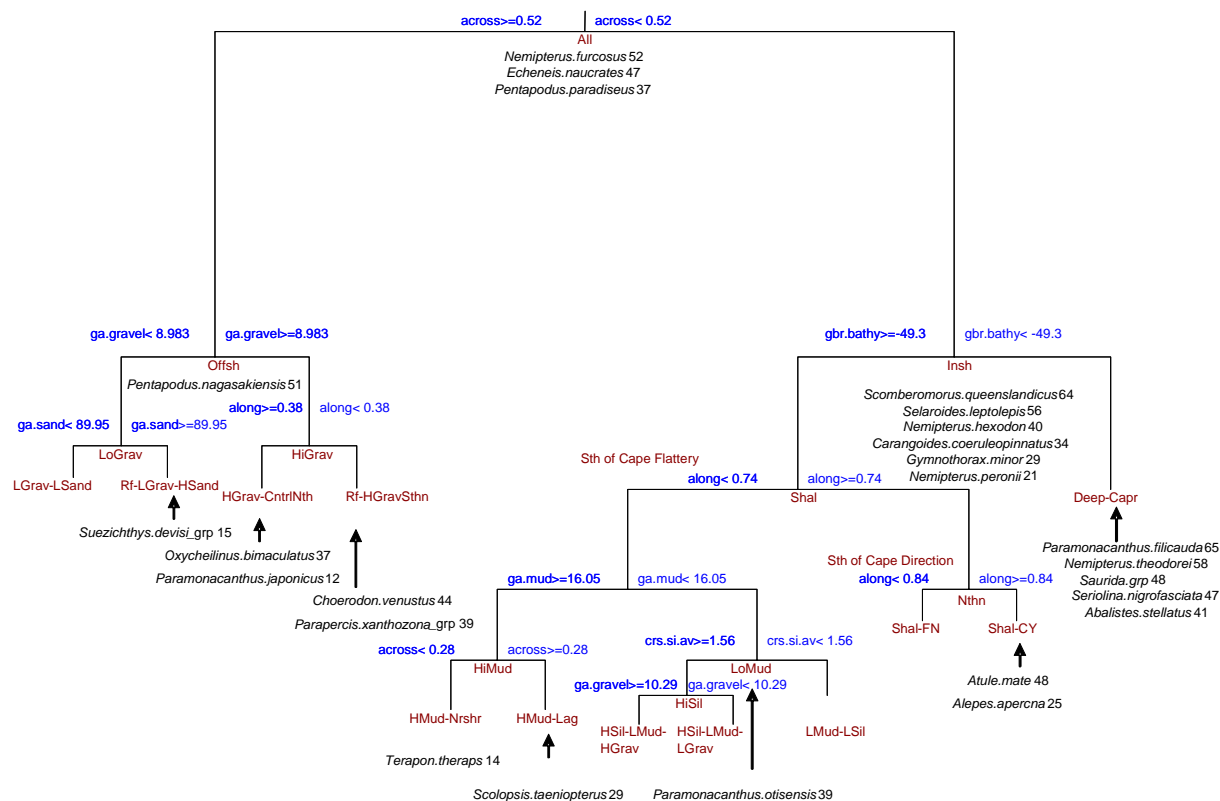


Figure 3-20 Multivariate regression tree analysis defining abundance (transformed by 4th root) of vertebrate assemblages (top 25 species) in terms of the top 20 environmental covariates in the GBRMP (366 sites). The terminal nodes represent 12 assemblages (see Table 3-5 for definitions of nodes), corresponding with various levels of mud, sand, gravel and silica and different regions of the GBRMP. The indicator species are shown with the DLI value for nodes where maxima in DLI occurred.

An assemblage characterised by high mud hugged the nearshore northern coast to the vicinity Bowen, but then showed a notable extension to deeper waters offshore from Mackay and the Shoalwater Bay-Broad Sound region. The small, demersal microcarnivore *Terapon theraps* was an indicator species for this group. It was remarkable to find it restricted to the shallowest nearshore sites in the central section, but then record it in deeper [>40 m] sites far offshore in the southern region outside the macrotidal bays. The high tidal energy in the Shoalwater Bay and Broad Sound was expected to produce scoured demersal habitats with coarse sediments. Indeed, the fish assemblage recognised there was influenced most by high gravel and low mud fractions in the sediments and high silica in the water column. A mix of sites offshore from Gladstone to the Whitsundays was influenced by low mud and low gravel in the sediments and high silica in the water column.

The offshore assemblages (see Figure 3-21) were less distinct spatially. In the eastern Swains Reefs for example there were a mix of three assemblages – two near reefs and one in channels and passes influenced by low gravel and low sand fractions. An assemblage near reefs in the southern region is influenced by high gravel, with DLI indicator species the Venus Tuskfish (*Choerodon venustus*), a large carnivore of benthic invertebrates, and *Parapercis xanthozona_grp*, a small ambush predator. Some adjacent sites in areas of high sand and low gravel, such as channels and passes, form a separate assemblage with the small wrasse *Suezichthys devisi_grp* being the sole indicator species. In the

central-north, north of about Bowen, an assemblage defined by high gravel offshore has two indicator species – the small wrasse, *Oxycheilinus bimaculatus*, and the small monacanthid *Paramonacanthus japonicus*. These species were often seen on video footage from sites with much marine plant growth.

The most distinctive assemblage, in terms of number of indicator species and spatial restriction, occurred in the deep Capricorn Channel northward into deeper lagoonal waters below 49 m. The indicator species there were from a variety of functional groups: the small schooling *Paramonacanthus filicauda*, which was restricted almost solely to sites south of Cape Upstart in BRUVS footage; the benthic microcarnivore *Nemipterus theodori*, again mainly a southern species; the ambush predator *Saurida*_grp; the mobile semi-pelagic predator *Seriolina nigrofasciata*; and the demersal omnivorous triggerfish *Abalistes stellatus*.

Table 3-5 Hierarchy of nodes in the multivariate tree using spatial and environmental covariates to represent the location of species assemblages. The number of species with maxima in DLI values are listed for each node. Terminal nodes are in bold font.

| node | abbrvn | split | N sites | Description | Boundary Landmarks | DLI |
|------|------------------------|------------------|---------|--|--|-----|
| 1 | All | root | 366 | | | 3 |
| 2 | Offsh | across>=0.52 | 170 | More than halfway across the shelf | | 1 |
| 4 | LoGrav | ga.gravel<8.98 | 84 | Low gravel, offshore | | 0 |
| 8 | LGrav-LSand | ga.sand<89.94 | 64 | low sand, low gravel, offshore | | 0 |
| 9 | Rf-LGrav-HSand | ga.sand>=89.94 | 20 | High sand, low gravel, near reefs | Offshore reefs, mostly southern - to north | 1 |
| 5 | HiGrav | ga.gravel>=8.98 | 86 | High gravel, offshore | | 0 |
| 10 | HGrav-CntrlNth | along>=0.38 | 31 | Offshore, High gravel, | Cape Upstart – Cape Melville | 2 |
| 11 | Rf-HGrav-Sthn | along<0.38 | 55 | Offshore, high gravel, southern region | Near reefs offshore between Bowen and Capricorn-Bunker group | 2 |
| 3 | Insh | across<0.52 | 196 | Less than halfway across the shelf | | 6 |
| 6 | Shal | gbr.bathy>=-49.3 | 164 | Under 49 metres depth | | 0 |
| 12 | Sth-Cntrl | along<0.74 | 125 | | South of Cape Flattery | 0 |
| 24 | HiMud | ga.mud>=16.04 | 70 | | | 0 |
| 48 | HMud-Nrshr | across<0.28 | 48 | Nearshore, high mud | Cape Flattery to Gladstone | 1 |
| 49 | HMud-Lag | across>=0.28 | 22 | Lagoon region, high mud | Cape Flattery to Palm Islands | 1 |
| 25 | LoMud | ga.mud<16.04 | 55 | | | 1 |
| 50 | HiSil | crs.si.av>=1.56 | 29 | | | 0 |
| 100 | HSil-LMud-HGrav | ga.gravel>=10.29 | 12 | High gravel, Low mud, High Silica | Shoalwater Bay to Broad Sound | 0 |
| 101 | HSil-LMud-LGrav | ga.gravel<10.29 | 17 | Low gravel, Low mud, High Silica | Whitsundays to Gladstone | 0 |
| 51 | LMud-LSil | crs.si.av<1.56 | 26 | Low Mud, Low Silica | Cardwell to Curtis Channel | 0 |
| 13 | Nthn | along>=0.74 | 39 | | | 0 |
| 26 | Shal-FN | along<0.84 | 21 | Shallow, far northern region | Cape Sidmouth [Princess Charlotte Bay] to Cape Flattery | 0 |
| 27 | Shal-CY | along>=0.84 | 18 | Shallow, tip of Cape York | North of Cape Direction to tip | 2 |
| 7 | Deep-Capr | gbr.bathy<-49.3 | 32 | | Capricorn Channel | 5 |

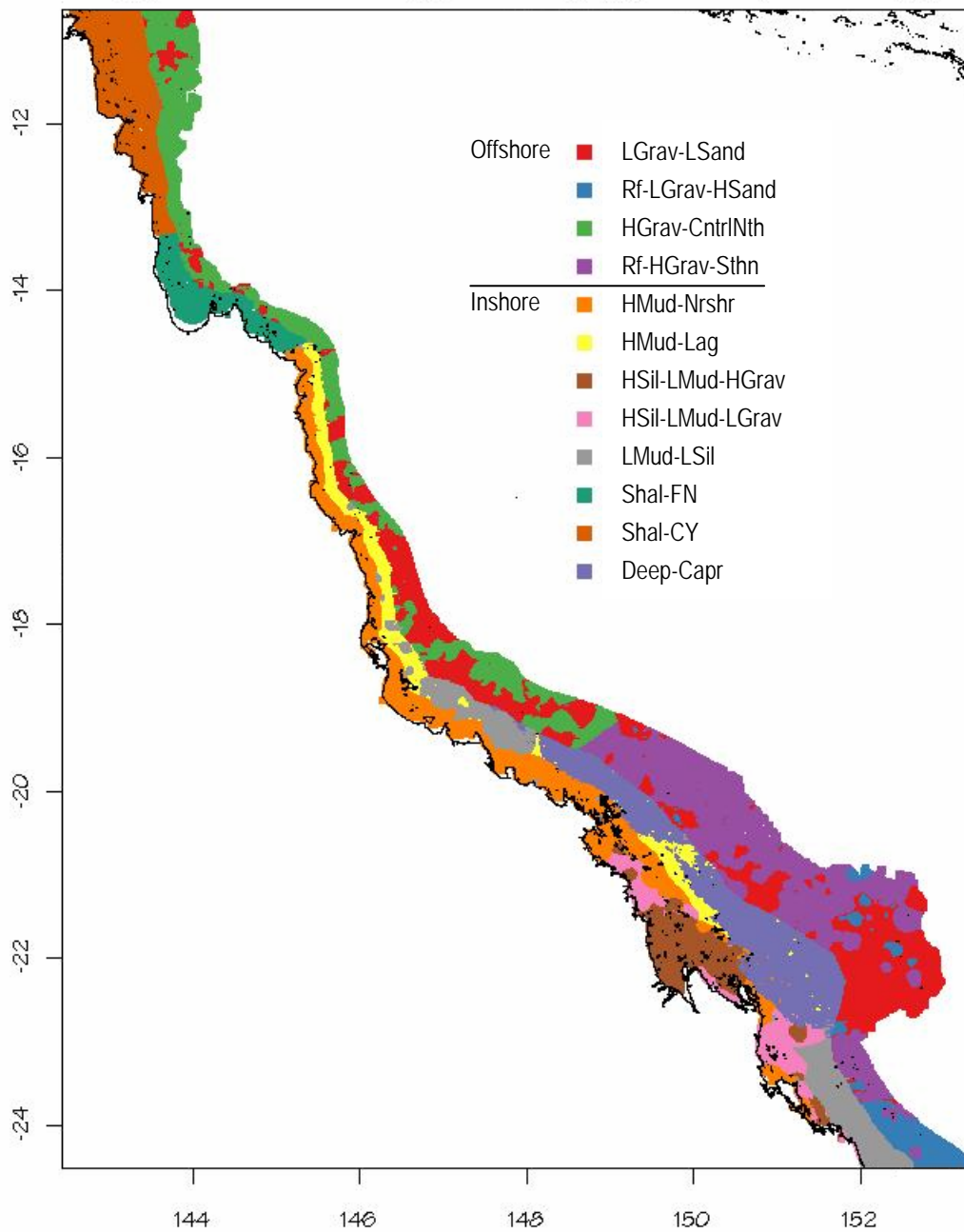


Figure 3-21 Predicted distribution of 12 fish assemblages (terminal nodes from Table 3-5) as defined by the top 20 explanatory environmental variables and location.

3.2. SINGLE SPECIES, BIOPHYSICAL MODELS AND PREDICTION

The GBR epibenthic sled dataset comprised 70,860 site-by-species records of 4,723 species (OTUs) from 1,190 sites. The sled biota were from more than 15 phyla of marine plants, invertebrates and vertebrates (Table 3-6). Taking into account that sorting of hydroids, annelids, crinoids and ascidians was not completed due to resourcing, this was a highly diverse biota dominated by sponges, molluscs, crustaceans, fishes, echinoderms, corals, bryozoans and algae (Table 3-6).

The GBR research trawl dataset comprised 39,702 site-by-species records of 3,510 species (OTUs) from 457 sites. The trawl biota were from more than 12 phyla of marine plants, invertebrates and vertebrates (Table 3-6). Taking into account that sorting of hydroids, annelids, crinoids, ascidians and marine plants was not completed due to resourcing, this was also a very diverse biota, in this case dominated by fishes, sponges, crustaceans, molluscs, echinoderms, corals, bryozoans and algae (Table 3-6).

Table 3-6: Number of OTUs by Phyla sampled by the epibenthic sled and research trawl, and in the merged dataset.

| Phylum | Sled OTUs | Phylum | Trawl OTUs | Phylum | Merged OTUs |
|---------------|-----------|---------------|------------|---------------|-------------|
| Porifera | 952 | Chordata | 993 | Porifera | 1121 |
| Mollusca | 913 | Porifera | 768 | Mollusca | 1036 |
| Arthropoda | 575 | Arthropoda | 410 | Chordata | 869 |
| Chordata | 563 | Mollusca | 401 | Arthropoda | 589 |
| Echinodermata | 443 | Echinodermata | 374 | Echinodermata | 509 |
| Cnidaria | 435 | Cnidaria | 358 | Cnidaria | 375 |
| Bryozoa | 361 | Bryozoa | 117 | Bryozoa | 321 |
| Rhodophyta | 210 | Chlorophyta | 31 | Rhodophyta | 214 |
| Chlorophyta | 152 | Annelida | 18 | Chlorophyta | 167 |
| Phaeophyta | 47 | Rhodophyta | 17 | Phaeophyta | 54 |
| Magnoliophyta | 18 | Phaeophyta | 11 | Annelida | 29 |
| Annelida | 17 | Magnoliophyta | 3 | Magnoliophyta | 18 |
| Brachiopoda | 15 | | | Brachiopoda | 15 |
| Cyanophyta | 8 | | | Cyanophyta | 8 |
| Hemichordata | 2 | | | Hemichordata | 2 |

For analyses, the sled and trawl datasets were merged. This required the reconciliation of synonymous OTUs between the two devices and taking all OTUs up to a common taxonomic level at which sorting and identification was consistent among the different laboratories. This merged reconciled dataset comprised 121,334 site-by-species records of 5,344 species (OTUs) from both Sled and Trawl sampled sites (Table 3-6). Of these species, 2,435 were unique to the sled, 1,085 were unique to the trawl and 1,824 were common to both devices.

The relative sampling rates per swept area of the two devices also differed markedly among different biota. The swept area of the sled was ~0.03 Ha and that of the research trawl was ~1.02 Ha, but when samples from both were each scaled to a per Ha basis, the sled had higher sampling rates for most biota, except crustaceans for which the sampling rates were similar, fishes for which the trawl sampling rate was >7-fold greater than the sled, and elasmobranchs, which were not well sampled by the prawn trawl but hardly at all by the sled (Table 3-7).

Table 3-7: Overall total and mean sampling rates (g per Ha) for the major Phyla sampled by the epibenthic Sled and research Trawl, indicating overall composition and relative catchability. Ratio shows the trawl sampling rate relative to the sled.

| Sled | | | | | Trawl | | | | | |
|---------------|-------------|------|--------|-------|---------------|------------|-----|--------|--------|-------|
| Group | Sum_Wt (g) | N | Mean | % | Group | Sum_Wt (g) | N | Mean | Ratio | % |
| Green algae | 35,905,360 | 1187 | 30,249 | 19.54 | Fishes | 4,789,876 | 457 | 10,481 | 7.27 | 39.56 |
| Sponges | 32,617,604 | 1187 | 27,479 | 17.75 | Sponges | 2,235,381 | 457 | 4,891 | 0.18 | 18.46 |
| Echinoderms | 24,609,197 | 1187 | 20,732 | 13.39 | Echinoderms | 2,040,998 | 457 | 4,466 | 0.22 | 16.86 |
| Ascidians | 18,986,710 | 1187 | 15,996 | 10.33 | Crustaceans | 937,739 | 457 | 2,052 | 1.04 | 7.74 |
| Red algae | 16,791,467 | 1187 | 14,146 | 9.14 | Molluscs | 891,499 | 457 | 1,951 | 0.18 | 7.36 |
| Cnidarians | 16,039,343 | 1187 | 13,513 | 8.73 | Cnidarians | 507,847 | 457 | 1,111 | 0.08 | 4.19 |
| Molluscs | 12,599,413 | 1187 | 10,615 | 6.86 | Ascidians | 441,504 | 457 | 966 | 0.06 | 3.65 |
| Bryozoans | 12,193,301 | 1187 | 10,272 | 6.63 | Elasmobranchs | 181,258 | 457 | 397 | 132.21 | 1.50 |
| Seagrasses | 5,410,059 | 1187 | 4,558 | 2.94 | Bryozoans | 79,669 | 457 | 174 | 0.02 | 0.66 |
| Brown algae | 3,426,676 | 1187 | 2,887 | 1.86 | Worms | 2,344 | 457 | 5 | 0.01 | 0.02 |
| Crustaceans | 2,348,077 | 1187 | 1,978 | 1.28 | TOTAL | 12,108,115 | | | | |
| Fishes | 1,710,445 | 1187 | 1,441 | 0.93 | | | | | | |
| Worms | 1,139,923 | 1187 | 960 | 0.62 | | | | | | |
| Elasmobranchs | 3,629 | 1187 | 3 | 0.00 | | | | | | |
| TOTAL | 183,781,203 | | | | | | | | | |

3.2.1. Sled and Trawl samples species richness

As is typical of benthic sampling, most of the species recorded were rare or uncommon, occurring in only a very small percentage of the sites surveyed. Most of the Sled species (~95%) were recorded in less than 5% of Sled sites; 1,347 OTUs (~29%) were recorded at only one site, 1,571 OTUs (~33%) were recorded at only 2-5 sites (Figure 3-22a). Only <1% of the species were prevalent at more than $\geq 20\%$ of the sites and, of these, only 5 species had a prevalence $>50\%$. Similarly, most of the Trawl species (~92%) were recorded in less than 8% of Trawl sites; 1,059 OTUs (~30%) were recorded at only one site, 1,213 OTUs (~35%) were recorded at only 2-5 sites (Figure 3-23a). Only ~2.5% of the species were prevalent at more than $\geq 20\%$ of the sites and, of these, only 2 species had a prevalence $>50\%$. The implications for analysis were that a relatively small proportion of the biota were abundant enough for analyses: only 850 species occurred at more than 25 sites, which was considered adequate for developing biophysical models for predicting broad-scale distributions without over-fitting.

There was an average of 59.5 ± 44.2 (s.d.) species per Sled site, ranging from 1 to 268. Ordering of the most diverse sites produced a sigmoid curve (Figure 3-22b). About 50% of the sites had high species richness (≥ 50 species per site), ~43% had moderate richness and only <7% had relatively low richness (≤ 10 species). Similarly, there was an average of 86.7 ± 30.9 (s.d.) species per Trawl site, ranging from 6 to 193. Ordering of the most diverse sites produced a sigmoid curve (Figure 3-23b). More than 90% of the sites had high species richness (≥ 50 species per site), ~9% had moderate richness and only <1% had relatively low richness (≤ 20 species). While the Sled had greater total species richness, it was more variable than the Trawl, which consistently sampled a representative number of species though it accumulated fewer species in total.

There were some clear spatial patterns in species richness of the Sled samples (Figure 3-24). Areas of high richness included the offshore Halimeda beds north of Princess Charlotte Bay and near Lizard Island, the *Halophila spinulosa* seagrass beds near the Turtle Island Group and in the Capricorn Region, the mixed algal-seagrass beds in the mid-shelf off Townsville extending north almost to Cairns, high current areas near Broad Sound/Shoalwater Bay, Torres Strait, Whitsunday Passage and offshore passages, most outer shelf areas including the Swains. Areas of low richness included most inshore and muddy areas, with lowest richness in the deep muddy entrance to the Capricorn Channel.

The spatial patterns in species richness of the Trawl samples were similar, though less clear due to the lower density of sampled sites and difficulty of sampling in more structured habitats (Figure 3-25).

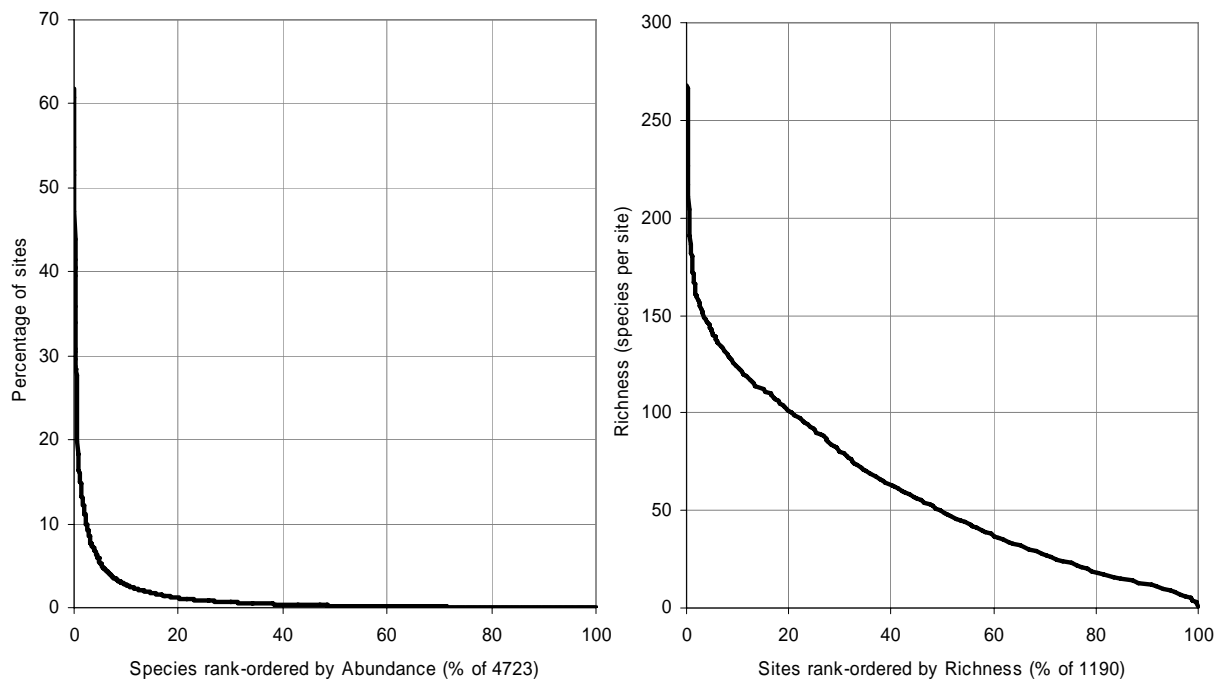


Figure 3-22: Patterns of prevalence and richness of 4,723 species at 1,190 Sled stations.

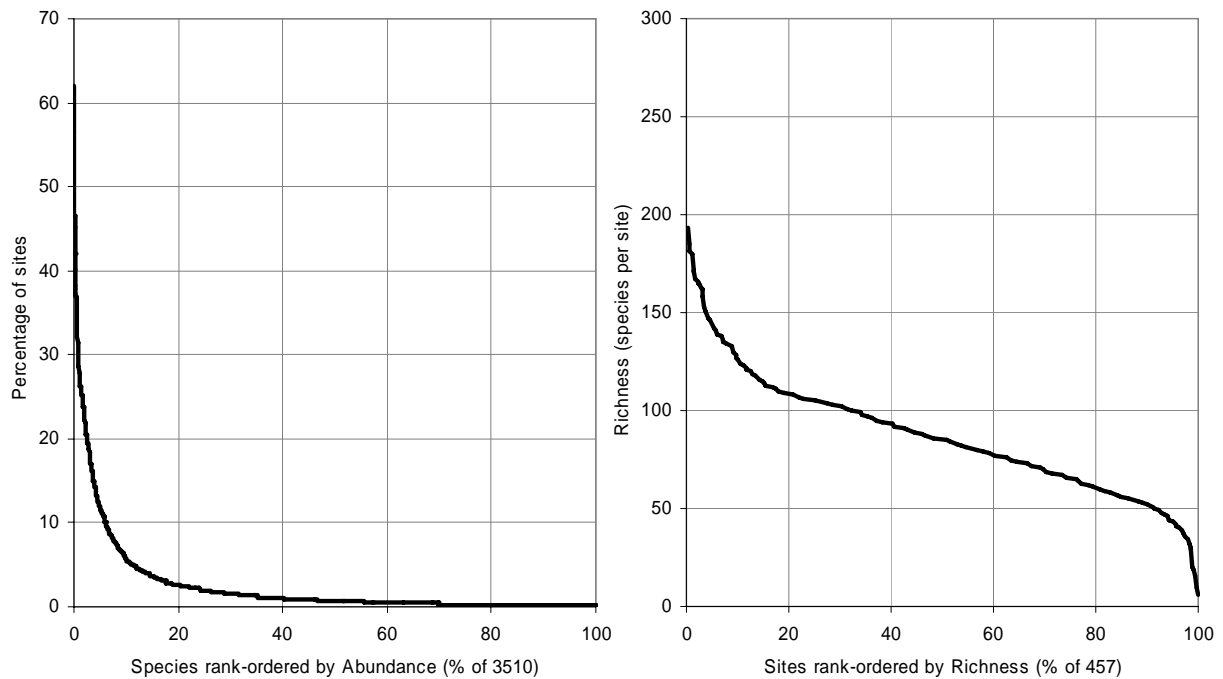


Figure 3-23: Patterns of prevalence and richness of 3,510 species at 457 Trawl stations.

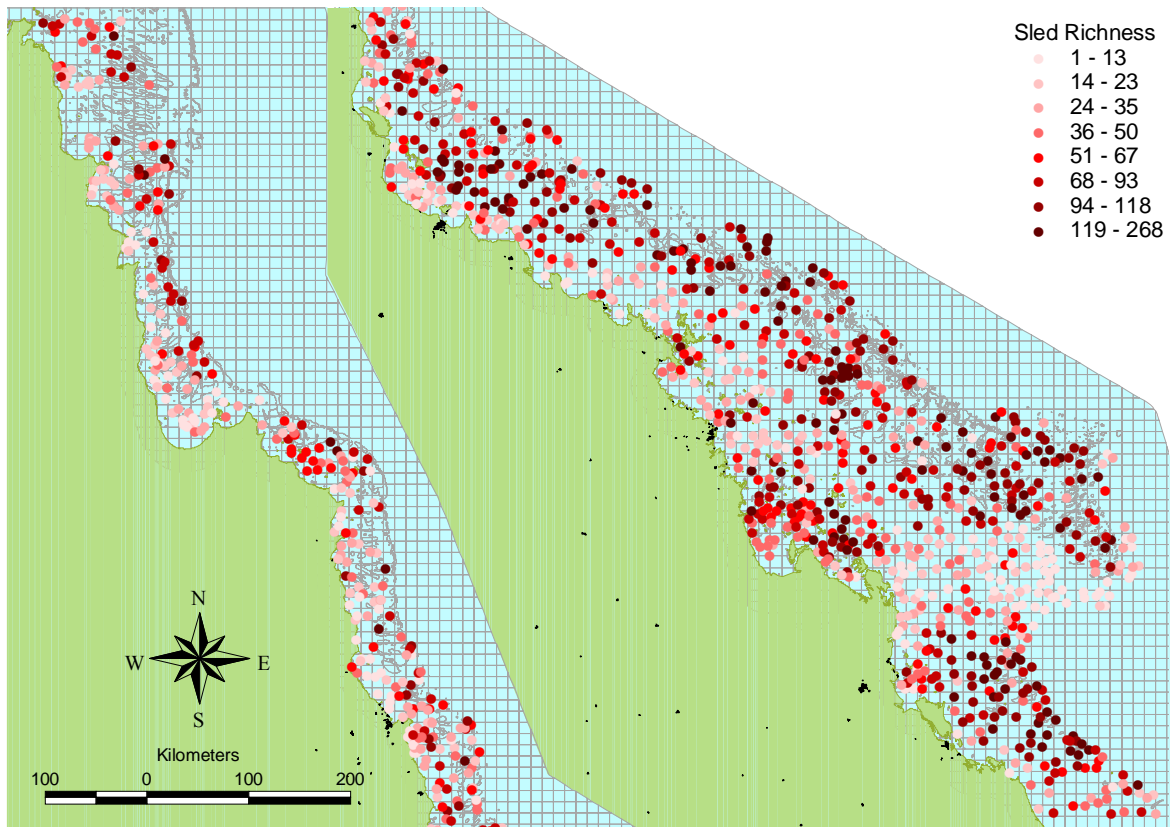


Figure 3-24: Species richness from epibenthic Sled data by location in the GBRMP.

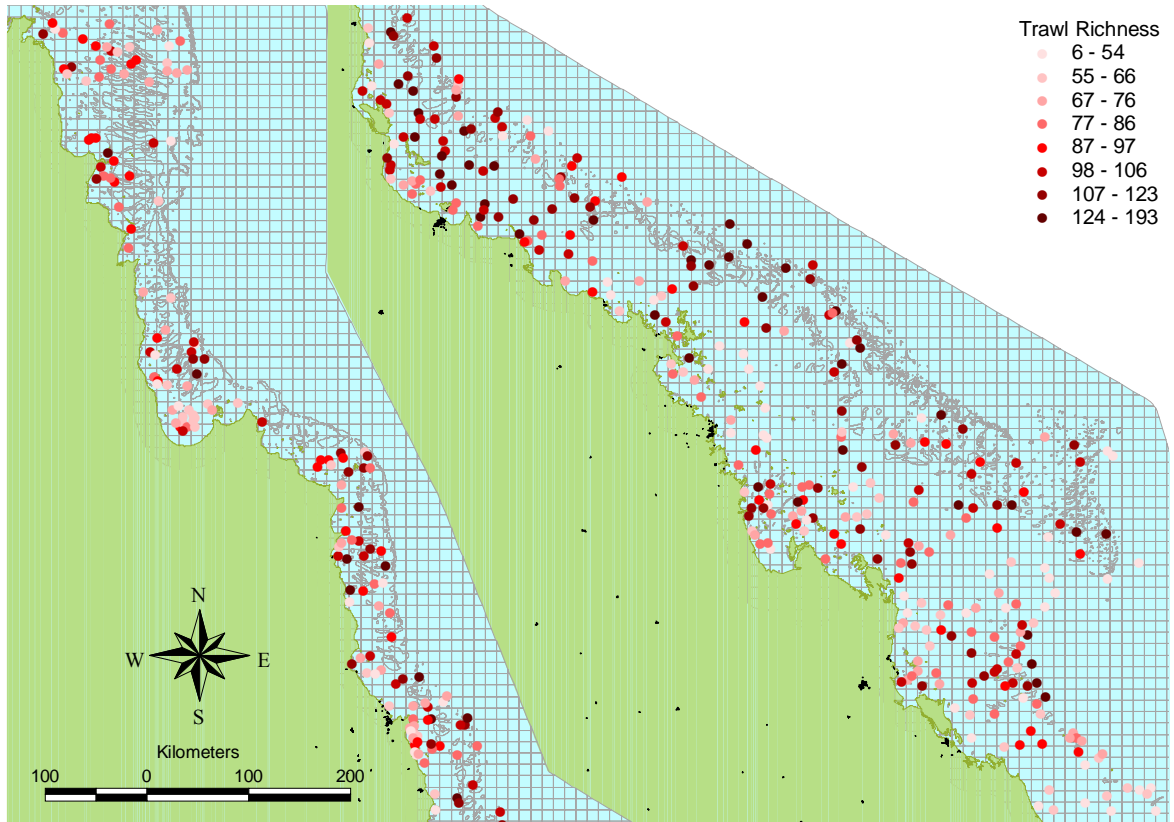


Figure 3-25: Species richness from research Trawl data by location in the GBRMP.

3.2.2. Single species models (M Browne & R Pitcher)

Single species distribution models and maps were generated for the 851 species that were observed at >25 sites. Species observed at less than 25 sites were considered to possess inadequate sample power to adequately estimate the array of measurement, temporal, physical and spatial effects considered in this study. Figure 3-26 provides just one of many possible examples of a single-species data / model / map summary, in this case for the relatively prevalent species Class: Actinopterygii, Family: Platycephalidae, *Elates ransonnetii*. In the upper left-hand side of the plot there are notes on the basic survey counts and weights. In this case, a total of 14.9 kg of the species was sampled with the scientific trawl at 94 locations and 100 g with the sled at 5 sites. In this case, the data from both the trawl and sled samples was included in the modelling.

A number of circles have been plotted on the distribution map to indicate the relative size of the raw sample weights at each of the survey sites. The area of the circle is directly proportional to the quantity of biomass observed, but the relative scale of circles was necessarily different for each species. The table on the right hand side of the map provides a key to interpret the biomass catch circles. The first column indicates the percentile of the biomass-only data set, the second indicates the corresponding circle size, and in the final column is the corresponding biomass. Note that the biomass circle overlay was provided to complement the model information, and does not indicate any modelling on the data, and are not standardized in any way (e.g. in order to compensate for covariate effects).

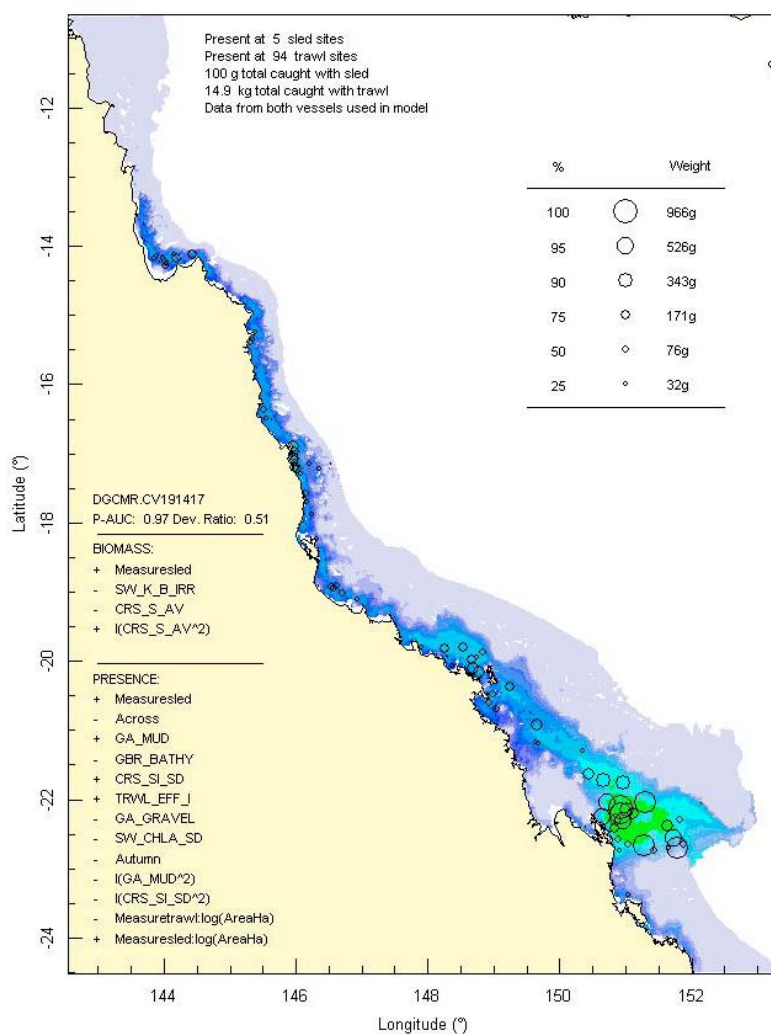


Figure 3-26: Example of a single species distribution map, for the Platycephalid fish, *Elates ransonnetii*.

Information about the model is provided in each single species map in three ways. Firstly, model estimates over the entire GBR region are shown. As stated previously, the model estimates reflect an inference based on the pattern of observed presence / biomass, considering the physical and spatial relationships, while controlling for temporal / measurement effects. Since the generated model-map is independent of temporal effects (such as time of year) it might correctly estimate a high prevalence in areas where nothing was actually caught, if this absence can be well explained by (for example) season and the physical and spatial properties of that area in question are similar to areas where the species was actually found to be abundant.

In the bottom left corner of the map is a list of variables chosen by the stepwise variable selection procedure with BIC criterion. For both stages, biomass and presence, the list of included variables is provided. The +/- signs indicate either a positive or negative relationship between the variable and either the probability of presence or log-biomass. In the example shown in Figure 3-26, the variable +GA_MUD (indicating percentage mud fraction) appears twice in the presence / absence model, with a positive linear effect and a negative quadratic effect (indicated by $-I(GA_MUD^2)$). This indicates that there is a non-linear relationship between mud fraction and species presence — the probability of observing this species first increases and then decreases with larger mud fraction. The P-AUC and Dev.Ratio relate to model performance and are described below.

3.2.2.1. Estimates of model performance: AUCs and ROCs

The confidence that should be placed in the modelled distribution map is naturally related to the degree of model fit. Two measures of model performance are provided on the left hand side of each map just below the species code. They are Presence / Absence: Area Under the Curve (P-AUC) and Biomass: Deviance Ratio (Dev.Ratio). These measures of model performance relate to the two stages of the modelling procedure and capture how well the model estimated whether a species is likely to be present or not, and the biomass given that the species was present. Both measures are calculated by comparing model estimates on the sites that were visited with the actual catch on those sites. It was somewhat difficult to quantify robustly the quality of the fit of the biomass component of the models because the data was distributed approximately log-normally and standard measures such as linear correlation do not apply. The deviance ratio, or relative deviance explained, was calculated as $1 - \text{residual deviance} / \text{null deviance}$ of the biomass models, which yielded a standardised variance ratio statistic, interpretable similar to that of a correlation as the proportional reduction in deviance explained by the biomass stage of the model. However, this statistic is intended as a rough guide to performance only.

The P-AUC was a little more difficult to describe concisely, but is a popular and well-regarded method for threshold-independent assessment of classifier performance. The P-AUC is calculated from the Receiver Operating characteristic Curve (ROC) which itself is a non-parametric summary of how a classifier responds given a list of target decisions (in this case actual observed presence-absence or 0-1 data), and an associated estimator output (in this case, the probability of presence model estimate p). The presence-absence data may be ranked so that estimate p is ordered from largest to smallest. The ROC is generated by starting at the bottom left corner of a $[0,1]$ box and proceeding through the ordered presence-absence data. Each time a 'presence' is encountered the curve moves up by $1/N$, each time an absence is encountered the curve moves right by $1/M$, where N and M are the number of presences and absences, respectively. A well-performing presence-absence model will have the 'presences' grouped towards the beginning of the list ordered from largest to smallest probability, and therefore tend to move up before moving right towards $[1,1]$. The area under the ROC (i.e. AUC) will therefore tend toward 1 as performance becomes perfect. A poorly performing estimator will move approximately diagonal from $[0,0]$ to $[1,1]$ and will therefore tend have an area of approximately 0.5. Figure 3-27 displays the ROC for the species in the previous distribution map example. The ideal predictor of presence-absence given the available variables is located at the intersection of the red lines, indicating that it would correctly predict this species to be present at 91% of the sites at which it was actually observed, and incorrectly estimate it to be present at 4% of sites at which it was not

actually observed. By standard interpretation guidelines of ROC and AUC, this is usually considered rather good estimation performance.

The median AUC observed for all species was 0.844, which indicates that overall, the models were relatively successful in explaining the presence or absence of species given the explanatory variables. The 25% and 75% quantiles of the AUC measure for all species were 0.785 and 0.894, indicating that reasonable to good performance was obtained on at least 75% of species considered. However, it is important to note that there was considerable variation in model performance: the presence distributions of some species were estimated very well, while that of others could not be explained adequately given the explanatory variables. Therefore, the model and associated map for each individual species should be evaluated. For the estimates of biomass where present, the median relative deviance explained was 0.315, with the lower and upper quartiles (25%, 75%) being 0.136 and 0.482 respectively, but for 132 species none of the deviance could be explained by the given models for biomass where present. Thus, summarizing over all species, while it was possible to explain some of the variation in biomass, a significant proportion of variability could not be explained given the input data. Although the two stages in the modelling procedure are qualitatively different and cannot be directly compared, it may be argued that the presence / absence of a species in an area can be estimated with more certainty than the likely biomass observed, given that it is present.

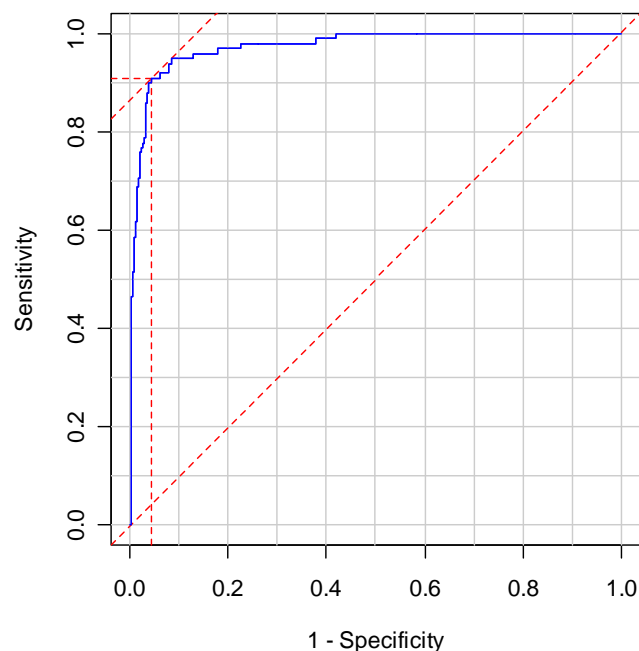


Figure 3-27: ROC curve for presence-absence estimation of *Actinopterygii: Elates ransonnetii*. As noted in the previous figure, this ROC has an AUC of 0.97

If desired, it is possible to weight the vertical ROC step size by another variable, about which information was available. In this case, weighting the ‘presence’ step sizes (going vertical on the ROC) by the actual biomass of the species measured at that site was considered. Instead of each vertical step being equal ($1/N$), the vertical steps were weighted proportional to the biomass observed at that site. Considering only the sites at which a species was actually observed, if a presence-absence model was more likely to correctly classify a site with relatively high biomass than one with a relatively low biomass, then the weighted AUC (P_AUCW) would be larger than the unweighted AUC. It may be argued that high biomass sites should be more likely to be closer to the centre of species preferred habitat range, then the P_AUCW should be higher than the AUC for any given species. From this point of view, comparing the P_AUCW to the AUC represents an independent validation of model efficacy, since the biomass ‘weightings’ were not incorporated in any way to the construction of the presence-absence models.

Figure 3-28 compares weighted versus unweighted AUCs for all species. Overall, the mean P_AUCW (0.851) was significantly higher than the mean AUC (0.837), with $t = 4.7$. This means that over all species, sites with high observed biomasses were relatively more likely to be correctly classified as a 'presence' than sites with low observed biomass. This was in accordance with expectations and was taken as an independent indication that the presence / absence models were performing properly. This can be explored further as noted from Figure 3-28 that the P_AUCWs tended to be relatively higher when the AUC was relatively high (e.g. > 0.9). Of the low to moderately highly effective models (those with an AUC < 0.9), the P_AUCW $>$ AUC 61% of the time. Of the highly effective models (AUC > 0.9), the P_AUCW $>$ AUC 81% of the time. Finally, it can be demonstrated explicitly that models with high AUC will tend to have a higher P_AUCW by transforming both of these logistically distributed variables so to have approximately normal distributions via the logit link:

$$g(x) = \log\left(\frac{x}{1-x}\right)$$

and modelling the transformed P_AUCW as a linear function of the transformed AUC. We establish that the slope of $g(\text{P_AUCW})$ with respect to $g(\text{AUC})$ is 1.24 (SD= 0.027) which is significantly higher than the null hypothesis (i.e. that the slope = 1), with $t = 8.59$. Thus, not only do P_AUCW tend to be higher than AUC overall, but stronger models tend to have relatively higher P_AUCW. This was again consistent with the view that high biomass sites ought to conform, on average, more strongly with characteristics associated with species presence. Stronger models should better reflect the underlying relationship of covariates to biomass, and this explains why the differential between AUC and P_AUCW should be stronger for stronger models. In summary, the overall strong presence / absence modelling results, as well as the meta-analyses conducted on the AUC and P_AUCW statistics, show quite strong support for the modelling effectiveness.

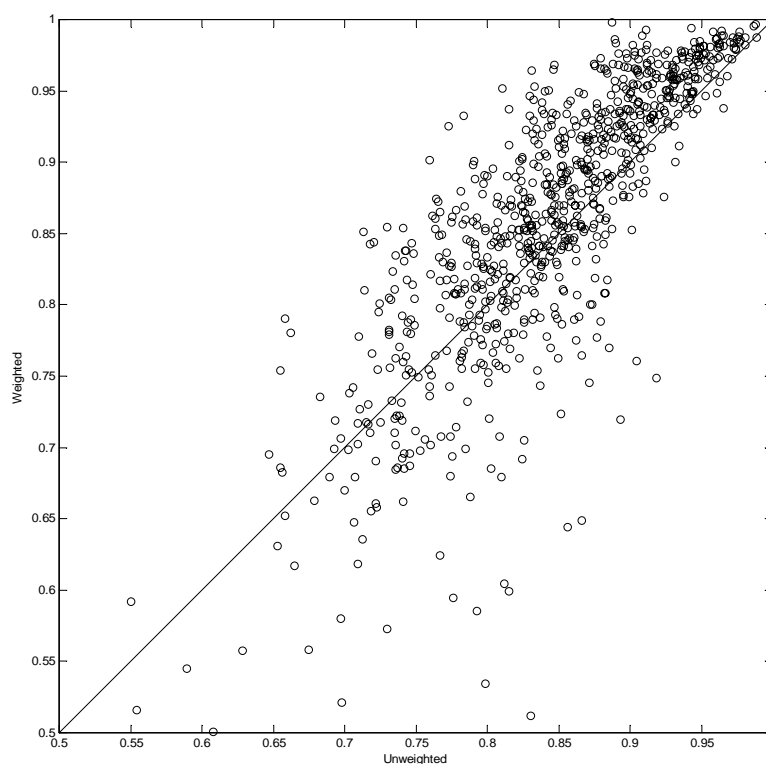


Figure 3-28: Scatter plot of the weighted versus unweighted AUCs for all species.

Having demonstrated that weighted AUC provided a more sensitive diagnostic of model performance against sampled biomass, the performance of all species model fits was examined for both the weighted AUC of the presence model and the deviance ratio of the biomass model at all sites (Figure 3-29). The presence model weighted AUC (P_AUCW) was > 0.75 for 699 of 838 species modelled

(~83%) with a median of 0.87, which represents good agreement between the actual samples and the model predictions for the majority of species. The deviance ratio was >0.3 for 439 of 838 species modelled (~52%) with a mean of 0.32, which represents reasonable agreement between the actual sample biomass and the model predictions for many species, though 15% of models could do no better than the grand mean where present. There was some correspondence between the presence model weighted AUC and the biomass model deviance ratio ($p=0.001$, Figure 3-30). However, there was no indication that frequency of occurrence had a strong influence on model performance (Figure 3-30).

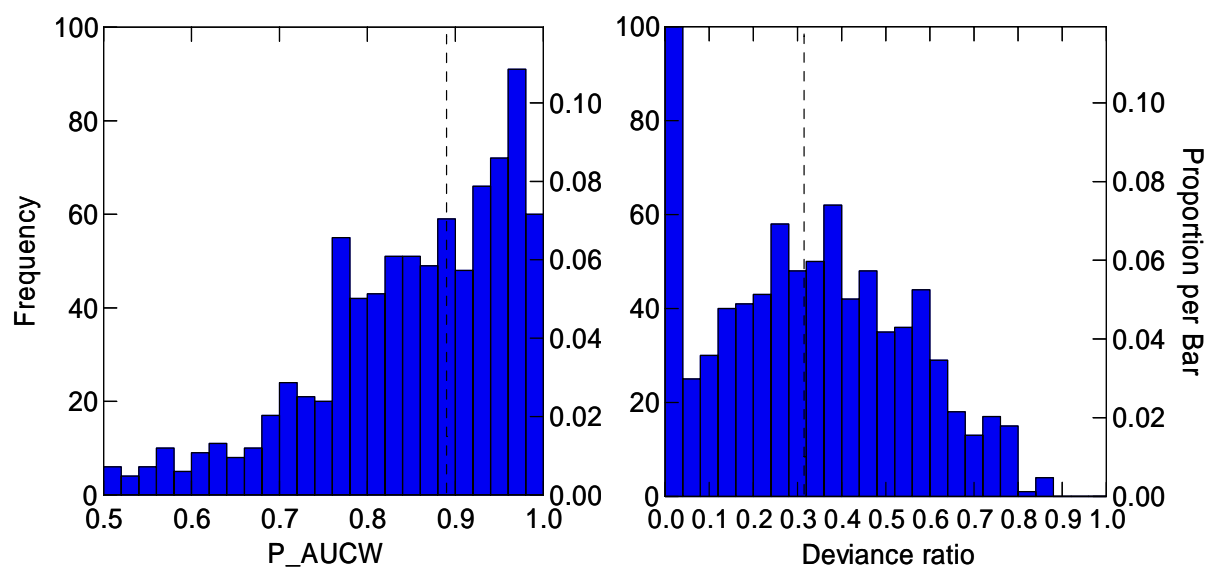


Figure 3-29: Frequency distributions of species biomass distribution model performance diagnostics for the presence model weighted AUC (P_AUCW) and for the biomass model relative deviance explained (Deviance ratio). The median is indicated by the dashed vertical lines.

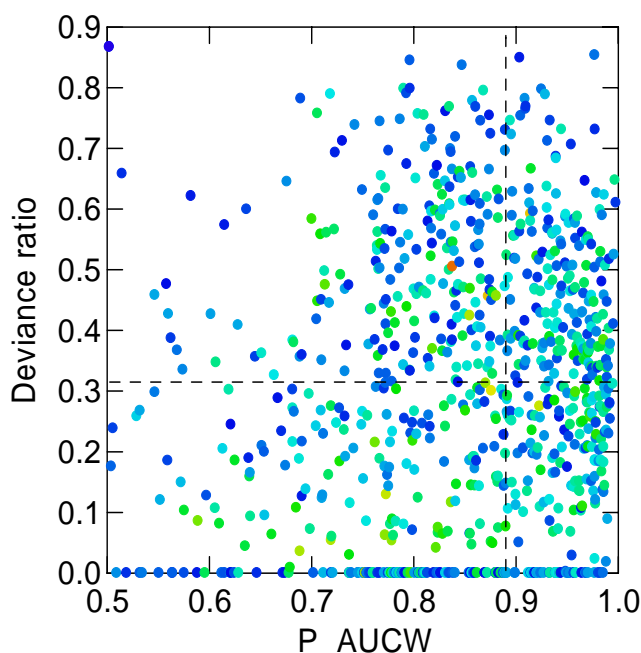


Figure 3-30: Relationship between species biomass distribution model performance diagnostics for presence model weighted AUC (P_AUCW) and for biomass model Deviance ratio. The medians are indicated by the dashed lines. Symbol colour indicates species frequency: least frequent=dark blue to most frequent=red.

The fit of the biomass model was typically less than that of the presence model, largely because the biomass model could be fit only on sites where a species was present — less than 60 sites for half the species (but >25 sites, the lower limit for modelling). For similar reasons, the biomass stage of the modelling often did not select any physical covariates (intercept only for 131 species, plus device only in 205 cases, plus temporal variables only in 33 cases), leading to ‘flat’ biomass predictions given presence (thus patterns in biomass distribution were determined solely by the probability of presence and average biomass where present). Only rarely did this occur with the more powerful presence stage model; physical covariates were not selected in only 11 cases leading to ‘flat’ probability of presence predictions.

Thus, while the majority of species were modelled satisfactorily, not all species were seen to have a good relationship with the available physical environment or spatial covariates with the consequence that their broader distribution beyond actual presence at sampled sites could not be estimated adequately. To illustrate, high, poor and median model performance, a selection of examples is provided below.

Examples of distribution maps of some species with higher performing models are shown in Figure 3-31. The fish *Kanekonia queenslandica* has P_AUC=0.88 and dev.ratio=0.80; another four species have diagnostics greater than these. The decapod crustacean *Solenocera pectinata* has P_AUC=0.92 and dev.ratio=0.73; another nine species have diagnostics greater than these. The gastropod *Xenophora cerea* has P_AUC=0.91 and dev.ratio=0.68; another 25 species have diagnostics greater than these. The fish *Paramonacanthus filicauda* has P_AUC=0.88 and dev.ratio=0.65; another 45 species have diagnostics greater than these.

Examples of distribution maps of some species with among the poorest performing models are shown in Figure 3-32. The bivalve *Corbula fortisulcata* had P_AUC=0.69 and dev.ratio=0; eight other species had both diagnostics lower/equal to these. The bryozoan *Synnotum* spp had P_AUC=0.66 and dev.ratio=0.12; three other species had both diagnostics lower than these. The Asteroid starfish *Goniasteridae* spp had P_AUC=0.64 and dev.ratio=0; one other species had both diagnostics lower/equal to these. The model for the small ray *Dasyatis leylandi* selected no physical or spatial covariates and was a flat prediction with P_AUC=0.52 and dev.ratio=0 — its pattern of occurrence did not correspond consistently with any physical or spatial covariate; no species had diagnostics lower than this species.

Examples of distribution maps of some species with typical model performance are shown in Figure 3-33. The crab *Portunus rubromarginatus* has P_AUC=0.89 and dev.ratio=0.38; the urchin *Prionocidaris bispinosa* has P_AUC=0.83 and dev.ratio=0.39; the fish *Priacanthus tayenus* has P_AUC=0.85 and dev.ratio=0.37; and the bryozoan *Celleporaria* spp has P_AUC=0.85 and dev.ratio=0.30. In general about half the model fits were poorer than these and about half were stronger.

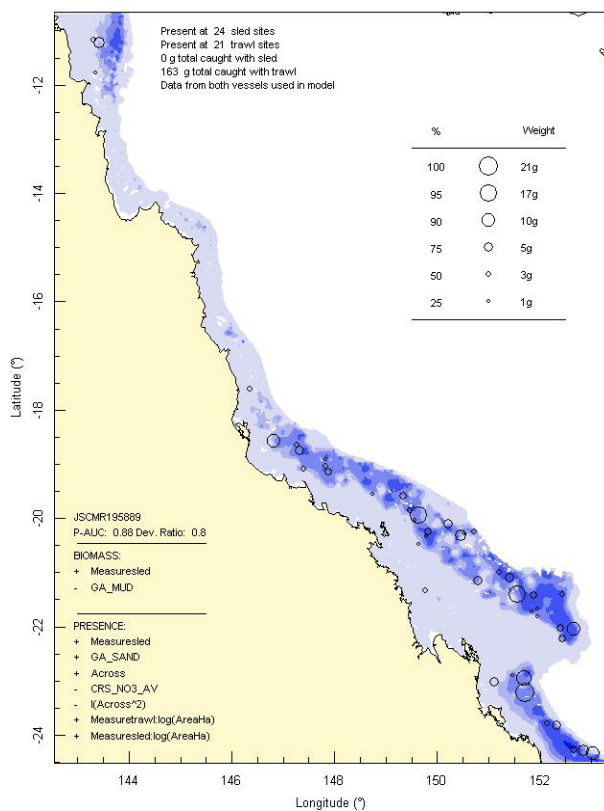
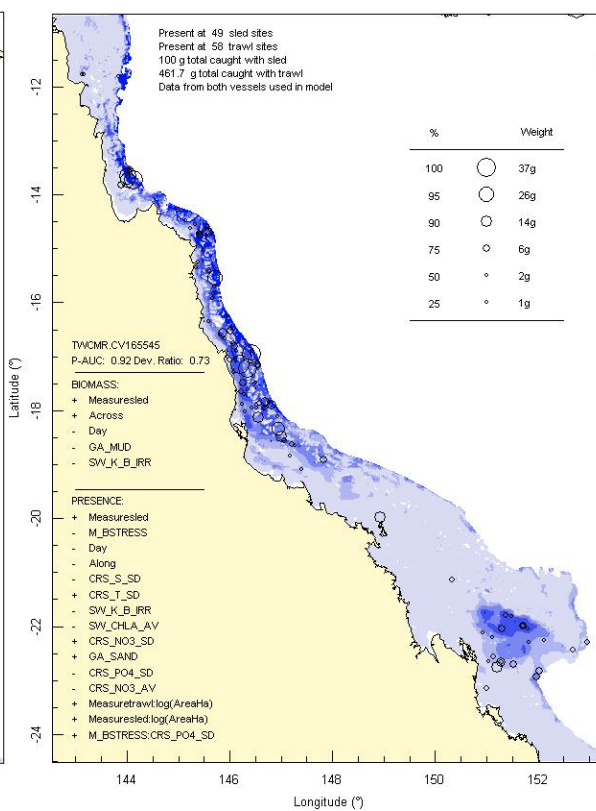
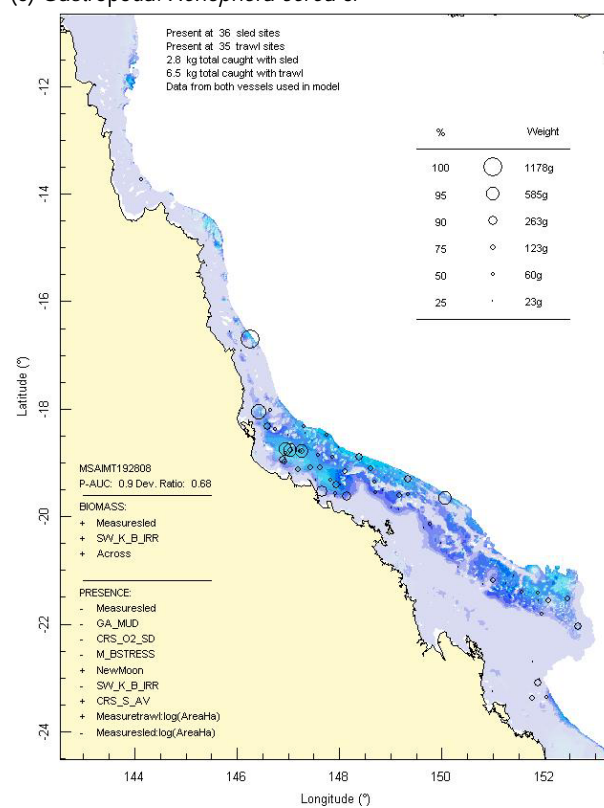
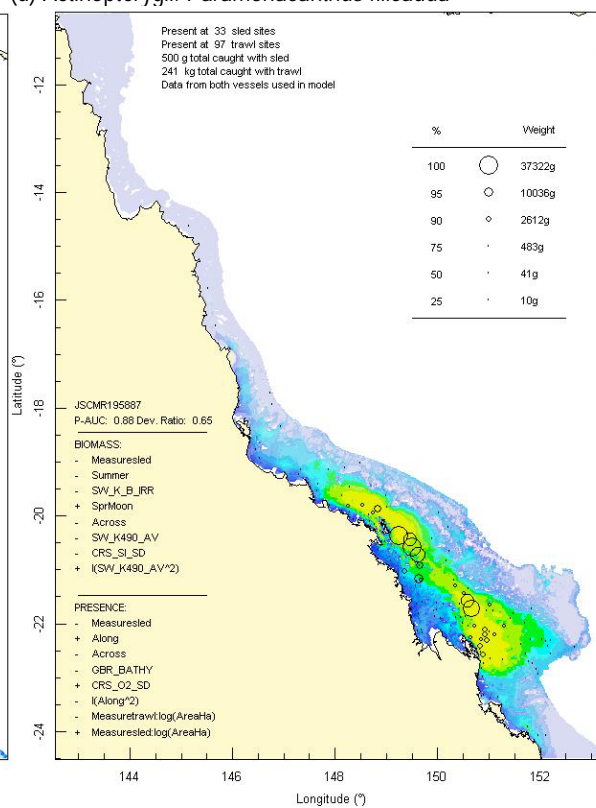
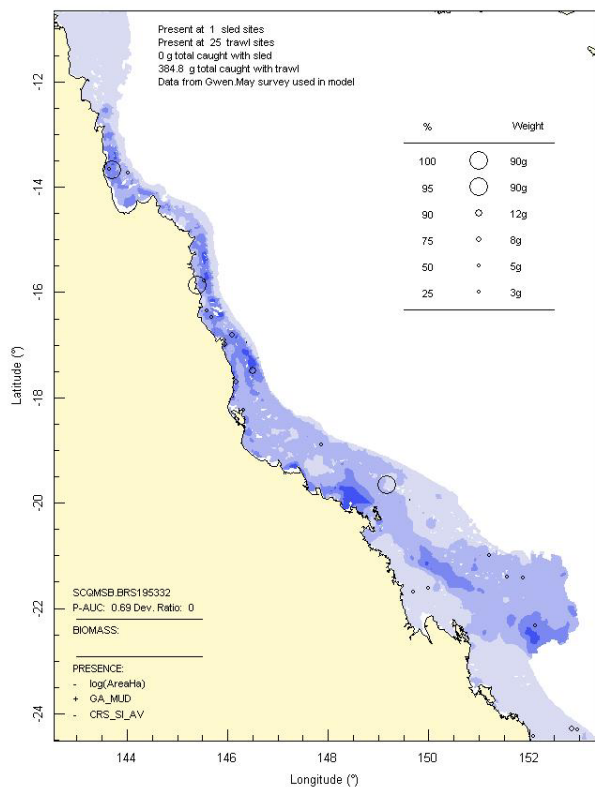
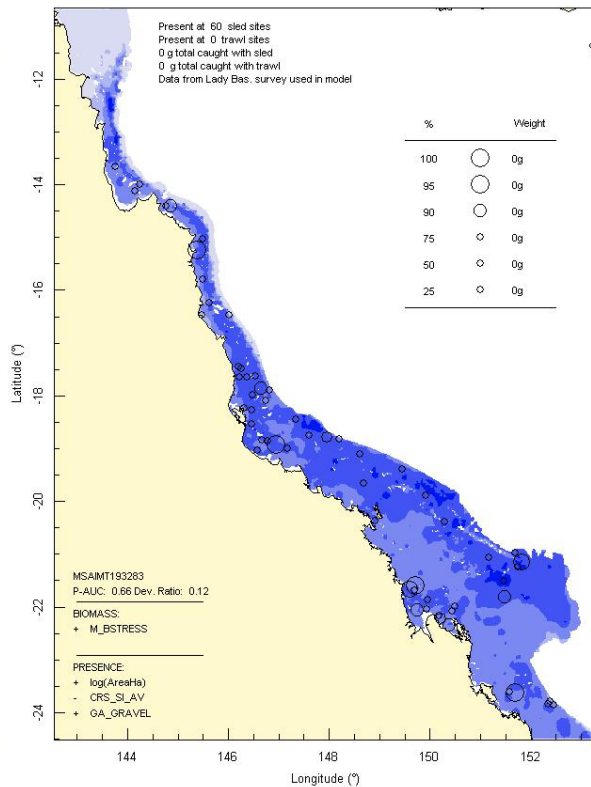
(a) Actinopterygii: *Kanekonia queenslandica*(b) Crustacea: *Solenocera pectinata*(c) Gastropoda: *Xenophora cerea* cf(d) Actinopterygii: *Paramonacanthus filicauda*

Figure 3-31: Model distribution maps of selected species with higher performing diagnostics.

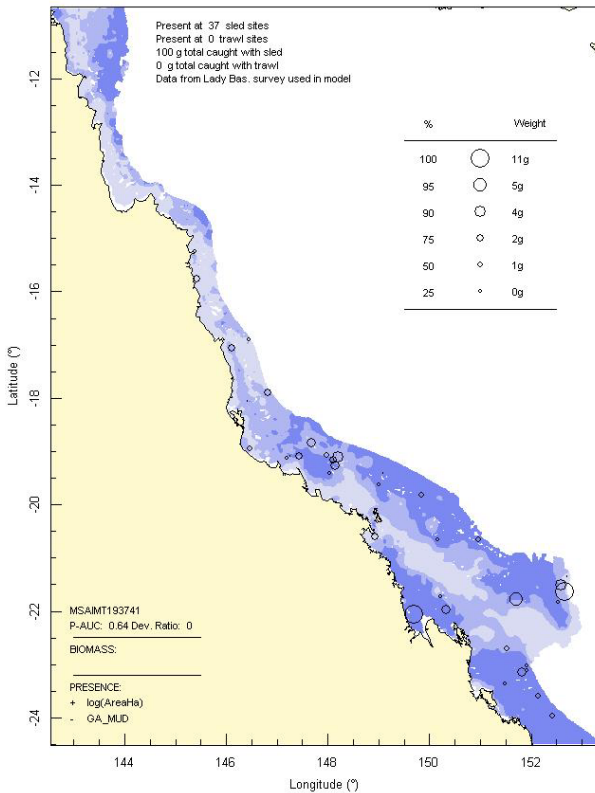
(a) Bivalvia: *Corbula fortisulcata*



(b) Gymnolaemata: *Synnotum* spp



(c) Asteroidea: *Goniasteridae* spp



(d) Chondrichthyes: *Dasyatis leylandi*

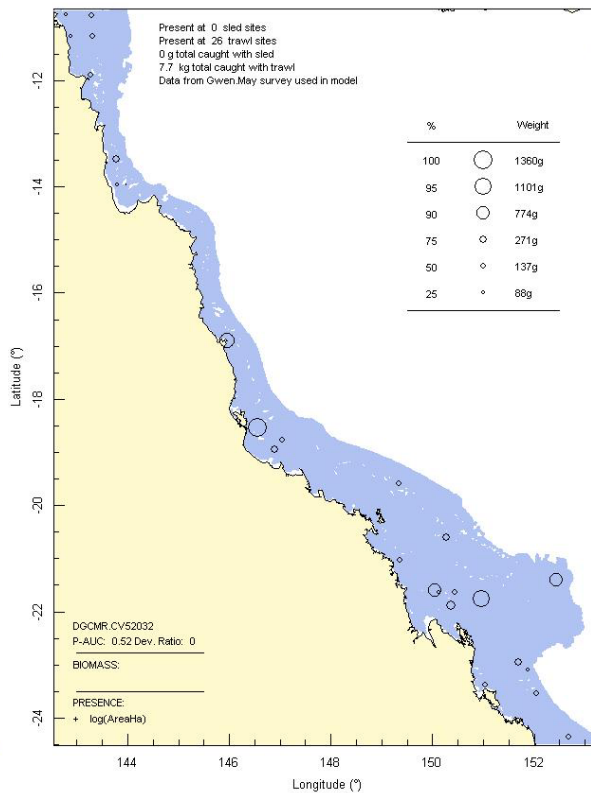


Figure 3-32: Model distribution maps of selected species with among the poorest performing diagnostics.

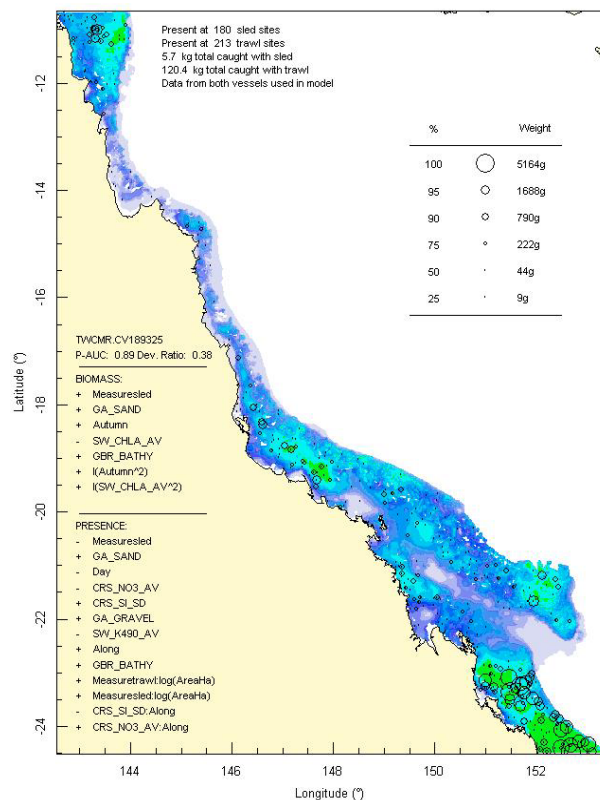
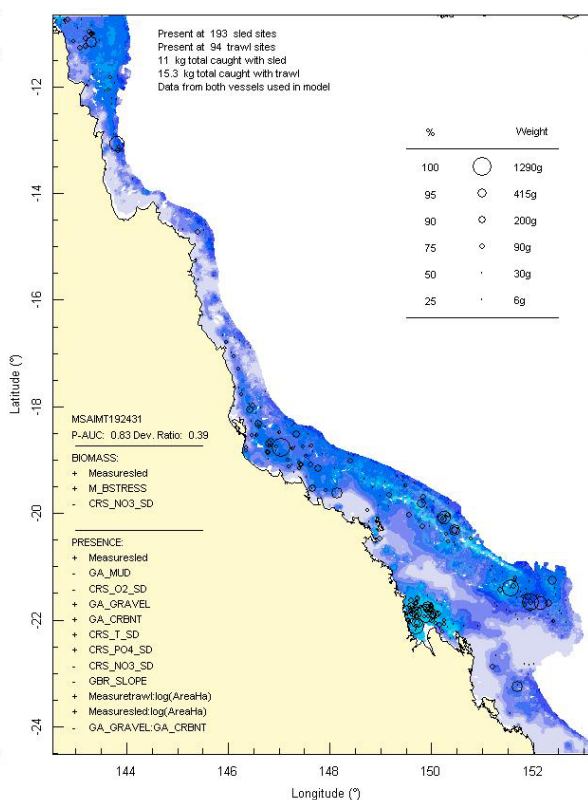
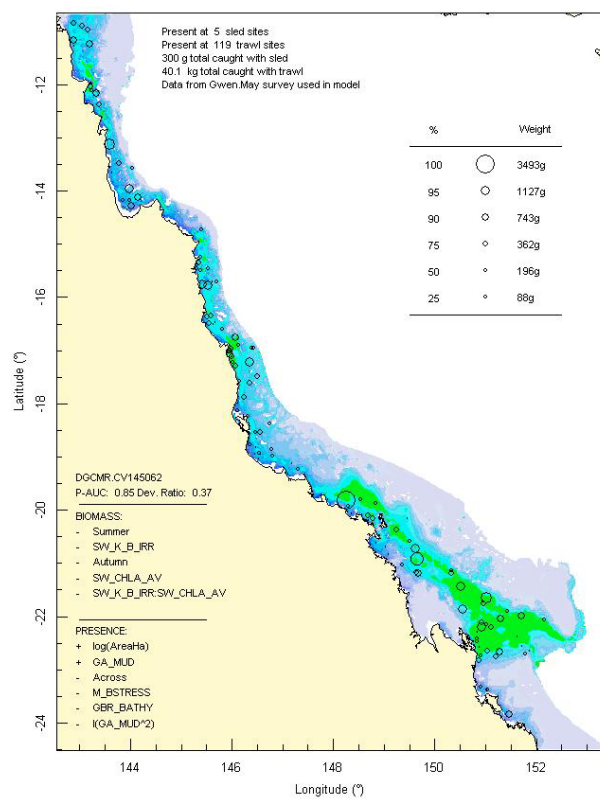
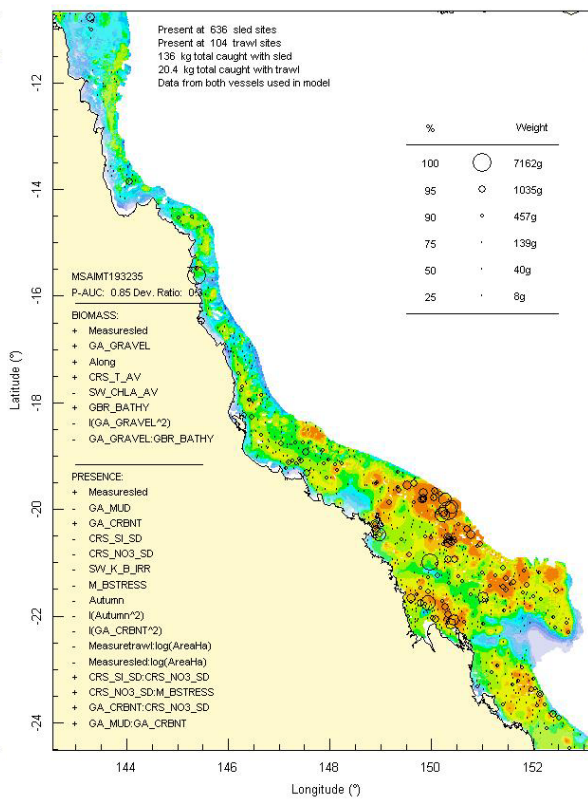
(a) Crustacea: *Portunus rubromarginatus*(b) Echinoidea: *Prionocidaris bispinosa*(c) Actinopterygii: *Priacanthus tayenus*(d) Gymnolaemata: *Celleporaria* spp

Figure 3-33: Model distribution maps of selected species with median performing diagnostics.

3.2.3. Selected single species distribution maps

With model distribution maps available for more than 800 species, it was not possible to present them all in this report. When particular species become of interest due to, for example, outcomes of the risk assessment (Section 3.7.2) then maps are presented where appropriate. In this section selected maps are presented to illustrate a variety of contrasting species distribution patterns with respect to some of the important physical environment covariates and between species within genera. Other distribution maps not presented in this report, as well as information about distribution of less frequently occurring species that were not modelled, can be made available for agreed purposes if required.

The first series of distribution maps show divergent distributions against key physical environment covariates. Figure 3-34 shows two species with positive relationships for muddy sediments (a fish *Nemipterus hexodon* and a bivalve *Anadara ferruginea* cf) and two species with negative relationships for muddy sediments (a brittle star *Euryale asperum* and a Gastropod *Conus ammiralis*).

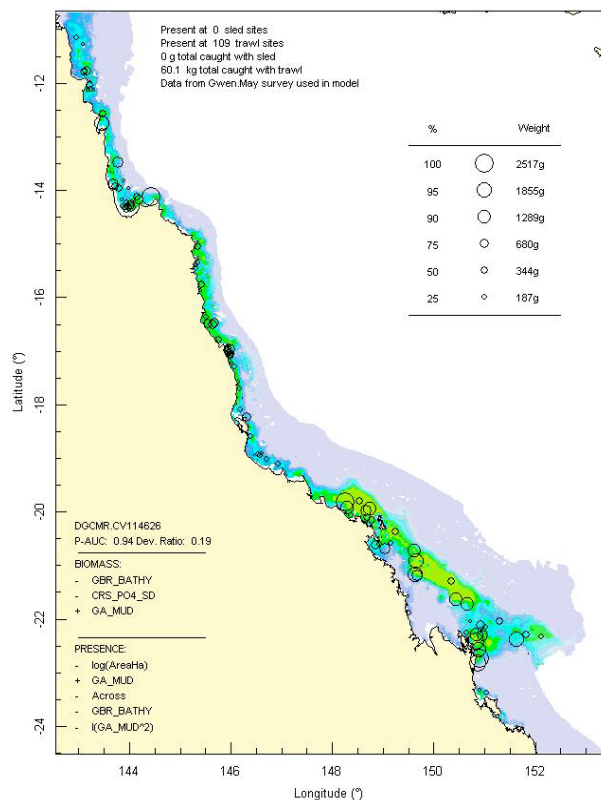
Figure 3-35 shows two species with positive relationships for benthic irradiance (green algae *Caulerpa taxifolia* and *Halimeda bikensis*) and two species with negative relationships for benthic irradiance (a fish *Lepidotrigla calodactyla* and a crustacean *Myra eudactyla*). It was not surprising that benthic irradiance arises as an important covariate for marine plants, which form important vegetated structural habitats that appear to support a high biodiversity (Figure 3-24).

Figure 3-36 shows two species with positive relationships for seabed current stress (a gorgonian *Echinogorgia* sp3 and a sponge *Callyspongia* sp23) and two species with negative relationships for seabed current stress (a holothurian *Stichopus ocellatus* and a crab *Charybdis truncata*). Gorgonians and other sessile epibenthic fauna (e.g. sea whips, soft corals and sponges) often formed seabed gardens in medium-high (but not extreme) current areas where harder substratum was often exposed and the currents facilitate feeding by these animals. Low current areas usually had fine sediment and a completely different biota.

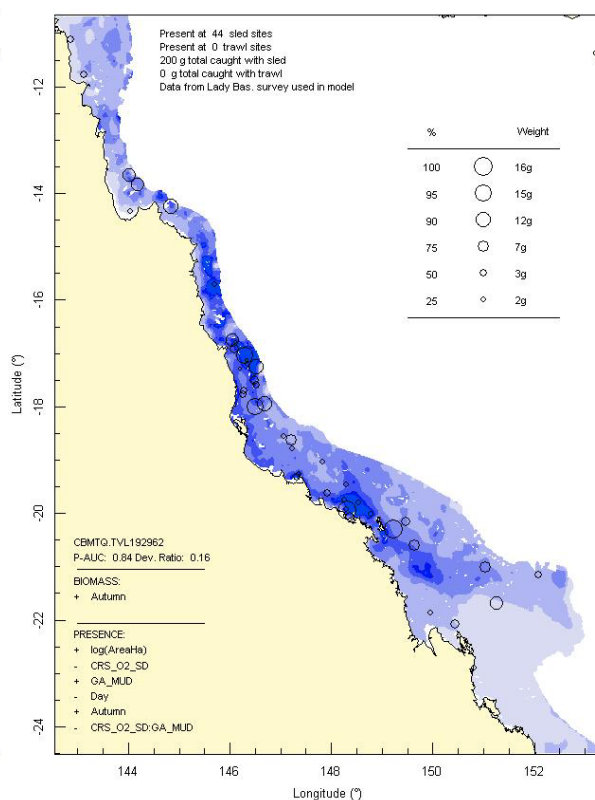
Figure 3-37 shows two species with relationships for shallow seabed (a fish *Pseudorhombus arsius* and a green algae *Caulerpa serrulata*) and two species with relationships for deep seabed (a stomatopod *Quollastria gonypetes* and a shrimp Carid sp4931).

The following series of distribution maps show divergent distributions of different species within the same genera. The threadfin bream, *Nemipterus furcosus*, had a strong northerly distribution extending south to the Swains, whereas *Nemipterus theodorei* had strong southerly distribution centred in the Capricorn Channel extending north past Cairns (Figure 3-38ab). The crab, *Portunus tenuipes*, had low abundance in the southern GBR and was distributed primarily from off Cape Upstart north along the midshelf into the far northern GBR — *Portunus sanguinolentus* occurred almost exclusively on the innershelf south of Shoalwater Bay with a few scattered records from coastal areas further north (Figure 3-38cd). The flounder, *Pseudorhombus argus*, was distributed in the northern GBR, primarily the far north midshelf, with a few innershelf records further south — *Pseudorhombus dupliciocellatus* occurred primarily in the southern GBR, primarily on the mid/outer shelf south of Cardwell, with a few records further north (Figure 3-39ab). The gastropod, *Strombus campbelli*, occurred in sandy inner-shelf areas along the length of the GBR — *Strombus dilatatus* occurred in sandy outer-shelf areas throughout the GBR (Figure 3-39cd). The cardinal fish, *Apogon fasciatus*, occurred in gravelly areas on the fringes of the Shoalwater Bay and Broad Sound high current area as well as muddy areas in the deeper Capricorn Channel and innershelf elsewhere — *Apogon timorensis* occurred primarily in carbonate sandy areas along the outer-shelf (Figure 3-40ab). The flatfish *Cynoglossus* sp4 occurred primarily in four sandy mid/outer-shelf areas, the far north, central, Swains and Capricorn — *Cynoglossus kopsi* occurred primarily on the inner-shelf with lower abundance in the central and Capricorn sections (Figure 3-40cd). These few examples indicate how different the distribution patterns of closely related species can be and demonstrate the importance of identifying specimens to species level in order to understand spatial patterns of biodiversity and develop predictive models of distributions.

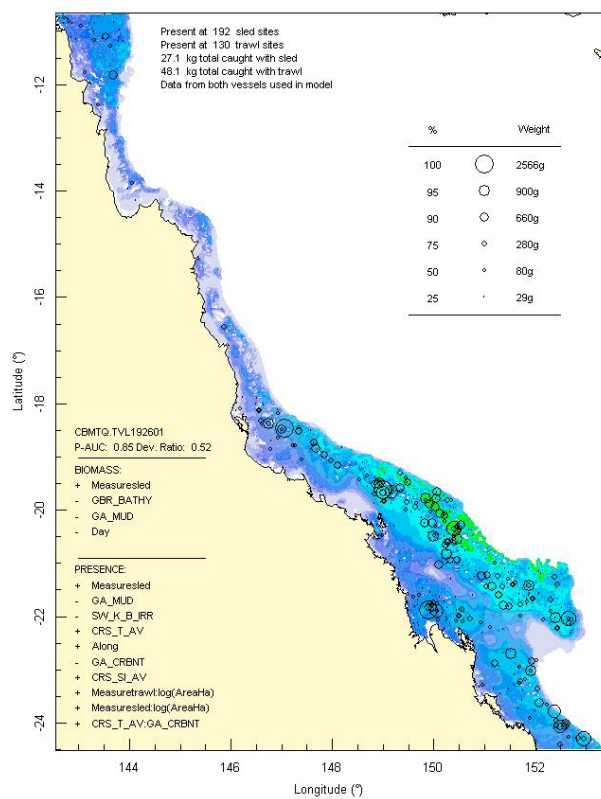
(a) Actinopterygii: *Nemipterus hexodon*



(b) Bivalvia: *Anadara ferruginea* cf



(c) Ophiuroidea: *Euryale asperum*



(d) Gastropoda: *Conus ammiralis*

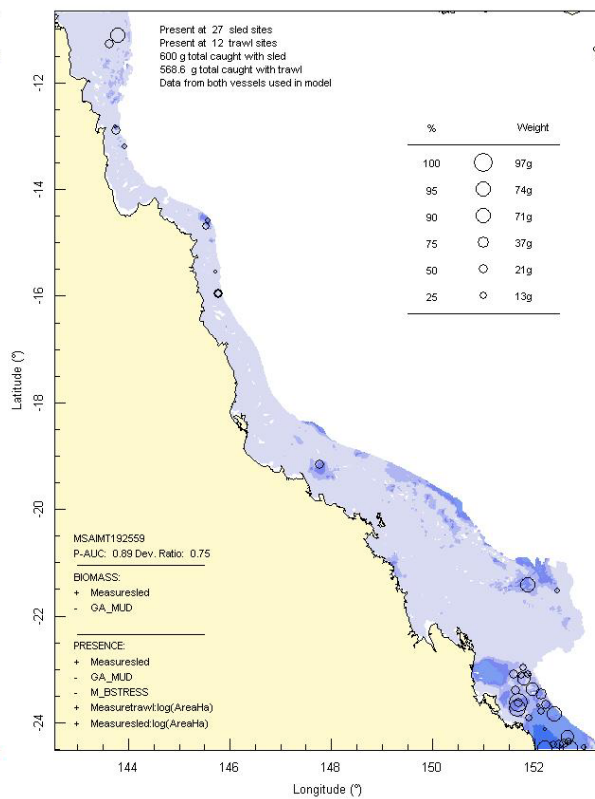
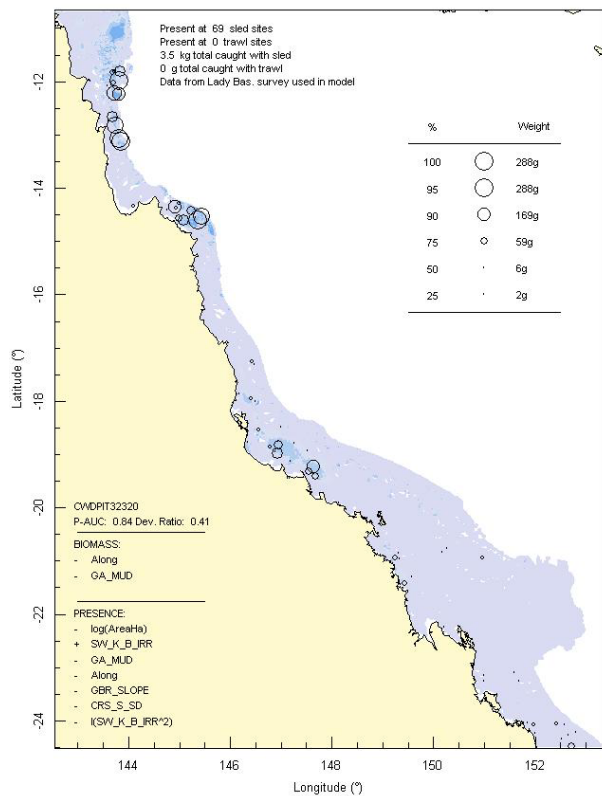
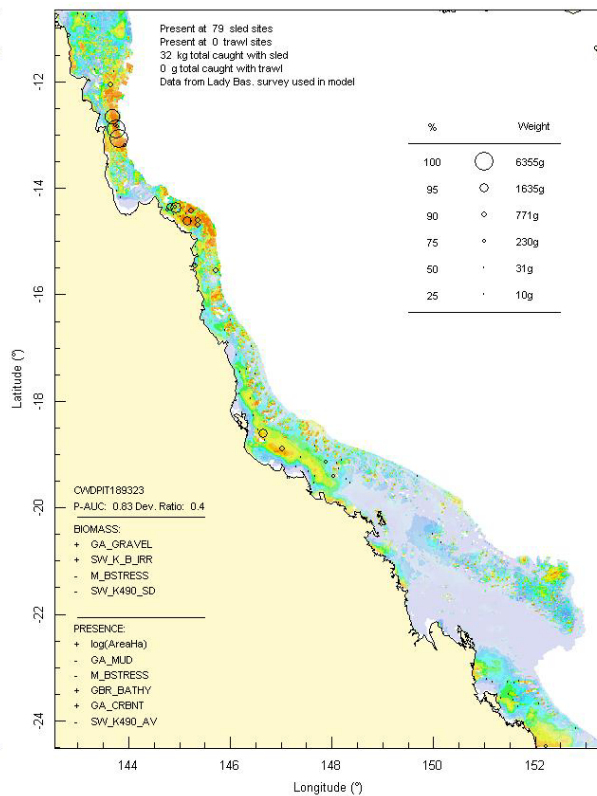


Figure 3-34: Model distribution maps of selected species with positive and negative affinities for mud.

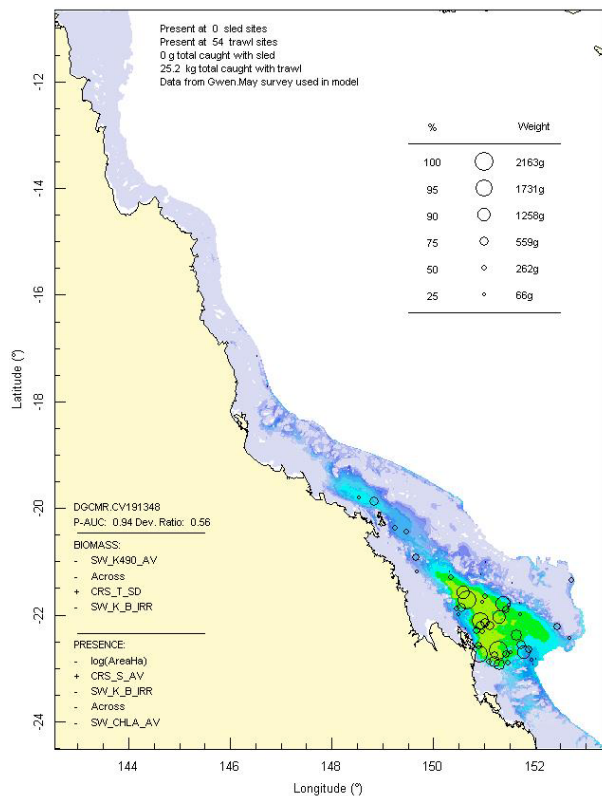
(a) Chlorophyceae: *Caulerpa taxifolia*



(b) Chlorophyceae: *Halimeda bikensis*



(c) Actinopterygii: *Lepidotrigla calodactyla*



(d) Crustacea: *Myra eudactyla*

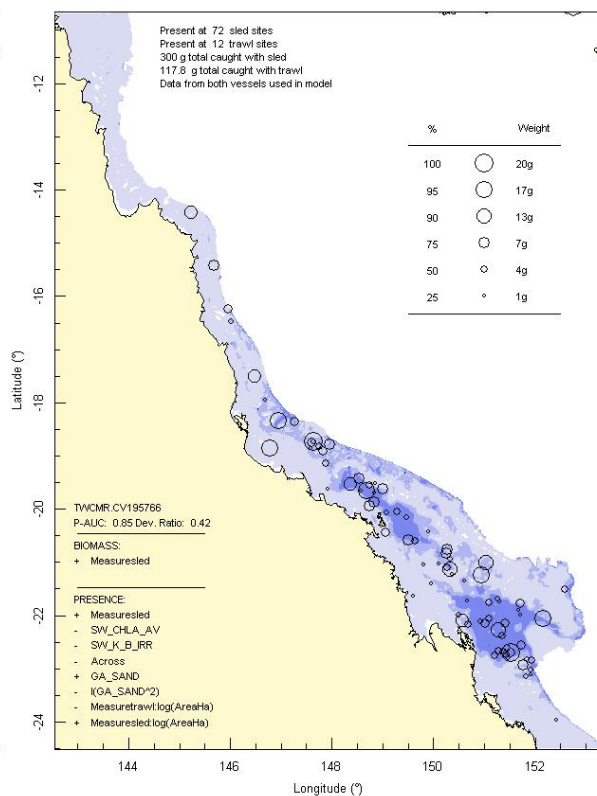
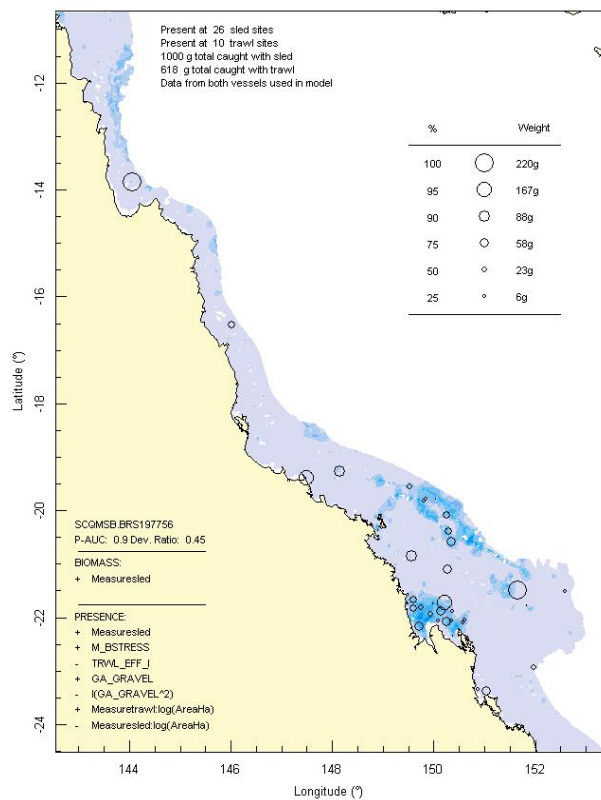
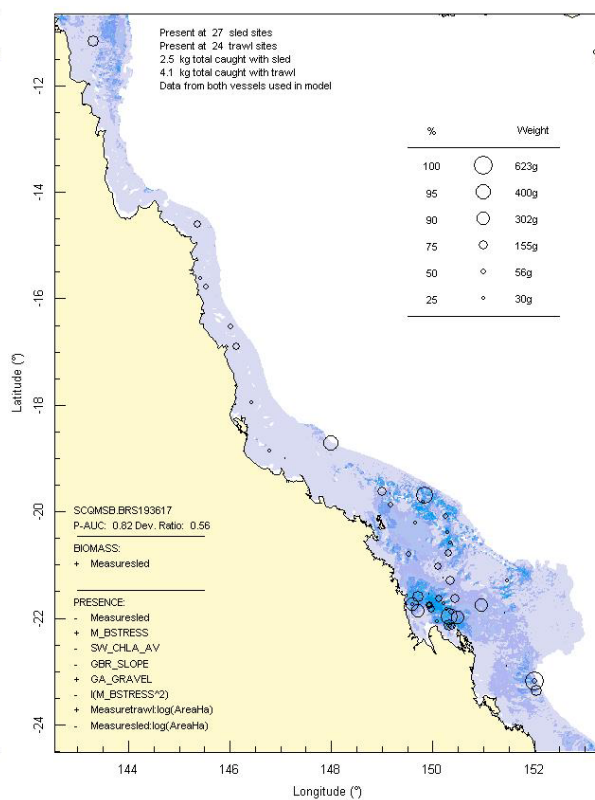


Figure 3-35: Model distribution maps of selected species with positive and negative affinities for benthic irradiance.

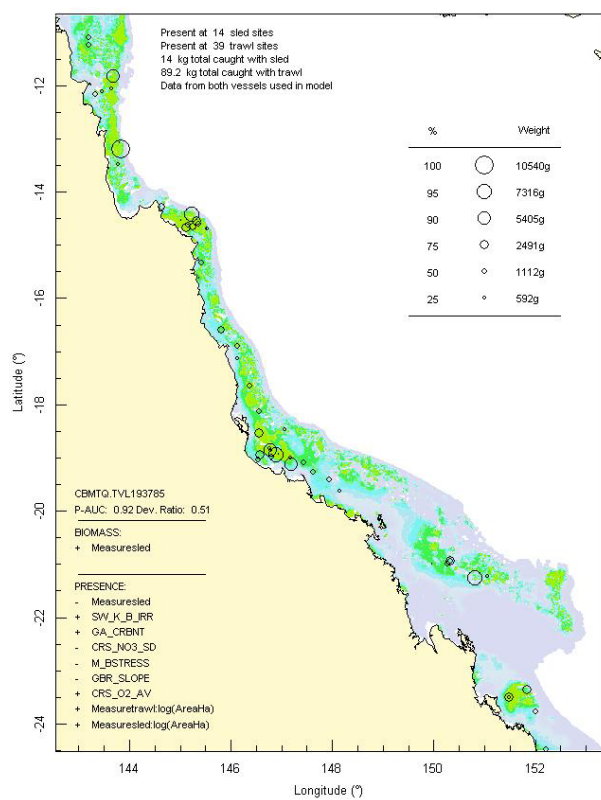
(a) Anthozoa: *Echinogorgia* sp3



(b) Demospongiae: *Callyspongia* sp23



(c) Holothuroidea: *Stichopus ocellatus*



(d) Crustacea: *Charybdis truncata*

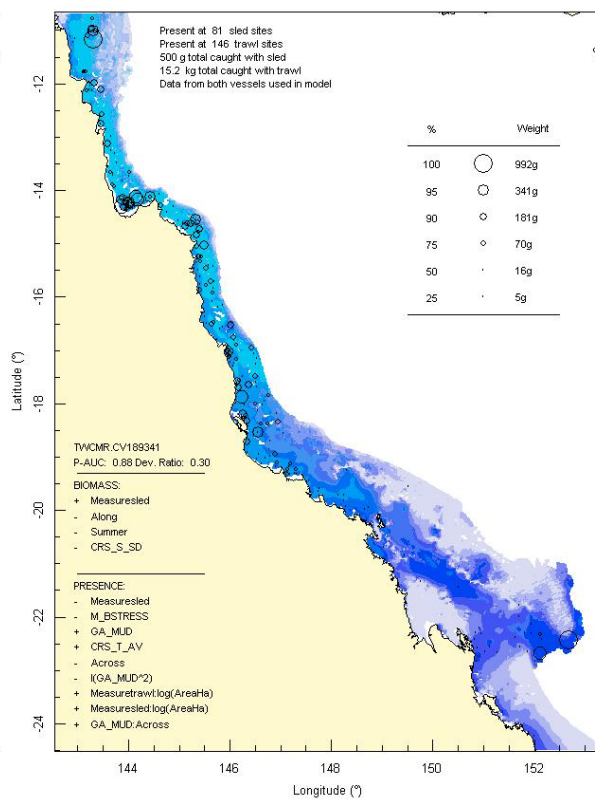
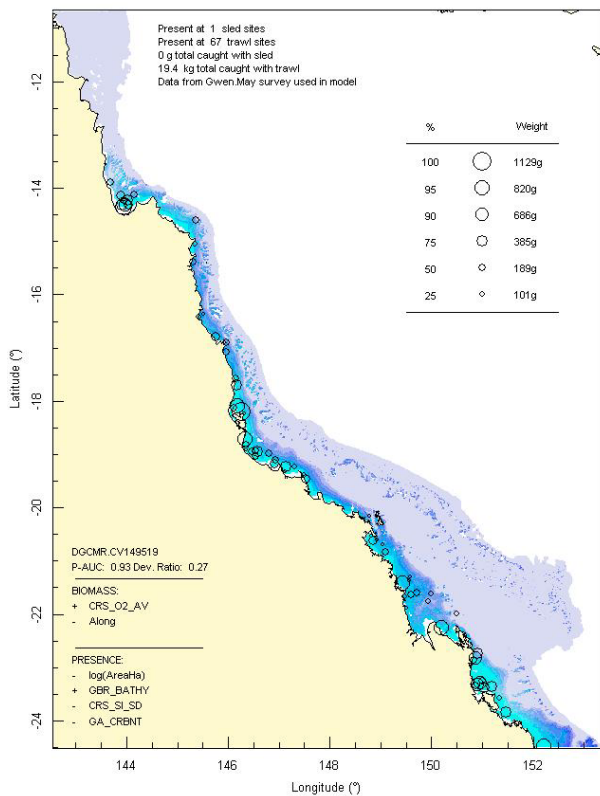
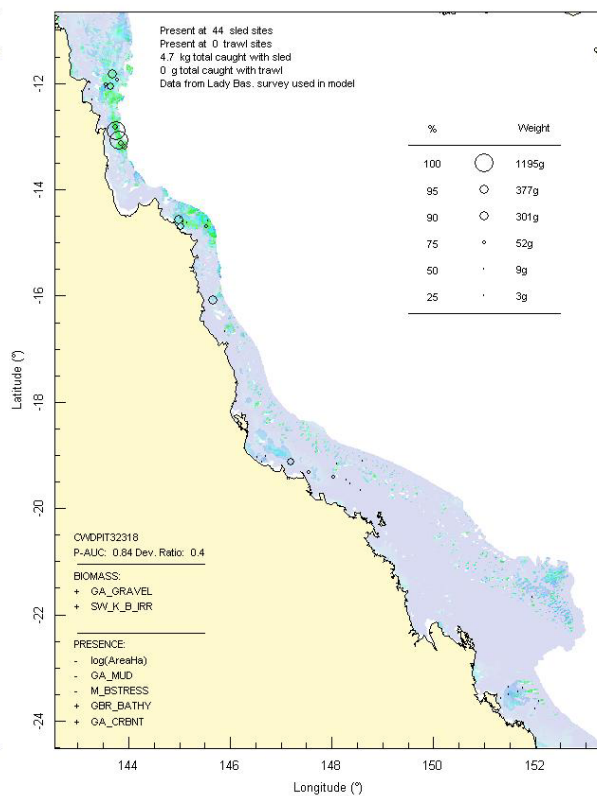


Figure 3-36: Model distribution maps of selected species with positive and negative affinities for seabed current stress.

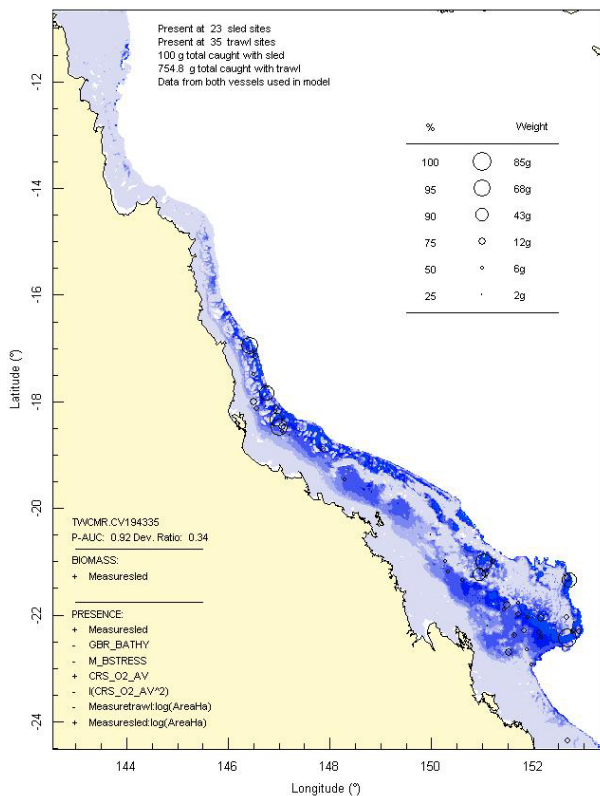
(a) Actinopterygii: *Pseudorhombus arsius*



(b) Chlorophyceae: *Caulerpa serrulata*



(c) Crustacea: *Quollastria gonypetes*



(d) Crustacea: Carid sp4931

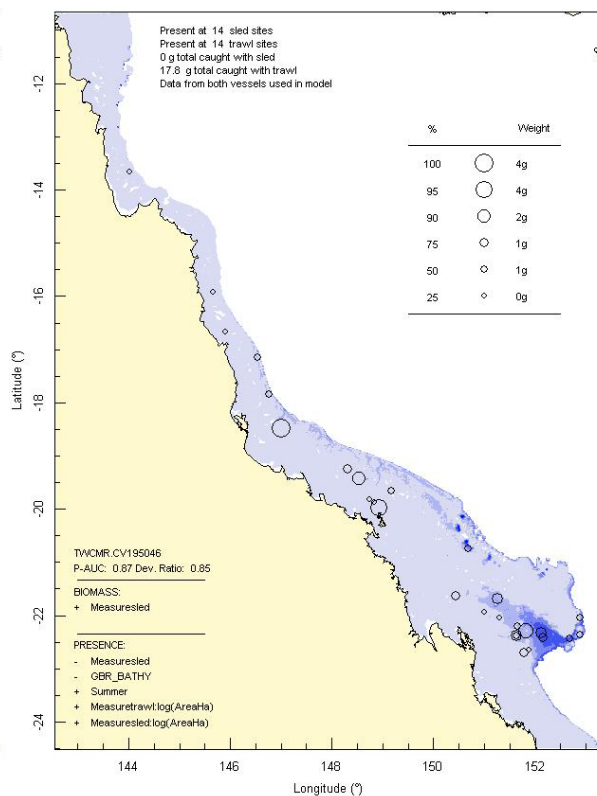
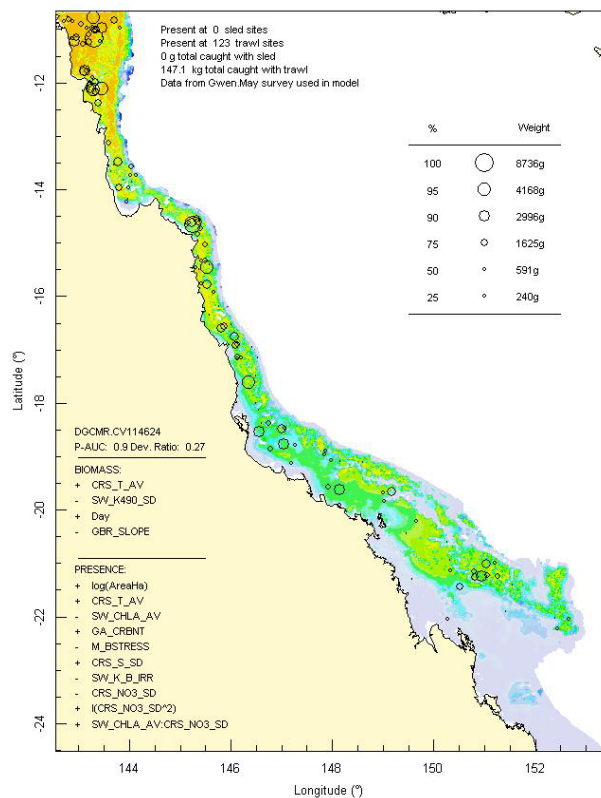
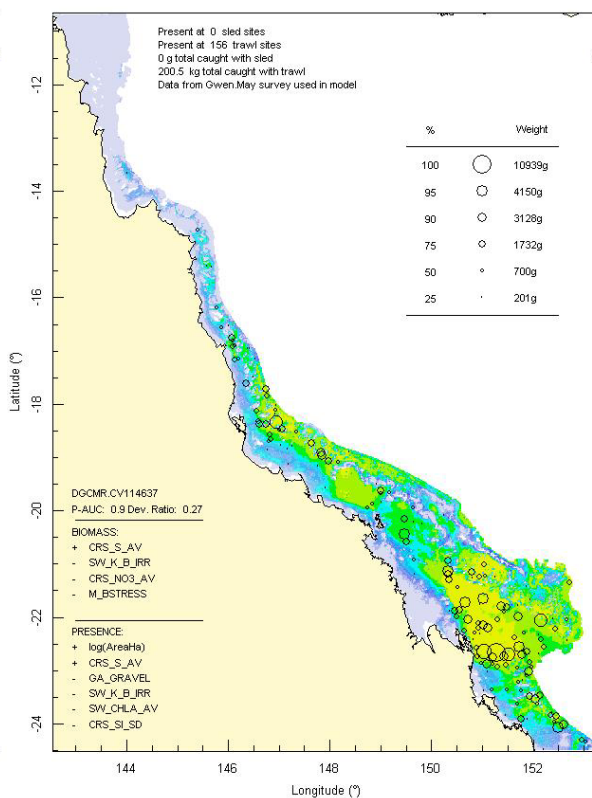


Figure 3-37: Model distribution maps of selected species with affinities for shallow and deep bathymetry.

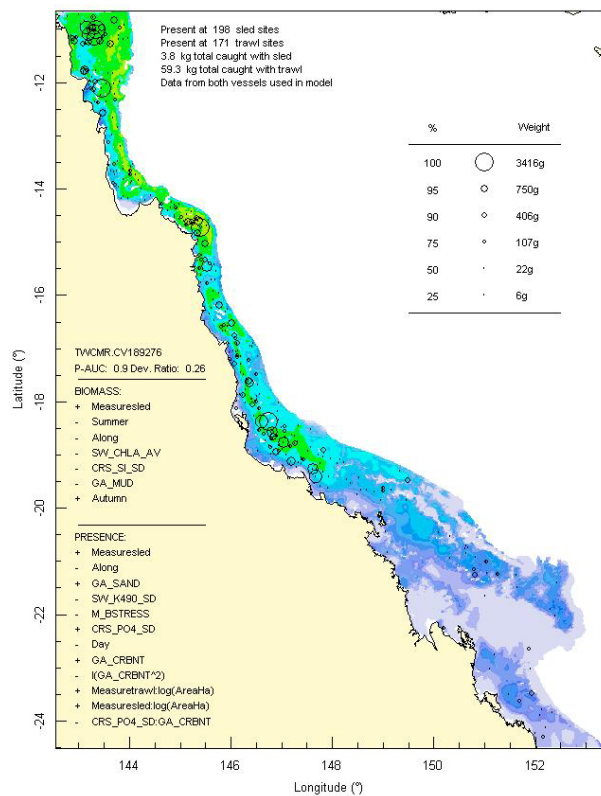
(a) Actinopterygii: *Nemipterus furcosus*



(b) Actinopterygii: *Nemipterus theodorei*



(c) Crustacea: *Portunus tenuipes*



(d) Crustacea: *Portunus sanguinolentus*

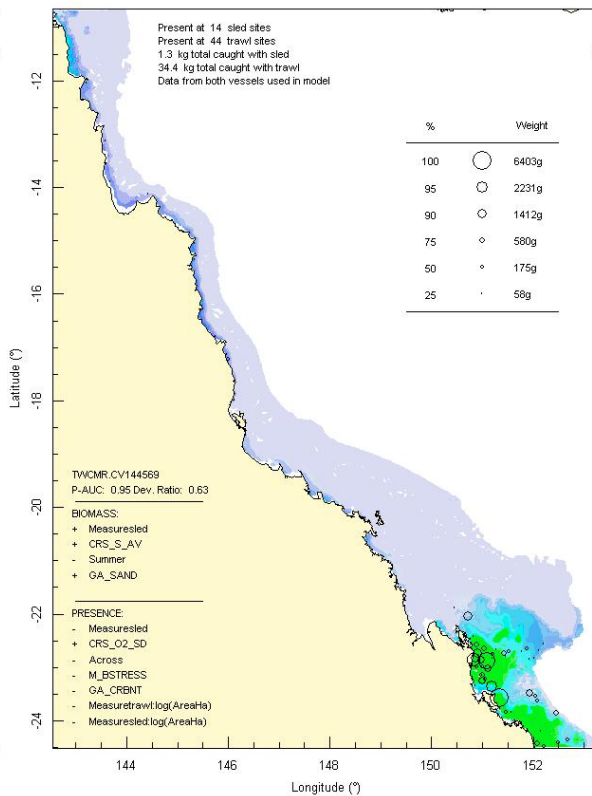
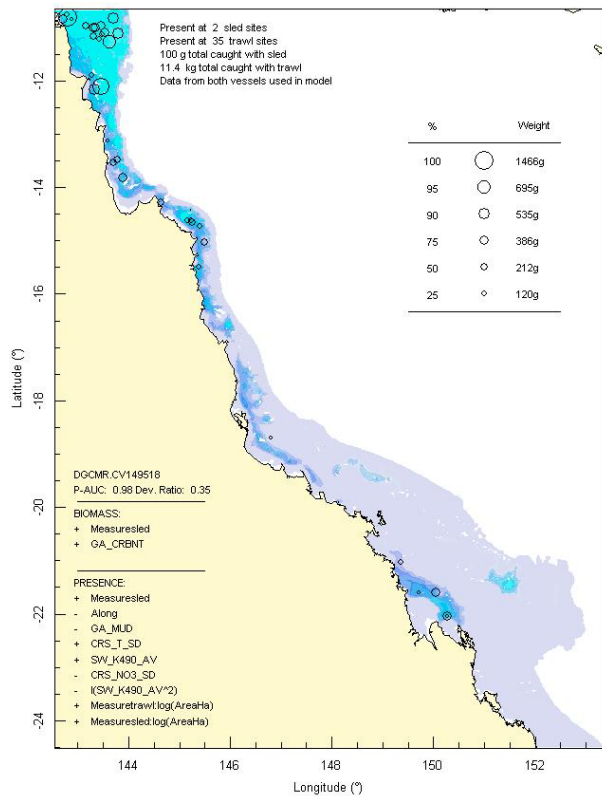
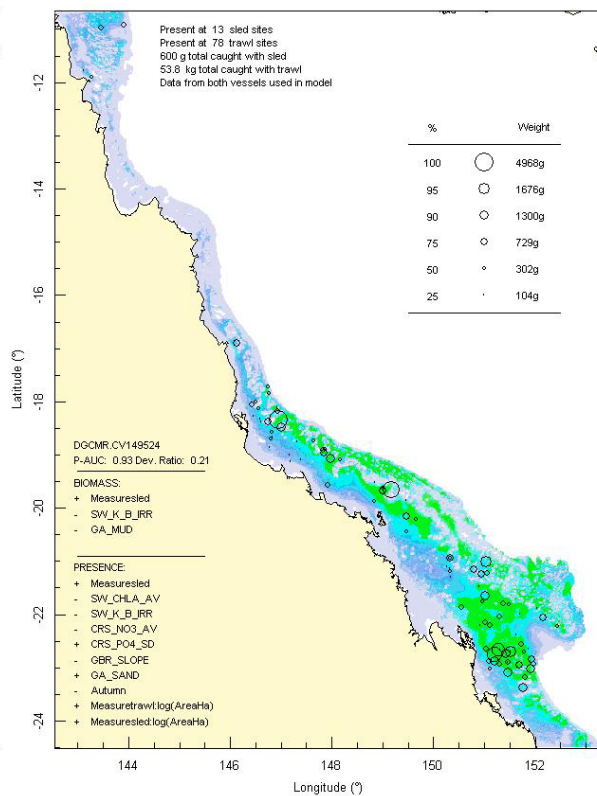


Figure 3-38: Model distribution maps of selected species within genera having contrasting distributions.

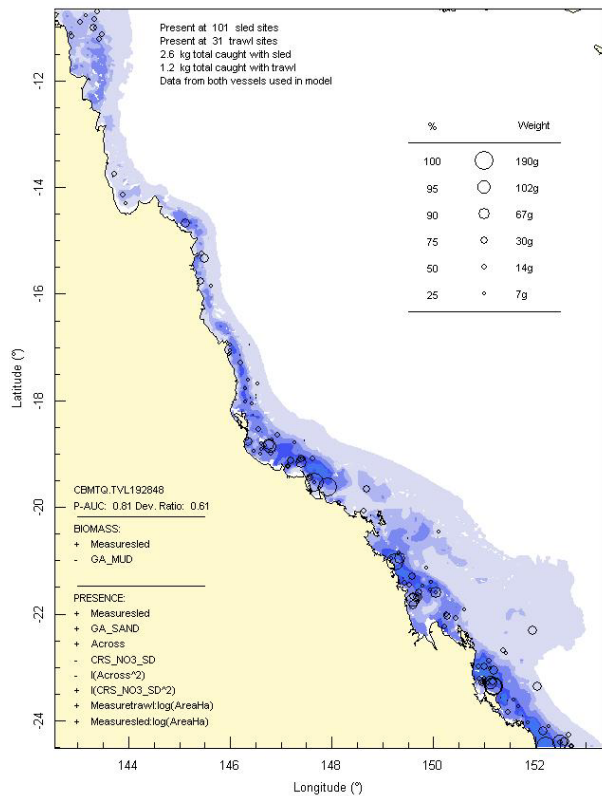
(a) Actinopterygii: *Pseudorhombus argus*



(b) Actinopterygii: *Pseudorhombus dupliciocellatus*



(c) Gastropoda: *Strombus campbelli*



(d) Gastropoda: *Strombus dilatatus*

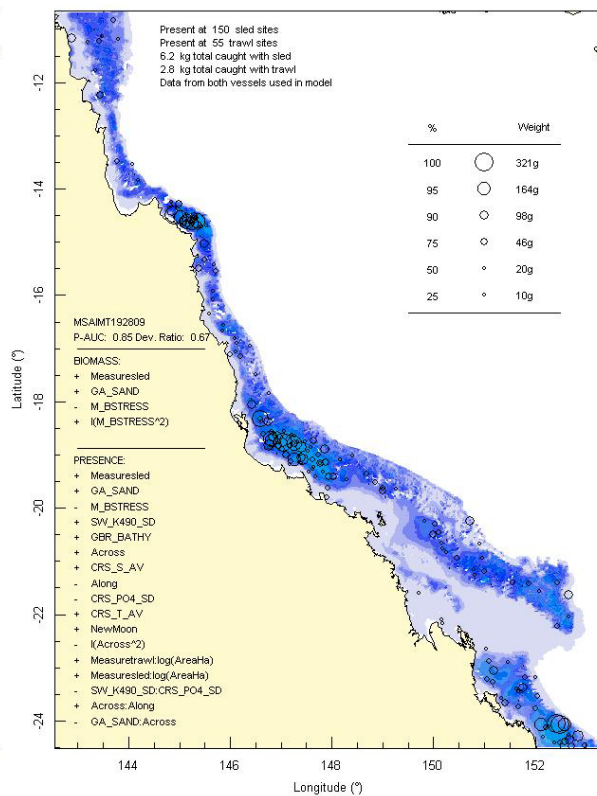
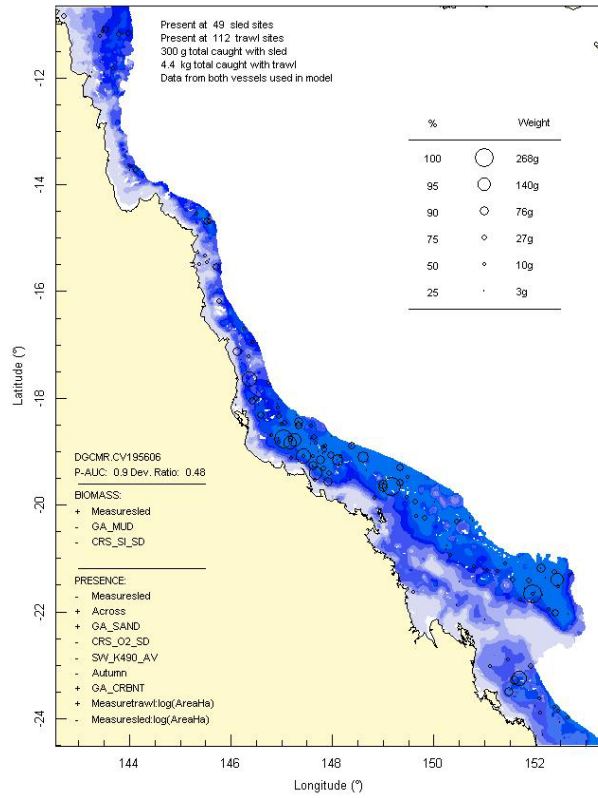
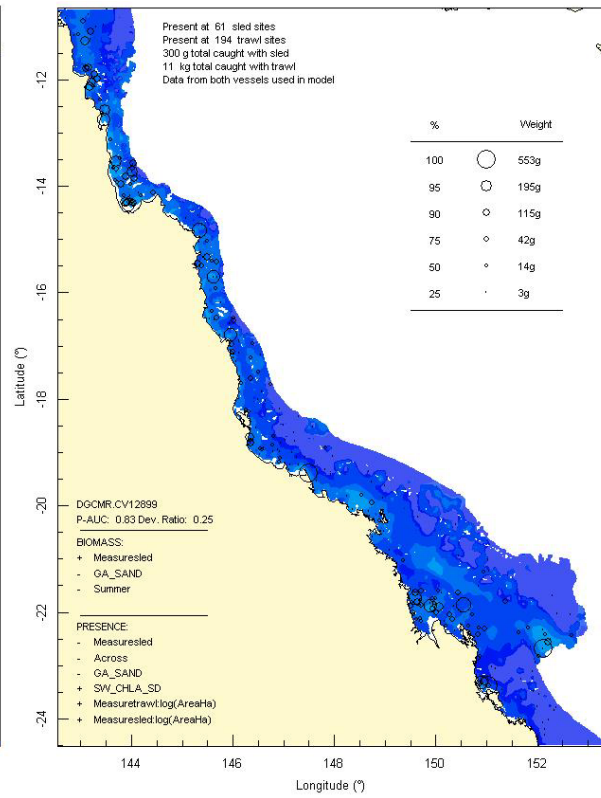
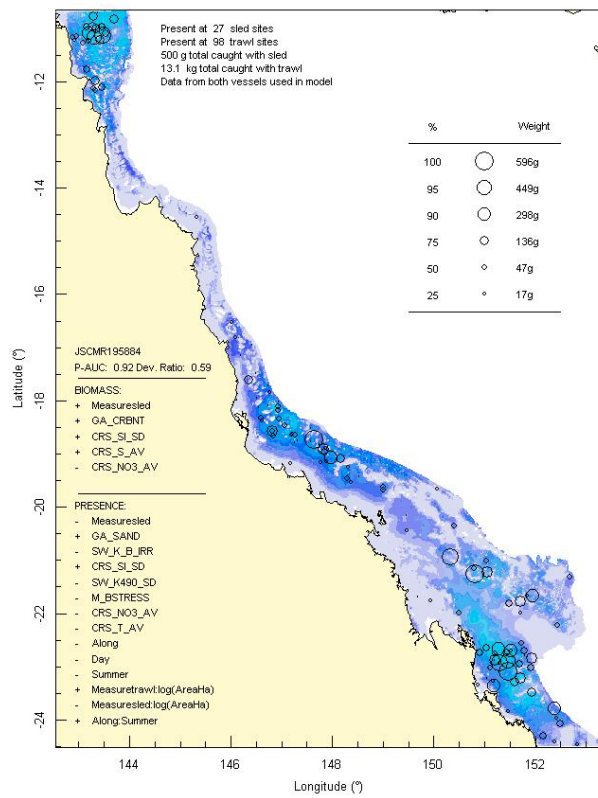
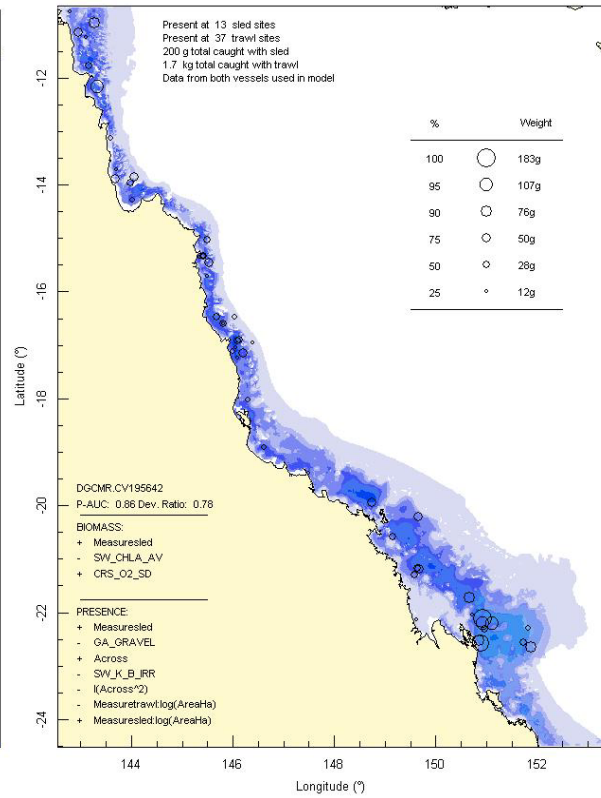


Figure 3-39: Model distribution maps of selected species within genera having contrasting distributions.

(a) Actinopterygii: *Apogon timorensis*(b) Actinopterygii: *Apogon fasciatus*(c) Actinopterygii: *Cynoglossus* sp4(d) Actinopterygii: *Cynoglossus kopsi***Figure 3-40:** Model distribution maps of selected species within genera having contrasting distributions.

3.3. SPECIES GROUPS CHARACTERIZATION AND PREDICTION (M Browne & R Pitcher)

3.3.1. Characterization and Prediction Model performance

Figure 3-41 shows the overall cluster structure produced by the clustering algorithm. Note that the hierarchical nature of the dendrogram allows for the definition of a range of possible subsets of the data. Choosing the level of the dendrogram at which to ‘cut’ so as to agglomerate all nodes below into a single cluster may be done with respect to the cost function, shown on the y axis. Further information may be gained by considering silhouette plots for a range of candidate clusterings, as the number of groups is increased as the critical ‘cut height’ (on the y axis) is lowered.

From a traditional clustering point of view (Kaufman and Rousseeuw 1990) the diagnostics for ‘objective clusters’ show relatively few strong clusters. However, the purpose here does not require a clustering this kind of objective basis. The objective here was small groups of species with estimated physical distributions that were strongly correlated to make modelling their aggregated distribution a useful and insightful exercise for the purposes of the project. In this sense the clustering tools used do give a useful basis for achieving this. It is not claimed that the resulting groups have any stronger objective basis than this utilitarian one.

Another way of viewing this is to note that single species models form a limiting case for modelling groups of species, that is, the case when each group consists of just one species. Our aim here is to move away from this limiting case in a meaningful way by combining species which appear to have correlated distributions and ‘borrowing strength’ from their combined data to obtain a clearer picture of the properties of this approximately common distribution pattern.

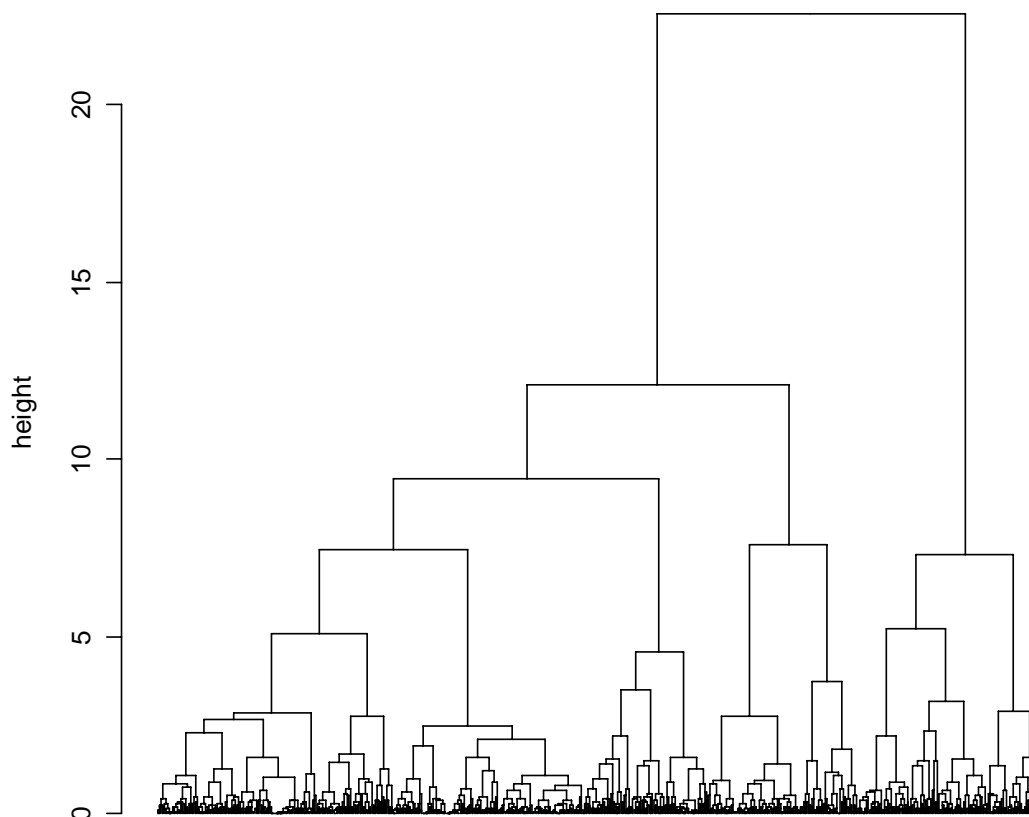


Figure 3-41: Cluster dendrogram of the single species estimates illustrating the hierarchical cluster structure determined by Ward’s method.

The high measurement uncertainty, the relative sparsity of data, and the large number of distinct species seen in this study was typical of marine biological sampling in general, and especially for places of high species diversity such as the GBR. These considerations motivate the aggregation of species providing that the group models were sufficiently representative of their member species models. In deciding the extent of aggregation to perform, it was decided to set a criterion that the resulting intra-cluster species estimate correlation at sites be $>.5$. Aggregating into 38 groups led to an overall average intra-cluster species estimate correlation of $.58$. Averaging with respect to groups lead to an average of $r = 0.55$, with a range of $0.4 < r < 0.69$.

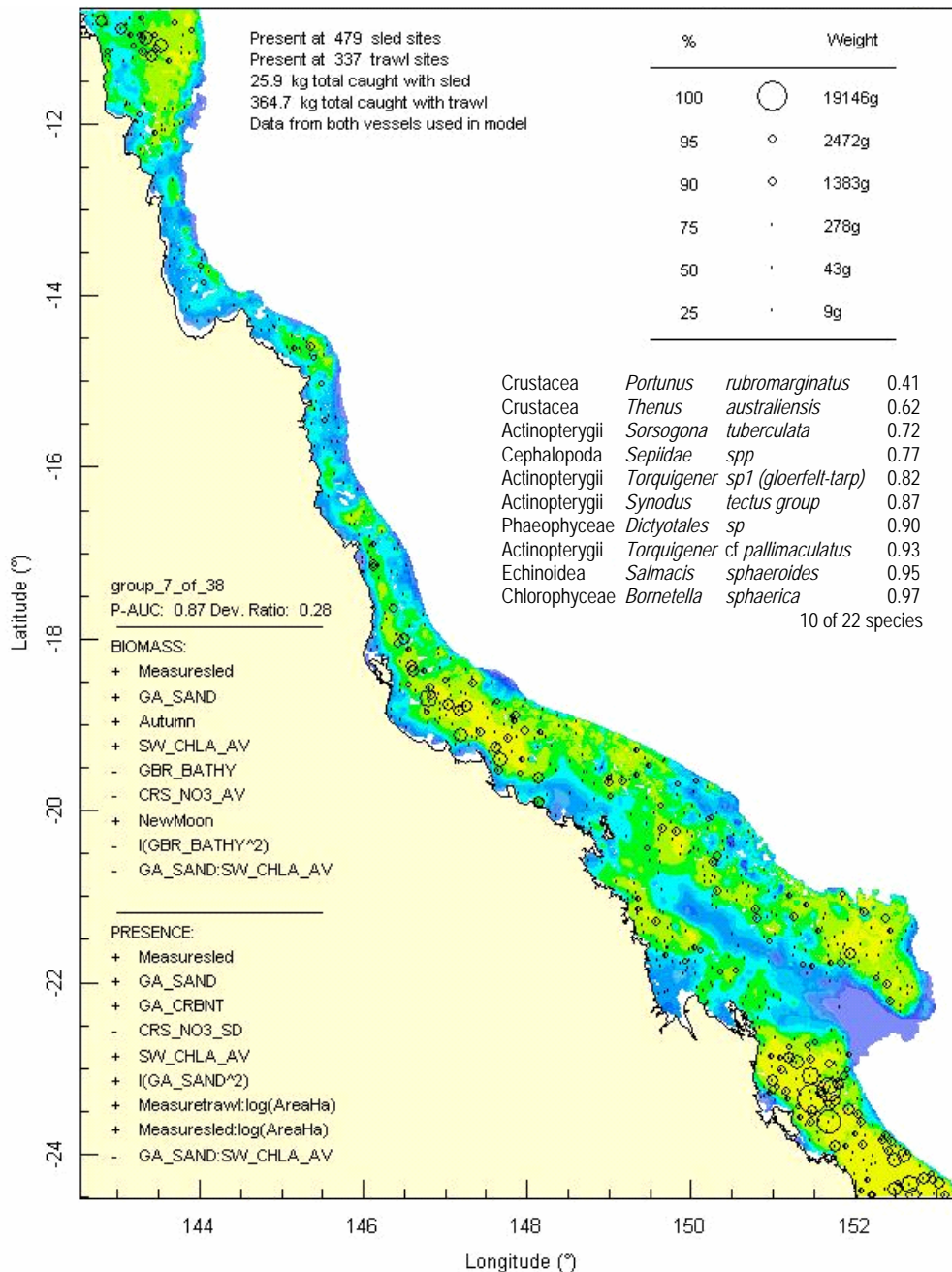


Figure 3-42: Aggregated biomass map and model for an example species-group ("7"). The top 10 of 22 species is tabulated with cumulative biomass.

The biomass data for each species was aggregated within each of the 38 clusters to create a group biomass that was then treated in the same way as the individual species. To provide an example,

Figure 3-42 shows the model predictions for a relatively typical species group#7. The individual species comprising the group are listed in Table 3-8. The mix of high and low estimated biomass densities illustrate that despite the relatively large number of members, the model is able to specify with some confidence the areas of high and low prevalence. Compared to individual species maps, the overall estimated biomass is obviously higher (since the estimate is of the sum of many individual species). The intensity of the colours is also high compared to most estimates for single species, reflecting the relatively higher confidence in the estimates (when considered with respect to the mean fit). The large number of predictor variables in the biomass component of the model is a result of the data set being comprised of far fewer zero entries than an individual species model. This provides more data to generate a more sophisticated model of the biomass. Despite the fact that a large number of species are being modelled simultaneously, the AUC model performance measure in particular was quite reasonable (0.87). This suggests that the constituent species possess sufficiently similar biophysical responses so as to permit a relatively effective common model.

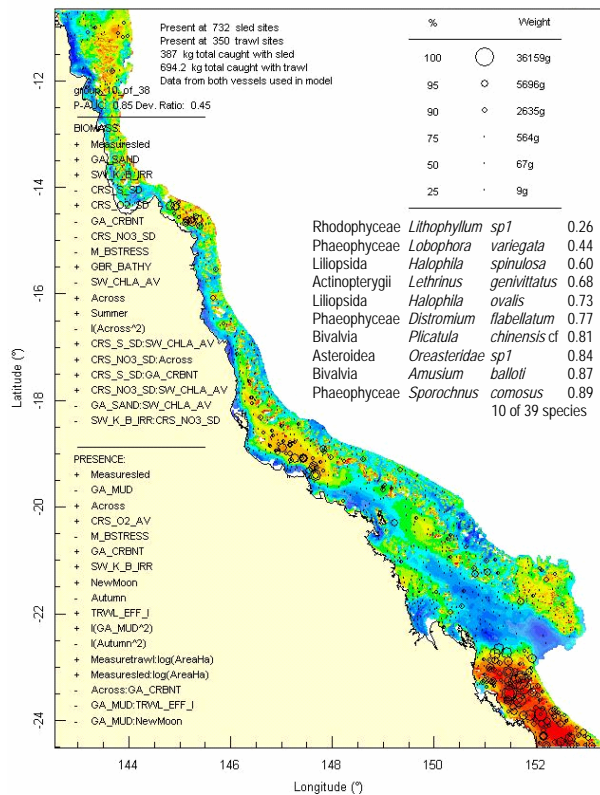
Table 3-8. List of species comprising species group 7.

| Class | Genus | Species | Class | Genus | Species |
|----------------|--------------------|-------------------------------|----------------|-----------------------|-----------------------|
| Crustacea | <i>Portunus</i> | <i>rubromarginatus</i> | Actinopterygii | <i>Calliurichthys</i> | <i>ogilbyi</i> |
| Crustacea | <i>Thenus</i> | <i>australiensis</i> | Gastropoda | <i>Strombus</i> | <i>vittatus</i> |
| Actinopterygii | <i>Sorsogona</i> | <i>tuberculata</i> | Chlorophyceae | <i>Cladophora</i> | sp |
| Cephalopoda | <i>Sepiidae</i> | spp | Actinopterygii | <i>Cynoglossus</i> | <i>maccullochi</i> |
| Actinopterygii | <i>Torquigener</i> | sp1 (<i>gloerfelt-tarp</i>) | Crustacea | <i>Dardanus</i> | <i>callichela var</i> |
| Actinopterygii | <i>Synodus</i> | <i>tectus group</i> | Cephalopoda | <i>Sepiadariidae</i> | sp5 |
| Phaeophyceae | <i>Dictyotales</i> | sp | Gastropoda | <i>Volva</i> | <i>volva</i> |
| Actinopterygii | <i>Torquigener</i> | cf <i>pallimaculatus</i> | Chlorophyceae | <i>Halimeda</i> | <i>cuneata</i> |
| Echinoidea | <i>Salmacis</i> | <i>sphaeroides</i> | Actinopterygii | <i>Kanekonia</i> | <i>queenslandica</i> |
| Chlorophyceae | <i>Bornetella</i> | <i>sphaerica</i> | Crustacea | <i>Leucosia</i> | <i>formosensis</i> |
| Actinopterygii | <i>Orbonymus</i> | <i>rameus</i> | Crustacea | <i>Sicyonia</i> | <i>rectirostris</i> |

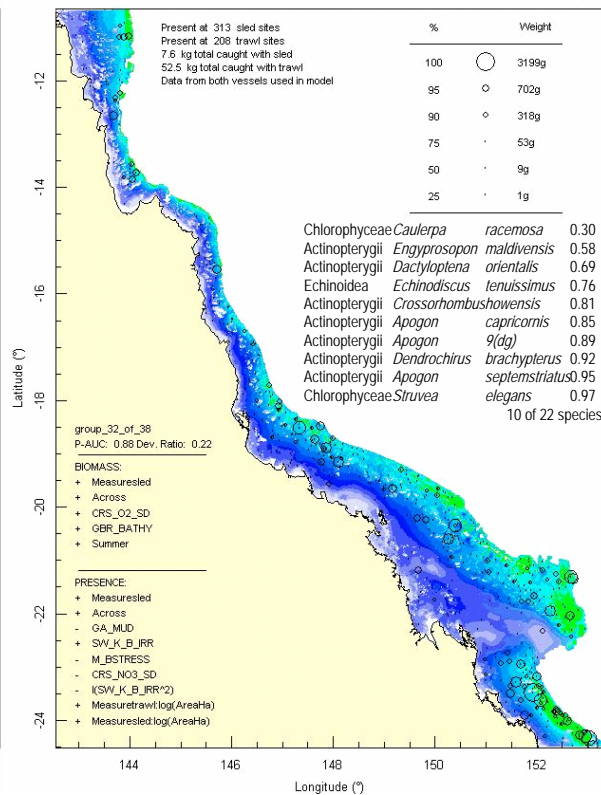
3.3.2. Selected species group distribution maps

Species grouped together in this way share approximately similar biophysical responses, and may or may not reflect some functional association, such as between a species that provides biological structural habitat and another species that uses that habitat. Average group membership was ~22 species and ranged from 3 to 80 species. Group 10 was one of the larger with 39 species and a distribution (Figure 3-44) that appeared to be largely coincident with some of the most vegetated areas in the region (see Section 3.5.2). This group included the largest biomass and number of marine plant species (14), such as *Halophila spinulosa* and *Halophila ovalis* and a dozen other species of green, red and brown algae. It is possible that some of the dominant fauna in this group, such as *Lethrinus genivittatus* and Oreasteridae sp1 may have some functional dependencies on the habitat forming biota, but this would need further ecological investigation. Group 32 was dominated by another common algae *Caulerpa racemosa* along with 21 other species of mostly fish and bryozoans, with a strong outer shelf distribution pattern. Group 4 species appeared to favour carbonate sand areas in mid/outer-shelf areas and included the commercial redspot prawn, *Penaeus longistylus*, the coral prawn, *Trachypenaeus curvirostris*, the flounder, *Pseudorhombus diplospilus*, and 25 other species. Group 24 was one of the smaller groups with only 12 species dominated by just two species, *Paramonacanthus filicauda* and *Priacanthus tayenus*, and a distribution that favoured low gravel, intermediate mud areas, particularly in the southern GBR lagoon. Group 23 included the lumped ascidians and hydroids and Group 18 included the lumped crinoids; three faunal classes which could not be fully sorted and identified within the scope of the project, coincidentally having similar distributions. Group 16 was dominated by bryozoans in terms of number of species (47 of 80). Group 37 was dominated by sponges, both in terms of biomass (~99%) and number of species (22 of 29).

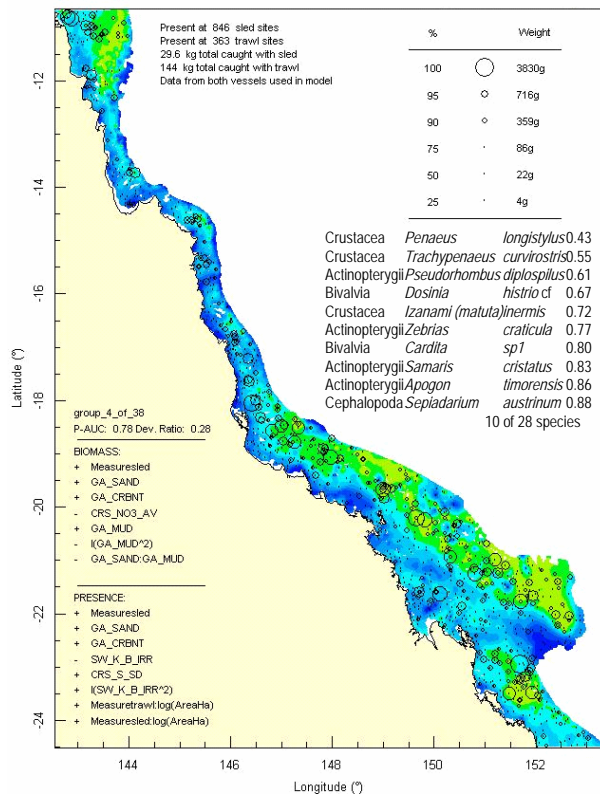
(a) Group 10



(b) Group 32



(c) Group 4



(d) Group 24

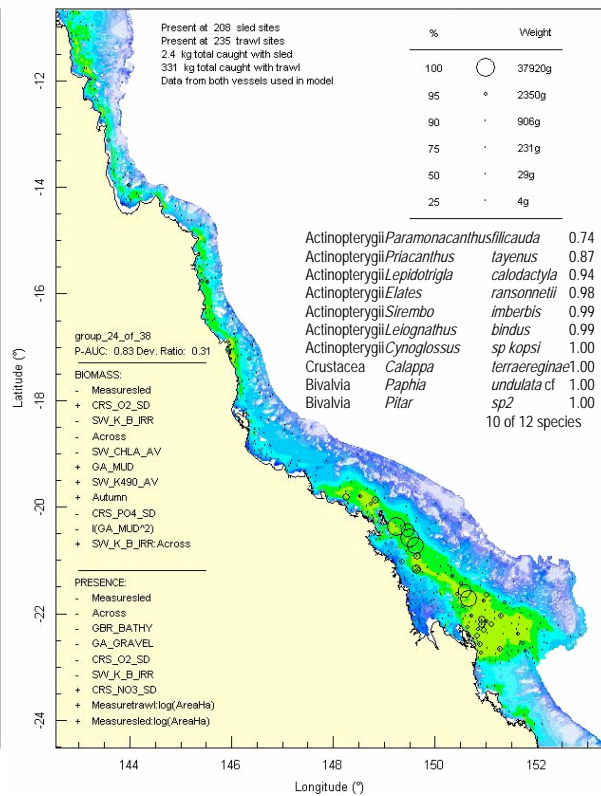
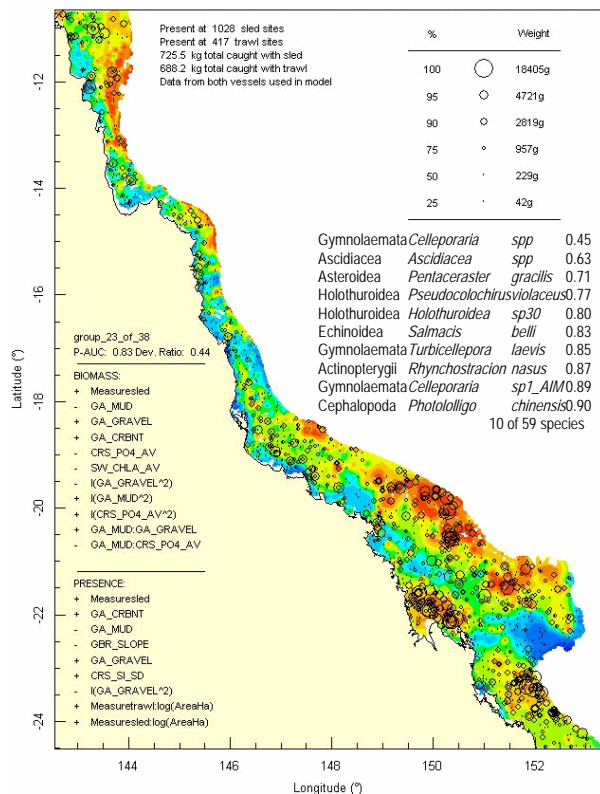
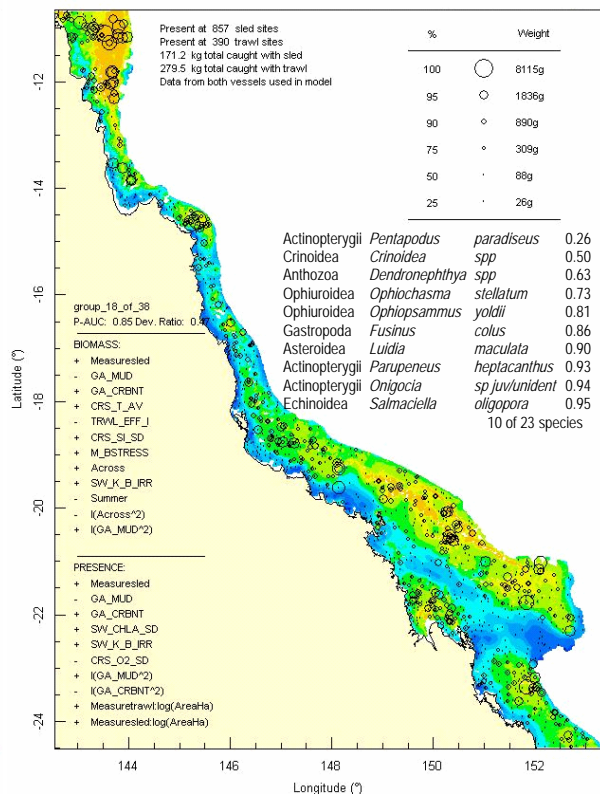


Figure 3-43: Model distribution maps of selected species groups.

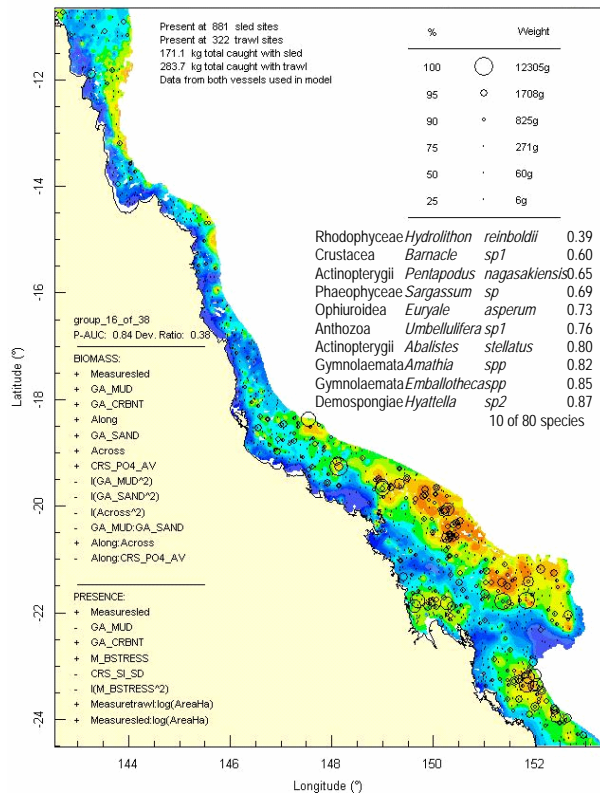
(a) Group 23



(b) Group 18



(c) Group 16



(d) Group 37

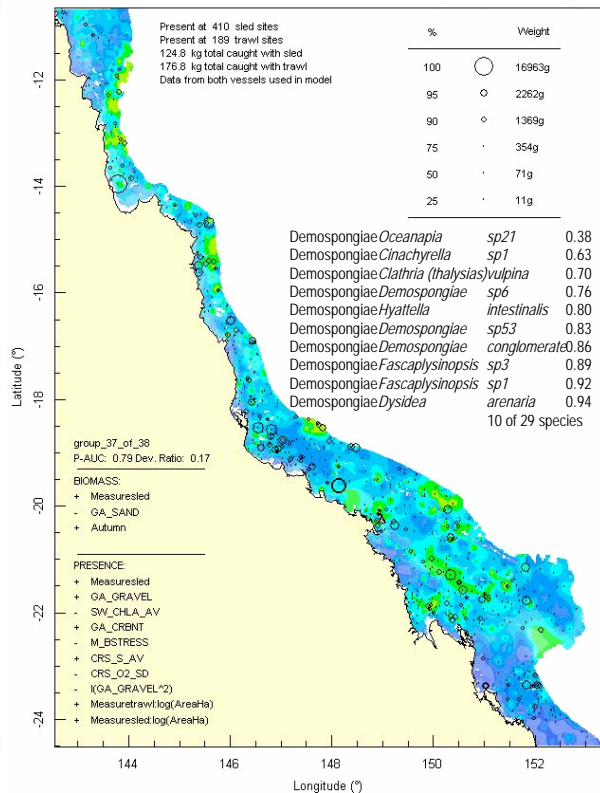


Figure 3-44: Model distribution maps of selected species groups.

3.4. SITE GROUPS CHARACTERIZATION AND PREDICTIONS (W Venables & R Pitcher)

3.4.1. Decision tree results

The recursive splitting on the physical variables, to achieve reduction in deviance of the sites Bray-Curtis matrix, produced 16 groups with the given stopping criteria. The resulting graphical decision tree is shown in Figure 3-45. The primary split was at 25% mud fraction, and mud or another sediment attribute accounted for several other splits, suggesting the importance of sediment grain size composition in structuring seabed assemblages. Given the correlation between variables and that other variables may be good surrogates to split at each node, caution is necessary in interpreting the importance of variables. Nevertheless, percent mud and other sediment attributes were often the most frequently selected in a wide range of biophysical analyses. Other variables likely to be important included bathymetry, oxygen variability, current stress, chlorophyll and/or light attenuation (K490), nutrients and temperature.

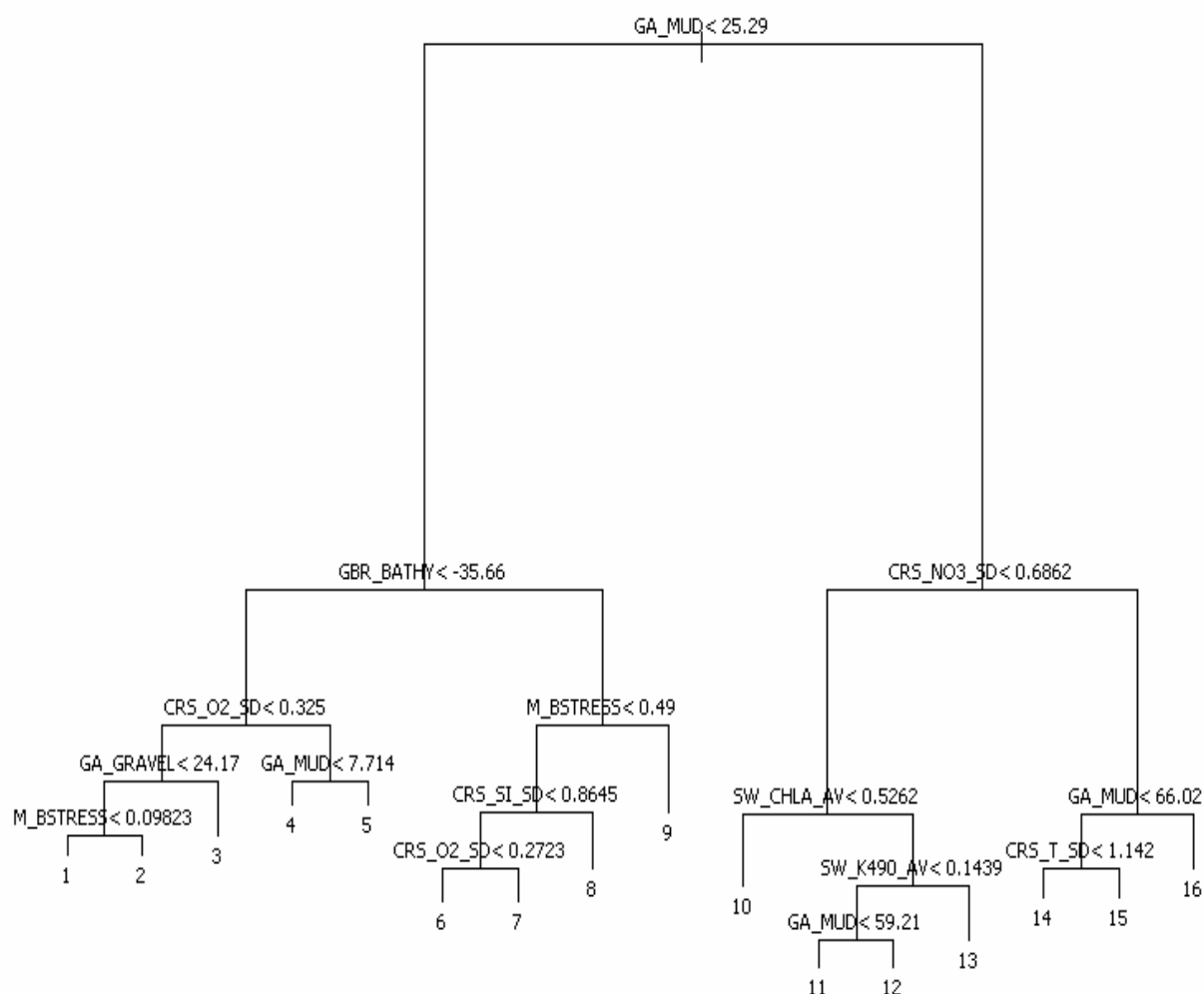


Figure 3-45: Recursive decision tree partitioning the sites into 16 groups, corresponding to the terminal nodes. The labels indicate the split variable and threshold for the group corresponding to the left hand branch in each case. The distances used were Bray-Curtis dissimilarities on $1/8^{\text{th}}$ root transforms of the predicted site species biomass data.

While the decision tree did split a Bray-Curtis matrix to group together sites with similar biota, nevertheless, the splits were on physical variables and so constrained the tree structure and may not necessarily have represented the structure of biological similarities between the 16 site groups. The representation of the biological similarities of the site groups, by hierarchical clustering of the Bray-Curtis dissimilarities of the medoid sites using Ward's method, demonstrated a similar structure, particularly between site-groups 1–9 and 10–16, and within site-groups 1-9 (Figure 3-46). However, the biological similarities of the site medoids within site-groups 10–16 was rather different from the structure of the decision tree, with groups 10–11 and 12–13 being placed biologically close and 11–12 moderately dissimilar. It is important to note that the GBR seabed assemblages are not distinct, but have fuzzy gradients of biotic composition and different transformations, distance metrics, and clustering methods will produce somewhat different results — sometimes transposing some site-groups across the primary mud split. Nevertheless, low-mud and high-mud site-groups typically were separated.

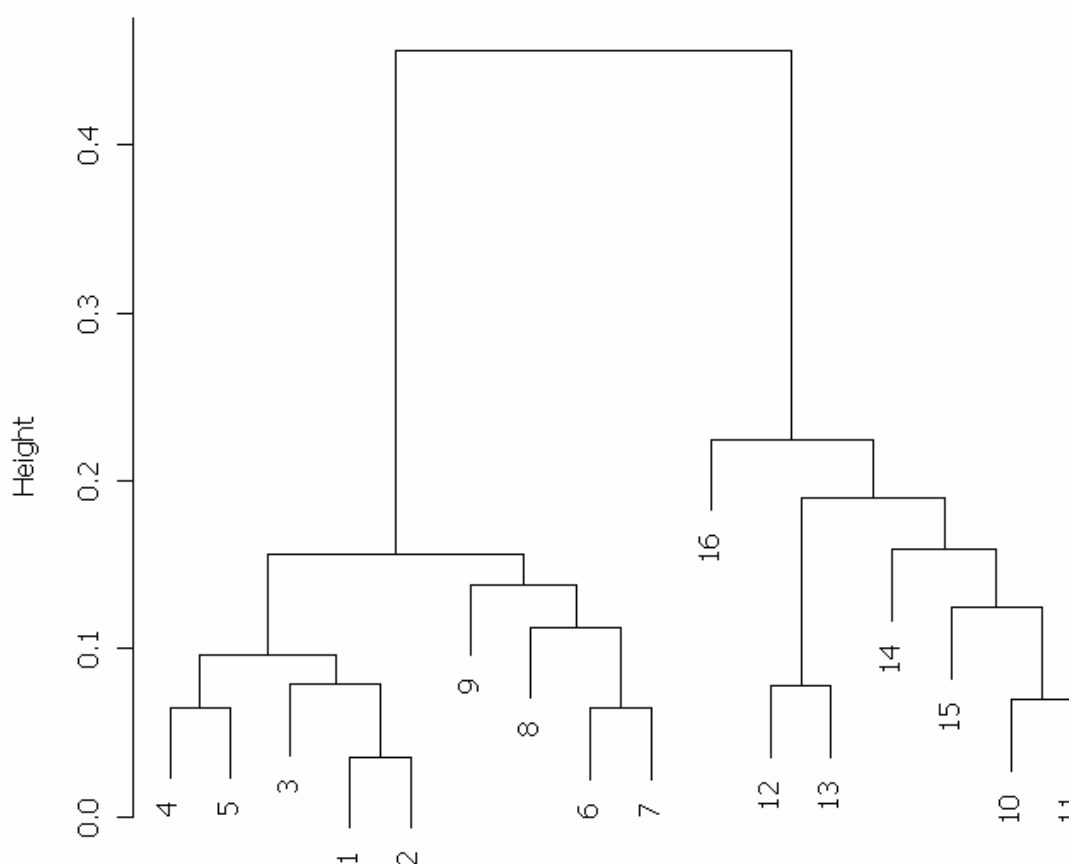


Figure 3-46: Dendrogram of biological similarities between the medoids of the site groups, as defined by the tree Figure 3-45, based on hierarchical clustering of Bray-Curtis dissimilarities using Ward's method.

The set of decision rules for splitting physical variables, defined on data from >1,000 sites, was straightforward to apply to the remaining >170,000 grids cells of the GBR study area and map the result (Figure 3-47). Overall, several rather distinct regions with little if any assemblage representation elsewhere were apparent, including: the Capricorn Section, the Capricorn Channel, Shoalwater Bay and Broad Sound, Swains and Pompey Reefs regions, central/Townsville area, and the northern GBR from about Hinchinbrook Is/Cairns. The composition of the site-group assemblages is discussed in more detail below (Section 3.4.3).

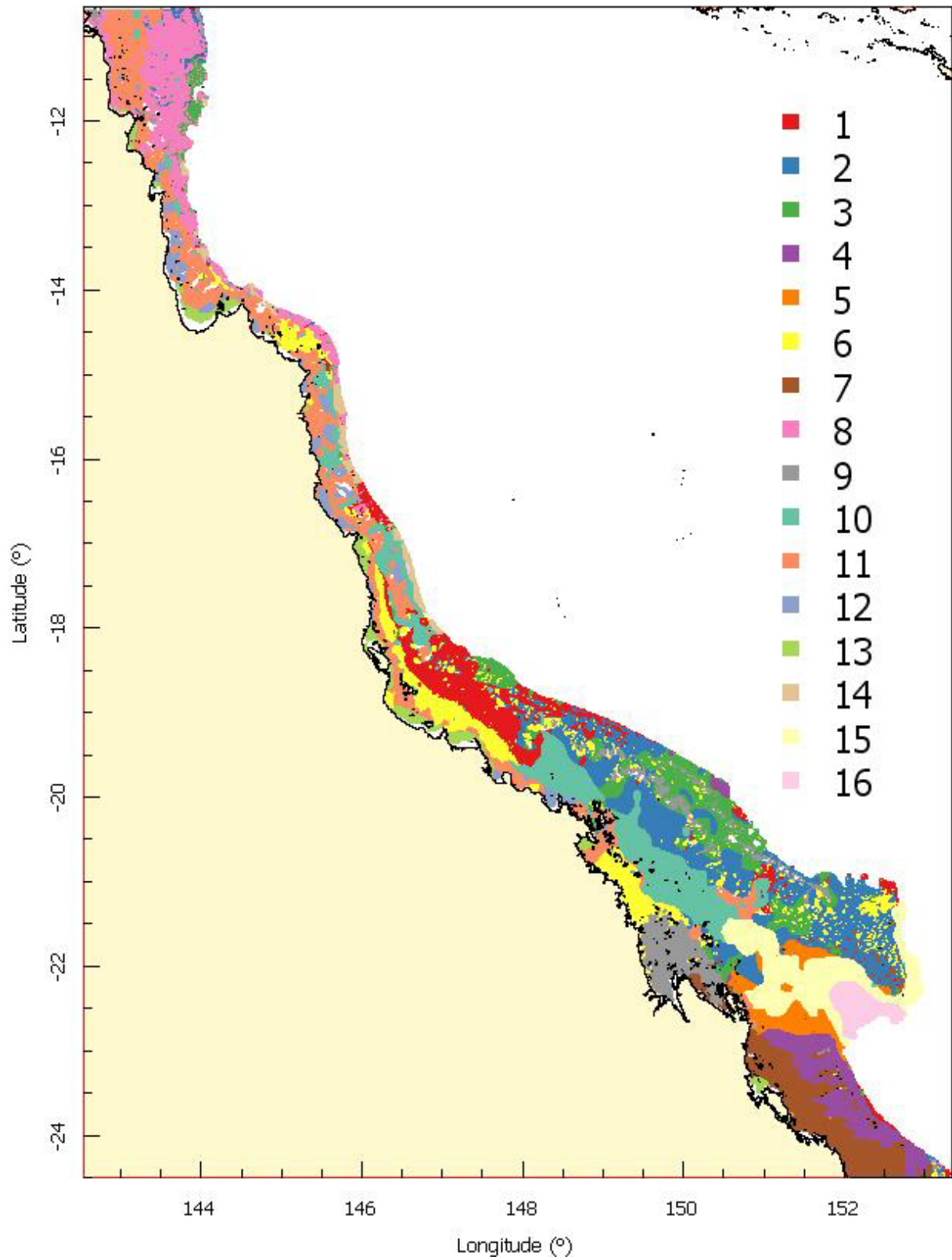


Figure 3-47: Map of predicted distributions of 16 seabed assemblages (site groups clusters).

3.4.2. Species affinity groups

The dendrogram of distances between species with respect to their affinities for the site-group assemblages is shown in Figure 3-48, for all 839 taxa for which prediction models were possible. The distance that defines the 12 species groups for purposes of this analysis is shown by cutting the dendrogram at the dashed red line in the diagram.

The first left branch represents those species with higher affinity for muddier site-groups. Of the right main branch, the smaller left branch represents those species with higher affinity for high current site-groups, and the rightmost branches represent those species with higher affinity for the remaining (coarser, vegetated and/or offshore) site-groups.

The relative biomasses of the 12 species affinity groups across the 16 site-group assemblages are shown in Figure 3-49. While the distribution and composition of the site-group assemblages are described in more detail below, there appear to be about 4–7 relatively distinct mixtures over the 16 site-group assemblages on the basis of summary patterns of relative biomasses of about five sets of the 12 species affinity groups (Figure 3-49). Most distinctive was site-group #8, which was dominated by species affinity group #L — most similar was site-group #6. The coastal/inshore muddy site-groups 11, 12, 13 were characterised primarily by species affinity groups E, G, C. Another, less distinct group of (deeper) muddy sites comprised site-groups 10, 15, 16 and 14 and 5, which were characterised primarily by species affinity groups D, F, H. The remaining site-groups were less distinctly structured; nevertheless, site-groups #1–2 were most similar, characterised primarily by the low biomass of species affinity groups G, E. Next were site-groups #4 & 7, characterised primarily by the species affinity groups K, I, B. Site-group #6 was somewhat similar to #1, 7, 8. Site-groups #9, 3 had the highest abundance of affinity group J.

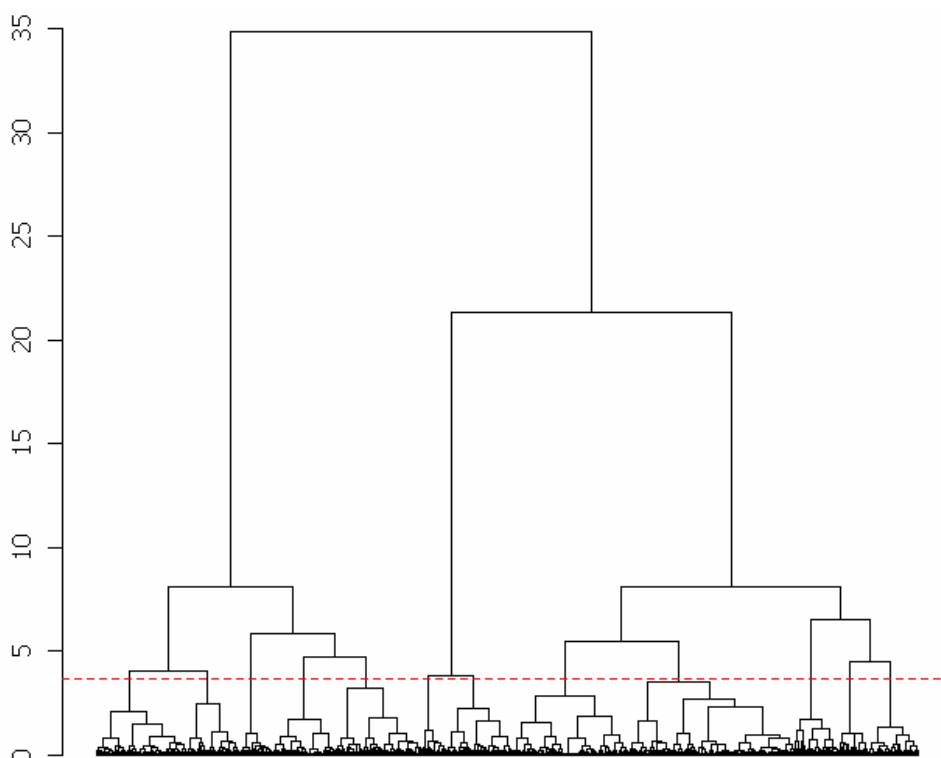


Figure 3-48: Dendrogram for species, defining clusterings based on inter-species distances that reflect affinities between species and site-groups. The red line shows a cut-off that defines the 12 groups used in this analysis. The dendrogram was constructed using Ward's method.

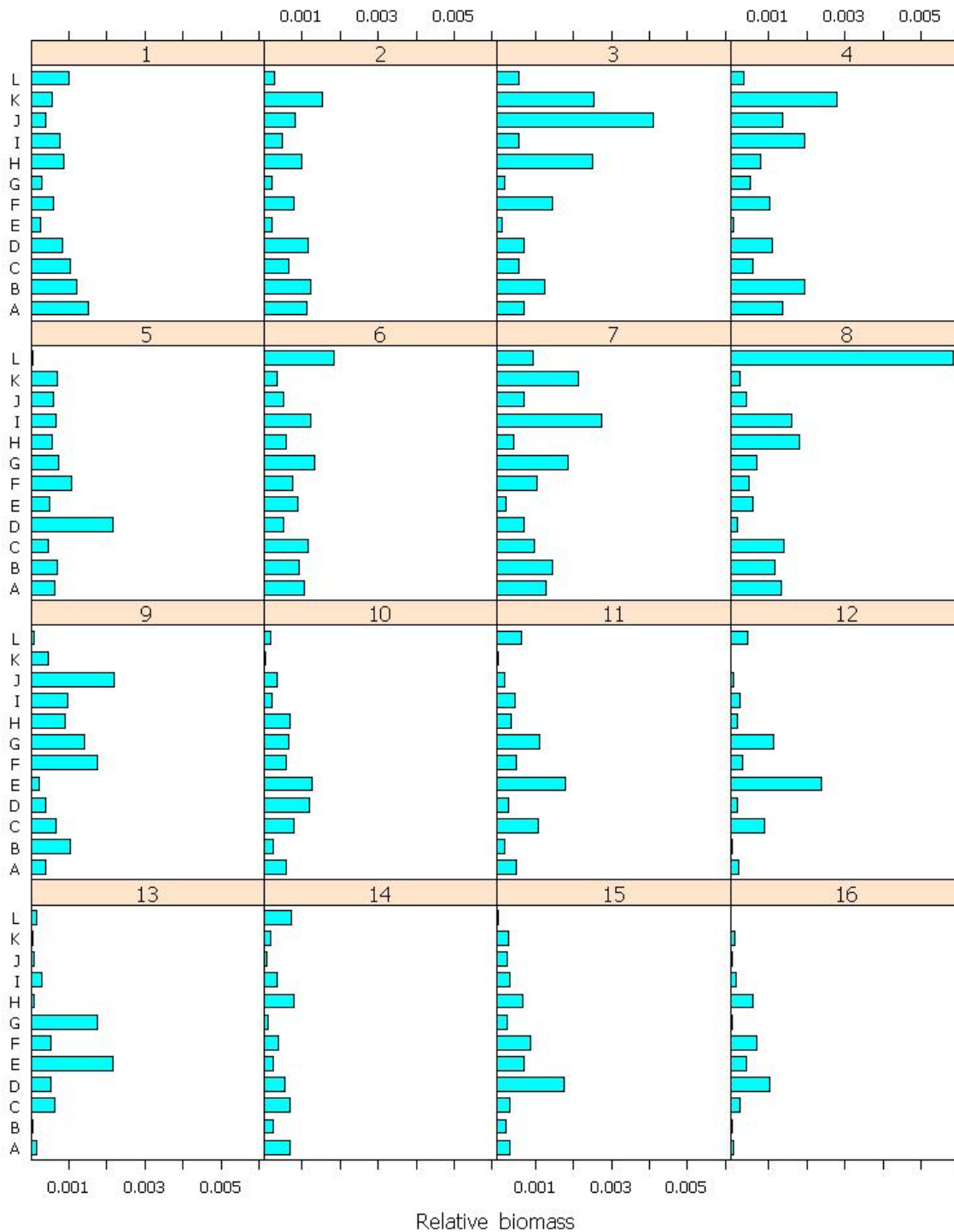


Figure 3-49: Plot of relative biomass of 12 species affinity groups (labeled A–L) across the 16 site-group assemblages mapped in Figure 3-47.

3.4.3. Description of site-group assemblages

Site cluster, or species **Assemblage#1**, occurred in low mud, deep, low gravel, low current stress areas (Figure 3-45) represented by the red areas in Figure 3-47, primarily on the outer shelf off Townsville. No particular species group stood-out in terms of relative biomass associated with assemblage#1 areas, except perhaps A — and lack of G, E, J. Similarly, no particular species had very strong affinities for

assemblage#1; those most aligned were Asteroidea: *Poraster superbus* (species affinity group A), Crustacea: *Portunus argentatus* (group A) and Gastropoda: *Atys cylindricus* cf (L).

Assemblage#2, occurred in low mud, deep, low gravel, slightly higher current stress areas (Figure 3-45) represented by the dark blue areas primarily on the outer shelf of the southern GBR.

Assemblage#2 areas were also characterised by lack of species groups, but groups A, K, B, D had some affinity and slightly higher relative biomass associated with Assemblage#2. A number of species had moderately strong affinities for assemblage#2; those most aligned were: Gymnolaemata: *Retiflustra* spp (A), *Hippopetraliella magna* cf (A), *Tetraplaria immerse* (K), *Nellia tenella* cf (D), Echinoidea: Temnopleuridae sp2_QMS (A), Ophiuroidea: *Euryale asperum* (B), Crustacea: *Parthenope* sp32091 (K), *Takedana eriphoides* (A), *Myrine kesslerii* (A), Actinopterygii: *Samaris cristatus* (A), *Hippocampus queenslandicus* (A), *Engyprosopon maldivensis* (B), *Kanekonia queenslandica* (B), Bivalvia: *Cardita* sp1 (A).

Assemblage#3, occurred in low mud, deep, high gravel areas (Figure 3-45) represented by the dark green areas in Figure 3-47, primarily on the outer shelf offshore from the Whitsundays and Mackay, with a patch occurring on the shelf edge offshore from Townsville. Species groups J, H, K stood-out in having higher affinity and/or relative biomass associated with assemblage#3 areas. At the species level, some of strongest affinities were seen for assemblage#3; those most aligned were: Gymnolaemata: *Adenifera armata* (H), *Hippomenella avicularis* (H), *Celleporaria* spp (J), *Euthyrisella obtecta* (J), *Macropora* spp (K), *Sinupetraliella* spp (H), Calcarea: *Clathrina* sp1 (H), Demospongiae: *Demospongiae* sp10 (H), *Demospongiae* sp26 (J), *Callyspongia* sp26 (J), *Demospongiae* sp27 (H).

Assemblage#4, occurred in very low mud, deep areas (Figure 3-45) represented by the purple areas in Figure 3-47, primarily on the outer shelf of the Capricorn Section of the GBR. Species groups K, B, I stood-out in having higher affinity and/or relative biomass distributed in assemblage#4 areas. A number of species had moderate affinities for assemblage#4; those most aligned were: Gymnolaemata: *Orthoscuticella* spp (K), *Arachnopusia* spp (K), *Scuticella plagiostoma* (K), Actinopterygii: *Ambiserrula jugosa* (K), Demospongiae *Xenospongia patelliformis* (K).

Assemblage#5, occurred in intermediate low mud, deeper areas (Figure 3-45) represented by the orange areas in Figure 3-47, on the flanks of the Capricorn Channel in the southern GBR. Species group D had the highest affinity and relative biomass distributed in assemblage#5 areas. At the species level, some of weakest affinities were seen for assemblage#5; those most aligned were: Actinopterygii: *Lepidotrigla calodactyla* (D), Foraminifera: *Discobotellina biperforata* (K).

Assemblage#6, occurred in low mud, shallower, low current stress areas (Figure 3-45) represented by the yellow areas in Figure 3-47, primarily on the inner/mid shelf off Townsville from Cape Upstart to Fitzroy Island, the inner shelf of the Mackay Coast, the mid shelf from Lizard Is to Turtle Is, and smaller scattered areas of the outer shelf and Swains. Although these were some of the more vegetated areas in the GBR, no particular species group stood-out in terms of affinity with assemblage#6, but L had elevated relative biomass. Again, at the species level, some of weakest affinities were seen for assemblage#6; those most aligned were: Actinopterygii: *Scorpaenopsis furneauxi* (G), Chlorophyceae: *Caulerpa taxifolia* (L), *Avrainvillea* sp1 (A), *Udotea flabellum* (A), Gastropoda: *Strombus campbelli* (G), *Dolabella* sp1 (I), Liliopsida: *Halophila spinulosa* (I).

Assemblage#7, occurred in somewhat similar areas as #6 (Figure 3-45), but primarily on the inner shelf of the Capricorn Coast indicated by the brown areas in Figure 3-47. These were also some of the more vegetated areas in the GBR, and species groups I, K, G stood-out in terms of affinity and/or relative biomass associated with assemblage#7. A number of species had moderate affinities for assemblage#7; those most aligned were: Crustacea: *Portunus sanguinolentus* (K), Asteroidea: *Oreasteridae* sp1 (I), Holothuroidea: *Holothuria* sp2 (I), Actinopterygii: *Ambiserrula jugosa* (K), *Suezichthys gracilis* (K), *Aploactis aspera* (I), *Paramonacanthus otisensis* (I), Rhodophyceae: *Chondrophyucus* sp1 (K), Phaeophyceae: *Padina* sp. (K).

Assemblage#8, also occurred in low mud, shallower, low current stress areas (Figure 3-45) represented by the pink areas in Figure 3-47, primarily on the outer shelf of the far northern GBR, extending south inside the barrier to about Lizard Island; the coastal silica sand strip from Shelbourne Bay north was also included. Some of the most extensive Halimeda banks occurred in some of these areas. Species group L was a stand-out in having higher affinity and relative biomass associated with

assemblage#8 areas; followed by species groups H, I and C, A. A number of species had moderate-high affinities for assemblage#8; those most aligned were: Chlorophyceae: *Dictyosphaeria cavernosa* (L), *Halimeda gigas* (L), *Halimeda opuntia* (L), *Caulerpa sertularioides* (L), *Caulerpa serrulata* (L), Actinopterygii: *Pseudorhombus argus* (L), Gastropoda: *Terebellum terebellum* (L), *Atys* sp1, Echinoidea: *Breynia desorii* (L), *Peronella lesueuri* (H), Anthozoa: *Heteropsammia cochlea* (L).

Assemblage#9, occurred in low mud, shallower, high current stress areas (Figure 3-45) represented by the grey areas in Figure 3-47, primarily in the vicinity of Broad Sound and Shoalwater Bay, but including offshore narrow inter-reef channels and the approaches to Torres Strait. Some of the most extensive epibenthic faunal gardens occurred in some of these areas. Species group J stood-out clearly in terms of relative biomass associated with assemblage#9, followed by F, G. At the species level, some the strongest affinities were seen for assemblage#9; those most aligned were: Actinopterygii: *Centrogenys vaigiensis* (G), *Inegocia harrisii* (G), Crustacea: *Metapenaeopsis novaeguineae* (G), *Paradorippe australiensis* (G), *Hyastenus elatus* (J), Gymnolaemata: *Micropora angusta* cf (J), Bivalvia: *Arca navicularis* (J), *avellana*_MTQ (J), Asteroidea: *Goniasteridae* sp5 (J), Demospongiae: *Callyspongia schultzi* (F), Anthozoa: *Melithaea* sp2 (J), *Mopsella* sp2 (J).

Assemblage#10, occurred in high mud, low nitrate variability, low chlorophyll areas (Figure 3-45) represented by the aqua-blue areas in Figure 3-47, primarily in the mid-Lagoon of the Whitsunday region and re-occurring on the outer shelf offshore from Hinchinbrook to Cape Flattery. Some of the most barren habitats occurred in some of these areas, although the sled and trawl revealed significant biodiversity. Species groups E, D had the highest relative biomass in this assemblage, but none had high affinity. At the species level, weak affinities were seen for assemblage#10; those most aligned with were: Actinopterygii: *Nemipterus hexodon* (E), Crustacea: *Cloridina chlorida* (E), *Iphiculus spongiosus* (E), Demospongiae: *Fascaplysinopsis* sp3 (H), Bivalvia: *Anadara ferruginea* cf (E).

Assemblages #11, 12, 13, occurred in high mud, low nitrate variability, high chlorophyll areas (Figure 3-45), with 12 being in the muddiest habitats and 13 in the most turbid, represented respectively by the salmon, grey-blue and pale-green areas in Figure 3-47, primarily in shallower inner shelf areas extending from ~Whitsunday Islands to Torres Strait, and broader north of about Cairns. Again, some of the most barren habitats occurred in some of these areas, although the sled and trawl revealed significant biodiversity. Species groups E, G were associated with these assemblages. At the species level, the affinities were moderate-weak (weakest for assemblage#12); those most aligned with assemblage #11 were: Actinopterygii: *Scolopsis taeniopterus* (E), *Terapon theraps* (E), *Leiognathus leuciscus* (E), Crustacea: *Charybdis truncata* (E), Crustacea: *Metapenaeus endeavouri* (E); those most aligned with assemblage #12 were: Crustacea: *Cryptolutea arafurensis* (E), Actinopterygii: *Saurida argentea/tumbil* (E); and those most aligned with assemblage #13 were: Actinopterygii: *Leiognathus splendens* (E), *Leiognathus moretoniensis* (G), *Gerres filamentosus* (G), *Tripodichthys angustifrons* (E), *Terapon puta* (E), *Apogon poecilopterus* (E), Crustacea: *Trachypenaeus anchoralis* (G), Crustacea *Metapenaeus ensis* (E), *Penaeus semisulcatus* (E).

Assemblages #14, 15, 16 occurred in high mud, high nitrate variability areas (Figure 3-45) represented by the deeper pale-khaki, pale-yellow and pale-pink areas in Figure 3-47. Assemblage #14 was located along the far outer shelf offshore from Hinchinbrook to Cairns; #15, 16 occurred near the entrance of the Capricorn Channel. Some of the most barren habitats occurred in some of these areas, although the sled and trawl revealed significant biodiversity. No species group or individual species had a clear association with Assemblage #14 in terms of relative biomass or affinity. Species groups D, F showed somewhat higher relative biomass in assemblages 15, 16, and D had some affinity with 15. Affinities were weak at the species level; those most aligned with assemblage#15 were: Crustacea: *Arcania heptacantha* (D), *Solenocera choprai* (D), Actinopterygii: *Upeneus moluccensis* (D), *Lepidotrigla calodactyla* (D), *Elates ransonnetii* (E); and those most aligned with assemblage#16 were: Crustacea: *Solenocera choprai* (D), Actinopterygii: *Upeneus moluccensis* (D).

3.5. VIDEO HABITAT CHARACTERIZATION AND PREDICTION

The data from the towed video camera, entered in real-time in the field ("tappity") and from post-analysis of random frames in the laboratory, was used to provide information on seabed habitats — in the form of maps summarizing the data and as a statistical characterisation.

3.5.1. Seabed substratum

The real-time tappity data showed that inshore areas along much of the length of the GBR were muddy or silty (Figure 3-50, Figure 3-52a), and comprised terrestrial sediments. Typically, with distance across the shelf, the substratum becomes sandier or even coarser (Figure 3-50, Figure 3-52d), and comprised of carbonate of biological origin. In offshore areas, coralline outcrops, reefs and shoals may occur in deep areas between emergent coral reefs (Figure 3-52k).

The strong tidal current areas among the dense reef matrix offshore in the central-southern GBR were rubbly or stony, with rocks and limestone bedrock often exposed. Much of the rubble in these areas is formed by encrusting bryozoans (Figure 3-52o). The inshore strong tide areas of Broad Sound and Shoalwater Bay are also very coarse or rocky. Between these lies the Capricorn Channel, a wide area of GBR lagoon with a very silty and muddy seabed. The south-eastern entrance to this channel is the deepest area on the GBR shelf, at 100-130 m.

The Capricorn Region, the southernmost part of the GBR, is typically sandy right across the shelf. It lies at the northern end of the Great Sandy Region, just beyond Fraser Island, the source of large quantities of terrestrial sand.

3.5.2. Seabed biological habitat

The majority of the seabed in the GBR was devoid of visible biological habitat attached to the surface of the substratum; however, most of these areas were bioturbated indicating the activity of animals in the sediments (Figure 3-51, white and grey areas; Figure 3-52 cf. bm). In offshore sandy areas with medium currents, crinoid feather stars were sometimes extremely abundant on the seabed (Figure 3-52n).

Marine plants form dominant cover over large areas of the GBR shelf (Figure 3-53, e.g. Figure 3-52f). A long band of mixed algae and patchy seagrass (primarily *Halophila spinulosa*) occurs along the mid-shelf off Townsville (Figure 3-51). Dense beds of *H. spinulosa* also occur over much of the shelf in the Capricorn region (Figure 3-52e) as well as around the Turtle Is Group in the central northern GBR (Figure 3-54). Vast banks of *Halimeda* algae (Figure 3-52g) occur just inside the outer barrier reef near Lizard Is, also in the central northern GBR, as well as in the far northern GBR (Figure 3-53). These *Halimeda* banks may be up to 15 m thick, comprised of the deposited carbonate skeletons of these algae. Other types of algae, including crustose corallines, are prolific along some sections of the outer shelf in water up to 80-100 m deep (Figure 3-53, Figure 3-52eh).

Epibenthic fauna such as alcyonarian soft corals, whips & gorgonians and sponges may occur in patchy gardens (Figure 3-51, Figure 3-52ij, Figure 3-57, Figure 3-56, Figure 3-55), particularly in medium-strong current areas corresponding to red areas in Figure 2-14; bryozoans are important in similar areas (Figure 3-58). Hard corals may grow on some of the hard ground areas, typically offshore (Figure 3-52, Figure 3-59).

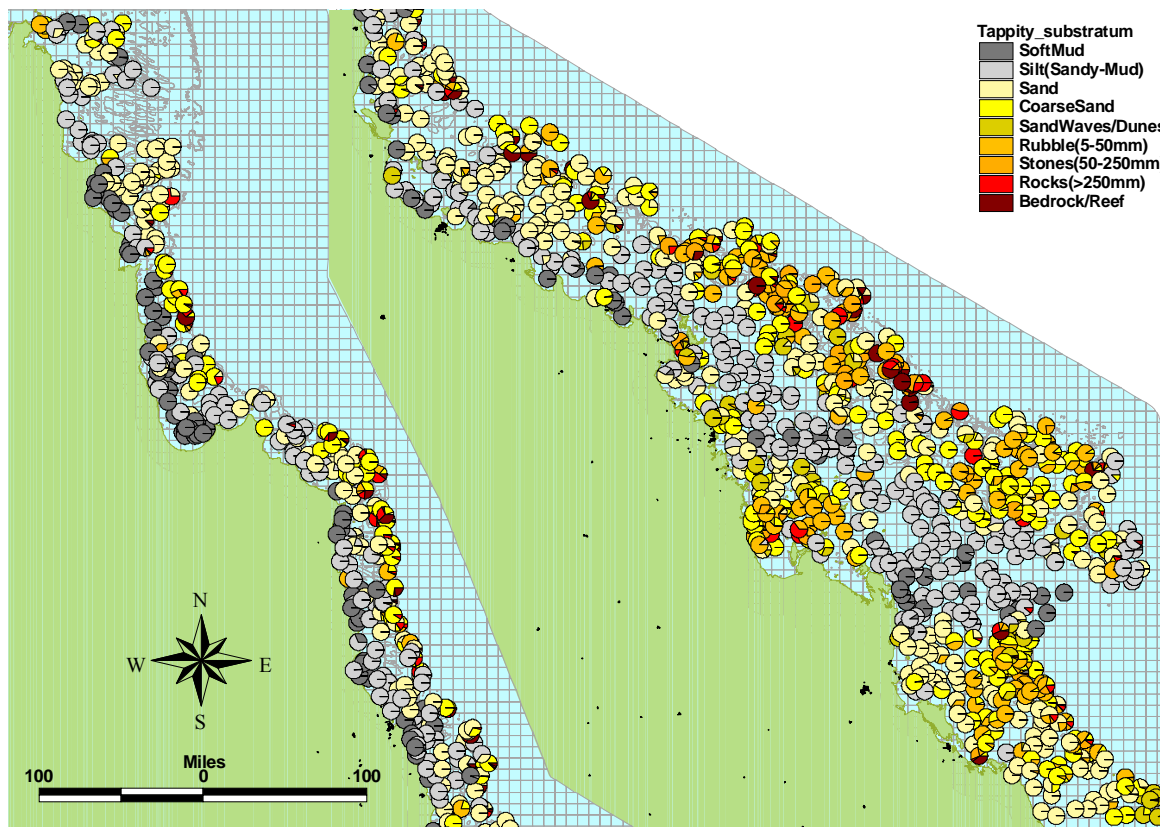


Figure 3-50: Map of the distribution of seabed substratum types summarized as percent of transect length observed by towed video camera.

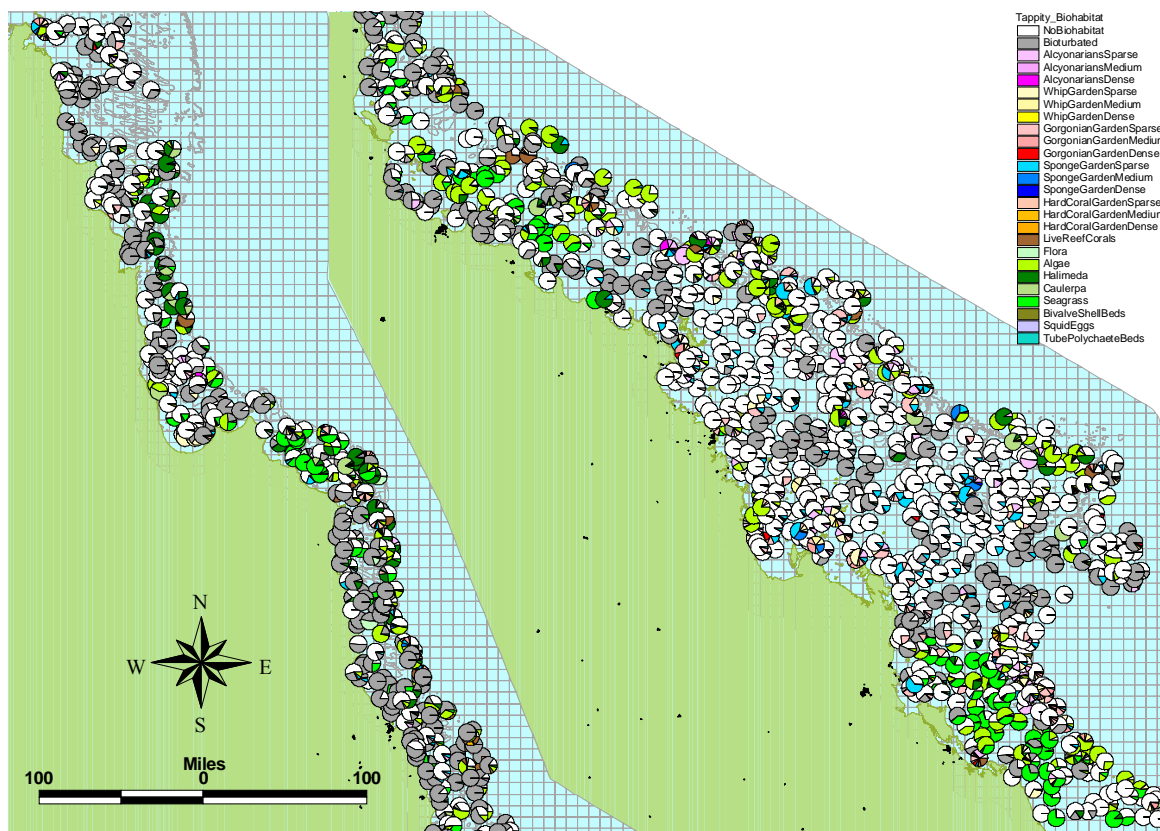


Figure 3-51: Map of the distribution of broad biological seabed habitat types summarized as percent of transect length observed by towed video camera.



a) Muddy inshore seabed, with filefish.



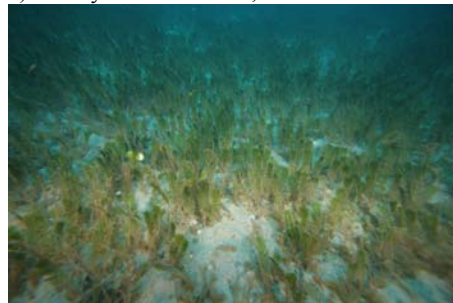
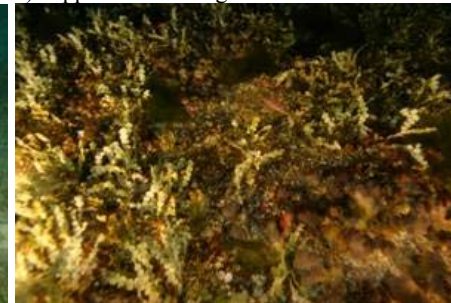
b) Bioturbated silty inner shelf seabed



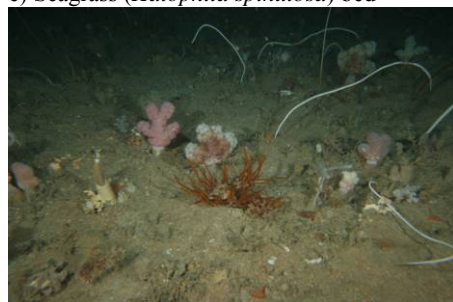
c) Rippled sand in high current area



d) Coarse outer shelf sediment with soft corals

e) Seagrass (*Halophila spinulosa*) bedf) Dense algal bed (*Caulerpa*)

g) Halimeda bank

h) *Ulva* growing on coralline algae at shelf edge

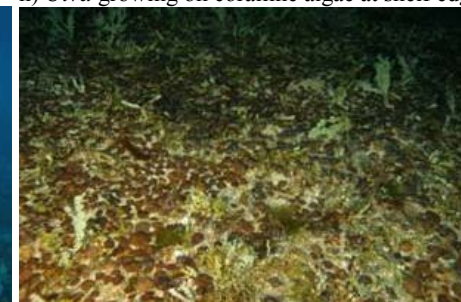
i) Soft corals in strong current channel



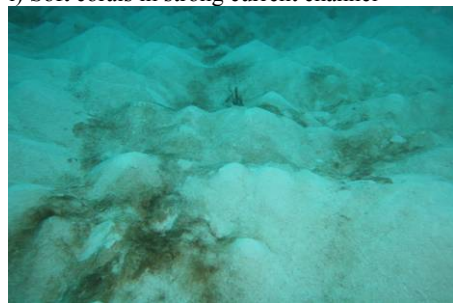
j) Gorgonian garden on hard ground



k) Shoal ground in deep water



l) Solitary coral and algae near shelf edge



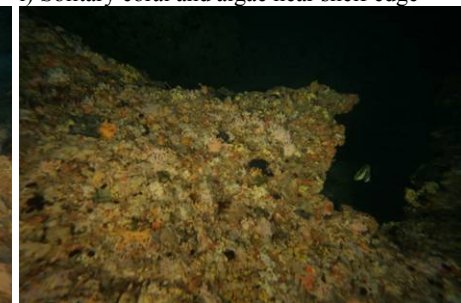
m) Large bioturbation mounds in offshore sand



n) Crinoids on sand in strong current area



o) Bryozoan rubble in strong current channel



p) Scoured rocky seabed in extreme current area

Figure 3-52: Photos of some example habitat types observed by towed video camera.

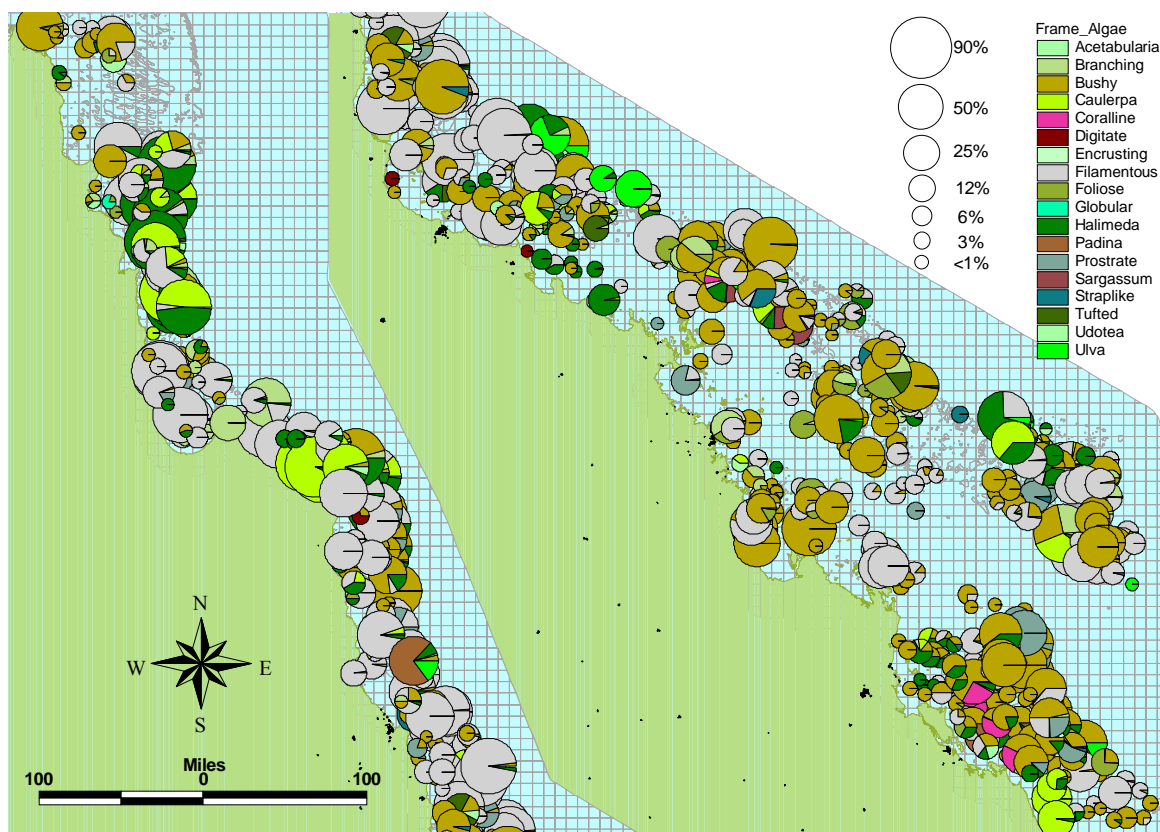


Figure 3-53: Map of the distribution and cover of conspicuous genera and other morpho-types of algae.

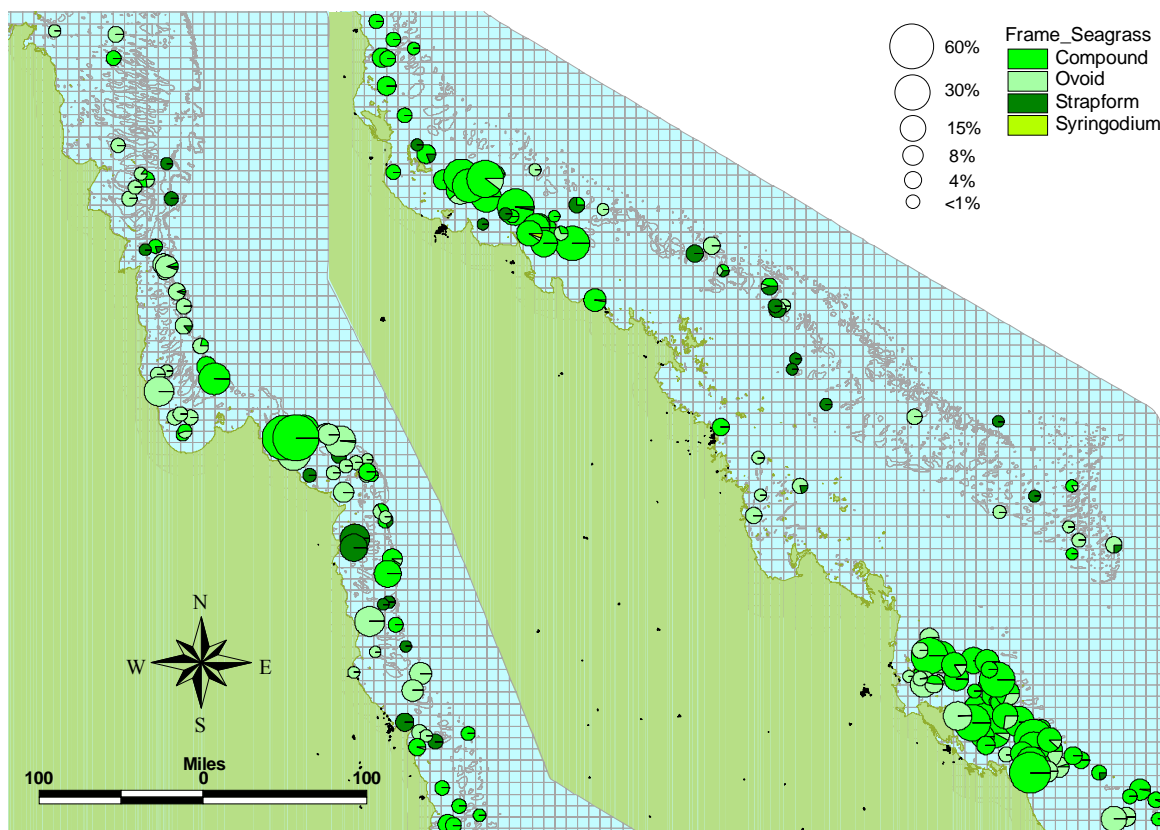


Figure 3-54: Map of the distribution and cover of morpho-types of seagrasses.

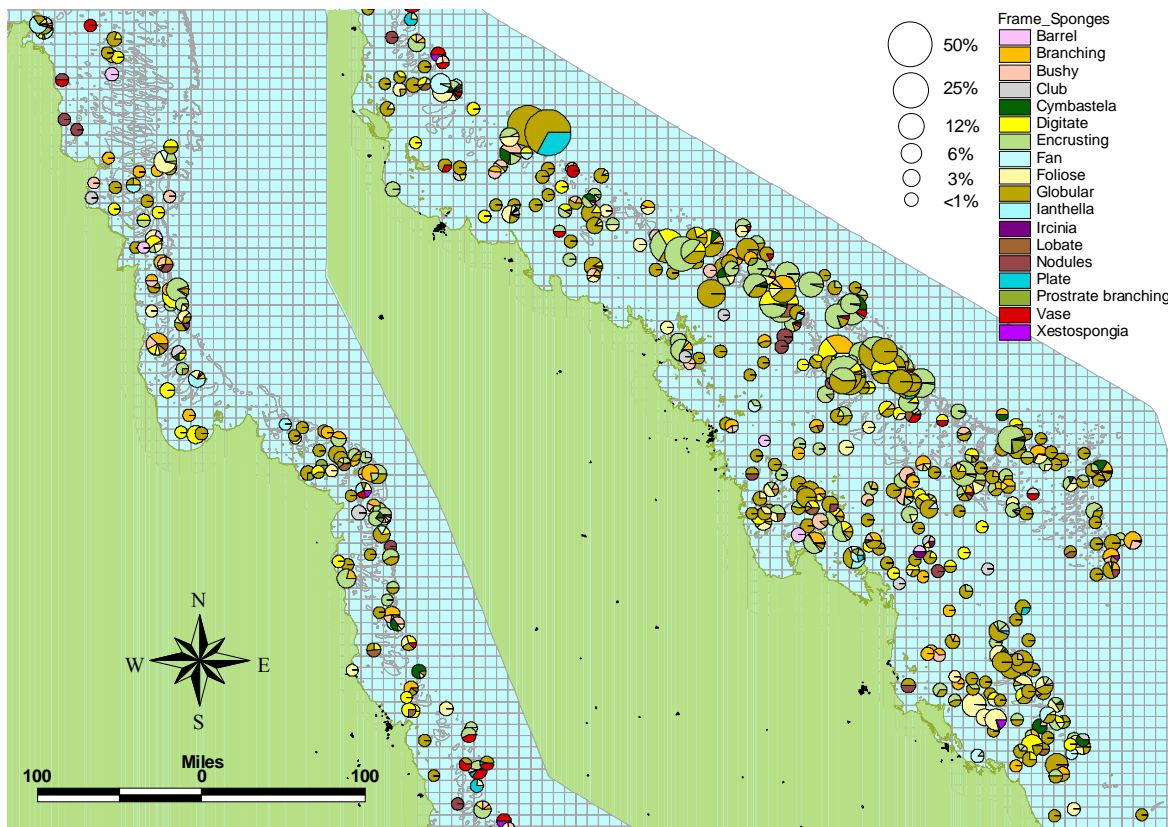


Figure 3-55: Map of the distribution and cover of conspicuous genera and other morpho-types of sponges.

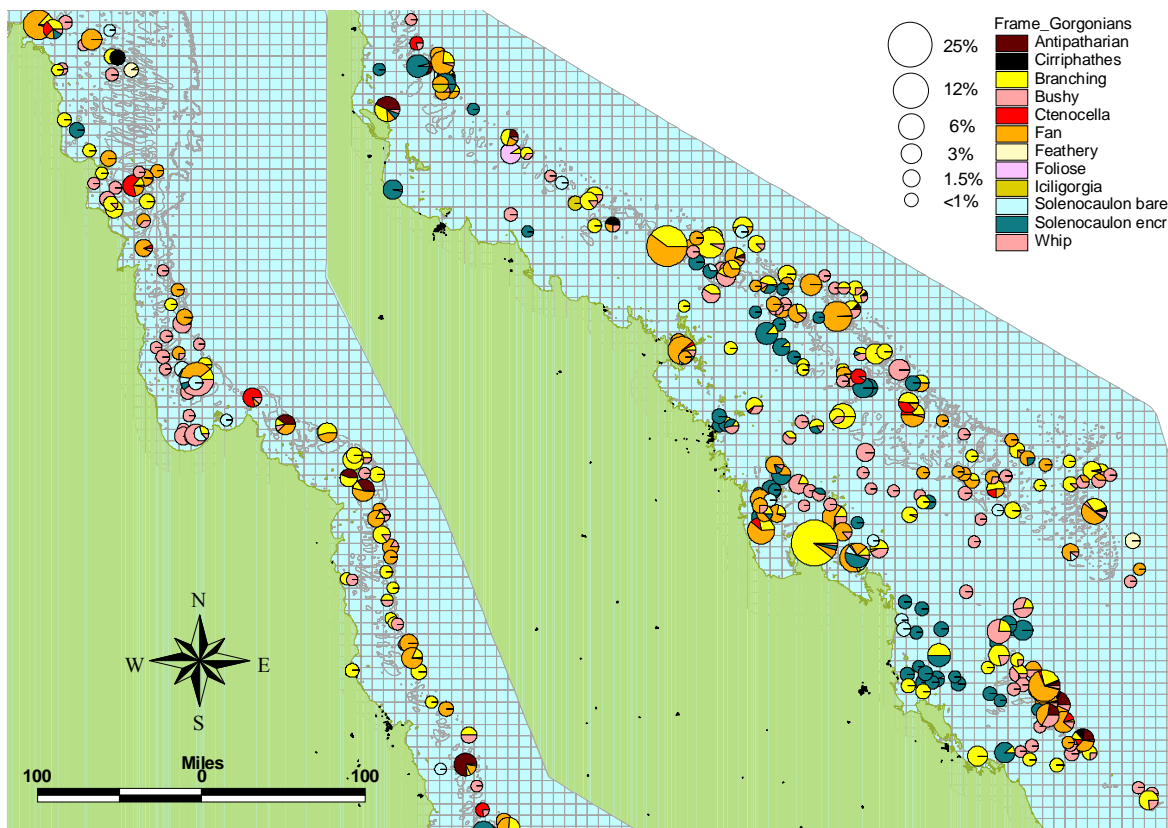


Figure 3-56: Map of the distribution and cover of conspicuous genera and other morpho-types of gorgonians.

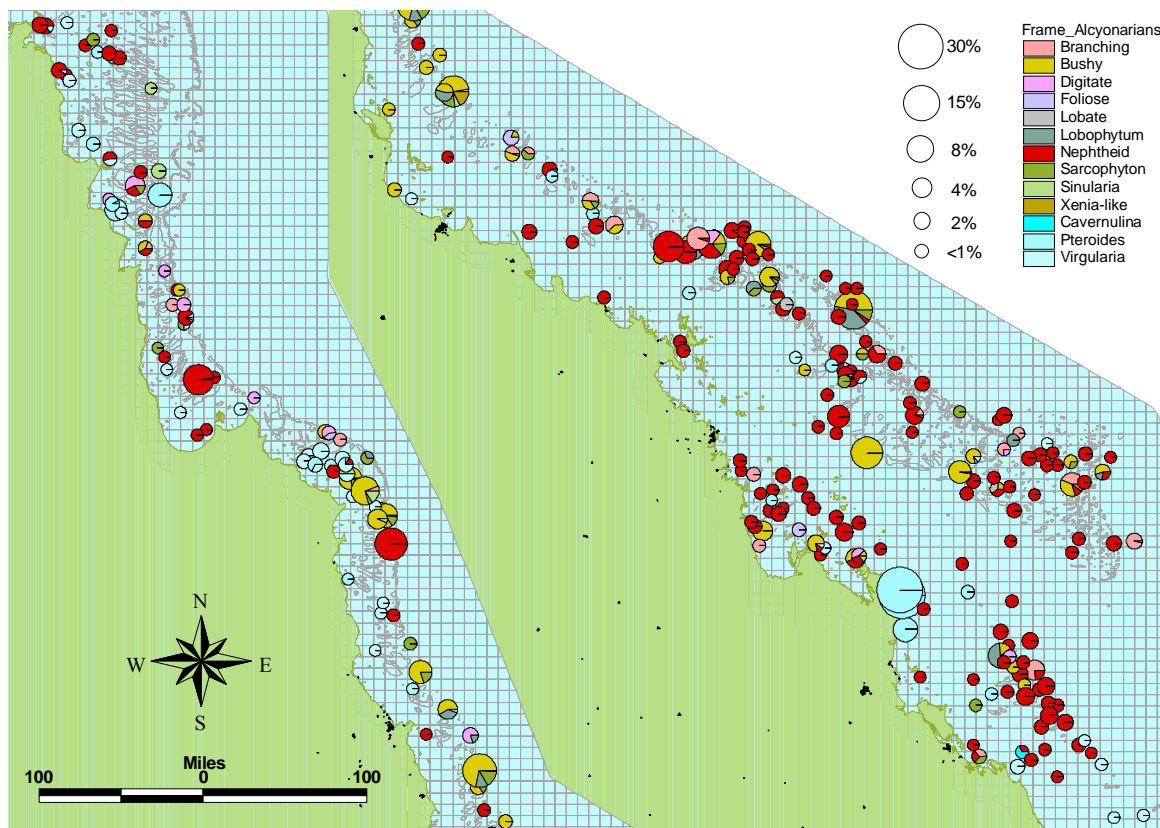


Figure 3-57: Map of the distribution and cover of conspicuous genera and other morpho-types of alcyonarian soft-corals.

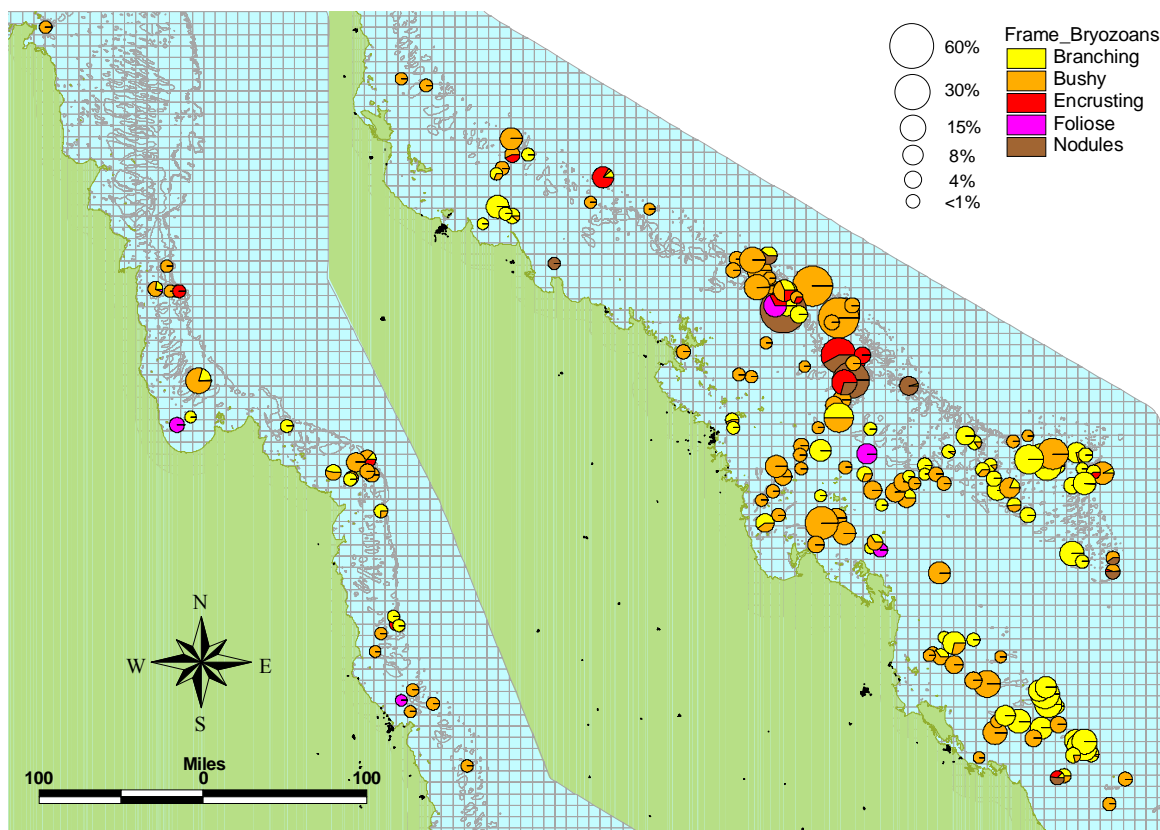


Figure 3-58: Map of the distribution and cover of morpho-types of bryozoans.

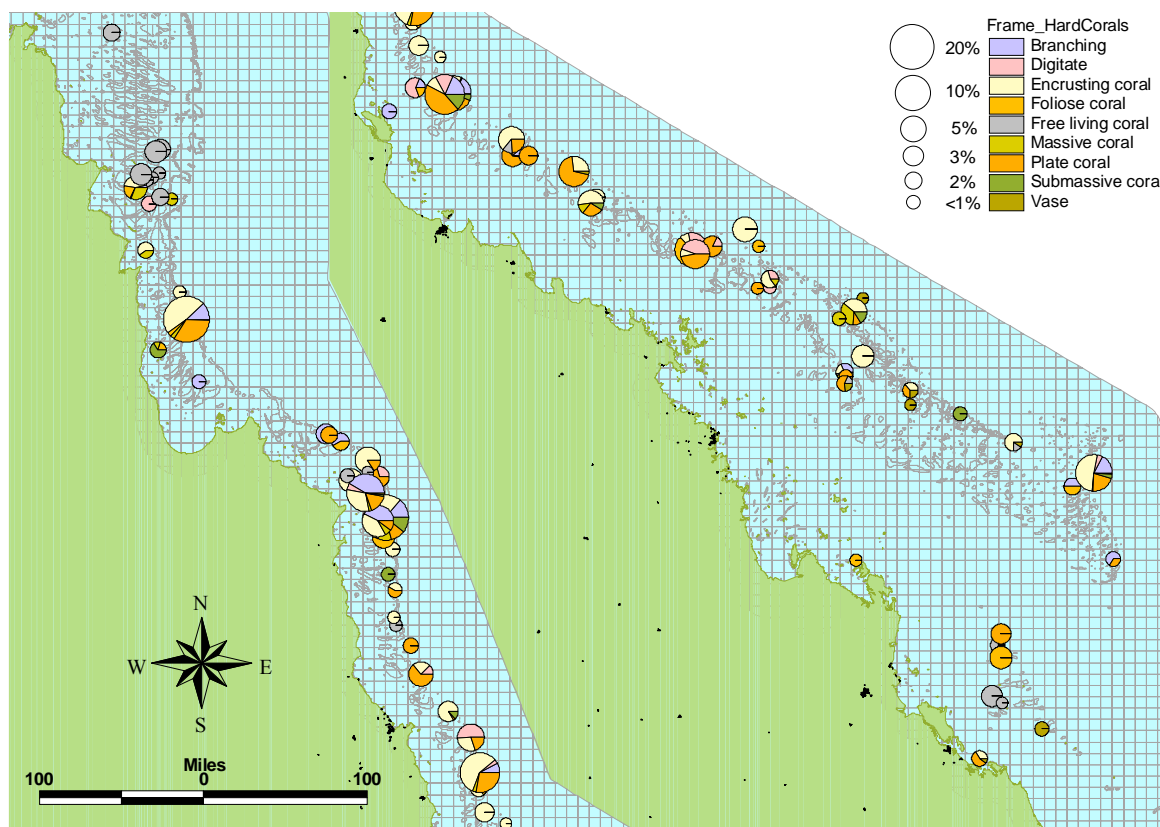


Figure 3-59: Map of the distribution and cover of morpho-types of hard corals.

3.5.3. Statistical characterization and prediction (W Venables & R Pitcher)

The medoid `rpart` algorithm, using the Manhattan (Bray-Curtis) distance metric applied to the vessel biological data (with the three densities of epibenthos grouped), produced the tree shown in Figure 3-60 — a result which appeared to capture more of the known habitat distributions, compared with the other tree metrics. The improvement (proportional reduction) in deviance achieved by any node is reflected by the height of the vertical lines descending from the node. Hence the most primary and most substantial cut is on the sediment variable `GA_MUD` with sites for which this value is less than 15.51% proceeding down to the left hand node and the remainder to the right hand node. In general, the labelling of each interior node indicated the cases going to the left hand node and the complement to the right. The labelling of the terminal nodes is with an arbitrary group number used only for identification purposes in the following descriptions

Experience with the `mvpart` algorithm using both the Euclidean and Hellinger metrics suggested that a complexity, in those cases, of about 6 or 7 groups was justified on the basis of cross-validation. The stopping rules of the `rpart` algorithm terminated the Manhattan (Bray-Curtis) tree at 9 groups, a similar though perhaps somewhat more optimistic number compared to the others and possibly with cross-validation of Manhattan if that was available.

Information on the biological habitat character of these 9 groups could be obtained from either the group medoids, or nearly equivalently, the group centroids. The latter are shown as horizontal bar graphs in Figure 3-61 and are described in more detail below. Nevertheless, it is clear from Figure 3-61 that while the biological habitat profiles of some of the groups stand out as different from others, some are not strikingly dissimilar. For example, there are degrees of similarity between 6 and 7, 3 and 4, and 5 and 9.

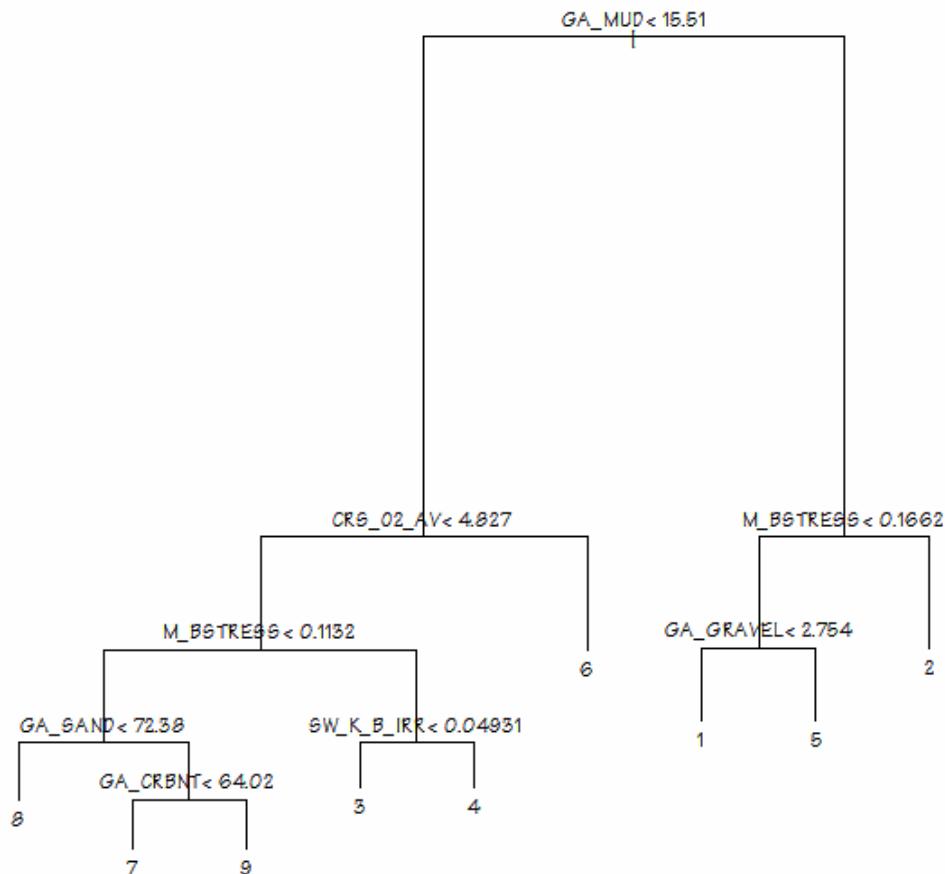


Figure 3-60: Recursive partitioning of sites based on the grouped vessel biological cover proportions, the Manhattan (Bray-Curtis) distance metric and the medoid partitioning algorithm.

3.5.3.1. Effectiveness of the substratum video data as predictors of biology

The check on the effectiveness of the external physical predictors, by including the substratum profile proportions as additional predictors and noting whether any were chosen in advance of the external physical variables. The resulting tree was mostly identical to the previous one (Figure 3-60), with the following exceptions: the previous clusters 3 and 4 were divided into three, with splits on the video substratum variable `Bedrock.Reef` and `M_BSTRESS`, and group 5 was further split into two on the video substratum variable, `Rocks.250mm`. The added predictors are only selected at a low level in the tree and the effect is to isolate similar subgroups within groups already present rather than to isolate different groups.

3.5.3.2. Predictions to the GBR grid

The predictions of node membership on the entire GBR covariate grid, based on the splits of the Manhattan (Bray-Curtis) tree, are shown in Figure 3-62, colour coded according to the scheme in the attached legend and numbered according to the tree (Figure 3-60).

With reference to the cluster profiles (Figure 3-61), the Manhattan (Bray-Curtis) tree (Figure 3-60) and the distribution map (Figure 3-62), the clusters were broadly characterised as follows: Cluster 1 represented the most barren seabed type, almost entirely bare and bioturbated with very little

biohabitat, distributed in muddy areas of the inshore and midshelf and the deep end of the Capricorn Channel. Cluster 2 was also very barren, with some bioturbation and very little epibenthos or algae, distributed in muddy-sand areas of the southern midshelf and far north. Cluster 3 had significant patches of epibenthic gardens separated by tracts of bare seabed, distributed in low mud higher current areas, primarily in the southern GBR. Cluster 4 was similar to cluster 3, but with more algae, and distributed in similar low mud higher current areas with higher benthic irradiance, in both the southern and far northern GBR. Cluster 5 represented mostly bioturbated and bare seabed with a little algae and seagrass algal habitat distributed over much of the shelf in the central and northern sections of the GBR. Cluster 6 represented seagrass and algal habitat distributed along much of the inner half of the shelf in the southern Capricorn section of the GBR. Cluster 7 represented similar patchy seagrass and algal habitat distributed along the mid-shelf from Cape Upstart to Innisfail. Cluster 8 represented much of the *Halimeda* algal habitat, as well as some other algae and epibenthos, distributed in various patches along the outer shelf, including the *Halimeda* banks inside the ribbon reefs near Lizard Is and in the far north. Cluster 9 represented patchy algae (including some *Halimeda*) with some bioturbation and a little other biohabitat, distributed primarily in the outer-shelf offshore from Townsville.

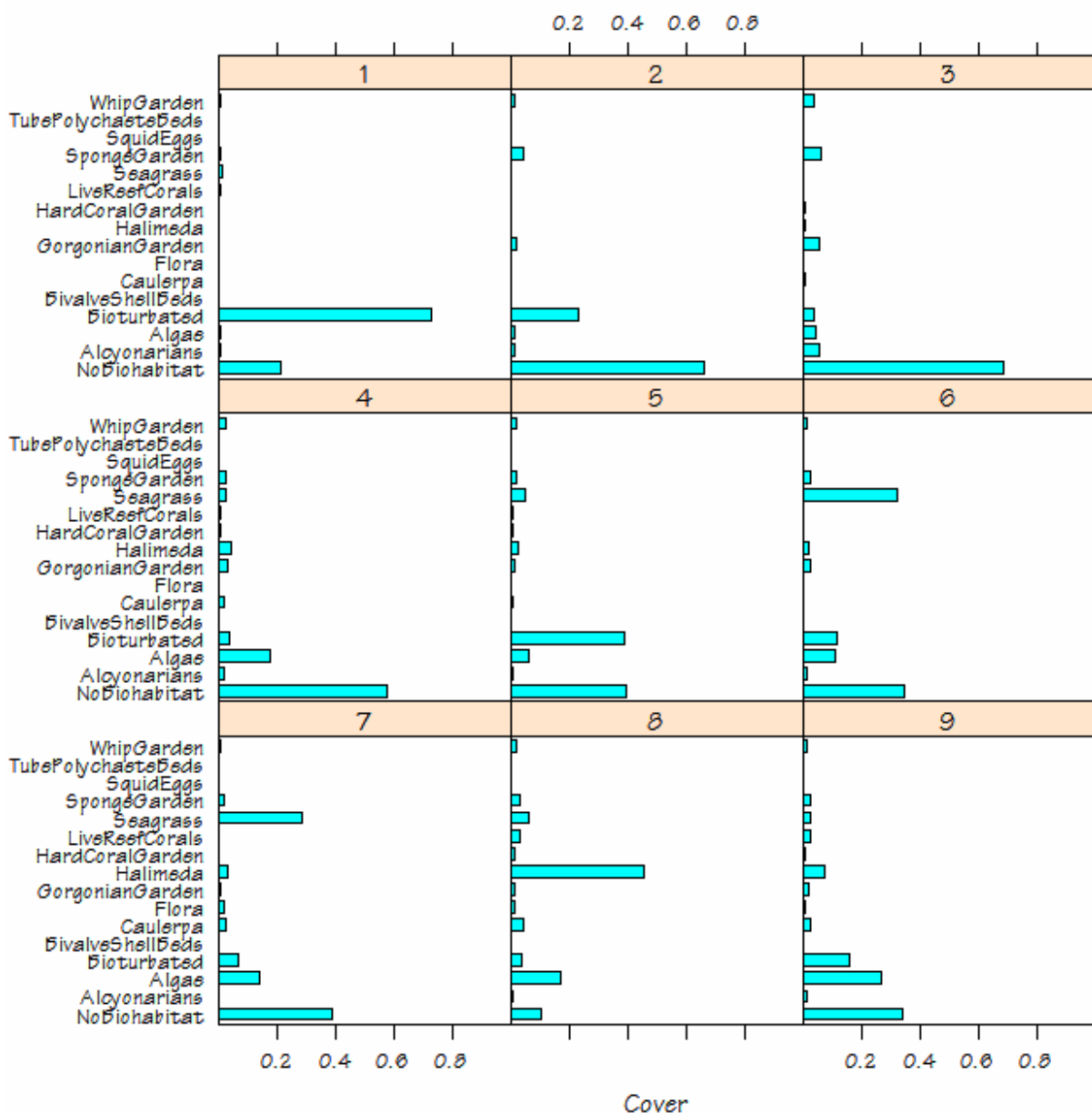


Figure 3-61: Mean profiles (centroids) of the 9 site groups as defined by the recursive partitioning algorithm.

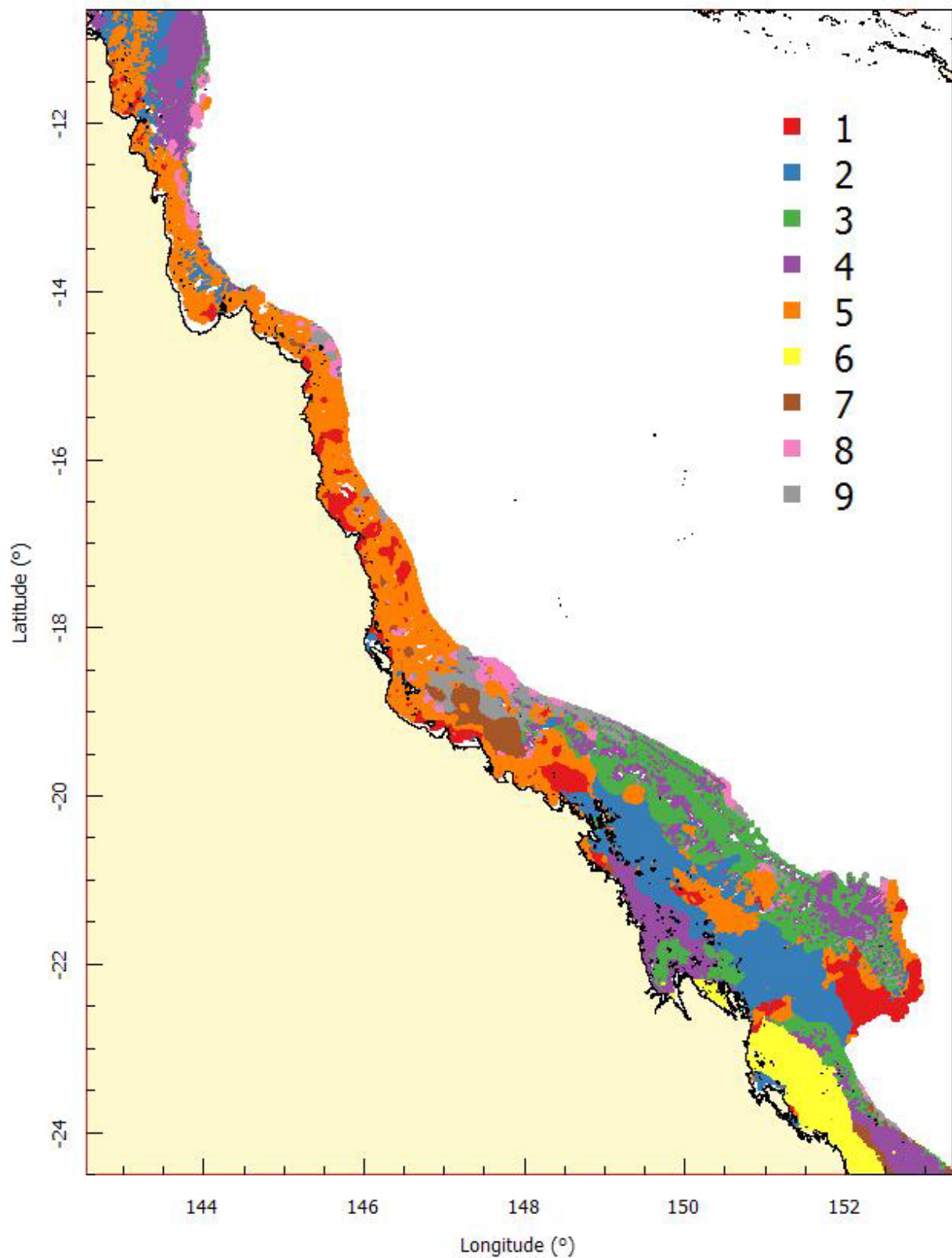


Figure 3-62: Map of predictions of group membership to the entire GBR grid. The groups are those from the medoid algorithm with grouped vessel biological data and Manhattan distances shown in (Figure 3-60).

3.6. ACOUSTICS DISCRIMINATION AND CLASSIFICATION

3.6.1. Wavelet Packet-Based Techniques Applied to Data in the Angular Domain (D H Smith)

3.6.1.1. Two Class Seabed Classification

This is the simplest classification case on which basic understanding of the data behaviour and applied techniques is sought before progressing to the more complex cases involving larger numbers of classes.

3.6.1.1.1 Sand Substratum with and without Biohabitat

For initial study and analysis purposes, sites containing large continuous blocks of each seabed type have been selected. Table 3-10 indicates a set of 18 sites possessing at least 1,000 consecutive samples with sand substratum and no biohabitat, while Table 3-11 lists three available sites with a similar number of (sand, seagrass) data samples.

A single classification experiment for the two class case refers to a given pair of sites from which training data is extracted and another distinct pair of sites from which a similar quantity of test data is also extracted. Such site-wise experiments can be considered as local, as opposed to global in the sense of training and test sets comprising data from multiple sites.

Table 3-9: A sample confusion matrix for the two-class case of sand and seagrass.

| | Sand | Seagrass |
|----------|------|----------|
| Sand | 98.0 | 2.0 |
| Seagrass | 5.7 | 94.3 |

Table 3-10: Sites with at least 1,000 consecutive samples of (sand, no biohabitat) seabed type with indices (6,17).

| Site | Mean Depth (m) |
|------|----------------|
| 897 | 41 |
| 2583 | 16 |
| 1701 | 51 |
| 2016 | 30 |
| 1580 | 61 |
| 2018 | 33 |
| 2631 | 21 |
| 828 | 63 |
| 2380 | 24 |
| 1917 | 14 |
| 2100 | 46 |
| 1647 | 42 |
| 833 | 50 |
| 1939 | 20 |
| 744 | 42 |
| 2626 | 27 |
| 1719 | 54 |
| 2005 | 26 |

Once the feature extraction scheme has been established on the training data, feature extraction is performed on the entire test set and subsequent classification is attempted, starting with just one feature and progressing to the full original data size. Every test data item is classified into one of the

two classes under consideration, and since the actual classes are known, mis-classification rates can be calculated to assess the overall procedure. These are derived from the calculated confusion matrix, which indicates what proportion of each class type is correctly classified, through its diagonal elements, with rows representing actual classes and columns representing predictions made by the classifier. The confusion matrix displayed below shows strong diagonal behaviour for both classes, with 98% of the sand correctly classified and 94.3% of the seagrass correctly classified.

Table 3-11: Sites with at least 1,000 consecutive samples of (sand, seagrass) seabed type with indices (6,21).

| Site | Mean Depth (m) |
|------|----------------|
| 2083 | 33 |
| 2084 | 31 |
| 2441 | 28 |

Pairwise combinations of the site data from Table 3-10 and Table 3-11 yielded a total of 54 training/test sets, on which 2916 individual classification experiments were performed, and selected results are presented. Results for a typical two-class classification experiment are shown in Figure 3-63, where the horizontal axis indicates the number of features used and the three curves represent the two confusion matrix diagonal elements and the associated overall mis-classification rate as percentages. Training data for the two seabed classes (sand, no biohabitat) and (sand, seagrass) comes from sites 1701 and 2441, while test data comes from sites 1580 and 2083, further details of which are given in Table 3-10 and Table 3-11. Best results in this picture occur just below 40 features, where the sand is perfectly classified and the seagrass is classified to over 90% accuracy, with overall mis-classification rate below 10%. Initial step activity visible in all three curves produced good results below 20% mis-classification with less than 10 features, offering a significant reduction from the original data size of 64.

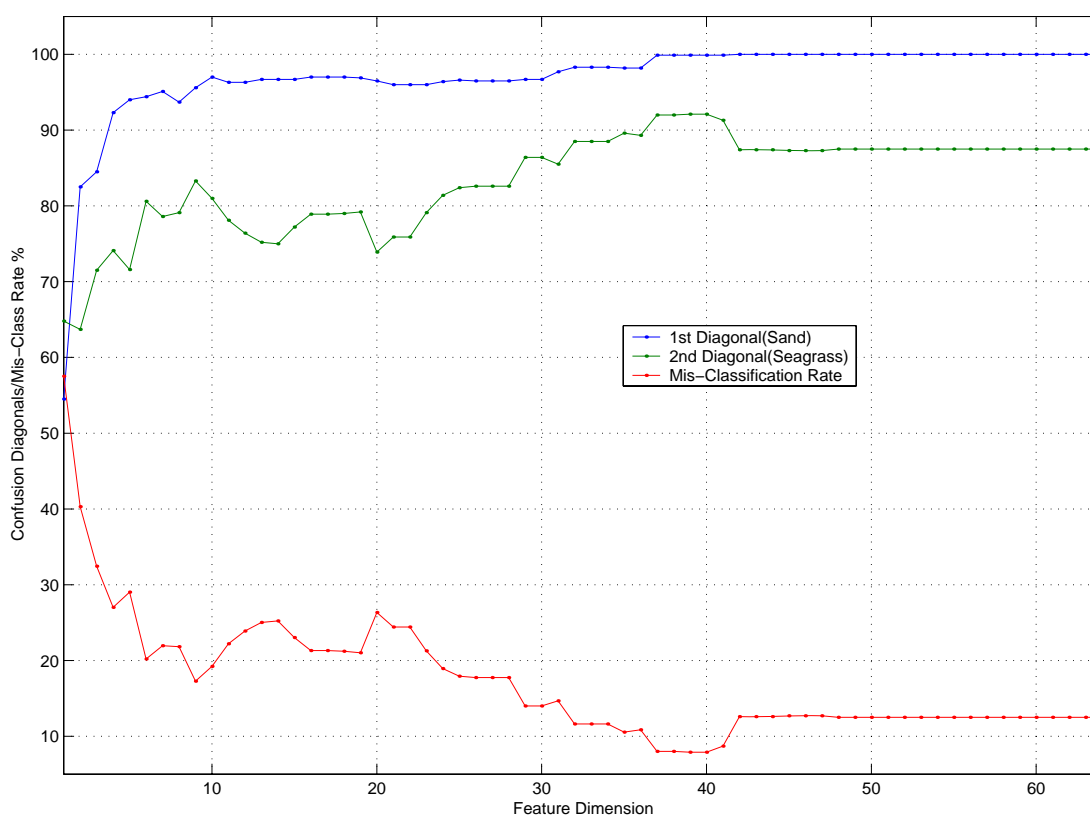


Figure 3-63: Results for a single two-class classification experiment for sand substratum with no biohabitat and sand substratum with seagrass, calculated with a Tree classifier. Training data is from sites 1701 and 2441 and test data is from sites 1580 and 2083.

Repeating the single classification experiment represented in Figure 3-63 across all 54 test sets produced the result in Figure 3-64, which indicates the lowest mis-classification rate with respect to feature dimension for each test set together with the confusion matrix diagonal elements. Circles and squares on this plot denote those test sets which are completely distinct from the training set, containing no data contribution from sites 1701 or 2441. A number of good results below 20% mis-classification have been recorded along with some poor results as high as 80% mis-classification rate. Sand being mis-classified as seagrass is responsible for the poor overall results at some sites, while seagrass remains well classified across the test set range with strong diagonal behaviour above 90%.

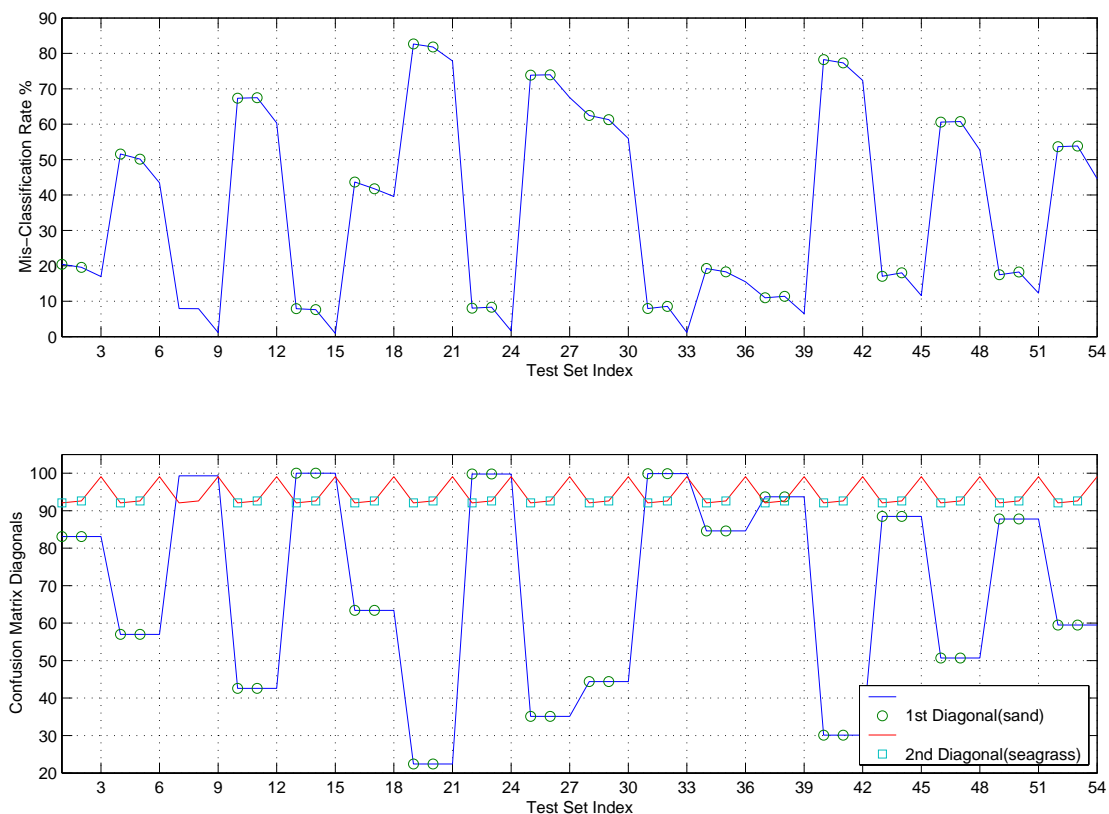


Figure 3-64: Classification results across 54 different test sets for training data from sites 1701 and 2441, calculated with a Tree classifier. Circles and squares indicate test sets containing no contributions in common with the training set.

The variation in classification performance seen in Figure 3-64 is accompanied by a variation in mean depth of the sand contribution from 14 to 63 m across the test sets, compared with 51 m mean depth for the corresponding training set contribution. An alternative view of Figure 3-64, plotting the same mis-classification rates against the actual depth departure between the training and test set sand components appears in Figure 3-65, showing a distinct depth divide separating the good and poor results. Inspection of the associated acoustic data for sand with no biohabitat reveals obvious structural differences with depth, which are in fact consistent with calculated predictions based on a model equation derived from underwater acoustic theory (Sternlicht and de Moustier, 2003). Depth variation between training and test data demands careful attention in the classification process, with pictures such as Figure 3-65 suggesting a depth partitioning strategy which limits allowable depth mismatches between training and test data.

Replacing the sand component of the training set with data from site 2005, which has a lower mean depth of 26 m, and repeating the classification calculations across all 54 test sets produced the mis-classification rates displayed in Figure 3-66. This training set produced a more steady behaviour than that previously observed in Figure 3-64, with a maximum mis-classification rate of just over 60% and

most values residing in a band between 20 and 30%. As with the previous training set, large errors in some test sets are the result of sand being mis-classified as seagrass.

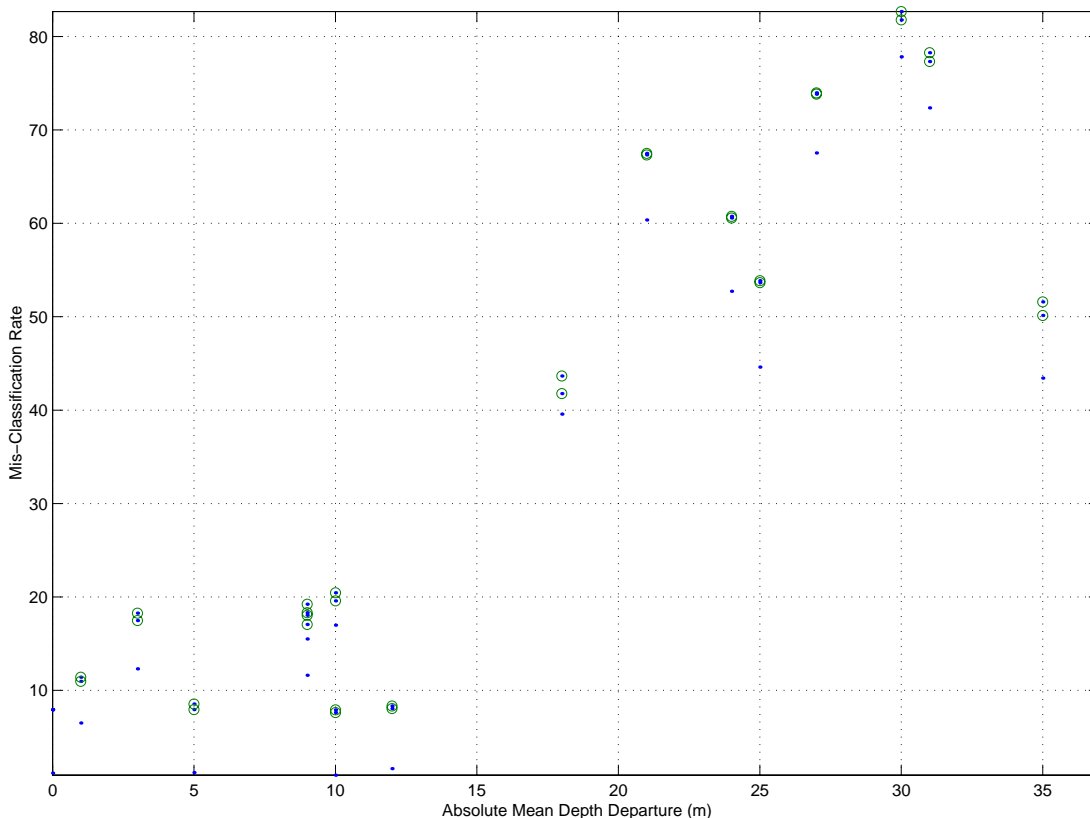


Figure 3-65: Mis-classification results from Figure 5 plotted against absolute depth difference between the sand components of the training and test sets, showing a distinct depth divide near 15 m separating the good and poor results.

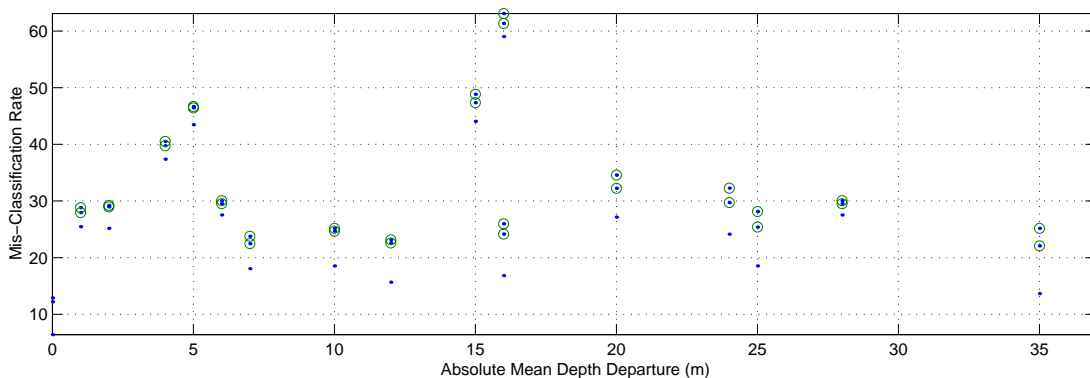
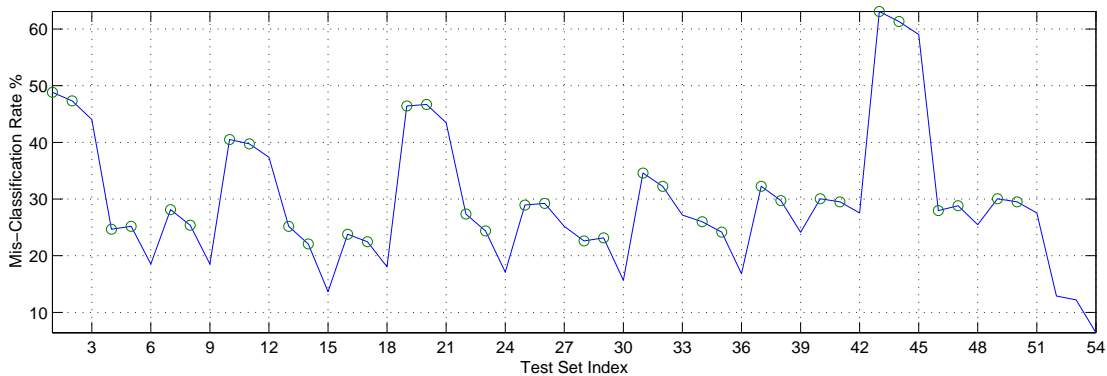


Figure 3-66: Tree classification results for (sand, no biohabitat) and (sand, seagrass) seabed types across 54 test sets with training data from sites 2005 and 2441.

In terms of depth departure between the sand component of the training and test sets, an entirely different behaviour is observed in Figure 3-66 whereby reasonable results occur across a wide range of departures, in stark contrast to the previous result of Figure 3-65. The largest mis-classification rate occurred roughly half way through the interval, and other large values were also seen near 5 m departure, signaling caution in the future application of any depth partitioning process.

3.6.1.1.2 Different Biohabitats on Sand Substratum

A second two-class classification study involved retaining the sand substratum and attempting to discriminate between two different biohabitats, namely sponge garden dense, which is available from five sites as indicated in Table 3-12, and seagrass as in the previous case. A total of 15 different training/test pairs were available, allowing 225 individual classification experiments.

Computed results for a single classification experiment with training data from sites 2580 and 2441 and test data from sites 2593 and 2084 are displayed in Figure 3-67, including both confusion matrix diagonal elements and the overall mis-classification rate. An abrupt change were observed just after 40 features, marking a transition to steady behaviour with strong diagonals and corresponding low mis-classification rates near 10%. Seagrass results, which reach well above 90%, are slightly superior to their sponge garden counterparts which remain just below 90%.

Table 3-12: Sites with 1,000 consecutive samples of (sand, sponge garden dense) seabed type with indices (6,18).

| Site | Mean Depth (m) |
|------|----------------|
| 2009 | 41 |
| 2593 | 33 |
| 2023 | 35 |
| 2584 | 31 |
| 2580 | 29 |

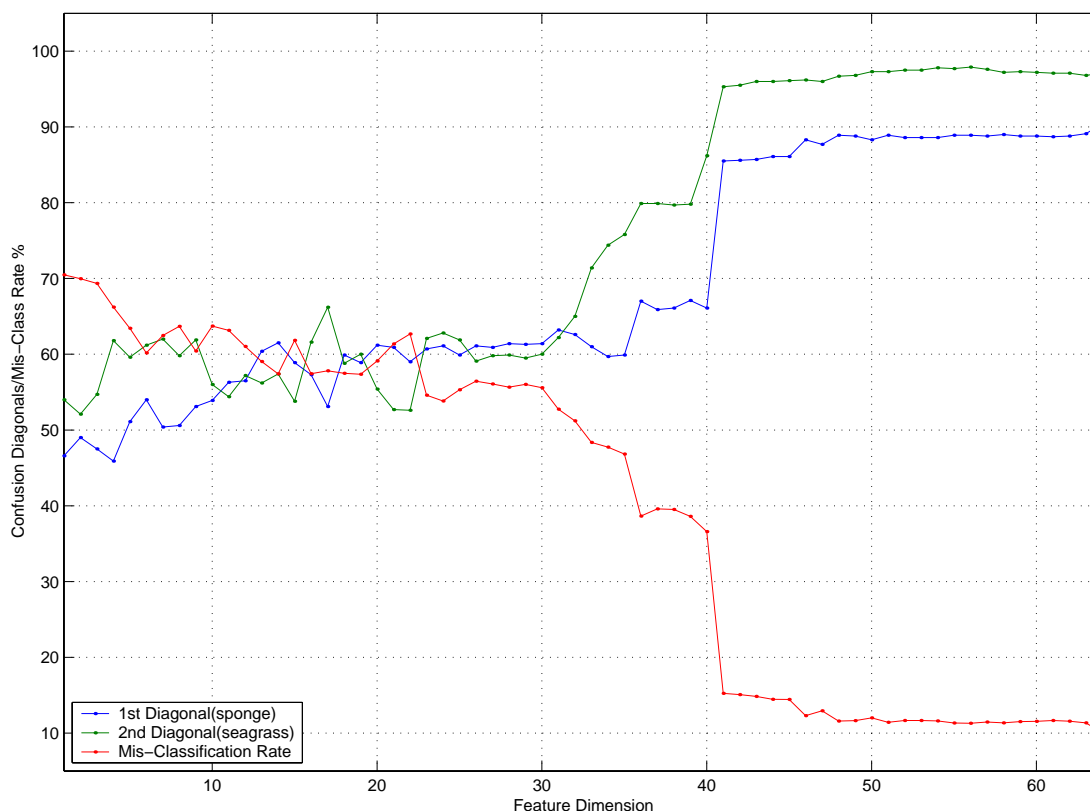


Figure 3-67: Results of a single two-class classification experiment for (sand, sponge garden dense) and (sand, seagrass) seabed types, generated with a Tree classifier. Training data is from sites 2580 and 2441 and test data is from sites 2593 and 2084.

Combining the three (sand, seagrass) sites in Table 3-11 with the five (sand, sponge garden) sites from Table 3-12 yielded a total of 15 training/test pairs for consideration. Repeating the classification calculations across all 15 test sets with the same training set produced the results summary in Figure 3-68. This indicates minimum mis-classification rates and maximum individual confusion diagonal elements with respect to feature dimension for each test set. Strong seagrass performance of over 90% is maintained across all test sets, as in the previous two-class case, with overall mis-classification rates residing between approximately 10 and 50%. For those test sets that were not well classified, where sponge garden being mis-classified as seagrass was clearly the dominant source of error.

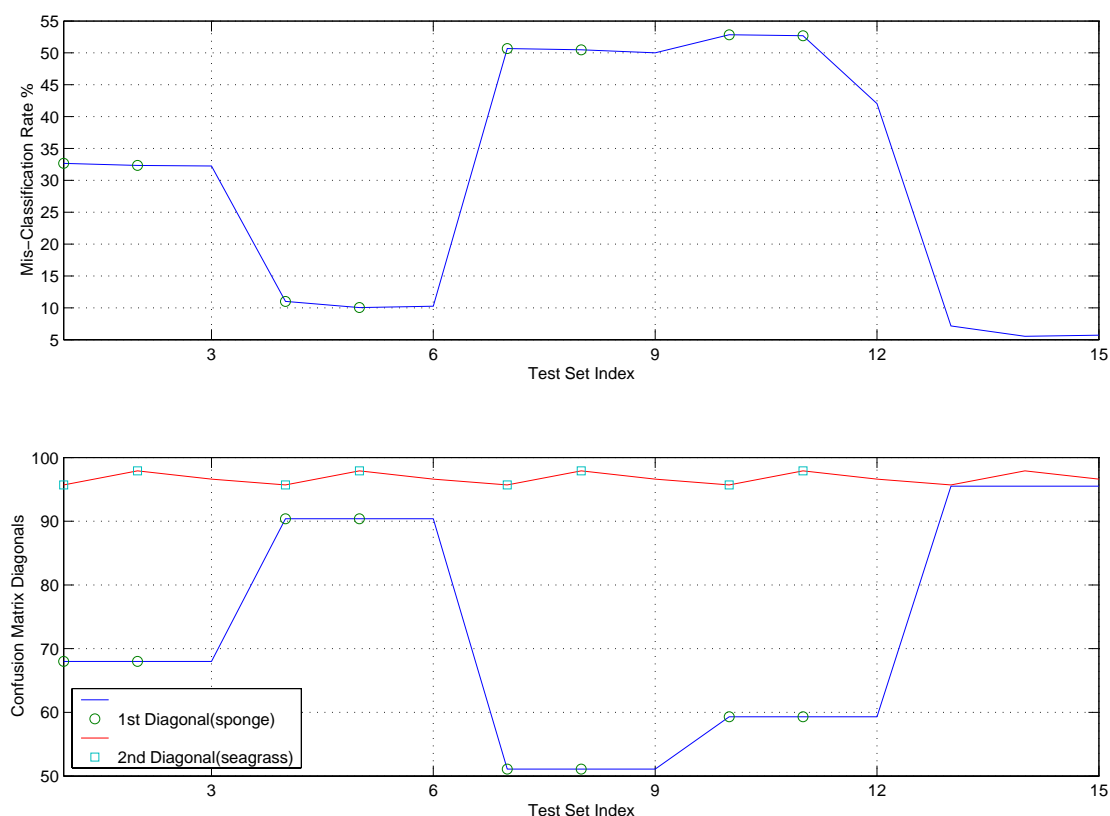


Figure 3-68: Tree classification results across 15 different test sets for training data from sites 2580 and 2441. Circles indicate test sets containing no contribution in common with the training set. Seagrass is well classified across the full test set range, while sponge garden undergoes larger variation to be the dominant error source for those test sets with high mis-classification rates

3.6.1.2. More than Two Seabed Classes

Taking all three of the previously considered seabed classes together now offered an extra dimension of complexity, to which the feature extraction methods must be subjected as part of the study and development process. Constructing a training set with data from sites 1701, 2009 and 244, and performing classification on a test set comprising data from sites 1580, 2593 and 2083 produced the results in Figure 3-69. This shows all three confusion matrix diagonal elements and the associated mis-classification rate against feature dimension. All three seabed types were classified to higher than 80% accuracy provided enough features are used, with sand returning the best result followed by sponge garden and seagrass. Abrupt jumps present in the sponge garden and seagrass curves between 30 and 40 features were not seen in the sand curve, which underwent a steady climb to reach above 95%

accuracy. With 50 features the overall mis-classification rate dropped to approximately 15%, providing an effective dimension reduction of smaller magnitude to that previously observed in the two-class cases.

Table 3-13: The calculated confusion matrix at feature dimension 50 from Figure 3-69.

| | Sand | Sponge Garden | Seagrass |
|---------------|------|---------------|----------|
| Sand | 99.1 | 0.4 | 0.5 |
| Sponge Garden | 0.0 | 89.4 | 10.6 |
| Seagrass | 13.5 | 4.1 | 82.4 |

The actual computed confusion matrix at 50 features shown above indicates precisely how the sponge garden and seagrass were mis-classified via the corresponding off-diagonal elements, which do not appear in Figure 3-69. Inspection of the second row shows the sponge garden error of approximately 10% to result entirely from mis-classification of this biohabitat as seagrass. Total seagrass errors of just under 20% are divided between sand and sponge garden, with sand taking the major share of almost 15% and sponge garden taking the remaining 5%. For sand, the very small total error of approximately 1% is essentially equally split between sponge garden and seagrass.

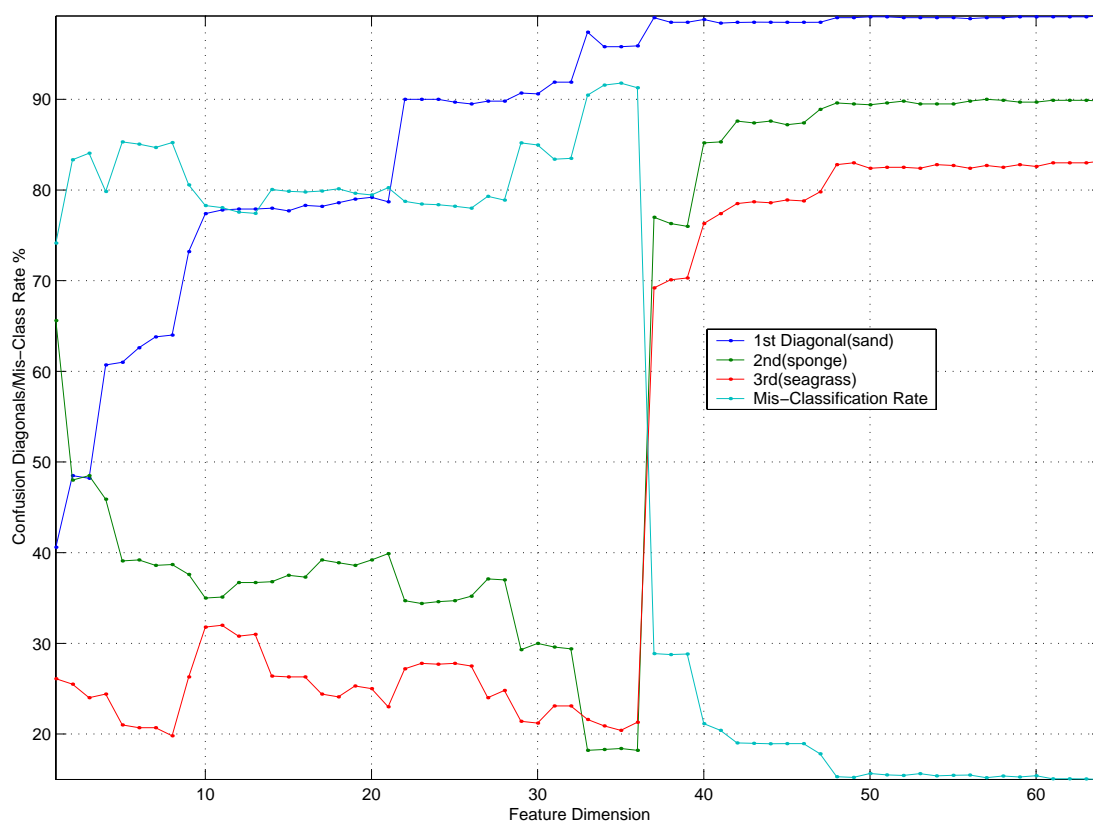


Figure 3-69: Results for a single classification experiment on three seabed classes comprising (sand, no biohabitat), (sand, sponge garden dense) and (sand, seagrass), calculated via Linear Discriminant Analysis. Training data is from sites 1701, 2009 and 2441, and test data is from sites 1580, 2593 and 2083.

Retaining the same training set, additional calculations were carried out on test sets containing all available data contributions from the same three seabed classes indicated in Table 3-10, Table 3-11 and Table 3-12, with maximum diagonal confusion matrix elements chosen as performance indicators for each test set. Viewing these values against their respective absolute depth departures between training and test set contributions under the application of Tree and Linear Discriminant Analysis classifiers produced the results shown in Figure 3-70, also offering a useful performance comparison. As in the initial two class case of Figure 3-65, a distinct depth divide has emerged in the (sand, no biohabitat) results, with a cluster of strong diagonal behaviour occurring below 15 m depth departure,

and poor results below 50% essentially confined to test sites with large depth departures. Recovery of the training set is also evident from the high values at zero depth departure, when the two sets coincide, and little performance difference was observed between the two classifiers. In sharp contrast, very noticeable differences have appeared for the remaining two seabed classes, with Linear Discriminant Analysis proving clearly superior in both cases for all test sets excluding the training set. Seagrass has been well classified to over 80% accuracy, as seen previously in the two class case, with similar success for sponge garden on all but one test set where a moderate 60% is achieved. Depth departures were also considerably lower for these two seabed types, reaching up to approximately 12 m for sponge garden and 5 m for seagrass.

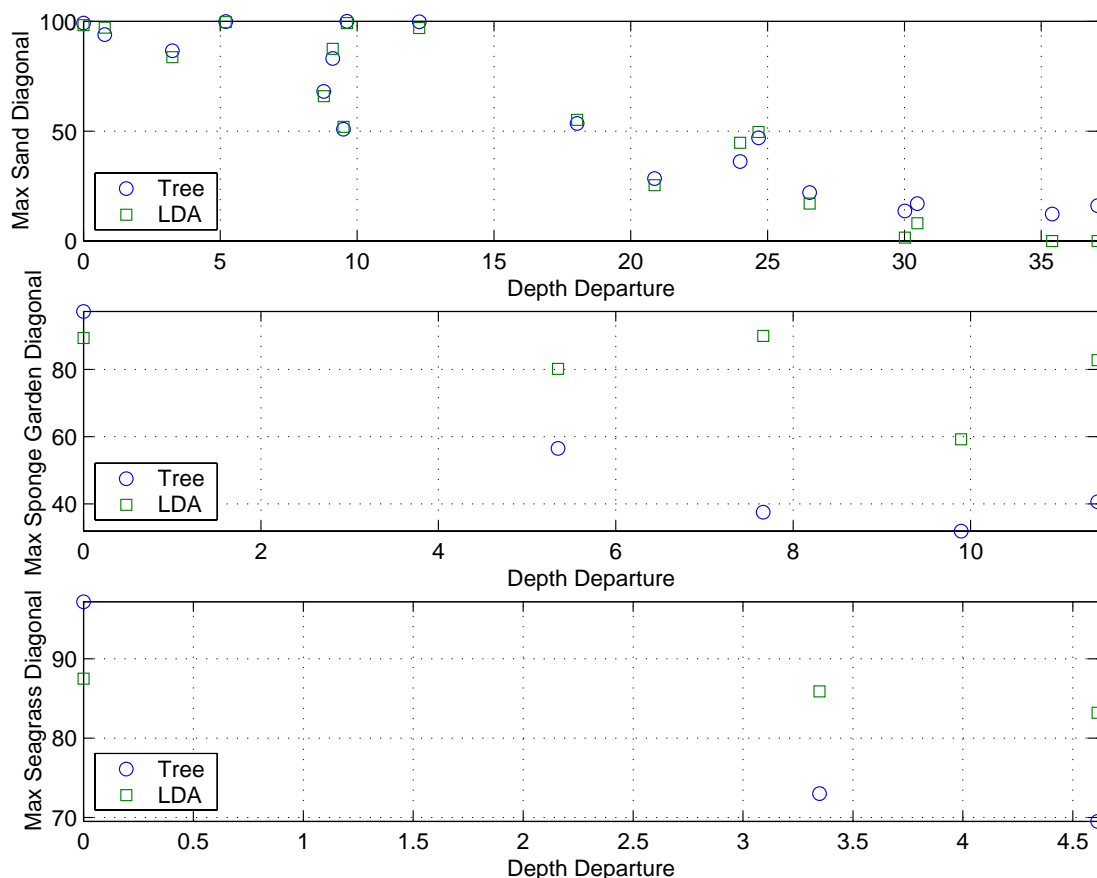


Figure 3-70: Additional classification results for the three classes (sand, no biohabitat), (sand, sponge garden dense) and (sand, seagrass), showing maximum confusion matrix diagonal elements against training/test depth departure, for test sets containing contributions from all available sites.

Continuing with the sand substratum, there was one more biohabitat type with at least 1,000 consecutive data samples available, namely bioturbated, which is indicated in Table 3-14. Adding data from sites 2191 and 2447 to the previous training and test sets and performing a single classification experiment gave the four confusion matrix diagonals and associated mis-classification rate curves displayed in Figure 3-71. The first two classes in this experiment, namely bioturbated and sand, had immediately distinguished themselves with exceptional performance of above 95% accuracy at feature dimension of 40, where a clear transition was observed. Bioturbated has further distinguished itself by its behaviour at low feature dimension, achieving above 90% accuracy with less than 10 features in comparison to 70% for sand. For the remaining two classes, seagrass reached approximately 65% at 40 features, while sponge garden produced the only poor result of approximately 30% to dominate an overall mis-classification rate of just above 50%.

To provide a closer look at the mis-classification behaviour and identify how the actual errors were distributed, the actual confusion matrix at feature dimension 40 from Figure 3-71 is displayed in Table 3-15. Small errors present in the bioturbated and sand results were essentially due to mis-classification

as seagrass and bioturbated respectively, while the relatively large sponge garden error of approximately 70% was entirely due to mis-classification as seagrass. Errors for seagrass are dominated by mis-classification as sponge garden, with small, almost equal contributions of less than 10% attributed to both bioturbated and sand.

Table 3-14: Sites with 1,000 consecutive samples of (sand, bioturbated) seabed type (6,5).

| Site | Mean Depth (m) |
|------|----------------|
| 2191 | 31 |
| 2447 | 30 |
| 2563 | 23 |
| 735 | 43 |
| 1847 | 24 |
| 1594 | 31 |
| 1743 | 48 |
| 1600 | 28 |
| 739 | 40 |
| 2322 | 52 |
| 1139 | 42 |
| 150 | 84 |
| 181 | 41 |
| 139 | 70 |
| 653 | 46 |

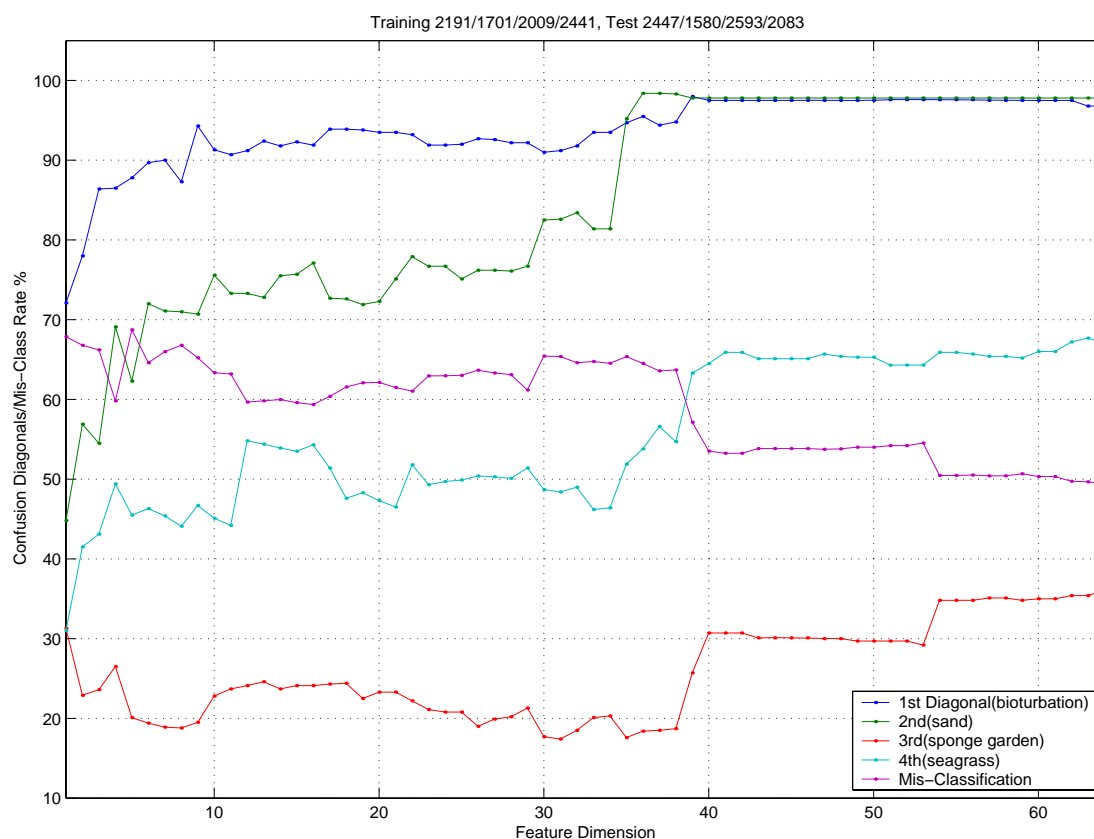


Figure 3-71: Results for a single classification experiment on four seabed classes, with training data taken from sites 2191, 1701, 2009 and 2441, and test data from sites 2447, 1580, 2593 and 2083, calculated via a Tree classifier.

Table 3-15: The calculated confusion matrix at feature dimension 40 from Figure 3-71.

| | Bioturbated | Sand | Sponge Garden | Seagrass |
|---------------|-------------|------|---------------|----------|
| Bioturbated | 97.5 | 0.1 | 0.0 | 2.4 |
| Sand | 2.2 | 97.8 | 0.0 | 0.0 |
| Sponge Garden | 0.0 | 0.0 | 30.7 | 69.3 |
| Seagrass | 7.7 | 6.0 | 21.8 | 64.5 |

As in the previous three-class case, additional calculations have been performed with the same training set on a collection of test sets containing all available contributions from each of the four classes under consideration, with results for both classifiers summarised in Figure 3-72. Bioturbated results have shown an exceptional performance from Linear Discriminant Analysis, which produced a cluster of strong diagonal elements above 95% for depth departures up to almost 20 m, and never dropped below 50% across the entire range. By contrast, corresponding Tree results reach as low as 20% at large depth departures, and as low as 40% below 20 m departure where Linear Discriminant Analysis excelled. For sand with no biohabitat, a familiar decline in performance with depth departure was observed, with the Tree classifier showing superiority, particularly at low departures where Linear Discriminant Analysis gave some poor results below 20%. Performance declines with depth departure were also recorded for the sponge garden and seagrass, with Linear Discriminant Analysis superior in the former case and clearly inferior to Tree classification in the latter case.

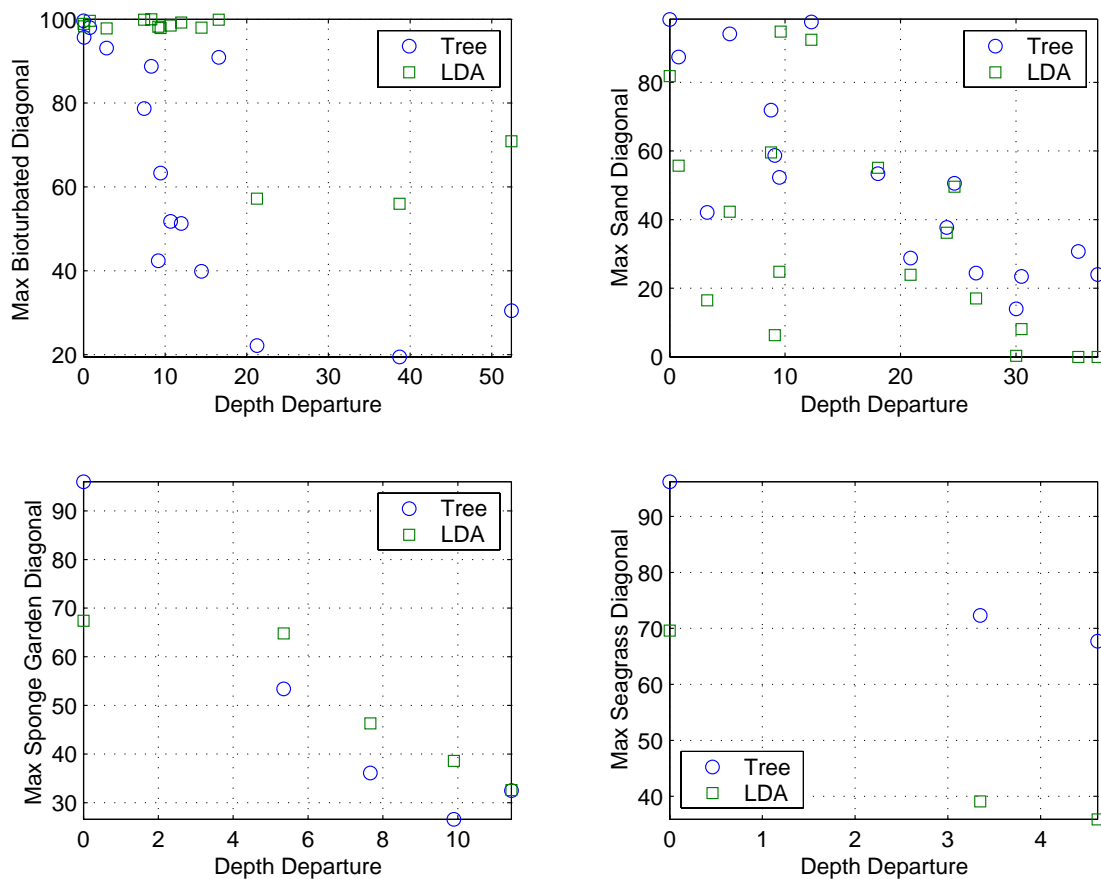


Figure 3-72: Computed four-class classification results for additional test sets, displayed as maximum confusion matrix diagonal elements for each of the four seabed classes.

3.6.1.2.1 Different Substrata in the Absence of Biohabitat

With over 250 possible seabed classes present in the original specification, merging of classes will be necessary in order to produce a smaller, computationally practical set of working seabed classes. A useful starting point in this direction involves the consideration of selected substrata in the absence of biohabitat. Accompanying the previously considered sand without biohabitat are the four substrata

types of coarse sand, sand waves/dunes, silt and soft mud, for which sites are available with at least 1,000 consecutive data samples as indicated in Table 3-16, Table 3-17, Table 3-18 and Table 3-19. An initial classification experiment on these five classes, using training data from sites 1828, 1701, 2458, 2407 and 2163, and test data from sites 2315, 1580, 2750, 1897 and 1940, has yielded the confusion diagonal elements and mis-classification rate curves shown in Figure 3-73.

Table 3-16: Sites with 1,000 consecutive samples of (coarse sand, no biohabitat) seabed type (2,17).

| Site | Mean Depth (m) |
|------|----------------|
| 1828 | 55 |
| 2315 | 55 |
| 1644 | 59 |

Table 3-17: Sites with 1,000 consecutive samples of (sand waves/dunes, no biohabitat) seabed type (7,17).

| Site | Mean Depth (m) |
|------|----------------|
| 2458 | 20 |
| 2750 | 14 |
| 1758 | 13 |

Table 3-18: Sites with 1,000 consecutive samples of (silt, no biohabitat) seabed type (8,17).

| Site | Mean Depth (m) |
|------|----------------|
| 2407 | 34 |
| 1897 | 20 |
| 1728 | 35 |

Table 3-19: Sites with 1,000 consecutive samples of (soft mud, no biohabitat) seabed type (9,17).

| Site | Mean Depth (m) |
|------|----------------|
| 2163 | 15 |
| 1940 | 29 |
| 2564 | 17 |

While the overall mis-classification rates were high (>60%), some noteworthy discrimination behaviour has taken place, dominated by strong performance of the sand waves/dunes diagonal element, which clearly distinguished itself by reaching above 90% with just over 40 features. The next best result belongs to coarse sand, which reached above 70% with less than 25 features, while silt started poorly at low feature dimension then underwent a very slow climb to finally reach over 60% with 50 features. Sand did not rise above 50% and soft mud reached just above 40% with less than 10 features before undergoing a decline. Of particular importance here is the actual mis-classification structure, as indicated by the calculated confusion matrix at feature dimension of 40 (Table 3-20).

In the first row, approximately two thirds of the coarse sand was correctly classified, with mis-classification as sand being the principal error contributor, and silt responsible for the remaining smaller contribution. Confusion between sand and coarse sand persists to a larger extent in the second row, showing almost equal amounts of the sand being classified as sand and coarse sand, with silt making up most of the remaining small error contribution. These two rows immediately suggest a possible merging of the sand and coarse sand substrata types, subject to further testing. Strong diagonal performance near 90% in the third row belongs to sand waves/dunes, as observed in Figure 3-73, none of which was mis-classified as either sand or coarse sand, with soft mud responsible for most of the remaining error. In the final two rows, almost 60% of the silt was mis-classified as soft mud and approximately 70% of the soft mud was mis-classified as silt, indicating strong confusion between this substrata pair, which can also be seen as potential candidates for merging, subject to additional testing. Additional tests on these five classes without biohabitat need to be carried out, followed by further calculations on the same substrata with various biohabitats present.

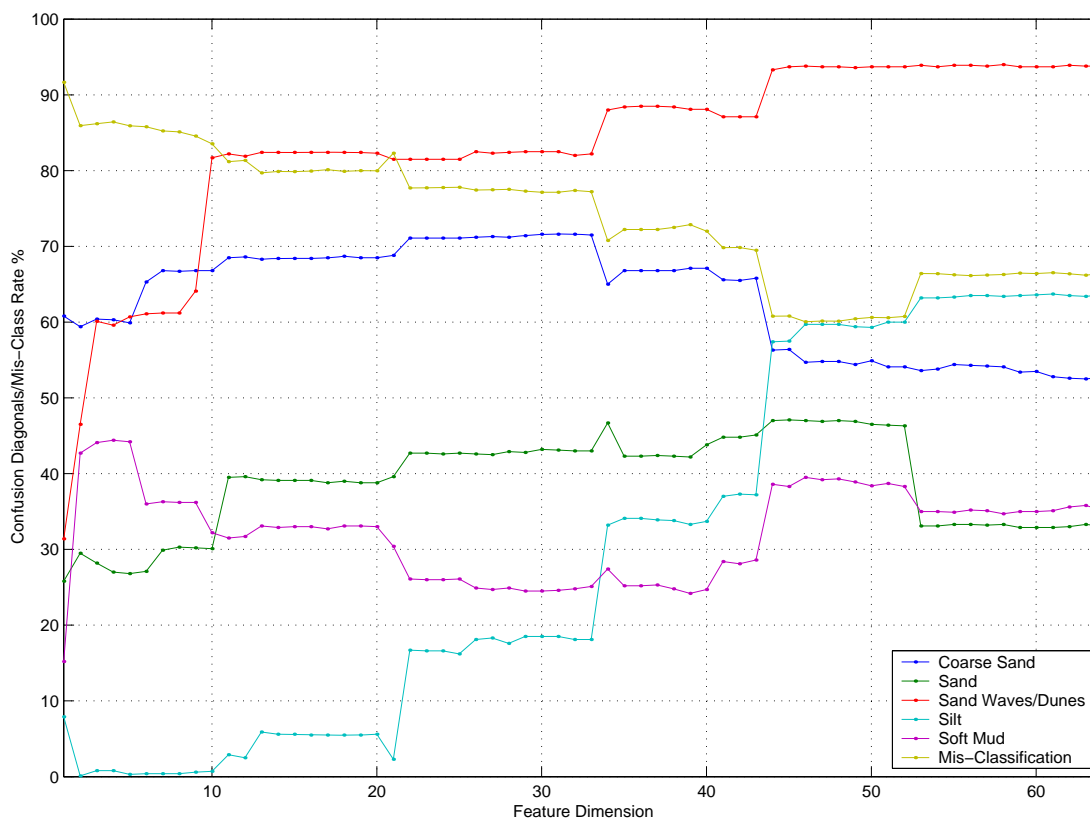


Figure 3-73: Confusion matrix diagonals and overall mis-classification rates for a 5-class classification experiment on selected substrata without biohabitat, generated with Linear Discriminant Analysis. Training data is supplied from sites 1828, 1701, 2458, 2407 and 2163, with test data from sites 2315, 1580, 2750, 1897 and 1940.

Table 3-20: The calculated confusion matrix at feature dimension 40 from Figure 3-73.

| | Coarse Sand | Sand | Sand Waves | Silt | Soft Mud |
|-------------|-------------|------|------------|------|----------|
| Coarse Sand | 67.1 | 25.6 | 0.0 | 6.6 | 0.7 |
| Sand | 45.0 | 43.8 | 0.0 | 9.9 | 1.3 |
| Sand Waves | 0.0 | 0.0 | 88.1 | 1.0 | 10.9 |
| Silt | 0.0 | 0.0 | 7.4 | 33.7 | 58.9 |
| Soft Mud | 0.0 | 3.5 | 1.1 | 70.7 | 24.7 |

3.6.2. Canonical Variate Analysis of Acoustic Data (N Campbell & D Devereux)

3.6.2.1. Depth Normalisation

Prior to analysis, the acoustic data were normalised to a constant depth so that signatures could be compared over the whole range of the data. Figure 3-74 and Figure 3-75 show plots of the original pelagic data and the depth-normalised data for a shallow sand site and a deeper sand site. The plot scales for the abscissa have been chosen to provide a good visual match. Since the depth normalisation involves only a linear transformation followed by nearest neighbour or linear or cubic resampling, there is strong agreement between the shapes for the original and depth-normalised plots, which is to be expected.

Figure 3-76 shows that after the linear scaling which arises during the depth normalisation, the main echo and second echo are essentially aligned for the depth-normalised pelagic data.

Plots of the pelagic data and the bottom data for a shallow site for a sand / algae group in Figure 3-77 show essentially the same shape; there was no apparent loss of features arising from the lower sampling rate for the pelagic data. There was no change in the shape of the ping response with depth as a result of the depth normalisation.

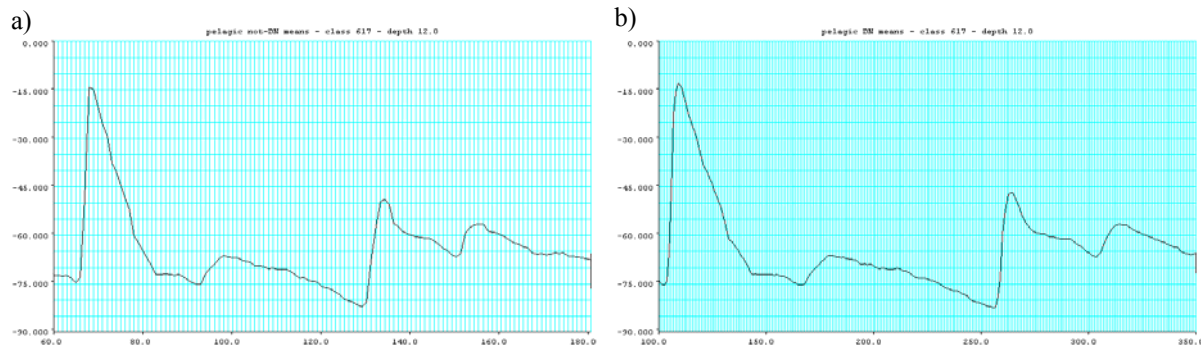


Figure 3-74: (a) Plot of the original pelagic data against sample time for a shallow sandy site (depth = 12 m); and (b) plot of depth-normalised data against sample number for the same site.

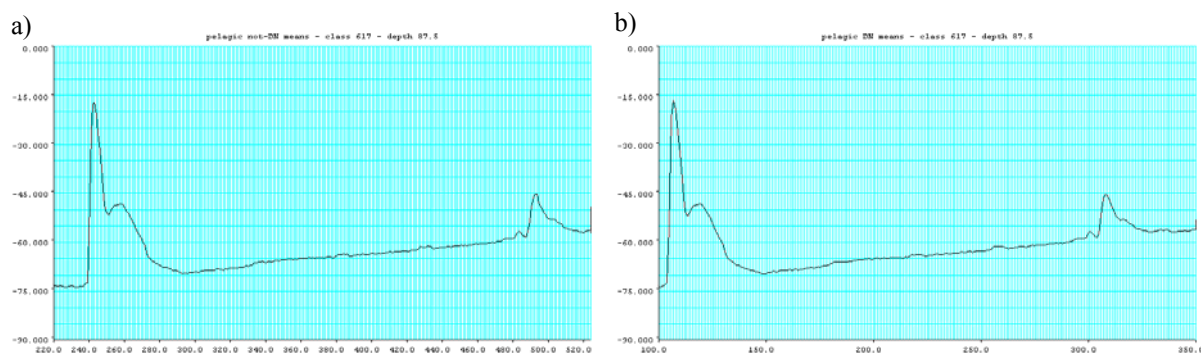


Figure 3-75: (a) Plot of the original pelagic data against sample time for a deep sandy site (depth = 87 m); and (b) plot of depth-normalised data against sample number for the same site.

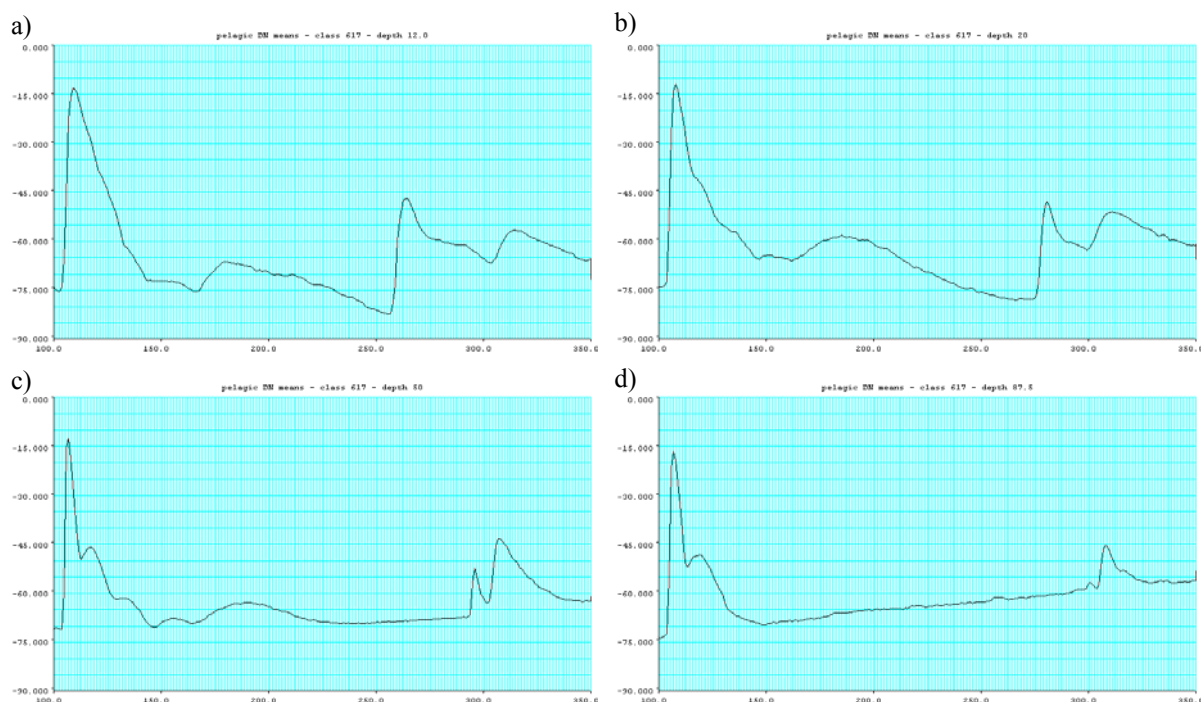


Figure 3-76: Plot of the depth-normalised pelagic data against sample number for sand sites for a range of depths: (a) 12 m; (b) 20 m; (c) 50 m; and (d) 87.5 m.

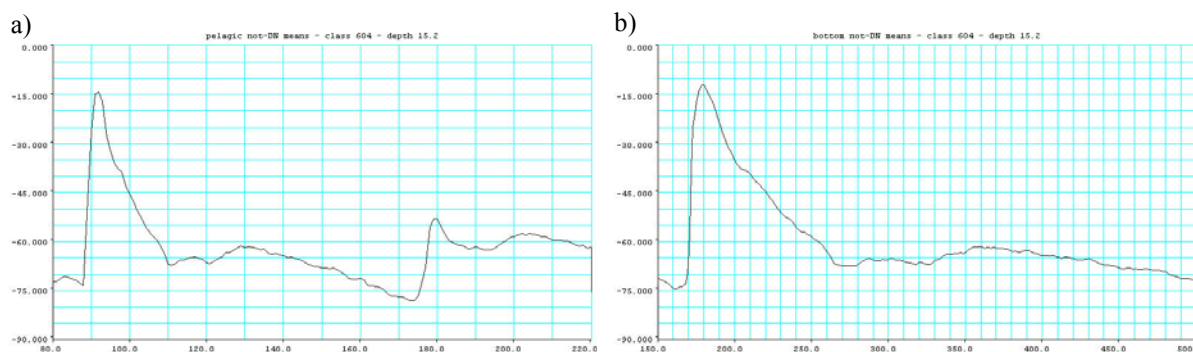


Figure 3-77: (a) Plot of the original pelagic data against sample time for a sand/algae group; and (b) plot of the corresponding bottom data for the same group.

Initial discriminant analyses were conducted on data for all groups of more than 100 contiguous echo responses from the same nominal substrate and biohabitat classes. The initial discriminant analyses of the 4519 such groups from 117 classes, without regard to the class labels, showed groupings into clusters. However, closer examination of the resulting plots showed that the differences between groups for the same habitat cover class were often as large as the differences between the cover classes. Extensive examination of the data suggested that even after depth normalisation there were depth-related differences in the shapes of the profiles, particularly at shallower depths (< 25 m), which required additional adjustment.

3.6.2.2. Depth Adjustment

Figure 3-74 and Figure 3-75 for the depth-normalised data for a shallow sand site and a deeper sand site show obvious shape differences related to depth. There are also obvious and marked differences in the profile responses for a shallow site and a deep site for two groups of >100 contiguous pings for class index 617 (sand:no biohabitat) in Figure 3-78 (see also the plots in Figure 3-81).

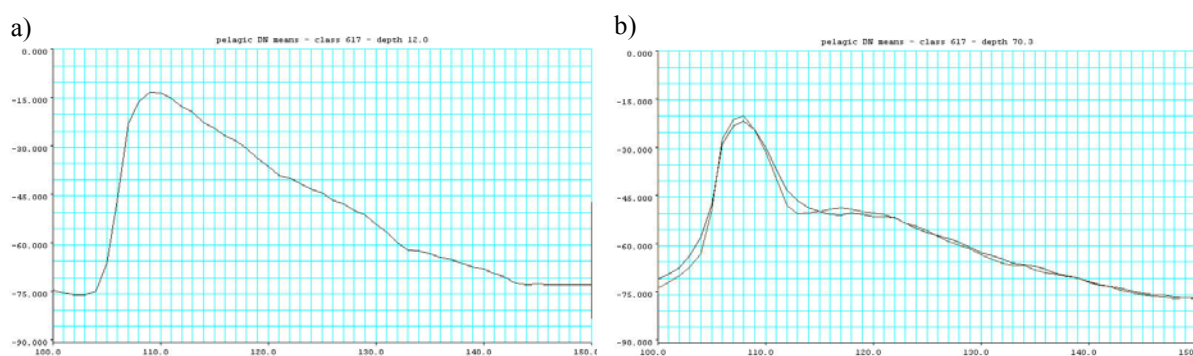


Figure 3-78: Plot of the depth-normalised pelagic data against sample number for (a) a shallow sandy site (depth = 12 m); and (b) a deep sandy site (depth = 70 m).

Plots of the response averaged over depth normalised sample numbers 110 – 112 against depth in (a) of Figure 3-79 and Figure 3-80 show a marked initial decrease until a depth of 20 – 25 m, followed by a much more gradual decrease; there appeared to be a systematic decrease in the width of the first echo with increasing depth.

Figure 3-74 and Figure 3-75 suggest that there was no obvious bias in the depth normalisation procedure; curves at shallower depths are not scaled differently to those at greater depths.

Figure 3-76 shows that after the linear scaling which arises during the depth normalisation, the main echo and second echo are essentially aligned for the depth-normalised pelagic data.

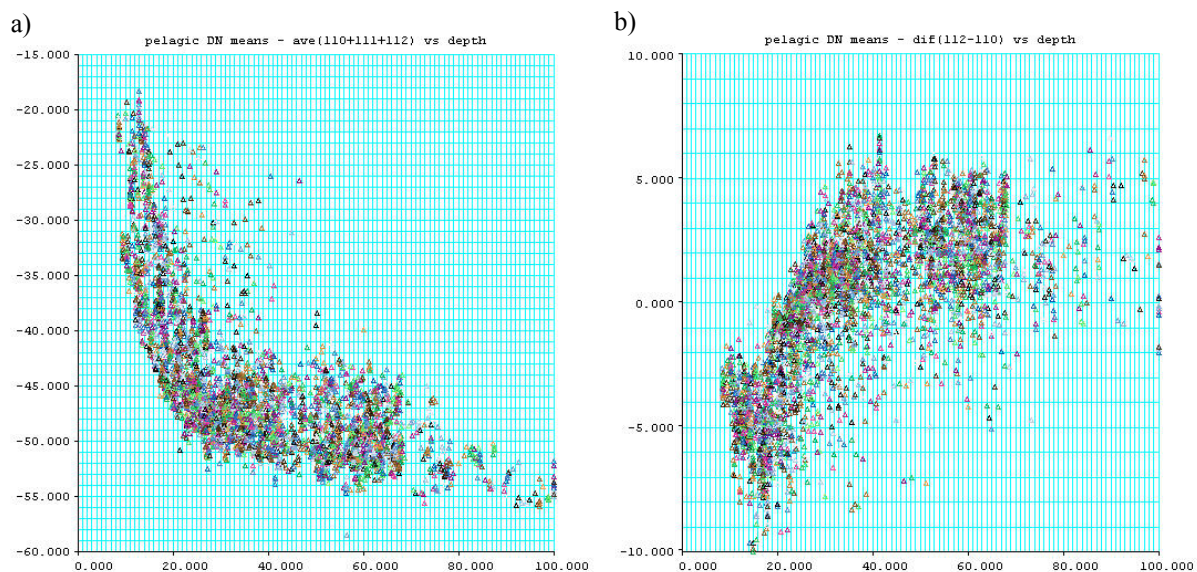


Figure 3-79: (a) Plot of the response averaged over sample numbers 110 – 112 against depth for all groups of >100 contiguous pings for all classes; and (b) plot of the difference in response for sample numbers 110 – 112 against depth for the same data.

Figure 3-77 shows that the pelagic data and the bottom data show essentially the same shape, and that there was no apparent loss of features arising from the lower sampling rate for the pelagic data.

Hence it seems reasonable to conclude that there is an obvious change in the shape of the ping response with depth; for shallower depths, the response for the first echo is much broader than it is at greater depths. This does not appear to be an artefact of the depth normalisation procedure, or of the use of the lower-resolution pelagic data.

The plots in Figure 3-82 show reasonably linear relationships of the response at sample numbers 113 and 115 with inverse depth. Note that the slopes of the relationships for the sand class are greater than those for the mud class.

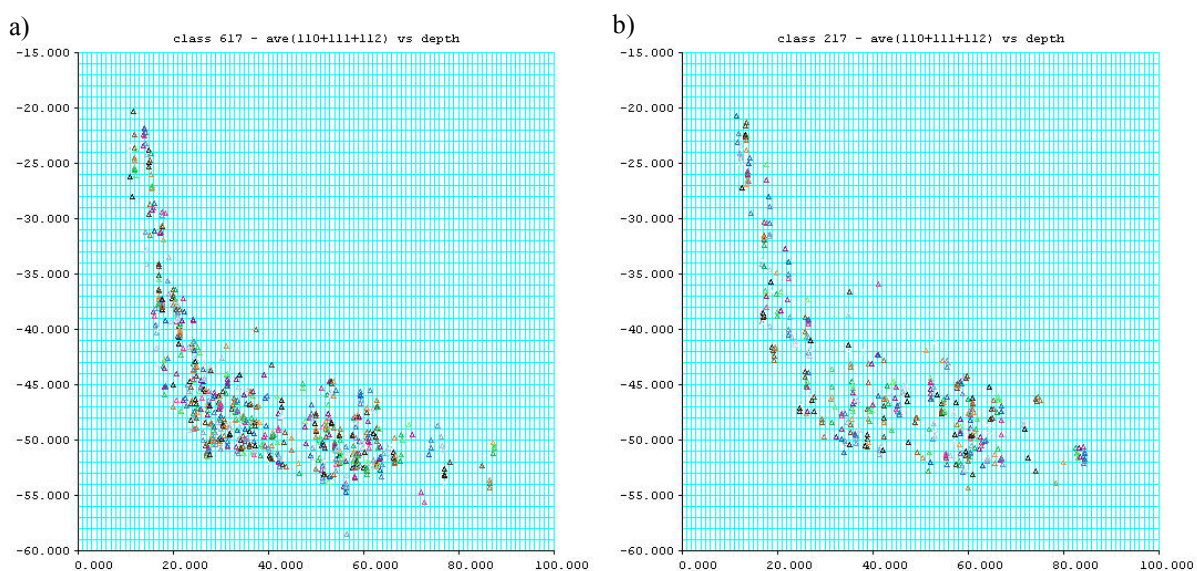


Figure 3-80: Plot of the response averaged over sample numbers 110 – 112 against depth for (a) class 617 (sand) and (b) class 217 (coarse sand).

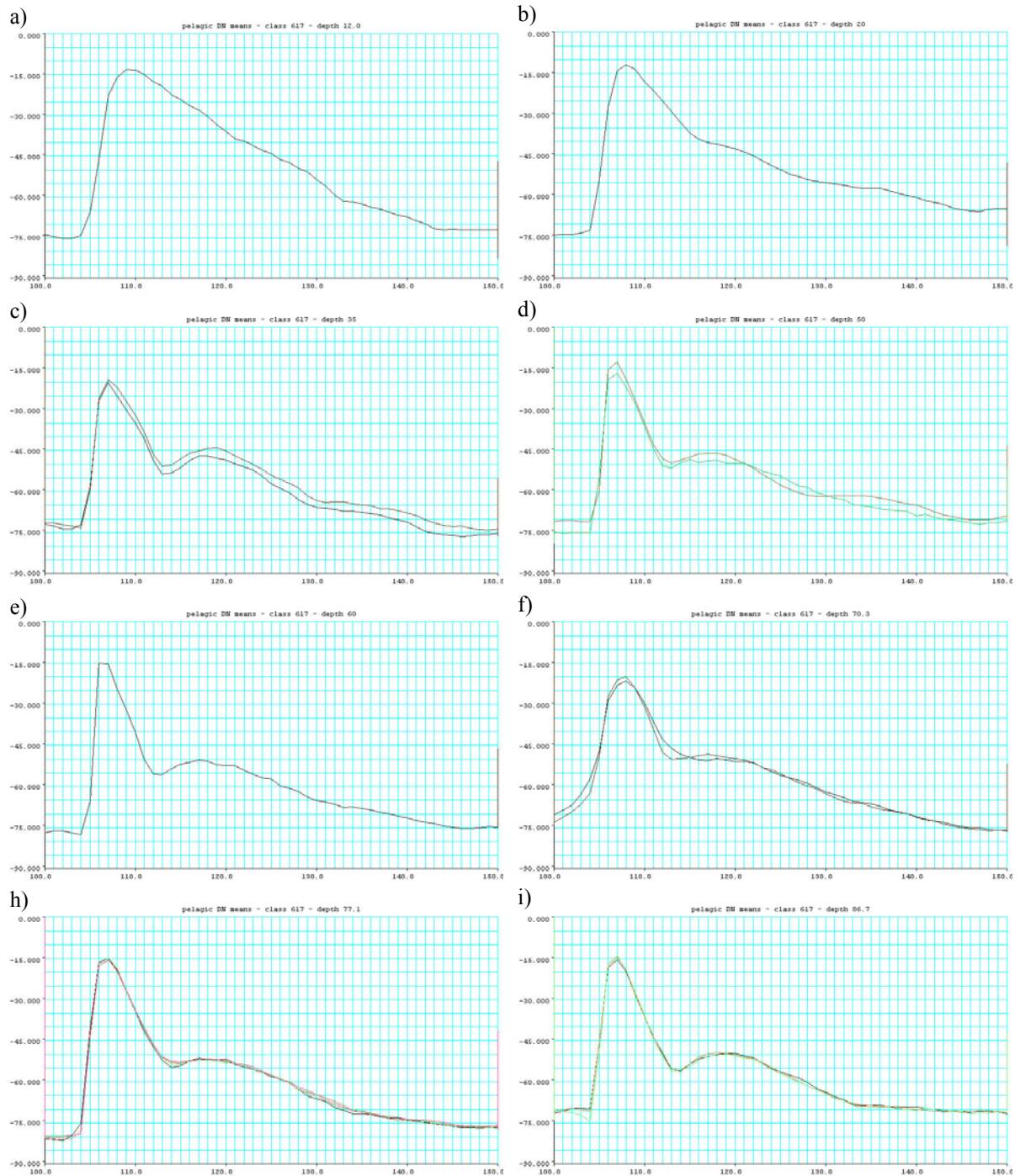


Figure 3-81: Plots of the depth-normalised pelagic data against sample number for sand sites for depths ranging from 12 m (a) to 85 m in (h).

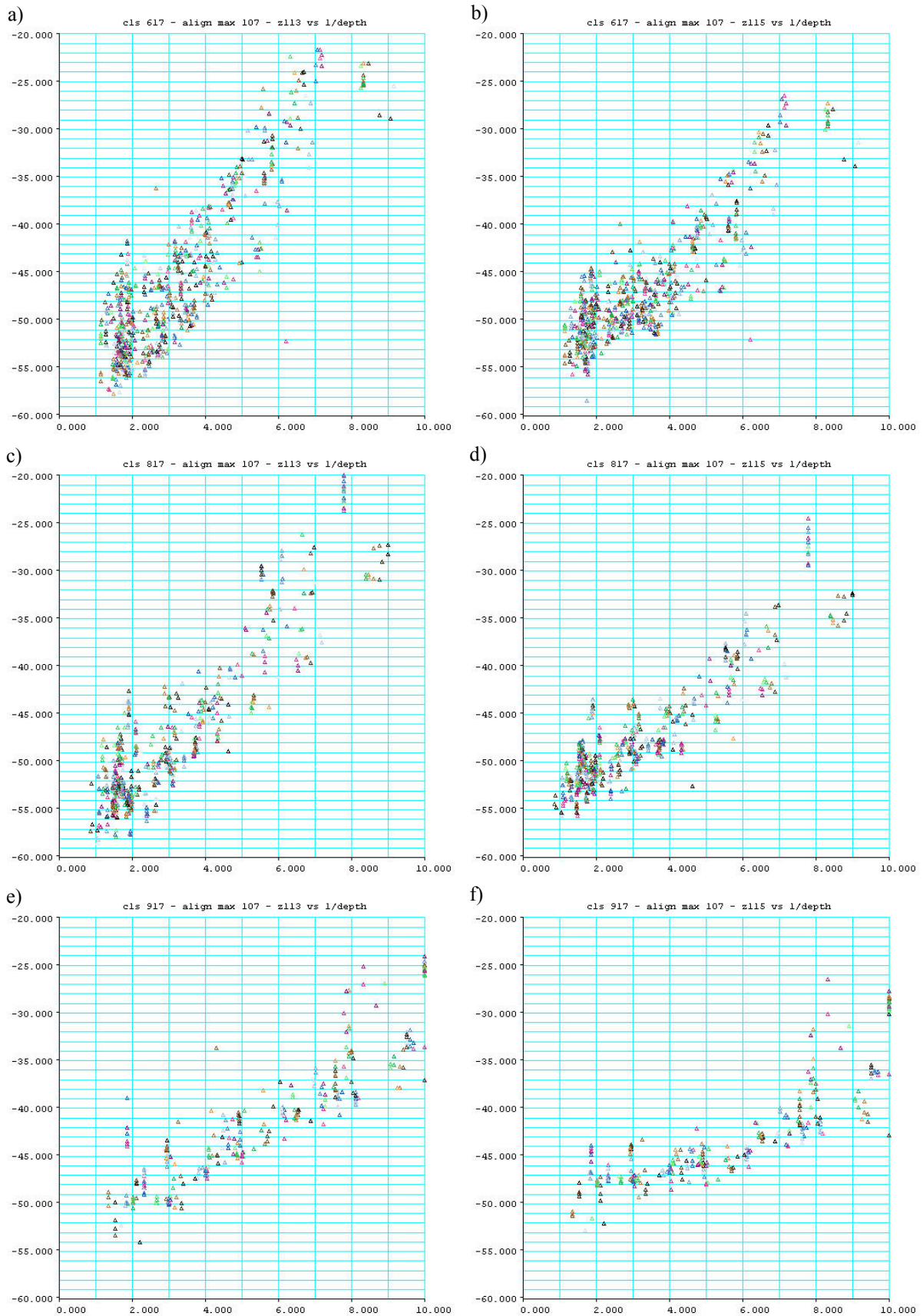


Figure 3-82: Plot of the response for the peak-aligned data against 100/depth for (a) sand class 617 for sample number 113; (b) sand class 617 for sample number 115; (c) silt class 817 for sample number 113; (d) silt class 817 for sample number 115; (e) mud class 917 for sample number 113; and (f) mud class 917 for sample number 115.

Table 3-21: Intercept, slope and r^2 values for regressions of the response at various sample numbers for the peak-aligned depth-normalised pelagic data on $1/\text{depth}$.

| Time | intercept | slope | r^2 |
|------|-----------|---------|--------|
| 101 | -73.1729 | -0.2186 | 0.0057 |
| 102 | -74.6114 | 0.3777 | 0.0131 |
| 103 | -79.4014 | 2.4815 | 0.2387 |
| 104 | -86.2605 | 6.4673 | 0.5882 |
| 105 | -78.9563 | 8.8755 | 0.6630 |
| 106 | -31.8452 | 2.5684 | 0.1629 |
| 107 | -17.1195 | 0.2755 | 0.0111 |
| 108 | -23.0639 | 1.0738 | 0.1408 |
| 109 | -31.6964 | 2.0394 | 0.3753 |
| 110 | -40.4079 | 2.8949 | 0.5301 |
| 111 | -49.1043 | 3.7135 | 0.6329 |
| 112 | -56.4091 | 4.2980 | 0.7250 |
| 113 | -60.0027 | 4.3289 | 0.7817 |
| 114 | -59.0950 | 3.7213 | 0.7837 |
| 115 | -56.6323 | 3.0226 | 0.7570 |
| 116 | -54.5358 | 2.4534 | 0.7020 |
| 117 | -53.3320 | 2.0885 | 0.6375 |
| 118 | -52.8377 | 1.8351 | 0.5619 |
| 119 | -52.8877 | 1.6525 | 0.4833 |
| 120 | -53.3637 | 1.5095 | 0.4132 |
| 121 | -54.1319 | 1.3700 | 0.3375 |
| 122 | -55.2195 | 1.2790 | 0.2816 |
| 123 | -56.5394 | 1.2252 | 0.2494 |
| 124 | -57.8636 | 1.1609 | 0.2238 |
| 125 | -59.3030 | 1.1419 | 0.2247 |
| 126 | -60.7373 | 1.1353 | 0.2349 |
| 127 | -62.1345 | 1.1370 | 0.2540 |
| 128 | -63.3999 | 1.1364 | 0.2710 |
| 129 | -64.5797 | 1.1588 | 0.2928 |
| 130 | -65.5028 | 1.1619 | 0.3019 |
| 131 | -66.2810 | 1.1759 | 0.3082 |
| 132 | -67.0064 | 1.2074 | 0.3199 |
| 133 | -67.4714 | 1.1793 | 0.3056 |
| 134 | -67.8956 | 1.1448 | 0.2902 |
| 135 | -68.2446 | 1.0849 | 0.2668 |
| 136 | -68.4714 | 0.9746 | 0.2290 |
| 137 | -68.7402 | 0.8539 | 0.1880 |
| 138 | -69.0259 | 0.7077 | 0.1403 |
| 139 | -69.2736 | 0.5300 | 0.0846 |
| 140 | -69.6341 | 0.3543 | 0.0382 |

3.6.2.3. Discriminant Analyses of the Depth-adjusted Data

The initial discriminant analyses of the 4500+ groups, without regard to the class labels, showed that the differences between groups for the same cover class were as large as the differences between the cover classes, and that there was no consistent discrimination between any of the cover classes.

Closer examination of the data indicated that there were depth-related differences in the shapes of the profiles, particularly at the shallower depths (< 25 m). There is also a small but reasonably consistent change in the position of the peak with depth.

In this section, the mean profiles are peak-aligned to remove one effect of depth. An attempt is made to remove the obvious effect of depth on the shape of the group means by regressing the echo response values against $1/\text{depth}$.

Another correction considered was to remove the so-called “size” effect, and focus on differences in shape. This is done by calculating a row mean (a simple measure of the average area under the curve), and subtracting this mean from all the values across an echo response curve; dividing by this mean is also advocated to equalise the area under the echo response curve.

3.6.2.3.1 Regressions of Peak-Aligned Responses against $1/\text{Depth}$

Table 3-21 lists the intercept, slope and r^2 values for the regressions of the peak-aligned depth-normalised pelagic data on $1/\text{depth}$. There is a reasonably strong relationship for sample numbers 110 – 120, but other parts of the ping have little relationship with $1/\text{depth}$.

3.6.2.3.2 Canonical Variate Analyses of the Peak-Aligned and Depth-Adjusted Data

The first five canonical roots for the canonical variate analysis of the 4519 groups from 117 classes, without regard to the class labels, for the peak-aligned and depth-adjusted data are 6.329, 4.225, 1.129, 0.6273 and 0.3591.

The first five canonical roots for the peak-aligned, depth-adjusted and row-corrected data are 4.332, 1.787, 0.6470, 0.3938 and 0.2862.

Both plots show two clusters, in one case along the second canonical variate for the peak-aligned and depth-adjusted data, and along the first canonical variate for the peak-aligned, row-corrected and depth-adjusted data.

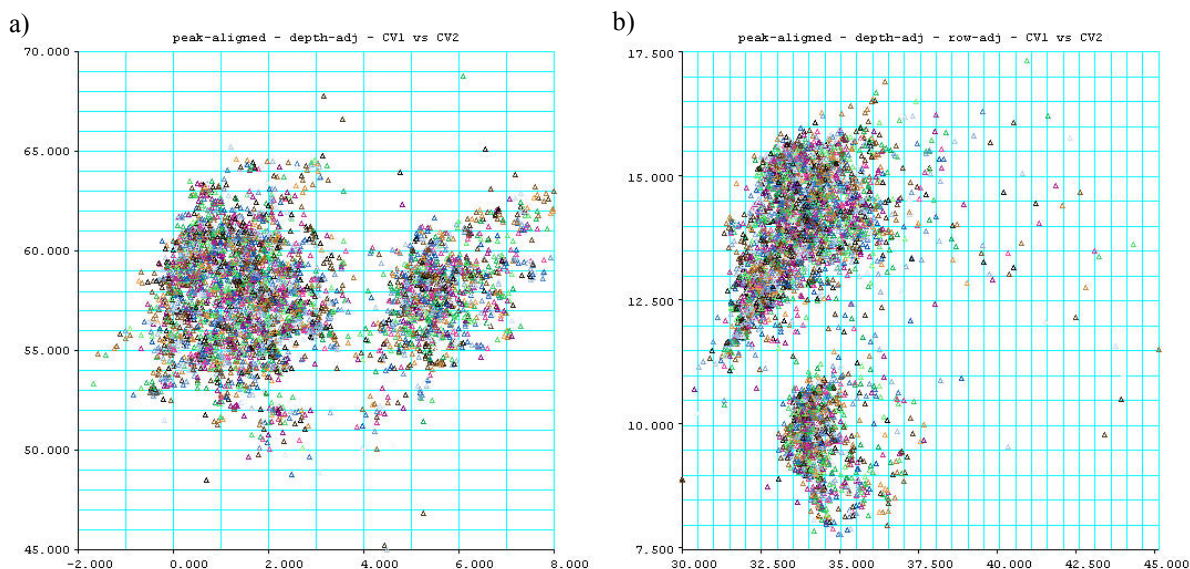


Figure 3-83: Plot of the group means for the first two canonical variates for the canonical variate analysis of the 4519 groups from 117 classes, without regard to the class labels, for (a) the peak-aligned and depth-adjusted data; and (b) the peak-aligned, row-corrected and depth-adjusted data.

A plot of the first canonical vector for the peak-aligned and depth-adjusted data in Figure 3-84 shows a clear summing or “size” effect – all the values are positive, and very roughly the same.

Plots of the subsequent canonical vectors for the peak-aligned and depth-adjusted data, and the canonical vectors for the peak-aligned, row-corrected and depth-adjusted data — Figure 3-85, Figure 3-86 and Figure 3-87 — show obvious visual similarities (remember that reversing the sign of a vector has no effect on the relative positions of the groups along an axis).

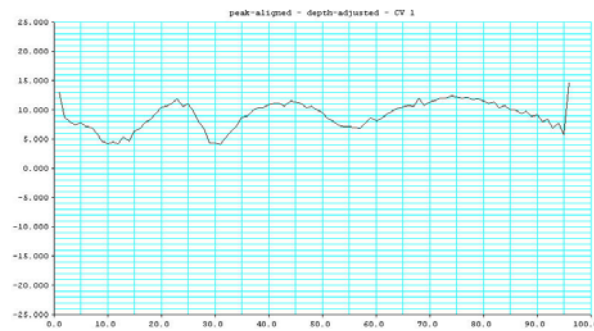


Figure 3-84: Plot of the first canonical vector for the canonical variate analysis of the 4519 groups from 117 classes, without regard to the class labels, for the peak-aligned and depth-adjusted data.

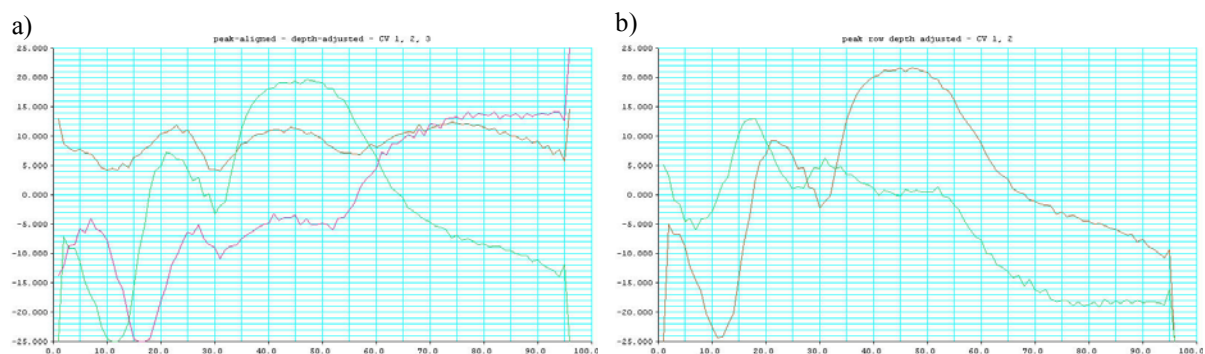


Figure 3-85: Plot of the canonical vectors for the canonical variate analysis of the 4519 groups, for (a) the peak-aligned and depth-adjusted data; and (b) the peak-aligned, row-corrected and depth-adjusted data.

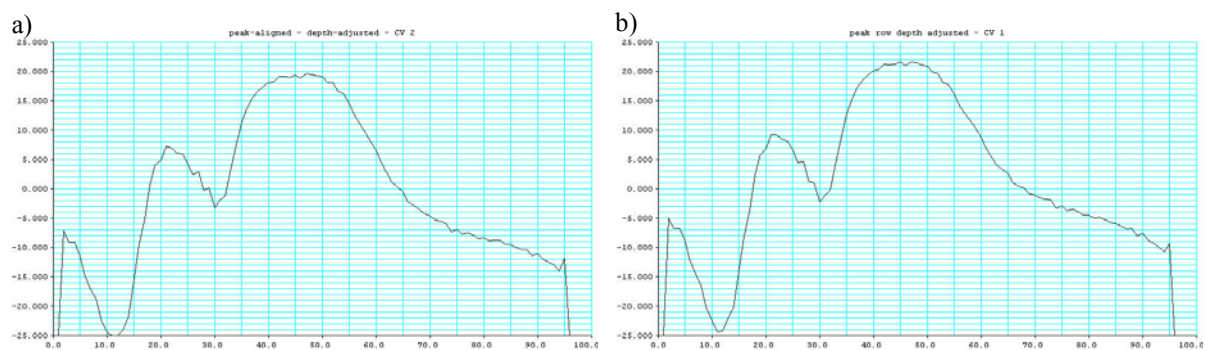


Figure 3-86: Plot of (a) the second canonical vector for the canonical variate analysis of the 4519 groups for the peak-aligned and depth-adjusted data; and (b) the first canonical vector the peak-aligned, row-corrected and depth-adjusted data.

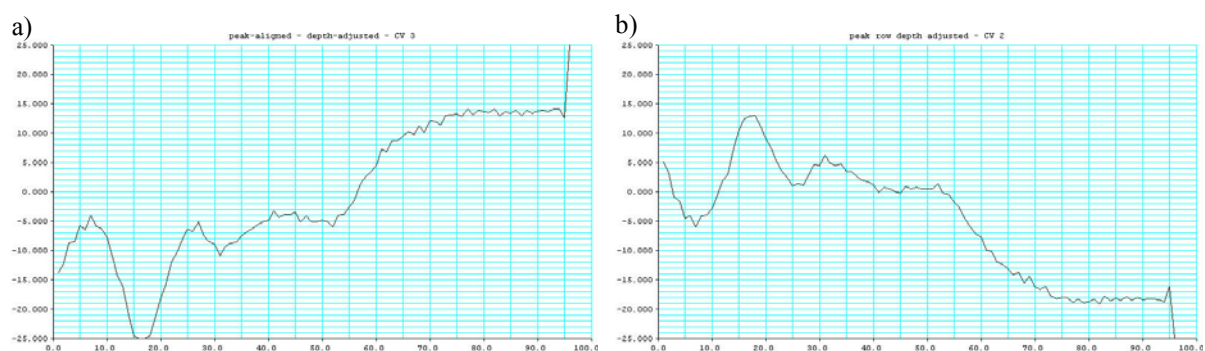


Figure 3-87: Plot of (a) the third canonical vector for the canonical variate analysis of the 4519 groups for the peak-aligned and depth-adjusted data; and (b) the second canonical vector the peak-aligned, row-corrected and depth-adjusted data.

For the usual analysis of the peak-aligned and depth-adjusted data, it seems clear that the first canonical vector is reflecting mainly size differences between the echo response profiles. Shape differences are evident in the successive canonical vectors for the peak-aligned and depth-adjusted data, and for all the canonical vectors for the peak-aligned, row-corrected and depth-adjusted data.

The plot of the group means for the first two canonical variates for the canonical variate analysis of the 4519 groups from 117 classes, without regard to the class labels, for the peak-aligned, row-corrected and depth-adjusted data in Figure 3-83 (b) showed two obvious clusters separated along the first canonical variate. However, plots for the group means from the individual classes in Figure 3-88 show that for all of the 117 classes, there are groups which fall within the two main clusters, and that there is no obvious separation between any of the classes.

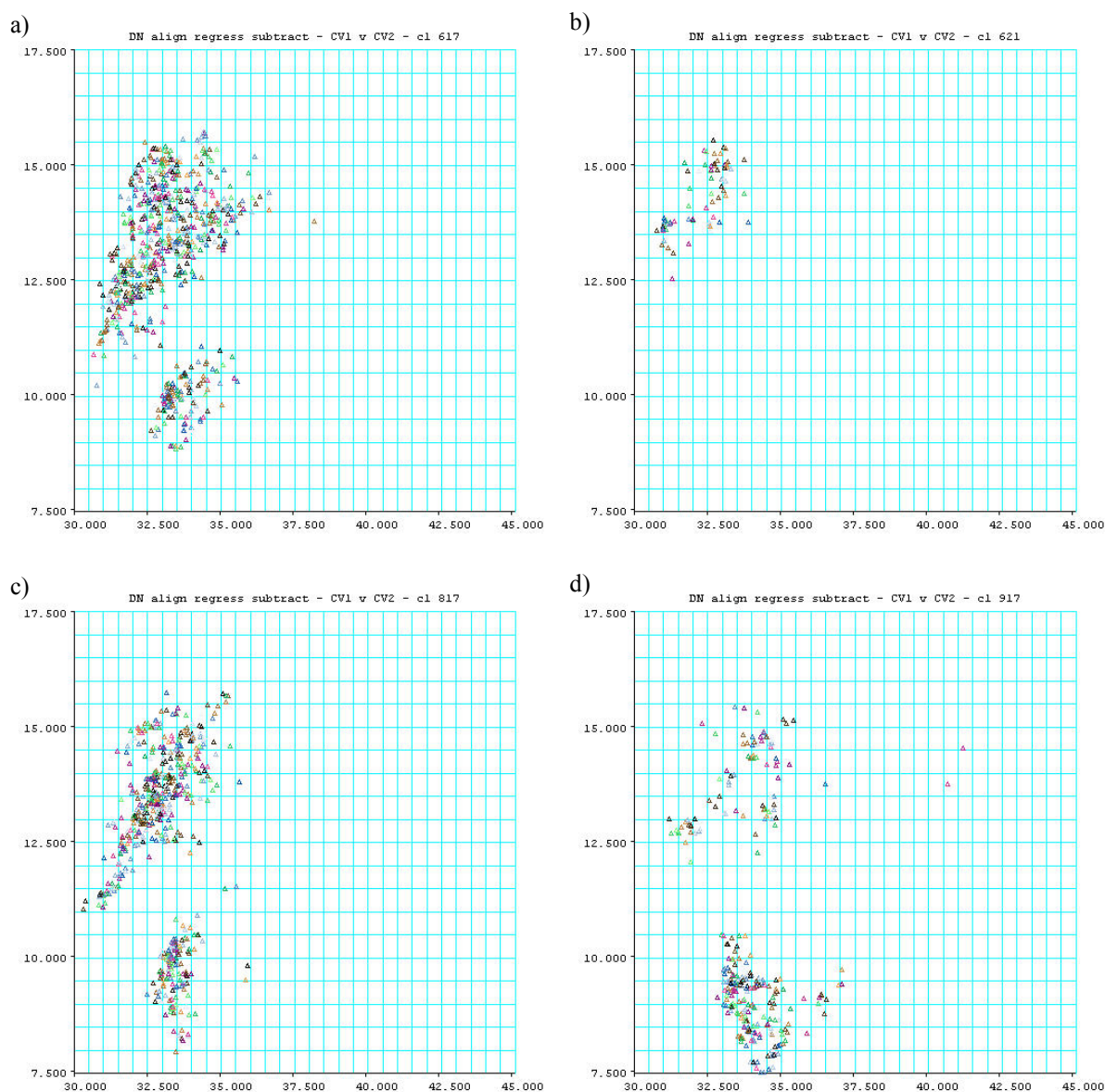


Figure 3-88: Plot of the group means for the first two canonical variates for the canonical variate analysis of the 4519 groups from 117 classes, without regard to the class labels, for the peak-aligned, row-corrected and depth-adjusted data for (a) sand class 617; (b) seagrass class 621; (c) silt class 817; and (d) mud class 917.

3.6.2.3.3 Directed Contrasts for the Peak-Aligned, Depth-Adjusted and Row-Corrected Data

Directed contrasts can be defined between classes of interest to calculate those canonical variates which best separate the specified classes. Figure 3-89 shows a plot (top-left) of the group means for the two canonical variates which result from contrasts between class 617 vs classes 618 and 621, and class 618 vs class 621.

Canonical variate plots for the groups for the classes involved in the contrast calculations — 617 (top-right), 618 (bottom-left) and 621 (bottom-right) — show that, for two of the three classes, there are groups which fall within the two main clusters. There is considerable overlap between class 617 and classes 618 and 621, and some overlap between classes 618 and 621. There is evidence of two clusters in the canonical variate group plots for most classes.

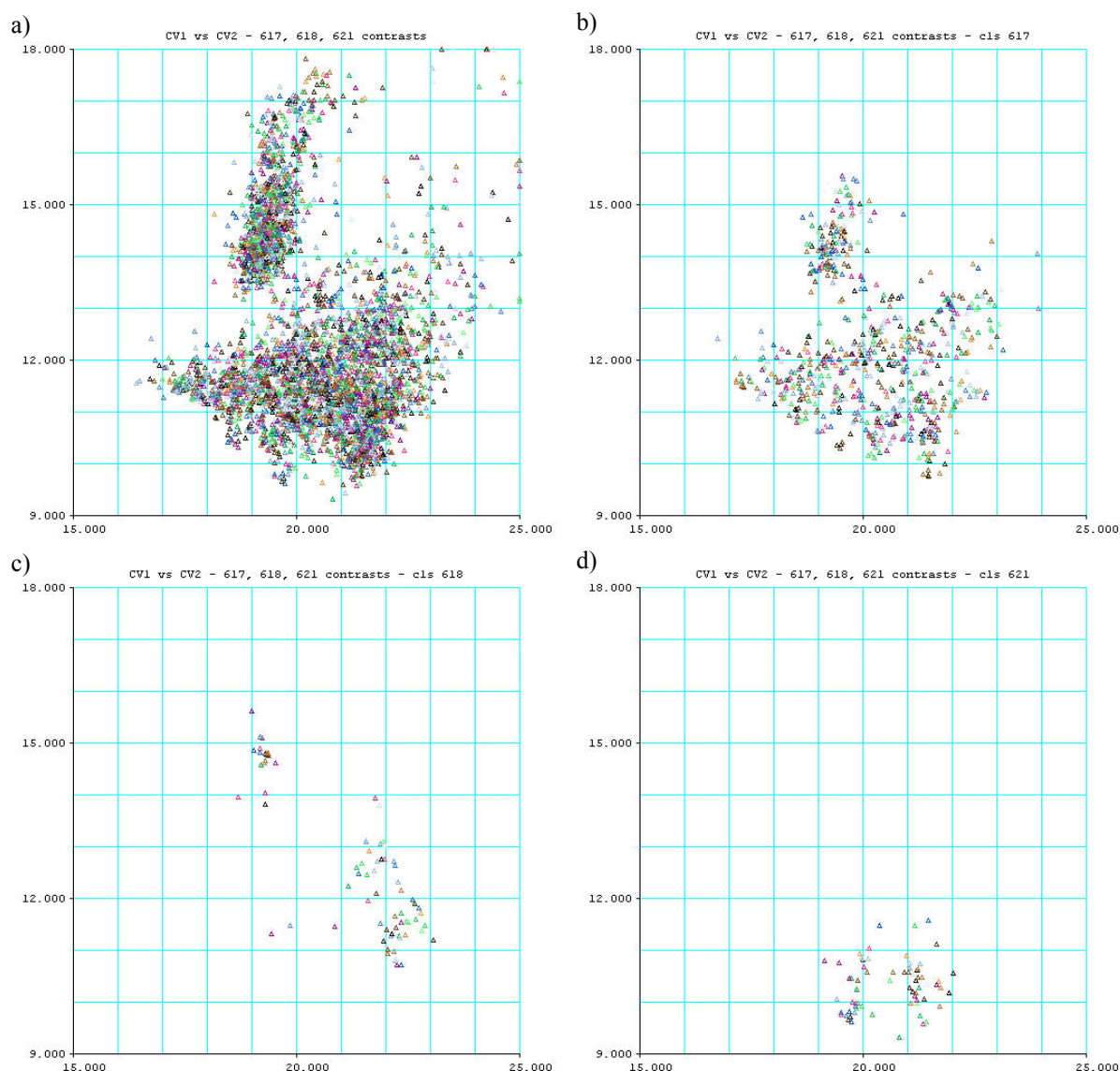


Figure 3-89: Plot of the group means for the first two canonical variates for the canonical variate analysis of the 4519 groups which result from contrasts between class 617 vs classes 618 and 621, and class 618 vs class 621, for the peak-aligned, row-corrected and depth-adjusted data for (a) all groups for all classes; (b) sand class 617; (c) sponge class 618; and (d) seagrass class 621.

The regressions of the echo response values on $1/\text{depth}$ were designed to remove or minimise depth-related effects. However, plots of the scores for the first canonical variate against depth and $100/\text{depth}$ in Figure 3-90 and Figure 3-91 show an unusual pattern. Clearly for the groups which have canonical

variate scores which fall within the top cluster in the overall plot of the first two canonical variates, there is a relationship between the scores for the first canonical variate and depth. Moreover, this pattern is really only clearly evident when the data for all the groups are plotted (see Figure 3-92). The pattern is again evident when the data for all the groups are plotted against 100/depth in Figure 3-93.

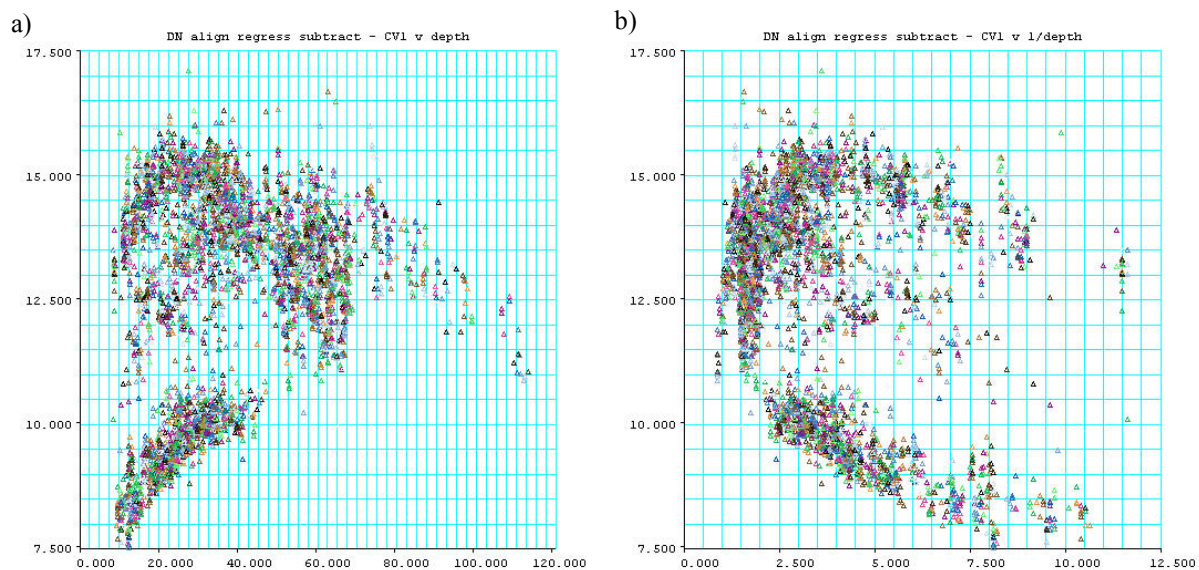


Figure 3-90: Plot of the group means for the first canonical variate for the canonical variate analysis of the 4519 groups for the peak-aligned, row-corrected and depth-adjusted data (a) against depth; and (b) against 1/depth.

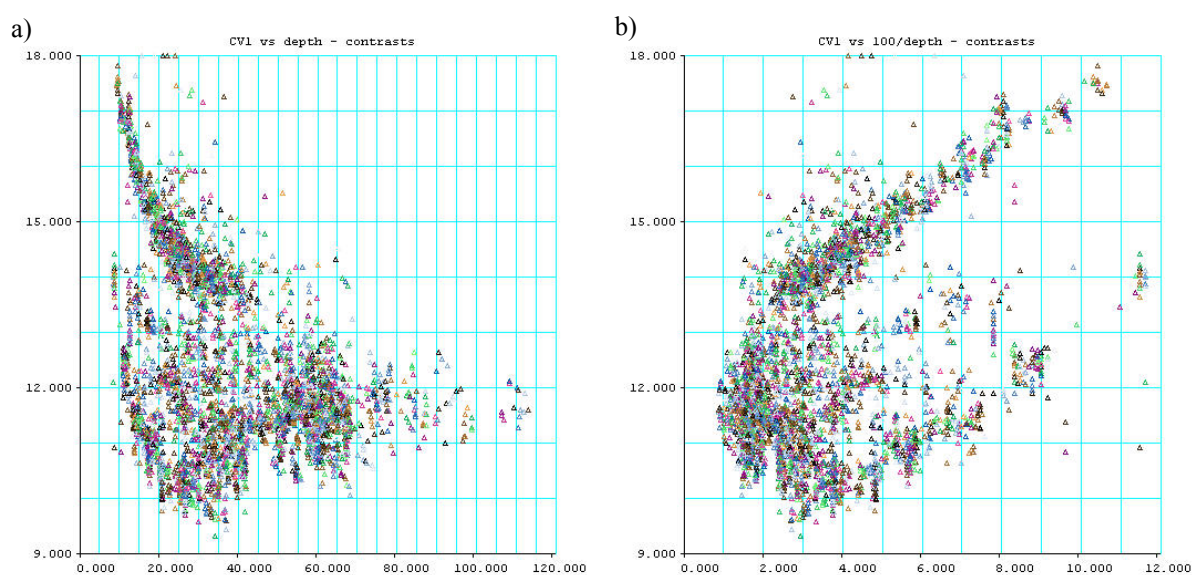


Figure 3-91: Plot of the group means for the first canonical variate for the canonical variate analysis of the 4519 groups which result from contrasts between class 617 vs classes 618 and 621, and class 618 vs class 621, for the peak-aligned, row-corrected and depth-adjusted data (a) against depth; and (b) against 1/depth.

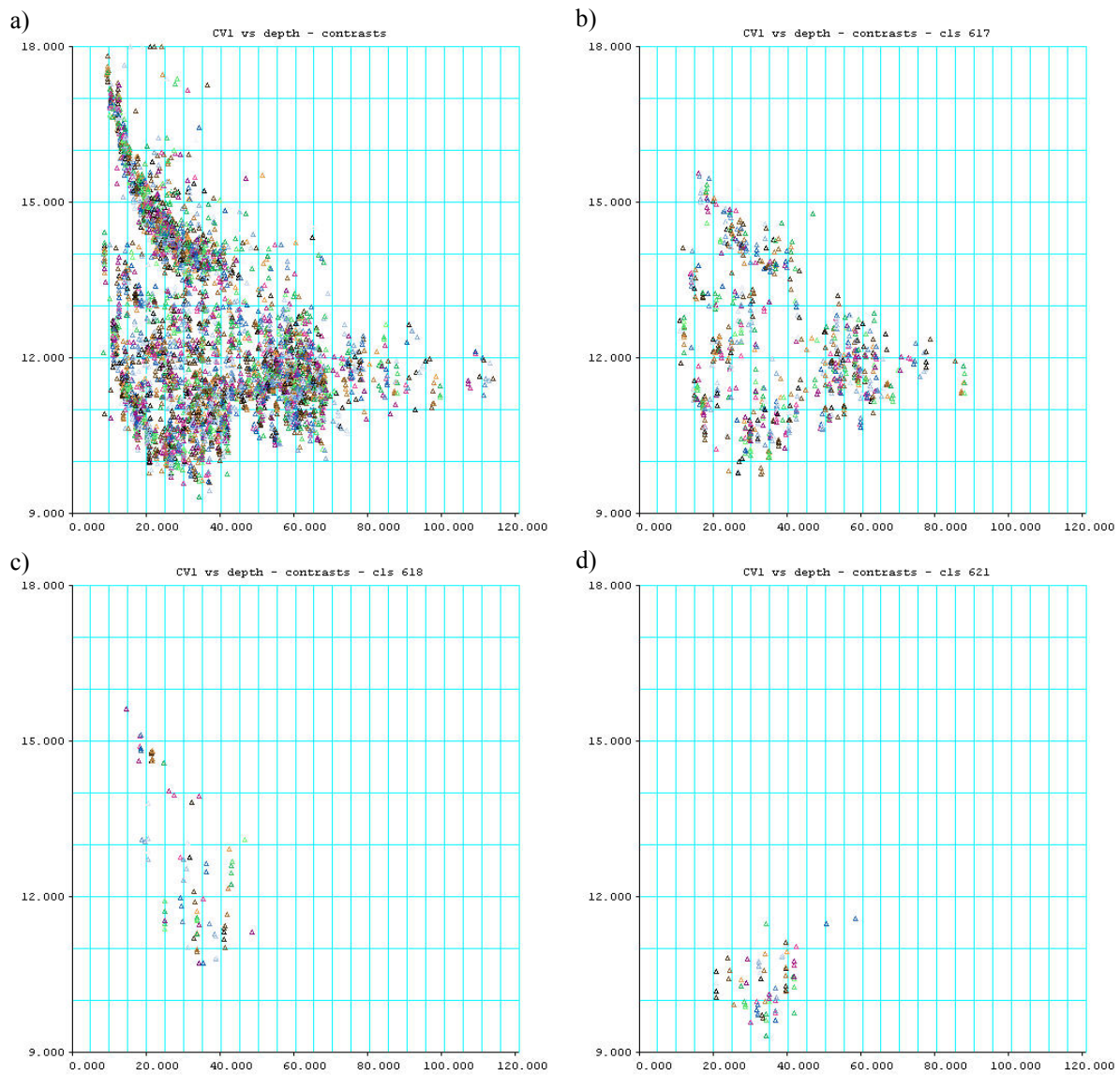


Figure 3-92: Plot of the group means for the first canonical variate for the canonical variate analysis of the 4519 groups which result from contrasts between class 617 vs classes 618 and 621, and class 618 vs class 621, for the peak-aligned, row-corrected and depth-adjusted data against depth for (a) all groups for all classes; (b) sand class 617; (c) sponge class 618; and (d) seagrass class 621.

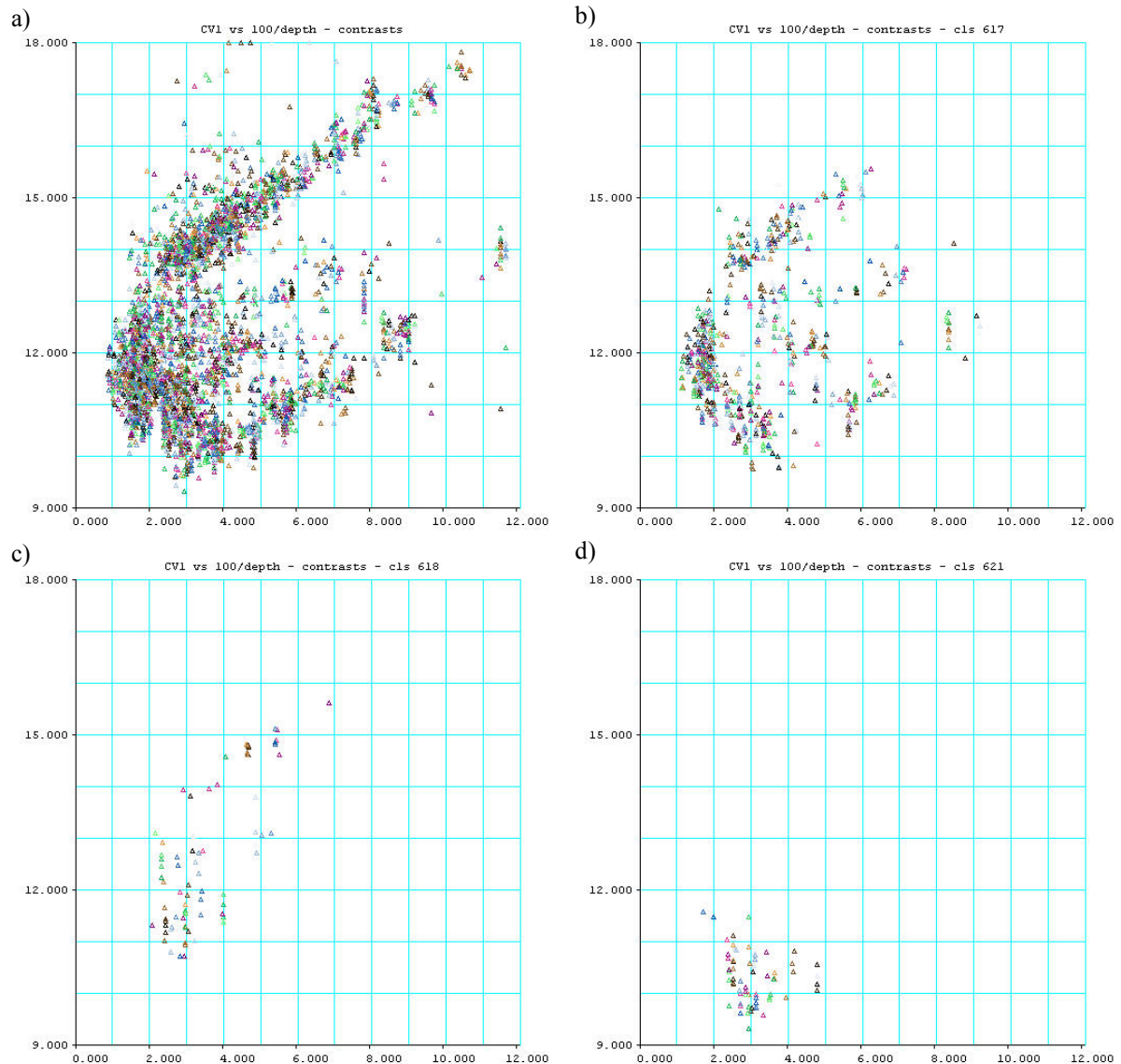


Figure 3-93: Plot of the group means for the first canonical variate for the canonical variate analysis of the 4519 groups which result from contrasts between class 617 vs classes 618 and 621, and class 618 vs class 621, for the peak-aligned, row-corrected and depth-adjusted data against $1/\text{depth}$ for (a) all groups for all classes; (b) sand class 617; (c) sponge class 618; and (d) seagrass class 621.

3.6.2.3.4 Canonical Variate Analyses for the Two Clusters

Clearly for the groups which have canonical variate scores which fall within the smaller cluster in the overall CV1-CV2 plots, there is a relationship between their CV1 scores and depth.

The CV1 vs CV2 plot was used to define two clusters. Groups were assigned to the larger cluster if $\text{CV1} \geq 11.5$. If $\text{CV1} < 10.5$, then groups were assigned to the smaller cluster. If $10.5 < \text{CV1} < 11$ and $\text{CV2} \geq 32$, then groups were assigned to the smaller cluster. Other groups with CV1 scores < 11.5 were assigned to the smaller cluster.

Figure 3-94(a) shows a plot of the canonical variate scores for the 3358 groups in the larger cluster. Canonical variate plots for the individual classes again show no obvious separation between any of the classes. Examples for sand (class 617), seagrass (class 621) and mud (class 917) are shown in Figure 3-94.

Figure 3-95 shows that there is no obvious pattern of the scores for the first canonical variate for the larger cluster with depth.

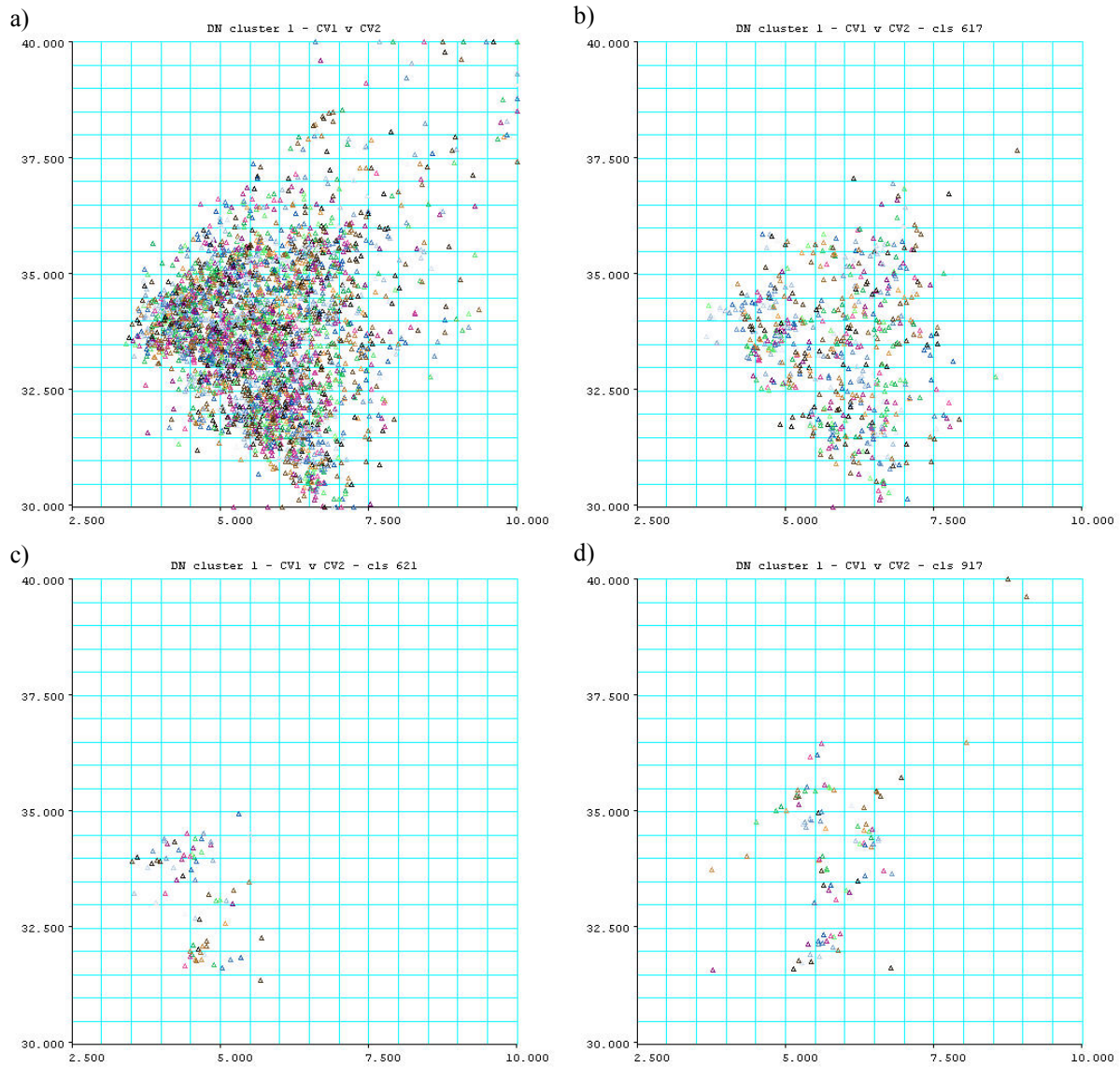


Figure 3-94: Plot of the group means for the first two canonical variates for the canonical variate analysis of the 3358 groups in the larger CV1-CV2 cluster for the peak-aligned, row-corrected and depth-adjusted data for (a) all groups; (b) sand class 617; (c) seagrass class 621; and (d) mud class 917.

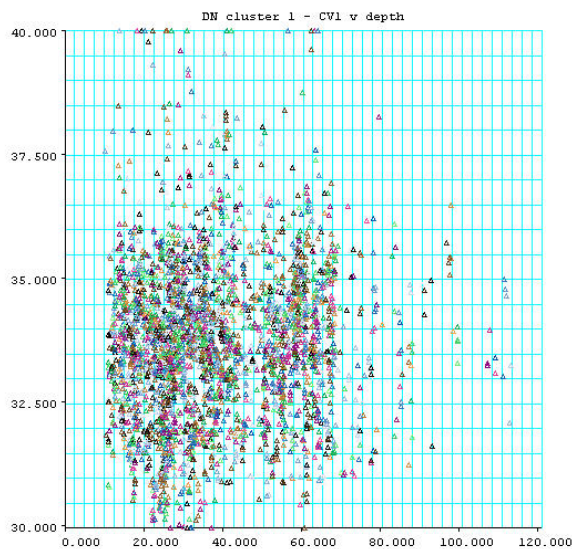


Figure 3-95: Plot of the group means for the first canonical variate for the canonical variate analysis of the 3358 groups for the peak-aligned, row-corrected and depth-adjusted data against depth.

Figure 3-96 (a) shows a plot of the canonical variate scores for the 1161 groups in the smaller cluster. Canonical variate plots for the individual classes again show no obvious separation between any of the classes. Examples for sand (class 617) and mud (class 917) are shown in Figure 3-96.

Figure 3-97 shows that there is no obvious pattern of the scores for the first canonical variate for the smaller cluster with depth.

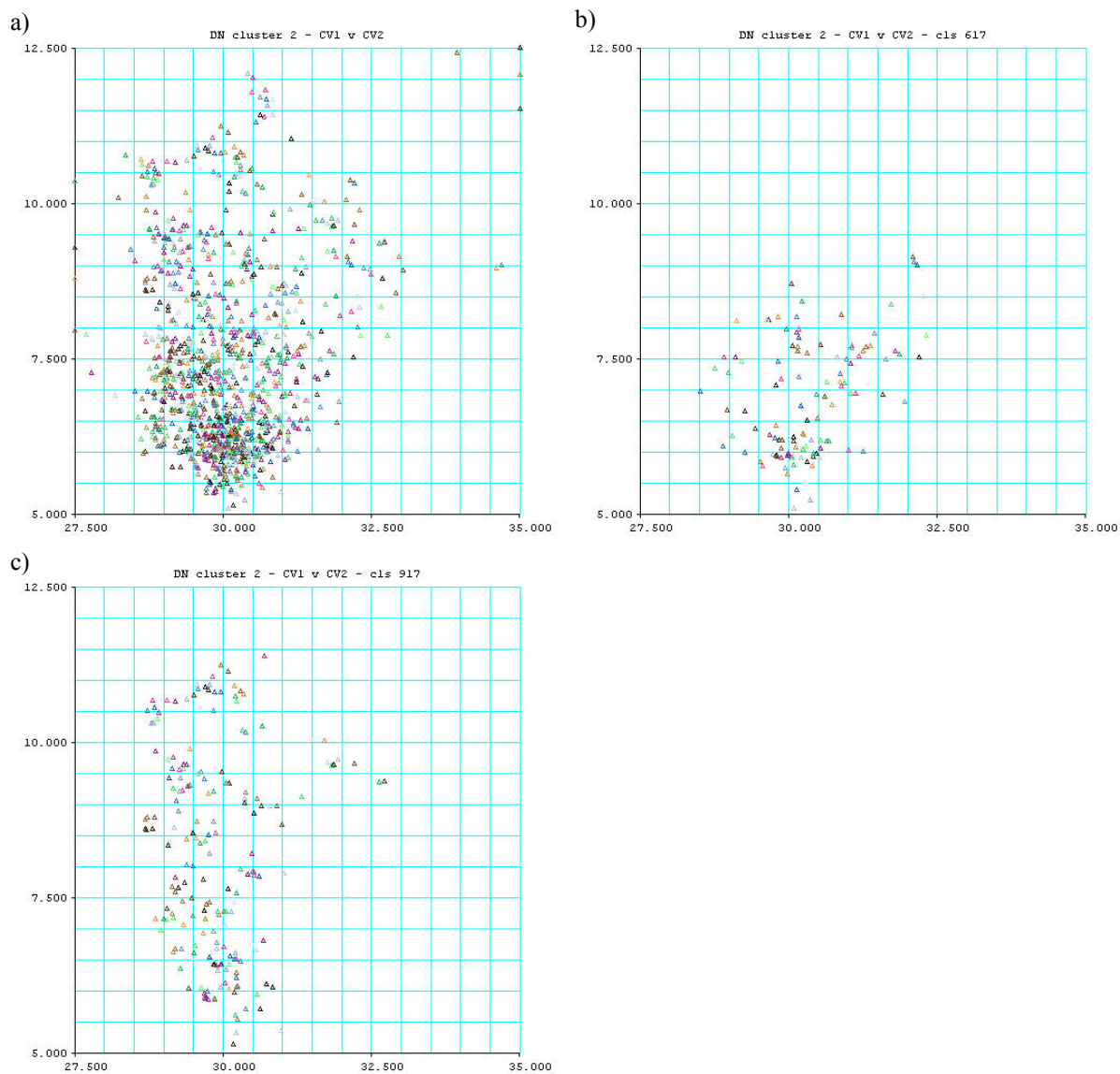


Figure 3-96: Plot of the group means for the first two canonical variates for the canonical variate analysis of the 1161 groups in the smaller CV1-CV2 cluster for the peak-aligned, row-corrected and depth-adjusted data for (a) all groups; (b) sand class 617; and (c) mud class 917

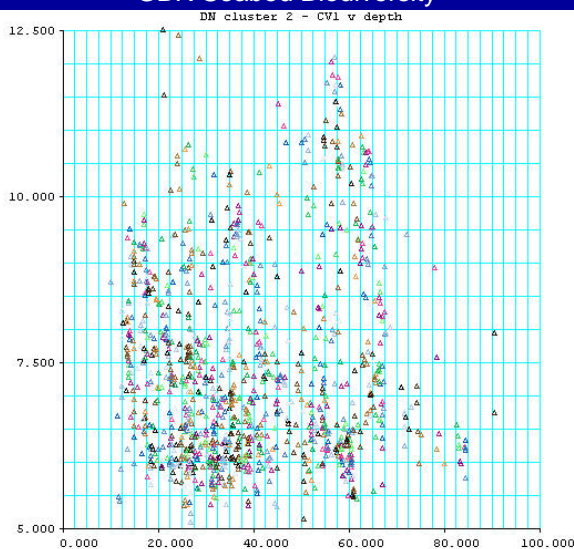


Figure 3-97: Plot of the group means for the first canonical variate for the canonical variate analysis of the 1161 groups for the peak-aligned, row-corrected and depth-adjusted data against depth

3.6.2.3.5 Site Contrast Canonical Variate Analyses

The data analysed here were from sites which were collected close together in time and hence geographically, concentrating on potential extremes of cover, such as sand and seagrass, and mud, silt and sand.

Sites 1631 vs 2552 – Seagrass vs Sand

There were 12 groups for class 621 (seagrass) from site 1631, and 30 groups for class 617 (sand) from site 2552. The first four canonical roots were 7.04, 0.383, 0.163 and 0.071. Figure 3-98 shows two obvious clusters along the first canonical variate, corresponding to groups from the seagrass site (on the left) and from the sand site (on the right).

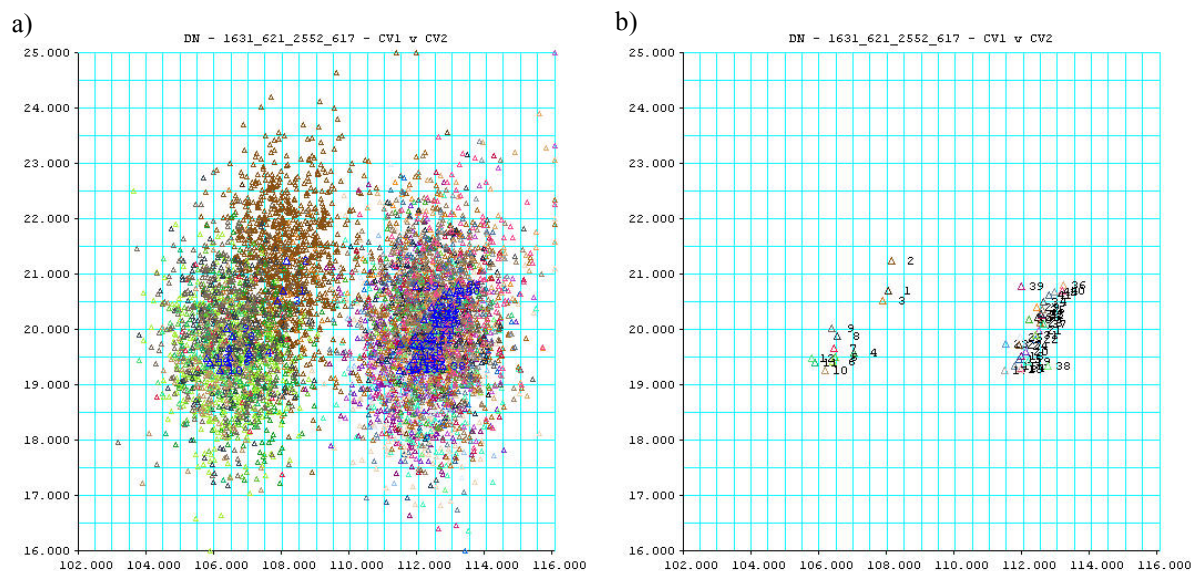


Figure 3-98: Plots of (a) the canonical variate scores and (b) the group means for the first two canonical variates for a canonical variate analysis of the depth-normalised data for 42 groups from sites 1631 and 2552, without regard to the class labels.

Aligning the peaks reduces the first canonical root from 7.04 to 6.57. The two sites are at average depths of 37 m (1631 - seagrass) and 30 m (2552 - sand). Adjusting the responses for the regressions

on inverse depth further reduces the first canonical root to 5.89. Aligning the peaks and correcting for size by subtracting the row means removes much of the class separation, reducing the first canonical root to 1.13; adjusting area under the curve by dividing by the row means reduces the first canonical root to 0.79. These analyses and the plots in Figure 3-99 suggest that the responses for seagrass and sand are quite similar in their shapes, and that the discrimination in Figure 3-98 results from differences in the magnitudes of the responses between the two classes.

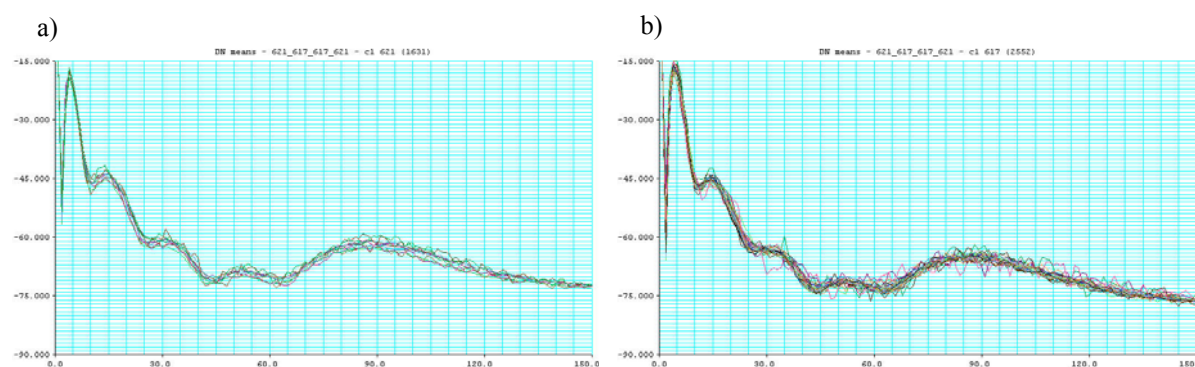


Figure 3-99: Plots of the depth-normalised pelagic data against sample number for group means for (a) 12 groups for the seagrass site 1631 (class 621); and (b) 30 groups for the sand site 2552 (class 617).

Sites 1631 vs 2552 vs 2224 – Seagrass vs Sand vs Sand

There were 12 groups for class 621 (seagrass) from site 1631, 30 groups for class 617 (sand) from site 2552, and 14 groups for class 617 (sand) from site 2224. The first four canonical roots were 9.26, 1.402, 0.253 and 0.154. Figure 3-100 shows that when sand groups from site 2224 collected on 23/09/2004 are included in an analysis of the depth-normalised data, there is marked separation between the two sand sites along the first canonical variate, and separation of the sand and seagrass sites along the second canonical variate. Figure 3-101 shows plots of group means for the two sand sites; the obvious differences in the shapes are reflected in the canonical variate scores in Figure 3-100. These plots of mean profiles for the two sand sites show greater differences in shape than do plots of the first sand site and the seagrass site (Figure 3-99). Note also the cluster of scores with low CV2 and high CV1 values in Figure 3-100, which do not correspond to defined sand groups. The top profile in Figure 3-102 is from sand group 53, but its canonical variate score plots in the low CV2 – high CV1 cluster, whereas the canonical variate scores for the other two profiles plot in the nominally correct high CV1 – high CV2 cluster.

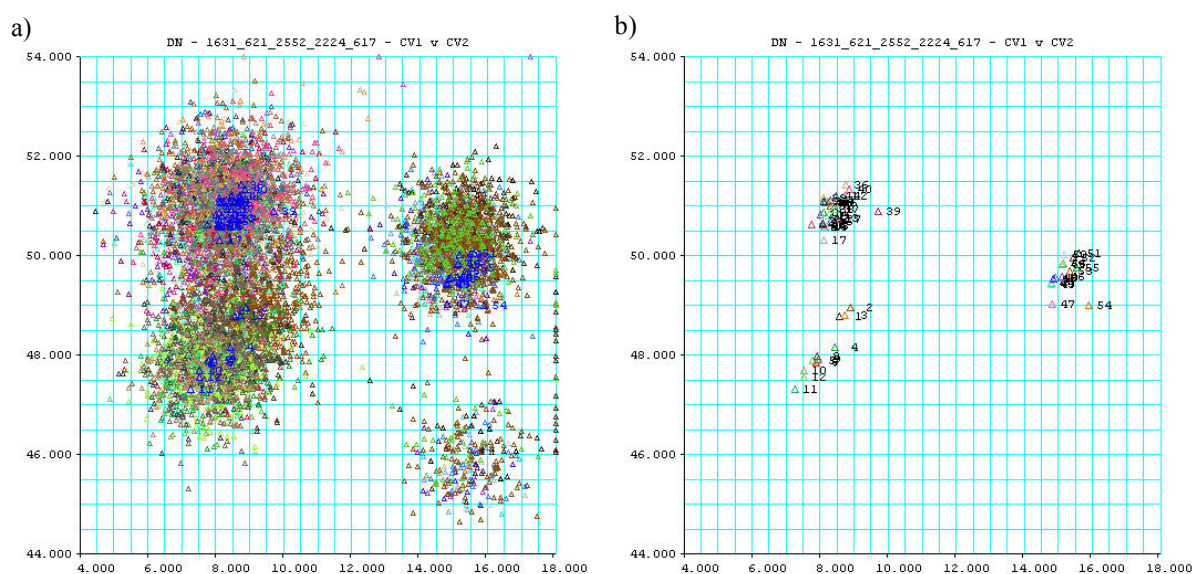


Figure 3-100: Plots of (a) the canonical variate scores and (b) the group means for the first two canonical variates for a canonical variate analysis of the depth-normalised data for 56 groups from sites 1631, 2552 and 2224, without regard to the class labels.

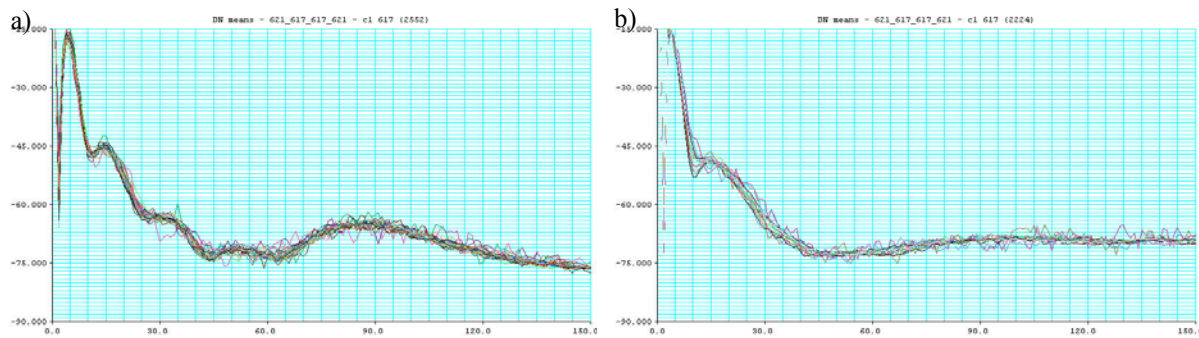


Figure 3-101: Plots of the depth-normalised pelagic data against sample number for group means for (a) 30 groups for class 617 (sand) from site 2552, and (b) 14 groups for class 617 (sand) from site 2224.

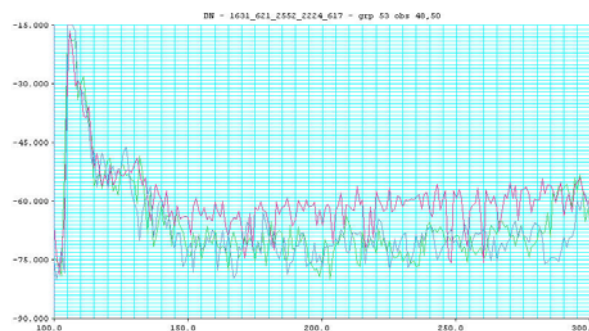


Figure 3-102: Plots of the echo responses for the depth-normalised pelagic data against sample number for profiles 48 – 50 for group 53 (from the sand site 2552 - class 617).

Sites 1631 vs 2552 vs 2224 vs 2441 – Seagrass vs Sand vs Sand vs Seagrass

In addition to the seagrass groups from site 1631, the sand groups from site 2552, and the sand groups site 2224, there are 5 groups for class 621 (seagrass) from site 2441 (the fifth group nominally consists of 59 contiguous pings from class 617 sand). The first four canonical roots are 9.38, 1.696, 0.488 and 0.188. Figure 3-103 shows that the new site 2441 seagrass groups 57 – 61 cluster with the initial site 1631 seagrass groups 1 – 12 along both CV1 and CV2. Note that group 61 (sand) is not separated from groups 57 – 60 along any of the canonical variates. There are obvious similarities in the shapes of the group mean ping profiles for the two seagrass sites in Figure 3-104.

As can be seen from Figure 3-104 (b), there are no obvious differences in shape between the four nominal seagrass groups and the nominal sand group from site 2441 — this sand group from the same predominantly seagrass site also clusters with the seagrass groups from the same site (Figure 3-103). This pattern was also observed for the analyses of the first pair of sites (1631 vs 2552) above, where there were a number of groups of contiguous pings, typically less than 20, from other classes. For these analyses, the CV scores for these groups always clustered with the respective groups for the dominant class for that site.

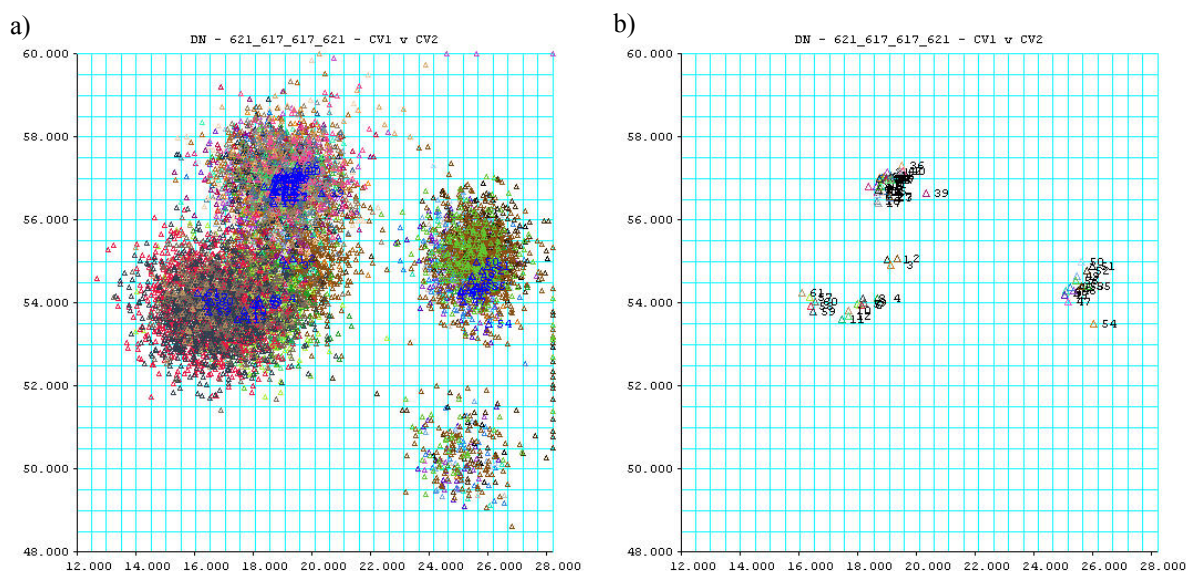


Figure 3-103: Plots of (a) the canonical variate scores and (b) the group means for the first two canonical variates for a canonical variate analysis of the depth-normalised data for 61 groups from sites 1631, 2552, 2224 and 2441, without regard to the class labels.

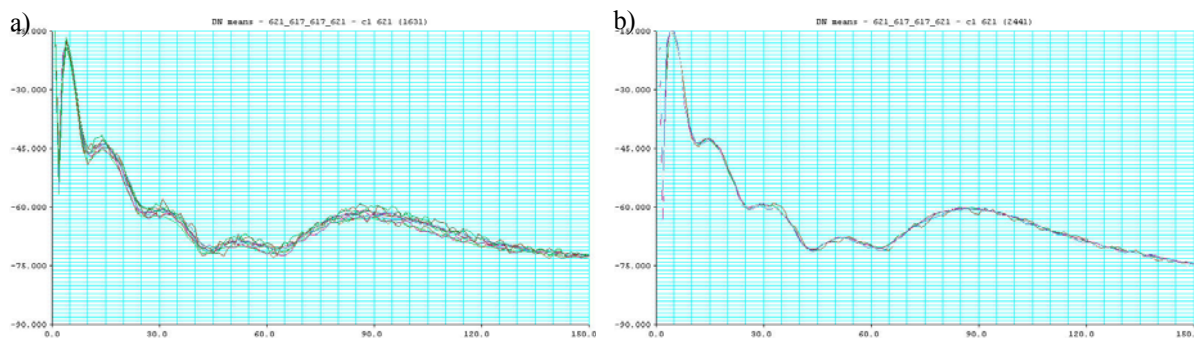


Figure 3-104: Plots of the depth-normalised pelagic data against sample number for group means for (a) 12 groups for class 621 (seagrass) from site 1631, and (b) 5 groups for class 621 (seagrass) from site 2441.

Variability of sand sites

Plots of the group mean ping profiles for the sand sites are shown in Figure 3-101 and Figure 3-105. Figure 3-105(b) shows that the group for nominal class 617 from site 1580 is obviously different from the groups from site 2224. The canonical variate scores for the group from site 1580 plot with the cluster of scores with low CV2 and high CV1 values noted earlier.

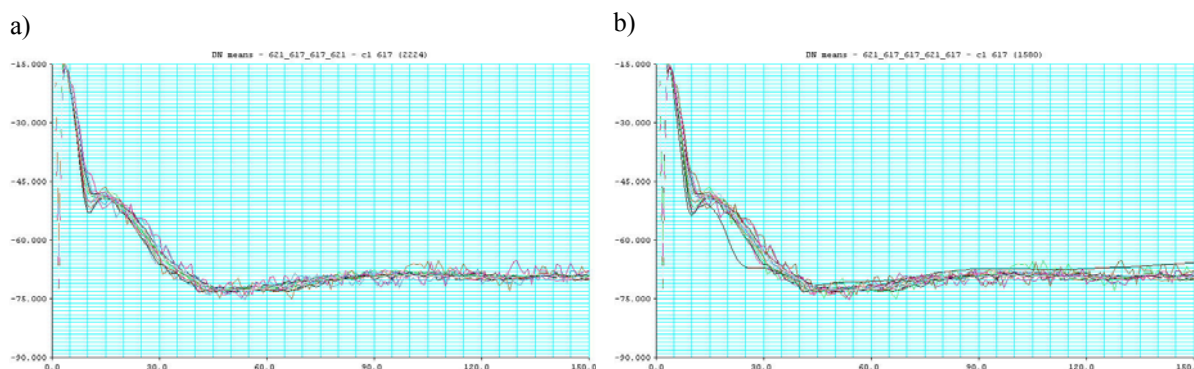


Figure 3-105: Plots of the depth-normalised pelagic data against sample number for group means for (a) 14 groups for class 617 (sand) from site 2224 and (b) the group for class 617 from site 1580 superimposed on the groups from site 2224.

3.6.3. Linear Discriminant Analyses of QTC View data (I McLeod)

3.6.3.1. *Substratum and BioHabitat combinations v2*

The full combination of the original 24 BioHabitat by 9 substratum event classes (v1) did not converge, so the combination of the original substratum 9 class coding (Table 2-6) and the first 12 class biohabitat re-coding (Table 2-10) schema was investigated. This potentially had 108 classes of which 102 classes were expressed.

The completed linear discriminant analysis (LDA) produced a confusion matrix (as described in Section 3.6.1) of 103 rows by 103 columns, which was too large to tabulate within this report. Instead an abridged version is presented (Table 3-22), that shows the relevant information from the diagonals of the relevant confusion matrices for all but the most infrequent habitat event class combinations.

The “Observed” are analogous to the row totals from the full confusion matrices. “Observed Counts” are original number of observations in each class and the “Observed % of Total” are the observed counts as a percentage of the total observations. The three right hand columns indicate the classification results. The “Observed vs Predicted Counts” are the number of observations of a given class correctly classified as that class. The “OvsP % of total” are the correctly classified counts as a percentage of the total observations. The “OvsP % of Row” are the correctly classified counts as a percentage of the observed counts, giving the percentage within class prediction skill.

Superficially, it seems that a number of the classes are reasonably accurately classified. However, these are relatively infrequent and the overall classification success is only ~3.4%. The most frequently occurring classes have very low classification success and were incorrectly classified to other (off-diagonal) habitat classes (not tabulated in the above abridged version). In particular, the more common classes, such as the no biohabitat classes, were almost always incorrectly classified as a range of other biohabitat combinations.

This poor performance with this number of classes was not unexpected, and further aggregation was necessary, but nevertheless clearly demonstrates that acoustics data are not able to discriminate a modest number of basic habitat types that are readily recognised by observers

3.6.3.2. *Substratum and BioHabitat combinations v3*

The next combination of the re-coding classes investigated was the combination of the second substratum re-coding (7 classes, Table 2-13) and the first biohabitat re-coding (12 classes, Table 2-10). This potentially had 84 classes of which 79 were expressed.

Again, the full confusion matrix from the cross-validated LDA was too large to present within this report, and an abridged table (Table 3-23) is again presented, which shows the relevant information from the diagonals of the relevant confusion matrices for all but the most infrequent habitat event class combinations. The table columns are as described for the previous table.

Again, a number of the relatively infrequent classes appear to have been reasonably accurately classified, but the overall classification showed little improvement at approximately 6%. Again, the most frequently occurring classes, such as the no biohabitat and bioturbated classes, had very low classification success and were incorrectly classified to other (off-diagonal) habitat class combinations (not tabulated in the abridged Table 3-23). Clearly, a much greater level of aggregation was required.

Table 3-22. Sub1_Hab2: Observed (Row Totals) counts and percentage contribution, Observed versus Predicted Diagonal counts and percentages.

| Sub1_Hab2 Description | Observed | | Observed vs Predicted | | |
|-----------------------------|---------------|------------|-----------------------|------------|----------|
| | Counts | % of total | Counts | % of total | % of Row |
| Reef : No BioHabitat | 140 | 0.10 | 4 | 0.00 | 2.86 |
| Reef : Sparse garden | 195 | 0.13 | 22 | 0.02 | 11.28 |
| Reef : Gorgonian | 94 | 0.06 | 10 | 0.01 | 10.64 |
| Reef : Sponge | 74 | 0.05 | 64 | 0.04 | 86.49 |
| Reef : Algae | 195 | 0.13 | 17 | 0.01 | 8.72 |
| Reef : Coral Dense | 891 | 0.61 | 125 | 0.09 | 14.03 |
| Boulders : No BioHabitat | 624 | 0.43 | 85 | 0.06 | 13.62 |
| Boulders : Sparse garden | 626 | 0.43 | 23 | 0.02 | 3.67 |
| Boulders : Gorgonian | 170 | 0.12 | 11 | 0.01 | 6.47 |
| Boulders : Sponge | 56 | 0.04 | 2 | 0.00 | 3.57 |
| Boulders : Algae | 218 | 0.15 | 55 | 0.04 | 25.23 |
| Boulders : Coral Sparse | 193 | 0.13 | 50 | 0.03 | 25.91 |
| Cobbles : No BioHabitat | 1007 | 0.69 | 201 | 0.14 | 19.96 |
| Cobbles : Sparse garden | 950 | 0.65 | 305 | 0.21 | 32.11 |
| Cobbles : Gorgonian | 92 | 0.06 | 28 | 0.02 | 30.43 |
| Cobbles : Algae | 323 | 0.22 | 23 | 0.02 | 7.12 |
| Gravel : No BioHabitat | 5834 | 3.98 | 3 | 0.00 | 0.05 |
| Gravel : Sparse garden | 2186 | 1.49 | 7 | 0.00 | 0.32 |
| Gravel : Gorgonian | 197 | 0.13 | 24 | 0.02 | 12.18 |
| Gravel : Sponge | 134 | 0.09 | 13 | 0.01 | 9.70 |
| Gravel : Algae | 2207 | 1.51 | 19 | 0.01 | 0.86 |
| Gravel : Caulerpa | 120 | 0.08 | 33 | 0.02 | 27.50 |
| Gravel : Halimeda | 216 | 0.15 | 13 | 0.01 | 6.02 |
| Gravel : Seagrass | 344 | 0.23 | 28 | 0.02 | 8.14 |
| Gravel : Bioturbated | 236 | 0.16 | 24 | 0.02 | 10.17 |
| Coarse Sand : No BioHabitat | 10567 | 7.21 | 0 | 0.00 | 0.00 |
| Coarse Sand : Sparse garden | 1214 | 0.83 | 2 | 0.00 | 0.16 |
| Coarse Sand : Alcyonarians | 1618 | 1.10 | 511 | 0.35 | 31.58 |
| Coarse Sand : Gorgonian | 198 | 0.14 | 4 | 0.00 | 2.02 |
| Coarse Sand : Algae | 2864 | 1.95 | 12 | 0.01 | 0.42 |
| Coarse Sand : Caulerpa | 226 | 0.15 | 73 | 0.05 | 32.30 |
| Coarse Sand : Halimeda | 2584 | 1.76 | 28 | 0.02 | 1.08 |
| Coarse Sand : Seagrass | 1579 | 1.08 | 16 | 0.01 | 1.01 |
| Coarse Sand : Bioturbated | 1643 | 1.12 | 28 | 0.02 | 1.70 |
| Fine Sand : No BioHabitat | 20055 | 13.69 | 2 | 0.00 | 0.01 |
| Fine Sand : Sparse garden | 1735 | 1.18 | 8 | 0.01 | 0.46 |
| Fine Sand : Alcyonarians | 394 | 0.27 | 207 | 0.14 | 52.54 |
| Fine Sand : Algae | 3719 | 2.54 | 117 | 0.08 | 3.15 |
| Fine Sand : Caulerpa | 500 | 0.34 | 1 | 0.00 | 0.20 |
| Fine Sand : Halimeda | 1613 | 1.10 | 54 | 0.04 | 3.35 |
| Fine Sand : Seagrass | 3802 | 2.59 | 62 | 0.04 | 1.63 |
| Fine Sand : Bioturbated | 10825 | 7.39 | 6 | 0.00 | 0.06 |
| Sand Waves : No BioHabitat | 4069 | 2.78 | 14 | 0.01 | 0.34 |
| Sand Waves : Sparse garden | 227 | 0.15 | 60 | 0.04 | 26.43 |
| Sand Waves : Gorgonian | 1021 | 0.70 | 283 | 0.19 | 27.72 |
| Sand Waves : Caulerpa | 108 | 0.07 | 50 | 0.03 | 46.30 |
| Silt : No BioHabitat | 15201 | 10.37 | 14 | 0.01 | 0.09 |
| Silt : Sparse garden | 1287 | 0.88 | 3 | 0.00 | 0.23 |
| Silt : Alcyonarians | 666 | 0.45 | 169 | 0.12 | 25.38 |
| Silt : Algae | 1011 | 0.69 | 31 | 0.02 | 3.07 |
| Silt : Caulerpa | 165 | 0.11 | 21 | 0.01 | 12.73 |
| Silt : Halimeda | 222 | 0.15 | 20 | 0.01 | 9.01 |
| Silt : Seagrass | 1456 | 0.99 | 297 | 0.20 | 20.40 |
| Silt : Bioturbated | 18398 | 12.56 | 299 | 0.20 | 1.63 |
| Mud : No BioHabitat | 8141 | 5.56 | 44 | 0.03 | 0.54 |
| Mud : Sparse garden | 1089 | 0.74 | 52 | 0.04 | 4.78 |
| Mud : Alcyonarians | 341 | 0.23 | 265 | 0.18 | 77.71 |
| Mud : Sponge | 118 | 0.08 | 115 | 0.08 | 97.46 |
| Mud : Seagrass | 480 | 0.33 | 81 | 0.06 | 16.88 |
| Mud : Bioturbated | 8689 | 5.93 | 374 | 0.26 | 4.30 |
| Total | 146533 | | | 3.4 | |

Table 3-23. Sub2_Hab2: Observed (Row Totals) counts and percentage contribution, Observed verse Predicted Diagonal counts and percentages.

| Sub2_Hab2 Description | Observed | | Observed vs. Predicted | | |
|--------------------------|---------------|------------|------------------------|-------------|----------|
| | Counts | % of total | Counts | % of total | % of Row |
| Reef : No BioHabitat | 140 | 0.10 | 51 | 0.03 | 36.4 |
| Reef : Sparse garden | 194 | 0.13 | 39 | 0.03 | 20.1 |
| Reef : Gorgonian | 94 | 0.06 | 50 | 0.03 | 53.2 |
| Reef : Sponge | 74 | 0.05 | 44 | 0.03 | 59.5 |
| Reef : Algae | 193 | 0.13 | 61 | 0.04 | 31.6 |
| Reef : Coral Dense | 887 | 0.61 | 56 | 0.04 | 6.3 |
| Reef : Coral Sparse | 80 | 0.05 | 43 | 0.03 | 53.8 |
| Boulders : No BioHabitat | 621 | 0.43 | 125 | 0.09 | 20.1 |
| Boulders : Sparse garden | 621 | 0.43 | 54 | 0.04 | 8.7 |
| Boulders : Gorgonian | 170 | 0.12 | 61 | 0.04 | 35.9 |
| Boulders : Sponge | 56 | 0.04 | 35 | 0.02 | 62.5 |
| Boulders : Algae | 218 | 0.15 | 34 | 0.02 | 15.6 |
| Boulders : Coral Dense | 96 | 0.07 | 56 | 0.04 | 58.3 |
| Boulders : Coral Sparse | 193 | 0.13 | 36 | 0.02 | 18.7 |
| Cobbles : No BioHabitat | 1005 | 0.69 | 87 | 0.06 | 8.7 |
| Cobbles : Sparse garden | 940 | 0.64 | 219 | 0.15 | 23.3 |
| Cobbles : Gorgonian | 92 | 0.06 | 39 | 0.03 | 42.4 |
| Cobbles : Algae | 321 | 0.22 | 70 | 0.05 | 21.8 |
| Gravel : No BioHabitat | 5813 | 3.98 | 218 | 0.15 | 3.8 |
| Gravel : Sparse garden | 2176 | 1.49 | 22 | 0.02 | 1.0 |
| Gravel : Gorgonian | 195 | 0.13 | 41 | 0.03 | 21.0 |
| Gravel : Sponge | 134 | 0.09 | 39 | 0.03 | 29.1 |
| Gravel : Algae | 2201 | 1.51 | 274 | 0.19 | 12.4 |
| Gravel : Caulerpa | 120 | 0.08 | 64 | 0.04 | 53.3 |
| Gravel : Halimeda | 216 | 0.15 | 62 | 0.04 | 28.7 |
| Gravel : Sea grass | 343 | 0.24 | 145 | 0.10 | 42.3 |
| Gravel : Bioturbated | 232 | 0.16 | 58 | 0.04 | 25.0 |
| Sand : No BioHabitat | 34543 | 23.68 | 452 | 0.31 | 1.3 |
| Sand : Sparse garden | 3165 | 2.17 | 36 | 0.02 | 1.1 |
| Sand : Alcyonarians | 2003 | 1.37 | 186 | 0.13 | 9.3 |
| Sand : Gorgonian | 1293 | 0.89 | 184 | 0.13 | 14.2 |
| Sand : Sponge | 76 | 0.05 | 39 | 0.03 | 51.3 |
| Sand : Algae | 6595 | 4.52 | 245 | 0.17 | 3.7 |
| Sand : Caulerpa | 829 | 0.57 | 98 | 0.07 | 11.8 |
| Sand : Halimeda | 4168 | 2.86 | 130 | 0.09 | 3.1 |
| Sand : Sea grass | 5368 | 3.68 | 243 | 0.17 | 4.5 |
| Sand : Bioturbated | 12408 | 8.51 | 250 | 0.17 | 2.0 |
| Silt : No BioHabitat | 15137 | 10.38 | 203 | 0.14 | 1.3 |
| Silt : Sparse garden | 1279 | 0.88 | 59 | 0.04 | 4.6 |
| Silt : Alcyonarians | 658 | 0.45 | 181 | 0.12 | 27.5 |
| Silt : Gorgonian | 70 | 0.05 | 45 | 0.03 | 64.3 |
| Silt : Sponge | 62 | 0.04 | 35 | 0.02 | 56.5 |
| Silt : Algae | 1005 | 0.69 | 87 | 0.06 | 8.7 |
| Silt : Caulerpa | 165 | 0.11 | 99 | 0.07 | 60.0 |
| Silt : Halimeda | 219 | 0.15 | 84 | 0.06 | 38.4 |
| Silt : Sea grass | 1447 | 0.99 | 263 | 0.18 | 18.2 |
| Silt : Bioturbated | 18339 | 12.57 | 880 | 0.60 | 4.8 |
| Mud : No BioHabitat | 8109 | 5.56 | 336 | 0.23 | 4.1 |
| Mud : Sparse garden | 1086 | 0.74 | 138 | 0.09 | 12.7 |
| Mud : Alcyonarians | 340 | 0.23 | 184 | 0.13 | 54.1 |
| Mud : Sponge | 118 | 0.08 | 105 | 0.07 | 89.0 |
| Mud : Algae | 90 | 0.06 | 59 | 0.04 | 65.6 |
| Mud : Sea grass | 475 | 0.33 | 151 | 0.10 | 31.8 |
| Mud : Bioturbated | 8674 | 5.95 | 1420 | 0.97 | 16.4 |
| TOTAL | 145886 | | | 6.02 | |

3.6.3.3. BioHabitat v2

The re-coding of habitat events from the original 26 class biohabitat code to the reduced 12 class set (Habitat_Code2, Table 2-10) was at least partly based on taxonomy. Due to the much smaller number of classes, it is possible to present here the confusion matrix, which is the cross-tabulation of the observed versus LDA classified results (Table 3-24). The diagonal of this matrix (left to right down the page) reports the observations that were correctly classified by the LDA. The row totals (far right column) show the total number of observations in each habitat class. The column totals (bottom row) show the total number of cases that were classified to each habitat class by LDA. The grand total (bottom right cell) shows the total number of observations that were classified. The other cells (off-diagonals) report the misclassification or confusion.

The next matrix (Table 3-25) is similar except that the numbers are shown as percentages of the row totals from Table 3-24. The diagonal now shows the relative classification success for each biohabitat class. A number of the biohabitat classes appear to have good classification performance; however, as was the case for the combinations examined above, these are the relatively infrequent types and performance is poor for the common seabed class types, such as No BioHabitat and Bioturbated, which tend to get classified as seagrass or algae or various types of epibenthos.

Table 3-24. Habitat_Code2: Confusion matrix of total counts observed vs. predicted

| Observed | Predicted | | | | | | | | | | | | Total | |
|---------------|-----------|-------|-------|-------|-------|------|-------|------|-------|-------|-------|-------|-------|--------|
| | 0 | 1 | 2 | 3 | 4 | 5 | 6 | 7 | 8 | 9 | 10 | 11 | | |
| No BioHabitat | 0 | 10259 | 5884 | 6290 | 7011 | 2837 | 5395 | 4140 | 6052 | 7615 | 5452 | 3506 | 1166 | 65607 |
| Sparse garden | 1 | 484 | 2809 | 872 | 1200 | 466 | 487 | 540 | 545 | 876 | 365 | 641 | 222 | 9507 |
| Alcyonarians | 2 | | 9 | 2402 | 50 | 48 | | 339 | 91 | 24 | | 130 | 30 | 3123 |
| Gorgonian | 3 | | 1 | 32 | 1567 | 132 | 6 | 72 | 6 | 1 | | 38 | 61 | 1916 |
| Sponge | 4 | | | | 5 | 528 | | | | | | | 21 | 554 |
| Algae | 5 | 395 | 638 | 579 | 1113 | 397 | 3632 | 503 | 727 | 963 | 360 | 1048 | 312 | 10667 |
| Caulerpa | 6 | | | 23 | 31 | 34 | | 1015 | | 1 | | 33 | 13 | 1150 |
| Halimeda | 7 | | 174 | 694 | 281 | 129 | 117 | 523 | 2256 | 219 | 14 | 268 | 91 | 4766 |
| Seagrass | 8 | 105 | 292 | 535 | 569 | 217 | 421 | 573 | 422 | 3534 | 236 | 622 | 124 | 7650 |
| Bioturbated | 9 | 1901 | 2156 | 4084 | 2743 | 956 | 2665 | 2252 | 4127 | 4426 | 10991 | 2904 | 674 | 39879 |
| Coral Dense | 10 | | | 6 | 20 | 24 | | 4 | | | | 1043 | 35 | 1132 |
| Coral Sparse | 11 | | | | | 4 | | | | | | | 482 | 486 |
| Total | | 13144 | 11963 | 15517 | 14590 | 5772 | 12723 | 9961 | 14226 | 17659 | 17418 | 10233 | 3231 | 146437 |

Table 3-25. Habitat_Code2: Confusion matrix of percentage contribution as a percentage of row totals

| Observed | Predicted | | | | | | | | | | | | Total | |
|---------------|-----------|------|------|------|------|------|------|------|------|------|------|------|-------|-----|
| | 0 | 1 | 2 | 3 | 4 | 5 | 6 | 7 | 8 | 9 | 10 | 11 | | |
| No BioHabitat | 0 | 15.6 | 9.0 | 9.6 | 10.7 | 4.3 | 8.2 | 6.3 | 9.2 | 11.6 | 8.3 | 5.3 | 1.8 | 100 |
| Sparse garden | 1 | 5.1 | 29.5 | 9.2 | 12.6 | 4.9 | 5.1 | 5.7 | 5.7 | 9.2 | 3.8 | 6.7 | 2.3 | 100 |
| Alcyonarians | 2 | | 0.3 | 76.9 | 1.6 | 1.5 | | 10.9 | 2.9 | 0.8 | | 4.2 | 1.0 | 100 |
| Gorgonian | 3 | | 0.1 | 1.7 | 81.8 | 6.9 | 0.3 | 3.8 | 0.3 | 0.1 | | 2.0 | 3.2 | 100 |
| Sponge | 4 | | | | 0.9 | 95.3 | | | | | | | 3.8 | 100 |
| Algae | 5 | 3.7 | 6.0 | 5.4 | 10.4 | 3.7 | 34.0 | 4.7 | 6.8 | 9.0 | 3.4 | 9.8 | 2.9 | 100 |
| Caulerpa | 6 | | | 2.0 | 2.7 | 3.0 | | 88.3 | | 0.1 | | 2.9 | 1.1 | 100 |
| Halimeda | 7 | | 3.7 | 14.6 | 5.9 | 2.7 | 2.5 | 11.0 | 47.3 | 4.6 | 0.3 | 5.6 | 1.9 | 100 |
| Seagrass | 8 | 1.4 | 3.8 | 7.0 | 7.4 | 2.8 | 5.5 | 7.5 | 5.5 | 46.2 | 3.1 | 8.1 | 1.6 | 100 |
| Bioturbated | 9 | 4.8 | 5.4 | 10.2 | 6.9 | 2.4 | 6.7 | 5.6 | 10.3 | 11.1 | 27.6 | 7.3 | 1.7 | 100 |
| Coral Dense | 10 | | | 0.5 | 1.8 | 2.1 | | 0.4 | | | | 92.1 | 3.1 | 100 |
| Coral Sparse | 11 | | | | | 0.8 | | | | | | | 99.2 | 100 |

The third matrix (Table 3-26) shows the classification results as percentages of the total number of observations. A comparison of the row and column total percentages, in particular, highlight the overall confusion — those biohabitats that were infrequent in the original observations are far too frequent in the classified results (by up to 10 times). In the case of seagrass, for example, the observed frequency was 5.2% whereas the classified frequency was 12.1% — clearly a large number of No biohabitat and bioturbated Observations were being classified as Seagrass. Conversely, those Habitats that were very frequent in the original observations are far too infrequent in the classified results. For example, the observed frequency of bioturbated was 27.2% whereas the classified frequency was 11.9% — clearly a large number of bioturbated observations were being classified as other types of biohabitats. The overall classification success was only 27.7%.

Table 3-26. Habitat_Code2: Confusion matrix of percentage contribution as a percentage of totals

| Observed | Predicted | | | | | | | | | | | Total | | |
|---------------|-----------|------|------|------|------|------|------|------|------|------|------|-------|------|------|
| | 0 | 1 | 2 | 3 | 4 | 5 | 6 | 7 | 8 | 9 | 10 | | 11 | |
| No biohabitat | 0 | 7.01 | 4.02 | 4.30 | 4.79 | 1.94 | 3.68 | 2.83 | 4.13 | 5.20 | 3.72 | 2.39 | 0.80 | 44.8 |
| Sparse garden | 1 | 0.33 | 1.92 | 0.60 | 0.82 | 0.32 | 0.33 | 0.37 | 0.37 | 0.60 | 0.25 | 0.44 | 0.15 | 6.5 |
| Alcyonarians | 2 | | 0.01 | 1.64 | 0.03 | 0.03 | | 0.23 | 0.06 | 0.02 | | 0.09 | 0.02 | 2.1 |
| Gorgonian | 3 | | 0.00 | 0.02 | 1.07 | 0.09 | 0.00 | 0.05 | 0.00 | 0.00 | | 0.03 | 0.04 | 1.3 |
| Sponge | 4 | | | | 0.00 | 0.36 | | | | | | | 0.01 | 0.4 |
| Algae | 5 | 0.27 | 0.44 | 0.40 | 0.76 | 0.27 | 2.48 | 0.34 | 0.50 | 0.66 | 0.25 | 0.72 | 0.21 | 7.3 |
| Caulerpa | 6 | | | 0.02 | 0.02 | 0.02 | | 0.69 | | 0.00 | | 0.02 | 0.01 | 0.8 |
| Halimeda | 7 | | 0.12 | 0.47 | 0.19 | 0.09 | 0.08 | 0.36 | 1.54 | 0.15 | 0.01 | 0.18 | 0.06 | 3.3 |
| Seagrass | 8 | 0.07 | 0.20 | 0.37 | 0.39 | 0.15 | 0.29 | 0.39 | 0.29 | 2.41 | 0.16 | 0.42 | 0.08 | 5.2 |
| Bioturbated | 9 | 1.30 | 1.47 | 2.79 | 1.87 | 0.65 | 1.82 | 1.54 | 2.82 | 3.02 | 7.51 | 1.98 | 0.46 | 27.2 |
| Coral Dense | 10 | | | 0.00 | 0.01 | 0.02 | | 0.00 | | | | 0.71 | 0.02 | 0.8 |
| Coral Sparse | 11 | | | | | 0.00 | | | | | | | 0.33 | 0.3 |
| Total | | 9.0 | 8.2 | 10.6 | 10.0 | 3.9 | 8.7 | 6.8 | 9.7 | 12.1 | 11.9 | 7.0 | 2.2 | 27.7 |

3.6.3.4. Biohabitat v3

An alternative, and more severe, aggregation of the original habitat event codes reduced the number of habitat classes to eight by lumping all epibenthos by density and all marine plants (Table 2-11). Very sparse epibenthos was considered to differ little from “No biohabitat”.

Again, cross-tabulations of observed versus classified results are presented as a series of confusion matrices. Table 3-27 shows the counts, Table 3-28 shows the percentages of row total observations and Table 3-29 shows the percentages of the total observations.

Table 3-27. Habitat_Code3: Confusion matrix of total counts observed vs. predicted

| Observed | Predicted | | | | | | | Total | | |
|--------------------|-----------|-------|------|-------|-------|-------|-------|-------|------|--------|
| | 0 | 1 | 2 | 3 | 4 | 5 | 6 | | 7 | |
| No biohabitat | 0 | 15716 | 1631 | 10763 | 16027 | 9282 | 10795 | 2454 | 769 | 67437 |
| Soft – Dense | 1 | | 444 | | | | | | 1 | 445 |
| Soft – Medium | 2 | | 143 | 4347 | 157 | 1 | | 146 | 60 | 4854 |
| Soft – Sparse | 3 | | 221 | 994 | 6046 | 130 | 72 | 357 | 110 | 7930 |
| Algae and Seagrass | 4 | 1657 | 461 | 3610 | 4470 | 9831 | 2545 | 1380 | 326 | 24280 |
| Bioturbated | 5 | 2251 | 574 | 5363 | 6516 | 4526 | 18288 | 2030 | 421 | 39969 |
| Coral – Dense | 6 | | 14 | | | | | 1094 | 24 | 1132 |
| Coral – Sparse | 7 | | 21 | | | | | | 465 | 486 |
| Total | | 19624 | 3509 | 25077 | 33216 | 23770 | 31700 | 7461 | 2176 | 146533 |

Again, the less frequent biohabitat types appeared to have been reasonably well classified whereas the more frequent types were poorly classified. For example, unaccepted proportions of No BioHabitat and Bioturbated were classified as epibenthos or Seagrass. The overall classification success was somewhat improved with fewer classes, at 38.4%.

Table 3-28. Habitat_Code3: Confusion matrix of percentage contribution as a percentage of row totals

| Observed | | Predicted | | | | | | | | Total |
|--------------------|---|-----------|------|------|------|------|------|------|------|-------|
| | | 0 | 1 | 2 | 3 | 4 | 5 | 6 | 7 | |
| No BioHabitat | 0 | 23.3 | 2.4 | 16.0 | 23.8 | 13.8 | 16.0 | 3.6 | 1.1 | 100 |
| Soft – Dense | 1 | | 99.8 | | | | | | 0.2 | 100 |
| Soft – Medium | 2 | | 2.9 | 89.6 | 3.2 | 0.0 | | 3.0 | 1.2 | 100 |
| Soft – Sparse | 3 | | 2.8 | 12.5 | 76.2 | 1.6 | 0.9 | 4.5 | 1.4 | 100 |
| Algae and Seagrass | 4 | 6.8 | 1.9 | 14.9 | 18.4 | 40.5 | 10.5 | 5.7 | 1.3 | 100 |
| Bioturbated | 5 | 5.6 | 1.4 | 13.4 | 16.3 | 11.3 | 45.8 | 5.1 | 1.1 | 100 |
| Coral - Dense | 6 | | 1.2 | | | | | 96.6 | 2.1 | 100 |
| Coral – Sparse | 7 | | 4.3 | | | | | | 95.7 | 100 |

Table 3-29. Habitat_Code3: Confusion matrix of percentage contribution as a percentage of totals

| Observed | | Predicted | | | | | | | | Total |
|--------------------|---|-----------|------|-------|-------|-------|-------|------|------|-------|
| | | 0 | 1 | 2 | 3 | 4 | 5 | 6 | 7 | |
| No BioHabitat | 0 | 10.73 | 1.11 | 7.35 | 10.94 | 6.33 | 7.37 | 1.67 | 0.52 | 46.02 |
| Soft – Dense | 1 | | 0.30 | | | | | | 0.00 | 0.30 |
| Soft – Medium | 2 | | 0.10 | 2.97 | 0.11 | 0.00 | | 0.10 | 0.04 | 3.31 |
| Soft – Sparse | 3 | | 0.15 | 0.68 | 4.13 | 0.09 | 0.05 | 0.24 | 0.08 | 5.41 |
| Algae and Seagrass | 4 | 1.13 | 0.31 | 2.46 | 3.05 | 6.71 | 1.74 | 0.94 | 0.22 | 16.57 |
| Bioturbated | 5 | 1.54 | 0.39 | 3.66 | 4.45 | 3.09 | 12.48 | 1.39 | 0.29 | 27.28 |
| Coral - Dense | 6 | | 0.01 | | | | | 0.75 | 0.02 | 0.77 |
| Coral – Sparse | 7 | | 0.01 | | | | | | 0.32 | 0.33 |
| Total | | 13.39 | 2.39 | 17.11 | 22.67 | 16.22 | 21.63 | 5.09 | 1.48 | 38.4 |

3.6.3.5. Substratum v1

The first analysis of substratum alone attempted to classify the original 9 sediment substratum event classes (Table 2-6) at the observed sites. As above, cross-tabulations of observed versus classified results are presented as a series of confusion matrices. Table 3-30 shows the counts, Table 3-31 shows the percentages of row total observations and Table 3-32 shows the percentages of the total observations.

Results similar to those for biohabitat types were obtained, in that the less frequent substratum types appeared to have been reasonably well classified whereas the more frequent types were poorly classified. The best result was ~99% success in predicting reef where it was observed; the residual 1% was spread over less-rough substrata and sand waves. However, Reef was only a very small component of the dataset (<1.2%), so in reality the high accuracy of the classification Reef is lost amid the mass of smooth or soft sediments — and incorrectly classified sands and silt inflates the predicted reef by more than 5-fold. The smooth and soft sediments displayed high levels of confusion with, for example, observed sand being classified correctly only 25% of the time and incorrectly being labelled in significant proportions in all other classes. Further, sand was observed 29% of the time but was predicted correctly only 7.5% the time.

Overall, the rough substratum types had >80% classification success whereas the more common smoother substratum types had <30% classification success and unacceptable proportions of smoother classes were classified as rougher classes. The overall classification success was 36.6%, that is, in ~37% of cases the classified result matched the observed, whereas in 63% of cases the classified result did not match the observed (i.e. the classification was confused).

Table 3-30. Substratum_Code1: Confusion matrix of total counts observed vs. predicted

| Observed | | Predicted | | | | | | | | | Total |
|-------------|---|-----------|-------|-------|-------|-------|-------|-------|-------|-------|--------|
| | | 1 | 2 | 3 | 4 | 5 | 6 | 7 | 8 | 9 | |
| Reef | 1 | 1682 | 6 | 11 | | | | 3 | | | 1702 |
| Rocks | 2 | 193 | 1904 | 44 | 1 | | | 53 | | | 2195 |
| Stones | 3 | 146 | 171 | 2141 | 8 | | | 53 | | | 2519 |
| Rubble | 4 | 983 | 1012 | 1265 | 3907 | 641 | 494 | 2361 | 408 | 516 | 11587 |
| Coarse Sand | 5 | 1781 | 1699 | 1525 | 1655 | 5842 | 1475 | 4434 | 1548 | 2614 | 22573 |
| Sand | 6 | 3640 | 3047 | 2954 | 2955 | 3059 | 10926 | 7014 | 3286 | 5942 | 42823 |
| Sand Waves | 7 | 196 | 348 | 385 | 110 | 47 | 4 | 4356 | 23 | 103 | 5572 |
| Silt | 8 | 2424 | 2470 | 2186 | 1877 | 2543 | 2794 | 6617 | 10390 | 7256 | 38557 |
| Mud | 9 | 967 | 763 | 460 | 358 | 591 | 810 | 1786 | 731 | 12539 | 19005 |
| Total | | 12012 | 11420 | 10971 | 10871 | 12723 | 16503 | 26677 | 16386 | 28970 | 146533 |

Table 3-31. Substratum_Code1: Confusion matrix of percentage contribution as a percentage of row totals

| Observed | | Predicted | | | | | | | | | Total |
|-------------|---|-----------|------|------|------|------|------|------|------|------|-------|
| | | 1 | 2 | 3 | 4 | 5 | 6 | 7 | 8 | 9 | |
| Reef | 1 | 98.8 | 0.4 | 0.6 | | | | 0.2 | | | 100 |
| Rocks | 2 | 8.8 | 86.7 | 2.0 | 0.0 | | | 2.4 | | | 100 |
| Stones | 3 | 5.8 | 6.8 | 85.0 | 0.3 | | | 2.1 | | | 100 |
| Rubble | 4 | 8.5 | 8.7 | 10.9 | 33.7 | 5.5 | 4.3 | 20.4 | 3.5 | 4.5 | 100 |
| Coarse Sand | 5 | 7.9 | 7.5 | 6.8 | 7.3 | 25.9 | 6.5 | 19.6 | 6.9 | 11.6 | 100 |
| Sand | 6 | 8.5 | 7.1 | 6.9 | 6.9 | 7.1 | 25.5 | 16.4 | 7.7 | 13.9 | 100 |
| Sand Waves | 7 | 3.5 | 6.2 | 6.9 | 2.0 | 0.8 | 0.1 | 78.2 | 0.4 | 1.8 | 100 |
| Silt | 8 | 6.3 | 6.4 | 5.7 | 4.9 | 6.6 | 7.2 | 17.2 | 26.9 | 18.8 | 100 |
| Mud | 9 | 5.1 | 4.0 | 2.4 | 1.9 | 3.1 | 4.3 | 9.4 | 3.8 | 66.0 | 100 |

Table 3-32. Substratum_Code1: Confusion matrix of percentage contribution as a percentage of totals

| Observed | | Predicted | | | | | | | | | Total |
|-------------|---|-----------|------|------|------|------|-------|-------|-------|-------|-------|
| | | 1 | 2 | 3 | 4 | 5 | 6 | 7 | 8 | 9 | |
| Reef | 1 | 1.15 | 0.00 | 0.01 | | | | 0.00 | | | 1.16 |
| Rocks | 2 | 0.13 | 1.30 | 0.03 | 0.00 | | | 0.04 | | | 1.50 |
| Stones | 3 | 0.10 | 0.12 | 1.46 | 0.01 | | | 0.04 | | | 1.72 |
| Rubble | 4 | 0.67 | 0.69 | 0.86 | 2.67 | 0.44 | 0.34 | 1.61 | 0.28 | 0.35 | 7.91 |
| Coarse Sand | 5 | 1.22 | 1.16 | 1.04 | 1.13 | 3.99 | 1.01 | 3.03 | 1.06 | 1.78 | 15.40 |
| Sand | 6 | 2.48 | 2.08 | 2.02 | 2.02 | 2.09 | 7.46 | 4.79 | 2.24 | 4.06 | 29.22 |
| Sand Waves | 7 | 0.13 | 0.24 | 0.26 | 0.08 | 0.03 | 0.00 | 2.97 | 0.02 | 0.07 | 3.80 |
| Silt | 8 | 1.65 | 1.69 | 1.49 | 1.28 | 1.74 | 1.91 | 4.52 | 7.09 | 4.95 | 26.31 |
| Mud | 9 | 0.66 | 0.52 | 0.31 | 0.24 | 0.40 | 0.55 | 1.22 | 0.50 | 8.56 | 12.97 |
| Total | | 8.20 | 7.79 | 7.49 | 7.42 | 8.68 | 11.26 | 18.21 | 11.18 | 19.77 | 36.6 |

3.6.3.6. *Substratum v2*

In the previous analysis, there was considerable confusion among the several classes of sand, causing poor overall performance. Consequently, the three separate classes of sand were aggregated into a single class “Sand”. This yielded seven classes, with separate classes for gravel, silt and mud (Table 2-12).

Again, cross-tabulations of observed versus classified results are presented as a series of confusion matrices. Table 3-33 shows the counts, Table 3-34 shows the percentages of row total observations and Table 3-35 shows the percentages of the total observations.

The sands were correctly classified in 30.4% of cases, but large proportions of observed sand were misclassified into gravel, silt or mud substratum classes. Observed Silt was also classified into anything from Gravel to Mud. Again, the more frequent observed classes (Sand 48.4% and Silt 26.3%) had the poorest classification success and were markedly under-classified in the results (18.2% and 18.8% respectively). On the other hand, while the less frequently observed classes appeared to have good classification success (75% to 99%), they were seriously over-classified in the results — erroneously indicating a much higher occurrence of harder/rougher substratum types than was observed. Overall classification success was ~45%.

Table 3-33. Substratum_Code2: Confusion matrix of total counts observed vs. predicted

| Observed | | Predicted | | | | | | | Total |
|----------|---|-----------|------|------|-------|-------|-------|-------|--------|
| | | 1 | 2 | 3 | 4 | 5 | 6 | 7 | |
| Reef | 1 | 1690 | 4 | 8 | | | | | 1702 |
| Boulders | 2 | 158 | 2006 | 31 | | | | | 2195 |
| Cobbles | 3 | 109 | 149 | 2260 | 1 | | | | 2519 |
| Gravel | 4 | 766 | 828 | 1090 | 7923 | | 390 | 590 | 11587 |
| Sand | 5 | 4374 | 4215 | 4139 | 16540 | 21543 | 9721 | 10436 | 70968 |
| Silt | 6 | 1850 | 2003 | 1805 | 5156 | 4015 | 16353 | 7375 | 38557 |
| Mud | 7 | 752 | 601 | 377 | 818 | 1126 | 1101 | 14230 | 19005 |
| Total | | 9699 | 9806 | 9710 | 30438 | 26684 | 27565 | 32631 | 146533 |

Table 3-34. Substratum_Code2: Confusion matrix of percentage contribution as a percentage of row totals

| Observed | | Predicted | | | | | | | Total |
|----------|---|-----------|------|------|------|------|------|------|-------|
| | | 1 | 2 | 3 | 4 | 5 | 6 | 7 | |
| Reef | 1 | 99.3 | 0.2 | 0.5 | | | | | 100 |
| Boulders | 2 | 7.2 | 91.4 | 1.4 | | | | | 100 |
| Cobbles | 3 | 4.3 | 5.9 | 89.7 | 0.0 | | | | 100 |
| Gravel | 4 | 6.6 | 7.1 | 9.4 | 68.4 | | 3.4 | 5.1 | 100 |
| Sand | 5 | 6.2 | 5.9 | 5.8 | 23.3 | 30.4 | 13.7 | 14.7 | 100 |
| Silt | 6 | 4.8 | 5.2 | 4.7 | 13.4 | 10.4 | 42.4 | 19.1 | 100 |
| Mud | 7 | 4.0 | 3.2 | 2.0 | 4.3 | 5.9 | 5.8 | 74.9 | 100 |

Table 3-35. Substratum_Code2: Confusion matrix of percentage contribution as a percentage of totals

| Observed | | Predicted | | | | | | | Total |
|----------|---|-----------|------|------|-------|-------|-------|-------|-------|
| | | 1 | 2 | 3 | 4 | 5 | 6 | 7 | |
| Reef | 1 | 1.15 | 0.00 | 0.01 | | | | | 1.16 |
| Boulders | 2 | 0.11 | 1.37 | 0.02 | | | | | 1.50 |
| Cobbles | 3 | 0.07 | 0.10 | 1.54 | 0.00 | | | | 1.72 |
| Gravel | 4 | 0.52 | 0.57 | 0.74 | 5.41 | | 0.27 | 0.40 | 7.91 |
| Sand | 5 | 2.98 | 2.88 | 2.82 | 11.29 | 14.70 | 6.63 | 7.12 | 48.43 |
| Silt | 6 | 1.26 | 1.37 | 1.23 | 3.52 | 2.74 | 11.16 | 5.03 | 26.31 |
| Mud | 7 | 0.51 | 0.41 | 0.26 | 0.56 | 0.77 | 0.75 | 9.71 | 12.97 |
| Total | | 6.62 | 6.69 | 6.63 | 20.77 | 18.21 | 18.81 | 22.27 | 45.04 |

3.6.3.7. Substratum v3

In the ‘Substratum v1’ analysis, the sand waves class had reasonable classification success, so as an alternative aggregation, “Sand Waves” were retained as a separate class but coarse sand, fine sand and silt were aggregated in a third substratum-only recoding schema (Table 2-13) of seven classes. Again, cross-tabulations of observed versus classified results are presented as a series of confusion matrices. Table 3-36 shows the counts, Table 3-37 shows the percentages of row total observations and Table 3-38 shows the percentages of the total observations.

In this aggregation, the Sand-Silt class represented about 71% of the observations and the classification success for this class remained a rather poor 35.5%, as well as being grossly under-represented in the classification results due large number of observations being classified as other substrata. Given the values of the diagonals, the other observed classes appeared to have much greater classification success and the overall classification success was 45.8%. However, as before, these classes were seriously over-classified in the results — erroneously indicating a much higher occurrence of harder/rougher or muddy substratum types than was observed.

Table 3-36. Substratum_Code3: Confusion matrix of total counts observed vs. predicted

| Observed | Predicted | | | | | | | Total | |
|------------|-----------|------|------|------|-------|-------|-------|-------|--------|
| | 1 | 2 | 3 | 4 | 5 | 6 | 7 | | |
| Reef | 1 | 1689 | 4 | 8 | | | | 1 | 1702 |
| Boulders | 2 | 158 | 1979 | 31 | | | | 27 | 2195 |
| Cobbles | 3 | 109 | 148 | 2235 | 1 | | | 26 | 2519 |
| Gravel | 4 | 767 | 817 | 1075 | 6108 | | 495 | 2325 | 11587 |
| Sand Silt | 5 | 6059 | 5757 | 5467 | 16789 | 37181 | 15946 | 16754 | 103953 |
| Mud | 6 | 752 | 603 | 375 | 702 | 1595 | 13287 | 1691 | 19005 |
| Sand Waves | 7 | 159 | 325 | 353 | 74 | | 58 | 4603 | 5572 |
| Total | | 9693 | 9633 | 9544 | 23674 | 38776 | 29786 | 25427 | 146533 |

Table 3-37. Substratum_Code3: Confusion matrix of percentage contribution as a percentage of row totals

| Observed | Predicted | | | | | | | Total | |
|------------|-----------|------|------|------|------|------|------|-------|-----|
| | 1 | 2 | 3 | 4 | 5 | 6 | 7 | | |
| Reef | 1 | 99.2 | 0.2 | 0.5 | | | | 0.1 | 100 |
| Boulders | 2 | 7.2 | 90.2 | 1.4 | | | | 1.2 | 100 |
| Cobbles | 3 | 4.3 | 5.9 | 88.7 | 0.0 | | | 1.0 | 100 |
| Gravel | 4 | 6.6 | 7.1 | 9.3 | 52.7 | | 4.3 | 20.1 | 100 |
| Sand Silt | 5 | 5.8 | 5.5 | 5.3 | 16.2 | 35.8 | 15.3 | 16.1 | 100 |
| Mud | 6 | 4.0 | 3.2 | 2.0 | 3.7 | 8.4 | 69.9 | 8.9 | 100 |
| Sand Waves | 7 | 2.9 | 5.8 | 6.3 | 1.3 | | 1.0 | 82.6 | 100 |

Table 3-38. Substratum_Code3: Confusion matrix of percentage contribution as a percentage of total

| Observed | Predicted | | | | | | | Total | |
|------------|-----------|------|------|------|-------|-------|-------|-------|-------|
| | 1 | 2 | 3 | 4 | 5 | 6 | 7 | | |
| Reef | 1 | 1.15 | 0.00 | 0.01 | | | | 0.00 | 1.16 |
| Boulders | 2 | 0.11 | 1.35 | 0.02 | | | | 0.02 | 1.50 |
| Cobbles | 3 | 0.07 | 0.10 | 1.53 | 0.00 | | | 0.02 | 1.72 |
| Gravel | 4 | 0.52 | 0.56 | 0.73 | 4.17 | | 0.34 | 1.59 | 7.91 |
| Sand Silt | 5 | 4.13 | 3.93 | 3.73 | 11.46 | 25.37 | 10.88 | 11.43 | 70.94 |
| Mud | 6 | 0.51 | 0.41 | 0.26 | 0.48 | 1.09 | 9.07 | 1.15 | 12.97 |
| Sand Waves | 7 | 0.11 | 0.22 | 0.24 | 0.05 | | 0.04 | 3.14 | 3.80 |
| Total | | 6.61 | 6.57 | 6.51 | 16.16 | 26.46 | 20.33 | 17.35 | 45.78 |

3.6.3.8. Substratum v3 with depth partitioning

The raw acoustics data was observed to have a substantial depth dependency (Sections 3.6.1, 3.6.2), and though the QTC View has a patented proprietary algorithm intended to compensate for the depth effect, most of the 166 QTC features had a positive or negative correlation (r) with depth of 0.2–0.5 — thus, the QTC data also had a strong depth dependency. Consequently, the data was partitioned into six depth classes, 5-10 m, 10-15 m, 15-20 m, 20-30 m, 30-40 m, and 40-60 m, for separate training and classification analyses of the third substratum recoding schema (Table 2-13) of seven classes. As above, cross-tabulations of observed versus classified results are presented as a series of confusion matrices. Table 3-39 shows the counts, Table 3-40 shows the percentages of row total observations and Table 3-41 shows the percentages of the total observations.

Table 3-39. Substratum_Code3 Depth Partitioned: Confusion matrix of total counts observed vs. predicted

| Observed | Predicted | | | | | | | Total | |
|------------|-----------|------|------|------|-------|-------|-------|-------|--------|
| | 1 | 2 | 3 | 4 | 5 | 6 | 7 | | |
| Reef | 1 | 1595 | 60 | 15 | | | | 2 | 1672 |
| Boulders | 2 | 62 | 1995 | 12 | | | 2 | 24 | 2095 |
| Cobbles | 3 | 55 | 139 | 1964 | 28 | | 4 | 172 | 2362 |
| Gravel | 4 | 706 | 930 | 914 | 6376 | 341 | 293 | 1690 | 11250 |
| Sand Silt | 5 | 5257 | 5477 | 4613 | 15298 | 40207 | 13549 | 14743 | 99144 |
| Mud | 6 | 667 | 607 | 317 | 1320 | 1758 | 12685 | 1585 | 18939 |
| Sand Waves | 7 | 150 | 360 | 212 | 144 | | 37 | 4667 | 5570 |
| Total | | 8492 | 9568 | 8047 | 23166 | 42306 | 26570 | 22883 | 141032 |

Table 3-40. Substratum_Code3 Depth Partitioned: Confusion matrix of contribution as a percentage of rows

| Observed | Predicted | | | | | | | Total | |
|------------|-----------|------|------|------|------|------|------|-------|-----|
| | 1 | 2 | 3 | 4 | 5 | 6 | 7 | | |
| Reef | 1 | 95.4 | 3.6 | 0.9 | 0.0 | 0.0 | 0.0 | 0.1 | 100 |
| Boulders | 2 | 3.0 | 95.2 | 0.6 | 0.0 | 0.0 | 0.1 | 1.1 | 100 |
| Cobbles | 3 | 2.3 | 5.9 | 83.1 | 1.2 | 0.0 | 0.2 | 7.3 | 100 |
| Gravel | 4 | 6.3 | 8.3 | 8.1 | 56.7 | 3.0 | 2.6 | 15.0 | 100 |
| Sand Silt | 5 | 5.3 | 5.5 | 4.7 | 15.4 | 40.6 | 13.7 | 14.9 | 100 |
| Mud | 6 | 3.5 | 3.2 | 1.7 | 7.0 | 9.3 | 67.0 | 8.4 | 100 |
| Sand Waves | 7 | 2.7 | 6.5 | 3.8 | 2.6 | 0.0 | 0.7 | 83.8 | 100 |

Table 3-41. Substratum_Code3 Depth Partitioned: Confusion matrix of contribution as a percentage of total

| Observed | Predicted | | | | | | | Total | |
|------------|-----------|-----|-----|-----|------|------|------|-------|------|
| | 1 | 2 | 3 | 4 | 5 | 6 | 7 | | |
| Reef | 1 | 1.1 | 0.0 | 0.0 | 0.0 | 0.0 | 0.0 | 0.0 | 1.2 |
| Boulders | 2 | 0.0 | 1.4 | 0.0 | 0.0 | 0.0 | 0.0 | 0.0 | 1.5 |
| Cobbles | 3 | 0.0 | 0.1 | 1.4 | 0.0 | 0.0 | 0.0 | 0.1 | 1.7 |
| Gravel | 4 | 0.5 | 0.7 | 0.6 | 4.5 | 0.2 | 0.2 | 1.2 | 8.0 |
| Sand Silt | 5 | 3.7 | 3.9 | 3.3 | 10.8 | 28.5 | 9.6 | 10.5 | 70.3 |
| Mud | 6 | 0.5 | 0.4 | 0.2 | 0.9 | 1.2 | 9.0 | 1.1 | 13.4 |
| Sand Waves | 7 | 0.1 | 0.3 | 0.2 | 0.1 | 0.0 | 0.0 | 3.3 | 3.9 |
| Total | | 6.0 | 6.8 | 5.7 | 16.4 | 30.0 | 18.8 | 16.2 | 49.3 |

As in the previous section, the Sands-Silt class represented about 71% of the observations and the classification success for this class improved from 35.5% to a still rather poor 40.6%, as well as remaining grossly under-represented in the classification results due large number of observations being classified as other substrata. Again, given the values of the diagonals, the other observed classes

appeared to have much greater classification success and the overall classification success improved to 49.3%. However, despite the small improvement, as before these classes were seriously over-classified in the results — again erroneously indicating a much higher occurrence of harder/rougher or muddy substratum types than was observed.

3.6.3.9. QTC results summary

The depth partitioned analyses were conducted on all of the re-coding schemas presented above, though details of all have not been discussed. However, a condensed version of the overall classification success results from the separate analyses yields a summary performance table (Table 3-42). Spatial partitioning of the data into 1 by 1 degree blocks was also attempted, but did not yield perceptible improvements and has not been presented.

It is clear that the depth partitioning generally leads to some improvement in classification performance and performance decreases inversely with the number of seabed class types. It is also clear that substantial further reduction in the number of classes (<5 to 3) would be necessary in an attempt to raise the level of classification success to a satisfactory level. However, so few distinguishable classes would have little information content of value in terms of broad scale seabed habitat mapping as only a few classes of substratum (i.e. mud, sand, rocks, reef) intersecting with only very basic biological habitats (i.e. none, bioturbation, vegetation, epibenthos, hard-coral) would realize at least 8 of 16 possible combinations.

Table 3-42. Summary of LDA classification performance of QTC View data.

| Analysis | Name | Potential classes | Actual classes | No partitioning | Depth partitioning |
|--------------------------|--------------|-------------------|----------------|-----------------|--------------------|
| Substrate v1, Habitat v2 | sub_hab_cod2 | 108 | 102 | 3.4% | 4.6% |
| Substrate v2, Habitat v2 | sub_hab_cod3 | 84 | 79 | 6.0% | 5.8% |
| Substrate v3, Habitat v2 | sub_hab_cod4 | 84 | 78 | | 5.9% |
| BioHabitat v2 | habitat_cod3 | 12 | 12 | 27.7% | 29.5% |
| BioHabitat v3 | habitat_cod2 | 8 | 8 | 38.4% | 40.5% |
| Substrate v1 | sbstrt_code | 9 | 9 | 36.6% | 39.0% |
| Substrate v2 | sbstrt_cod2 | 7 | 7 | 45.0% | 49.1% |
| Substrate v3 | sbstrt_cod3 | 7 | 7 | 45.8% | 49.3% |

3.7. ECOLOGICAL RISK INDICATORS

The basic approach to establishing the ecological risk indicators involved estimating the proportion of area or biomass of an assemblage, species group or species in various zones of the GBRMP or exposed to trawling and at various intensities of effort. The study area on the continental shelf of the GBRMP (excluding islands, coral reefs and shallow shoals < ~12 m, and coastal shallows < ~7 m) was almost 200,000 km², of which 44% was zoned General Use, 28% was Habitat Protection, 28% was Marine National Park (and Conservation Park), and <1% was Preservation (Table 3-43).

Table 3-43: Total area and percentage of the study area on the continental shelf of the GBRMP in various management zones considered for estimating ecological risk indicators.

| ZONE | General Use | Habitat Protection | Marine National Park | Preservation | TOTAL |
|----------------------|-------------|--------------------|----------------------|--------------|---------|
| Area km ² | 87,016 | 56,709 | 55,535 | 383 | 199,644 |
| Area % | 44 | 28 | 28 | <1 | 100 |

Of the almost 200,000 km² study area, just over 47,000 km² of 0.01° study grid cells had trawl effort recorded by VMS in 2005. For most of this area, the level of effort was very low and only fractions of these grid cells were swept by trawl gear. At the other extreme, about 10,000 km² of 0.01° grid cells were trawled with ≥8 hours of effort, which if distributed uniformly was roughly sufficient to cover a 0.01° cell one or more times. In these areas, the effective area trawled was approximately the same as the grid cell area even though the total swept area was greater (Table 3-44). Thus, while the total area of seabed swept in 2005 was approximately 38,500 km², the actual area of seabed potentially affected was much less (at approximately 17,200 km²) because of aggregation of the majority of effort (~80%) into a small area (~5%), with consequent environmental benefit to the vast remainder of the seabed environment. Further, because of the assumption here of uniformly distributed effort within grid cells, the estimate of 17,200 km² is likely to be an upper estimate. In reality, trawling at this scale would be random or even aggregated with the consequence that slightly less seabed would be potentially affected (Ellis & Pantus 2001); possibly only ~13,000 km² in the case of random distribution within cells. On the other hand, such very small scale randomness or aggregations are unlikely to be consistent from year to year, even though the larger scale pattern is very consistent. Thus, over time periods of years the total area of seabed affected would be greater than that in any single year, but the true area is uncertain. The estimates provided here indicate a likely range for the area of seabed affected by trawling.

Table 3-44: Total area of the study area on the continental shelf of the GBRMP exposed to various levels of trawl effort, measured by VMS in 2005, considered for estimating ecological risk indicators. The total effective area trawled and total area swept are also estimated.

| Effort interval (hrs / 0.01° cell) | Area km ² | Effort hrs | Effective area km ² | Swept area km ² |
|---------------------------------------|-------------------------|---------------|-----------------------------------|-------------------------------|
| 0 | 152,419 | 0 | 0 | 0 |
| 0.125 | 10,554 | 1,175 | 171 | 171 |
| 0.25 | 6,054 | 1,840 | 268 | 268 |
| 0.5 | 5,718 | 3,486 | 507 | 507 |
| 1 | 5,139 | 6,302 | 917 | 917 |
| 2 | 4,804 | 11,870 | 1,727 | 1,727 |
| 4 | 4,839 | 24,059 | 3,500 | 3,500 |
| 8 | 4,746 | 46,680 | 4,746 | 6,790 |
| 16 | 3,198 | 61,670 | 3,198 | 8,971 |
| 32 | 1,533 | 57,168 | 1,533 | 8,316 |
| 64 | 593 | 43,576 | 593 | 6,339 |
| 128 | 44 | 5,900 | 44 | 858 |
| 256 | 5 | 1,266 | 5 | 184 |
| Total | 199,644 | 264,991 | 17,207 | 38,546 |

3.7.1. Indicators for species-groups biomass

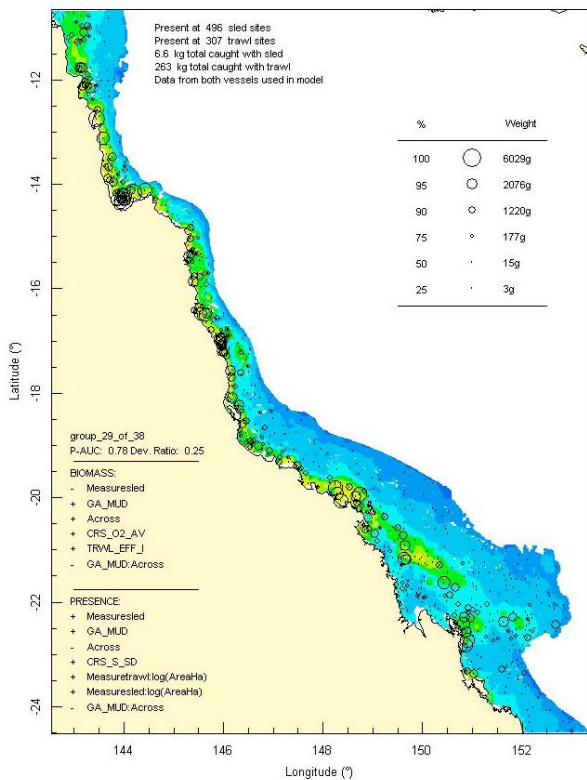
On the basis of the biophysical model predictions of species-group biomass distributions, the first indicator considered was the amount of biomass of each group located in various marine park zones, in particular the percentage of the total located in General Use (GU) zones was available to trawling and potentially at risk (Table 3-45). Thirty six of the 38 species groups had more than 25% of their biomass in GU zones (Table 3-45, pale orange) and 12 groups had more than 50% of their biomass in GU zones (Table 3-45, dark orange). The lowest level of availability was 23% and the highest level was 65%.

The next indicator considered was the percentage of biomass of each species-group located in grid cells where trawl effort was present — regardless of the intensity of effort in the grid cells (Table 3-45). Fifteen of the 38 species groups had more than 25% of their biomass in grid cells with trawl effort (Table 3-45, pale orange) and none had more than 50% of their biomass in grid cells with trawl effort. The lowest level of exposure was 10% and the highest level was 41%. This indicator is more specific and more sensitive than the previous.

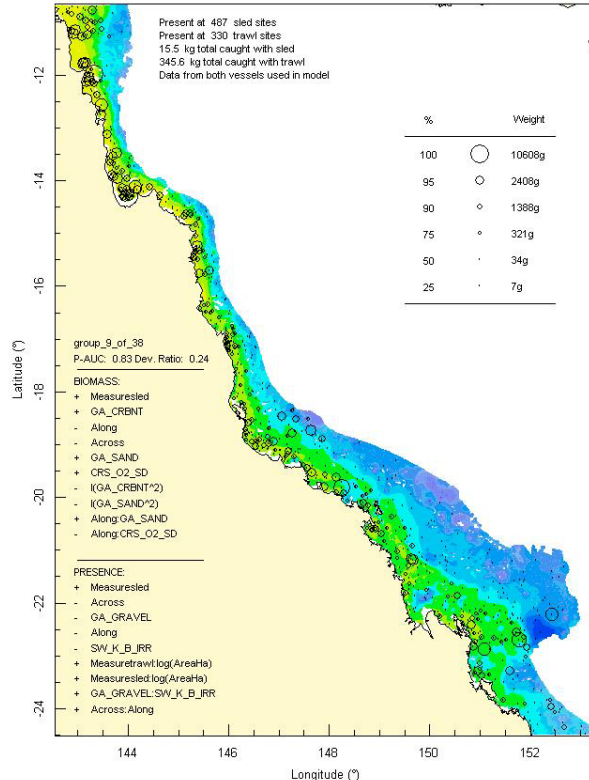
The third indicator for species-groups was the percentage of biomass of each group directly exposed to trawl effort taking into account the intensity of trawl effort (Table 3-45). The table shows the amount of biomass exposed at several different levels of effort intensity, as well as the final total exposure as a percentage. Recall that as ~8 hrs of effort is sufficient to cover a 0.01° grid cell once, all biomass in cells with 8 hrs was considered exposed, whereas in cells with say 4 hrs only half the biomass was exposed and in cells with say 16 hrs the biomass was exposed 2 times. This method was an approximation and leads to an upper limit. That is, the level of exposure was unlikely to exceed the estimates provided. Only seven of the 38 species groups had more than 25% of their biomass directly exposed to trawl effort in 2005 (Table 3-45, pale orange) and only one had more than 50% of biomass directly exposed (Table 3-45, dark orange) (Figure 3-106, Figure 3-107). The lowest level of exposure to effort was 7% and the highest level was 60%. This most specific and sensitive indicator suggested that 713 of 840 OTUs (85%) represented by the 38 species-groups have very low risk of exposure, 94 (11%) have moderately low risk of exposure, and 22 (3%) have moderately high risk of exposure. For each of the higher exposure groups, the potential risk for each member species was examined in further detail (Section 3.7.2).

Finally, the trawl effort coefficient of the biophysical models for species-groups was considered where included. Trawl effort was selected in 12 of the 38 group models and was significant in 11 cases. For the highest exposure-ranked group#29, the trawl effort coefficient was positive 0.009 for the biomass component of the model, suggesting that this group was ~0.9% more abundant per annual hour of effort per 0.01° grid cell, with a possible implication that this group was almost 5% more abundant as a result of trawling. For the 8th exposure-ranked group#10 (with an exposure of 24%), the trawl effort coefficient was positive for the presence component of the model, but there was a negative interactive with mud, with a possible implication that this group had + ~0.1% overall change in abundance as a result of trawling. For the 12th exposure-ranked group#1 (with an exposure of 21%), the trawl effort coefficient was -0.019 for the presence component of the model, suggesting that this group was ~1.9% less likely to be present per annual hour of effort per 0.01° grid cell, with a possible implication that this group was ~0.2% less abundant as a result of trawling. For the 15th exposure-ranked group#8 (Figure 3-107, with an exposure of 20%), the trawl effort coefficient was -0.08 for the presence model, but there was a negative interactive with carbonate, with a possible implication that this group had ~1.2% overall decrease in abundance as a result of trawling. The remaining eight groups with significant trawl effort terms had coefficients ranging from -0.01 to -0.04 and possible decreases in abundance as a result of trawling of -0.1% to -6%; their exposures to trawl effort ranged from 14% to 7%. Those groups with greatest potential negative change in biomass are shown in Figure 3-107. For each of the groups with significant trawl coefficients, the potential risk for each member species was examined in further detail below (Section 3.7.2).

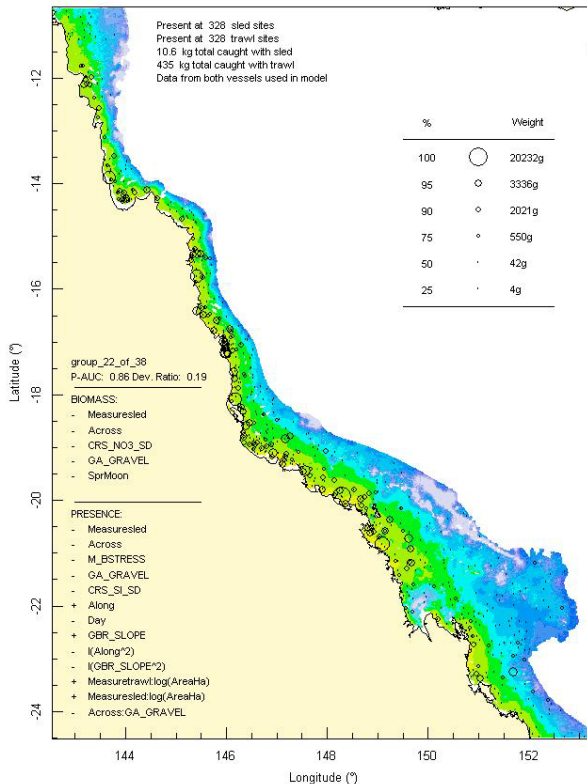
(a) Group 29



(b) Group 9



(c) Group 22



(d) Group 14

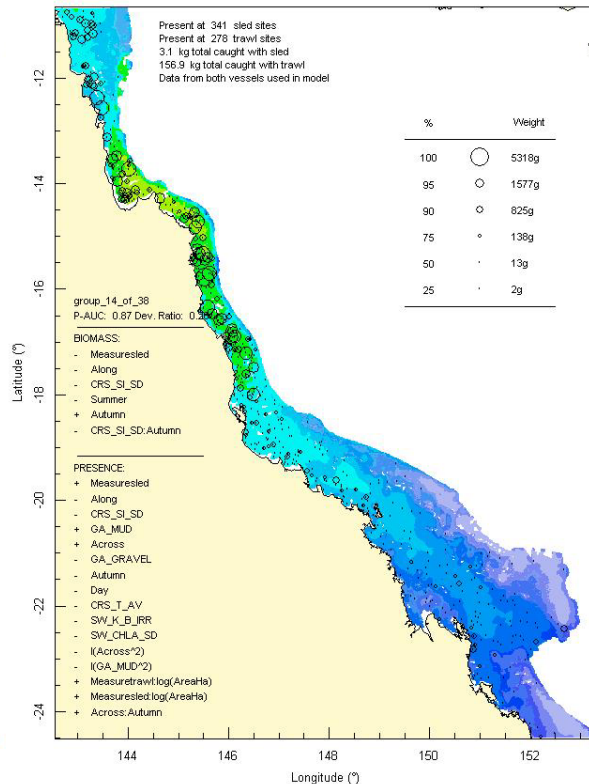
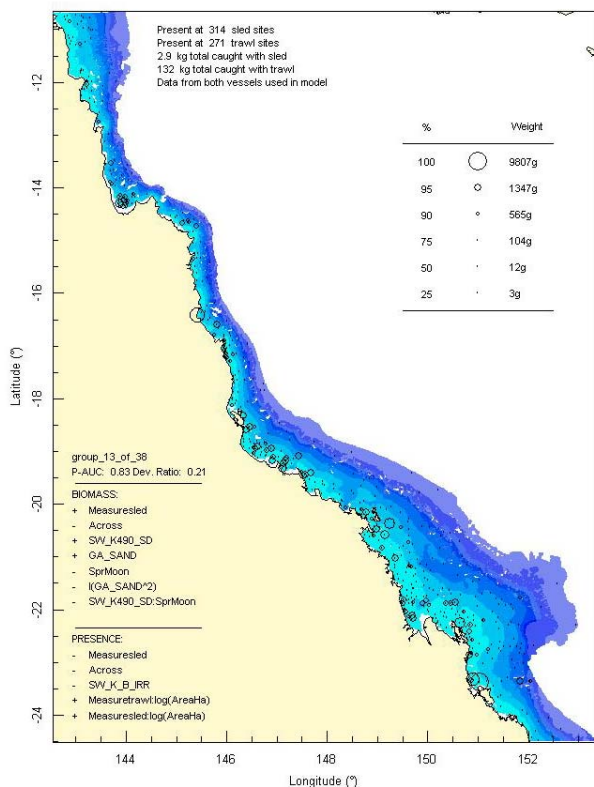
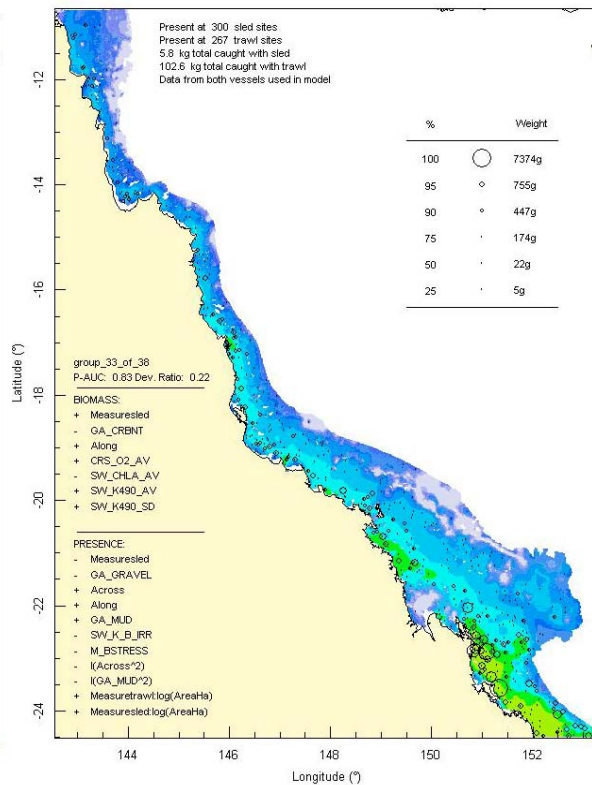


Figure 3-106: Distribution maps of the most exposed species groups (a) exposed over 50 %, (b) – (d) exposed by 25-50%

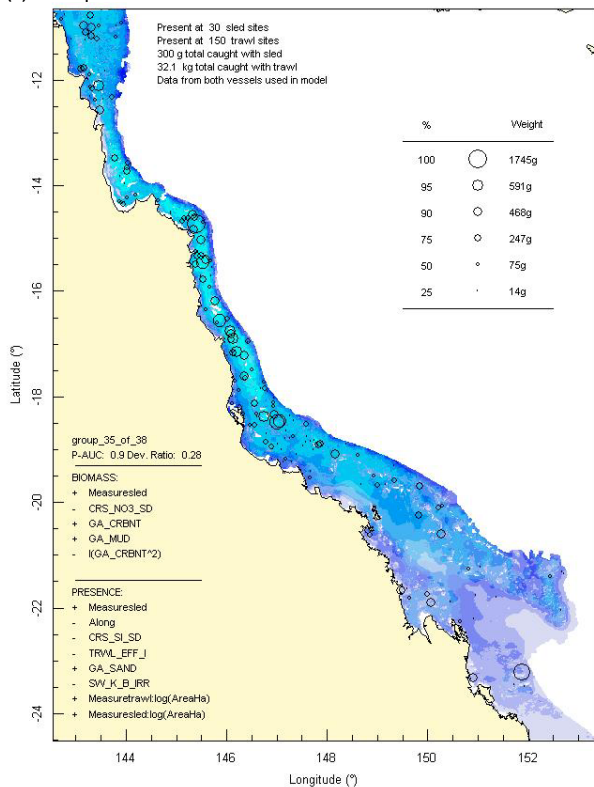
(a) Group 13



(b) Group 33



(c) Group 35



(d) Group 6

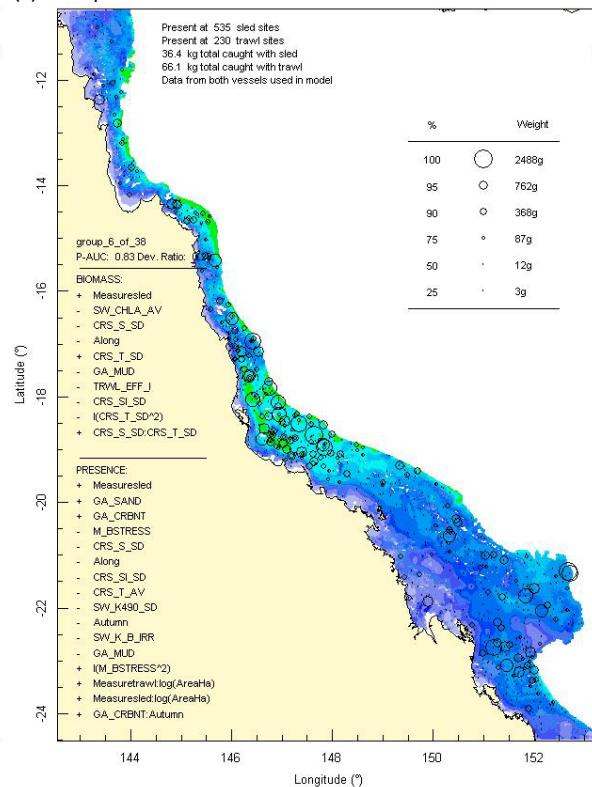


Figure 3-107: Distribution maps of the most exposed species groups: (a) and (b) exposed by 25-50%; and species groups with negative trawl effort coefficients and possible population decreases in abundance as a result of trawling of >5%; (c) -5.3% and (d) -6% respectively.

3.7.2. Indicators for individual species biomass

Risk indicators were estimated for all individual species that were members of the species groups that appeared to be at higher levels of potential risk. The results for group #29 species are shown in Table 3-46, in a similar though abbreviated form as for species groups in Table 3-45. All but one of the 22 species in this group had high proportions of their exposed biomass in areas of high effort, so that their total effort exposed biomass was greater than their trawled biomass. Four species appear to have very high levels of exposure — greater than 100% of their standing biomass. Given that group 29 had the greatest overlap with the highest levels of trawl effort, it is not surprising a key prawn target species, *Penaeus semisulcatus* (grooved tiger prawn), was a member of this group and had a very high level of exposure — even though 26% of its biomass was protected by zoning and 36% of its biomass was not exposed to any effort, the exposed 64% of biomass was trawled an average of more than 2.7 times in 2005, contributing to a total indicator of 174% of standing biomass exposed to trawl effort (Figure 3-108a). The second most exposed species in group 29 was *Cryptolutea arafurensis* (a Pilumnid Crab), with 57% of its biomass available in GU zones, 41% in cells with recorded effort that was trawled an average of ~3.1 times giving a total of ~128% total direct exposure to trawling (Figure 3-108b). The third most exposed species in group 29 was *Brachirus muelleri* (a Pleuronectiform flatfish), with 69% of its biomass available in GU zones, 59% in cells with recorded effort that was trawled an average of ~2 times giving a total of 119% exposure to trawling (Figure 3-108c). The fourth most exposed species in group 29 was *Pentaprion longimanus* (a Gerreid fish), with 62% of its biomass available in GU zones, 48% in cells with recorded effort that was trawled an average of ~2.4 times giving a total of 117% exposure to trawling (Figure 3-108d). Another two species had high levels of exposure — between 75% and 100% of their standing biomass. *Terapon puta* (a Terapontid fish), had 56% of its biomass available in GU zones, 47% in cells with recorded effort that was trawled an average of ~1.6 times giving a total of 78% exposure to trawling (Figure 3-109a). The Bivalve mollusc *Enisiculus cultellus* had 61% of its biomass available in GU zones, 46% in cells with recorded effort that was trawled an average of ~1.6 times giving a total of 75% exposure to trawling (Figure 3-109b). Four species had moderate-high levels of exposure — between 50% and 75% of their standing biomass. The prawn *Metapenaeus ensis* had 67% of its biomass available in GU zones, 49% in cells with recorded effort that was trawled an average of ~1.4 times giving a total of 67% exposure to trawling (Figure 3-109c). The lizardfish *Saurida argentea/tumbil* had 58% of its biomass available in GU zones, 38% in cells with recorded effort that was trawled an average of ~1.6 times giving a total of 63% exposure to trawling (Figure 3-109d). The Bivalve mollusc *Placamen tiara* had 55% of its biomass available in GU zones, 35% in cells with recorded effort that was trawled an average of ~1.6 times giving a total of 55% exposure to trawling (Figure 3-110a). *Euristhmus nudiceps* (a Plotosid fish) had 56% of its biomass available in GU zones, 33% in cells with recorded effort that was trawled an average of ~1.6 times giving a total of 55% exposure to trawling (Figure 3-110a). Ten species had moderate-low exposures of 25-50% and one species had low exposure <25% (Table 3-46).

The results for group #9 species are shown in Table 3-47. All of the 23 species in this group had high proportions of their exposed biomass in areas of high effort, so that their total effort exposed biomass was greater than their trawled biomass. While as a correlated species group, group#9 had moderate-low exposure, three individual species appeared to have high levels of exposure: *Leiognathus leuciscus* (a Leiognathid ponyfish), with 59% of its biomass available in GU zones, 43% in cells with recorded effort that was trawled an average of ~2.2 times giving a total of 95% exposure to trawling (Figure 3-110b); *Upeneus sundaicus* (a Mullid fish), with 63% of its biomass available in GU zones, 50% in cells with recorded effort that was trawled an average of ~1.9 times giving a total of 93% exposure to trawling (Figure 3-110c); and *Portunus gracilimanus* (a crab), with 59% of its biomass available in GU zones, 38% in cells with recorded effort that was trawled an average of ~2.2 times giving a total of 86% exposure to trawling (Figure 3-110d). Five species from group 9 had a moderate-high exposure, including fishes *Calliurichthys grossi* and *Cynoglossus maculipennis*, bivalves *Amusium pleuronectes* cf and *Melaxinaea vitrea*, and the bug lobster *Thenus parindicus* — with 54–60% of their biomass available in GU zones, 36–39% in cells with recorded effort that was trawled an average of ~1.4–1.7 times giving totals of 52–59% exposure to trawling (see Figure 3-111a-d and Figure 3-112a).

The results for group #22 species are shown in Table 3-48. Again, all of the species in this group had high proportions of their exposed biomass in areas of high effort, so that their total effort exposed biomass was greater than their trawled biomass. While as a correlated group, group#22 had moderate-low exposure, seven individual species appeared to have moderate-high levels of exposure, including fishes: *Leiognathus splendens*, *Psettodes erumei*, *Terapon theraps*, *Upeneus sulphureus*, crustaceans: *Erugosquilla woodmasoni*, *Myra tumidospina*, and a gastropod: *Nassarius cremmatus* cf — with 54–70% of their biomass available in GU zones, 38–49% in cells with recorded effort that was trawled an average of ~1.2–1.6 times giving totals of 54–65% exposure to trawling (see Figure 3-112b-d and Figure 3-113a-d). Sixteen group #22 species had moderate-low exposures of 30–50% and none had low exposure <25%.

The results for group #14 species are shown in Table 3-49. All but two of the 16 species in this group had high proportions of their exposed biomass in areas of high effort, so that their total effort exposed biomass was greater than their trawled biomass. One species, *Scolopsis taeniopterus* (a Nemipterid fish), appeared to have a moderate-high level of exposure with 51% of its biomass available in GU zones, 33% in cells with recorded effort that was trawled an average of ~1.7 times giving a total of 54% exposure to trawling (Figure 3-114a). Ten species had moderate-low exposures between 25-50% and five species had low exposure <25%.

The results for group #13 species are shown in Table 3-50. Twelve of the 19 species in this group had high proportions of their exposed biomass in areas of high effort, so that their total effort exposed biomass was greater than their trawled biomass. Two species from group 13 had a moderate-high exposures including: *Repomucenus belcheri* (a Callionymid fish) and *Trachypenaeus anchoralis* (a prawn) — with 64% of their biomass available in GU zones, 42–44% in cells with recorded effort that was trawled an average of ~1.3–1.5 times giving totals of 53–67% exposure to trawling (see Figure 3-114 bc). Ten species had moderate-low exposures between 25-50% and seven species had low exposure <25%.

The results for group #33 species are shown in Table 3-51. All eight species appeared to have moderate-low levels of exposure, with 49–67% of their biomass available in GU zones, 28–40% in cells with recorded effort that was trawled an average of about 0.9 times giving a total of 27–35% exposure to trawling.

Group #27 overall had a low level of exposure (Table 3-45) and the results for species in this group are shown in Table 3-52. Two of the five species in this group had high proportions of their exposed biomass in areas of high effort, so that their total effort exposed biomass was somewhat greater than their trawled biomass. No species had high exposure; four species appeared to have moderate-low levels of exposure, with 50–59% of their biomass available in GU zones, 25–33% in cells with recorded effort that was trawled an average of about 1.1 times giving a total of 25–37% exposure to trawling. Only one species had low exposure <25%.

While the remaining 31 of the 38 groups, representing 713 (85%) of the 840 species examined, as groups had low levels of exposure (<25%) (Table 3-45), the species members of each were examined in more detail and key summary results are presented (Table 3-53). Of these remaining species, 91 had 50-69% of their biomass available in General Use, 568 had 25-50% of their biomass available and 52 had <25%. Only three species had more than 50% (51%, 54% and 60%) of their biomass in cells with recorded effort, 235 species had 25-50% of their biomass in trawled cells and 474 species had <25%. One additional species had high total direct exposure to trawl effort: *Pelates quadrilineatus* (a Terapontid fish), with 69% of its biomass available in GU zones, 47% in cells with recorded effort that was trawled an average of ~2.2 times giving a total of 103% exposure to trawling (Figure 3-114d). Four species had moderate-high levels of direct exposure (Table 3-53): *Brachaluteres taylori* (a Monacanthid filefish), with 71% of its biomass available in GU zones, 60% in cells with recorded effort that was trawled an average of ~1.2 times giving a total of 72% exposure to trawling (Figure 3-115a), *Leiognathus bindus* (a Leiognathid pony fish), with 42% of its biomass available in GU zones, 28% in cells with recorded effort that was trawled an average of ~2.3 times giving a total of 63% exposure to trawling (Figure 3-115b), *Yongeichthys nebulosus* (a Gobiid fish), with 42% of its biomass available in GU zones, 25% in cells with recorded effort that was trawled an average of ~2.1 times giving a total of 51% exposure to trawling (Figure 3-115c), and *Apogon poecilopterus* (a Cardinal fish), with 50% of its biomass available in GU zones, 34% in cells with recorded effort that

Table 3-48: Ecological Risk Indicators with respect to trawling for estimated Biomass (kg) of species in group#22: biomass available in General Use zone; biomass potentially exposed in trawled cells; and biomass directly exposed to trawl effort. Pale orange: >25% biomass exposed; dark orange: >50% biomass exposed; red: >50% biomass exposed.

| Class | Genus | Species | Biomass | Gen Use | % Available | Not trawled | Trawled | % Exposed | Effort Exp | Effort Exp% |
|----------------|----------------------|---------------------|---------|---------|-------------|-------------|---------|-----------|------------|-------------|
| Actinopterygii | <i>Caranx</i> | <i>bucculentus</i> | 1236784 | 797276 | 64 | 754020 | 482764 | 39 | 580618 | 47 |
| Actinopterygii | <i>Gerrus</i> | <i>filamentosus</i> | 84315 | 47619 | 56 | 49621 | 34695 | 41 | 41978 | 50 |
| Actinopterygii | <i>Leiognathus</i> | <i>splendens</i> | 270168 | 145446 | 54 | 151522 | 118646 | 44 | 145528 | 54 |
| Actinopterygii | <i>Nemipterus</i> | <i>peronii</i> | 1355758 | 865424 | 64 | 851889 | 503869 | 37 | 651640 | 48 |
| Actinopterygii | <i>Nemipterus</i> | sp juv/unident | 6496 | 3035 | 47 | 4705 | 1791 | 28 | 2009 | 31 |
| Actinopterygii | <i>Psettodes</i> | <i>erumei</i> | 361247 | 221081 | 61 | 215737 | 145511 | 40 | 204453 | 56 |
| Actinopterygii | <i>Sillago</i> | <i>burrus</i> | 307944 | 140790 | 46 | 215146 | 92797 | 30 | 115526 | 37 |
| Actinopterygii | <i>Sugggrundus</i> | <i>macracanthus</i> | 559472 | 330620 | 59 | 375946 | 183525 | 33 | 253496 | 45 |
| Actinopterygii | <i>Terapon</i> | <i>theraps</i> | 359964 | 227353 | 63 | 206648 | 153316 | 43 | 224795 | 62 |
| Actinopterygii | <i>Torquigener</i> | <i>whitleyi</i> | 150537 | 78812 | 52 | 99749 | 50788 | 34 | 57201 | 38 |
| Actinopterygii | <i>Upeneus</i> | <i>sulphureus</i> | 723274 | 504361 | 70 | 390634 | 332639 | 46 | 423359 | 58 |
| Anthozoa | <i>Sea pen</i> | sp1 | 507 | 287 | 57 | 318 | 189 | 37 | 252 | 50 |
| Crustacea | <i>Erugosquilla</i> | <i>woodmasoni</i> | 19542 | 12829 | 66 | 10017 | 9525 | 49 | 12819 | 65 |
| Crustacea | <i>Myra</i> | <i>tumidospina</i> | 14791 | 8393 | 57 | 9237 | 5555 | 38 | 8930 | 60 |
| Crustacea | <i>Paguristes</i> | sp2358-2 | 30865 | 15957 | 52 | 21256 | 9609 | 31 | 11286 | 36 |
| Crustacea | <i>Portunus</i> | <i>hastatoides</i> | 5197 | 2846 | 55 | 3264 | 1933 | 37 | 2261 | 43 |
| Crustacea | <i>Portunus</i> | <i>tuberculatus</i> | 1226 | 570 | 46 | 882 | 344 | 28 | 391 | 32 |
| Echinoidea | <i>Chaetodiadema</i> | <i>granulatum</i> | 80329 | 38799 | 48 | 58367 | 21962 | 27 | 24544 | 30 |
| Gastropoda | <i>Aplysia</i> | sp1_QMS | 450338 | 227820 | 51 | 307454 | 142885 | 32 | 170472 | 38 |
| Gastropoda | <i>Bufonaria</i> | <i>rana</i> | 19213 | 10701 | 56 | 12811 | 6402 | 33 | 7564 | 39 |
| Gastropoda | <i>Gemmula</i> | sp2 | 7259 | 3372 | 46 | 5226 | 2033 | 28 | 2314 | 32 |
| Gastropoda | <i>Nassarius</i> | <i>crematus</i> cf | 35852 | 19832 | 55 | 22024 | 13827 | 39 | 20331 | 57 |
| Holothuroidea | <i>Holothuria</i> | <i>ocellata</i> | 858968 | 445403 | 52 | 587871 | 271098 | 32 | 307892 | 36 |

Table 3-49: Ecological Risk Indicators with respect to trawling for estimated Biomass (kg) of species in group#14: biomass available in General Use zone; biomass potentially exposed in trawled cells; and biomass directly exposed to trawl effort. Pale orange: >25% biomass exposed; dark orange: >50% biomass exposed; red: >50% biomass exposed.

| Class | Genus | Species | Biomass | Gen Use | % Available | Not trawled | Trawled | % Exposed | Effort Exp | Effort Exp% |
|----------------|--------------------|----------------------|---------|---------|-------------|-------------|---------|-----------|------------|-------------|
| Actinopterygii | <i>Fistularia</i> | <i>petimba</i> | 135435 | 59846 | 44 | 100778 | 34657 | 26 | 43146 | 32 |
| Actinopterygii | <i>Nemipterus</i> | <i>nematopus</i> | 693470 | 255198 | 37 | 546854 | 146616 | 21 | 250954 | 36 |
| Actinopterygii | <i>Scolopsis</i> | <i>taeniopterus</i> | 1016419 | 517873 | 51 | 685276 | 331143 | 33 | 549892 | 54 |
| Bivalvia | <i>Anadara</i> | <i>ferruginea</i> cf | 11718 | 5388 | 46 | 9089 | 2630 | 22 | 2563 | 22 |
| Bivalvia | <i>Fulvia</i> | <i>scalata</i> | 3799 | 1503 | 40 | 3075 | 723 | 19 | 896 | 23 |
| Cephalopoda | <i>Sepia</i> | <i>pharaonis</i> | 139386 | 71540 | 51 | 92518 | 46868 | 34 | 67431 | 48 |
| Crustacea | <i>Charybdis</i> | <i>truncata</i> | 437520 | 210733 | 48 | 303449 | 134071 | 31 | 201102 | 46 |
| Crustacea | <i>Cloridina</i> | <i>chlorida</i> | 374 | 110 | 29 | 362 | 12 | 3 | 9 | 2 |
| Crustacea | <i>Diogenidae</i> | sp356-1 | 442 | 200 | 45 | 331 | 111 | 25 | 162 | 36 |
| Crustacea | <i>Metapenaeus</i> | <i>endeavouri</i> | 534272 | 275629 | 52 | 367939 | 166333 | 31 | 246691 | 46 |
| Crustacea | <i>Portunus</i> | <i>spinipes</i> | 5017 | 1764 | 35 | 4436 | 582 | 12 | 678 | 13 |
| Crustacea | <i>Portunus</i> | <i>tuberculosis</i> | 394 | 187 | 47 | 270 | 123 | 31 | 181 | 46 |
| Crustacea | <i>Scyllarus</i> | sp3418 | 29264 | 11114 | 38 | 23714 | 5550 | 19 | 5861 | 20 |
| Gastropoda | <i>Lophiotoma</i> | <i>acuta</i> | 4385 | 2383 | 54 | 2897 | 1488 | 34 | 1944 | 44 |
| Gastropoda | <i>Vexillum</i> | <i>obeliscus</i> cf | 2302 | 1007 | 44 | 1730 | 572 | 25 | 910 | 39 |
| Liliopsida | <i>Halophila</i> | <i>tricostata</i> | 911642 | 413948 | 45 | 682405 | 229238 | 25 | 270360 | 30 |

Table 3-50: Ecological Risk Indicators with respect to trawling for estimated Biomass (kg) of species in group#13: biomass available in General Use zone; biomass potentially exposed in trawled cells; and biomass directly exposed to trawl effort. Pale orange: >25% biomass exposed; dark orange: >50% biomass exposed; red: >50% biomass exposed.

| Class | Genus | Species | Biomass | Gen Use | % Available | Not trawled | Trawled | % Exposed | Effort Exp | Effort Exp% |
|----------------|----------------------|----------------------|---------|---------|-------------|-------------|---------|-----------|------------|-------------|
| Actinopterygii | <i>Apogon</i> | <i>cavitiensis</i> | 7972 | 3738 | 47 | 6186 | 1786 | 22 | 1164 | 14 |
| Actinopterygii | <i>Cynoglossus</i> | sp juv/unident | 14818 | 7957 | 54 | 10208 | 4610 | 31 | 5389 | 36 |
| Actinopterygii | <i>Leiognathus</i> | cf <i>bindus</i> | 22870 | 13528 | 59 | 14551 | 8319 | 36 | 10329 | 45 |
| Actinopterygii | <i>Leiognathus</i> | <i>moretoniensis</i> | 47237 | 24755 | 52 | 31263 | 15974 | 34 | 19323 | 41 |
| Actinopterygii | <i>Parapercis</i> | <i>diplospilus</i> | 3855 | 2275 | 59 | 2477 | 1378 | 36 | 1733 | 45 |
| Actinopterygii | <i>Polydactylus</i> | <i>multiradiatus</i> | 418667 | 127018 | 30 | 335464 | 83203 | 20 | 93241 | 22 |
| Actinopterygii | <i>Pomadasys</i> | <i>maculatus</i> | 1542585 | 1000058 | 65 | 1007063 | 535523 | 35 | 549160 | 35 |
| Actinopterygii | <i>Repomucenus</i> | <i>belcheri</i> | 98260 | 63114 | 64 | 57470 | 40790 | 42 | 52407 | 53 |
| Actinopterygii | <i>Siganus</i> | <i>canaliculatus</i> | 377618 | 160420 | 42 | 304851 | 72767 | 19 | 45039 | 12 |
| Actinopterygii | <i>Triphichthys</i> | <i>weberi</i> | 59106 | 33297 | 56 | 39951 | 19155 | 32 | 23536 | 40 |
| Bivalvia | <i>Solen</i> | <i>siphons only</i> | 69535 | 34171 | 49 | 53272 | 16263 | 23 | 11424 | 16 |
| Bivalvia | <i>Solen</i> | sp3 | 35340 | 15962 | 45 | 29504 | 5836 | 17 | 3313 | 9 |
| Crustacea | <i>Cryptopodia</i> | <i>queenlandi</i> | 5162 | 2767 | 54 | 3530 | 1632 | 32 | 1971 | 38 |
| Crustacea | <i>Eucrate</i> | <i>affinis</i> | 2137 | 1022 | 48 | 1745 | 392 | 18 | 235 | 11 |
| Crustacea | <i>Leucosia</i> | <i>ocellata</i> | 13523 | 8034 | 59 | 8713 | 4811 | 36 | 5981 | 44 |
| Crustacea | <i>Pagurid</i> | sp2358-1 | 15945 | 6996 | 44 | 12791 | 3154 | 20 | 2867 | 18 |
| Crustacea | <i>Trachypenaeus</i> | <i>anchoralis</i> | 45119 | 29038 | 64 | 25097 | 20022 | 44 | 30501 | 67 |
| Gastropoda | <i>Murex</i> | <i>brevispina</i> | 4747 | 2906 | 61 | 3087 | 1660 | 35 | 1691 | 35 |
| Gastropoda | <i>Natica</i> | <i>vitellus</i> | 8642 | 4609 | 53 | 6049 | 2593 | 30 | 2560 | 29 |

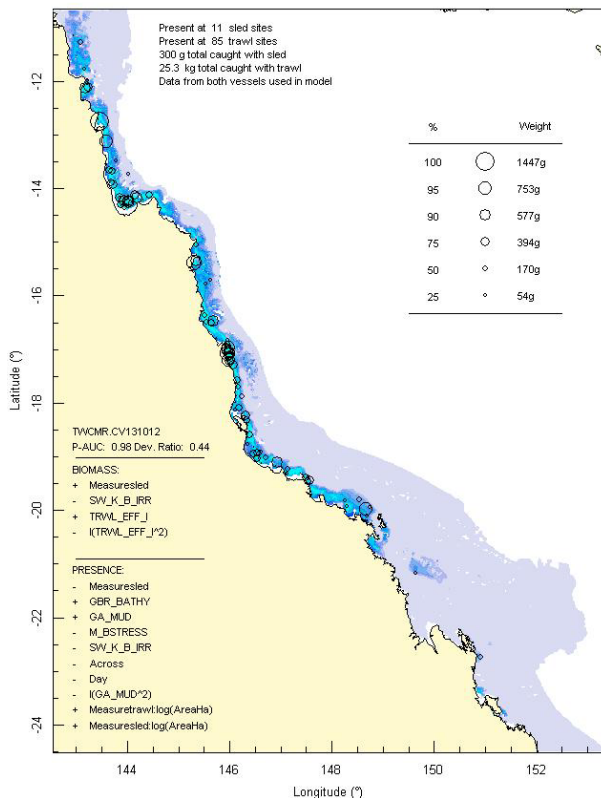
Table 3-51: Ecological Risk Indicators with respect to trawling for estimated Biomass (kg) of species in group#33: biomass available in General Use zone; biomass potentially exposed in trawled cells; and biomass directly exposed to trawl effort. Pale orange: >25% biomass exposed; dark orange: >50% biomass exposed; red: >50% biomass exposed.

| Class | Genus | Species | Biomass | Gen Use | % Available | Not trawled | Trawled | % Exposed | Effort Exp | Effort Exp% |
|----------------|-----------------------|-----------------------|---------|---------|-------------|-------------|---------|-----------|------------|-------------|
| Actinopterygii | <i>Apistus</i> | <i>carinatus</i> | 1073477 | 604069 | 56 | 708259 | 365218 | 34 | 359383 | 33 |
| Actinopterygii | <i>Minous</i> | <i>versicolor</i> | 92283 | 53586 | 58 | 60500 | 31783 | 34 | 30116 | 32 |
| Actinopterygii | <i>Pseudorhombus</i> | <i>elevatus</i> | 775731 | 522838 | 67 | 496676 | 279055 | 36 | 270665 | 35 |
| Asteroidea | <i>Luidia</i> | <i>hardwicki</i> | 26743 | 15522 | 58 | 17560 | 9183 | 34 | 8964 | 33 |
| Crustacea | <i>Portunus</i> | <i>sanguinolentus</i> | 1018755 | 666215 | 65 | 611257 | 407498 | 40 | 349207 | 34 |
| Foraminifera | <i>Discobotellina</i> | <i>biperforata</i> | 151281 | 88000 | 58 | 97759 | 53522 | 35 | 47083 | 31 |
| Gastropoda | <i>Nassarius</i> | <i>conoidalis</i> cf | 2625 | 1378 | 52 | 1869 | 756 | 29 | 702 | 27 |
| Polychaeta | <i>Chloea</i> | <i>flava</i> | 15742 | 7784 | 49 | 11292 | 4450 | 28 | 4432 | 28 |

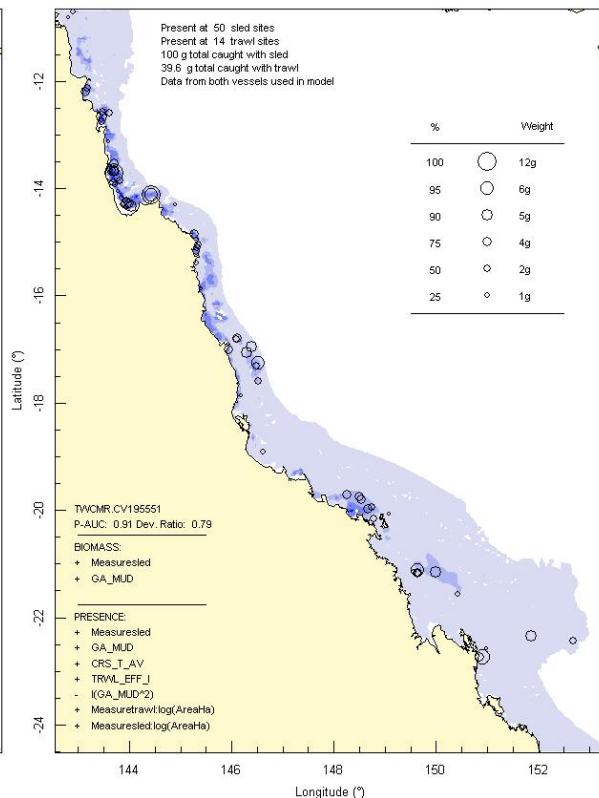
Table 3-52: Ecological Risk Indicators with respect to trawling for estimated Biomass (kg) of species in group#27: biomass available in General Use zone; biomass potentially exposed in trawled cells; and biomass directly exposed to trawl effort. Pale orange: >25% biomass exposed; dark orange: >50% biomass exposed; red: >50% biomass exposed.

| Class | Genus | Species | Biomass | Gen Use | % Available | Not trawled | Trawled | % Exposed | Effort Exp | Effort Exp% |
|----------------|-----------------------|------------------------|---------|---------|-------------|-------------|---------|-----------|------------|-------------|
| Actinopterygii | <i>Grammatobothus</i> | <i>polyophthalmus</i> | 358459 | 211058 | 59 | 239915 | 118544 | 33 | 133790 | 37 |
| Actinopterygii | <i>Pseudochromis</i> | <i>quinquedentatus</i> | 1907 | 1024 | 54 | 1404 | 503 | 26 | 471 | 25 |
| Bivalvia | <i>Leionucula</i> | <i>superba</i> | 5499 | 3078 | 56 | 3738 | 1761 | 32 | 2069 | 37 |
| Crustacea | <i>Nursilia</i> | sp nov | 3789 | 1909 | 50 | 2800 | 989 | 26 | 984 | 26 |
| Crustacea | <i>Trachypenaeus</i> | <i>granulosus</i> | 424353 | 211608 | 50 | 316595 | 107758 | 25 | 108573 | 25 |

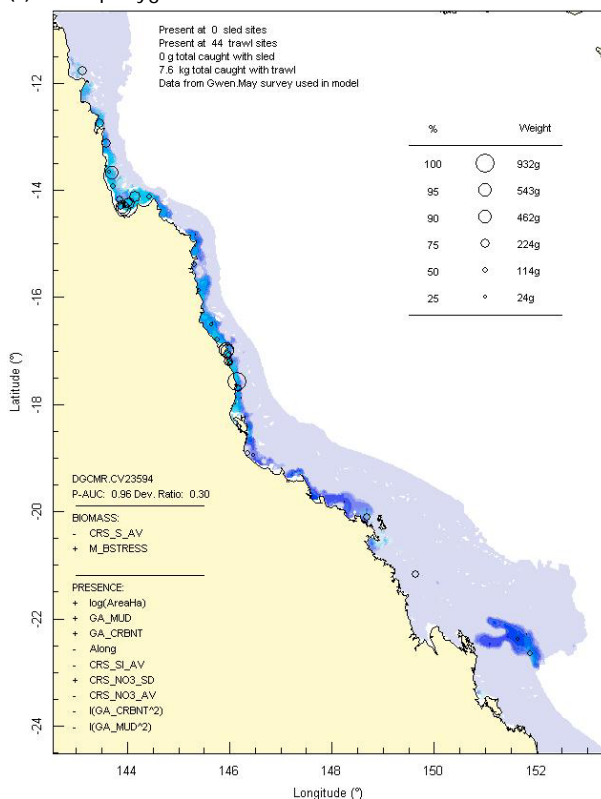
(a) Crustacea: *Penaeus semisulcatus*



(b) Crustacea: *Cryptolutea arafurensis*



(c) Actinopterygii: *Brachirus muelleri*



(d) Actinopterygii: *Pentaprion longimanus*

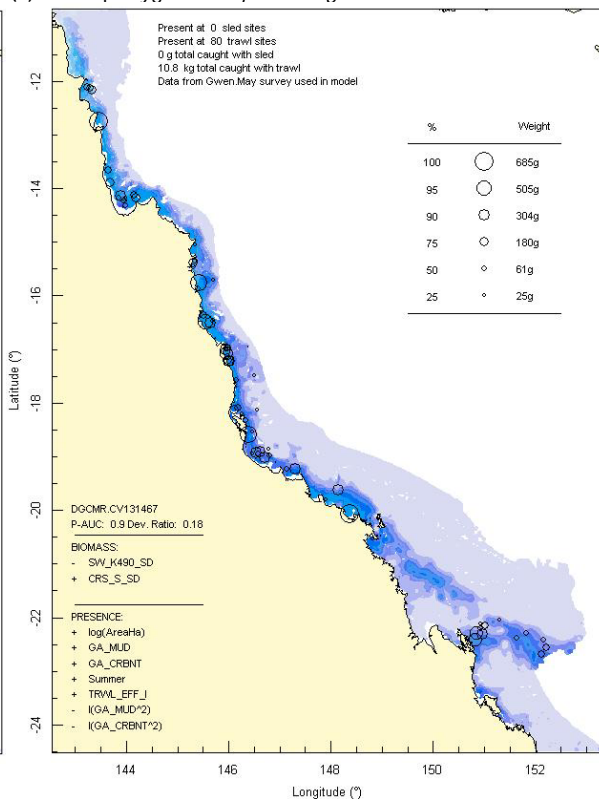
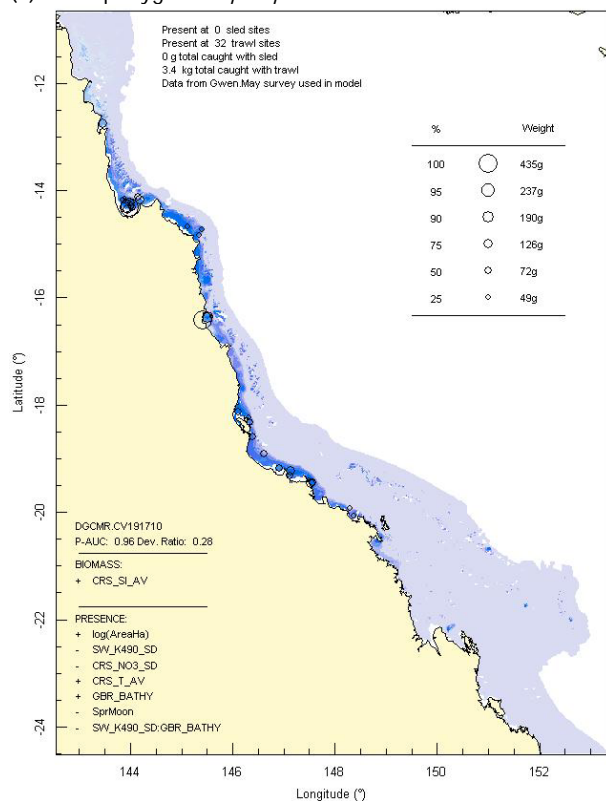
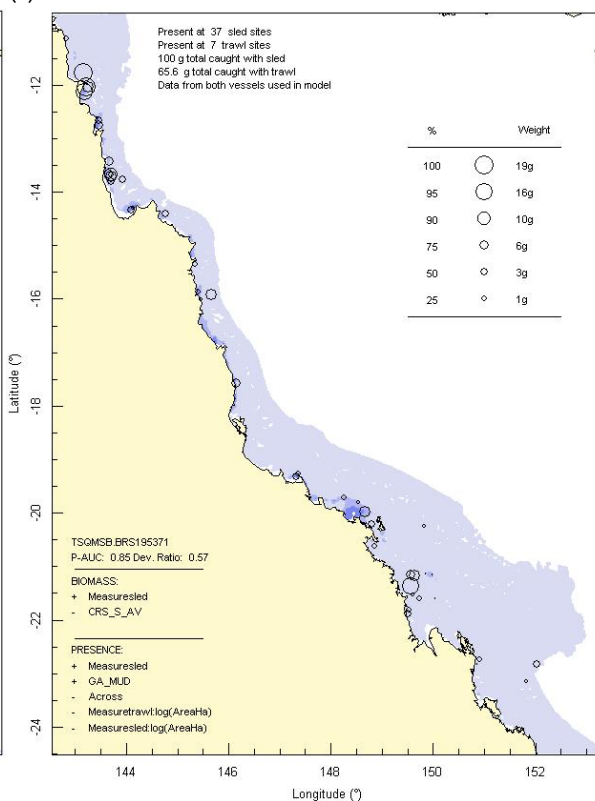


Figure 3-108: Model distribution maps of selected species with higher trawl exposure indicators.

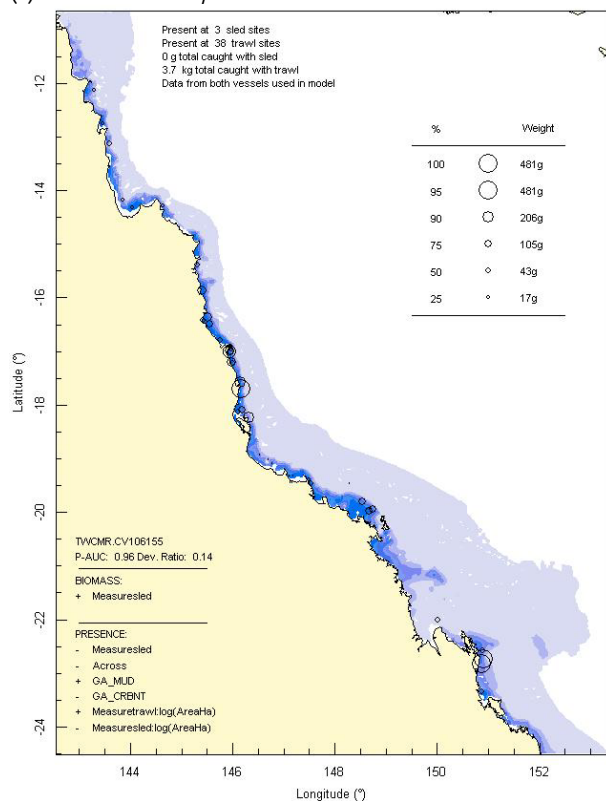
(a) Actinopterygii: *Terapon puta*



(b) Bivalvia: *Ensisculus cultellus*



(c) Crustacea: *Metapenaeus ensis*



(d) Actinopterygii: *Saurida argentea/tumbil*

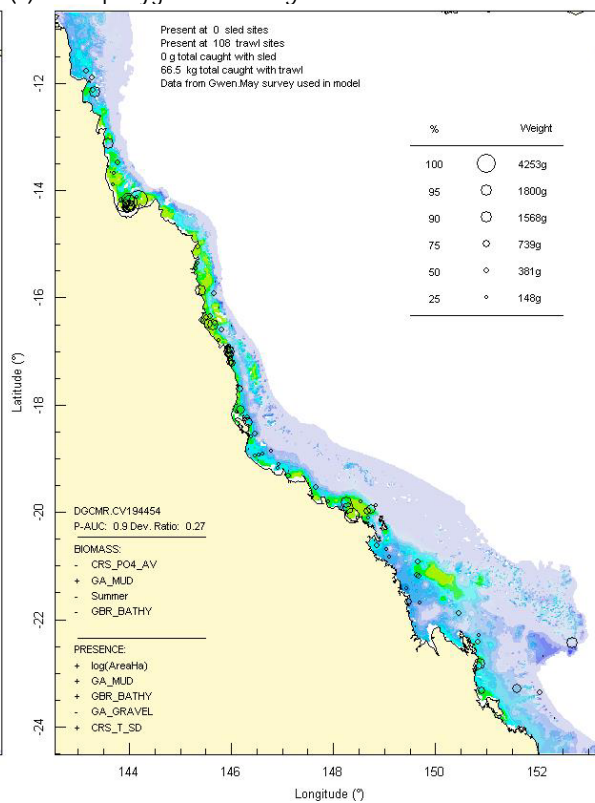
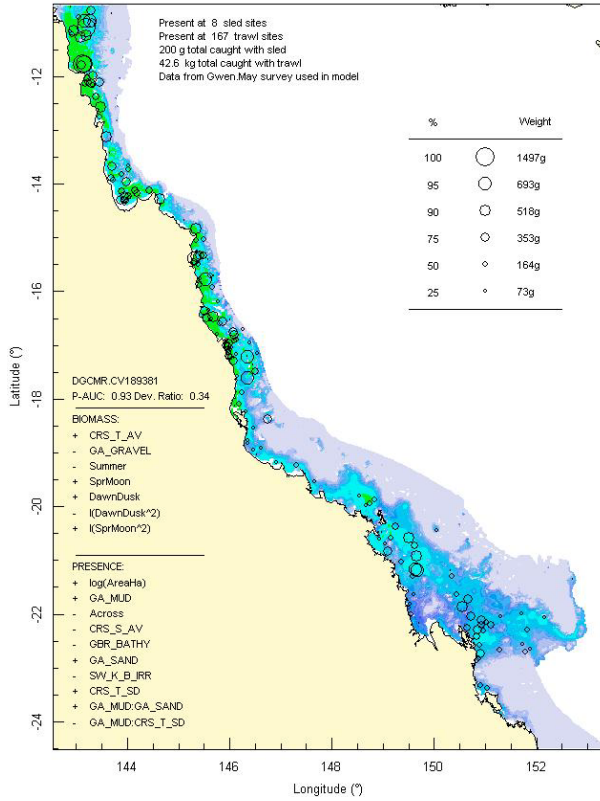
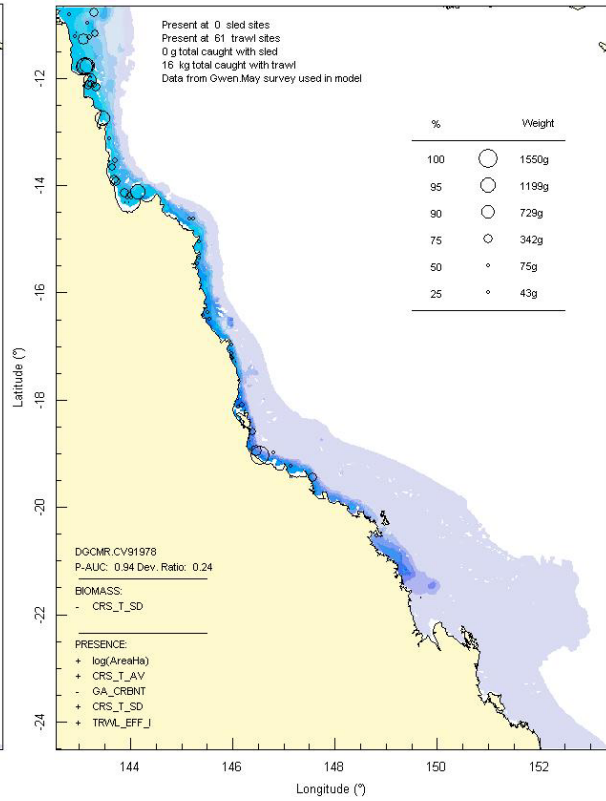


Figure 3-109: Model distribution maps of selected species with higher trawl exposure indicators.

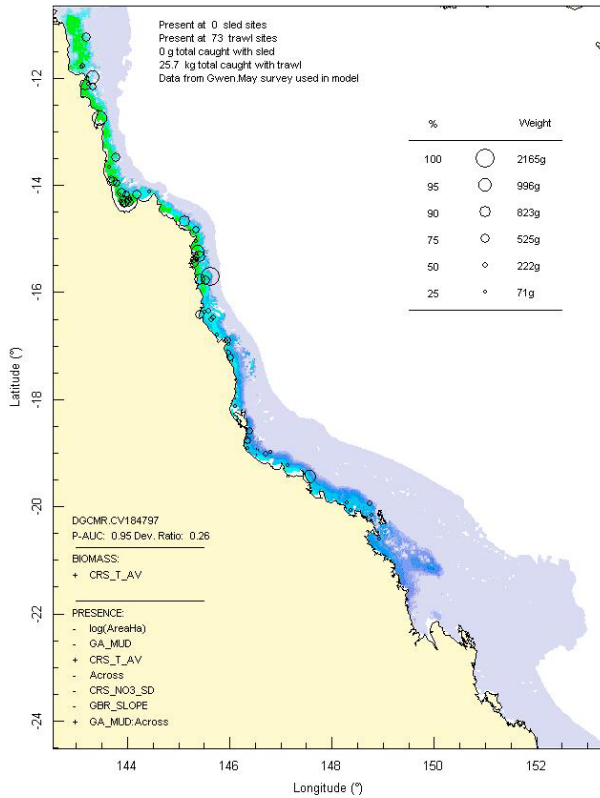
(a) Actinopterygii: *Euristhmus nudiceps*



(b) Actinopterygii: *Leiognathus leuciscus*



(c) Actinopterygii: *Upeneus sundaicus*



(d) Crustacea: *Portunus gracilimanus*

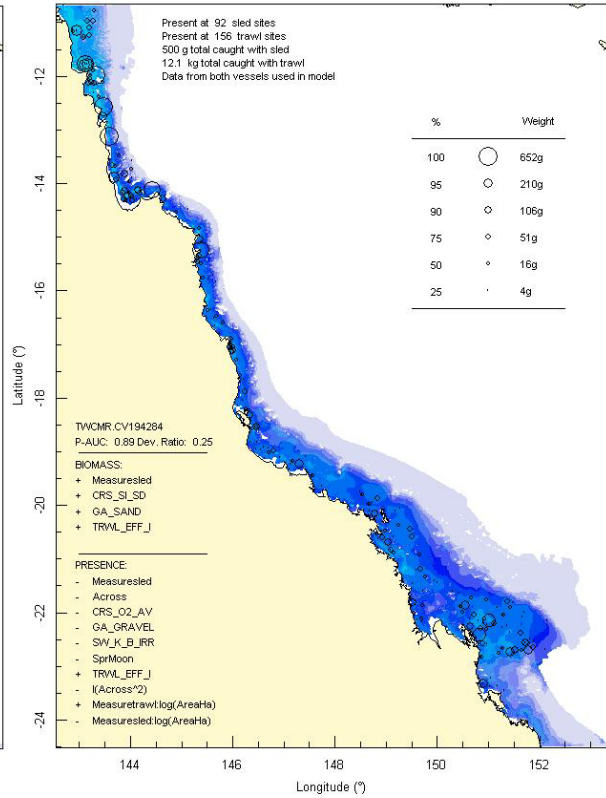
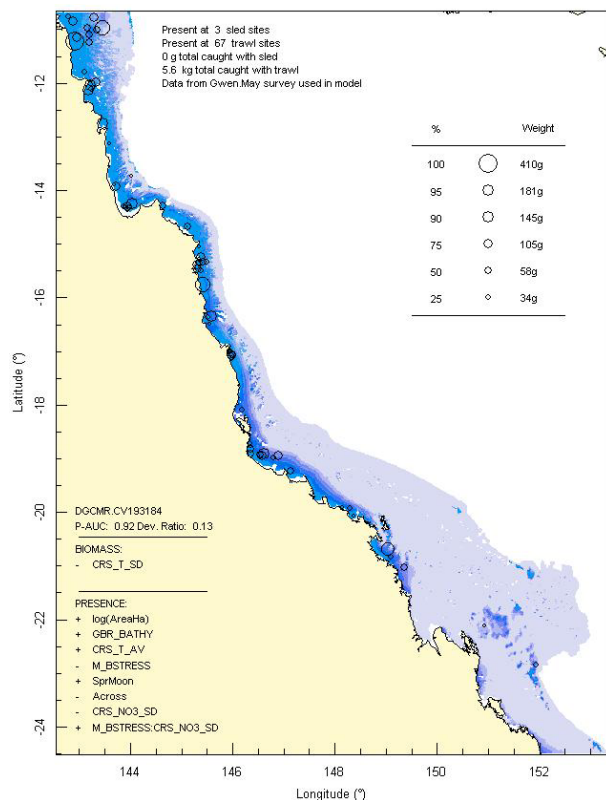
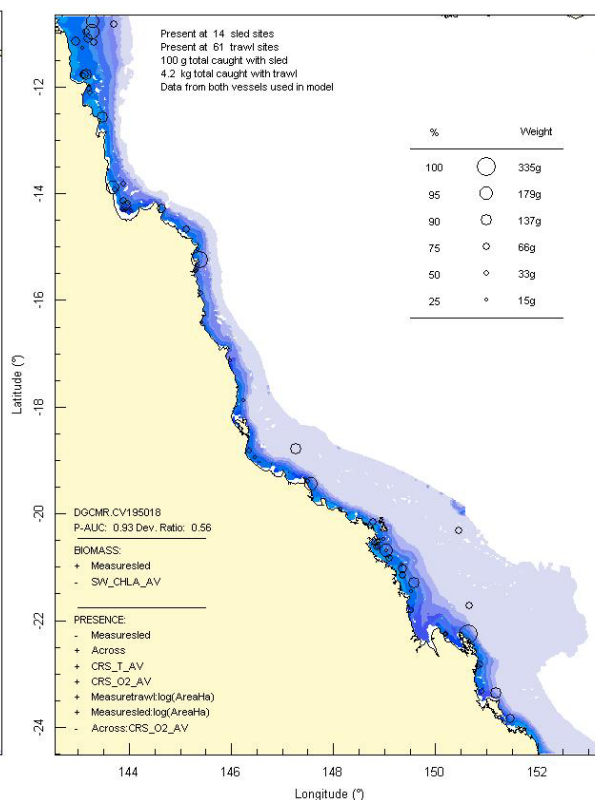


Figure 3-110: Model distribution maps of selected species with higher trawl exposure indicators.

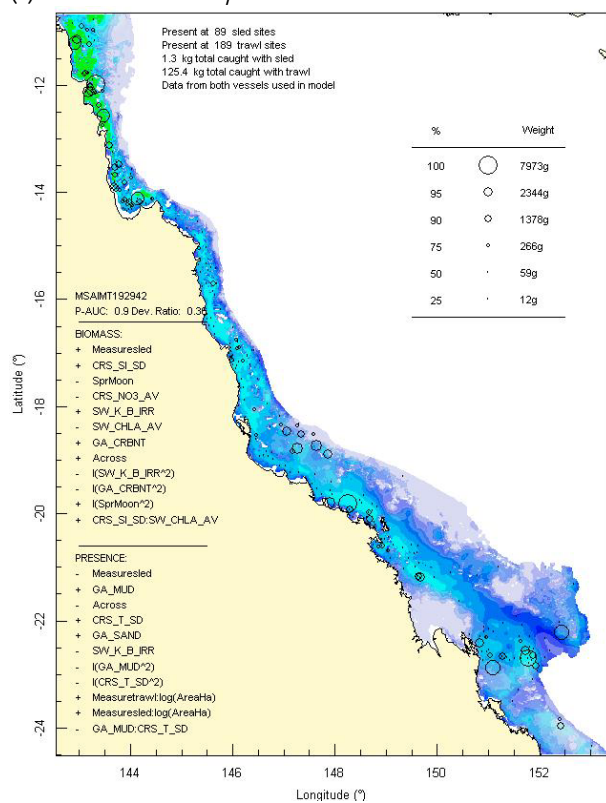
(a) Actinopterygii: *Callurichthys grossi*



(b) Actinopterygii: *Cynoglossus maculipinnis*



(c) Bivalvia: *Amusium pleuronectes* cf



(d) Bivalvia: *Melaxinaea vitrea*

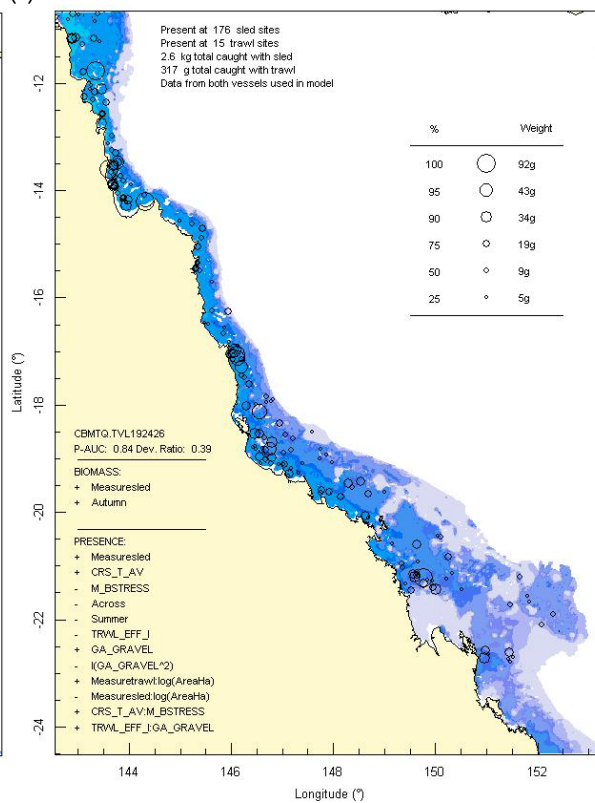
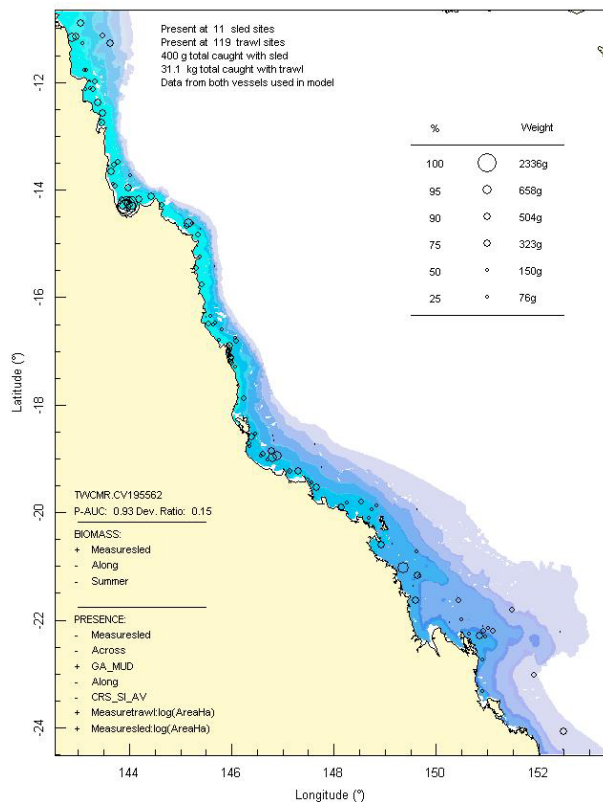
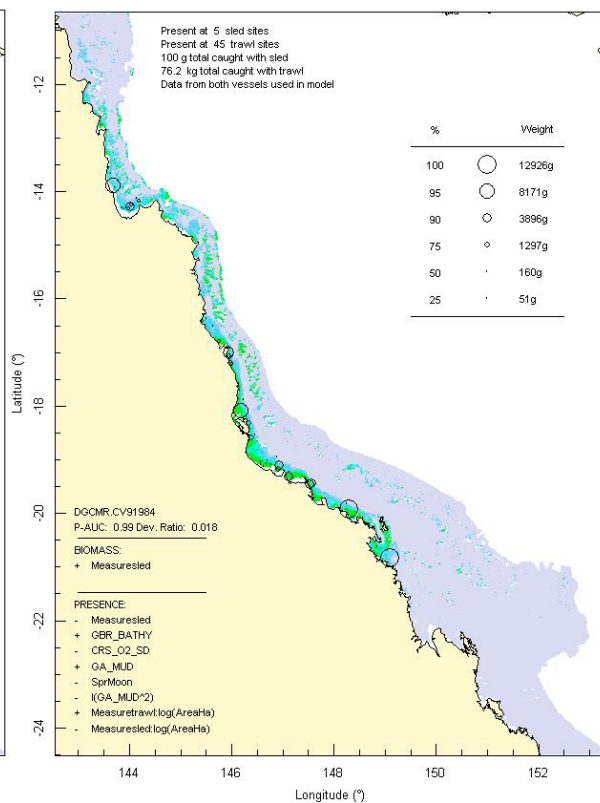


Figure 3-111: Model distribution maps of selected species with higher trawl exposure indicators.

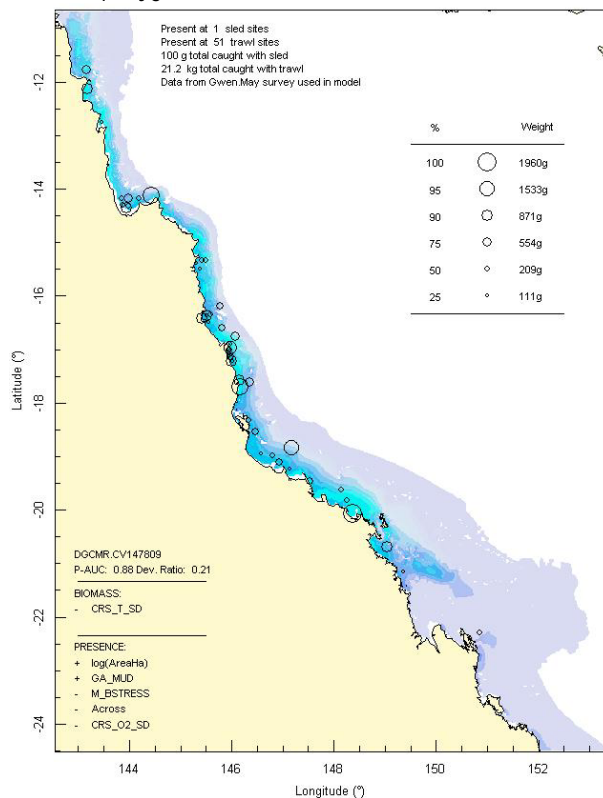
(a) Crustacea: *Thenus parindicus*



(b) Actinopterygii: *Leiognathus splendens*



(c) Actinopterygii: *Psettodes erumei*



(d) Actinopterygii: *Terapon theraps*

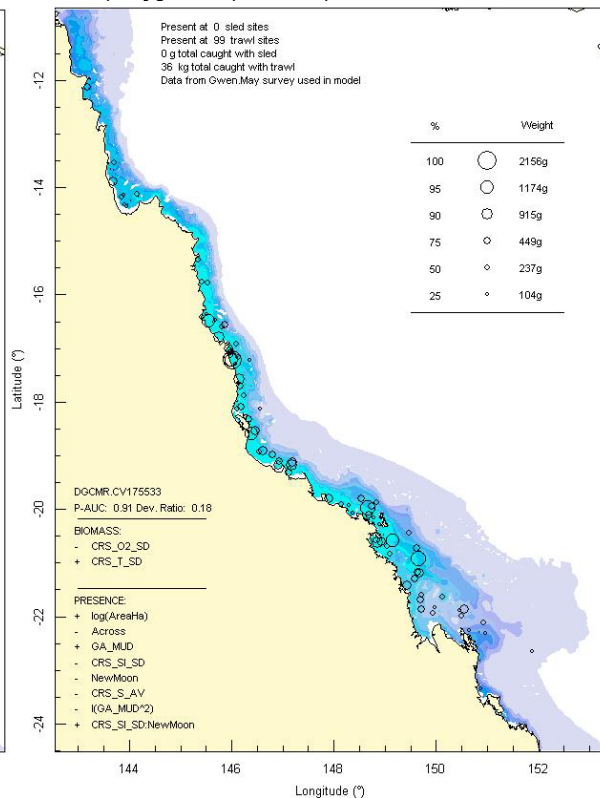
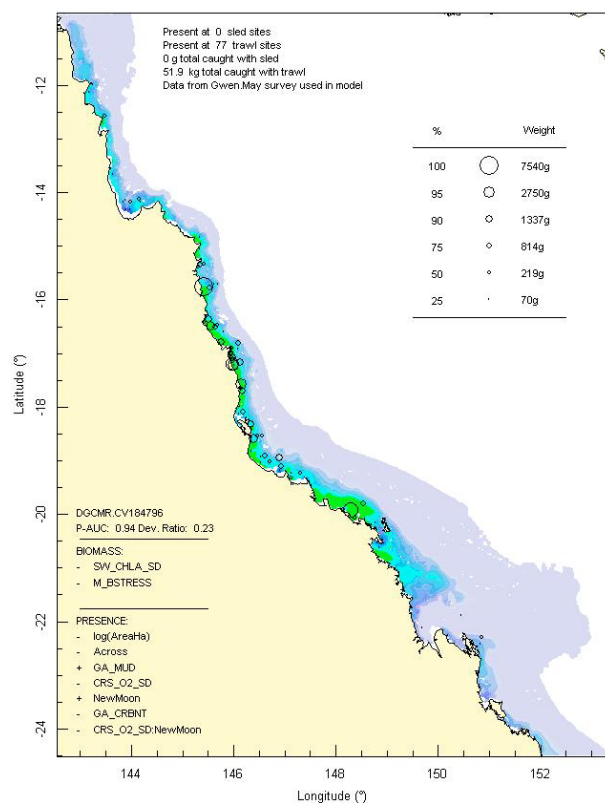
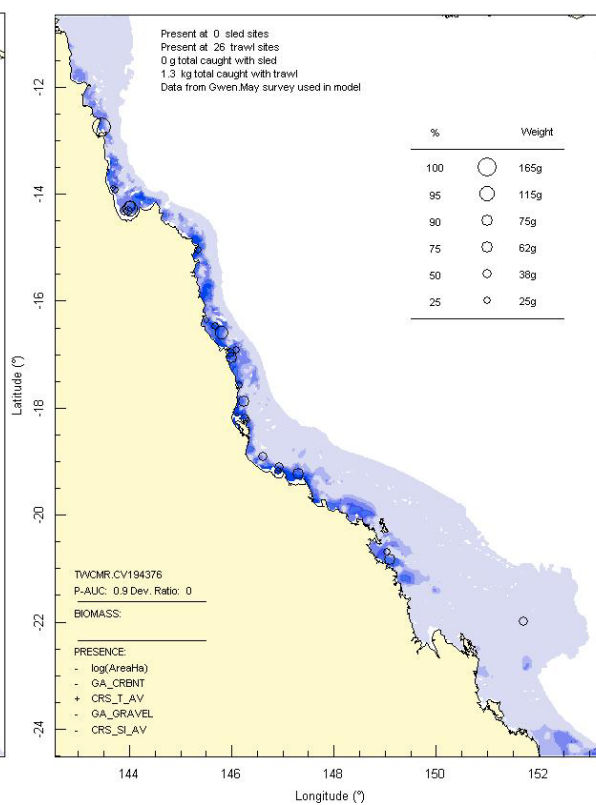
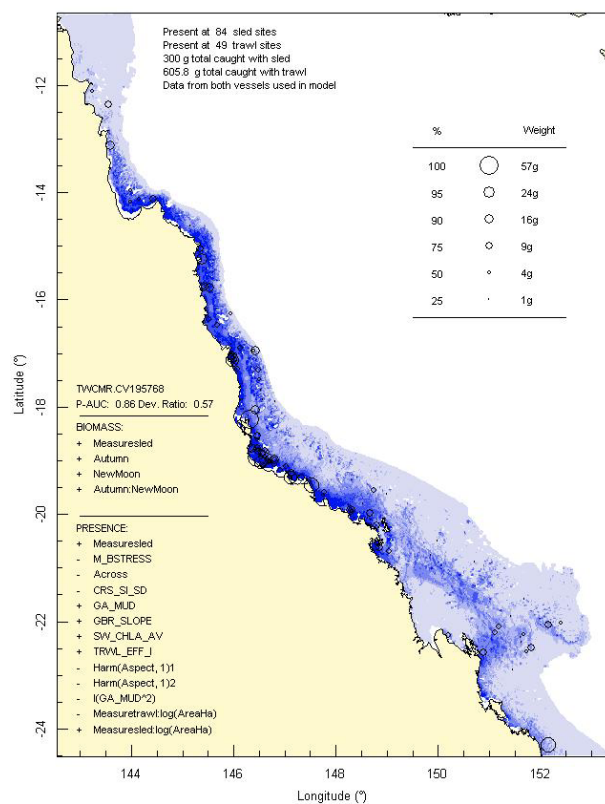
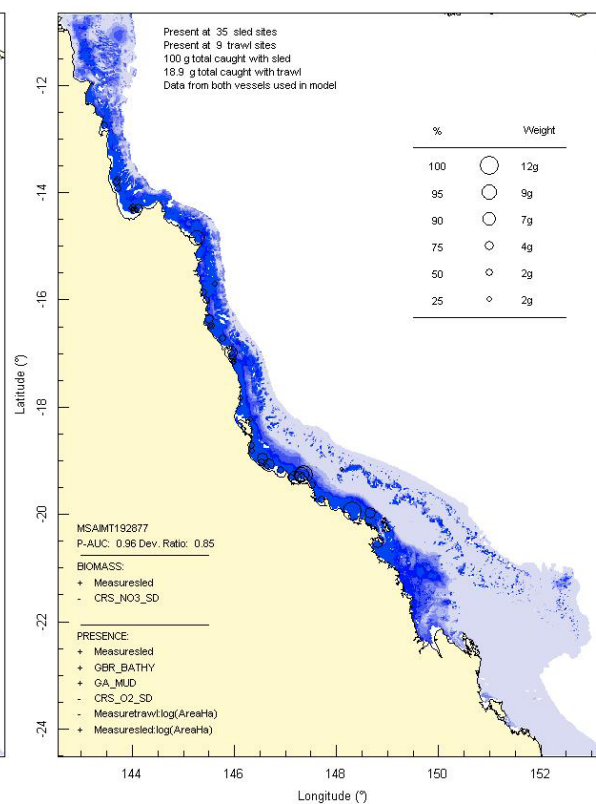
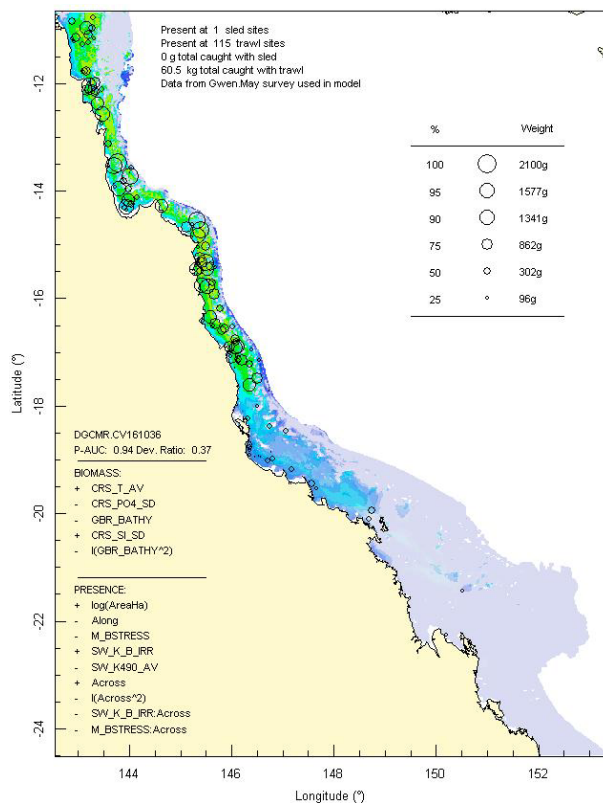


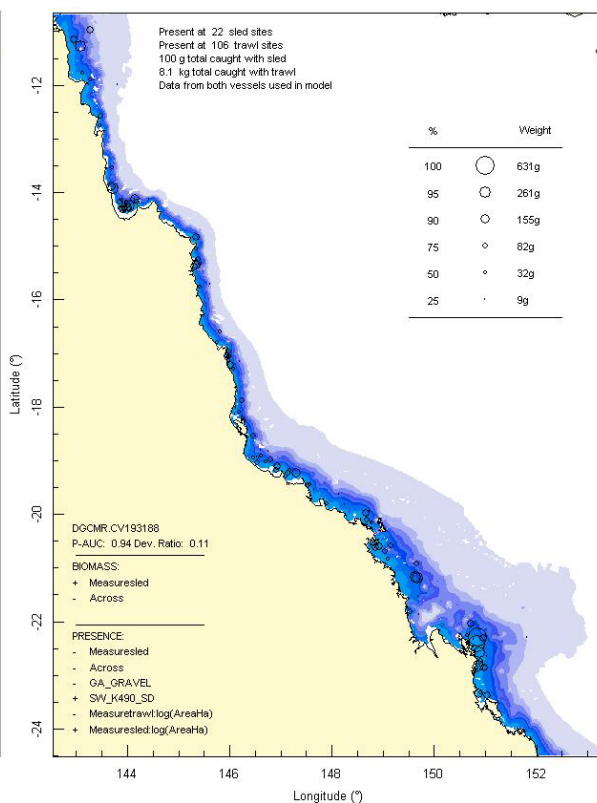
Figure 3-112: Model distribution maps of selected species with higher trawl exposure indicators.

(a) Actinopterygii: *Upeneus sulphureus*(b) Crustacea: *Erugosquilla woodmasoni*(c) Crustacea: *Myra tumidospina*(d) Gastropoda: *Nassarius cremmatus* cf**Figure 3-113:** Model distribution maps of selected species with higher trawl exposure indicators.

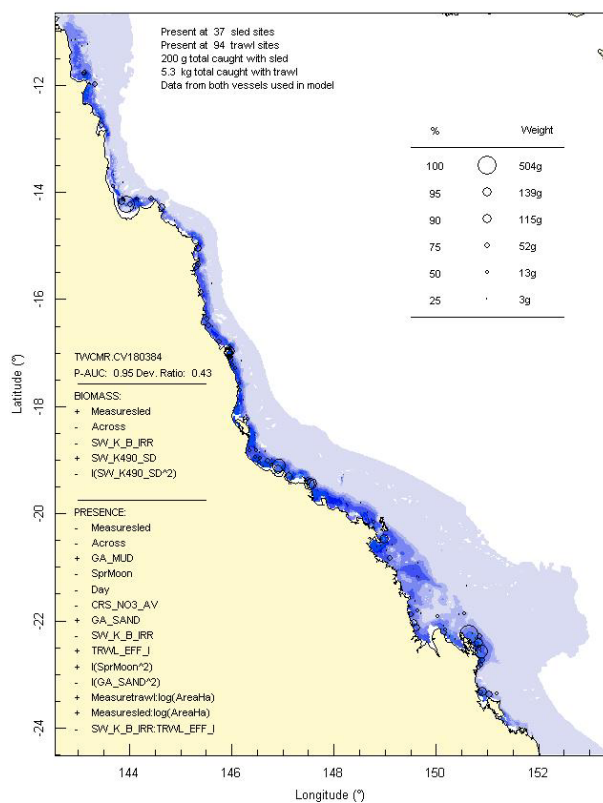
(a) Actinopterygii: *Scolopsis taeniopterus*



(b) Actinopterygii: *Repomucenus belcheri*



(c) Crustacea: *Trachypenaeus anchoralis*



(d) Actinopterygii: *Pelates quadrilineatus*

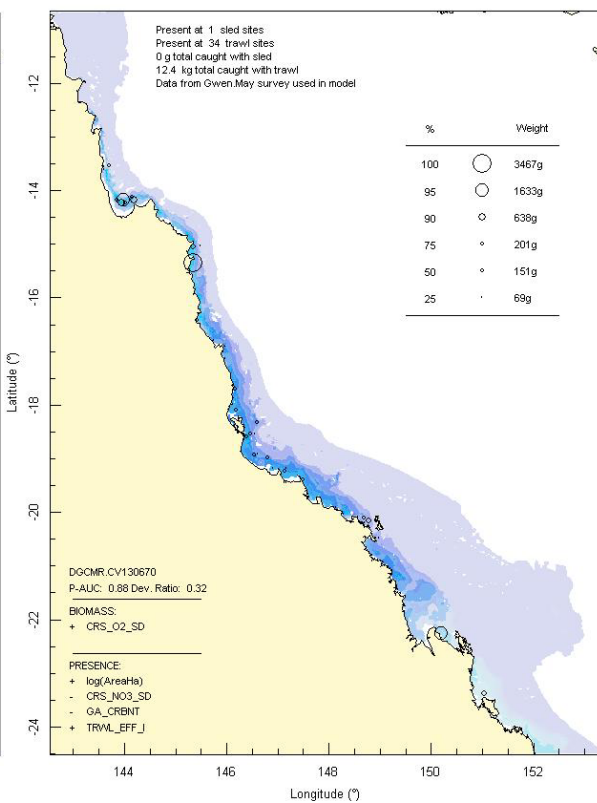
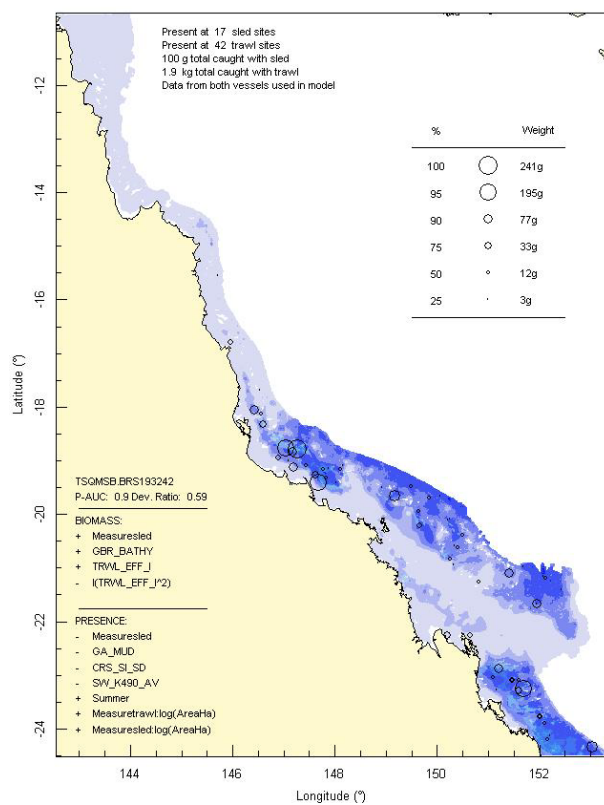
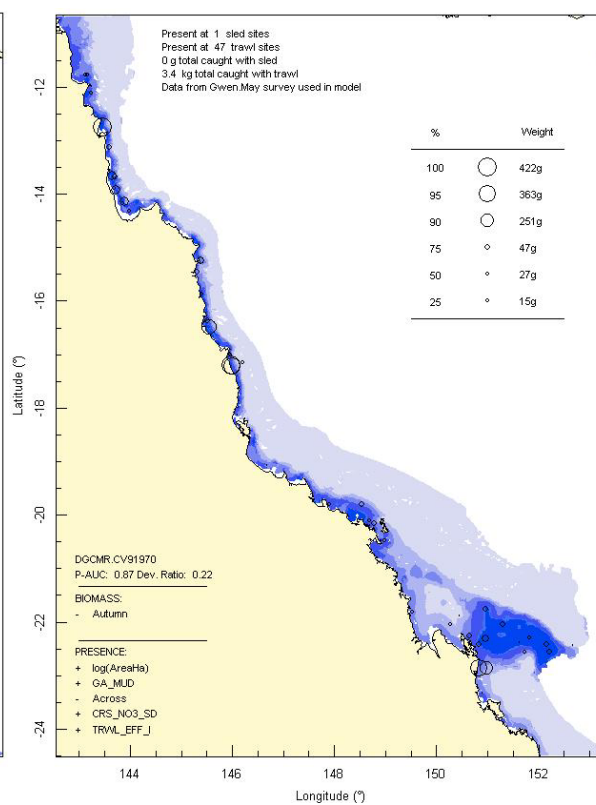
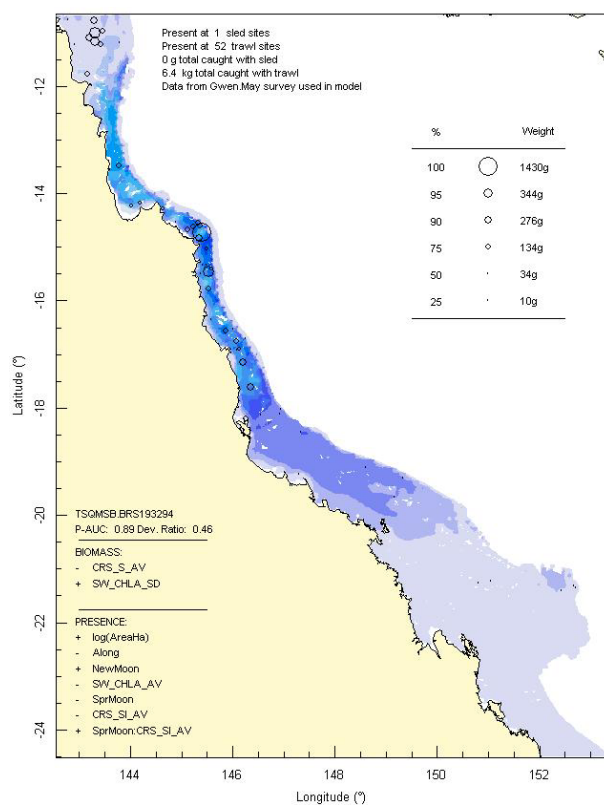
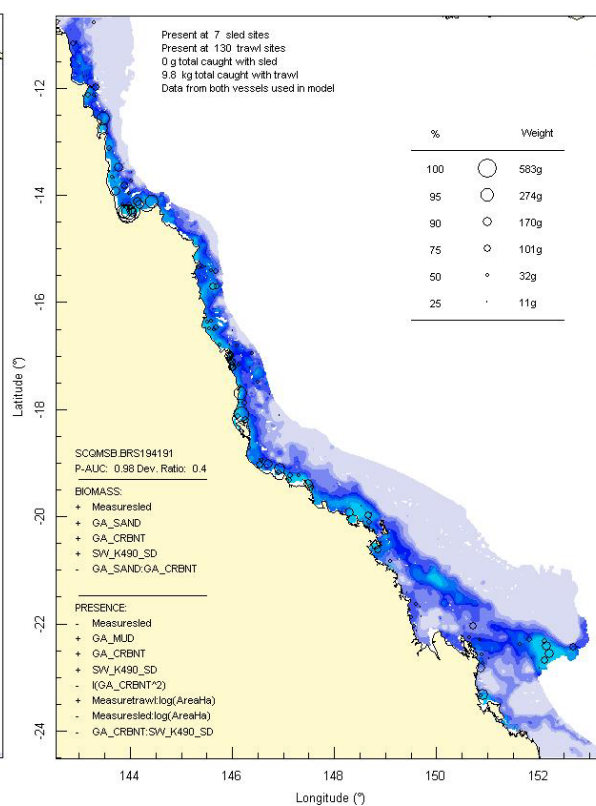


Figure 3-114: Model distribution maps of selected species with higher trawl exposure indicators.

(a) Actinopterygii: *Brachaluteres taylori*(b) Actinopterygii: *Leiognathus bindus*(c) Actinopterygii: *Yongeichthys nebulosus*(d) Actinopterygii: *Apogon poecilopterus***Figure 3-115:** Model distribution maps of selected species with higher trawl exposure indicators.

Modelling of the presences of BRUVS fishes provided distribution maps for a total of 25 species (Section 3.1.2), including 6 species that were infrequent in trawl data and not modelled, and 4 species were not sampled at all by the research trawl. The proportion of populations in GU zones for these 10 species ranged from 38–54%, the proportions in cells with recorded effort ranged from 20–33%, and proportions exposed to trawl effort ranged from 13–28%. These species in order of total effort exposure (%) included: *Gymnothorax minor* (28), *Alepes apercna* (27), *Scomberomorus queenslandicus* (27), *Echeneis naucrates* (26), *Carangoides coeruleopinnatus* (25), *Gnathanodon speciosus* (22), *Seriolina nigrofasciata* (19), *Carangoides gymnostethus* (19), *Decapterus russelli* (16) and *Carangoides fulvoguttatus* (13). As these species were rare or absent from the prawn trawl samples, it follows that their catchability was low or very low (as corroborated by relative catch rates of Fish Trawls from the Effects of Trawling Study, Poiner *et al.* 1998) and the proportions of their populations caught is likely to be considerably less than the proportions exposed.

In the case of those BRUVS fish species also analysed from research trawl data sources, the exposure assessments were similar and did not change the level of risk for any species — even though BRUVS were able to be deployed in areas too rugged for the trawl.

3.7.2.1. Trawl effort coefficients

The species modelling process selected the Trawl Effort Index covariate for 81 of 840 species analysed (9.6%), and was significant in 55 cases (6.5%). This frequency is little more than expected by chance and suggests that trawling does not have a strong influence on overall seabed distribution patterns. Nevertheless, taking each species model as an independent test, but recalling the caution expressed in Section 2.4.7, the probability of presence was negatively affected for 43 species, significant in 24 cases; biomass was negatively affected for 7 species, significant in each case (Table 3-54). Probability of presence was positively affected for 11 species, significant in all cases, and biomass was positively affected for 1 species, also significant (Table 3-55). Thirteen species had models with a second term involving the Trawl Effort covariate — in addition to a linear Trawl Effort term for presence or biomass — such as biomass, a quadratic or an interaction (Table 3-56).

The possible magnitude of the Trawl Effort coefficient where selected, in terms of predicted percent change in overall biomass, is also indicated in the Tables. Of the 50 negative Trawl Effort responses, five species (3 significant) were estimated to have moderate negative change in biomass of >25%–33%, compared with a model prediction with trawl effort set to zero over the entire region (Table 3-54). Another 15 species (9 significant) were estimated to have negative change in biomass of 15%–25%. The remaining 30 negative responses (19 significant) were between –1% and –15%. There was considerable uncertainty in these estimates. In the case of non-significant coefficients, the uncertainty was greater than the estimate and so includes the possibility of no (or even positive) change due to trawl effort. In the case of significant coefficients, the typical uncertainty was about 75% of the estimate. Not surprisingly, all species with negative trawl coefficients have low to very low exposure to current effort.

Species for which the negative trawl effect was larger and significant are examined in more detail below. The first point to note is that many of these species tended to be infrequent and low in abundance, which can present a challenge for the modelling. Further, while many of the AUC diagnostics were reasonable, the presence models for these species typically selected very few environmental covariates and the biomass models often did not select any environmental covariates — this tended to lead to rather smooth distribution predictions. On the other hand, those species with significant small negative coefficients (% change < -10%) were almost always more frequently sampled and more abundant, with more specific biophysical models.

The species with the largest significant predicted negative change (-33%) was the Majid crab *Thacanophrys* sp165 (Figure 3-116a). This species appears to have a widely scattered distribution in non-muddy environments, as indicated by the negative mud coefficient. Given the significant negative trawl coefficient, there was a statistical expectation that this species would have greater presence on

non-muddy seabeds in the absence of trawling. About three quarters of the estimated distribution of *Thacanophrys* sp165 was protected by the zoning and only ~3% annually was directly exposed to current effort.

Table 3-54: Results for the Trawl Effort covariate: species with negative coefficients for presence (P) or biomass (B), coefficients with $p>0.05$ are greyed, the magnitude of the coefficient in terms of overall % change in abundance is also indicated. The group membership, total estimated biomass (kg), % available, % exposed and effort exposed % are as above.

| Class | Genus | Species | Grp | Biomass | % Available | % Exposed | Effort Exp% | Model | Coefficient | p | % Change |
|----------------|---------------------------|-----------------------|-----|---------|-------------|-----------|-------------|-------|-------------|-------|----------|
| Crustacea | <i>Thacanophrys</i> | sp165 | 17 | 885 | 25 | 6 | 3 | P | -1.5918 | 0.021 | -33 |
| Anthozoa | <i>Euplexaura</i> | sp6 | 3 | 483859 | 36 | 15 | 9 | P | -0.7738 | 0.045 | -28 |
| Demospongiae | <i>Cinachyrella</i> | sp1 | 37 | 3327419 | 25 | 5 | 3 | P | -1.6453 | 0.084 | -27 |
| Crustacea | <i>Eucrate</i> | <i>affinis</i> | 13 | 2137 | 48 | 18 | 11 | P | -0.2340 | 0.029 | -27 |
| Ophiuroidea | <i>Ophioneis</i> | <i>semoni</i> cf | 15 | 7324 | 30 | 8 | 4 | P | -0.7199 | 0.064 | -26 |
| Bivalvia | <i>Solen</i> | sp3 | 13 | 35340 | 45 | 17 | 9 | P | -0.3686 | 0.066 | -25 |
| Demospongiae | <i>Demospongiae</i> | sp146 | 15 | 6870 | 31 | 9 | 5 | P | -0.5931 | 0.047 | -25 |
| Crustacea | <i>Pilumnus</i> | <i>spincarpus</i> | 15 | 1620 | 26 | 7 | 4 | P | -0.8290 | 0.042 | -24 |
| Anthozoa | <i>Echinogorgia</i> | sp5 | 23 | 11065 | 26 | 8 | 4 | P | -0.6230 | 0.088 | -22 |
| Anthozoa | <i>Iciligorgia</i> | sp1 | 17 | 129051 | 31 | 13 | 7 | P | -0.4120 | 0.039 | -20 |
| Crustacea | <i>Barnacle</i> | sp1 | 16 | 5009088 | 23 | 12 | 6 | P | -0.6110 | 0.035 | -20 |
| Demospongiae | <i>Oceanapia</i> | <i>tubes only</i> | 3 | 3664 | 33 | 13 | 7 | P | -0.2857 | 0.088 | -19 |
| Bivalvia | <i>Globivenus</i> | <i>embrithes</i> cf | 12 | 113931 | 42 | 15 | 9 | P | -0.2447 | 0.036 | -18 |
| Gymnolaemata | <i>Crassimarginatella</i> | spp | 31 | 222 | 27 | 14 | 8 | P | -0.5266 | 0.104 | -18 |
| Actinopterygii | <i>Lutjanus</i> | <i>vitta</i> | 20 | 316853 | 37 | 13 | 7 | P | -0.2158 | 0.066 | -18 |
| Demospongiae | <i>Demospongiae</i> | sp16 | 15 | 43858 | 34 | 12 | 7 | B | -0.2684 | 0.007 | -18 |
| Actinopterygii | <i>Siganus</i> | <i>canaliculatus</i> | 13 | 377618 | 42 | 19 | 12 | P | -0.1625 | 0.002 | -17 |
| Actinopterygii | <i>Apogon</i> | <i>cavitiensis</i> | 13 | 7972 | 47 | 22 | 14 | P | -0.1169 | 0.013 | -16 |
| Anthozoa | <i>Junceella</i> | sp2 | 16 | 137591 | 28 | 12 | 7 | P | -0.3584 | 0.066 | -16 |
| Gymnolaemata | <i>Telopora</i> | spp | 31 | 442 | 28 | 14 | 8 | P | -0.3682 | 0.049 | -16 |
| Astroidea | <i>Tamaria</i> cf | sp3 | 25 | 66687 | 43 | 20 | 12 | P | -0.1315 | 0.047 | -15 |
| Cephalopoda | <i>Loligo</i> | sp1 | 37 | 87486 | 30 | 11 | 6 | P | -0.2538 | 0.047 | -14 |
| Actinopterygii | <i>Sillago</i> | <i>ingenua</i> | 21 | 400298 | 48 | 24 | 16 | P | -0.1590 | 0.038 | -13 |
| Demospongiae | <i>Cinachyrella</i> | <i>australiensis</i> | 37 | 125583 | 20 | 5 | 3 | P | -0.5908 | 0.123 | -13 |
| Cephalopoda | <i>Photololigo</i> | sp1 | 35 | 126860 | 32 | 14 | 8 | P | -0.1871 | 0.066 | -12 |
| Anthozoa | <i>Echinogorgia</i> | sp3 | 23 | 110904 | 18 | 5 | 3 | P | -0.5701 | 0.196 | -12 |
| Actinopterygii | <i>Centrogenys</i> | <i>vaigiensis</i> | 3 | 20426 | 23 | 5 | 3 | P | -0.4504 | 0.245 | -11 |
| Crustacea | <i>Urnalana</i> | <i>whitei</i> | 12 | 41726 | 47 | 22 | 15 | P | -0.0797 | 0.033 | -11 |
| Crustacea | <i>Thalamita</i> | <i>intermedia</i> | 23 | 3456 | 22 | 8 | 4 | P | -0.3043 | 0.196 | -10 |
| Actinopterygii | <i>Paramonacanthus</i> | <i>oblongus</i> | 2 | 139092 | 41 | 20 | 13 | P | -0.0844 | 0.001 | -10 |
| Anthozoa | <i>Mopsella</i> | sp2 | 23 | 26395 | 24 | 9 | 5 | P | -0.2236 | 0.089 | -10 |
| Demospongiae | <i>Spirastrella</i> | sp2 | 15 | 528299 | 35 | 14 | 9 | P | -0.1009 | 0.044 | -9 |
| Crustacea | <i>Gonodactylaceus</i> | <i>graphurus</i> | 25 | 6851 | 49 | 26 | 18 | P | -0.0555 | 0.018 | -8 |
| Bivalvia | <i>Solen</i> | <i>siphons only</i> | 13 | 69535 | 49 | 23 | 16 | P | -0.0462 | 0.052 | -7 |
| Actinopterygii | <i>Upeneus</i> | <i>luzonius</i> | 20 | 584420 | 36 | 15 | 10 | P | -0.0705 | 0.058 | -7 |
| Crustacea | <i>Hyastenus</i> | <i>elatus</i> | 3 | 18772 | 33 | 13 | 8 | P | -0.0858 | 0.076 | -7 |
| Gymnolaemata | <i>Adeonella</i> | <i>lichenoides</i> cf | 17 | 84065 | 40 | 23 | 16 | P | -0.0554 | 0.008 | -6 |
| Astroidea | <i>Astropecten</i> | <i>zebra</i> | 20 | 12709 | 52 | 26 | 20 | B | -0.0274 | 0.000 | -6 |
| Actinopterygii | <i>Paramonacanthus</i> | <i>filicauda</i> | 24 | 8764207 | 39 | 11 | 7 | B | -0.0858 | 0.002 | -6 |
| Actinopterygii | <i>Choerodon</i> | <i>monostigma</i> | 12 | 285266 | 36 | 9 | 7 | P | -0.0711 | 0.157 | -6 |
| Crustacea | <i>Pandalidae</i> | sp916 | 15 | 11205 | 38 | 17 | 12 | P | -0.0580 | 0.022 | -5 |
| Chlorophyceae | <i>Udotea</i> | <i>orientalis</i> | 2 | 842312 | 34 | 16 | 10 | P | -0.0660 | 0.008 | -5 |
| Actinopterygii | <i>Lethrinus</i> | <i>genivittatus</i> | 10 | 6198005 | 45 | 24 | 17 | P | -0.0687 | 0.004 | -5 |
| Crustacea | <i>Lupocyclus</i> | <i>rotundatus</i> | 20 | 73747 | 44 | 21 | 17 | P | -0.0297 | 0.020 | -5 |
| Actinopterygii | <i>Lagocephalus</i> | <i>sceleratus</i> | 36 | 210666 | 44 | 22 | 17 | P | -0.0298 | 0.042 | -4 |
| Actinopterygii | <i>Apogon</i> | <i>truncatus</i> | 36 | 736274 | 42 | 20 | 17 | B | -0.0175 | 0.000 | -3 |
| Actinopterygii | <i>Rogadius</i> | <i>pristiger</i> | 35 | 447881 | 34 | 14 | 14 | P | -0.0225 | 0.078 | -3 |
| Annelida | <i>Annelida</i> | spp | 20 | 5213418 | 42 | 21 | 19 | B | -0.0183 | 0.008 | -2 |
| Anthozoa | <i>Dendronephthya</i> | spp | 18 | 1302022 | 29 | 13 | 10 | B | -0.0196 | 0.003 | -2 |
| Astroidea | <i>Astropecten</i> | spp | 20 | 76778 | 45 | 26 | 29 | B | -0.0414 | 0.009 | -1 |

The species with the second largest significant predicted negative change (-28%) was the gorgonian *Euplexaura* sp6 (Figure 3-116b). Like all gorgonians, this species tended to be associated with harder seabed; also indicated by the positive gravel coefficient. Given the significant negative trawl coefficient, there is a statistical expectation that this species would have greater presence on gravel seabeds in the absence of trawling, probably on patches of biogenic hard substratum. Almost two thirds of the estimated distribution of *Euplexaura* sp6 was protected by the zoning and only ~9% annually was directly exposed to current effort.

The species with the third largest significant predicted negative change (-27%) was the decapod crustacean *Eucrete affinis* (Figure 3-116c). This species appeared to have a widely scattered inner shelf but not inshore distribution. Again, given the significant negative trawl coefficient, there was a statistical expectation that this species would have greater presence on inner shelf seabeds in the absence of trawling. About 52% of the estimated distribution of *Eucrete affinis* was protected by the zoning and only 11% annually was directly exposed to current effort.

The species with the next largest significant predicted negative change (-25%) was Demospongiae sp146 (Figure 3-116d). This species appeared to have a very low predicted biomass (lowest colour from key everywhere) and, with no spatial variables other than effort, a very broad predicted distribution. Again, given the significant negative trawl coefficient, there was a statistical expectation that this species would have greater presence on the seabed in the absence of trawling. About 69% of the estimated distribution of Demospongiae sp146 was protected by the zoning and only ~5% annually was directly exposed to current effort.

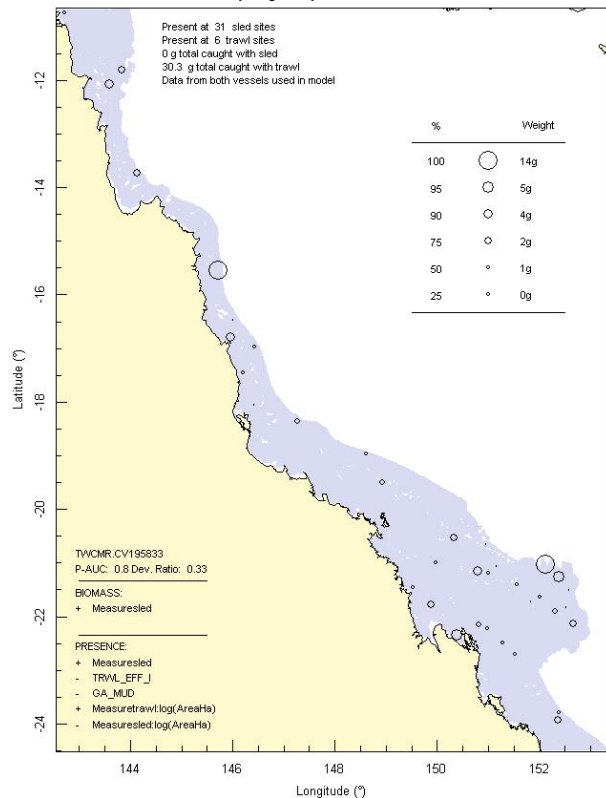
The species with the next largest predicted negative change (-24%) was the Xanthid crab *Pilumnus spinicarpus* (Figure 3-117a). This species appeared to have a very low predicted biomass (lowest colour from key ~everywhere). Again, given the significant negative trawl coefficient, there was a statistical expectation that this species would have greater presence on the seabed in the absence of trawling. About 74% of the estimated distribution of *Pilumnus spinicarpus* was protected by the zoning and only ~4% annually was directly exposed to current effort.

The species with the next largest predicted negative change (-20%) was the gorgonian *Iciligorgia* sp1 (Figure 3-117b). Like other gorgonians, this species was expected to be associated with harder seabed; and was predicted to be widely scattered in non-muddy seabeds. Given the significant negative trawl coefficient, there is a statistical expectation that this species would have greater presence on such seabeds in the absence of trawling, probably on patches of biogenic hard substratum. About 69% of the estimated distribution of *Iciligorgia* sp1 was protected by the zoning and only ~7% annually was directly exposed to current effort.

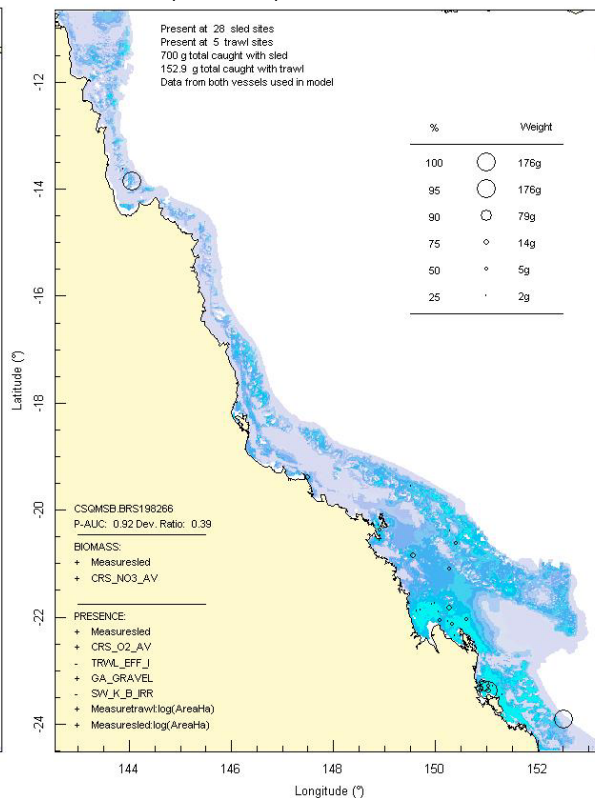
The species with the next largest predicted negative change (-21%) was an unidentified Barnacle sp1 (Figure 3-117c). This species appeared to have a more specific distribution in non-muddy carbonate gravel in the southern GBR and with the significant negative trawl coefficient, a statistical expectation of greater presence on these types of seabeds in the absence of trawling. About 77% of the estimated distribution of Barnacle sp1 was protected by the zoning and only ~6% annually was directly exposed to current effort.

The species with the next largest predicted negative change (-18%) was the bivalve *Globivenus embrithes* cf (Figure 3-117d). This species appeared to be associated with inshore low effort areas seabeds primarily in the southern GBR. Again, given the significant negative trawl coefficient, there is a statistical expectation that this species would have greater presence on such seabeds in the absence of trawling. About 58% of the estimated distribution of *Globivenus embrithes* cf was protected by the zoning and only ~9% annually was directly exposed to current effort.

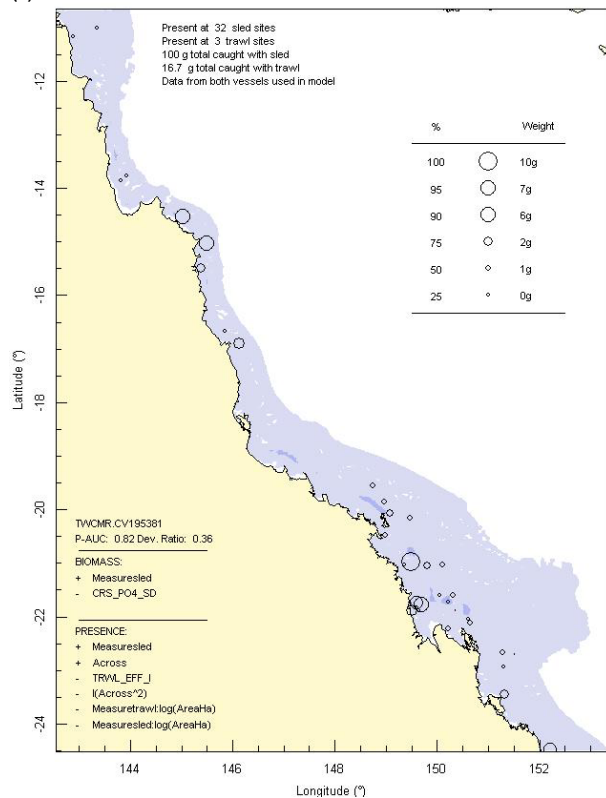
(a) Crustacea: *Thacanophrys* sp165



(b) Anthozoa: *Euplexaura* sp6.



(c) Crustacea: *Euclate affinis*



(d) Demospongiae: Demospongiae sp146

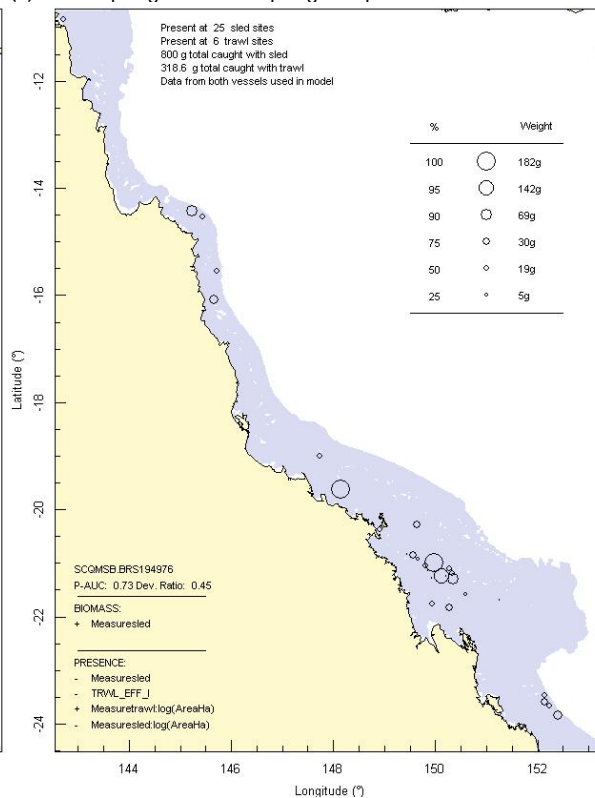
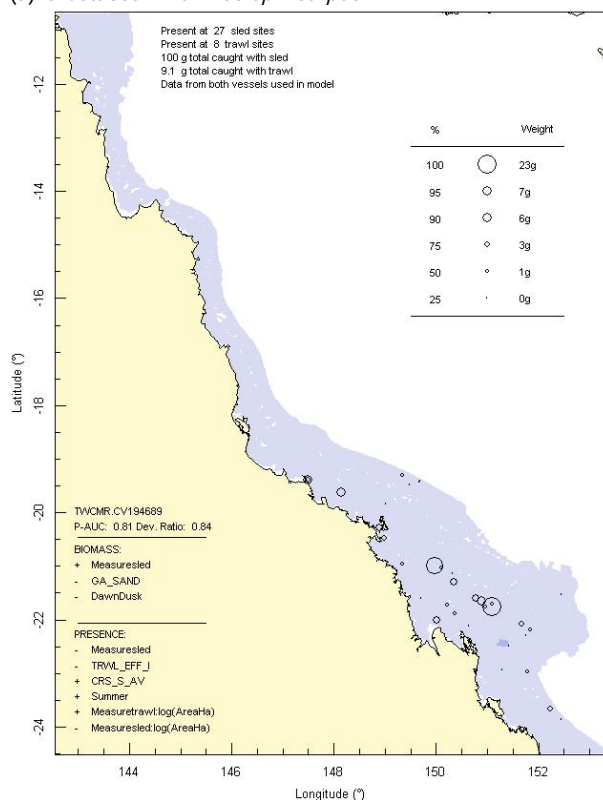
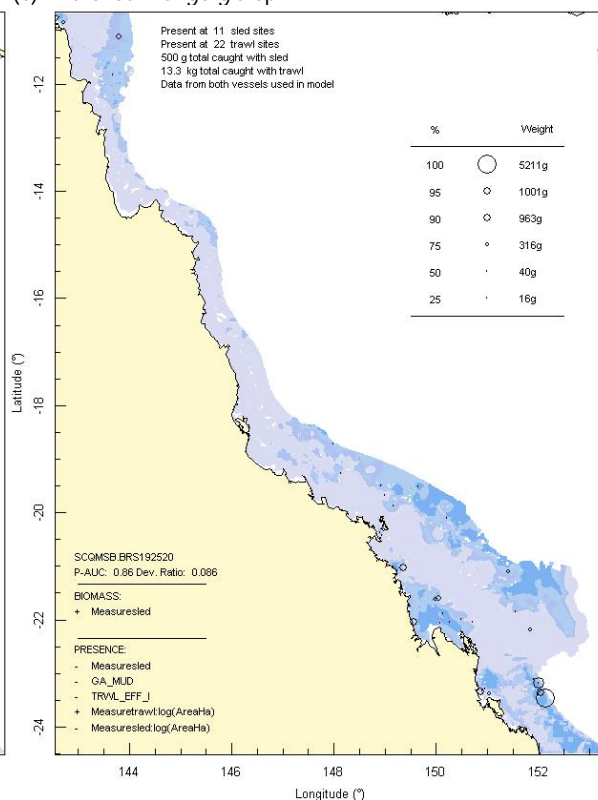
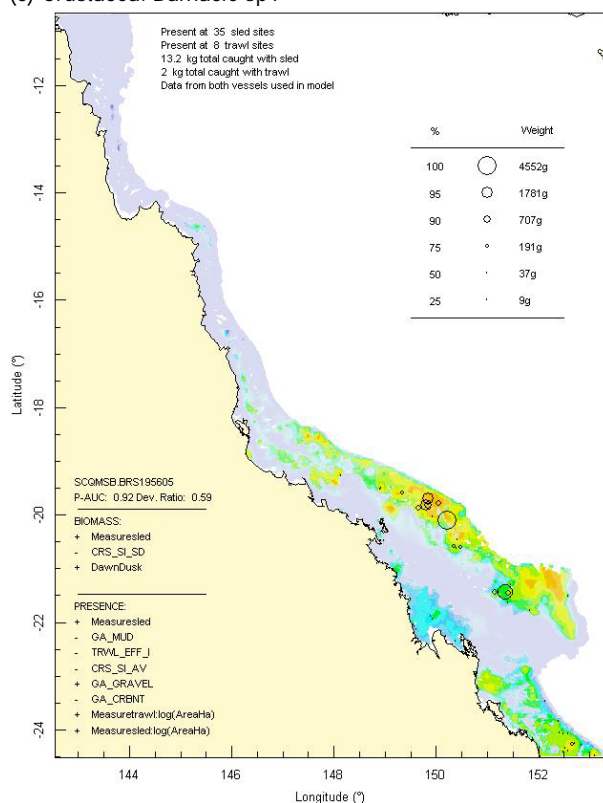
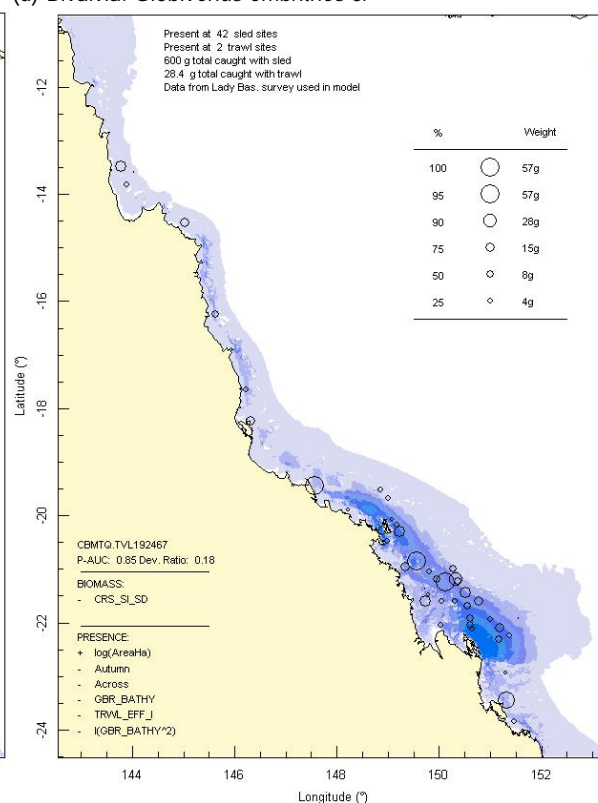


Figure 3-116: Model distribution maps of selected species with significant larger negative trawl coefficients.

(a) Crustacea: *Pilumnus spinicarpus*(b) Anthozoa: *Iciligorgia* sp1

(c) Crustacea: Barnacle sp1

(d) Bivalvia: *Globivenus embrithes* cf**Figure 3-117:** Model distribution maps of selected species with significant larger negative trawl coefficients.

The 12 positive Trawl Effort responses were relatively smaller, four species (all significant) were estimated to have positive change in biomass of >12%–19%, compared with a model prediction with trawl effort set to zero over the entire region (Table 3-55). The remaining 8 positive responses (all significant) were between >0% and +10%. The typical uncertainty in these estimates was about 70%

of the estimate. Not surprisingly, many species with positive trawl coefficients have high to very high exposure to current effort and most were highlighted in the previous section. Species for which the positive trawl effect was larger are examined in more detail below. The first point to note is that most of these species were sampled relatively frequently (though not necessarily abundant) and had relatively strong presence and biomass models.

The species with the largest predicted positive change (+19%) was the Pilumnid crab *Cryptolutea arafurensis* (Figure 3-108b above). This species was moderately frequent in sled samples and appeared to be common on muddy (but not extremely) seabeds. Given the significant positive trawl coefficient, there was a statistical expectation that this species would have lower presence on such seabeds in the absence of trawling. About 43% of the estimated distribution of *Cryptolutea arafurensis* was protected by the zoning but a high proportion of its biomass in GU zones was in high effort areas leading to an annual direct exposure to current effort of 128%.

The species with the second largest predicted positive change (+18%) was the Terapontid fish *Pelates quadrilineatus* (Figure 3-114d). This species was the least frequent of this group and appeared to be widely scattered on inshore substratums of terrestrial origin (low carbonate). Given the significant positive trawl coefficient, there was a statistical expectation that this species would have lower presence on such seabeds in the absence of trawling. About 31% of the estimated distribution of *Pelates quadrilineatus* was protected by the zoning but a high proportion of its biomass in GU zones was in high effort areas leading to an annual direct exposure to current effort of 103%.

The species with the third largest predicted positive change (+13%) was the Gerreid fish *Pentaprion longimanus* (Figure 3-108d). This species was moderately frequent in trawl samples and appeared to be common on intermediate carbonate muddy seabeds, mostly inner-shelf. Given the significant positive trawl coefficient, there was a statistical expectation that this species would have lower presence on such seabeds in the absence of trawling. About 38% of the estimated distribution of *Pentaprion longimanus* was protected by the zoning but a high proportion of its biomass in GU zones was in high effort areas leading to an annual direct exposure to current effort of 117%.

The species with the next largest predicted positive change (+12%) was the bivalve scallop *Amusium balloti* (Figure 3-118a). This species was very frequent in sled and trawl samples and was often abundant on sandy seabed in the southern GBR. Given the significant positive trawl coefficient, there was a statistical expectation that this species would have lower presence in these areas in the absence of trawling; however, given also that this scallop is also a target species, a plausible alternative explanation is that the searching ability of fisherman — as represented by the effort data — are a better indicator of the sampled distribution of scallops at a scale finer than that of spatial patterns in the physical environmental data, rather than indicating that scallops are more abundant because of trawling. About 45% of the estimated distribution of *Amusium balloti* was protected by the zoning and a somewhat high proportion of the biomass in GU zones lies in higher effort areas leading to an annual direct exposure to current effort of 45%.

The species with the next largest predicted positive change (+10%) was the Leiognathid ponyfish *Leiognathus leuciscus* (Figure 3-110b). This species was moderately frequent in trawl samples and appeared to be common on inshore substratums of terrestrial origin (low carbonate) on the northern two-thirds of the GBR. Given the significant positive trawl coefficient, there was a statistical expectation that this species would have lower presence on such seabeds in the absence of trawling. About 41% of the estimated distribution of *Leiognathus leuciscus* was protected by the zoning but a high proportion of its biomass in GU zones was in high effort areas leading to an annual direct exposure to current effort of 95%.

The species with the next largest predicted positive change (+9%) was another Leiognathid ponyfish *Leiognathus bindus* (Figure 3-115b). This species was moderately infrequent in trawl samples and appeared to be common on muddy substratums mostly inshore but extending offshore in the Capricorn Channel. Given the significant positive trawl coefficient, there was a statistical expectation that this species would have lower presence on such seabeds in the absence of trawling. About 58% of the estimated distribution of *Leiognathus bindus* was protected by the zoning but a somewhat higher proportion of its biomass in GU zones was in high effort areas leading to an annual direct exposure to current effort of 63%.

The Gastropod, *Xenophora indica* had a predicted positive change of +8% and was moderately frequent in sled and trawl samples and appeared to be common on clearer sandy seabeds, distributed offshore in the southern half of the GBR (Figure 3-118b). Again, given the significant positive trawl coefficient, there was a statistical expectation that this species would have lower presence on such seabeds in the absence of trawling. About 56% of the estimated distribution of *Xenophora indica* was protected by the zoning and its biomass in trawled GU zones had an annual direct exposure to current effort of 30%.

Another notable species in this group is the commercial western king prawn, *Penaeus latisulcatus*, which was moderately frequent in trawl samples at sites in clear shallow sandy areas particularly in the southernmost GBR (Figure 3-118c). With a significant positive trawl coefficient corresponding to predicted positive change of 6%, there was a statistical expectation that this species would have lower presence in these areas in the absence of trawling. However, like scallops, this prawn is also a target species and the same alternative explanation cannot be excluded. About 41% of the estimated distribution of *Penaeus latisulcatus* was protected by the zoning and a somewhat high proportion of the biomass in GU zones lies in higher effort areas leading to an annual direct exposure to current effort of 49%.

The Leucosiid crab, *Myra tumidospina* had a predicted positive change of +6% and was relatively frequent in sled and trawl samples and appeared to be common in muddy high-chlorophyll areas, primarily in inshore region along much of the GBR but also in some muddy offshore areas (Figure 3-113c). Again, given the significant positive trawl coefficient, there was a statistical expectation that this species would have lower presence on such seabeds in the absence of trawling. About 43% of the estimated distribution of *Myra tumidospina* was protected by the zoning but a somewhat higher proportion of its biomass in GU zones was in high effort areas leading to an annual direct exposure to current effort of 60%.

The Xanthid crab, *Liagore rubromaculata* had a predicted positive change of +5% and was moderately frequent in trawl and sled samples and appeared to be common in muddy high-chlorophyll areas, primarily on deeper muddy substratums mostly inshore but extending offshore in the Capricorn Channel (Figure 3-118d). Again, given the significant positive trawl coefficient, there was a statistical expectation that this species would have lower presence on such seabeds in the absence of trawling. About 52% of the estimated distribution of *Liagore rubromaculata* was protected by the zoning but a somewhat higher proportion of its biomass in GU zones was in high effort areas leading to an annual direct exposure to current effort of 43%.

Table 3-55: Results for the Trawl Effort covariate: species with positive coefficients for presence (P) or biomass (B), coefficients with $p > 0.05$ are greyed, the magnitude of the coefficient in terms of overall % change in abundance is also indicated. The group membership, total estimated biomass (kg), % available, %exposed and effort exposed are as above.

| Class | Genus | Species | Group | Biomass | % Available | % Exposed | Effort Exp% | Model | Coefficient | p | % Change |
|----------------|--------------------|-----------------------|-------|---------|-------------|-----------|-------------|-------|-------------|-------|----------|
| Crustacea | <i>Cryptolitea</i> | <i>arafurensis</i> | 29 | 480 | 57 | 41 | 128 | P | 0.0213 | 0.001 | 19 |
| Actinopterygii | <i>Pelates</i> | <i>quadrilineatus</i> | 21 | 129842 | 69 | 47 | 103 | P | 0.0299 | 0.001 | 18 |
| Actinopterygii | <i>Pentaprion</i> | <i>longimanus</i> | 29 | 61963 | 62 | 48 | 117 | P | 0.0189 | 0.048 | 13 |
| Bivalvia | <i>Amusium</i> | <i>balloti</i> | 10 | 2355308 | 55 | 37 | 45 | B | 0.0424 | 0.003 | 12 |
| Actinopterygii | <i>Leiognathus</i> | <i>leuciscus</i> | 9 | 171753 | 59 | 43 | 95 | P | 0.0235 | 0.026 | 10 |
| Actinopterygii | <i>Leiognathus</i> | <i>bindus</i> | 24 | 76017 | 42 | 28 | 63 | P | 0.0279 | 0.003 | 9 |
| Gastropoda | <i>Xenophora</i> | <i>indica</i> | 8 | 25049 | 44 | 27 | 30 | P | 0.0451 | 0.000 | 7 |
| Crustacea | <i>Penaeus</i> | <i>latisulcatus</i> | 21 | 235627 | 59 | 39 | 49 | P | 0.0265 | 0.004 | 6 |
| Crustacea | <i>Myra</i> | <i>tumidospina</i> | 22 | 14791 | 57 | 38 | 60 | P | 0.0169 | 0.006 | 6 |
| Crustacea | <i>Liagore</i> | <i>rubromaculata</i> | 29 | 49419 | 48 | 25 | 43 | P | 0.0275 | 0.001 | 5 |
| Actinopterygii | <i>Elates</i> | <i>ransonnetii</i> | 24 | 431203 | 30 | 12 | 17 | P | 0.0213 | 0.038 | 1 |
| Rhodophyceae | <i>Haloplegma</i> | <i>duperreyi</i> | 1 | 3474678 | 44 | 24 | 20 | P | 0.0392 | 0.004 | 0 |

In the case of the 15 species with more complex responses to the Trawl Effort covariate involving an additional term, the magnitude and direction varied widely and could not be inferred simply from the

coefficients (Table 3-56). Seven species were estimated to have significant negative change in biomass of -5% to -36% and five species were estimated to have significant positive change in biomass of +4% to +96%, compared with a model prediction with trawl effort set to zero over the entire region. The typical uncertainty in these estimates was about 70% of the estimate. As before, species predicted to had a positive change with trawling had moderately high to high exposure to current effort, while species with a negative change had low to very low exposure. Six species with the largest effects are examined in more detail below.

The species with the largest predicted positive change (+96%) was the Monacanthid fish *Brachaluteres taylori* (Figure 3-115a). This species was not uncommon in trawl samples at sites in shallow clear non-muddy areas, particularly in the southern half of the GBR, with intermediate intensity of trawl effort. With a positive trawl effort term and a negative squared term for the biomass model, giving an overall large positive predicted trawl effect, there was a statistical expectation that this species would have lower presence on those types of seabeds in the absence of trawling. About 29% of the estimated distribution of *Brachaluteres taylori* is protected by the zoning and 72% annually is directly exposed to current effort.

The species with the second largest predicted positive change (+50%) was the commercial grooved tiger prawn, *Penaeus semisulcatus* (Figure 3-108a). This species was common in trawl samples at sites in shallow muddy (but not extreme) low-light inshore areas, mostly in the northern two-thirds of the GBR, with intermediate intensity of trawl effort. With a positive trawl effort term and a negative squared term for the biomass model, giving an overall large positive predicted trawl effect, there was a statistical expectation that this species would have lower presence on those types of seabeds in the absence of trawling. About 26% of the estimated distribution of *Penaeus semisulcatus* was protected by the zoning and a high proportion of its biomass in GU zones was in high effort areas leading to an annual direct exposure to current effort of 174%. Like *Penaeus latisulcatus* and *Amusium balloti* discussed above, *Penaeus semisulcatus* is also a target species and the same alternative explanation cannot be excluded. The negative Biomass:Trawl_Eff² term was indicative of reduced standing biomass at very high levels of effort.

The species with the largest predicted negative change (-36%) was a gorgonian soft coral *Carijoa* sp1 (Figure 3-119a). This species appeared to have a widely scattered patchy distribution and with a negative trawl effort term for both the presence and the biomass model giving a strong negative predicted trawl effect, there is a statistical expectation that this species would have higher abundance in the absence of trawling. Three-quarters of the estimated distribution of *Carijoa* sp1 was protected by the zoning and only ~3% annually is directly exposed to current effort.

The species with the next largest predicted change (-27%) was *Inegocia harrisii* (a Platycephalid fish) (Figure 3-119b). This species was common at sites in low-light inshore areas, particularly in the vicinity of the very high tidal range areas of Shoalwater Bay, Broad Sound and the Whitsunday Islands. With a negative trawl effort term for both the presence and the biomass model, giving an overall negative predicted trawl effect, there was a statistical expectation that this species would have higher abundance on those types of seabeds in the absence of trawling. About 78% of the estimated distribution of *Inegocia harrisii* was protected by the zoning and only ~3% annually was directly exposed to current effort.

The species with the next largest predicted change (-26%) was the sediment infaunal sponge *Oceanapia* sp21 (Figure 3-119c). This species was not uncommon in sled samples at widely scattered sites in clear intermediate-gravel areas (mostly mid-to-outer shelf). With a negative trawl effort term and a positive effort*gravel interaction term in the presence model, giving an overall negative predicted trawl effect, there was a statistical expectation that this species would have higher abundance on those types of seabeds in the absence of trawling. It is possible that the interaction indicates that the negative trawl effect is less as gravel increases. About 75% of the estimated distribution of *Oceanapia* sp21 was protected by the zoning and only 3% annually was directly exposed to current effort.

The species with the next largest predicted change (-20%) was the Majid crab *Austrolabidia gracilipes* (Figure 3-119d). This species was not uncommon in sled samples at particularly off Mackay and the Whitsunday Islands, with scattered records elsewhere. With a positive trawl effort term and a negative effort*temp_SD interaction term in the presence model, giving an overall negative predicted trawl effect, there was a statistical expectation that this species would have higher abundance in the region

in the absence of trawling. It was possible that the interaction indicates that the negative trawl effect is greater where temperature is more variable. About two-thirds of the estimated distribution of *Austrolabidia gracilipes* was protected by the zoning and only 7% annually was directly exposed to current effort.

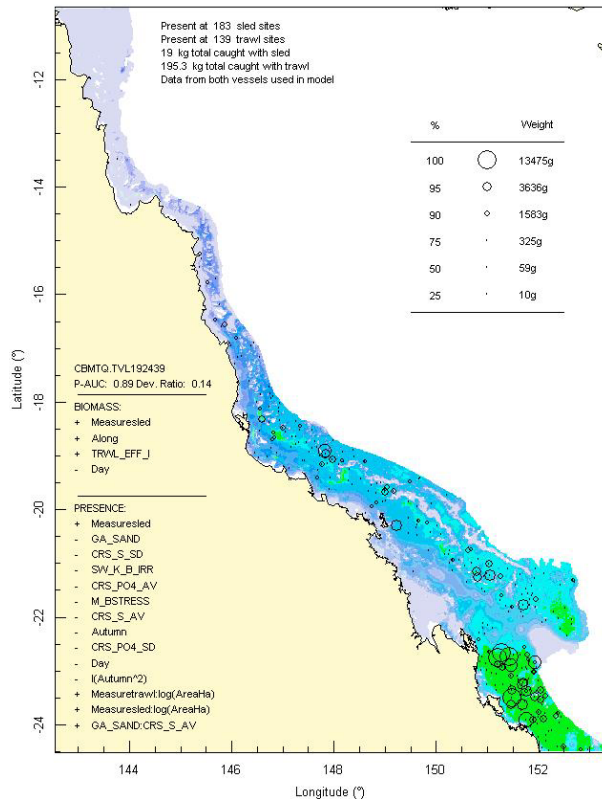
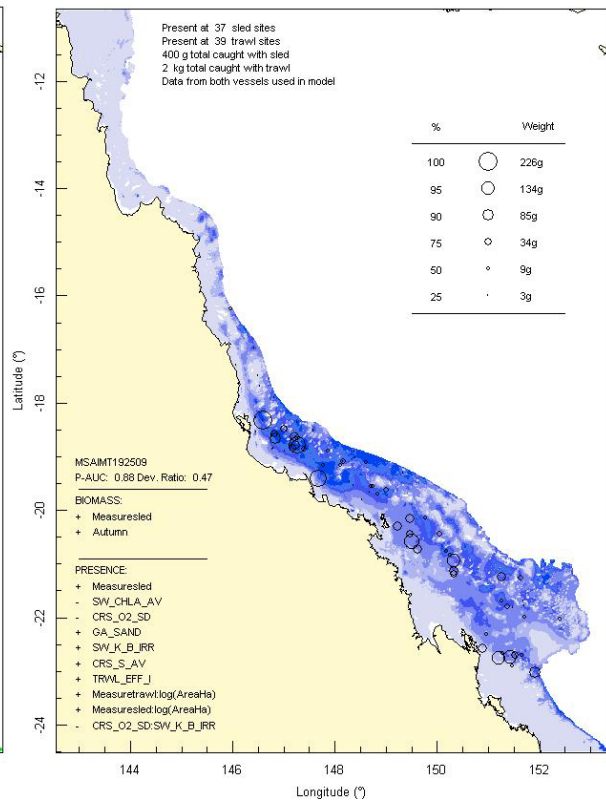
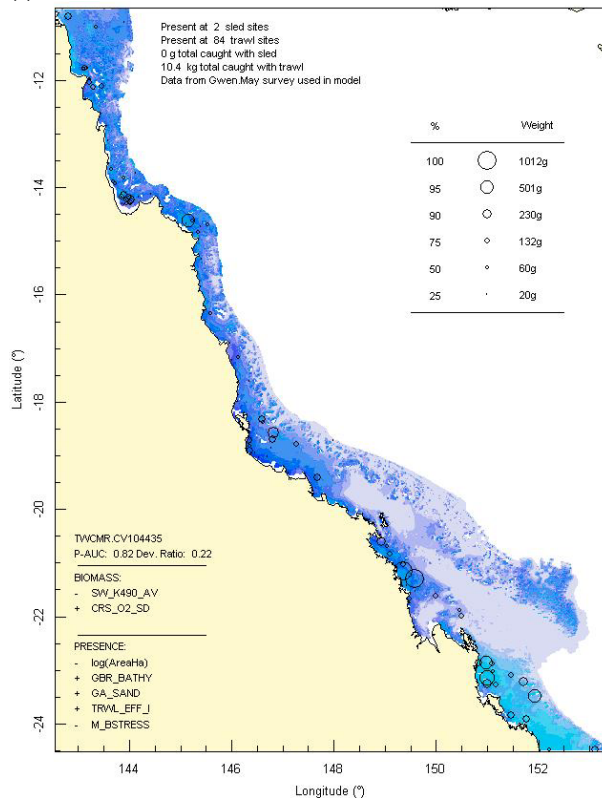
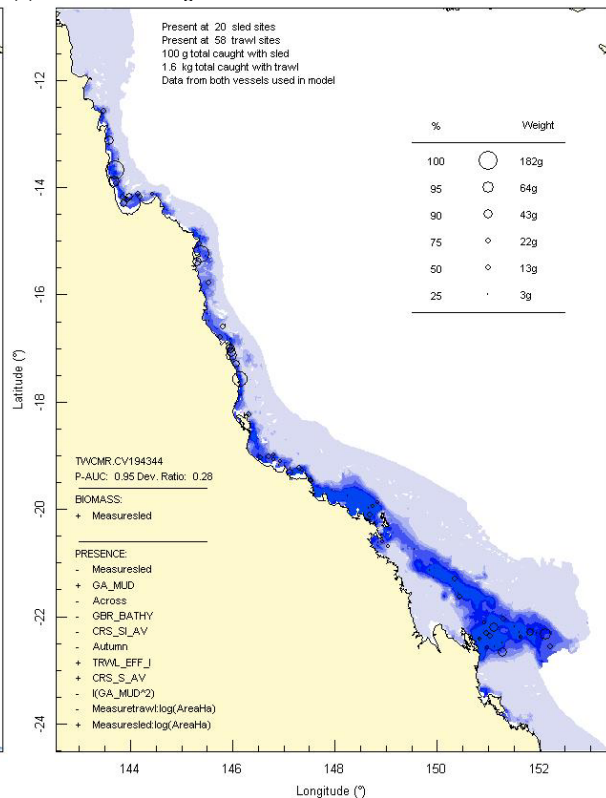
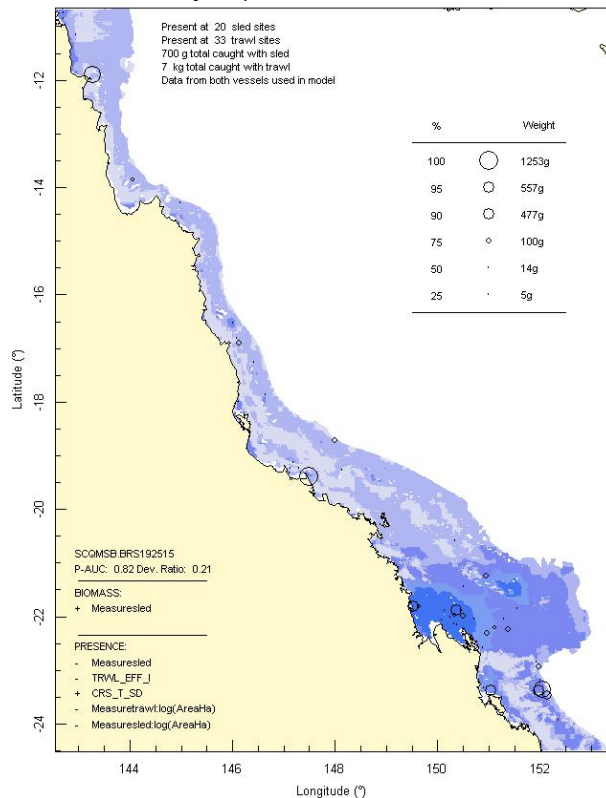
(a) Bivalvia: *Amusium balloti*(b) Gastropoda: *Xenophora indica*(c) Crustacea: *Penaeus latissulcatus*(d) Crustacea: *Liagore rubromaculata*

Figure 3-118: Model distribution maps of selected species with significant larger positive trawl coefficients.

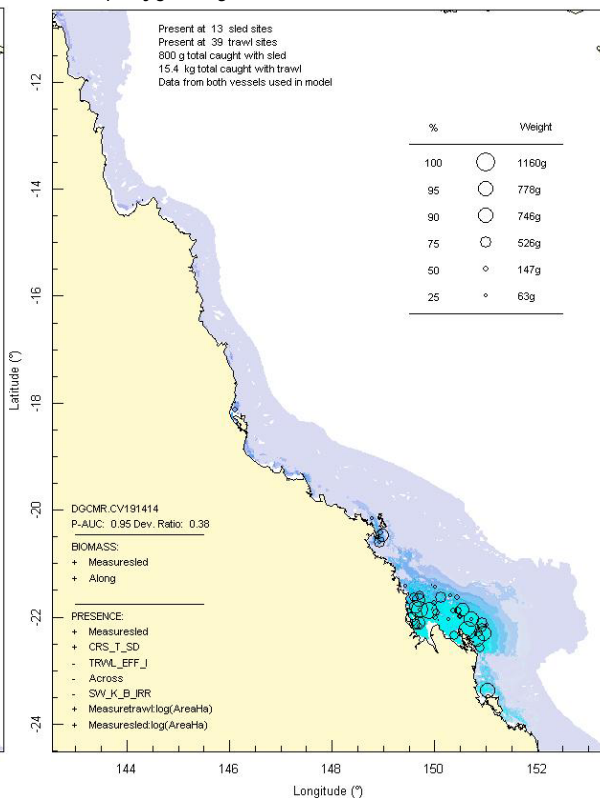
Table 3-56: Results for the Trawl Effort covariate: species with an additional term involving the Trawl Effort covariate, as well as coefficients for presence (P) or biomass (B), coefficients with $p > 0.05$ are grayed, the magnitude of the coefficient in terms of overall % change in abundance is also indicated. The group membership, total estimated biomass (kg), % available, % exposed and effort exposed are as above.

| Class | Genus | Species | Group | Biomass kg | % Available | % Exposed | Effort Exp % | Model | Trawl Effort Coefficient | p | Second term | Coefficient | p | % Change |
|----------------|----------------------|---------------------|-------|------------|-------------|-----------|--------------|-------|--------------------------|-------|-----------------------|-------------|-------|----------|
| Actinopterygii | <i>Brachaluteres</i> | <i>taylori</i> | 8 | 62129 | 71 | 60 | 72 | B | 0.2436 | 0.000 | I(TRWL_EFF_I^2) | -0.0047 | 0.001 | 96 |
| Crustacea | <i>Penaeus</i> | <i>semisulcatus</i> | 29 | 301314 | 74 | 64 | 174 | B | 0.0513 | 0.000 | I(TRWL_EFF_I^2) | -0.0004 | 0.004 | 50 |
| Crustacea | <i>Portunus</i> | <i>gracilimanus</i> | 9 | 204641 | 59 | 38 | 86 | P | 0.0154 | 0.009 | biomass: TRWL_EFF_I | 0.0148 | 0.001 | 11 |
| Actinopterygii | <i>Saurida</i> | <i>grandi/undo</i> | 21 | 8331858 | 59 | 37 | 46 | P | 0.0348 | 0.031 | biomass: TRWL_EFF_I | 0.0116 | 0.009 | 7 |
| Bivalvia | <i>Melaxinaea</i> | <i>vitrea</i> | 9 | 171979 | 59 | 38 | 63 | P | -0.0002 | 0.980 | TRWL_EFF_I:GA_GRAVEL | 0.0022 | 0.008 | 6 |
| Crustacea | <i>Trachypenaeus</i> | <i>anchoralis</i> | 13 | 45119 | 64 | 44 | 67 | P | 0.0773 | 0.001 | SW_K_B_IRR:TRWL_EFF_I | -0.4881 | 0.008 | 4 |
| Actinopterygii | <i>Pentapodus</i> | <i>paradiseus</i> | 18 | 2615371 | 34 | 16 | 11 | P | 0.1900 | 0.007 | TRWL_EFF_I:SW_CHLA_AV | -0.5093 | 0.001 | -5 |
| Demospongiae | Demospongiae | sp109 | 37 | 119911 | 25 | 6 | 4 | P | 0.3294 | 0.001 | TRWL_EFF_I:GA_CRBNT | -0.0106 | 0.001 | -10 |
| Crustacea | Pagurid | sp2358-1 | 13 | 15945 | 44 | 20 | 18 | P | 0.0693 | 0.024 | Across:TRWL_EFF_I | -1.1173 | 0.002 | -16 |
| Echinoidea | <i>Mespilia</i> | <i>globulus</i> | 30 | 22836 | 12 | 3 | 2 | P | 0.1490 | 0.464 | GA_GRAVEL:TRWL_EFF_I | -0.1363 | 0.008 | -17 |
| Crustacea | <i>Austrolabidia</i> | <i>gracilipes</i> | 3 | 12992 | 33 | 12 | 7 | P | 0.7857 | 0.006 | CRS_T_SD:TRWL_EFF_I | -0.7849 | 0.006 | -20 |
| Crustacea | <i>Cloridina</i> | <i>chlorida</i> | 14 | 374 | 29 | 3 | 2 | P | 0.0578 | 0.569 | M_BSTRESS:TRWL_EFF_I | -20.8768 | 0.124 | -22 |
| Demospongiae | <i>Oceanapia</i> | sp21 | 37 | 5236461 | 25 | 5 | 3 | P | -2.3602 | 0.010 | TRWL_EFF_I:GA_GRAVEL | 0.0539 | 0.011 | -26 |
| Actinopterygii | <i>Inegocia</i> | <i>harrisii</i> | 3 | 217420 | 22 | 5 | 3 | P | -0.5655 | 0.010 | biomass: TRWL_EFF_I | -0.4681 | 0.001 | -27 |
| Anthozoa | <i>Carrijoa</i> | sp1 | 3 | 78340 | 25 | 5 | 3 | P | -0.6098 | 0.004 | biomass: TRWL_EFF_I | -1.4558 | 0.006 | -36 |

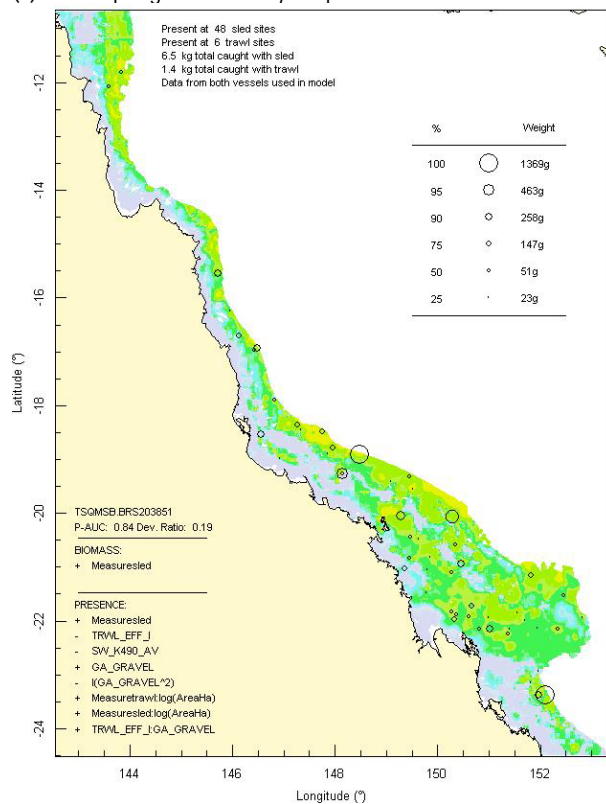
(a) Anthozoa: *Carijoa* sp1



(b) Actinopterygii: *Inegocia harrisii*



(c) Demospongiae: *Oceanapia* sp21



(d) Crustacea: *Austrolabidia gracilipes*

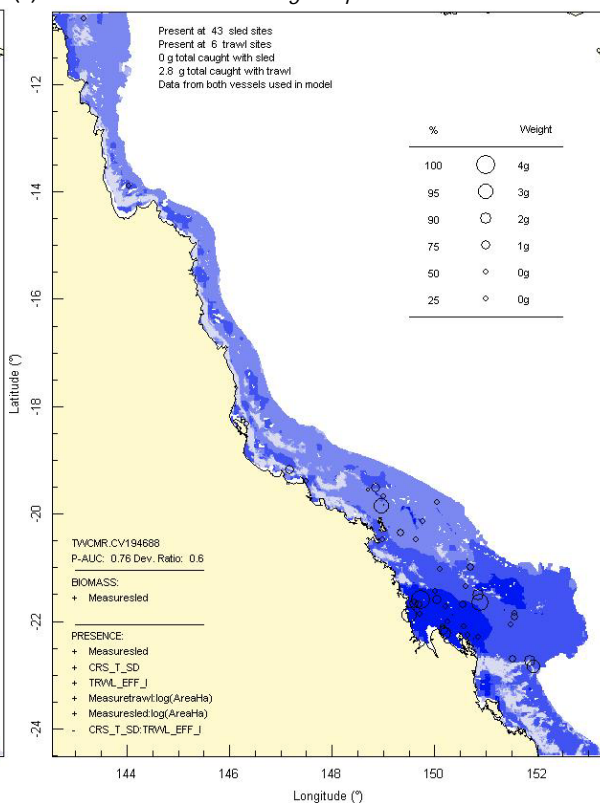


Figure 3-119: Model distribution maps of selected species with multiple trawl coefficients.

The trawl effort covariate was included in all 25 BRUVS fish species presence models, although significance tests were not possible, and the potential population change due to the influence of trawling was estimated for all species. Most (16) of the estimated changes were small ($\leq \pm 5\%$) and most (18) were positive. The largest negative estimates were for *Carangoides fulvoguttatus* (-9%) and *Abalistes stellatus* (-8). The largest estimated changes were all positive: *Nemipterus peronii* (17%), *Gymnothorax minor* (17%), *Parapercis nebulosa_grp* (16%), *Paramonacanthus otisensis* (11%), *Echeneis naucrates* (11%), *Lagocephalus sceleratus* (10%). Of the above named species, only *Carangoides fulvoguttatus*, *Echeneis naucrates* and *Gymnothorax minor* were not assessed from the research trawl data; however, the uncertainty in these estimates from BRUVS is unknown.

3.7.2.2. Species exposure rank, catchability, and recovery indicators

The species exposure estimates from the previous sections were tabulated and ranked in order of most exposed to trawl effort intensity (Table 3-57). This exposure ranking is the primary output of the Seabed Project with respect to risk indicators for the trawl fishery in the GBR region. All of those species with effort exposure $>50\%$ have been discussed above, as well as several with exposure $<50\%$. In this section, these exposure rankings were developed further with additional information from the Project and/or from external sources. By multiplying the effort exposure by the relative catch rate and BRD effect (if appropriate), an estimate of the percentage of population caught annually is tabulated (Table 3-57). Note that this estimate is not a true ‘catchability’ and there has not been a formal analysis of catchability as part of this Project. Where data from both sled and trawl was included in the modelling for a given species the coefficient of the device term was taken (indicated by “Model” in the table) and the range of \pm SE was taken as an indicator of the uncertainty. Where model coefficients were not available at the species level, the mean of genus level coefficients was taken (indicated by “MdlGen” in the table) and similarly for the uncertainty. If model coefficients were not available, a simple ratio of average catch rates between devices, at the species or genus level (“Mean” or “MnGen” respectively), was used. If there was evidence that a fish trawl net had a higher catch rate in the earlier “Green Zone Effects of Trawling Study” then a simple ratio of average catch rates from that source, again at the species or genus level (“GZFsh” or “GZMn” respectively), was used. Often, there was considerable variability in relative catch rate among sources, which was taken as an indicator of uncertainty where the model result was not available. The estimated relative catch rate usually was less than 1 and the estimated percentage of populations caught annually was usually less than the estimated percentage exposed to trawl effort. The estimated effect of relative catch rate varied widely among species and substantially altered the ranking of species potentially at risk in terms of estimated percentage caught. At this point, the highest ranked species was the Pleuronectiform flatfish *Brachirus muelleri* (~110% caught), followed by other small fishes *Terapon puta* (59%), *Saurida argentea/tumbil* (58%), *Psettodes erumei* (52%) and the commercial prawn *Penaeus semisulcatus* (55%). Of the 33 species with effort exposure $>50\%$, only 5 had $>50\%$ caught and 19 had $<25\%$ caught (Table 3-57). Of the 218 species with effort exposure between 25% and 50%, only 19 had $>25\%$ caught and 199 had $<25\%$ caught (Table 3-57). While these estimates of potential relative incidental (or in some cases target) catch make a critical contribution to understanding potential environmental risk, they do not provide a definitive indication of sustainability risk. For this, some indication of population recovery (the propensity for the population to replenish) is required.

Information on potential population recovery that was available were the “recovery” rankings for fishes from the NPF Bycatch Sustainability Project approach (Stobutzki *et al.* 2001) and for invertebrates from the NPF Ecological Surrogates Project (Hill *et al.* 2002). Where recovery ranks were available, weighted mean added ranks were tabulated (Table 3-57) for matching fish species genera. In the case of invertebrates, recovery ranks were available at the family level only. Low ranks (1.5–1.875, shaded red) indicate lower relative potential recovery and high ranks (2.65–3.0, not shaded) indicate higher relative potential recovery (low-moderate 1.875–2.25 and moderate 2.25–2.65 ranks are shaded orange and pale respectively). The available mean recovery rank for 422 species was plotted against the estimated percentage of population caught (Figure 3-120). The species at greatest relative risk should plot towards the upper left quadrant of the graph. The top ranking species were: *Brachirus muelleri*, *Sepia pharaonis*, *Terapon puta*, *Saurida argentea/tumbil*, *Penaeus semisulcatus*, *Euristhmus nudiceps*, *Apogon poecilopterus*, *Sepia elliptica*, *Scolopsis taeniopterus*, *Psettodes erumei*,

Amusium pleuronectes cf, *Tripodichthys angustifrons*, *Saurida grandi/undo*, *Yongeichthys nebulosus*, *Sepia whitleyana*, *Upeneus sundaicus*, *Leiognathus leuciscus*, *Sepia smithi*, *Portunus gracilimanus*, *Chaetodermis penicilligera* and *Sepia plangon* (see species distribution maps Figure 3-108 to Figure 3-115 above and Figure 3-121, Figure 3-122 below). While these species have higher relative risk on the basis of their recovery attributes, such that management attention as to their future status is warranted, it is nevertheless unclear whether these species are currently at sustainability risk or not.

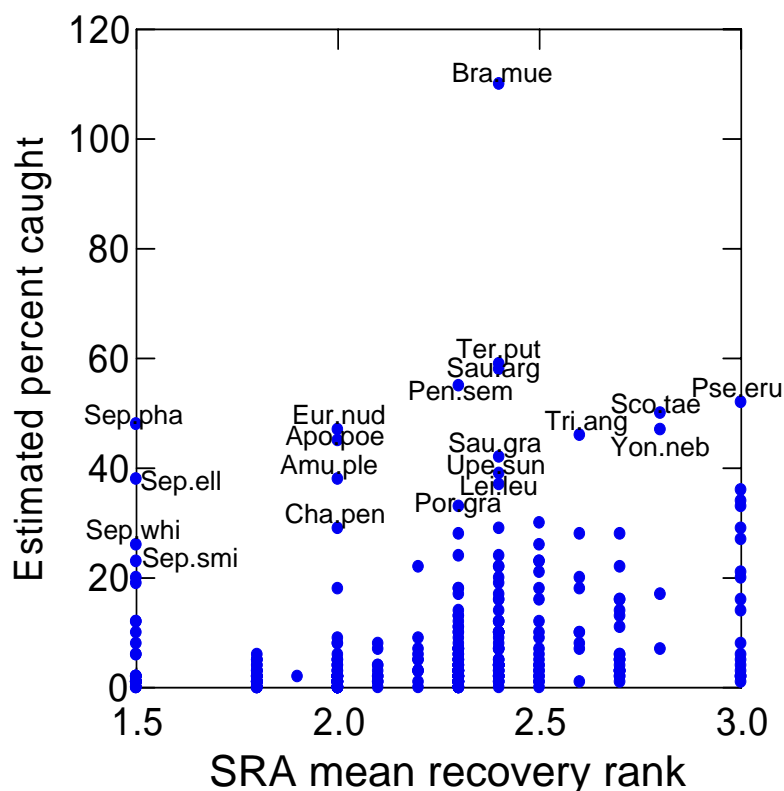


Figure 3-120: Plot of estimated percentage of population caught against mean RSA recovery rank. Species at greatest potential risk should plot towards the upper left quadrant. The top ranking species are labeled with the first three letters of their genus and species name (see Table 3-57).

In this report, a sustainability indicator — analogous to that of Zhou & Griffiths (2007) was estimated, where natural mortality rates have been collated in Brewer *et al.* (2007) or were available from other sources — as the proportion of the total population caught/natural mortality (Table 3-57). Where this indicator exceeded the reference points 0.6 and 0.8, and the limit reference point 1.0, the indicator was highlighted (pale, orange, and red, respectively). Three species exceeded the limit reference point: *Fistularia petimba*, the Rough Flutemouth (at 1.12); *Brachirus muelleri*, the Tufted Sole (at 1.11) and *Trixiphichthys weberi*, the Blacktip Tripodfish (at 1.09). *Fistularia petimba* was moderately frequent in trawl samples and was distributed along the length of the GBR, though more to the north, in low current stress, low light areas (Figure 3-123a). Most individuals caught were small (average: 15.5 g, range: 2–58 g) compared to adults, which would usually be considered a reef associated species. *Brachirus muelleri* was moderately infrequent in trawl samples and was distributed on intermediate carbonate mud sediments innershelf from Shelbourne Bay to the Whitsundays, and near the mouth of the Capricorn Channel (Figure 3-108c). Individuals caught ranged in size from 4–189 g (average: 61 g). *Brachirus muelleri* was also listed among the highest risk SRA species. *Trixiphichthys weberi* was infrequent in trawl samples and was distributed along most of the length of the GBR in inner-shelf but not inshore areas (Figure 3-123b). Most individuals caught were small (average: 25 g, range: 6–79 g).

One species exceeded the first conservative reference point: *Pomadasy maculatus*, the Blotched Javelin (a grunter bream) (at 0.96). *Pomadasy maculatus* was moderately frequent in trawl samples and was distributed along most of the length of the GBR in inshore areas with low-light levels on the seabed (Figure 3-123c). Most individuals caught were relatively small (average: 35 g, range: 4–104 g).

Two species exceeded the second conservative reference point: *Psettodes erumei*, the Australian Halibut or Spiny Turbot (at 0.75) and *Sillago burrus*, the Western Trumpeter Whiting (at 0.60). *Psettodes erumei* occurred in 51 trawl samples and was distributed along most of the length of the GBR, from about Mackay northwards, in inshore muddy areas with low current stress (Figure 3-112c). Individuals caught averaged 220 g, range: 21–1960 g. *Psettodes erumei* was also listed among the highest risk RSA species. *Sillago burrus* was relatively infrequent in trawl samples and was distributed along most of the length of the GBR in shallow areas with low turbidity, primarily inshore (Figure 3-123d). Individuals caught ranged in weight from 14–129 g (average: 50 g).

The next 10 ranked species were below the natural mortality based sustainability reference points, but included seven species ranked highly by the SRA method (indicated by *): *Dasyatis leylandi* (0.59), *Nemipterus furcosus* (0.56), *Tripodichthys angustifrons** (0.53), *Terapon puta** (0.53), *Euristhmus nudiceps** (0.52), *Saurida argentea/tumbil** (0.52), *Nemipterus peronii* (0.41), *Sepia pharaonis** (0.39), *Saurida grandi/undosquamis** (0.38) and *Amusium pleuronectes* cf* (0.35). The highest ranked target species were *Thenus parindicus* (at 0.31), *Penaeus semisulcatus* (at 0.24) and *Amusium balloti* (at 0.16).

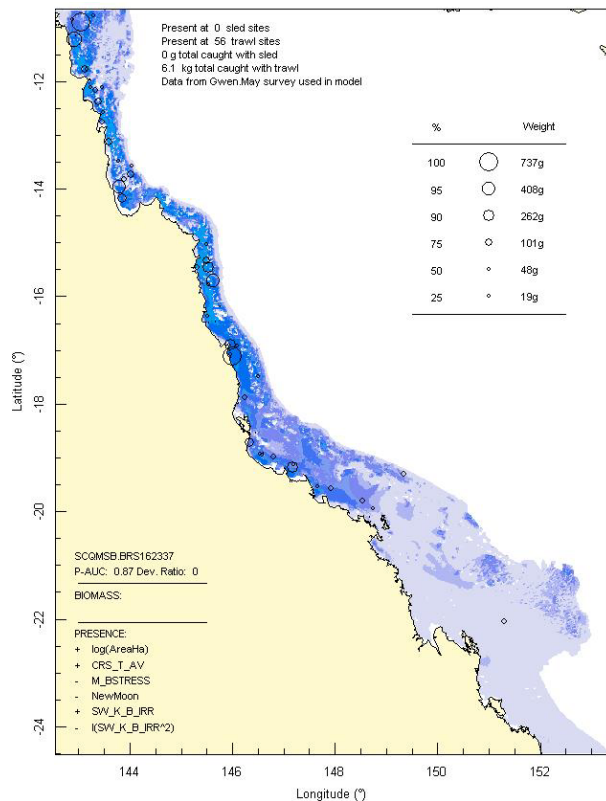
The final column (*) in Table 3-57 indicates the importance of the catchability parameter in altering the sustainability indicator outcome. It assumed that catchability was 1 and showed “!!!” if the $1 \times M$ limit reference point would be exceeded and “!!” and “!” if the $0.8 \times M$ and $0.6 \times M$ reference points would be exceeded; if M was unknown, then the importance of catchability was also unknown (“u”) in this respect. The uncertainty in catchability was particularly critical for *Pomadasyss maculatus*, which would exceed the limit reference point at the higher end of the catchability uncertainty range.

Psettodes erumei would be above the first conservative reference point; and *Nemipterus peronii*, *Terapon puta* and *Nemipterus furcosus* would be above the second conservative reference point at the higher end of the catchability uncertainty range. On the other hand, at the lower end of the catchability uncertainty range, *Trixiphichthys weberi* would drop from exceeding the limit reference point to the lowest reference point. Further investigation of catchability is required to have greater confidence in the sustainability risk indicators for these species, as well as others flagged in Table 3-57. The estimates of natural mortality from other sources are also accompanied by unspecified uncertainty.

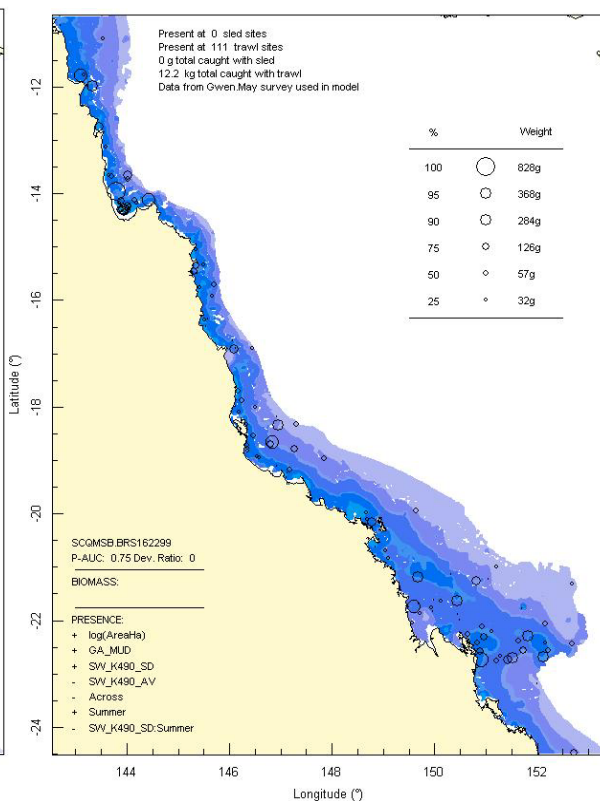
Of the species for which M was unknown, only three had an estimated % caught >25% and these were considered further because of the uncertainty regarding their sustainability in the absence of M . The highest ranking was the anaspid gastropod *Aplysia* sp1_QMS with an estimated catch of 38%. While uncertain, the relative catch rate of 1 for this species may be erroneous due identification issues between sled and trawl samples as, at the family level, the relative catch rate was 0.35 and if realistic, this suggests an actual % caught of ~13%. No information on mortality was found. Next was the sorbeoconch gastropod *Lamellaria* sp1 with an estimated catch of 37%. Again, while uncertain, the relative catch rate of 1 for this species may be erroneous due identification issues between sled and trawl samples as, at the order level, the relative catch rate was 0.08 and if realistic, this suggests an actual % caught of ~3%. No information on mortality was found. Finally, the polychaete bristle worm *Chloeia flava* had an estimated catch of 21% and again, the relative catch rate of 1 for this species may be erroneous as the sled worm samples were not sorted. Further, this group is known to respond positively to trawl disturbance by feeding on carrion (Engel & Kvitek 1998), has regeneration capacity and multiple reproductive modes, and is very likely to have a short lifespan and corresponding high natural mortality rate, so is unlikely to be at risk.

Indicators for all other species with modelled distributions were tabulated in APPENDIX 4: SINGLE SPECIES TRAWL EXPOSURE — ranked by species level exposure, if known.

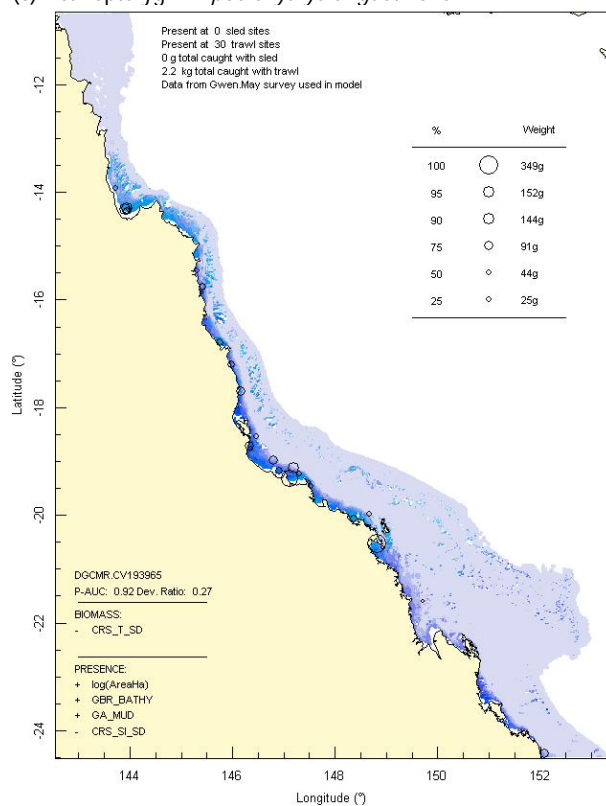
(a) Cephalopoda: *Sepia phararonis*



(b) Cephalopoda: *Sepia elliptica*



(c) Actinopterygii: *Tripodichthys angustifrons*



(d) Actinopterygii: *Saurida grand/undosquamis*

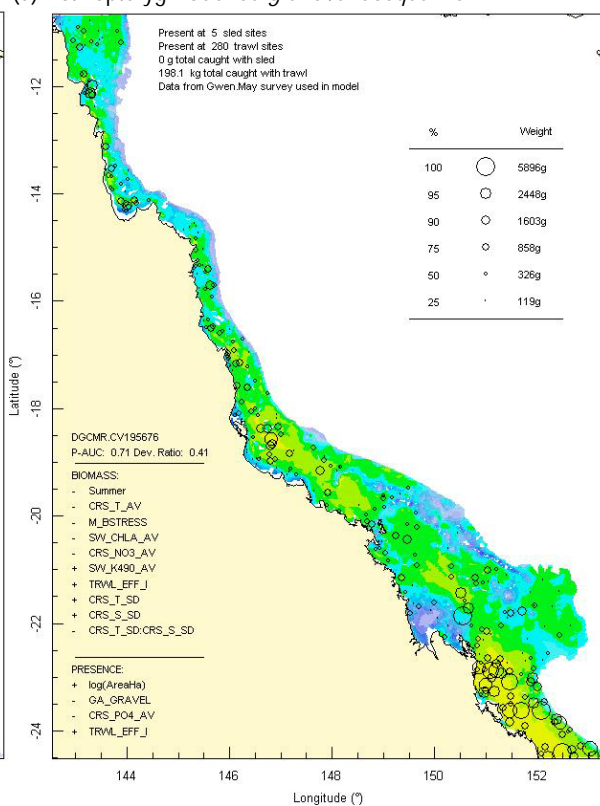
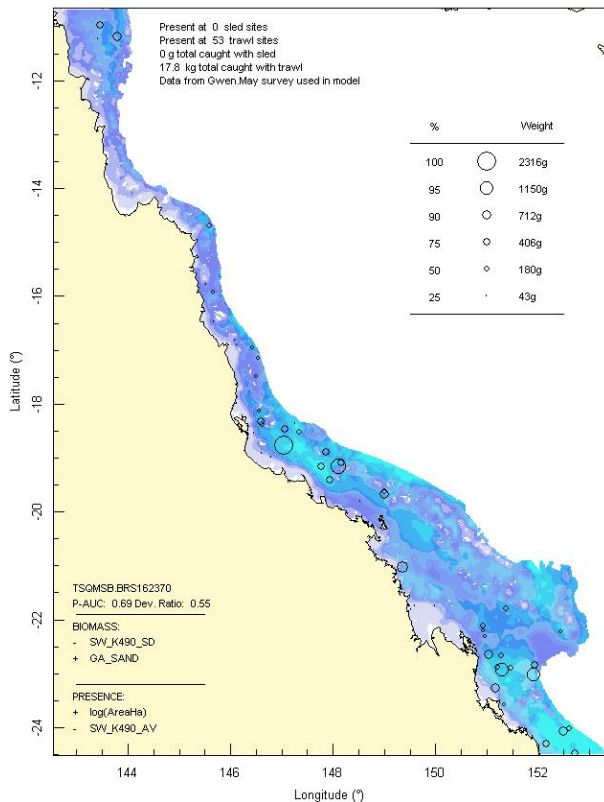
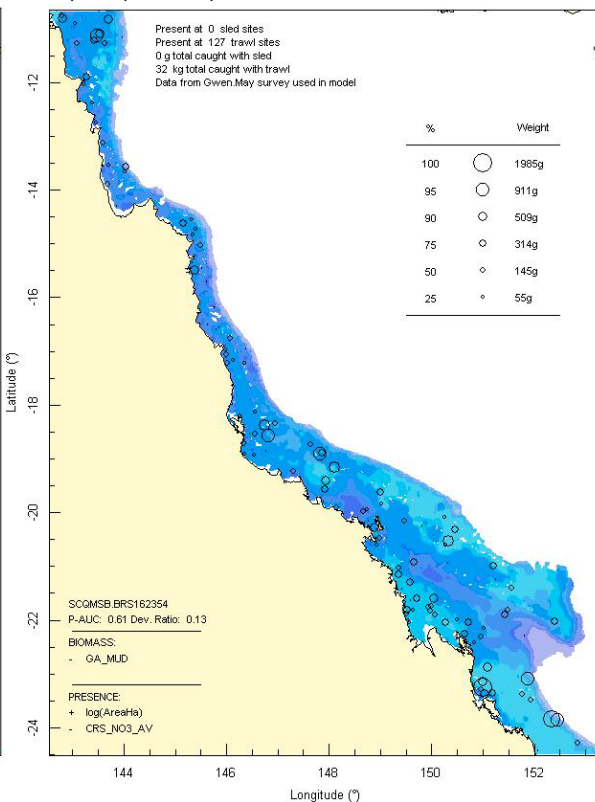


Figure 3-121: Model distribution maps of selected species with higher relative risk identified from exposure and SRA recovery attributes.

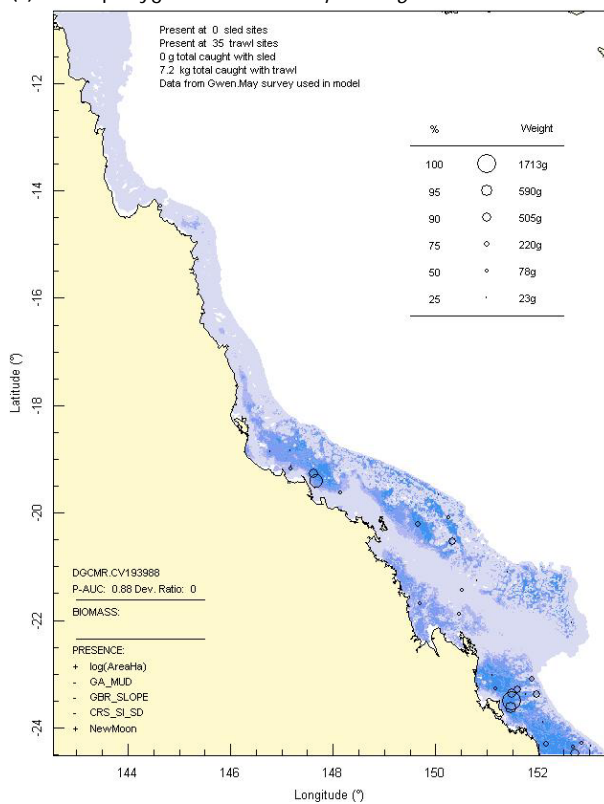
(a) Cephalopoda: *Sepia whiteleyana*



(b) Cephalopoda: *Sepia smithi*



(c) Actinopterygii: *Chaetodermis penicilligera*



(d) Cephalopoda: *Sepia plangon*

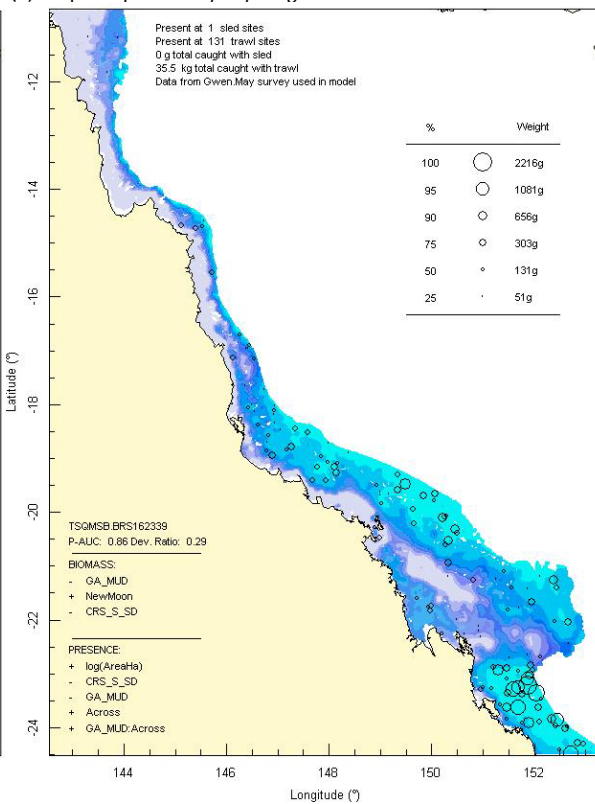
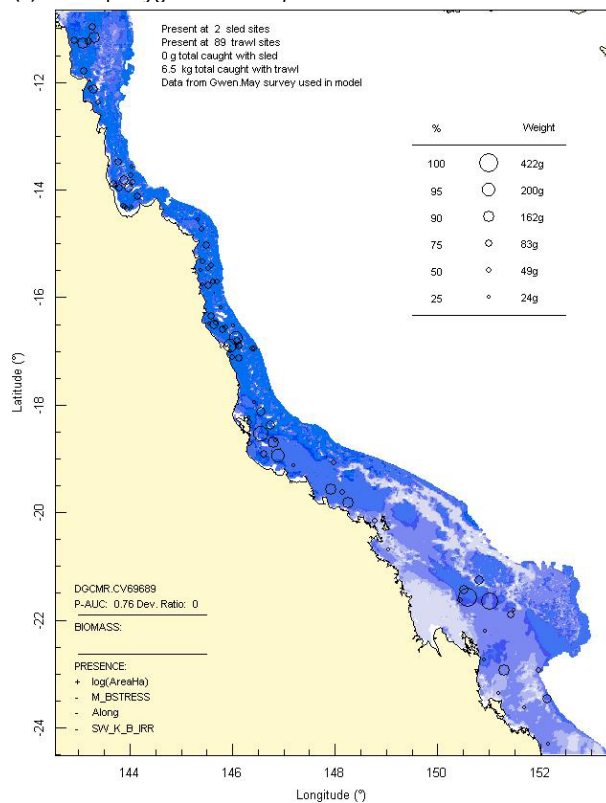
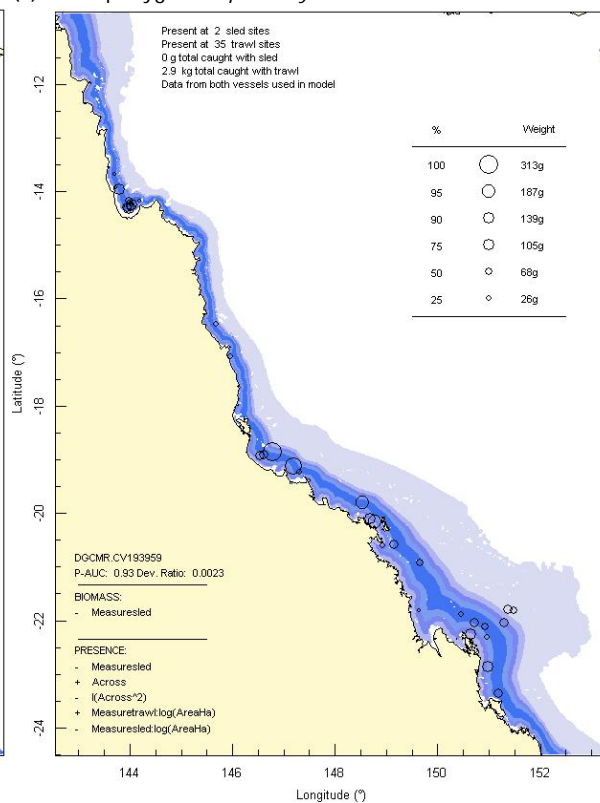


Figure 3-122: Model distribution maps of selected species with higher relative risk identified from exposure and SRA recovery attributes.

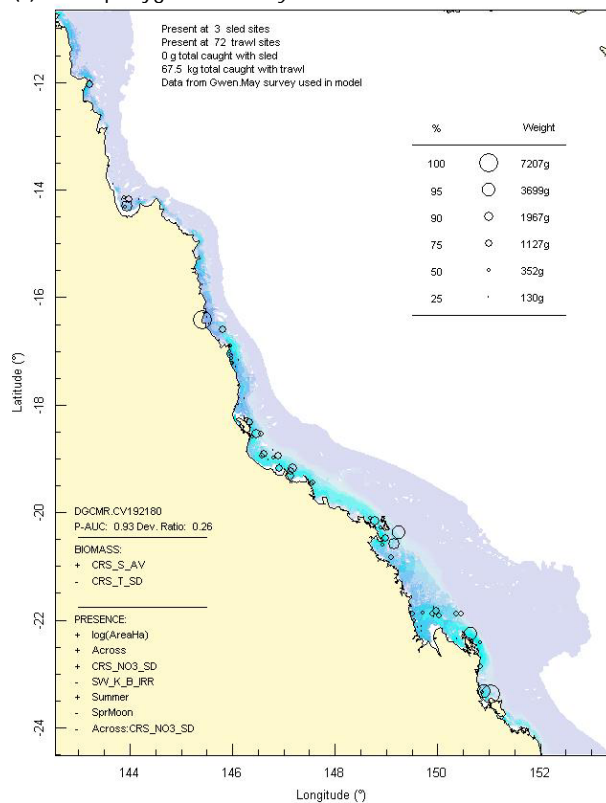
(a) Actinopterygii: *Fistularia petimba*



(b) Actinopterygii: *Trixiphichthys weberi*



(c) Actinopterygii: *Pomadasys maculatus*



(d) Actinopterygii: *Sillago burrus*

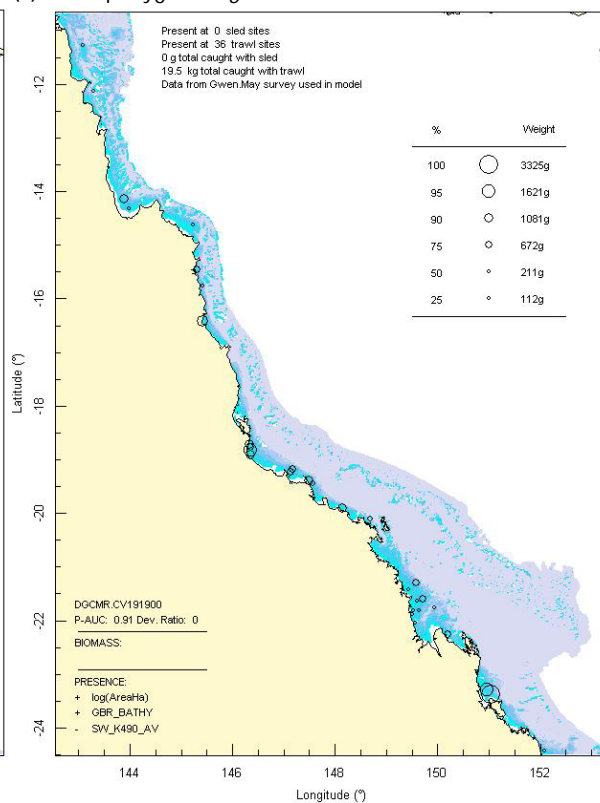


Figure 3-123: Model distribution maps of selected species with highest sustainability risk indicators.

3.7.3. Assemblage indicators

On the basis of the sites-groups characterisation and biophysical predictions of the species assemblage data in Section 3.4, area-based (number of grid cells) exposure indicators were estimated similar to those considered for species-group biomass (Section 3.7.1). First was the amount of area of each assemblage type located in various marine park zones, in particular the percentage of the total area located in GU zones was available to trawling and potentially at risk (Table 3-58).

Eleven of the 16 assemblages had more than 25% of their area in GU zones (Table 3-58, % Available, pale orange), 9 of those had more than 50% of their area in GU zones (dark orange) and none had more than 75% of its area in GU zones. The lowest level of availability was 5% and the highest level was 73%.

The next indicator was the percentage of area of each assemblage located in grid cells where trawl effort was present — regardless of the intensity of effort in the grid cells (Table 3-58, % Exposed). Seven assemblages had more than 25% of their area in grid cells with trawl effort (pale orange) and three of those had more than 50% of their area in grid cells with trawl effort. The lowest level of exposure was 0% and the highest level was 58%. This indicator is more specific and more sensitive than the previous.

The third indicator was the percentage of area of each assemblage directly exposed to trawl effort taking into account the intensity of trawl effort (Table 3-58, Effort Exposed %). The table shows the amount of area exposed at several different levels of effort intensity, as well as the final total exposure as a percentage. Five of the 16 assemblages had more than 25% of their area directly exposed to trawl effort in 2005 (Table 3-58, pale orange), two had more than 50% of area directly exposed (dark orange) and one had more than 100% of area directly exposed due to being trawled multiple times (red). The lowest level of exposure was 0% and the highest level was 108%. The exposures between 32% and 41% indicate moderate-low risk, exposure of 58% indicates moderate-high risk, and exposure of 108% indicates high potential risk.

The highest exposure, at 108%, was assemblage 12 representing primarily group E species (Figure 3-49) — including *Cryptolutea arafurensis*, *Saurida argentea/tumbil*, *Enisiculus cultellus* and *Placamen tiara* (see Table 3-60 for list of 40 species with greatest affinity for assemblage 14) — followed by groups G and C species. Assemblage 12 was distributed in patches along the coastal/inner-shelf from the Whitsundays to Cape Upstart and from Cairns north (Figure 3-47).

The next most exposed, at 58%, was assemblage 11 representing primarily group E species (Figure 3-49) — including *Scolopsis taeniopterus*, *Charybdis truncata*, *Terapon theraps*, *Leiognathus leuciscus*, *Metapenaeus endeavouri* and *Calliurichthys grossi* (see Table 3-60 for top 40 species) — followed by groups G and C species. Assemblage 11 was distributed along coastal areas north of Mackay and more broadly across the inner/mid-shelf from Cairns north (Figure 3-47).

Next was assemblage 4, at 41%, representing primarily group K species (Figure 3-49) — including *Orthoscuitella* spp, *Ambiserrula jugosa*, *Arachnopusia* spp, *Xenospongia patelliformis* and *Scuticella plagiostoma* (see Table 3-60 for top 40 species) — followed by groups G and C species. Assemblage 4 was distributed over much of the mid/outer shelf in the Capricorn section of the GBR (Figure 3-47).

Next was assemblage 13, at 41%, representing primarily groups E and G species (Figure 3-49) — including *Leiognathus splendens*, *Leiognathus moretoniensis*, *Trachypenaeus anchoralis*, *Gerres filamentosus* and *Metapenaeus ensis* (see Table 3-60 for top 40 species) — and was scattered patchily close inshore from the Whitsundays north (Figure 3-47).

Assemblage 1 had 32% exposure and represented primarily group A species (Figure 3-49) — including *Poraster superbus*, *Portunus argentatus*, *Atys cylindricus* cf, *Richardsonichthys leucogaster* and *Caulerpa brachypus* (see Table 3-60 for top 40 species) — and was distributed in the mid/outer shelf in the central section offshore from about Cape Upstart to Hinchinbrook Is (Figure 3-47).

The remaining clusters had low to zero levels of exposure and included a number of species affinity groups, particularly K, J, but also L, H, B, D (Figure 3-49).

A number of species occurred repeatedly across the more highly exposed assemblages. As an indication of their cumulative exposure, species were ranked by the sum of the products of their assemblage exposure by assemblage affinity — so that species with higher affinities for several more exposed assemblages would have a higher ranking. The top 40 species with highest exposure are also listed in Table 3-60 and primarily includes group E species, with some G and C. Many of these species are the same as those ranked with higher exposure in the singles species assessment (Section 3.7.2.2, Table 3-57).

3.7.4. Habitat indicators

On the basis of the characterisation and biophysical predictions of the video habitat data in Section 3.5.3, area-based (number of grid cells) exposure indicators were estimated similar to those considered for species-group biomass (Section 3.7.1) and assemblage distribution (Section 3.7.3). First was the amount of area of each habitat cluster type located in various marine park zones, in particular the percentage of the total located in GU zones was available to trawling and potentially at risk (Table 3-59).

Eight of the 9 habitat clusters had more than 25% of their area in GU zones (Table 3-59, % Available, pale orange), 2 of those groups had more than 50% of their area in GU zones (dark orange) and one group (cluster 6) had more than 75% of its area in GU zones (red). The lowest level of availability was 12% and the highest level was 80%.

The next indicator was the percentage of area of each cluster located in grid cells where trawl effort was present — regardless of the intensity of effort in the grid cells (Table 3-59, % Exposed). Four clusters had more than 25% of their area in grid cells with trawl effort (pale orange) and two of those had more than 50% of their area in grid cells with trawl effort. The lowest level of exposure was 6% and the highest level was 64%. This indicator is more specific and more sensitive than the previous.

The third indicator was the percentage of area of each cluster directly exposed to trawl effort taking into account the intensity of trawl effort (Table 3-59, % Effort Exposed). The table shows the amount of area exposed at several different levels of effort intensity, as well as the final total exposure as a percentage. Five of the 9 clusters had more than 25% of their area directly exposed to trawl effort in 2005 (Table 3-59, pale orange) and none had more than 50% of area directly exposed. The lowest level of exposure was 3% and the highest level was 39%. Exposures between 25% and 39% indicate moderate-low risk. The highest, at 39%, was cluster 7 representing patchy seagrass and algal habitat (Figure 3-61) distributed along the mid-shelf from Cape Upstart to Innisfail (Figure 3-62). The next most exposed, at 34%, was cluster 6 also representing patchy seagrass and algal habitat (Figure 3-61) distributed along much of the inner-shelf in the southern Capricorn section of the GBR (Figure 3-62). Next was cluster 5, also at 34%, representing mostly bioturbated and bare seabed with a little algae and seagrass algal habitat (Figure 3-61) distributed over much of the shelf in the central and northern sections of the GBR (Figure 3-62). Next was cluster 1, at 26%, representing the most barren seabed type — almost entirely bare and bioturbated with very little biohabitat (Figure 3-61) — distributed in inshore muddy areas and the Capricorn Channel (Figure 3-62). Cluster 9 had 25% exposure and represented patchy algae (including limited *Halimeda*) with some bioturbation and a little other biohabitat distributed offshore from Townsville (Figure 3-62). The remaining clusters included most of the *Halimeda* banks and epibenthic garden biohabitats and had low levels of exposure.

The exposure of habitat components identified from the frame-level video post-analysis (Section 3.5.2) was examined from the point data (i.e. not from models of predicted distributions), which carries some risk of bias due to the purposeful stratification of the sampling design. Overall, 62% of the observed seagrass occurred in GU zones and 47% was observed in grid cells where trawl effort was present; but given the intensity of trawl effort the total exposure was 21%. The majority of observed seagrass was *Halophila spinulosa* and like-species, with indicators of 67%, 54% and 24% respectively, which is a very similar exposure outcome as the modelled sample distribution for this species (22%, Table 3-49). Ovoid leaf *Halophila*'s were ranked next at 54%, 33%, and 15%, which is also a very similar exposure outcome as the modelled sample distribution for *Halophila ovalis* (18%, Table 3-49). The concordance between these two completely independent sources of data, and raw

versus modelled distributions, gives confidence to the estimates of exposure. Other observed morphotypes of seagrass had very low exposure.

Thirty four percent of observed algae, overall growth forms combined, occurred in GU zones and 18% was observed in grid cells where trawl effort was present; given the intensity of trawl effort the total exposure was 14%. The exposure of the diversity of different morphotypes of algae varied considerably. The most exposed form was crustose coralline algae (total exposure 44%); primarily in the trawl grounds off Gladstone. Crustose coralline algae nodules can be considered a robust growth form. The next most exposed form was filamentous blue-green algae (total exposure 25%). All other growth forms were $\leq 17\%$ and most (including *Halimeda*'s) were $< 5\%$.

Thirty eight percent of observed gorgonians, overall growth forms combined, occurred in GU zones and 15% was observed in grid cells where trawl effort was present; given the intensity of trawl effort the total exposure was 3%. The exposure of the diversity of different morphotypes of gorgonians was $\leq 2\%$ for all but *Solenocaulon*, with forms covered with epifauna having 20% exposure and those without having 14% exposure.

Twenty two percent of observed soft corals, overall growth forms combined, occurred in GU zones and 9% was observed in grid cells where trawl effort was present; given the intensity of trawl effort the total exposure was 4%. The exposure of the diversity of different morphotypes of soft corals was $\leq 4\%$ for all but *Pteroides*, which had 15% exposure. This is also a very similar exposure outcome as the modelled sample distribution for this genus of sea pen (16%). Sea pens appear to have a low catchability (~ 0.06) with narrow uncertainty (~ 0.05), so would appear to be at low risk.

Seventeen percent of observed sponges, overall growth forms combined, occurred in GU zones and 10% was observed in grid cells where trawl effort was present; given the intensity of trawl effort the total exposure was 3%. The exposure of the diversity of different morphotypes of sponges was $\leq 6\%$ for all but barrel forms, which had 14% exposure (excluding *Ircinia* and *Xestospongia*) and foliose forms, which had 10% exposure.

Twenty nine percent of observed bryozoans, overall growth forms combined, occurred in GU zones and 14% was observed in grid cells where trawl effort was present; given the intensity of trawl effort the total exposure was 7%. The exposure of the diversity of different morphotypes of bryozoans varied between 0–11%.

Six percent of observed hard corals, overall growth forms combined, occurred in GU zones and 6% was observed in grid cells where trawl effort was present; given the intensity of trawl effort the total exposure was $\sim 1\%$. The exposure of the diversity of different morphotypes of hard corals was mostly close to zero (but $\leq 3\%$) for all forms except solitary corals, which had 12% exposure. The most common sampled solitary corals were of the genus *Cycloseris* with a total exposure of $\sim 17\%$ and low catchability (~ 0.07) with narrow uncertainty (~ 0.06), so would appear to be at low risk.

Table 3-58: Ecological Risk Indicators with respect to trawling for estimated area (km²) of predicted distributed of species assemblages (site clusters): by GBRMP Zoning indicating percent of area available; by area not trawled/trawled indicating percent area potentially exposed; by trawl intensity (ann_hrs/0.01° cell) indicating percent area exposed to effort.

| Assemblage | General Use | Habitat Protection | Marine Nat Park | Preservation | TOTAL | % Available | Not trawled | Trawled | % Exposed | 0 | 0.125 | 0.25 | 0.5 | 1 | 2 | 4 | 8 | 16 | 32 | 64 | 128 | 256 | Effort Exp% |
|------------|-------------|--------------------|-----------------|--------------|-------|-------------|-------------|---------|-----------|---|-------|------|-----|-----|-----|-----|------|------|------|------|-----|-----|-------------|
| 1 | 7521 | 3960 | 3212 | 16 | 14709 | 51 | 8556 | 6154 | 42 | 0 | 12 | 25 | 61 | 134 | 303 | 812 | 1337 | 1229 | 640 | 132 | 0 | 0 | 32 |
| 2 | 10736 | 11496 | 6287 | 45 | 28565 | 38 | 23098 | 5467 | 19 | 0 | 22 | 38 | 68 | 110 | 210 | 365 | 610 | 663 | 279 | 27 | 0 | 0 | 8 |
| 3 | 2336 | 6308 | 5717 | 13 | 14374 | 16 | 13157 | 1217 | 8 | 0 | 7 | 9 | 16 | 28 | 32 | 41 | 84 | 58 | 59 | 0 | 0 | 0 | 2 |
| 4 | 6670 | 573 | 2240 | 23 | 9506 | 70 | 4175 | 5331 | 56 | 0 | 15 | 25 | 54 | 109 | 231 | 496 | 1048 | 1326 | 538 | 51 | 0 | 0 | 41 |
| 5 | 2900 | 548 | 1844 | 17 | 5310 | 55 | 4285 | 1025 | 19 | 0 | 4 | 7 | 9 | 21 | 41 | 61 | 157 | 159 | 66 | 0 | 0 | 0 | 10 |
| 6 | 8369 | 4409 | 3718 | 49 | 16545 | 51 | 11870 | 4676 | 28 | 0 | 23 | 30 | 48 | 90 | 172 | 286 | 542 | 548 | 374 | 42 | 0 | 0 | 13 |
| 7 | 8934 | 1015 | 2955 | 37 | 12940 | 69 | 7329 | 5611 | 43 | 0 | 25 | 39 | 65 | 105 | 178 | 317 | 709 | 773 | 529 | 29 | 0 | 0 | 21 |
| 8 | 4082 | 4990 | 5061 | 38 | 14172 | 29 | 13656 | 516 | 4 | 0 | 3 | 3 | 9 | 11 | 14 | 16 | 31 | 41 | 29 | 210 | 59 | 0 | 3 |
| 9 | 1523 | 4511 | 3513 | 29 | 9576 | 16 | 9369 | 207 | 2 | 0 | 2 | 2 | 1 | 3 | 1 | 3 | 0 | 0 | 0 | 0 | 0 | 0 | 0 |
| 10 | 12004 | 4344 | 5154 | 35 | 21537 | 56 | 19475 | 2062 | 10 | 0 | 15 | 14 | 23 | 35 | 47 | 69 | 115 | 84 | 31 | 13 | 21 | 0 | 2 |
| 11 | 13934 | 4501 | 5912 | 20 | 24367 | 57 | 14161 | 10206 | 42 | 0 | 30 | 52 | 109 | 194 | 356 | 690 | 1378 | 2543 | 3968 | 4041 | 699 | 184 | 58 |
| 12 | 2668 | 1284 | 712 | 42 | 4706 | 57 | 2247 | 2459 | 52 | 0 | 5 | 9 | 17 | 38 | 67 | 191 | 449 | 1119 | 1406 | 1696 | 80 | 0 | 108 |
| 13 | 2827 | 92 | 929 | 3 | 3851 | 73 | 1634 | 2217 | 58 | 0 | 8 | 14 | 25 | 40 | 75 | 151 | 331 | 428 | 396 | 96 | 0 | 0 | 41 |
| 14 | 208 | 1258 | 630 | 14 | 2110 | 10 | 2110 | 0 | 0 | 0 | 0 | 0 | 0 | 0 | 0 | 0 | 0 | 0 | 0 | 0 | 0 | 0 | 0 |
| 15 | 2124 | 6889 | 4677 | 0 | 13690 | 16 | 13620 | 70 | 1 | 0 | 1 | 1 | 1 | 0 | 0 | 0 | 0 | 0 | 0 | 0 | 0 | 0 | 0 |
| 16 | 179 | 532 | 2973 | 0 | 3684 | 5 | 3676 | 8 | 0 | 0 | 0 | 0 | 0 | 0 | 0 | 0 | 0 | 0 | 0 | 0 | 0 | 0 | 0 |

Table 3-59: Ecological Risk Indicators with respect to trawling for estimated area (km²) of predicted distributed of video habitat clusters: by GBRMP Zoning indicating percent of area available; by area not trawled/trawled indicating percent area potentially exposed; by trawl intensity (ann_hrs/0.01° cell) indicating percent area directly exposed to effort.

| Cluster | General Use | Habitat Protection | Marine Nat Park | Preservation | TOTAL | % Available | Not trawled | Trawled | % Exposed | 0 | 0.125 | 0.25 | 0.5 | 1 | 2 | 4 | 8 | 16 | 32 | 64 | 128 | 256 | % Effort Exp |
|---------|-------------|--------------------|-----------------|--------------|-------|-------------|-------------|---------|-----------|---|-------|------|-----|-----|-----|------|------|------|------|------|-----|-----|--------------|
| 1 | 6669 | 2979 | 5586 | 10 | 15244 | 44 | 11606 | 3639 | 24 | 0 | 13 | 17 | 36 | 56 | 114 | 279 | 590 | 1229 | 1161 | 351 | 55 | 47 | 26 |
| 2 | 15208 | 9397 | 9023 | 41 | 33670 | 45 | 30004 | 3667 | 11 | 0 | 20 | 27 | 52 | 71 | 107 | 140 | 150 | 246 | 280 | 206 | 0 | 0 | 4 |
| 3 | 9639 | 11538 | 8994 | 42 | 30213 | 32 | 24461 | 5752 | 19 | 0 | 22 | 36 | 64 | 120 | 223 | 424 | 805 | 884 | 297 | 20 | 0 | 0 | 10 |
| 4 | 10426 | 11239 | 9328 | 97 | 31089 | 34 | 26720 | 4370 | 14 | 0 | 19 | 28 | 47 | 95 | 154 | 268 | 511 | 642 | 417 | 67 | 0 | 0 | 7 |
| 5 | 25857 | 14870 | 13874 | 113 | 54714 | 47 | 39217 | 15497 | 28 | 0 | 54 | 84 | 161 | 291 | 525 | 1012 | 2076 | 3335 | 4785 | 5521 | 803 | 137 | 34 |
| 6 | 10737 | 385 | 2234 | 3 | 13360 | 80 | 5729 | 7632 | 57 | 0 | 28 | 45 | 84 | 144 | 299 | 576 | 1339 | 1423 | 605 | 41 | 0 | 0 | 34 |
| 7 | 4541 | 165 | 1469 | 0 | 6175 | 74 | 2239 | 3936 | 64 | 0 | 10 | 17 | 36 | 79 | 187 | 510 | 904 | 439 | 177 | 27 | 0 | 0 | 39 |
| 8 | 779 | 2706 | 2892 | 38 | 6414 | 12 | 6035 | 379 | 6 | 0 | 2 | 2 | 3 | 6 | 16 | 33 | 29 | 29 | 64 | 0 | 0 | 0 | 3 |
| 9 | 3158 | 3431 | 2134 | 38 | 8761 | 36 | 6407 | 2354 | 27 | 0 | 5 | 10 | 24 | 55 | 100 | 261 | 386 | 744 | 531 | 105 | 0 | 0 | 25 |

Table 3-60. Species with greatest affinity (top 40) for site-group assemblages identified in Section 3.4, with the highest levels of trawl exposure.

| Assemblage 12 | | Assemblage 11 | | Assemblage 4 | | Assemblage 13 | | Assemblage 1 | | Exposure across Assemblages | |
|-----------------------|------------------------|-----------------------|------------------------|-------------------------|---------------------------|-----------------------|------------------------|--------------------------|-----------------------|-----------------------------|------------------------|
| <i>Cryptolutea</i> | <i>arafurensis</i> | <i>Scolopsis</i> | <i>taeniopterus</i> | <i>Orthoscuitella</i> | spp | <i>Leiognathus</i> | <i>splendens</i> | <i>Poraster</i> | <i>superbus</i> | <i>Enisiculus</i> | <i>cultellus</i> |
| <i>Saurida</i> | <i>argentea/tumbil</i> | <i>Charybdis</i> | <i>truncata</i> | <i>Ambiserrula</i> | <i>jugosa</i> | <i>Leiognathus</i> | <i>moretoniensis</i> | <i>Portunus</i> | <i>argentatus</i> | <i>Cryptolutea</i> | <i>arafurensis</i> |
| <i>Enisiculus</i> | <i>cultellus</i> | <i>Terapon</i> | <i>theraps</i> | <i>Arachnopusia</i> | spp | <i>Trachypenaeus</i> | <i>anchoralis</i> | <i>Alys</i> | <i>cylindricus</i> cf | <i>Saurida</i> | <i>argentea/tumbil</i> |
| <i>Pentaprion</i> | <i>longimanus</i> | <i>Leiognathus</i> | <i>leuciscus</i> | <i>Xenospongia</i> | <i>patelliformis</i> | <i>Gerres</i> | <i>filamentosus</i> | <i>Richardsonichthys</i> | <i>leucogaster</i> | <i>Pentaprion</i> | <i>longimanus</i> |
| <i>Placamen</i> | <i>tiara</i> | <i>Metapenaeus</i> | <i>endeavouri</i> | <i>Scuticella</i> | <i>plagiostoma</i> | <i>Metapenaeus</i> | <i>ensis</i> | <i>Caulerpa</i> | <i>brachypus</i> | <i>Thenus</i> | <i>parindicus</i> |
| <i>Tripodichthys</i> | <i>angustifrons</i> | <i>Calliurichthys</i> | <i>grossi</i> | <i>Iodictyum</i> | spp | <i>Penaeus</i> | <i>semisulcatus</i> | <i>Takedana</i> | <i>eriphioides</i> | <i>Nassarius</i> | <i>crematus</i> cf |
| <i>Upeneus</i> | <i>sundaicus</i> | <i>Thenus</i> | <i>parindicus</i> | <i>Annachlamys</i> | <i>kuhnholzii</i> | <i>Tripodichthys</i> | <i>angustifrons</i> | <i>Palicoides</i> | <i>whitei</i> | <i>Placamen</i> | <i>tiara</i> |
| <i>Brachirus</i> | <i>muelleri</i> | <i>Upeneus</i> | <i>sundaicus</i> | <i>Exochella</i> | <i>conjuncta</i> cf | <i>Terapon</i> | <i>puta</i> | <i>Xenophora</i> | <i>indica</i> | <i>Tripodichthys</i> | <i>angustifrons</i> |
| <i>Metapenaeus</i> | <i>ensis</i> | <i>Euristhmus</i> | <i>nudiceps</i> | <i>Junceella</i> | <i>juncea</i> | <i>Apogon</i> | <i>poecilopterus</i> | <i>Demospongiae</i> | sp11 | <i>Upeneus</i> | <i>sundaicus</i> |
| <i>Nassarius</i> | <i>crematus</i> cf | <i>Dougaloplus</i> | <i>echinata</i> | <i>Codium</i> | <i>geppii</i> | <i>Leiognathus</i> | cf <i>bindus</i> | <i>Solenocera</i> | <i>pectinata</i> | <i>Erugosquilla</i> | <i>woodmasoni</i> |
| <i>Apogon</i> | <i>poecilopterus</i> | <i>Vexillum</i> | <i>obeliscus</i> cf | <i>Emballotheca</i> | spp | <i>Enisiculus</i> | <i>cultellus</i> | <i>Sicyonia</i> | <i>lancifer</i> | <i>Penaeus</i> | <i>semisulcatus</i> |
| <i>Penaeus</i> | <i>semisulcatus</i> | <i>Penaeus</i> | <i>semisulcatus</i> | <i>Suezichthys</i> | <i>gracilis</i> | <i>Nassarius</i> | <i>crematus</i> cf | <i>Alys</i> | sp1 | <i>Psettodes</i> | <i>erumei</i> |
| <i>Erugosquilla</i> | <i>woodmasoni</i> | <i>Sepia</i> | <i>pharaonis</i> | <i>Paguridae</i> | sp213 | <i>Chaetodiadema</i> | <i>granulatum</i> | <i>Phyllodictyon</i> | sp1 | <i>Charybdis</i> | <i>truncata</i> |
| <i>Nemipterus</i> | <i>nematopus</i> | <i>Melaxinaea</i> | <i>vitrea</i> | <i>Penaeus</i> | <i>plebejus</i> | <i>Erugosquilla</i> | <i>woodmasoni</i> | <i>Actumnus</i> | <i>squamosus</i> | <i>Aplysia</i> | sp1_QMS |
| <i>Diogenidae</i> | sp356-1 | <i>Selaroides</i> | <i>leptolepis</i> | <i>Robertsonidra</i> | spp | <i>Oratosquillina</i> | <i>gravieri</i> | <i>Mycale</i> | <i>mirabilis</i> | <i>Metapenaeus</i> | <i>ensis</i> |
| <i>Psettodes</i> | <i>erumei</i> | <i>Amusium</i> | <i>pleuronectes</i> cf | <i>Trachinocephalus</i> | <i>myops</i> | <i>Terapon</i> | <i>theraps</i> | <i>Trachypenaeus</i> | <i>curvirostris</i> | <i>Calliurichthys</i> | <i>grossi</i> |
| <i>Leiognathus</i> | <i>leuciscus</i> | <i>Penaeus</i> | <i>esculentus</i> | <i>Retelepralla</i> | <i>mosaica</i> | <i>Portunus</i> | <i>hastatooides</i> | <i>Didymozoum</i> | spp | <i>Melaxinaea</i> | <i>vitrea</i> |
| <i>Thenus</i> | <i>parindicus</i> | <i>Lophiotoma</i> | <i>acuta</i> | <i>Choerodon</i> | <i>venustus</i> | <i>Repomucenus</i> | <i>belcheri</i> | <i>Strombus</i> | <i>dilatatus</i> | <i>Diogenidae</i> | sp356-1 |
| <i>Charybdis</i> | <i>truncata</i> | <i>Cynoglossus</i> | <i>maculipinnis</i> | <i>Bohadschia</i> | <i>marmorata</i> cf | <i>Pseudorhombus</i> | <i>arsius</i> | <i>Xenophora</i> | <i>cerea</i> cf | <i>Portunus</i> | <i>tuberculosis</i> |
| <i>Yongeichthys</i> | <i>nebulosus</i> | <i>Nemipterus</i> | <i>peronii</i> | <i>Inimicus</i> | <i>caledonicus</i> | <i>Saurida</i> | <i>argentea/tumbil</i> | <i>Parthenope</i> | <i>turriger</i> | <i>Sea pen</i> | sp1 |
| <i>Upeneus</i> | <i>sulphureus</i> | <i>Psettodes</i> | <i>erumei</i> | <i>Batrachomoeus</i> | <i>dubius/trispinosus</i> | <i>Brachirus</i> | <i>muelleri</i> | <i>Paraperis</i> | <i>snyderi</i> | <i>Portunus</i> | <i>hastatooides</i> |
| <i>Portunus</i> | <i>tuberculosis</i> | <i>Pronotoxyx</i> | <i>leavis</i> | <i>Chama</i> | spp | <i>Upeneus</i> | <i>sundaicus</i> | <i>Udotea</i> | <i>flabellum</i> | <i>Terapon</i> | <i>theraps</i> |
| <i>Leiognathus</i> | <i>splendens</i> | <i>Diogenidae</i> | sp356-1 | <i>Aploactis</i> | <i>aspera</i> | <i>Torquigener</i> | <i>whitleyi</i> | <i>Udotea</i> | <i>argentea</i> | <i>Dosinia</i> | <i>altenai</i> |
| <i>Euristhmus</i> | <i>nudiceps</i> | <i>Nemipterus</i> | <i>furcosus</i> | <i>Annachlamys</i> | <i>flabellata</i> | <i>Myra</i> | <i>tumidospina</i> | <i>Scyllarus</i> | sp3418 | <i>Leiognathus</i> | <i>leuciscus</i> |
| <i>Scolopsis</i> | <i>taeniopterus</i> | <i>Nassarius</i> | <i>crematus</i> cf | <i>Brachiopoda</i> | sp1_MTO | <i>Caranx</i> | <i>bucculentus</i> | <i>Conescharella</i> | spp | <i>Holothuria</i> | <i>ocellata</i> |
| <i>Calliurichthys</i> | <i>grossi</i> | <i>Portunus</i> | <i>tuberculosis</i> | <i>Beania</i> | <i>discodermiae</i> cf | <i>Polydactylus</i> | <i>multiradiatus</i> | <i>Naxoides</i> | <i>taurus</i> | <i>Myra</i> | <i>tumidospina</i> |
| <i>Gerres</i> | <i>filamentosus</i> | <i>Ova</i> | <i>lacunosus</i> | <i>Struvea</i> | <i>elegans</i> | <i>Pentaprion</i> | <i>longimanus</i> | <i>Choerodon</i> | <i>frenatus</i> | <i>Sepia</i> | <i>elliptica</i> |
| <i>Leiognathus</i> | <i>bindus</i> | <i>Inegocia</i> | <i>japonica</i> | <i>Plicatula</i> | <i>chinensis</i> cf | <i>Calliurichthys</i> | <i>grossi</i> | <i>Calappa</i> | sp 1984 | <i>Sepia</i> | <i>pharaonis</i> |
| <i>Terapon</i> | <i>puta</i> | <i>Modiolus</i> | <i>elongatus</i> | <i>Upeneus</i> | <i>filifer</i> | <i>Leucosia</i> | <i>ocellata</i> | <i>Calliurichthys</i> | <i>ogilbyi</i> | <i>Euristhmus</i> | <i>nudiceps</i> |
| <i>Portunus</i> | <i>hastatooides</i> | <i>Brissopsis</i> | <i>luzonica</i> | <i>Telopora</i> | spp | <i>Psettodes</i> | <i>erumei</i> | <i>Apogon</i> | <i>timorensis</i> | <i>Vexillum</i> | <i>obeliscus</i> cf |
| <i>Apogon</i> | <i>fasciatus</i> | <i>Pentaprion</i> | <i>longimanus</i> | <i>Macropora</i> | spp | <i>Sillago</i> | <i>burrus</i> | <i>Demospongiae</i> | sp13 | <i>Apogon</i> | <i>poecilopterus</i> |
| <i>Nemipterus</i> | <i>hexodon</i> | <i>Dosinia</i> | <i>altenai</i> | <i>Conus</i> | <i>ammiralis</i> | <i>Upeneus</i> | <i>sulphureus</i> | <i>Myrine</i> | <i>kesslerii</i> | <i>Selaroides</i> | <i>leptolepis</i> |
| <i>Terapon</i> | <i>theraps</i> | <i>Trisidos</i> | <i>semitortata</i> | <i>Lepralia</i> | <i>elimata</i> | <i>Paraperis</i> | <i>diplospilus</i> | <i>Microdictyon</i> | <i>umbilicatum</i> | <i>Nemipterus</i> | sp juv/unident |
| <i>Metapenaeus</i> | <i>endeavouri</i> | <i>Yongeichthys</i> | <i>nebulosus</i> | <i>Beania</i> | <i>plurispinosa</i> cf | <i>Thenus</i> | <i>parindicus</i> | <i>Avrainvillea</i> | sp1 | <i>Metapenaeus</i> | <i>endeavouri</i> |
| <i>Dosinia</i> | <i>altenai</i> | <i>Astropecten</i> | spp | <i>Padina</i> | sp | <i>Leiognathus</i> | <i>leuciscus</i> | <i>Portunus</i> | <i>tenuipes</i> | <i>Portunus</i> | <i>tuberculatus</i> |
| <i>Vexillum</i> | <i>obeliscus</i> cf | <i>Sea pen</i> | sp1 | <i>Amusium</i> | <i>balloti</i> | <i>Sea pen</i> | sp1 | <i>Rogadius</i> | <i>patriciae</i> | <i>Gemmula</i> | sp2 |
| <i>Corbula</i> | <i>fortisulcata</i> | <i>Carangidae</i> | sp juv/unident | <i>Figularia</i> | <i>clithridiata</i> cf | <i>Placamen</i> | <i>tiara</i> | <i>Scyllarus</i> | <i>martensii</i> | <i>Apogon</i> | <i>fasciatus</i> |
| <i>Sepia</i> | <i>elliptica</i> | <i>Astropecten</i> | <i>zebra</i> | <i>Erosa</i> | <i>erosa</i> | <i>Euristhmus</i> | <i>nudiceps</i> | <i>Callyspongia</i> | sp6 | <i>Scolopsis</i> | <i>taeniopterus</i> |
| <i>Epinephelus</i> | <i>sexfasciatus</i> | <i>Cynoglossus</i> | sp 1 punctate | <i>Crepidacantha</i> | spp | <i>Leiognathus</i> | <i>bindus</i> | <i>Temnopleuridae</i> | sp2_QMS | <i>Torquigener</i> | <i>whitleyi</i> |
| <i>Sea pen</i> | sp1 | <i>Nemipterus</i> | <i>nematopus</i> | <i>Onigocia</i> | cf <i>macrolepis</i> | <i>Cryptopodia</i> | <i>queenslandi</i> | <i>Crella</i> | 1525 | <i>Dougaloplus</i> | <i>echinata</i> |

3.8. TRAWL MANAGEMENT SCENARIO MODEL (N Ellis, R Pitcher)

Total trawl effort in the region increased gradually after the fishery initially commenced, but grew rapidly in the early 1990s, before peaking in 1996/1997 and falling rapidly in the late 1990s (by ~25%) (Figure 2-42) — even before implementation of the management scenarios evaluated here. The average simulated effort is shown in Figure 3-124. The status quo 2001 model scenario (SQ2001) maintained these effort levels through until 2025. The first intervention was the 2001 spatial closure (CL2001) with the same effort levels. The second intervention was the latter closure plus the 2001 buy-back (CL/BB2001), which reduced effort by a further ~30% (down ~45% from the 1990s peak). The third intervention was the latter plus the progressive penalty (CL/BB2001+P), which reduced effort by a further ~30% again (down ~60% from the 1990s peak). The fourth intervention added the RAP re-zoning CL/BB2001+P+RAP) at the same effort levels. The fifth intervention added the RAP-associated buy-back (CL/BB2001+P+RAP+BB2005), which reduced effort again by almost ~10% (down ~65% from the 1990s peak). The final scenario was the actual effort observed through this period, including all management interventions — the status quo 2006 (SQ2006).

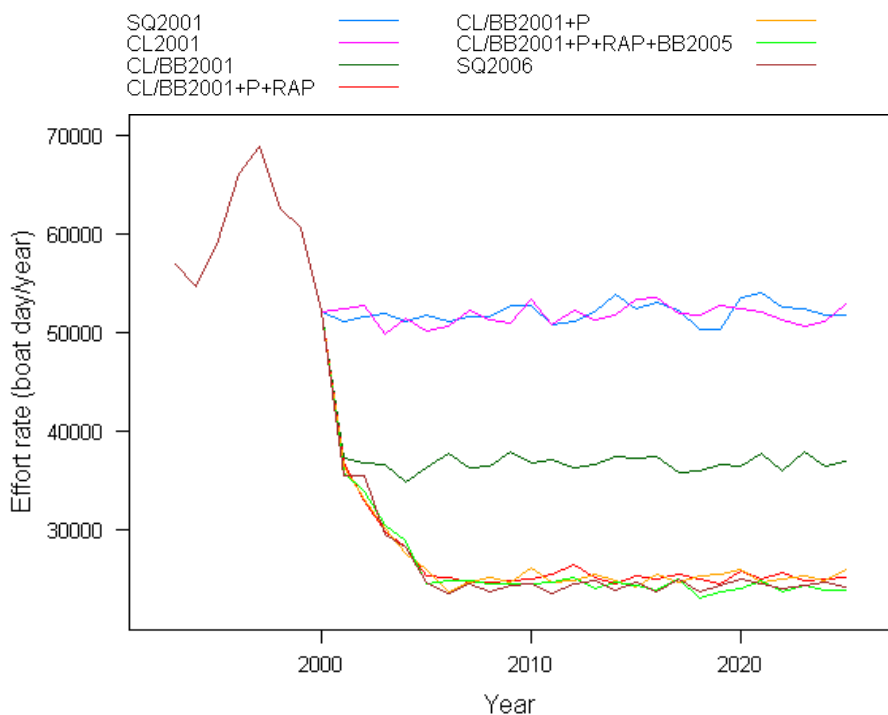


Figure 3-124. Total annual effort averaged over 20 replicate simulations for the 7 scenarios.

Each scenario was replicated 20 times to encompass a range of realized behaviours of the fleet and the results reported here are averages over the 20 replicates. The variation of the trawl model response within scenario is shown in Figure 3-125. This variation arises entirely from random variation in the realized effort. The variation in biomass is larger when the value approaches 50% and would be smaller as the value approached 0% or 100%. The variation in relative biomass is fairly small because it is an average over all model cells.

All the MSE results presented herein are subject to uncertainty, which arises from different sources. First, given values of r and d , the MSE simulations are subject to process error due to variation in the effort allocation. According to Figure 3-125, this is a fairly small effect. The uncertainty in the r and d values themselves is likely to be more important. The error in r is likely to be greater than that in d , as replication from Figure 2-45 suggests. The effect of variation in these parameters can be assessed from Figure 3-126, which encompass the extremes of behaviour. The largest uncertainty is in the pristine

biomass values; the standard errors for individual cell predictions from the GLM models are typically of the same order of magnitude as the estimates themselves.

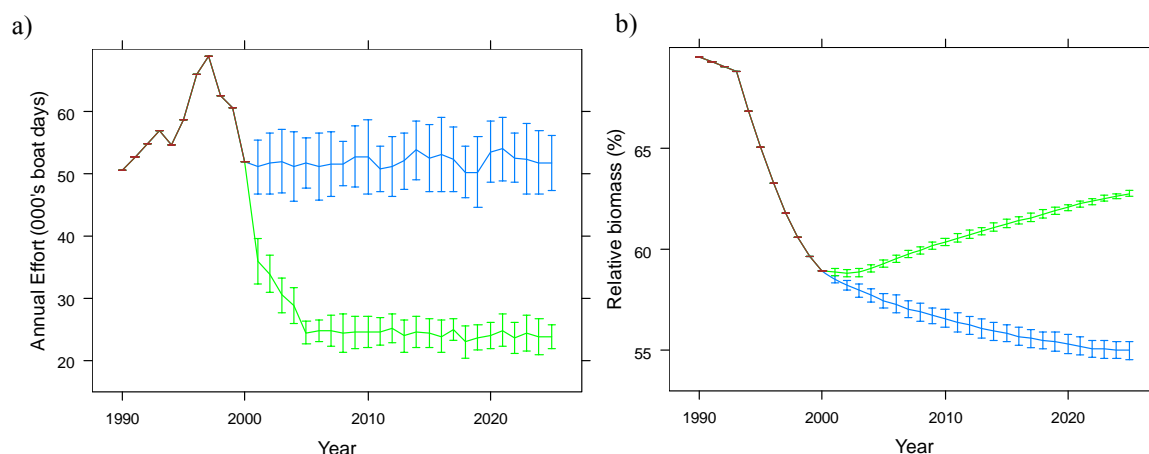


Figure 3-125. Average and standard deviations over 20 replicates for scenarios SQ2001 (*blue*) and CL/BB2001+P+RAP+BB2005 (*green*) of (a) effort and (b) relative biomass.

Although the absolute results from the MSEs are subject to large errors, the comparison across scenarios is much more robust. For instance, the ranking of the scenarios by impact on the benthos is largely unaffected by these errors. The ratios of the indicators across scenarios depended to some extent on r and d , mainly through r/d .

While keeping in mind the uncertainty, the general pattern of relative population status (equivalent to a hypothetical uniform pristine distribution across the region) across a range of observed depletion-recovery parameters was slow decline until ~1990, then more dramatic decline through the high effort period of the 1990s. The falling effort in the late 1990s arrested or reversed the decline for all except the most vulnerable depletion-recovery combinations, which would have continued to decline under status quo 2001 (Figure 3-126). Given all of the actual management interventions that were implemented over the period, the status quo 2006 indicates recovery trends for the most vulnerable fauna, while the least vulnerable recovered almost completely. Individually, each intervention made varying contributions to the overall response: the 2001 low-effort areas closure made almost no contribution; the 2001 buy-back contributed about half of the recovery response; the progressive penalty contributed about half to most of the remainder, depending on vulnerability (high to low, respectively); the RAP re-zoning made some contribution, particularly in the case of higher vulnerability fauna, and the 2005 buy-back lead to a slight additional improvement.

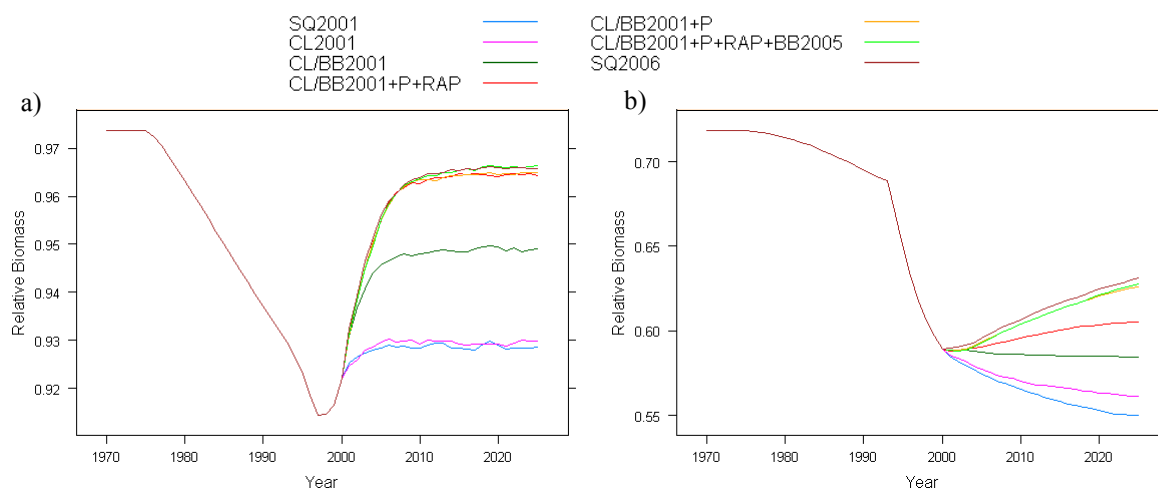


Figure 3-126. Relative biomass histories for all scenarios for two widely different vulnerability types: (*left*) a highly resilient taxon ($r, d = (0.7, 0.1)$); (*right*) a highly vulnerable taxon ($r, d = (0.1, 0.44)$).

After combining these relative status results with the newly available absolute abundance distribution predictions, estimates of regional absolute population status were possible. Thirty-eight cases were examined, including: all mapped species that could be matched with the previous trawl recovery project (Pitcher *et al.* 2004); all mapped species whose individual trawl exposure was examined and/or had a significant trawl effort covariate and could be matched with a morpho-typically similar recovery-project species; and all major invertebrate classes for which impact rate and recovery had been estimated. The overall patterns of individual responses were similar to the general case outlined above. That is, by 2000 almost all taxa had arrested or reversed the declines of the early-mid 1990s, all taxa responded positively to the management interventions of 2001–2005 with the 2001 buy-back contributing about half of the recovery response and the progressive penalty contributing most of the remainder (see Figure 3-127 and Figure 3-128).

However, differences were apparent because different species were distributed differently in relation to trawl effort and closed areas, as well as differing in estimates of their depletion and recovery parameters. The average lowest population status for sessile species, prior to these management interventions, was about 83% of pristine (range ~50% to 96%) and the average projection for 2025 with all current interventions in place was about 89% of pristine (range ~57% to 98%). Low points for mobile species ranged from ~83% to 96% (average ~88%) and projections for 2025 ranged from ~93% to 98% (average ~95%) (see Table 3-61).

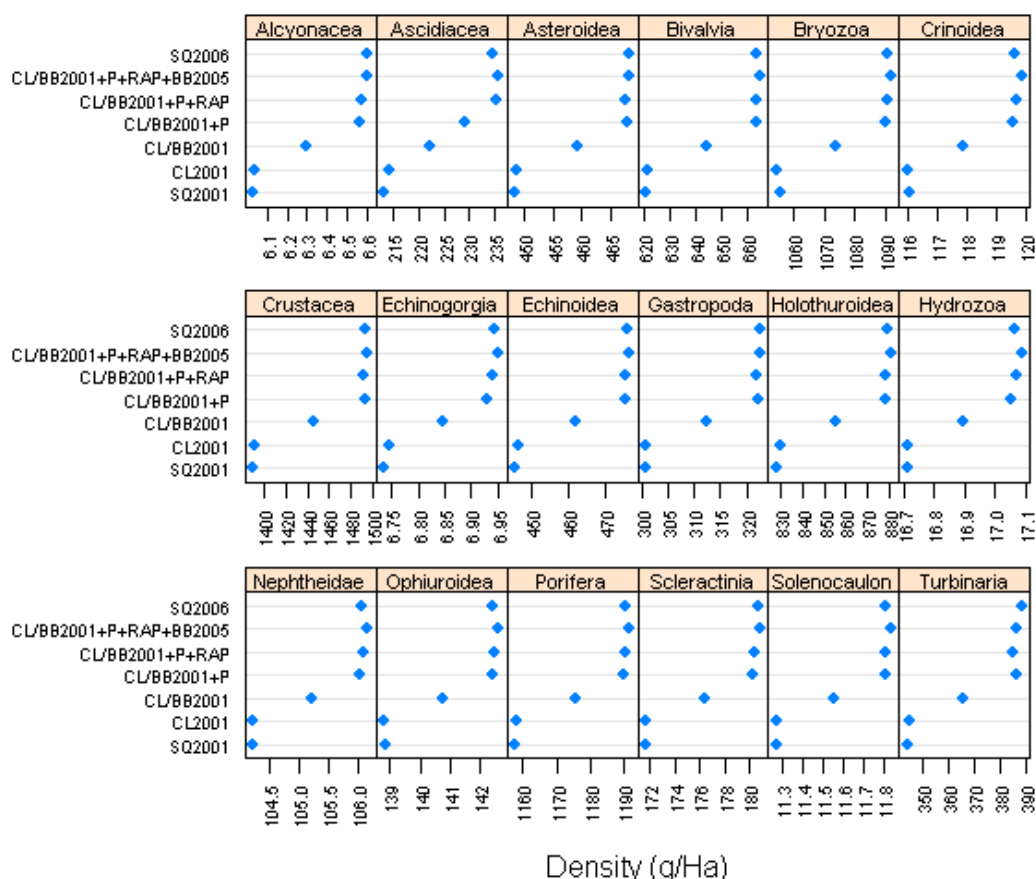


Figure 3-127. Average density of genus- and higher-level taxa in 2025 under each scenario.

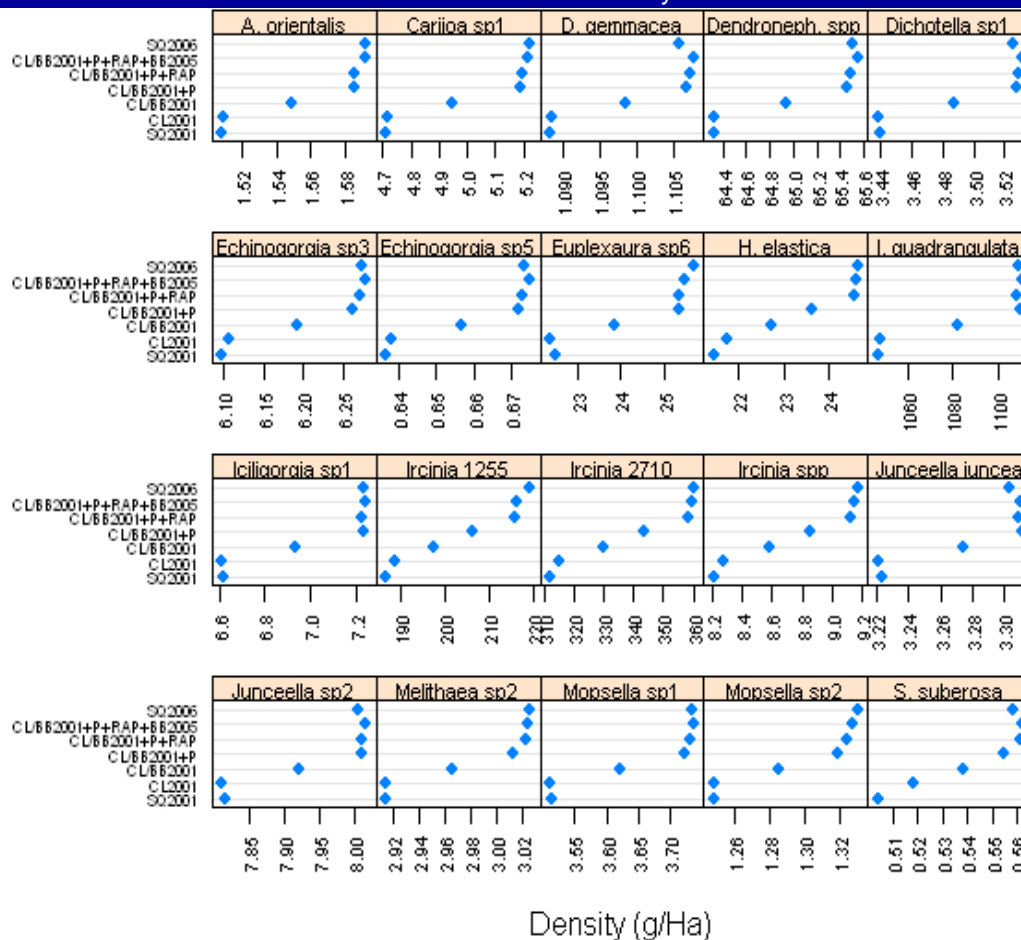


Figure 3-128. Average density of individual species in 2025 under each scenario.

Table 3-61. Lowest historical (pre-2001) percentage relative biomass and final relative biomass in 2025 under scenarios SQ2001 and SQ2006 for (left) species- and genus-level taxa and (right) coarse-level taxa.

| Species/Genus | lowest | SQ'01 | SQ'06 | OTU | lowest | SQ'01 | SQ'06 |
|--------------------------------|--------|-------|-------|--------------|--------|-------|-------|
| <i>Alertigorgia orientalis</i> | 88.5 | 90.8 | 95.8 | Alcyonacea | 79.7 | 82.3 | 89.4 |
| <i>Carijoa</i> sp1 | 74.2 | 77.3 | 85.6 | Ascidiacea | 71.8 | 70.3 | 77.3 |
| <i>Dendronephthya</i> spp | 95.8 | 96.6 | 98.4 | Asterozoa | 90.7 | 92.5 | 96.5 |
| <i>Dichotella gemmacea</i> | 95.8 | 96.7 | 98.3 | Bivalvia | 83.6 | 85.7 | 92.9 |
| <i>Dichotella</i> sp1 | 93.8 | 95.1 | 97.5 | Bryozoa | 92.1 | 93.4 | 96.8 |
| <i>Echinogorgia</i> sp3 | 93.3 | 94.8 | 97.5 | Crinoidea | 92.0 | 93.2 | 96.6 |
| <i>Echinogorgia</i> sp5 | 86.9 | 89.5 | 94.7 | Crustacea | 83.0 | 85.1 | 92.5 |
| <i>Euplexaura</i> sp6 | 65.0 | 67.3 | 77.0 | Echinozoa | 89.2 | 90.8 | 95.5 |
| <i>Hippospongia elastica</i> | 60.7 | 59.1 | 67.9 | Gastropoda | 87.1 | 89.2 | 94.6 |
| <i>Ianthella quadrangulata</i> | 87.2 | 89.1 | 94.4 | Holothurozoa | 85.3 | 87.1 | 93.7 |
| <i>Iciligorgia</i> sp1 | 78.1 | 82.0 | 89.6 | Hydrozoa | 95.1 | 95.9 | 98.1 |
| <i>Ircinia</i> 1255 | 49.6 | 48.6 | 57.1 | Nephtheidae | 93.8 | 95.1 | 97.6 |
| <i>Ircinia</i> 2710 | 59.8 | 58.2 | 67.1 | Ophiurozoa | 95.6 | 96.5 | 98.3 |
| <i>Ircinia</i> spp | 66.8 | 65.7 | 73.4 | Porifera | 93.6 | 94.7 | 97.6 |
| <i>Junceella juncea</i> | 93.6 | 94.9 | 97.3 | Scleractinia | 90.3 | 92.3 | 96.5 |
| <i>Junceella</i> sp2 | 94.0 | 95.3 | 97.6 | | | | |
| <i>Melithaea</i> sp2 | 90.6 | 91.7 | 95.2 | | | | |
| <i>Mopsella</i> sp1 | 83.2 | 84.8 | 90.2 | | | | |
| <i>Mopsella</i> sp2 | 83.1 | 84.5 | 90.1 | | | | |
| <i>Subergorgia suberosa</i> | 74.1 | 69.2 | 76.6 | | | | |
| <i>Echinogorgia</i> | 89.8 | 91.9 | 96.0 | | | | |
| <i>Solenocaulon</i> | 89.4 | 90.9 | 95.5 | | | | |
| <i>Turbinaria</i> | 73.3 | 77.3 | 87.7 | | | | |

For six of the 38 taxa examined, the reducing effort in the late 1990s was not sufficient to arrest or reverse the population decline projected for the preceding period, and the status quo 2001 would have seen these decline even further (Figure 3-129 and Figure 3-130). These taxa included two species of the sponge genus *Ircinia* and other unidentified *Ircinia*, the sponge *Hippospongia elastica*, the gorgonian *Subergorgia suberosa*, and lumped ascidians. While this result for ascidians may be an artefact of the pattern of their recruitment into the Trawl Recovery experiment, which substantially under-estimated their recovery potential (Pitcher *et al.* 2004), the result for the others was likely to be realistic. The sponges responded positively to the 2001 buy-back, and to the penalties by a similar amount, and to the re-zoning by a similar amount again; the response to the 2005 buy-back was imperceptible. *Ircinia* sp.1255 had 46% of its biomass in GU, 27% in trawled grids and 33% exposed to effort; having an estimated catchability of 0.23, its annual incidental bycatch would be about 7% (Section 3.7.2). *Ircinia* sp.2710 had 43% of its biomass in GU, 23% in trawled grids and 24% exposed to effort; having an estimated catchability of 0.10, its annual incidental bycatch would be about 2%. *Hippospongia elastica* was less abundant, and had 42% of its biomass in GU, 22% in trawled grids and 20% exposed to effort; having an estimated catchability of 0.14, its annual incidental bycatch would be about 3%. *Subergorgia suberosa* was projected to remain approximately static under the 2001 buy-back, but the subsequent penalties improved that with a projected positive response, and the re-zoning and the response to the 2005 buy-back was imperceptible. *Subergorgia suberosa* had 32% of its biomass in GU, 16% in trawled grids and 11% exposed to effort, and, with an estimated catchability of 0.10, its annual incidental bycatch would be about 1%.

The most exposed gorgonian modelled was *Alertigorgia orientalis*, with 50% of its biomass in GU, 27% in trawled grids and 29% exposed to effort; with an estimated catchability of 0.09, its annual incidental bycatch would be about 3% (Section 3.7.2). This species showed the same general pattern of positive response to the series of management interventions, and under status quo 2006 management was projected to reach close to pre-WHA abundance by 2025 (Figure 3-129).

Several species examined by the trawl scenario model had negative trawl effort terms in the biophysical modelling. The most negative trawl effect for a species modelled (−36%) was for the gorgonian soft coral *Carijoa* sp1; nevertheless, this species responded positively to the series of management interventions and under status quo 2006 management was projected to reach >90% of pre-WHA (~85% of pristine) abundance by 2025 (Figure 3-129). The current exposure of this species was 25% of its biomass in GU, 5% in trawled grids and 3% exposed to effort, and with an estimated catchability of 0.15, its annual incidental bycatch would be <1% (Section 3.7.2). The next most negative trawl effect for a species modelled (−28%) was for the gorgonian *Euplexaura* sp6; this species also responded positively to the series of management interventions and under status quo 2006 management was projected to reach ~90% of pre-WHA (~77% of pristine) abundance by 2025 (Figure 3-129). The current exposure of this species was 36% of its biomass in GU, 15% in trawled grids and 9% exposed to effort, and with an estimated catchability of 0.14, its annual incidental bycatch would be about 1% (Section 3.7.2). Other modelled species having negative (or possible) trawl effects included *Echinogorgia* sp5 (−22%, ns), *Iciligorgia* sp1 (−20%), *Junceella* sp2 (−16% ns), *Echinogorgia* sp3 (−12%, ns), *Mopsella* sp2 (−10%, ns) and *Dendronephthya* spp (−2%). Again, each of these species responded positively to the series of management interventions, and under status quo 2006 management were projected to reach 90%–98% of pristine abundance by 2025 (Figure 3-129, Table 3-61) — and each had low to very low exposure to current effort.

For a few species, e.g. the sea whip *Junceella juncea*, the sponge *Ianthella quadrangulata* and the coral *Turbinaria*, the positive effect of the 2001 buy-back and subsequent penalties was slightly greater than the additional re-zoning (Figure 3-129). This could be a result of displacement of effort out of newly closed areas, increasing effort in areas where these species were distributed. The effects, however, were very slight (<1%) and appeared to be rectified by the additional buyback.

Nine other species examined by the Effects of Trawling Recovery Project were too infrequent in the GBR Seabed Biodiversity samples for biophysical distribution modelling, though they were observed during towed video transects typically on hard ground not likely to be exposed to trawling.

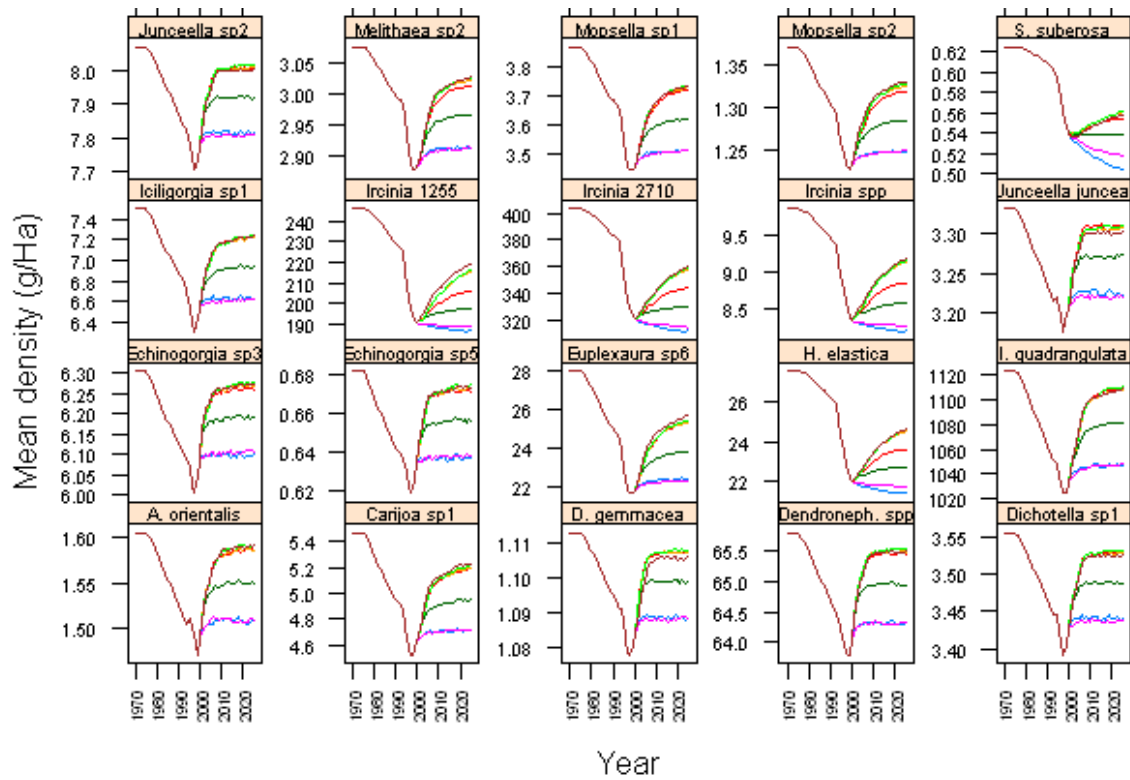


Figure 3-129. Time histories since 1990 of mean density 20 individual species under all scenarios.

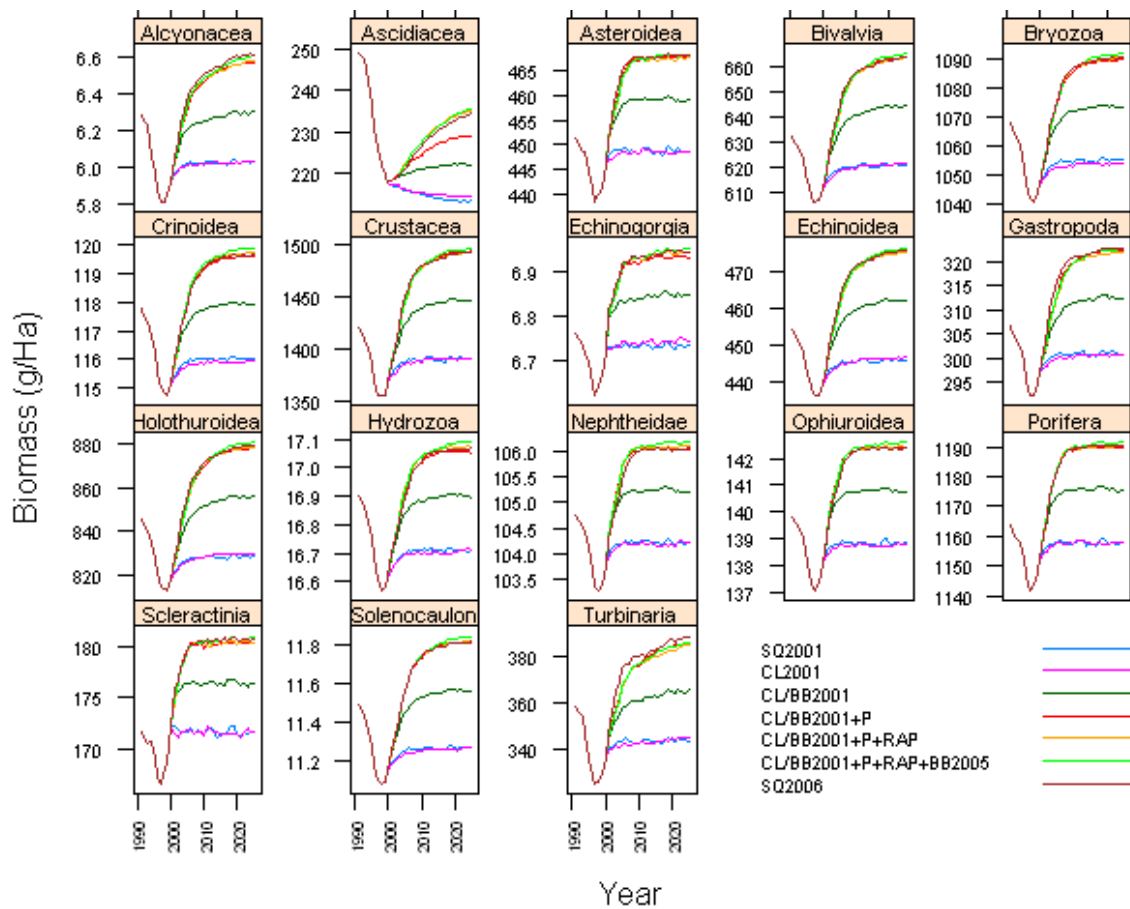


Figure 3-130. Time histories since 1990 of mean density of 18 genus- and higher-level taxa under all scenarios.

The common consistent result from the trawl management scenario modelling was that the omnipresent depletion trends of structural epibenthos up until the late 1990s all appear to have been arrested and reversed by the series of management interventions implemented between 2000 and 2005. The 2001 buyback and the subsequent progressive penalties appeared to make the biggest positive contributions. For ~7 of 38 representative taxa modelled, the rezoning made an observable additional positive contribution, and for a similar number of species a slight contribution of the 2005 buy-back was also observable.

4. DISCUSSION

The GBR seabed is a complex mix of physical environments. The component species and biological assemblages have been observed to respond significantly, though in different ways, to the multiple interacting physical gradients and few of these gradients have simple trends in 2-dimensional space. Much of the prior knowledge about seabed biodiversity has been sourced from the Central (Townsville) Section of the GBR where there are a series of relatively linear cross-shelf coastal to offshore gradients. Along with a gradient of progressively increasing depth, there is an inner shelf prism of terrigenous sandy-mud sediments that extends 15–20 km offshore to water depths of 20–22 m. Further offshore, the GBR lagoon in depths ~22–40 m has little terrigenous sediment but a thin veneer of mixed shelly, muddy-sand overlying weathered Pleistocene clay, which can be exposed by cyclones to form outcrops on the seabed. Amongst the mid-shelf and outer-shelf reefs, the seabed (40–80 m) has virtually no terrigenous sediment, but is covered thinly by shelly biogenic carbonate sand; here, old Pleistocene reef platforms are the foundations on which modern coral reefs emerge (Larcombe & Carter 2004). With these geological patterns, there is a gradient from high turbidity to clear water. The mid/outer shelf reef matrix off Townsville is relatively open and this permeability allows influx of the EAC oceanic water and induced upwellings, which penetrate as far as the mid-shelf (Wolanski 1994). The south-easterly trade winds drive a northward flowing coastal boundary layer that limits mixing of nearshore and offshore waters (Brinkman *et al.* 2002). As a result, there are cross shelf gradients in bottom water attributes coastal to offshore: warm to cooler temperature (high to low variability), low to high salinity (high to low variability), high to low oxygen (low to high variability), and low to high nutrients (low to high variability). Further, tidal currents are weak though most of the area. This has led to an established view of fixed across shelf zoning of the biota (discussed further in sections below).

However, these simple cross-shelf physical environment patterns largely apply only to the Townsville vicinity from about Cape Upstart to about Hinchinbrook Is. The physical covariates collated by the project showed that elsewhere, the physical environment does generally change more quickly in the cross-shelf direction than the along-shelf direction, but in ways that may be completely different to that in the Townsville vicinity. For example, about a third of the coast from about Mackay south is sandy not muddy, as is the far northern coast from Shelbourne Bay north (as well as a number of other locations). Conversely, much of the mid-shelf from about Mackay south is muddy not sandy, as is the far northern inner/mid-shelf from about Shelbourne Bay north; the outer shelf from about Innisfail to Cooktown has significant areas of high (carbonate) mud fraction. The Capricornia section is almost entirely sand; terrestrial silica sand along the coast and across the shelf in the south; carbonate to the northeast. While coastal areas are always shallow, much of the outer shelf north of about Cooktown is about as shallow as the inner and mid shelf, as is the Swains even though it is the most offshore area in the region. In the southern GBR, the mid-shelf is the deepest (Capricorn Channel). In much of the southern GBR, and far northern/Torres Strait, extreme tidal currents create forces on the seabed in both inshore and offshore areas that lead to sediment scoured and epibenthic habitats that rarely occur in the Townsville and Cairns Sections. The ribbon reefs extending north from about Cooktown to Torres Strait limit exchange and upwelling of cooler, saline, nutrient rich water onto the outer shelf; in the southern GBR, these occur well into the Capricorn Channel. These different physical environment patterns elsewhere contribute to the complexity in patterns of seabed biota observed by this project.

It has been noted previously that there are a wide range of inter-reef habitats dominating in different regions of the GBRMP due to varying riverine inputs, tides, currents and upwellings, seasonal winds, waves, and cyclonic events, with different combinations of these forces governing the topography, grain size and composition of sediments, the chemical properties of overlying waters (Larcombe & Carter 2004; Porter-Smith *et al.* 2004) and therefore, the nature of seabed assemblages and their dynamics. Local influences, such as tidal jetting of nutrients, facilitate the development of substantial *Halimeda* algal banks 15-20 m thick inside the ribbon reef passages of the northern GBR (Drew 2001). Porter-Smith *et al.* (2004) noted that in the macrotidal areas of Broad Sound and Shoalwater Bay, tidal currents were the dominant force influencing the mobility and grain size properties and contrasted with the rest of the GBRMP. The bifurcation of the South Equatorial Current (SEC) against

the outer reef (Wolanski 1994) between about Lizard Is and Cairns, which produces the EAC to the south and the NW Coral Sea gyre to the north, can influence the dispersal of species with oceanic larvae (Pitcher *et al.* 2005).

There are also latitudinal differences in flushing rates and the amplitude of seasonal variation in sea surface temperature (SST) and salinity. Hancock *et al.* (in Press) found that inner lagoon diffusivity was about 2.5 times higher in the central section compared to the northern, so that water within 20 km of coast is flushed with outer lagoon water on a time scale of 18-45 days, with greater flushing times in the north. Salinities in the southern lagoon are significantly higher than those in the central and northern sections, and seasonal variation is lower. Summer SST are ~2-3°C lower in the region south of Bowen compared to the far north, and in winter a relatively cold coastal water body forms there (Condie and Dunn 2006).

4.1. BRUVS SPECIES MODELS, CHARACTERIZATION & PREDICTION (M Cappel, G De'Ath)

4.1.1. BRUVS Fish species

Only 50 of the 347 species recorded by BRUVS occurred at 7% or more of the sampling sites. Univariate biophysical models of this subset produced many erroneous (negative) predictions of abundance. It was decided then to produce biophysical models and maps of the presence/absence (occurrence) of single species in relation to the environmental covariates. The occurrence of only 25 fish species could be predicted with errors of 20% or less, and a shortlist of 20 environmental covariates were useful as predictors.

The “nuisance” temporal variables such as moon phase, season and time of day had no effect on average rates of prediction, so they were dropped from the best models. This implied the biophysical maps of occurrence in the BRUVS dataset do not need to be adjusted for these temporal variables.

The spatial location (across, along, depth) and mud, gravel and carbonate content of sediments were the top six predictors of species occurrence. There were a variety of relationships between these physical parameters and the occurrence of particular species. The presence of some species was best explained by a single variable, including *Scomberomorus queenslandicus* found inshore, *Pentapodus paradiseus* influenced by gravelly sediments, and *Nemipterus furcosus* and *Alepes apercna* found in warmer temperatures. The presence of other species was influenced most most by a combination of spatial and environmental variables. *Nemipterus hexodon* was one of the most predictable species, occurring nearshore in sediments with high mud content. In contrast, *Pentapodus nagasakiensis* was found offshore in sediments with high carbonate. Within the same family *N. theodorei* was influenced most by deep water and high salinity. This species was not seen in the far north. A number of species were influenced most by environmental variables. The economically important *Choerodon venustus* occurred most in areas of higher current with sediments containing high carbonate. *Parapercis nebulosa* also occurred in higher current, over sediments with low mud content.

The trawl effort index explained a moderate proportion of the variability in occurrence of only a single species (*Nemipterus peronii*), but interpreting such relationships was very difficult because trawling occurs infrequently, or not at all, over most of the GBRMP and in high levels in some areas, such as Cape Flattery. Thus the 10th percentile in the trawl effort index had much leverage on the response by *N. peronii*. The relationship between the species responses and the environmental gradients in the GBRMP are discussed below with the characterisation of species groups.

4.1.2. BRUVS Fish Assemblages

Significant differences have been reported in the distribution and abundance of a range of faunal and floral groups in the GBRMP along the strong cross-shelf gradients readily measurable in salinity, nutrient input, water clarity and exposure to prevailing wind and waves with increasing distance from

the coast (Drew 2001, Wilkinson & Cheshire 1988, Newman *et al.* 1997, Gust *et al.* 2001). However, studies have incorporated the latitudinal gradient along the shelf (DeVantier *et al.* 2006, Fabricius & De'ath 2001, Williams 1991), and most have been restricted to the depth limits of SCUBA diving observations on shallow reefs. The results reported here are the first attempt at describing the patterns in fish communities in terms of both location in the GBRMP and critical environmental covariates.

The use of boosted and multivariate regression trees provided compelling results concerning the cross-shelf rise in species richness to “hotspots” about the shallow banks and shoals amongst the offshore reef matrix, the existence of spatially-contiguous fish communities along and across the shelf of the GBRMP, and the existence of major community boundaries near Bowen (20°S) in the south and Princess Charlotte Bay (13.3°S) in the north. These robust patterns were detected amongst a functionally diverse cross-section of the fish fauna by analysis of data collected with a simple, efficient baited video technique.

The majority of species recorded by the BRUVS occurred rarely and this pattern also seems characteristic of tropical fish faunas sampled by trawl. The widespread sampling with BRUVS recorded a similar number of species (347) to those recorded by trawling (300 – 350) in similar latitudes by Watson *et al.* (1990), Blaber *et al.* (1994), Wassenberg *et al.* (1997), and Stobutzki (2001b). Those trawl inventories were also dominated by species that occurred rarely and in low abundance. Stobutzki (2001b) found that 75% of species occurred in less than 10% of prawn trawls, and Blaber *et al.* (1994) found that 75% of the biomass in fish trawls comprised only 8% of the species caught. Like estuarine fish faunas (Magurran & Henderson, 2003), the vertebrates in the “inter-reef” waters of the GBRMP probably comprise “core species”, which are persistent, abundant and biologically associated with particular habitats, and “occasional species”, which occur infrequently in surveys, are typically low in abundance and have different habitat requirements.

Only 50 species occurred at 7% or more of the sampling sites and the abundance of only 25 of these species could be predicted, in terms of the 40 environmental covariates, with errors of 20% or less. This shortlist was chosen for preparation of biophysical maps relating communities to the environment. Multivariate trees were used within this shortlist of species to define a hierarchy of communities constrained by their spatial and environmental values that locate them in the GBRMP. This hierarchical approach identified groups of the 25 predictable species that co-occur at varying spatial scales to form communities.

A number of multivariate trees were assembled using different combinations of spatial and environmental variables. The simplest, most easily interpreted model chosen to produce biophysical maps used only position across and along the shelf as explanatory variables for the 25 most predictable species. The broad patterns identified by this tree largely coincide with the analysis of the entire species list by Cappo *et al.* (subm.) in a study that aimed to explain (not predict or map) communities in terms of location and depth.

The across and along tree produced spatially contiguous communities occurring around major faunal breaks in the nearshore half and middle of the lagoon, and alongshore. Latitudinal variation was greatest in the inner half of the shelf, where Bowen and Princess Charlotte Bay separated inner and outer shelf groups. The offshore communities were latitudinally more extensive showing that outer-shelf deep communities were more similar amongst latitudes than to inner-shelf communities at the same latitude and vice versa. These trends were also reported by Williams (1991) for reef fish communities on outer slopes of outer-shelf and mid-shelf coral reefs, with mid-shelf reefs in the far north being more similar to nearshore reefs elsewhere than to mid-shelf reefs at more southerly latitudes.

Cross-shelf gradients in demersal fish communities have been reported elsewhere in the southern Indo-Pacific. A “nearshore” group of sites (<24 m depth) was distinguished from a “mid-shelf” (outer lagoon 35-42 m depth) and an “inter-reef” group (mid-shelf reef matrix 43-56 m) in catches by prawn trawl in the central GBRMP (Watson *et al.* 1990). That study concluded the composition of the ‘inter-reef’ fauna remained strikingly uniform regardless of proximity (~0.5 to 10 km) to coral reef formations. In the Gulf of Carpentaria, Blaber *et al.* (1994) distinguished six main site groups and 15 fish community groups in fish trawls, correlated with depth but not with sediment type, salinity, temperature or turbidity. Letourneur *et al.* (1998) concluded that the effect of sediment type in shaping reef fish communities in lagoon waters was confounded by cross-shelf position, which acted as an

easily measured surrogate for the gradient from terrigenous to oceanic influences in New Caledonia. At broader scales, Ramm *et al.* (1990) found that a bycatch fauna from prawn trawls samples clustered along geographic and bathymetric gradients, forming distinct western and eastern groups separated near 132°E, either side of the 30 metre isobath. This longitudinal boundary separates the faunistic provinces of the Timor Sea to the west and the Arafura Sea to the east.

Reviews have concluded that sediment type, water clarity, seabed topography, the nature of epibenthic communities and thermal stratification all shape the composition of tropical, demersal fish communities (Longhurst & Pauly 1987, Sainsbury *et al.* 1997, Lowe-McConnell 1987). In the tropical western Atlantic, Lowe-McConnell (1987) characterised a cross-shelf gradient from a “brown water” zone (ariid catfishes, dasyatid rays) over mud, to a “golden fish” zone (sciaenid croakers) over sandy/mud, to a “silver fish” zone (carangid jacks, haemulid grunts) in “green water” (40–60 m deep), above a “red fish” zone (lutjanid snappers) over hard sand/rock in “blue” oceanic waters (~100 m). Similar patterns were reported in the eastern Atlantic, with the additional influence of a strong thermocline causing sub-tropical sparids to dominate in the cooler waters under the thermocline over sand, rock and Holocene reef edges (Fager & Longhurst 1968, Lowe-McConnell 1987).

We found that there were not strict cross-shelf differences in the occurrence of different families and that single families often contained a number of species that characterised different communities. Ubiquitous families such as the nemipterid threadfin breams, monacanthid file fishes, carcharhinid requiem sharks and tetraodontid pufferfish had representatives in both inshore and offshore, deep and shallow communities. The inshore community included many indicator species from the “small pelagic” functional groups, such as the piscivorous *Scomberomorus queenslandicus* and deep-bodied micro-invertebrate carnivores (Carangidae: *Atule mate*, *Selaroidesleptolepis* and *Carangoides coeruleopinnatus*). Demersal teraponid grunters and bathysaurid lizardfishes were also characteristic of inshore groups. These are known to inhabit soft sediments in the Indo-Pacific (Blaber *et al.* 1994; Sainsbury *et al.* 1997). Indicator species offshore included pinguipedid grubfishes (*Parapercis xanthozona_grp 40*) and labrid wrasses (*Choerodon venustus*, *Oxycheilinus bimaculatus*) thought to be associated with more complex seafloor topography, such as reefs, rocks and rubble.

The distributions of fishes and their assemblages are likely to be shaped by variation in sedimentary and oceanic processes and other influences that determine the wide range of seabed physical and biological habitats dominating in different regions of the GBRMP, as described above. In turn, these habitats may influence the recruitment, feeding success and mortality of fish communities inhabiting them. The nearshore and mid-shelf boundaries separating the fish assemblages appear related to sediment carbonate and grain-size composition particularly in the Central Section. The observed fish assemblage patterns fit well with knowledge of gradients and boundaries in sedimentary processes, water movement, and seafloor fish habitats such as erosional features, depositional banks and vegetated meadows.

Major latitudinal boundaries in the fish assemblages may be related to circulation patterns and their consequences. The latitudinal variation amongst the communities along the shelf, with boundaries near Mackay, Bowen, Cape Bowling Green, Princess Charlotte Bay and Cape Direction, may be explained by circulation patterns in a cooler, macrotidal southern region, a well-flushed central region with deepwater seagrass beds, and a warmer, constricted northern region where *Halimeda* algal banks thrive behind a dense reef matrix. The next step is to analyse these spatial groupings within a comprehensive suite of biotic measurements from other sampling gears to determine if predictions and explanations of the shelf-scale patterns in fish communities can be improved with knowledge of epibenthic communities now available from the Seabed Biodiversity dataset.

4.2. SINGLE SPECIES, BIOPHYSICAL MODELS AND PREDICTION

The epibenthic sled and research trawl both sampled a highly diverse seabed biota of more than 14 phyla and >5,300 species, of which about a third were sampled by both devices, almost half were unique to the sled, and just less than a quarter were unique to the trawl. While the Sled samples were rich with almost 60 taxa per site on average and had greater total species richness, the Trawl samples averaged about 87 taxa and were less variable (<1% sampled fewer than 20 species). Thus, the trawl

more consistently sampled local populations representatively (particularly fishes and crustaceans), whereas the Sled sampled all other biota better, though with greater variability, perhaps due to the greater number of sites and habitats sampled by the sled. These devices provided specimens that could be properly identified, showed that otherwise inseparable taxa could have strikingly different distribution patterns and revealed the enormous biodiversity of the region (even at sites where other devices observed no biota at all). They also provided excellent benefit:cost in terms of enormous information yield per unit investment and given the very small area sampled (~1/50000).

As is typical of biological sampling, a large proportion of these taxa occurred in only one or a very few sites. This, and patterns of species accumulation curves, indicated that many more seabed species remain to be discovered — despite the regional extent and number of sites sampled by the project — and confirms the significant biodiversity of the deeper lagoon and inter-reef seabed in the GBR.

There were some clear basic patterns of species richness: structured habitats were more diverse, and structure was provided by marine plants, epibenthic fauna, and rugose hard substrata. Key vegetated habitats occurred in a midshelf band in the central GBR, the inner/mid-shelf in the Capricorn region, the outer shelf in the far northern region and near the Turtle and Howick Island groups. Key epibenthic habitats occurred in the vicinity of Broad Sound and Shoalwater Bay, approaches to Torres Strait, inshore and offshore passages and hard ground. Topographically complex hard ground occurred primarily among the outer shelf reef matrix as relic reef growth from eras of lower sea levels. Muddy habitats, on the other hand, had relatively low biodiversity and tended to be dominated by smaller fishes. The structured areas also had steeper species accumulation curves, i.e. additional sites were more likely to yield additional species compared with muddy areas, which consequently tended to be more homogeneous.

Compared with the total number of species sampled, relatively fewer species were considered frequent enough for analyses (at >25 sites). Nevertheless, there were about 840 species that met this criterion. This presented considerable computational challenges for biophysical modelling, necessitating a consistent mechanistic approach and meant that in the available timeframe models could not be manually customized for individual species. The analyses also produced an enormous output, of which only summary distributional highlights can be presented, even in a large report, and future examination of the dataset and results would provide valuable specific information.

The two-stage presence-biomass GLMs provided a robust and flexible method of selecting physical covariates having statistical relationships with the biological data suitable for modelling biophysical responses and predicting distributions. More than 65% of the ~840 species analysed had good models; however, not all species could be modelled well. Up to ~10% had poor models though many of the latter were for species that could not be weighed readily, and 11 species had no statistical relationship with any of the physical or spatial variables. For the majority of species, i.e. those occurring at <25 sites, no analyses or modelling has been reported at this time, though point data will be available.

The biophysical modelling provided an indication of covariate importance in relation to patterns of species abundances. The most frequent covariates were sediment grain size and carbonate composition, followed by space, benthic irradiance, current stress, bathymetry, then bottom water physical attributes, seasonal effects, nutrients and turbidity, and other temporal effects. Trawl effort was selected infrequently, at about 10% and was significant in just over half these cases. Aspect was selected least. However, frequency of covariate selection is not necessarily a direct test of performance among the various individual physical or spatial covariates due to the high correlations between many of them. That is, a given covariate may be parsimoniously selected though it is merely a surrogate for a number of others with which it is correlated.

The environmental covariates have demonstrated utility for spatial prediction of the broad scale patterns of presence for the majority of species with occurrence >25 sites, although they do not often account for the majority of observed variation in local biomass. Other factors, including stochastic processes such as recruitment and mortality, biological interactions, and random sampling effects typically outweigh deterministic environmental relationships at the local site biomass scale.

The variety of biophysical responses, and hence distributions, expressed was almost as large as the number of species analysed, and while there were numerous highly contrasting responses there was a continuum of responses between the extremes. Some of the contrasting responses observed followed the more frequently occurring covariates, such as \pm mud or sand or gravel, shallow vs deep, low vs

high benthic irradiance, inshore vs offshore, northern vs southern, strong vs weak current stress, cool vs warm temperature etc. It is important to note that taxonomy provides little guide to patterns of distribution. For example, many similar con-generic species were observed to have highly contrasting distributions, demonstrating the importance of species-level identifications wherever possible, when assessing biophysical responses and physical surrogate performance, and when addressing management applications such as fisheries risk assessments and conservation planning.

4.3. SPECIES GROUPS CHARACTERIZATION AND PREDICTION

The ~840 modelled species were clustered into 38 groups largely to facilitate manageable processing of the trawl risk assessments rather than any particular attempt at this time to identify an objective number of functional “communities” of interacting species; though the methods used may be useful to facilitate initial identification of potential functional relationships between species, significant future ecological investigation would be required. As noted in the previous section, there was almost a continuum of distributional patterns with few strong clusters. The groups were constructed to comprise species with highly correlated distributions, given the stated purpose, leading to a greater number of groups than conventional applications of the method. The basic patterns of groups were similar to those of single species and though the models were more complex, covariate importance ranks were also similar to those of single species.

Species groups distributions were also not clearly related to taxonomic groupings, as noted above, with closely related species occurring in different groups and most groups comprising numerous unrelated taxa. Possible exceptions may have included some marine plants, sponges and bryozoans. Marine plants appeared to dominate in a number of rather specific areas determined at least in part by light availability; this and other shared constraints lead to a number of related species sharing similar distributions. Similarly, a number of encrusting bryozoan taxa were distributed in high current passages of the Pompey Reefs complex and a number of sponge taxa had similar distributions. Even in these constrained taxa, however, members of the same genus, family or class may have markedly different distributions.

4.4. SITE GROUPS CHARACTERIZATION AND PREDICTION

Due to the complex mix of physical environments described above, as well as additional variability remaining unexplained by the available covariates, the biodiversity assemblages of the GBR seabed are difficult to represent adequately in any single characterisation. The multitude of species respond in different, overlapping and varying ways to the multiple interacting physical gradients, which as noted above do not have simple trends in geographic space. Much of the prior biological sampling has been conducted in the Central (Townsville) Section of the GBR where the gradients are among the simplest in the region.

Seabed biological assemblages off Townsville were first sampled by Birtles and Arnold (1983 & 1988) using an epibenthic sled during a series of studies between 1977 and 1983. The shallower (<20 m) inshore muddy zone, to about 30 km offshore was characterised by low species richness of carnivorous and deposit feeding echinoderms, molluscs, crustaceans, fishes, bryozoans and algae, and low species evenness — i.e. a relatively low number of species was dominated by even fewer. Further offshore, from ~30 km to the mid-shelf reef-matrix at ~80 km, the deeper (20–50 m) carbonate sand lagoon zone was characterised by higher species richness of all faunal groups, due to increased habitat heterogeneity with patches of harder substratum that allow a wide variety of suspension feeders, such as sponges, ascidians, crinoids, holothurians, and bryozoans, a foothold in addition to the deposit feeders in the sediments between the patches. On the deeper gravely outer shelf (> ~80 km) offshore inter-reef zone the fauna was dominated by the suspension feeders (Birtles and Arnold, 1983). Temporal sampling showed that patterns of distribution remained essentially stable over the period. Greatest variability was apparent in the nearshore sites, due to physical instability of the sediments

caused by wind generated waves. Later, Watson and Geoden (1989) sampled around the Birtles and Arnold study area with somewhat greater alongshore coverage, using commercial prawn trawl gear, and found similar parallel zones that were stable over time. With few benthic studies conducted elsewhere, there has tended to exist a rather fixed view of simple cross-shelf zonation in the biota.

However, as already noted, the physical environment in other areas of the GBR has different combinations of physical environments and geographic gradients that may be completely different to that offshore from Townsville. These different physical environment patterns elsewhere explain why there have been reports of what had been regarded as nearshore faunas occurring in mid-shelf areas north of Cairns and even outer shelf areas (i.e. inner edge of Swains) (e.g. Williams, 1991). The Effects of Trawling Study in the far northern section (Poiner *et al.* 1998) noted that the coastal silica sand strip had fauna more similar to mid/outer-shelf areas than to the inner/mid-shelf high mud area. These "aberrant" patterns may now be understood more clearly with the extensive bio-physical information provided by the Seabed Biodiversity Project — the patterns are not aberrant at all but reflect the complex variety of environments manifest and distributed in different spatial patterns throughout the GBR region. The biotas are located largely (but not entirely) by environment than by cross-shelf position *per se*, or by latitude *per se*.

The biological assemblages observed by the Seabed Biodiversity Project are largely in line with the physical covariates found to be important in the single-species modelling and hence with the complex multidimensional physical environment patterns collated and mapped by the project and outlined at the beginning of the discussion. That is, the patterns are consistent with gradients between high and low mud areas, shallow and deep areas, high and low current areas, with further separations on sediments, water chemistry and turbidity. Note that each of these variables have surrogates that could separate assemblages, given the numerous correlations between the covariates. These broad patterns were largely unrelated to higher level taxonomic groupings; with members of most groups of biota occurring in most areas.

However, not all known patterns were captured within the stopping/cross-validation rules used by most statistical splitting algorithms, largely due to the variability in the data. For example, the inshore and offshore high current stress areas were grouped together and while they were similar in some respects there were nevertheless differences in species occurrences, depth and turbidity; the topographic shoal strata was not separated but was shown to differ from surrounding deeper seabed in a previous study (Poiner *et al.* 1998); and vegetated habitats were not separated precisely in the biophysical characterisation compared with the point species data.

4.5. VIDEO HABITAT CHARACTERIZATION AND PREDICTION

The physical habitats observed during towed video transect largely followed the physical environment patterns already discussed, not surprisingly given the similarity of the attributes quantified. Substratum was closely related to sediment grain size and carbonate, with exposed hard substratum occurring in high current areas, and deeper rocky areas amongst the outer shelf reefs. The biological habitats observed by video in part followed the physical substratum patterns, with bioturbated habitats occurring in many softer sediment areas and sessile epibenthic fauna and bryozoans common in high current hard ground areas. Vegetated habitats occurred on a variety of substrata and have constraints related more to irradiance and bottom water attributes. While some of the densest vegetated habitats were captured by the biophysical characterisation of video habitats, including much of the Townsville midshelf band, the Capricorn inner shelf area and far northern *Halimeda* banks, they were not separated very precisely. Furthermore, the biophysical characterisation confused intermediate density vegetated areas with some high density areas as well as with some very low density areas. Statistical stopping rules in conjunction with data variance contribute to this imprecise separation, and better broad scale data on relevant bottom water attributes would likely improve the biophysical characterisation.

A key issue with video, however, is the inability to identify most of the biota adequately. For example, hundreds of species of algae that comprise algal habitats can be identified to only a very few distinct genera and most to a handful of morpho-types, which blurs biophysical relationships that were

apparent at the species level and leads to inconsistent biophysical responses that are difficult to model with statistical methods, and thus difficult to map with biophysical spatial modelling.

A further issue was indicated by results of the first habitat characterisation strategy (first cluster the video biological data alone, then attempt to model their physical relationships), which had some difficulty representing the broader distribution of habitat clusters. Whereas, the second strategy found ‘habitats’ by using the biological profile together with and at the same time as the physical environment in which it resides. In this case, very similar biological habitats appeared in different tree nodes suggestive of different regions of environmental space. As an example from the results, two very similar seagrass dominated habitats (tree nodes 6 and 7, Figure 3-60, Figure 3-61,) were four nodes apart in the tree diagram suggesting different regions in environmental space. The mapped predictions (Figure 3-62) indicate a spatial divergence as well, with group 6 largely confined to the southern region of the GBR but with group 7 distributed in the mid-shelf off Townsville. Note that spatial predictors, however, played no direct part in the definition of these groups. However, the risk this brings to the second strategy is that essentially the same habitat, split in this way, may be interpreted as a different habitat — unless the composition is examined carefully. It is possible that if the habitat groups are initially defined in terms of biology only (the first strategy), sites such as those present in groups 6 and 7 may be clustered together, though this may make their prediction using the external physical variables more difficult because they are in different regions of environmental space. Note that the GLM method used in the single species modelling successfully modelled *H. spinulosa* distribution, the key species present in these two example seagrass dominated habitat cluster types and apparently occupying different regions of environmental space.

4.6. ACOUSTICS DISCRIMINATION AND CLASSIFICATION

Three approaches were taken to examine the performance of remotely sensed acoustic data, from a normal-incidence 120 kHz single beam digital echo sounder, for discriminating different seabed habitats and hence, as a surrogate for patterns in habitats and their constituent biodiversity.

- (1) wavelet-based methods on angular transformed and re-sampled EY500 digital data, initially on simple pair-wise habitat class comparisons between few sites then progressively adding more habitat classes and sites.
- (2) canonical variate-based methods on dilation-translation transformed and re-sampled EY500 digital data, initially on the entire ground-truthed dataset including all available sites and classes, then directed contrasts between fewer sites and fewer habitat classes.
- (3) linear discriminant analysis methods on the QTC View proprietary 166 feature data, initially on the entire ground-truthed dataset including all available sites and classes, amalgamating classes, and by a moving window of restricted spatial and depth dimensions.

4.6.1. Wavelet Packet-Based Techniques Applied to Data in the Angular Domain (D H Smith)

Supervised classification experiments were performed on data in the angular domain via the Local Discriminant Basis in conjunction with Daubechies-2 filter coefficients and two different standard classifiers for up to five seabed habitat classes of long contiguous blocks of >1,000 pings, which tended to exclude certain habitats that were typically patchy in nature. Two-class testing on (sand,no biohabitat) and (sand,seagrass) seabeds with a single deep (sand,no biohabitat) training set produced very satisfactory classification results in a few pairwise site comparisons; however, addition of more sites demonstrated a strong sensitivity to the depth of the corresponding test set component, despite angular transformation of the data. This can be partially explained by the physics of acoustics, resulting in a distinct depth divide separating good and poor classification results. Substitution of a much shallower alternative training set for the (sand,no biohabitat) component produced no clear divide with less-variable classification accuracy lying between the extremes of the about experiment. In terms of overall mis-classification rates, the best results reached below 10% while the worst cases

reached just over 80% for these two-class cases. High mis-classification rates, when they did occur, were essentially the result of sand being mis-classified as seagrass.

Highly variable performance was also recorded in a second series of two-class experiments involving (sand, sponge garden dense) and (sand, seagrass) seabed types. Mis-classification rates for a selected training set ranged approximately between 10 and 55%, the upper limit caused by sponge garden being mis-classified as seagrass on many test sets. Little depth variation was present in these training and test sets, and the variable performance has little to do with the depth effect noted above.

A three-class classification test involving (sand, no biohabitat), (sand, sponge garden dense) and (sand, seagrass) seabed types produced satisfactory classification results on a particular single training/test set pair, with confusion matrix diagonals all exceeding 80% and a best overall mis-classification rate of approximately 15% achieved with Linear Discriminant Analysis. Sand produced the best classification result, followed by sponge garden and seagrass. Feature dimension reduction was also achieved, but to a smaller extent than that obtained on the two class cases. Additional calculations with the same training data on a collection of test sets, including all available data of >1,000 contiguous pings for each class, indicated some significant performance differences between the Linear Discriminant Analysis and Tree classifiers. For sponge garden and seagrass biohabitats the Linear Discriminant Analysis was clearly superior, while little difference was observed for sand without biohabitat. In each case a general decline in performance with depth departure between the training and test sets was observed, however only one single training set was applied and performance with multiple training sets would be needed to fully assess variability in performance.

Incorporating a fourth seabed habitat class, namely (sand, bioturbated), gave mixed results on a selected single training/test set combination, with good performance recorded for the (sand, no biohabitat) and (sand, bioturbated) classes accompanied by moderate performance for (sand, seagrass). Principal error contributions for the latter case were due to mis-classification as (sand, sponge garden), which in turn was poorly classified and largely mistaken as seagrass. Further calculations on a range of different test sets showed good results from Linear Discriminant Analysis on the bioturbated class for depth departures up to almost 20 m, beyond which above 50% accuracy was retained up to 50 m departure. On the remaining three classes the two classifiers demonstrated clear differences, with Linear Discriminant Analysis superior for sponge garden and inferior for sand and seagrass; whereas as, in the experiment above, LDA had performed better than Tree on the same seagrass datasets. Again, classification performance was observed to decline with depth differences.

For a single five-class experiment involving different substrata in the absence of biohabitat, evidence for the concept of class merging appeared, in which different nominal classes are merged to produce a workable reduced set of seabed classes. Specifically, this applied to coarse sand and sand substrata types, and also to silt and soft mud, which were strongly confused by Linear Discriminant Analysis. The fifth substrata type, namely sand waves/dunes was almost 90% correctly classified in this experiment, with the error primarily due to mis-classification as soft mud.

In these tests with training and test set class contributions from individual sites, the Local Discriminant Basis operating on angular transformed data was able in selected localised cases to extract features that provided a good basis for classification of a limited number of classes by methods such as Trees or LDA. However, as the number of sites involved in tests was increased, or as the depth departure between sites increased, or as the number of classes of biological habitat on a fixed substratum was increased, or as the number of substratum types was increased, classification performance declined to unsatisfactory levels. The increased ambiguity means that relatively few bottom types can be consistently classified and so included in a workable set of seabed classes, and then only within a limited range of depth variation.

4.6.2. Canonical Variate Analysis of Acoustic Data (N Campbell & D Devereux)

Canonical Variate Analyses were performed on digitised ping data, depth-normalised by the dilation method, and tested primarily with all available habitat classes and depths, but restricted to data representing classes with >100 contiguous pings.

A depth problem was again apparent and was examined in some detail. Depth-related differences in the shapes of normalised ping profiles were observed, at shallower depths (especially <25 m) the response for the first echo is much broader than it is at greater depths. This effect is due to the physics of echo-sounder operation and was seen to have a $1/\text{depth}$ relationship. Several methods to standardise for the effect were attempted, including an empirical regression of the echo response values on $1/\text{depth}$. While a physically-based correction would be useful, none exist in the literature and the issue remains unresolved.

Analyses of data from sites that were collected close together in time, space and depth, suggested that it may be possible to provide local separation of extremes of cover in some circumstances. However, analyses of the larger data set over an extensive geographic area showed that the differences among pings from the same cover class were often as large as the differences between the cover classes. Even the site-contrast analyses for localised areas show that differences between sand sites can be greater than differences between sand and seagrass sites. Sand classes were the most common, were highly variable and their range of variability included almost all other habitat classes to a greater or lesser extent. Data from almost all classes were seen to plot almost throughout the full range of variability of the principal CVs. This demonstrated very considerable ambiguity between the acoustic signatures of the same and different classes, even at the same depth.

The digital echo sounder system used to collect the data analysed here had a transducer with a nominal beam angle of 10° — with greatest sensitivity $< \pm 10^\circ$ and little sensitivity between 10° – 50° — as is fairly typical of single beam echo sounders. Relatively recent analyses of multibeam data show that much of the discrimination between cover classes occurs at angles 25° – 35° , where the backscatter response for this single-beam instrument was much less than at narrower angles. For the narrower angles, there was some discrimination, though context from neighbouring pings is needed to improve the reliability. Thus, in the data from this echo-sounder, while some local scale discrimination in shape was observed, most discrimination would seem to depend on differences in the magnitudes of the responses at narrow angles, and not from consistent differences in the broader shape between the various cover classes.

4.6.3. Linear Discriminant Analyses of QTC View data

Linear Discriminant Analyses were performed on the QTC View proprietary 166 feature data, and initially on the entire set of ground-truth seabed type classes, including all available sites and substratum and biological habitat types. Subsequently, similar types of habitat classes were amalgamated on the basis of ambiguity observed in LDA confusion matrices. The depth problem found in other types of data and analyses was also present in the QTC data and was addressed by partitioning the data by depth (and restricted spatial dimensions) to limit data selected for iterative training and testing trials, with some small improvement in amalgamated classification success.

Overall, the QTC data also had low levels of success in classifying the observed seabed classes, based upon its 166 acoustic parameters, and that success increased inversely as the number of classes was reduced. The fewest number of substratum classes analysed was seven, yet it was clear that a reduction to as few as 3–5 would be necessary in an attempt to raise classification success.

The best result achieved (~49%) was with a simple set of seven substratum classes (after partitioning into 6 depth strata). The majority of the confusion involved the most frequent substratum class (the sands), which accounted for ~70% of the observed seabed types, yet sands could be classified correctly in significantly less than half of observed cases, with the result that most sand was classified as either a more structured class type (gravel, rock, reef) or as mud.

It is acknowledged that the ground truth (EVENTS) data was at times also subject to misclassification by human observers of the towed video; for example, on occasion it could be difficult to accurately determine the sub types of soft sediments (sand, silt, mud) from video. Further, sediments can vary in ways that affect their acoustic properties, which cannot be observed on the sediment surface. While the reliability of the EVENTS data with respect to visually similar substrata can at times be questioned, there was little doubt that extreme substrata (mud, sand, rocks, reef) were identified with certainty and yet these distinct classes are substantially confused in the analyses of the QTC data.

It appears that the signal to noise ratio of the acoustics data is not adequate to consistently distinguish readily observable basic habitat types. Any given class (especially sand) is so variable that its feature attributes overlap strongly with neighbouring categories. This is exacerbated by vessel pitch and roll, weather effects, and the relatively narrow angle (10 deg) of single beam acoustics.

4.6.4. Acoustics summary

Three different approaches were taken to examine the performance of normal-incidence single beam echo sounder data, for discriminating different seabed habitats and hence as a surrogate for patterns in habitats and their constituent biodiversity. Within each approach, several different techniques of analysing the data were attempted. Typically, localised contrasts among two or a few classes would sometimes yield satisfactory results, but inclusion of greater numbers of classes of interest over greater spatial and depth scales increased ambiguity, and hence mis-classification rates, to unsatisfactory levels.

This confusion can be explained at least partially by the physics of echo-sounder operation, whereby in shallow water the length of the ping pulse is large in relation to the difference between the slant range of the side lobes and the normal-incident range to the seabed — whereas in deep water, the slant range difference is much larger than the pulse length. This causes a continuous change of the shape of the returned pulse, in proportion to the factor $1/\text{depth}$, that cannot be removed by the angular or dilation transformations that normalise for different depths.

Attempts to remove the depth affect had limited success, and even restricting contrasts to similar depths, the acoustics data showed great variability within any habitat class across the broad range of available data. That is, habitats of the same type, as identified by video, do not consistently have the same shape of echo-return, as characterised by a range of types of features. Further, the range of variability in any acoustic features extracted for any given habitat overlap broadly with those extracted for other habitats. While some merging of habitat classes is reasonable where they are ecologically similar, such as merging mud and silt to say soft or fine substratum, or sand and coarse-sand to say coarse substratum, it is not reasonable to merge the biohabitat seagrass with sponge gardens.

After merging and with partitioning by space and depth, only a few extreme bottom types such as mud, rocks, reef could be consistently separated but overall errors were still in the vicinity of 50%. This was largely as a result of sand being erroneously classified as other more extreme substratum types. These results contrast with the claimed success of some other studies, usually of small areas, with more limited depth range and fewer habitat types. In this study, as the scale of coverage was increased in terms of area, number of habitat classes and depth, classification success quickly declined to unsatisfactory levels. This means that as a general guide, ground-truthing needs to be conducted regularly in space, by depth and by habitat type, and the number and types of classes that can be expected to be separated are few and simple, with limited information content.

The success rate here was similar to our previous results with normal-incidence single beam echo sounders, in studies on scales of a few 10s of sq km to a few 1,000s of sq km that used only two simple features — the Hardness and Roughness (E1 and E2) indices acquired by a RoxAnn™ system (e.g. Skewes *et al.* 1996; Long *et al.* 1997) or their equivalents implemented for digital data (e.g. McLeod *et al.* 2007) — to classify about 4–5 seabed types with about 60% success. Even recent analyses of swathe acoustics data have been able to separate reliably only about three seabed classes such as soft, hard, and rough (R. Kloser pers. comm., N. Campbell pers. comm.). With the greater range and detail of features analysed in this study, significant improvements in classification success were expected, particularly for biological habitats. However, the greater spatial scales, depth range, number of habitats, and variability conspired to limit the number of classes that can be separated with any consistency in this broad-scale mapping of seabed habitat.

4.7. ECOLOGICAL RISK INDICATORS

Trawl exposure indicators were estimated for 38 species groups representing ~840 species that were sufficiently abundant in sled and trawl samples for analyses. For the more exposed groups and those groups (and species) having significant trawl effort terms, their constituent species were assessed individually for estimated availability in GU zones, abundance in trawled areas and total exposure to trawl effort. For the more exposed species, further information was sought on their relative catch rates and possible BRD effects to estimate likely proportions of populations caught. Wherever available, Susceptibility-Recovery Analysis (SRA) “recovery” rank scores (from Stobutzki *et al.* 2001a) and natural mortality estimates (primarily from Zhou and Griffiths 2007) were sought to estimate, respectively, relative sustainability risk and a quantitative sustainability indicator against reference points — particularly for species with higher estimates of proportion caught. This represents the most extensive and detailed quantitative species-level risk assessment conducted for any fishery in Australia to date.

Of the ~840 species analysed, ~586 had total exposure to trawl effort of less 25%, ~218 species had exposure to trawl effort of between 25%-50%, 23 species had exposure between 50%-75%, and 10 species had exposure >75%. Of the latter 10 species, five had estimated exposure greater than their estimated standing stock and the most exposed of these was a key prawn target species, *Penaeus semisulcatus*. The majority of highly exposed species were smaller fishes typical of tropical trawl bycatch.

After taking into account available relative catch rate information, the potential risks were much reduced for the majority of species. Of the ~840 species analysed, ~804 had estimates of annual catch of less 25%, ~28 species had annual catch estimates of between 25%-50%, 4 species had catch estimates between 50%-75%, and 1 species had catch of ~110%. These estimates apply further focus on those species that may be at risk; however, understanding the potential for sustainability requires information on the propensity of populations to recover — two approaches were considered.

For the first approach, SRA recovery rank scores were available for a large number of bycatch species from previous ERA assessments in northern Australia (Stobutzki *et al.* 2001a). These provided a “recovery” axis orthogonal to the catch axis already discussed and allowed further differentiation of species risk in relation to their recovery attributes — those species orientated towards the higher catch:lower recovery quadrant are at greater relative risk. The top 20 ranking species were listed as having higher relative risk on the basis of their SRA recovery attributes, and while the SRA method does not confirm whether those species are actually at sustainability risk, it would be prudent that attention be given to their future status.

The northern Australia SRA risk assessment (Stobutzki *et al.* 2001a, 2002) also used a ranking method for susceptibility, unlike the quantitative exposures estimated for the GBR; nevertheless, it is of interest to consider any similarities between the northern Australia overall SRA risk ranking and those for the GBR. It is possible that similar fishes have similar habitat preferences in the two regions and those species that favour habitats also favoured by prawns are likely to be similar and hence, are exposed to trawling. However, only two species were among the top 20 relative risk ranks for both regions, *Saurida undosquamis* and *Chaetodermis penicilligera*, which may reflect the different assessment methods (for the susceptibility axis) or different relative distributions of bycatch species relative to prawns and trawling.

For the second approach, estimates of natural mortality rates had been collated for a large number of bycatch species from a recent bycatch risk assessment in Northern Prawn Fishery (Brewer *et al.* 2007). These, and estimates of natural mortality from other sources, enabled calculation of a sustainability indicator (catch/mortality), which could be compared against reference points, based on the Schaffer surplus production model, and allowed further differentiation of species risk in relation to their recovery potential — those species with higher catch/mortality are at greater relative risk. This was analogous to the Zhou & Griffiths (2007) approach — “sustainability assessment for fishing effects” (SAFE). The benefit of this method was that it provided an absolute estimate of sustainability rather

than a relative rank. It was nevertheless, only an approximation and not as robust as a thorough stock assessment.

Three species exceeded the limit reference point (set at $C/M=1$, \equiv MSY). The Rough Flutemouth, *Fistularia petimba*, with 44% of its biomass available in GU zones, an estimate of 29% caught and a low estimated natural mortality rate M of 0.26, the sustainability indicator for this species was 1.12. The Tufted Sole, *Brachirus muelleri*, with 69% of its biomass available in General Use, an estimate of 110% caught and a medium estimated natural mortality rate M of 0.98, the sustainability indicator for this species was 1.11. *Brachirus muelleri* was ranked highest by SRA. The Blacktip Tripodfish, *Trixiphichthys weberi*, with 56% of its biomass available in General Use, an estimate of 36% caught and a low estimated natural mortality rate M of 0.33, the sustainability indicator for this species was 1.09. One species exceeded the first conservative reference point (set at $C/M=0.8$), *Pomadasys maculatus* (a grunter bream) had 65% of its biomass available in General Use, an estimate of 33% caught and a low estimated natural mortality rate M of 0.34, giving a sustainability indicator of 0.96. Two species exceeded the second conservative reference point (set at $C/M=0.6$): *Psettodes erumei* and *Sillago burrus*. *Psettodes erumei* (Australian Halibut) had 61% of its biomass available in General Use, an estimate of 52% caught and a medium estimated natural mortality rate M of 0.69, giving a sustainability indicator of 0.75. *Psettodes erumei* was ranked ~10 by SRA. *Sillago burrus* (Western Trumpeter Whiting) had 46% of its biomass available in General Use, an estimate of 34% caught and a medium estimated natural mortality rate M of 0.57, giving a sustainability indicator of 0.60. Future attention should be directed at these species to clarify uncertainties and take actions to ensure their sustainability. A further 10 species of next highest risk rank below the reference points were also listed and included seven species also ranked highly by the SRA method — again, it would be prudent that attention be given to the future status of these species also.

There are uncertainties to consider in these estimates of sustainability risk, not only in the modelling of biomass distributions, but in the estimates of relative catch rates and natural mortality rates. For this reason, a larger number of top ranking species were also listed for future attention even though they were below conservative reference points. Where estimates of uncertainty in catchability were available, the implications were assessed. At the higher end of the catchability uncertainty range, *Pomadasys maculatus* and *Psettodes erumei* would step up one reference point and three additional species *Nemipterus peronii*, *Terapon puta* and *Nemipterus furcosus* fell above the first C/M reference point — *T. puta* was also listed by the SRA recovery rank approach.

It is notable that most of the species identified as most at risk by the quantitative C/M method did not coincide with the top ranked species by the qualitative RSA method. Further, most of species ranked highest by the RSA method did not appear to be at risk by the C/M method. Note also that in this application, only the recovery rank axis of the RSA method was used against the quantitative Catch axis. In its usual application, the RSA method uses a qualitative susceptibility rank axis instead of a quantitative Catch axis and, given the now widespread use of the RSA and similar methods, it would be timely to test the method against a fully quantitative approach to assess its reliability. Such an assessment is now possible with the availability of the Seabed Biodiversity dataset.

Natural mortality estimates were not available for all species. Nevertheless, those species for which natural mortality was unavailable had low estimates of annual catch. The highest of these were examined and on the basis of known life history of related species, or comparative catchability, were considered unlikely to have natural mortality rates low enough, or actual catch rates high enough, to put them at risk.

The selection and statistical significance of the trawl effort covariate was another potential risk indicator examined. The trawl covariate was selected for 77 of ~840 species analysed and was significant in 55 cases (~6.4%). Of the significant effects, 17 were overall positive and 38 were overall negative. Of the negative effects, 11 were indicative of changes of about -20% to -36% and 13 were indicative of changes of about -10% to -20% — these included several gorgonians and sponges that were addressed by the trawl scenario modelling, as well as a range of other fauna. It is possible that these negative effects are indicative of the magnitude of historical impacts of trawling in the region. Nevertheless, all species with negative coefficients had low to very low exposure to current distribution of effort and were unlikely to be at ongoing risk. Of the 17 positive effects, 2 were indicative of changes of >50% and 7 were indicative of changes of about 10% to 19%. These included three target species, and in these cases the positive trawl coefficient could reflect fishers ability to

focus their effort rather than a real positive response to trawling (however, there is evidence for the latter, Gribble 2003, 2004). All species showing trawl effects and having high exposure to trawl effort had positive trawl coefficients.

The sled and trawl species data at sites were statistically separated into 16 relatively homogeneous groups that were mapped to the GBR study area on the basis of their biophysical relationships. Area-based trawl exposure indicators were estimated for these assemblages similar to those considered for species biomass. Most of these assemblages had very low to low exposures to trawl effort; three had exposures between 32% and 41%, one had an exposure of 58%, and the highest was 108%. Species having highest affinity for these assemblages were identified and a number of species were seen to occur repeatedly across the more exposed assemblages. Their cumulative exposure was considered so that species with higher affinities for more exposed assemblages would have a higher ranking. The top ranking 40 species were listed and included many of the same species ranked with higher effort exposure in the single species assessment. While it has not been established whether there are any functional relationships among these species, consideration should be given to the potential need to monitor the ongoing status of these species.

The data from post-processing of video transects at sites were statistically separated into 9 somewhat homogeneous habitat mixture groups that were mapped to the region on the basis of their biophysical relationships. Area-based trawl exposure indicators were estimated for these habitat groups, similar to those considered for assemblages. Five of these habitats had medium exposures between 25% and 39%, the other four had low exposures between 3% and 10%. The highest exposures were for two relatively dense but patchy seagrass and algal habitat groups: one distributed in the mid-shelf of the central region with 39% exposure to effort; the other along much of the inner-shelf in the Capricorn section with 34% exposure. Another (sparsely) vegetated habitat group distributed well offshore from Townsville included patchy algae (with a little *Halimeda*) some bioturbation and occasional epibenthos had 25% exposure. The most wide-spread habitat group included mostly bioturbated and bare seabed with a little sparse algae and seagrass distributed over much of the shelf in the central and northern sections had 34% exposure. The most barren seabed type was mostly bioturbated and distributed in muddy areas of the inshore, midshelf and Capricorn Channel had 26% exposure. The remaining habitat mixture groups included those with most of the *Halimeda* banks and epibenthic garden biohabitats, as well as very extensive groups with mostly bare and bioturbated seabed, had low levels of exposure. While important seagrass and algal habitats were moderately exposed, such that their level of risk needs to be considered, there was no habitat group particularly associated with trawling areas and trawl effort was not selected by the statistical methods as a splitting variable for habitat groups. This suggests that trawling has not been a dramatic modifier of habitat state in the region.

The habitat components from the video data comprising the habitat groups were examined individually, particularly marine plants, due to their higher level of exposure. *Halophila spinulosa* and like-species had 24% exposure and ovoid leaf *Halophila*'s had 15%, which were very similar exposure outcomes as the modelled sample distributions for these species. The different morphotypes of algae varied in their exposure. Crustose coralline algae was most exposed (44%), primarily off Gladstone, though these nodules should be robust. Filamentous blue-green algae was the most extensive and had exposure of 25%. All other morphotypes were $\leq 17\%$ and most (including *Halimeda*'s) were $< 5\%$. The available information suggested that catchability of marine plants is low and the single species assessments indicated that the exposure risk of marine plant species was low. Seagrasses have persisted in these exposed areas since earlier surveys (Rob Coles pers comm.) and it has previously been found that trawling has not reduced the probability of seagrass occurrence and suggested that trawling may even facilitate seagrass (Coles *et al.* 2006). Of the other 57 habitat components examined, the majority had very low exposures to trawling. The exceptions included *Solenocaulon* (a gorgonian), with 14% to 20% exposure, *Pteroides* (a sea pen), which had 15% exposure and solitary corals, which had 12% exposure. Again, the available information suggested that catchability of these fauna was very low. The final exception was unidentified barrel sponges (excluding *Ircinia* and *Xestospongia*), which had 14% exposure; such sponges may have moderate catchability (based on known species) which may place their overall risk to trawl at about 3%-10%.

4.8. TRAWL MANAGEMENT SCENARIO MODEL

A dynamic model was applied to assess the effects of several major management interventions, including large scale closures and effort reductions, which were implemented between the years 2000 and 2006, on benthic fauna — particularly sessile benthic fauna that were the focus of experiments on trawl depletion rates (Poiner *et al.* 1998, Burridge *et al.* 2003) and subsequent recovery (Pitcher *et al.* 2004). The dynamic model applied depletion and recovery parameters estimated from previous experiments and annual trawl effort as provided by industry and management data, and estimated the relative status of fauna in the region. The model was run with and without the effects on effort of each management intervention. The relative status estimates were combined with the abundance distributions available from this project in order to estimate the regional absolute status of these fauna.

Total trawl effort in the region grew gradually after the fishery initially commenced, but increased rapidly in the early 1990s, before peaking in 1996/1997 and falling rapidly in the late 1990s (by ~25%) — even before implementation of the management scenarios evaluated here. The status quo 2001 model scenario maintained these effort levels through until 2525. The first intervention was the 2001 low effort areas spatial closure with the same effort levels. The second intervention was the latter closure plus the 2001 major effort reduction buy-back, which reduced effort by a further ~30% (down ~45% from the 1990s peak). The third intervention was the latter plus an effort trading penalty system operating over several years, which progressively reduced effort by a further ~30% again (down ~60% from the 1990s peak). The fourth intervention added the 2004 representative areas program (RAP) re-zoning of the GBR at the same effort levels. The fifth intervention added the 2005 RAP associated buy-back, which reduced effort again by almost ~10% (down ~65% from the 1990s peak). The final scenario was the actual effort observed throughout this period, including all management interventions — the status quo 2006.

The general pattern of relative (to a uniform pristine distribution) population status across a range of observed depletion-recovery parameters was slow decline until ~1990, then more dramatic decline through the high effort period of the 1990s. The decreasing effort in the late 1990s arrested or reversed the decline for all except the most vulnerable depletion-recovery combinations, which would have continued to decline under status quo 2001. With all of the management interventions actually implemented over the period, the status quo 2006 indicated recovery trends for the most vulnerable fauna while the least vulnerable recovered. Each intervention by itself made varying contributions to the overall response. The 2001 low effort areas closure made almost no contribution as only areas with very little or no recorded effort were closed; nevertheless, that action would have had the effect of preventing any possible expansion of effort into such areas. The 2001 buy-back contributed about half of the recovery response; and the progressive penalty contributed about half to most of the remainder depending on faunal vulnerability (high to low, respectively). The RAP re-zoning made some contribution (particularly in the case of higher vulnerability fauna), though more limited because the re-zoning policy was to minimize disruption to current activities, hence only a relatively small proportion of effort was affected spatially. The 2005 buy-back led to a slight additional improvement.

Estimates of regional absolute population status were possible by combining the relative status results for the observed range of faunal vulnerabilities, with this project's predicted absolute abundance distributions. The patterns of individual responses were similar to the general case outlined above: by 2000 almost all taxa had arrested or reversed the declines of the early-mid 1990s, all taxa responded positively to the management interventions of 2001–2005 with the 2001 buy-back contributing about half of the recovery response and the progressive penalty contributing most of the remainder. However, differences were apparent because different species were distributed differently in relation to trawl effort and closed areas, as well as differing in estimates of their depletion and recovery parameters. Prior to the management interventions evaluated, the average population low-points for sessile species were about 83% of pristine (range ~50% to 96%) and the average projection for 2025 with all current interventions in place was about 89% of pristine (range ~57% to 98%). Low points for mobile species ranged from ~83% to 96% (average ~88%) and projections for 2025 ranged from ~93% to 98% (average ~95%). Species with lower low points tended to benefit most from the interventions, typically by 5-15%.

For six of the 38 taxa examined, the falling effort in the late 1990s was not sufficient to arrest or reverse the population decline projected for the preceding period, and the status quo 2001 would have seen these decline even further. These taxa included two species of the sponge genus *Ircinia*, unidentified *Ircinia*, the sponge *Hippospongia elastica*, and the gorgonian *Subergorgia suberosa*. *Ircinia* sp1255 was the most exposed to trawl effort of the species modelled. Nevertheless, the management measures implemented were predicted to produce a positive recovery response for each — among the largest predicted. Each species had <46–32% of their biomass located in General Use and <33–11% exposed to current effort, and estimated incidental mortality of 7–1%.

The most exposed gorgonian was *Alertigorgia orientalis*, with 50% of its biomass in GU, 27% in trawled grids and 29% exposed to effort, and having an estimated catchability of 0.09 its annual incidental bycatch would be about 3%. This species showed the same general pattern of positive response to the series of management interventions and under status quo 2006 management was projected to reach close to pre-WHA abundance by 2025.

Several species examined by the trawl scenario model had negative trawl effort terms in the biophysical modelling. The most negative trawl effect (-36%) was for the gorgonian soft coral *Carijoa* sp1, nevertheless, this species was predicted to respond positively to the series of management interventions and under status quo 2006 management was projected to reach >90% of pre-WHA abundance by 2025. The current exposure of this species was 25% of its biomass in GU, 5% in trawled grids and 3% exposed to effort, and with an estimated catchability of 0.15, its current annual incidental bycatch would be <1. The next most negative trawl effect (-28%) was for the gorgonian *Euplexaura* sp6, nevertheless, this species also responded positively to the series of management interventions and under status quo 2006 management was projected to reach ~90% of pre-WHA abundance by 2025. The current exposure of this species was 36% of its biomass in GU, 19% in trawled grids and 9% exposed to effort, and with an estimated catchability of 0.14, its current annual incidental bycatch would be <1. Other modelled species having negative (or possible) trawl effects also responded positively (again, among the largest predicted) to the series of management interventions and under status quo 2006 management were projected to reach 90%–98% of pre-WHA abundance by 2025 — and each had low to very low exposure to current effort, suggesting little future risk to their current status.

For a few species, e.g. the sea whip *Junceella juncea*, the sponge *Ianthella quadrangulata* and the coral *Turbinaria*, the positive effect of the 2001 buy-back and subsequent penalties was slightly greater than the additional RAP re-zoning. This may be a possible result of displacement of effort out of newly closed areas, increasing effort in areas where these species were distributed. Though the effects were very slight (<1%), such consequences have been reported previously in the effects of trawling literature (e.g. Fogarty and Murawski 1998; Brendan Ball, Ireland, pers comm.) and are a consideration when planning and implementing closed-area management and/or marine protected areas. The 2005 buyback appeared to neutralize this predicted impact of displaced effort and highlights the importance of removing effort that is affected by closed area management.

The consistent prediction from the trawl management scenario modelling was that the ubiquitous depletion trends of structural epibenthos up until the late 1990s have all been arrested and reversed by the series of management interventions implemented between 2000 and 2005. The 2001 buyback and the subsequent progressive penalties appeared to make the biggest positive contributions. For ~7 of 38 representative taxa modelled, the rezoning made a small additional positive contribution, and for a similar number of species the contribution of the 2005 buy-back was also discernable.

5. BENEFITS

This project has produced comprehensive new scientific knowledge of seabed habitats, biodiversity, and bycatch — including species new to science — in the GBR region, and delivered to the highest 'High Priority' research areas identified by the Biological Diversity Advisory Council as well as the “areas of research of national importance” (Biodiversity Research: Australia’s Priorities — a Discussion Paper. Environment Australia 2000).

This knowledge-base has benchmarked the current status of the region’s assemblages and will raise the level of stakeholder knowledge of the nature and status of the region’s ecosystems. The outputs are already facilitating assessment of spatial management in the region and will benefit future planning and regional ecosystem management, including a basis for assessing issues such as climate change.

The outputs have enabled managers and stakeholders to identify the likely extent of past and current impacts of trawl fishery effort, as well as the environmental benefits of recent measures introduced in the region. If needed, the project has also provided the basis for evaluation of any future strategies to minimise identified impacts and further improve the environmental sustainability of the fishery. These assessments have provided a quantitative regional context that will benefit managers needing to respond effectively to industry and community concerns and achieve an objective balance between the pressures of exploitation and needs for conservation in a multiple-use environment. The community will be informed and benefit from independent information on the environmental sustainability of trawling.

Further benefits of this project’s outputs to the Queensland trawl fishery, its managers and the community include delivery of quantitative ecological risk and sustainability indicators, and lists of species potentially at risk, for responding to environmental assessment under the EPBC Act, as well as other State and Commonwealth fishery and environmental legislation, and national ESD reporting. It can be expected that these outputs, in combination with appropriate management and industry responses, will likely lead to positive assessment and exemption from export controls status.

6. FURTHER DEVELOPMENT

In order to fully adopt the outputs of the research, it will be necessary for project staff to present the results to appropriate fisheries/management committees, collaborate with fisheries/management staff and contribute as requested to ongoing revision of management arrangements regarding meeting the requirements of EPBC assessment, including strategies for the species identified to be at sustainability risk in this project. Some aspects of these activities may require additional support.

Presentations to marine park managers and committees, and collaboration with marine park managers/staff would contribute to adoption of results for zoning assessment and ongoing marine park planning arrangements with respect to meeting WHA obligations. Some aspects of these activities are being supported by the M&TSRF Project 1.1.1.

Further dissemination of results to other research providers, engaged in providing similar kinds of fishery management and marine planning outputs, could be achieved by presentations/contributions to relevant policy and/or scientific workshop/forums.

Broader dissemination of results will be achieved by seminars at scientific conferences, by scientific publications, through availability of data via OBIS, and potentially by relocation and further development of the project's former CRC Reef website with the addition of site data, images, video, and maps.

Further research is warranted to address key uncertainties in the risk assessments, such as catchability and natural mortality rates, particularly for higher risk species and those with higher exposures. The benefits of such research are likely to be widely applicable because similar suites of species are likely to be present in the trawled grounds of most tropical prawn fisheries due to their habitat preferences.

Ecological Risk Assessments for fisheries of type "Likelihood and Consequence" and SRA (or "Productivity Susceptibility Analysis") (Level 1 & 2 respectively, in Hobday *et al.* 2006) are now being conducted widely in many fisheries in Australia. However, the hybrid SRA method examined herein produced results that had little in common with the much more quantitative C/M approach also applied, which raises concerns about the reliability of the qualitative approaches. Similar concerns were raised by Griffiths *et al.* (2006), which lead them to develop the quantitative "SAFE" approach (Zhou and Griffiths 2007). The reliability of the Level 1 and 2 methods has never been fully benchmarked, largely because of the lack of a suitable test bed, but now the GBR Seabed Biodiversity species distribution dataset provides a powerful opportunity to assess of the performance of these methods.

It is widely held that physical environmental variables, or distribution patterns of a broadly sampled taxonomic group (e.g. fishes), are useful surrogates for the distribution patterns of biodiversity more generally for the purposes of regional marine planning. While environmental variables had utility for spatial prediction of many species herein, the more general inter-regional utility of physical variables has not been tested and neither have cross-taxonomic patterns, or the spatial scales at which they may or may not be effective. Again, the GBR Seabed Biodiversity dataset provides a powerful opportunity to assess of the performance of these as surrogates for application in marine planning in other regions. Aspects of such an assessment are being supported by the CERF National Marine Biodiversity Hub.

The project was unable to complete sorting and identification of all samples, with the resources and timeframe available to the project, even though considerable extra resources were applied. The samples that remain unsorted include: annelid, ascidian, crinoid, and hydroid samples from both the epibenthic sled and scientific trawl, and all marine plants sampled by the trawl. Completion of sorting these samples and further taxonomic work to move beyond the macroscopic OTU identifications possible within the scope of the project would provide full utilization of the samples and specimens and deliver additional value to science and end-users.

Similarly, 140 sites were videoed by towed camera but were too rough for the epibenthic sled or trawl. While the habitat for these sites was characterised from the video, there is essentially no species information for these sites comparable with that available from the sled or trawl, which has limited the

project's ability to model distributions of structural habitat species that were the subject of the Trawl Scenario Modelling completed herein, and possibly underestimated their population sizes in areas inaccessible to industry. Quantification of species from the available video and digital stills photos would provide information on the abundance of visible species in areas not sampled by other methods, as well as further develop the non-extractive methods.

This project has developed and applied population level sustainability indicators, which have identified species potentially at risk. Nevertheless, with the increasing requirement for ecosystem-based management, there is a need to develop condition and trend and vulnerability indicators for seabed communities and ecosystems — not only in relation to fisheries but also other issues such as climate change. A wide range of potential indicators have been suggested (e.g. production/biomass, trophic indices, functional redundancy, diversity, size ratios, size spectra, dominance, habitat complexity and fragmentation, susceptibility and productivity. Fulton *et al.* 2004) — the extensive Seabed Biodiversity sample collections and dataset provide an opportunity to research and examine such indicators for the region.

7. ACHIEVEMENT OF OUTCOMES

The project has produced all of the outputs as originally proposed. Preliminary outputs were presented during the course of the project and team members contributed to management/industry activities such as bycatch risk assessments, assessments of trawl plan targets and monitoring strategies. The nature of this project meant that the final results could be delivered only after the complete dataset had been analysed and synthesized, towards the end of the project. With this report and the delivery of the final outputs, and activities outlined in Section 6, it is largely from this time forward that the anticipated outcomes may be achieved. The planned potential industry, management and stakeholder outcomes include:

- Raising the level of stakeholder knowledge of the status of the region's ecosystems, facilitating development and improvement of regional ecosystem management plans.

Progress has been made through milestone reports, numerous presentations to management industry community and scientific audiences and delivery of preliminary results and images on the Project's website. Further dissemination activities are planned.

- Objective information on which stakeholders can base consultation with respect to:
 - reasonable use of the region that maintains the ecosystem, bycatch and benthos species
 - development and implementation of management plans leading to an ecologically sustainable fishery acceptable to stakeholders, sustainability of the seabed environment and future planning.

Again, progress has been made through reports, presentations, delivery of preliminary results and further activities are planned.

- Assessment of the current Trawl Plan targets by estimating (with specifiable uncertainty) performance against the 40% reduction in bycatch and 25% reduction in benthos, as required under State legislation to meet environmental sustainability objectives.

Team members have contributed to management/industry assessments of the trawl plan targets and bycatch risk assessments. The 40% and 25% reductions were considered largely with respect to reductions in trawl effort; the outputs from this project have provided an assessment of their likely sustainability.

- Facilitation of stakeholder development of reliable and widely accepted operational ecological risk/sustainability indicators for identification of marine species at risk, including both bycatch and seabed benthos species, filtering of low risk species and identifying high risk species that need further management or information, as required under Commonwealth legislation to meet environmental sustainability objectives. This will address a DEW condition that the fishery conduct a risk assessment and develop biologically meaningful target reference points for high risk species within 3 years. Significant progress against these criteria is required when the WTO is reviewed 3 yrs after its initial approval. The WTO is conditional on demonstrating adequate performance.

Ecological risk/sustainability indicators, with biologically reference points, have been developed with management and industry involvement. These outputs have contributed to an DEW condition on the WTO for this fishery.

- Assessment of the implications for sustainability of recent management changes (including the new GBRMPA RAP zoning changes due to be implemented in 2004) —current environmental targets, risk/sustainability indicators, and MSE modelling will be estimated both with/without, before/after recent management changes.

These assessments have demonstrated that the suite of recent management changes have had positive implications for sustainability of the fishery.

- Successful review of the adequacy of the current Qld East Coast Trawl Management Plan (1999) by provision of critical information. A key component of the review will be evaluation of the adequacy of the current suite of input controls in relation to ensuring the negative impacts of trawl on bycatch and benthos are maintained within acceptable limits. The TMP review will begin by Nov 2004 and completed by Nov 2006. Outputs from this project will help develop relevant and measurable environmental indicators to be incorporated into an improved Plan.

The project outputs provide indicators of the level of impact under the current management arrangements and have provided biological reference points. Further activities are planned with respect to revision of the TMP.

- Ability to evaluate alternative management strategies that may in future be needed to meet State and Commonwealth environmental sustainability legislation, in a MSE context that would estimate the outcomes for the environment and for the fishery for each option – and thus contribute to decision making by Managers and industry.

This capability has been demonstrated by assessments of the implications of recent management changes and can be available for evaluating future alternative management strategies.

8. CONCLUSIONS

The outputs from the project have delivered the "Form of Results" as originally proposed and as mapped against the objectives. These are outlined below:

The project proposed and has produced a library of videos of the seabed habitat types of the GBR shelf, including the QECTF in the region. Real-time on-vessel characterisation along video transect recognised 9 substratum types, 24 broad biological habitat types and 14 class-level animal events. Post-processing of randomised frames of these videos in the laboratory recognised 11 physical bottom types, 30 sediment types, and 114 biological habitat component types.

The project proposed and has produced an inventory of the benthos, bycatch and fish species of the GBR shelf, including the QECTF in the region, with catalogued museum voucher specimens to authenticate records. In total, more than 5,300 taxa were identified, many of which are new species, and further taxonomic work will identify additional species.

The project proposed and has produced a database of the distribution and abundance of seabed benthos species and bycatch species at each sampling station. In total there are more than 140,000 records of species weight and count at sampled sites. This dataset was the basis for the biophysical modelling and risk assessment.

The project proposed and developed predictive models of bio-physical relationships between benthos and bycatch species, seabed assemblages and communities and their physical environment. About 850 species have been successfully modelled in this way, and in the process the key environmental variables likely to be important in structuring biotic distributions have been identified and may be useful as surrogates.

The project proposed and has produced maps of the distribution and abundance of benthos and bycatch species, and their assemblages, based on the biophysical models, giving full coverage of the GBR shelf, including the QECTF in the region. Many preliminary maps were provided to trawl managers as the project progressed, and this report and subsequent dissemination activities will deliver the final maps to managers and industry to facilitate any further development of strategies that minimise effects of trawling on habitats.

The project proposed and has produced estimates of the large scale effects of trawling on benthos and bycatch quantified by measuring and analysing their abundances across a range of trawl effort intensities, within and outside trawl grounds in the GBR, while taking into account habitat differences. The Trawl Effort covariate was significant in 55 of ~840 species analysed (6.4%); little more than expected by chance and suggesting that trawling does not have a strong influence on overall seabed distribution patterns. Of these significant responses, 38 were negative and most effects were small; 6 species had significant moderate negative change in biomass of >25%–36%. Seventeen significant responses were positive and again most were small; one species had a significant moderate positive change in biomass of ~50% and one other species had a significant large positive change in biomass estimated at ~96%.

The project proposed and has produced quantitative sustainability risk indicators for bycatch species, developed from this projects' estimates of the proportion of bycatch populations exposed to trawling, estimates of the proportion of these populations removed by trawling (based on relative catch-rates from this and other projects, e.g. FRDC 93/096), and bycatch life-history characteristics (from SRA, FRDC 96/257 and FRDC 2000/160). Exposure risk was estimated for about 850 species: about half the species had very low exposure, about a third had low exposure, ~218 had moderate-low exposure, ~23 had moderate-high exposure and 10 species had high exposure. Of these species, 1 had very high estimates of proportion caught annually, 4 had moderate-high estimates of proportion caught, 28 had moderate-low proportions caught, and the remainder (>800) had low estimates. Inclusion of the SRA qualitative recovery ranks indicated that about 15 species (20 listed) stood out as being at higher relative risk. Additionally, the project included another quantitative absolute sustainability indicator (analogous to the "SAFE" method, FRDC 2004/024) based on the estimates of annual catch herein and estimates of natural mortality rates from other sources. This method indicated that three species

exceeded a limit reference point, and another three other species exceeded one or two conservative reference points. Another 10 species below the sustainability reference points included seven species ranked highly by the SRA method and were also listed due to uncertainty in parameters. Further research is recommended to address key uncertainties in estimates of catchability and natural mortality rates.

The project proposed and has produced quantitative status and sustainability risk indicators for selected seabed structural benthos in the region and evaluations of the environmental performance of different management options implemented over the duration by relevant authorities, developed from this projects' estimates of the proportion of benthos populations exposed to trawling, together with measurements of trawl-removal rates and recovery rates from other projects (FRDC 93/096, GBRMPA Trawl Recovery) in an MSE modelling framework (GBRMPA Trawl Scenario Modelling Project). The consistent result was that the generalized depletion trends up until the late 1990s have all been arrested and reversed by the series of management interventions implemented between 2000 and 2005. The 2001 buyback and the subsequent progressive penalties appeared to have made the biggest positive contributions; the 2004 rezoning made a small positive contribution for some species.

The project proposed and has produced transferable methodology and tools for regional marine planning nationally, including: cost-effective representative survey design and techniques (including use and assessment of video and acoustics), spatial-statistical classification and prediction methods, and biodiversity and bycatch species risk assessment methods. Reliable assessment methods required robust distribution and abundance data delivered by accurate identification of specimens collected by conventional sampling devices deployed at sites selected carefully by a biophysical stratified design strategy. Acquisition of video data delivered information on dominant visible habitat components, and contributed to understanding of the catchability of structural biota, though identifications were problematic and statistical treatment of data from video was less successful. BRUVS were capable of being deployed in more rugged terrain and could provide information on fishes from such areas where the trawl could not be deployed, but also had some identification issues. Acoustics was capable of reliably discriminating only a few substratum types, such a soft sediment, rough ground and intermediate sediments.

9. RECOMMENDATIONS

A key output from the project was the series of environmental risk indicators, which aimed to filter out species of little or no sustainability concern so that attention could be focussed on those species at risk or potentially at risk. Several lists were produced, based on different indicators, and species were ranked in order of risk or potential risk. The top 20 (an arbitrary threshold) ranked species for five of the indicators are reproduced below (Table 9-1). For two of the indicators (c and e), the ranking is relative and no reference points are possible. For two (a and b) of the other three, the indicator is clear and quantitative and though related to risk is not necessarily indicative of sustainability, and the reference points are arbitrary. The C/M indicator (d) is clear, quantitative and directly related to sustainability through well established population modelling, and the reference points are biologically based. While only three species appear to be at risk and another three species exceed conservative reference points, based on the C/M indicator, there is uncertainty in the indicators that requires a more precautionary response. Further, many species (27 of 48 listed below) have multiple occurrences across these five indicators: one species occur in all five lists, six species occur in four lists, five species occur in three lists, and 15 species occur in two lists — which also suggests a more inclusive response. It is recommended that the entire list, as well as the arbitrary top-20 cut off, should be considered for consultation regarding future action. Such management, industry and stakeholder consultation processes can decide the most appropriate strategies from options that may include clarification of the identified uncertainties, monitoring, management interventions that reduce impacts on these bycatch species or combinations of these actions.

As already noted, there are uncertainties in the risk assessments due to uncertainties in estimates of catchability and natural mortality rates. In one worst case scenario of catchability=1, some additional species would exceed the limit reference point, several would exceed the conservative reference points and many species with unknown mortality might be of concern. Similarly, in another worst case scenario of natural mortalities having been over-estimated by for example a factor of two, some additional species would exceed the limit reference point, several would exceed the conservative reference points and many species with unknown mortality might be of concern. Equally, it is possible that clarification of these uncertainties may show that species currently thought to be at risk or potentially at risk may be demonstrated to be of no sustainability concern. Thus, it is recommended that further analyses of relative catchability based on existing data from multiple sources and, if necessary, field studies of actual catchabilities be conducted to address this key uncertainty. Similarly, it is recommended that further analyses of natural mortality rates based on existing data and, if necessary, biological studies leading to more precise estimates of natural mortality rates be conducted to address this key uncertainty. Such results are likely to have wide application in risk assessments being conducted in multiple jurisdictions.

During the course of the project, preliminary recommendations for monitoring seabed areas affected by the rezoning have been provided and discussed with GBRMPA staff. In particular, this focussed on identifying 3-4 seabed soft-sediment areas where high levels of trawl effort have been excluded by rezoning, with suitable reference areas open and subject to trawling, in a management evaluation framework, with preliminary costings. Given the nature of the seabed habitats and fauna in potential candidate areas, it was noted that any possible trawl impact may be difficult to detect initially and observable recovery may occur quite rapidly. Therefore it would have been necessary to establish the sampling program for monitoring at the time of the rezoning, with a review of future sampling frequency based on the results of the initial monitoring. A monitoring program of this type was not supported by the first year's ARP of the M&TSRF.

On a less-immediate timeframe, it is recommended that key seabed habitats and constituent species be identified on the basis of the Seabed Biodiversity dataset, for long-term monitoring of trends in ecological condition and their responses to regional pressures, in particular climate change. Candidate habitats should include those that have been demonstrated to be particularly biodiverse such as vegetated areas and epibenthic gardens. The vegetated areas such as deepwater seagrass/algal beds in the mid-shelf off Townsville, the inner-shelf Capricorn region and the Turtle-Howick Is group vicinity; the offshore/shelf-edge algal beds of the Central Section and the northern Swains/T-Reef; and

the outer shelf *Halimeda* banks of the Northern and Far-northern Sections, may well be vulnerable to climate change as there is an expectation that the thermocline may deepen and upwellings may become weaker and less frequent with potential consequences for productive habitat dependent on nutrients from such sources. The potential consequences of changed runoff patterns for inner and midshelf vegetation and epibenthic gardens are unknown.

Other further development activities outlined in Section 6 are also recommended with expected benefits for greater understanding of the seabed ecosystem, sustainability of the trawl fishery, zoning assessment and ongoing marine park planning arrangements and nationally for fisheries risk assessments and regional marine planning more generally.

Table 9-1. Top 20 ranked species for four different indicators. (a) Percent of biomass directly exposed to effort (red = >75%, orange = >50%). (b) Estimated percent of biomass caught per annum (red = >75%, orange = >50%, pale = >25%). (c) highest relative risk ranked species from plotting 'Recovery' rank from 'SRA' against estimated catch from b (no reference points are possible). (d) Sustainability indicator: estimated catch b / natural mortality rate (red = exceeds limit reference point 1.0, orange = exceeds conservative reference point 0.8, pale = exceeds conservative reference point 0.6). (e) Highest ranked species from assemblage exposure and species affinities for assemblages (no reference points).

| (a) Effort exposed % | | (b) Est. % caught | | (c) SRA rank | | (d) C/M indicator | | (e) Assemblage exposure | |
|-----------------------|------------------------|----------------------|---------------------------|----------------------|---------------------------|----------------------|---------------------------|-------------------------|------------------------|
| Genus | species | Genus | species | Genus | species | Genus | species | Genus | species |
| <i>Penaeus</i> | <i>semisulcatus</i> | <i>Brachirus</i> | <i>muelleri</i> | <i>Brachirus</i> | <i>muelleri</i> | <i>Fistularia</i> | <i>petimba</i> | <i>Enisiculus</i> | <i>cultellus</i> |
| <i>Cryptolutea</i> | <i>arafurensis</i> | <i>Terapon</i> | <i>puta</i> | <i>Sepia</i> | <i>pharaonis</i> | <i>Brachirus</i> | <i>muelleri</i> | <i>Cryptolutea</i> | <i>arafurensis</i> |
| <i>Brachirus</i> | <i>muelleri</i> | <i>Saurida</i> | <i>argentea/tumbil</i> | <i>Terapon</i> | <i>puta</i> | <i>Triphichthys</i> | <i>weberi</i> | <i>Saurida</i> | <i>argentea/tumbil</i> |
| <i>Pentaprion</i> | <i>longimanus</i> | <i>Penaeus</i> | <i>semisulcatus</i> | <i>Saurida</i> | <i>argentea/tumbil</i> | <i>Pomadasys</i> | <i>maculatus</i> | <i>Pentaprion</i> | <i>longimanus</i> |
| <i>Pelates</i> | <i>quadrilineatus</i> | <i>Psettodes</i> | <i>erumei</i> | <i>Penaeus</i> | <i>semisulcatus</i> | <i>Psettodes</i> | <i>erumei</i> | <i>Thenus</i> | <i>parindicus</i> |
| <i>Leiognathus</i> | <i>leuciscus</i> | <i>Scolopsis</i> | <i>taeniopterus</i> | <i>Euristhmus</i> | <i>nudiceps</i> | <i>Sillago</i> | <i>burrus</i> | <i>Nassarius</i> | <i>crematus</i> cf |
| <i>Upeneus</i> | <i>sundaicus</i> | <i>Sepia</i> | <i>pharaonis</i> | <i>Apogon</i> | <i>poecilopterus</i> | <i>Dasyatis</i> | <i>leylandi</i> | <i>Placamen</i> | <i>tiara</i> |
| <i>Portunus</i> | <i>gracilimanus</i> | <i>Yongeichthys</i> | <i>nebulosus</i> | <i>Sepia</i> | <i>elliptica</i> | <i>Nemipterus</i> | <i>furcosus</i> | <i>Tripodichthys</i> | <i>angustifrons</i> |
| <i>Terapon</i> | <i>puta</i> | <i>Euristhmus</i> | <i>nudiceps</i> | <i>Scolopsis</i> | <i>taeniopterus</i> | <i>Polydactylus</i> | <i>multiradiatus</i> | <i>Upeneus</i> | <i>sundaicus</i> |
| <i>Enisiculus</i> | <i>cultellus</i> | <i>Tripodichthys</i> | <i>angustifrons</i> | <i>Psettodes</i> | <i>erumei</i> | <i>Tripodichthys</i> | <i>angustifrons</i> | <i>Erugosquilla</i> | <i>woodmasoni</i> |
| <i>Brachaluteres</i> | <i>taylori</i> | <i>Apogon</i> | <i>poecilopterus</i> | <i>Amusium</i> | <i>pleuronectes</i> cf | <i>Terapon</i> | <i>puta</i> | <i>Penaeus</i> | <i>semisulcatus</i> |
| <i>Trachypenaeus</i> | <i>anchoralis</i> | <i>Saurida</i> | <i>grandi/undosquamis</i> | <i>Tripodichthys</i> | <i>angustifrons</i> | <i>Euristhmus</i> | <i>nudiceps</i> | <i>Psettodes</i> | <i>erumei</i> |
| <i>Metapenaeus</i> | <i>ensis</i> | <i>Upeneus</i> | <i>sundaicus</i> | <i>Saurida</i> | <i>grandi/undosquamis</i> | <i>Saurida</i> | <i>argentea/tumbil</i> | <i>Charybdis</i> | <i>truncata</i> |
| <i>Erugosquilla</i> | <i>woodmasoni</i> | <i>Sepia</i> | <i>elliptica</i> | <i>Yongeichthys</i> | <i>nebulosus</i> | <i>Nemipterus</i> | <i>peronii</i> | <i>Aplysia</i> | <i>sp1_QMS</i> |
| <i>Leiognathus</i> | <i>bindus</i> | <i>Aplysia</i> | <i>sp1_QMS</i> | <i>Sepia</i> | <i>whitleyana</i> | <i>Sepia</i> | <i>pharaonis</i> | <i>Metapenaeus</i> | <i>ensis</i> |
| <i>Melaxinaea</i> | <i>vitrea</i> | <i>Amusium</i> | <i>pleuronectes</i> cf | <i>Upeneus</i> | <i>sundaicus</i> | <i>Saurida</i> | <i>grandi/undosquamis</i> | <i>Calliurichthys</i> | <i>grossi</i> |
| <i>Saurida</i> | <i>argentea/tumbil</i> | <i>Lamellaria</i> | <i>sp1</i> | <i>Leiognathus</i> | <i>leuciscus</i> | <i>Amusium</i> | <i>pleuronectes</i> cf | <i>Melaxinaea</i> | <i>vitrea</i> |
| <i>Terapon</i> | <i>theraps</i> | <i>Leiognathus</i> | <i>leuciscus</i> | <i>Sepia</i> | <i>smithi</i> | <i>Pristotis</i> | <i>obtusirostris</i> | <i>Diogenidae</i> | <i>sp356-1</i> |
| <i>Myra</i> | <i>tumidospina</i> | <i>Triphichthys</i> | <i>weberi</i> | <i>Portunus</i> | <i>gracilimanus</i> | <i>Nemipterus</i> | <i>sp juv/unident</i> | <i>Portunus</i> | <i>tuberculosis</i> |
| <i>Calliurichthys</i> | <i>grossi</i> | <i>Sillago</i> | <i>burrus</i> | <i>Chaetodermis</i> | <i>penicilligera</i> | <i>Nemipterus</i> | <i>hexodon</i> | <i>Sea pen</i> | <i>sp1</i> |

10. REFERENCES

- Birtles, A., Arnold, P. (1983) Between the Reefs: some patterns of soft substrate epibenthos on the GBR Shelf, pp. 159-163 in Baker, J.T., Carter, R.M., Sammarco, P.W., Stark, K.P. (Eds) *Proc GBR Conference, Townsville, 1983*.
- Birtles R.A., Arnold, P.W. (1988) Distribution of trophic groups of epifaunal echinoderms and molluscs in the soft sediment areas of the central Great Barrier Reef shelf. In Proceedings of the 6th International Coral Reef Symposium, Townsville, Australia, Volume 3: Contributed Papers (Choat, J.H. & Barnes, D. eds) 6th International Coral Reef Symposium Executive Committee, pp. 325-332
- Blaber S.J.M., Brewer D.T., Harris A.N. (1994). Distribution, biomass and community structure of demersal fishes of the Gulf of Carpentaria, Australia. *Aust J Mar Freshw Res* 45: 375-96
- Breiman, L. (2001). Random Forests, *Machine Learning* 45(1), 5–32.
- Brewer, D.T., Rawlinson, N., Eayrs, S., Burridge, C.Y., (1998). An assessment of bycatch reduction devices in a tropical Australian prawn trawl fishery. *Fish. Res.* 36, 195–215.
- Brewer, D.T., Griffiths, S., Heales, D.S., Zhou, S., Tonks, M., Dell, Q., Taylor, B.T., Miller, M., Kuhnert, P., Keys, S., Whitelaw, W., Burke, A., Raudzens, E. (2007). Design, trial and implementation of an integrated, long-term bycatch monitoring program, road tested in the Northern Prawn Fishery. Final Report on FRDC Project 2004/024. CSIRO Cleveland. pp. 416.
- Brinkman, R., Wolanski, E., Deleersnijder, E., McAllister, F., Skirving, W. (2002) Oceanic inflow from the Coral Sea into the Great Barrier Reef. *Est Coast Shelf Sci* 54: 655–668
- Burridge C.Y., Pitcher C.R., Wassenberg T.J., Poiner I.R., Hill, B.J. (2003). Measurement of the rate of depletion of benthic fauna by prawn (shrimp) otter trawls: an experiment in the Great Barrier Reef, Australia. *Fisheries Research* 60: 237–253
- Cappo, M., Harvey, E., Malcolm, H., Speare, P. (2003) Potential of video techniques to monitor diversity abundance and size of fish in studies of Marine Protected Areas. In: "Aquatic Protected Areas - what works best and how do we know?" (Eds Beumer JP, Grant A, Smith DC). World Congress on Aquatic Protected Areas Proceedings, Cairns Australia, August 2002. pp 455-464
- Cappo, M., Speare, P., D'earth, G. (2004) Comparison of Baited Remote Underwater Video Stations (BRUVS) and prawn (shrimp) trawls for assessments of fish biodiversity in inter-reefal areas of the Great Barrier Reef Marine Park. *J Exp Mar Biol Ecol* 302(2): 123-152
- Cappo, M., De'ath, G., Speare, P. (subm.) Shelf-scale patterns in communities of aquatic vertebrates in the inter-reefal waters of the Great Barrier Reef Marine Park determined by Baited Remote Underwater Video Stations. *Mar Ecol Progr Ser*
- Cohen, A., Daubechies, I., Vial, P., (1993). Wavelets on the Interval and Fast Wavelet Transforms, *Applied and Computational Harmonic Analysis*, 1 p54-81.
- Coles, R., McKenzie, L., De'ath, G., Roelofs, A., Lee Long, W. (2006) Modelling factors that influence the spatial distribution of deepwater seagrass in the inter reef lagoon of the Great Barrier Reef World Heritage Area, northern Australia. Submitted manuscript.
- Condie, S.A., Dunn, J.R. (2006). Seasonal characteristics of the surface mixed layer in the Australasian region: implications for primary production regimes and biogeography. *Mar Freshw Res* 57: 569–590
- Courtney, A.J., Haddy, J.A., Campbell, M.J., Roy, D.P., Tonks, M.L., Gaddes, S.W., Chilcott, K.E., O'Neill, M.F., Brown, I.W., McLennan, M., Jebreen, J.E., Van Der Geest, C., Rose, C., Kistle, S., Turnbull, C.T., Kyne, P.M., Bennett, M.B. and Taylor, J. (2006). Bycatch weight, composition and preliminary estimates of the impact of bycatch reduction devices in Queensland's trawl fishery. FRDC Project #2000/170 Final Report 353p.
-

- Courtney, A.J., Tonks, M.L., Campbell, M.J., Roy, D.P., Gaddes, S.W., Kyne, P.M., O'Neill, M.F. (2006). Quantifying the effects of bycatch reduction devices in Queensland's (Australia) shallow water eastern king prawn (*Penaeus plebejus*) trawl fishery. *Fisheries Research* 80:136–147
- De'ath, G. (2006) Boosted trees for ecological modeling and prediction. *Ecology*
- De'ath, G. (2002) Multivariate regression trees: a new technique for modeling species-environment relationships. *Ecology* 83:1105-1117.
- DeVantier, L.M., De'ath, G., Turak, E., Done, T.J., Fabricius, K.E. (2006). Species richness and community structure of reef-building corals on the nearshore Great Barrier Reef. *Coral Reefs* 25(3): 329-340
- Dredge, M.C.L. (1985) Estimates of natural mortality and yield-per-recruit for *Amusium japonicum balloti* Bernardi (Pectinidae) based on tag recoveries. *Journal of Shellfish Research*, 5:103–109.
- Drew, E.A. (2001). Ocean nutrients to sediment banks via tidal jets and Halimeda meadows. In: Wolanski, E. (Ed.), *Oceanographic processes of coral reefs: physical and biological links in the Great Barrier Reef*. CRC Press, Boca Raton, Florida, pp. 127-144
- Duda, R., Hart, P., Stork, D., (2001). *Pattern Classification*, 2nd Ed, Wiley.
- Dufrêne, M., Legendre, P. (1997) Species assemblages and indicator species: the need for a flexible asymmetrical approach. *Ecol Monogr* 67(3): 345-66
- Ellis, N., Pantus, F. (2001) Management strategy modelling: tools to evaluate trawl management strategies with respect to impacts on benthic biota within the Great Barrier Reef Marine Park area. CSIRO Marine Research Final Report to the Great Barrier Reef Marine Park Authority.
- Engel, J. & Kvitek, R. (1998) Effects of otter trawling on benthic community in Monterey Bay National Marine Sanctuary. *Cons.Biol.* 12(6):1204-214.
- Environment Australia, (2000). *Biodiversity Research: Australia's Priorities — a Discussion Paper*.
- Fabricius, K., De'ath, G. (2001) Biodiversity on the Great Barrier Reef: Large-scale patterns and turbidity-related local loss of soft coral taxa. In: Wolanski, E. (Ed.), *Oceanographic processes of coral reefs: physical and biological links in the Great Barrier Reef*. CRC Press, Boca Raton, Florida, pp. 127-144
- Fager, E.W., Longhurst, A.R. (1968) Recurrent group analysis of species assemblages of demersal fish in the Gulf of Guinea. *J Fish Res Board Can* 25(7): 1405–21
- Fogarty, M.P., and Murawski, S.A. 1998. Large-scale disturbance and the structure of marine systems: fishery impacts on Georges Bank. *Ecological Applications*, 8(1), Supplement: S6eS22.
- Friedman, J.H. (2001) Greedy function approximation: a gradient boosting machine. *Ann Stat* 29(5): 1189-1232
- Fulton, E.A., Smith, A.D.M., Webb H., Slater, J. (2004). *Ecological Indicators for the Impacts of Fishing on Non-Target Species, Communities and Ecosystems: Review of Potential Indicators*. AFMA Final Research Report Number R99/1546
- Gribble, N. A. (2003). GBR-prawn: modelling ecosystem impacts of changes in fisheries management of the commercial prawn (shrimp) trawl fishery in the far northern Great Barrier Reef. *Fisheries Research* 65(1-3): 493-506
- Gribble, N. A. (2004). A spatially explicit multi-competitor coexistence model of penaeid (shrimp) distribution on the Australian Great Barrier Reef. *Ecological Modelling*: Vol 177(1-2):61-74
- Gribble, N.A., Good, N., Peel, D., Tanimoto, M., and Officer, R. (2007). Innovative stock assessment and effort mapping using VMS and electronic logbooks. Final Report to FRDC 2002/056.
- Griffiths, S.P., Brewer, D.T., Heales, D.S., Milton, D.A., Stobutzki, I.C., (2006). Validating ecological risk assessments for fisheries: assessing the impacts of turtle excluder devices on
-

- elasmobranch bycatch populations in an Australian trawl fishery. *Marine and Freshwater Research*, 57, 395–401
- Gulland, J.A. (1983). *Fish Stock Assessment: a manual of basic methods*. FAO/Wiley Inter-Science, New York, 223 pp.
- Gust, N., Choat, J.H., and McCormick, M.I. (2001) Spatial variability in reef fish distribution, abundance, size and biomass: a multi-scale analysis. *Mar Ecol Prog Ser* 214, 237-251
- Hancock, G.J., Webster, I.T., Stieglitz, T.C. (In Press) Horizontal mixing of Great Barrier Reef waters: offshore diffusivity determined from radium isotope distribution. *JGR Oceans*
- Haywood, M., Hill, B., Donovan, A., Rochester, W., Ellis, N., Welna, A., Gordon, S., Cheers, S., Forcey, K., Mcleod, I., Moeseneder, C., Smith, G., Manson, F., Wassenberg, T., Thomas, Steve, Kuhnert, P., Laslett, G., Burrridge, C., and Thomas, Sarah, (2005). Quantifying the effects of trawling on seabed fauna in the Northern Prawn Fishery. Final Report on FRDC Project 2002/102. CSIRO, Cleveland. 488 pp.
- Hobday, A. J., Smith, A., Webb, H., Daley, R., Wayte, S., Bulman, C., Dowdney, J. Williams, A., Sporcic, M., Dambacher, J., Fuller, M., Walker, T. (2006) Ecological Risk Assessment for the Effects of Fishing: Methodology. Report R04/1072 for the Australian Fisheries Management Authority, Canberra
- Hilborn, R., Walters, C.J. (1992). *Quantitative fisheries stock assessment: choice, dynamics and uncertainty*. Chapman & Hall, London. 570p.
- Hill, B.J., Haywood, M., Venables, B., Gordon, S.R., Condie, S., Ellis, N.R., Tyre, A., Vance, D., Dunn, J., Mansbridge, J., Moeseneder, C., Bustamante, R. and Pantus, F., (2002). Surrogates I - Predictors, impacts, management and conservation of the benthic biodiversity of the Northern Prawn Fishery. Final Report on FRDC Project 2000/160. CSIRO, Cleveland. 437 pp.
- Jensen, A., la Cour-Harbo, A., (2001). *Ripples in Mathematics, the Discrete Wavelet Transform*, Springer.
- Kaufman, L. and Rousseeuw, P. J. (1990) *Finding Groups in Data*, Wiley, New York.
- Kaufman, L. and Rousseeuw, P. J. (1990). *Finding Groups in Data: An Introduction to Cluster Analysis*. Wiley, New York.
- Koch, V., Wolff, M. (2002) Energy budget and ecological role of mangrove epibenthos in the Caeté estuary, North Brazil. *Mar Ecol Prog Ser* 228: 119–130
- Kodama, K., Horiguchi, T., Kume, G., Nagayama, S., Shimizu, T., Shiraishi, H., Morita, M., Shimizu, M., (2006) Effects of hypoxia on early life history of the stomatopod *Oratosquilla oratoria* in a coastal sea. *Mar Ecol Prog Ser* Vol. 324: 197–206.
- Larcombe, P., Carter, R.M., (2004) Cyclone pumping, sediment partitioning and the development of the Great Barrier Reef shelf system: a review. *Quatern Sci Rev* 23:107–135
- Lee, H-H., Hsu, C-C. (2003). Population biology of the swimming crab *Portunus sanguinolentus* in the waters off northern Taiwan. *Journal of Crustacean Biology* 23:691–699
- Letourneur, Y., Kulbicki, M., Labrosse, P. (1998) Spatial structure of commercial reef fish communities along a terrestrial runoff gradient in the northern lagoon of New Caledonia. *Environ Biol Fish* 51: 141–159
- Long, B.G., Skewes, T.D., Taranto, T.J., Smith, G., Mcleod, I., Pitcher, C.R., Poiner, I.R. (1997) PNG Gas Project: Torres Strait Marine Infill Survey: Report To NSR Re Papua New Guinea–Queensland Gas Project. CSIRO Division of Marine Research.
- Longhurst, A.R., Pauly, D. (1987). *Ecology of tropical oceans*. Academic Press, San Diego, California (USA). 407p
- Lowe-McConnell, R.H. (1987). *Ecological studies in tropical fish communities*. Cambridge University Press. pp 213-223
-

- Magurran, A.E., Henderson, P.A. (2003) Explaining the excess of rare species in natural species abundance distributions. *Nature* 422(6933): 714-716
- Mathews, E.J. and Heap, A.D., (2006). Sedimentology and Geomorphology of Inter-reefal Seabed Environments of the Great Barrier Reef, northeast Australia. Geoscience Australia, Record 2006/11.
- McLeod, I., Skewes, T.D., Gordon, S.R., Pitcher, C.R. (2007). A method for seabed habitat mapping: Integrating acoustic information with biogeophysical observations; Case study – Scott Reef, in Todd, B.J., and Greene, H.G., eds. Mapping the Seafloor for Habitat Characterization: Geological Association of Canada, Special Paper 47, pp.
- Newman, S.J., Williams, D.M., Russ, G.R. (1997). Patterns of zonation of assemblages of the Lutjanidae, Lethrinidae and Serranidae (Epinephelinae) within and among mid shelf and outer shelf reefs in the central Great Barrier Reef. *Mar Freshw Res* 48:119–128
- Penn, J.W. (1976) Tagging Experiments with Western King Prawn, *Penaeus latisulcatus* Kishinouye II. Estimation of Population Parameters. *Aust. J. Mar. Freshwater Res.* 27, 239-50
- Pitcher, C.R., Venables, W., Ellis, N., McLeod, I., Pantus, F., Austin, M., Cappel, M., Doherty, P., Gribble, N. (2002). GBR Seabed Biodiversity Mapping Project: Phase 1. CSIRO/AIMS/QDPI Report to CRC-Reef, pp. 192.
- Pitcher C.R., Austin, M., Burrige, C.Y., Bustamante, R.H., Cheers, S.J., Ellis, N., Jones, P.N., Koutsoukos, A.G., Moeseneder, C.H., Smith, G.P., Venables, W., Wassenberg, T.J., (2004). Recovery of Seabed Habitat from the Impact of Prawn Trawling in the Far Northern Section of the Great Barrier Reef Marine Park. CSIRO Marine Research Final Report to GBRMPA, pp. 370
- Pitcher, C.R., Turnbull, C., Atfield, J., Griffin, D., Dennis, D.M., Skewes, T.D. (2005). Biology, larval transport modelling and commercial logbook data analysis to support management of the NE Queensland rock lobster *Panulirus ornatus* fishery. FRDC Project 2002/008 report to Fisheries Research and Development Corporation. CSIRO Marine & Atmospheric Research pp. 148
- Poiner, I.R., Glaister, J., Pitcher, C.R., Burrige, C., Wassenberg, T., Gribble, N., Hill, B., Blaber, S.J.M., Milton, D.A., Brewer, D., Ellis, N., (1998). The environmental effects of prawn trawling in the far northern section of the Great Barrier Reef Marine Park: 1991–1996. Final Report to GBRMPA and FRDC. CSIRO Division of Marine Research – Queensland Department of Primary Industries Report, 554 pp.
- Porter-Smith, R., Harris, P.T., Andersen, O.B., Coleman, R., Greenslade, D., Jenkins, C.J. (2004). Classification of the Australian continental shelf based on predicted sediment threshold exceedance from tidal currents and swell waves. *Mar Geol* 211: 1– 20
- R Development Core Team (2005) R: a language and environment for statistical computing. R Foundation for statistical computing, Vienna.
- Ramm, D.C., Pender, P.J., Willing, R.S., Buckworth, R.C. (1990). Large-scale spatial patterns of abundance within the assemblage of fish caught by prawn trawlers in northern Australian waters. *Aust J Mar Freshw Res* 41: 79-95
- Ridgway, K. R., J. R. Dunn and J. L. Wilkin, 2002. Ocean interpolation by four-dimensional least squares - Application to the waters around Australia. *Journal of Atmospheric and Oceanic Technology*, 19, 1357-1375.
- Robins, J.B. & McGilvray, J.G. (1999). The AustTED II, an improved trawl efficiency device 2. Commercial performance. *Fisheries Research* 40: 29-41.
- Robins-Troeger, J.B., Buckworth, R.C. & Dredge, M.C.L. (1995). Development of a trawl efficiency device (TED) for Australian prawn fisheries II. Field evaluations of the AustTED. *Fisheries Research*, 22: 107-117.
- Sainsbury KJ, Campbell RA, Lindholm R, Whitelaw AW (1997). Experimental management of an Australian multispecies fishery: Examining the possibility of trawl induced habitat
-

- modification. In: Pikitch EK, Huppert DD, Sissenwine MP (Eds) *Global Trends: Fisheries management*. pp 107-112. American Fisheries Society, Maryland, USA. John Wiley and Son
- Saito, N., Coifman, R., (1995). Local Discriminant Bases and their Applications. *Journal of Mathematical Imaging and Vision*, 5: 337-358.
- Schwarz, G. (1978). "Estimating the dimension of a model". *Annals of Statistics* 6, 461-464.
- Scott, D. W. (1992) *Multivariate Density Estimation: Theory, Practice, and Visualization*. Wiley.
- Simrad EY500 Operating Manual <http://www.simrad.com/html>
- Skewes, T.D., Pitcher, C.R., Long, B.G., Mcleod, I., Taranto, T.J. Gordon, S., Smith, G., Poiner, I.R. (1996) *Torres Strait Infill Survey: Report to IPC Re Pandora Gas Development Project*. CSIRO Division of Fisheries.
- Sternlicht, D., de Moustier, C., (2003). Time-dependent seafloor acoustic backscatter (10-100kHz), *J. Acous. Soc. Am.* 114 (5), p2709--2725 (2003).
- Stobutzki, I.C., Miller, M.J., Brewer, D.T. (2001a). Sustainability of fishery bycatch: a process for assessing highly diverse and numerous bycatch. *Environmental Conservation* 28, 167–181.
- Stobutzki IC, Miller MJ, Jones P, Salini JP (2001b) Bycatch diversity and variation in a tropical Australian penaeid fishery; the implications for monitoring. *Fish Res* 53(3): 283-301
- Stobutzki, I.C., Miller, M.J., Heales, D.S., Brewer, D.T. (2002). Sustainability of elasmobranchs caught as bycatch in a tropical shrimp trawl fishery. *Fish. Bull.* 100:800-821.
- Trefethen, L. N. 1980. Numerical Computation of the Schwarz-Christoffel Transformation, *Siam J. Sci. Stat. Comp.* 1, 82–102
- Wahba, G. (1990) *Spline Models for Observational Data*. National Science Foundation -Conference Board of Mathematical Sciences Regional Conference Series in Applied Mathematics, Philadelphia: Society for Industrial and Applied Mathematics.
- Ward, J.H. (1963). Hierarchical Grouping to optimize an objective function. *Journal of American Statistical Association*, 58(301), 236-244
- Wassenberg TJ, Blaber SJM, Burridge CY, Brewer DT, Salini JP, Gribble N (1997). The effectiveness of fish and shrimp trawls for sampling fish communities in tropical Australia. *Fish Res* 30: 229-240
- Watson RA, Dredge MLC, Mayer DG (1990). Spatial and seasonal variation in demersal trawl fauna associated with a prawn fishery on the central Great Barrier Reef, Australia. *Aust J Mar Freshw Res* 41: 65-77
- Watson, R.A., Goeden, G.B. (1989) Temporal and spatial zonation of the demersal trawl fauna of the central Great Barrier Reef. *Mem. Qld. Mus.* 27(2): 611-620
- Wilkinson, C.R., Cheshire, A.C. (1988). Cross shelf variations in coral reef structure and function— influences of land and ocean. In: *Proceedings of the 6th International Coral Reef Symposium*, Townsville, Australia, Volume 3: Contributed Papers (Choat, J.H. & Barnes, D. eds) 6th International Coral Reef Symposium Executive Committee, pp 227–233
- Williams, D.M. (1991). Patterns and processes in the distribution of coral reef fishes. In: Sale PF (ed) *The ecology of fishes on coral reefs*. Academic Press San Diego. pp 437–474
- Williams, A., Last, P.R., Gomon, M.F., & Paxton, J.R. (1996) Species composition and checklist of the demersal ichthyofauna of the continental slope off western Australia (20–35°S) *Rec. WA Mus.* 18, 135–155.
- Wolanski, E. (1994). *Physical oceanographic processes of the Great Barrier Reef*. CRC Press Marine Science Series.
- Zhou, S., Griffiths, S.P. (2007) Sustainability Assessment for Fishing Effects (SAFE): a new quantitative ecological risk assessment method and its application to elasmobranch bycatch in an Australian trawl fishery. *Fisheries Research* (In Press)
-

11. ABBREVIATIONS

BRUVS – Baited Remote Underwater Video Stations
CARS2000 – CSIRO Atlas of Regional Seas
CERF National Marine Biodiversity Hub
CLARA – Clustering for large Datasets
CRC – Cooperative Research Centre
CTD – Conductivity Temperature Depth sensor array
DEW – Department of Environment & Water Resources
DEM – Digital Elevation Model
DLI – Dufrêne-Legendre Index
EPBC – Environment Protection & Biodiversity Conservation
ERA – Ecological Risk Assessments
FRDC – Fisheries Research & Development Corporation
GA – Geoscience Australia
GBRWHA – Great Barrier Reef World Heritage Area
GPS – Global Positioning System
GU zone – General Use zone
HO – Hydrographic Office
HPA – Highly protected area
IQR – Inter-Quartile Range
JCU – James Cook University
MaxN – Maximum number of fish seen at any one time in field of view of BRUVS
MSE – Management Strategies Evaluations
NOO – National Oceans Office
NPF – Northern Prawn Fishery
NSRMPA – National Representative System of Marine Protected Areas
OSI – Ocean Sciences Institute, Sydney University
PAM – Partitioning Around Medoids
PAR – Photosynthetically Active Radiation
PC-space – Principal Components Space
SRA – Susceptibility-Recovery Analysis
QDPI&F – Queensland Department of Primary Industries & Fisheries
QECTF – Queensland East Coast Trawl Fishery
QSIA – Queensland Seafood Industry Association
RAP – Representative Areas Program
RMS – Residual Mean Square
SRA – Susceptibility Recovery Analysis
SVD – Singular Value Decomposition
VMS – Vessel Monitoring System
VTRs – Video Tape Recorders
WHA – World Heritage Area
WTO – Wildlife Trade Operation

12. APPENDIX 1: INTELLECTUAL PROPERTY

There is no intellectual property of a commercial nature arising from the outputs of this Project.



13. APPENDIX 2: STAFF

| | | | |
|----------------------|---|------------|------|
| Roland Pitcher | CSIRO Marine and Atmospheric Research | Cleveland | Qld. |
| Peter Doherty | Australian Institute of Marine Science | Townsville | Qld |
| Peter Arnold | Museum of Tropical Queensland | Townsville | Qld |
| John Hooper | Queensland Museum South Bank | Brisbane | Qld |
| Neil Gribble | Queensland Department of Primary Industries & Fisheries | Cairns | Qld |
| Chris Bartlett | Museum of Tropical Queensland | Townsville | Qld |
| Matthew Browne | CSIRO Maths and Information Sciences | Cleveland | Qld |
| Norm Campbell | CSIRO Maths and Information Sciences | Perth | WA |
| Toni Cannard | CSIRO Marine and Atmospheric Research | Cleveland | Qld |
| Mike Cappo | Australian Institute of Marine Science | Townsville | Qld |
| Giovannella Carini | Queensland Museum South Bank | Brisbane | Qld |
| Susan Chalmers | Queensland Department of Primary Industries & Fisheries | Cairns | Qld |
| Sue Cheers | CSIRO Marine and Atmospheric Research | Cleveland | Qld |
| Doug Chetwynd | CSIRO Marine and Atmospheric Research | Cleveland | Qld |
| Andrew Colefax | Queensland Museum South Bank | Brisbane | Qld |
| Rob Coles | Queensland Department of Primary Industries & Fisheries | Cairns | Qld |
| Stephen Cook | Queensland Museum South Bank | Brisbane | Qld |
| Peter Davie | Queensland Museum South Bank | Brisbane | Qld |
| Glenn De'ath | Australian Institute of Marine Science | Townsville | Qld |
| Drew Devereux | CSIRO Maths and Information Sciences | Perth | WA |
| Barbara Done | Museum of Tropical Queensland | Townsville | Qld |
| Tim Donovan | Australian Institute of Marine Science | Townsville | Qld |
| Barry Ehrke | Queensland Department of Primary Industries & Fisheries | Cairns | Qld |
| Nick Ellis | CSIRO Marine and Atmospheric Research | Cleveland | Qld |
| Gavin Ericson | Australian Institute of Marine Science | Townsville | Qld |
| Ida Fellegara | Queensland Museum South Bank | Brisbane | Qld |
| Karl Forcey | CSIRO Marine and Atmospheric Research | Cleveland | Qld |
| Melodyrose Furey | CSIRO Marine and Atmospheric Research | Cleveland | Qld |
| Dan Gledhill | CSIRO Marine and Atmospheric Research | Hobart | Tas |
| Norm Good | Queensland Department of Primary Industries & Fisheries | Cairns | Qld |
| Scott Gordon | CSIRO Marine and Atmospheric Research | Cleveland | Qld |
| Mick Haywood | CSIRO Marine and Atmospheric Research | Cleveland | Qld |
| Ian Jacobsen | University of Queensland | Brisbane | Qld |
| Jeff Johnson | Queensland Museum South Bank | Brisbane | Qld |
| Michelle Jones | Queensland Museum South Bank | Brisbane | Qld |
| Stuart Kinninmoth | Australian Institute of Marine Science | Townsville | Qld |
| Sarah Kistle | Queensland Department of Primary Industries & Fisheries | Cairns | Qld |
| Peter Last | CSIRO Marine and Atmospheric Research | Hobart | Tas |
| Anita Leite | Museum of Tropical Queensland | Townsville | Qld |
| Shona Marks | CSIRO Marine and Atmospheric Research | Cleveland | Qld |
| Ian McLeod | CSIRO Marine and Atmospheric Research | Cleveland | Qld |
| Sybilla Oczkowicz | Queensland Department of Primary Industries & Fisheries | Cairns | Qld |
| Cassandra Rose | Queensland Department of Primary Industries & Fisheries | Cairns | Qld |
| Denise Seabright | Museum of Tropical Queensland | Townsville | Qld |
| Jacquie Sheils | CSIRO Marine and Atmospheric Research | Cleveland | Qld |
| Matt Sherlock | CSIRO Marine and Atmospheric Research | Cleveland | Qld |
| Posa Skelton | Queensland Department of Primary Industries & Fisheries | Townsville | Qld |
| David H Smith | CSIRO Marine and Atmospheric Research | Cleveland | Qld |
| Greg Smith | CSIRO Marine and Atmospheric Research | Cleveland | Qld |
| Peter Speare | Australian Institute of Marine Science | Townsville | Qld |
| Marcus Stowar | Australian Institute of Marine Science | Townsville | Qld |
| Colleen Strickland | Queensland Museum South Bank | Brisbane | Qld |
| Patricia Hendriks | Queensland Museum South Bank | Brisbane | Qld |
| Claire Van der Geest | Queensland Department of Primary Industries & Fisheries | Cairns | Qld |

| | | | |
|----------------|---|------------|-----|
| Bill Venables | CSIRO Maths and Information Sciences | Cleveland | Qld |
| Cath Walsh | Queensland Department of Primary Industries & Fisheries | Townsville | Qld |
| Ted Wassenberg | CSIRO Marine and Atmospheric Research | Cleveland | Qld |
| Andrzej Welna | CSIRO Marine and Atmospheric Research | Cleveland | Qld |
| Gus Yearsley | CSIRO Marine and Atmospheric Research | Hobart | Tas |

14. APPENDIX 3: PROJECT STEERING COMMITTEE MEMBERS

Chairperson: Peter Doherty — AIMS, CRC-Reef Program C Leader

Task Leader: Roland Pitcher — CSIRO

Task Associate: David Williams — CRC-Reef

Task Associate: Dorothea Huber → Phil Cadwallader — GBRMPA

Task Associate: Brigid Kerrigan → Malcolm Dunning — QDPI&F

Task Associate: Duncan Souter → Martin Hicks — QSIA

Task Associate: Barry Ehrke — QSIA

Task Associate: Vicki Nelson — NOO

Task Associate: Vern Veitch — Sunfish

15. APPENDIX 4: SINGLE SPECIES TRAWL EXPOSURE

Table 15-1: Summary of species exposure estimates for all 840 modelled species, ranked in decending order by percent of biomass exposed to trawl effort intensity; showing also species group membership, total estimated biomass, percent of biomass available in General Use zone, percent of biomass potentially exposed in trawled cells. Pale orange: >25% biomass exposed; dark orange: >50% biomass exposed; red: >50% biomass exposed.

| Group | Class | Genus | Species | Biomass Kg | %Available | %Exposed | %EffortExp |
|-------|----------------|-----------------------|------------------------|------------|------------|----------|------------|
| 29 | Crustacea | <i>Penaeus</i> | <i>semisulcatus</i> | 301314 | 74 | 64 | 174 |
| 29 | Crustacea | <i>Cryptolutea</i> | <i>arafurensis</i> | 480 | 57 | 41 | 128 |
| 29 | Actinopterygii | <i>Brachirus</i> | <i>muelleri</i> | 80330 | 69 | 59 | 119 |
| 29 | Actinopterygii | <i>Pentaprion</i> | <i>longimanus</i> | 61963 | 62 | 48 | 117 |
| 21 | Actinopterygii | <i>Pelates</i> | <i>quadrilineatus</i> | 129842 | 69 | 47 | 103 |
| 9 | Actinopterygii | <i>Leiognathus</i> | <i>leuciscus</i> | 171753 | 59 | 43 | 95 |
| 9 | Actinopterygii | <i>Upeneus</i> | <i>sundaicus</i> | 370945 | 63 | 50 | 93 |
| 9 | Crustacea | <i>Portunus</i> | <i>gracilimanus</i> | 204641 | 59 | 38 | 86 |
| 29 | Actinopterygii | <i>Terapon</i> | <i>puta</i> | 60300 | 56 | 47 | 78 |
| 29 | Bivalvia | <i>Enisculus</i> | <i>cultellus</i> | 984 | 61 | 46 | 75 |
| 8 | Actinopterygii | <i>Brachaluteres</i> | <i>taylori</i> | 62129 | 71 | 60 | 72 |
| 13 | Crustacea | <i>Trachypenaeus</i> | <i>anchoralis</i> | 45119 | 64 | 44 | 67 |
| 29 | Crustacea | <i>Metapenaeus</i> | <i>ensis</i> | 31126 | 67 | 49 | 67 |
| 22 | Crustacea | <i>Erugosquilla</i> | <i>woodmasoni</i> | 19542 | 66 | 49 | 65 |
| 24 | Actinopterygii | <i>Leiognathus</i> | <i>bindus</i> | 76017 | 42 | 28 | 63 |
| 9 | Bivalvia | <i>Melaxinaea</i> | <i>vitrea</i> | 171979 | 59 | 38 | 63 |
| 29 | Actinopterygii | <i>Saurida</i> | <i>argentea/tumbil</i> | 1109937 | 58 | 38 | 63 |
| 22 | Actinopterygii | <i>Terapon</i> | <i>theraps</i> | 359964 | 63 | 43 | 62 |
| 22 | Crustacea | <i>Myra</i> | <i>tumidospina</i> | 14791 | 57 | 38 | 60 |
| 9 | Actinopterygii | <i>Calliurichthys</i> | <i>grossi</i> | 171819 | 54 | 39 | 59 |
| 22 | Actinopterygii | <i>Upeneus</i> | <i>sulphureus</i> | 723274 | 70 | 46 | 58 |
| 9 | Crustacea | <i>Thenus</i> | <i>parindicus</i> | 518607 | 55 | 36 | 57 |
| 22 | Gastropoda | <i>Nassarius</i> | <i>cremmatus</i> cf | 35852 | 55 | 39 | 57 |
| 22 | Actinopterygii | <i>Psettodes</i> | <i>erumei</i> | 361247 | 61 | 40 | 56 |
| 29 | Bivalvia | <i>Placamen</i> | <i>tiara</i> | 3225 | 55 | 35 | 55 |
| 14 | Actinopterygii | <i>Scolopsis</i> | <i>taeniopterus</i> | 1016419 | 51 | 33 | 54 |
| 22 | Actinopterygii | <i>Leiognathus</i> | <i>splendens</i> | 270168 | 54 | 44 | 54 |
| 13 | Actinopterygii | <i>Repomucenus</i> | <i>belcheri</i> | 98260 | 64 | 42 | 53 |
| 9 | Actinopterygii | <i>Cynoglossus</i> | <i>maculipinnis</i> | 78915 | 60 | 38 | 52 |
| 9 | Bivalvia | <i>Amusium</i> | <i>pleuronectes</i> cf | 824663 | 60 | 37 | 52 |
| 35 | Actinopterygii | <i>Yongeichthys</i> | <i>nebulosus</i> | 66438 | 42 | 25 | 51 |
| 38 | Actinopterygii | <i>Apogon</i> | <i>poecilopterus</i> | 121050 | 50 | 34 | 51 |
| 29 | Actinopterygii | <i>Euristhmus</i> | <i>nudiceps</i> | 1374323 | 56 | 33 | 51 |
| 29 | Actinopterygii | <i>Tripodichthys</i> | <i>angustifrons</i> | 43969 | 45 | 36 | 50 |
| 22 | Anthozoa | <i>Sea pen</i> | sp1 | 507 | 57 | 37 | 50 |
| 22 | Actinopterygii | <i>Gerres</i> | <i>filamentosus</i> | 84315 | 56 | 41 | 50 |
| 9 | Actinopterygii | <i>Selaroides</i> | <i>leptolepis</i> | 586810 | 56 | 36 | 49 |
| 21 | Crustacea | <i>Penaeus</i> | <i>latisulcatus</i> | 235627 | 59 | 39 | 49 |
| 14 | Cephalopoda | <i>Sepia</i> | <i>pharaonis</i> | 139386 | 51 | 34 | 48 |
| 22 | Actinopterygii | <i>Nemipterus</i> | <i>peronii</i> | 1355758 | 64 | 37 | 48 |
| 9 | Bivalvia | <i>Modiolus</i> | <i>elongatus</i> | 39291 | 56 | 35 | 47 |
| 9 | Crustacea | <i>Penaeus</i> | <i>esculentus</i> | 1031505 | 62 | 36 | 47 |
| 9 | Actinopterygii | <i>Cynoglossus</i> | sp 1 punctate | 80719 | 56 | 34 | 47 |
| 22 | Actinopterygii | <i>Caranx</i> | <i>bucculentus</i> | 1236784 | 64 | 39 | 47 |
| 14 | Crustacea | <i>Metapenaeus</i> | <i>endeavouri</i> | 534272 | 52 | 31 | 46 |
| 21 | Actinopterygii | <i>Saurida</i> | <i>grandi/undo</i> | 8331858 | 59 | 37 | 46 |
| 14 | Crustacea | <i>Charybdis</i> | <i>truncata</i> | 437520 | 48 | 31 | 46 |
| 14 | Crustacea | <i>Portunus</i> | <i>tuberculosis</i> | 394 | 47 | 31 | 46 |
| 10 | Bivalvia | <i>Amusium</i> | <i>balloti</i> | 2355308 | 55 | 37 | 45 |
| 22 | Actinopterygii | <i>Suggrundus</i> | <i>macracanthus</i> | 559472 | 59 | 33 | 45 |
| 13 | Actinopterygii | <i>Leiognathus</i> | cf <i>bindus</i> | 22870 | 59 | 36 | 45 |
| 13 | Actinopterygii | <i>Parapercis</i> | <i>diplospilus</i> | 3855 | 59 | 36 | 45 |
| 10 | Holothuroidea | <i>Bohadschia</i> | <i>marmorata</i> cf | 270670 | 69 | 54 | 44 |
| 14 | Gastropoda | <i>Lophiotoma</i> | <i>acuta</i> | 4385 | 54 | 34 | 44 |

| Group | Class | Genus | Species | Biomass Kg | %Available | %Exposed | %EffortExp |
|-------|----------------|------------------------|-----------------------|------------|------------|----------|------------|
| 21 | Actinopterygii | <i>Pseudorhombus</i> | <i>arsius</i> | 329560 | 68 | 41 | 44 |
| 9 | Actinopterygii | <i>Inegocia</i> | <i>japonica</i> | 1096930 | 60 | 36 | 44 |
| 21 | Crustacea | <i>Ixa</i> | <i>inermis</i> | 2544 | 62 | 40 | 44 |
| 13 | Crustacea | <i>Leucosia</i> | <i>ocellata</i> | 13523 | 59 | 36 | 44 |
| 29 | Crustacea | <i>Liagore</i> | <i>rubromaculata</i> | 49419 | 48 | 25 | 43 |
| 22 | Crustacea | <i>Portunus</i> | <i>hastatoides</i> | 5197 | 55 | 37 | 43 |
| 9 | Crustacea | <i>Calappa</i> | sp44 | 10969 | 57 | 34 | 43 |
| 10 | Actinopterygii | <i>Ambiserrula</i> | <i>jugosa</i> | 501376 | 68 | 51 | 43 |
| 38 | Crustacea | <i>Oratosquillina</i> | <i>gravieri</i> | 48611 | 48 | 30 | 42 |
| 13 | Actinopterygii | <i>Leiognathus</i> | <i>moretoniensis</i> | 47237 | 52 | 34 | 41 |
| 21 | Crustacea | <i>Portunus</i> | <i>pelagicus</i> | 2172862 | 60 | 37 | 40 |
| 10 | Actinopterygii | <i>Aploactis</i> | <i>aspera</i> | 21363 | 66 | 47 | 40 |
| 13 | Actinopterygii | <i>Trixiphichthys</i> | <i>weberi</i> | 59106 | 56 | 32 | 40 |
| 14 | Gastropoda | <i>Vexillum</i> | <i>obeliscus</i> cf | 2302 | 44 | 25 | 39 |
| 22 | Gastropoda | <i>Bufonaria</i> | <i>rana</i> | 19213 | 56 | 33 | 39 |
| 10 | Actinopterygii | <i>Inimicus</i> | <i>caledonicus</i> | 711097 | 65 | 47 | 39 |
| 9 | Echinoidea | <i>Brissopsis</i> | <i>luzonica</i> | 1377669 | 46 | 27 | 38 |
| 13 | Crustacea | <i>Cryptopodia</i> | <i>queenslandi</i> | 5162 | 54 | 32 | 38 |
| 22 | Actinopterygii | <i>Torquigener</i> | <i>whitleyi</i> | 150537 | 52 | 34 | 38 |
| 29 | Cephalopoda | <i>Sepia</i> | <i>elliptica</i> | 158747 | 51 | 30 | 38 |
| 22 | Gastropoda | <i>Aplysia</i> | sp1_QMS | 450338 | 51 | 32 | 38 |
| 21 | Actinopterygii | <i>Upeneus</i> | <i>asymmetricus</i> | 367368 | 60 | 37 | 38 |
| 27 | Bivalvia | <i>Leionucula</i> | <i>superba</i> | 5499 | 56 | 32 | 37 |
| 9 | Gastropoda | <i>Lamellaria</i> | sp1 | 5697 | 46 | 27 | 37 |
| 22 | Actinopterygii | <i>Sillago</i> | <i>burrus</i> | 307944 | 46 | 30 | 37 |
| 9 | Ophiuroidea | <i>Dougaloplus</i> | <i>echinata</i> | 2513 | 47 | 27 | 37 |
| 21 | Crustacea | <i>Dorippe</i> | <i>quadridens</i> | 3584 | 63 | 38 | 37 |
| 27 | Actinopterygii | <i>Grammatobothus</i> | <i>polyophthalmus</i> | 358459 | 59 | 33 | 37 |
| 29 | Bivalvia | <i>Dosinia</i> | <i>altenai</i> | 191530 | 50 | 27 | 37 |
| 14 | Crustacea | <i>Diogenidae</i> | sp356-1 | 442 | 45 | 25 | 36 |
| 22 | Crustacea | <i>Paguristes</i> | sp2358-2 | 30865 | 52 | 31 | 36 |
| 13 | Actinopterygii | <i>Cynoglossus</i> | sp juv/unident | 14818 | 54 | 31 | 36 |
| 14 | Actinopterygii | <i>Nemipterus</i> | <i>nematopus</i> | 693470 | 37 | 21 | 36 |
| 22 | Holothuroidea | <i>Holothuria</i> | <i>ocellata</i> | 858968 | 52 | 32 | 36 |
| 10 | Actinopterygii | <i>Suezichthys</i> | <i>gracilis</i> | 14695 | 61 | 44 | 36 |
| 7 | Gastropoda | <i>Strombus</i> | <i>vittatus</i> | 56120 | 57 | 38 | 36 |
| 10 | Actinopterygii | <i>Apogon</i> | <i>nigripinnis</i> | 59272 | 65 | 41 | 35 |
| 13 | Gastropoda | <i>Murex</i> | <i>brevispina</i> | 4747 | 61 | 35 | 35 |
| 13 | Actinopterygii | <i>Pomadasys</i> | <i>maculatus</i> | 1542585 | 65 | 35 | 35 |
| 10 | Gymnolaemata | <i>Iodictyum</i> | spp | 17890 | 56 | 45 | 35 |
| 25 | Gastropoda | <i>Strombus</i> | <i>campbelli</i> | 22441 | 64 | 40 | 35 |
| 21 | Actinopterygii | <i>Paramonacanthus</i> | <i>otisensis</i> | 402900 | 58 | 37 | 35 |
| 33 | Actinopterygii | <i>Pseudorhombus</i> | <i>elevatus</i> | 775731 | 67 | 36 | 35 |
| 24 | Crustacea | <i>Calappa</i> | <i>terraeereginae</i> | 10382 | 45 | 28 | 34 |
| 25 | Actinopterygii | <i>Scorpaenopsis</i> | <i>furneauxi</i> | 2174 | 60 | 41 | 34 |
| 33 | Crustacea | <i>Portunus</i> | <i>sanguinolentus</i> | 1018755 | 65 | 40 | 34 |
| 8 | Chlorophyceae | <i>Chaetomorpha</i> | <i>crassa</i> | 360585 | 52 | 34 | 34 |
| 9 | Bivalvia | <i>Trisidos</i> | <i>semitorata</i> | 402307 | 47 | 26 | 34 |
| 21 | Holothuroidea | <i>Holothuria</i> | sp2 | 110155 | 64 | 41 | 34 |
| 10 | Phaeophyceae | <i>Sporochnus</i> | <i>comosus</i> | 1515084 | 57 | 38 | 34 |
| 3 | Crustacea | <i>Paradorippe</i> | <i>australiensis</i> | 2758 | 49 | 27 | 33 |
| 2 | Anthozoa | <i>Virgularia</i> | sp1 | 2422 | 41 | 25 | 33 |
| 33 | Asteroidea | <i>Luidia</i> | <i>hardwicki</i> | 26743 | 58 | 34 | 33 |
| 33 | Actinopterygii | <i>Apistus</i> | <i>carinatus</i> | 1073477 | 56 | 34 | 33 |
| 31 | Demospongiae | <i>Xenosporgia</i> | <i>patelliformis</i> | 599 | 59 | 38 | 33 |
| 29 | Crustacea | <i>Pronotonyx</i> | <i>leavis</i> | 329 | 46 | 24 | 33 |
| 9 | Asteroidea | <i>Astropecten</i> | sp4_AIM | 11187 | 45 | 26 | 33 |
| 21 | Actinopterygii | <i>Paracentropogon</i> | <i>longispinus</i> | 89968 | 49 | 30 | 33 |
| 8 | Gastropoda | <i>Strombus</i> | <i>dilatatus</i> | 92276 | 53 | 38 | 33 |
| 19 | Actinopterygii | <i>Pseudorhombus</i> | <i>spinosus</i> | 969118 | 58 | 32 | 33 |
| 21 | Gymnolaemata | <i>Selenaria</i> | <i>maculata</i> cf | 288844 | 59 | 37 | 33 |
| 2 | Demospongiae | <i>Ircinia</i> | 1255 | 7482318 | 46 | 27 | 33 |
| 33 | Actinopterygii | <i>Minous</i> | <i>versicolor</i> | 92283 | 58 | 34 | 32 |
| 8 | Actinopterygii | <i>Asterorhombus</i> | <i>intermedius</i> | 154382 | 61 | 37 | 32 |

| Group | Class | Genus | Species | Biomass Kg | %Available | %Exposed | %EffortExp |
|-------|----------------|-------------------------|-----------------------|------------|------------|----------|------------|
| 25 | Actinopterygii | <i>Paraploactis</i> | <i>kagoshimensis</i> | 18985 | 62 | 38 | 32 |
| 20 | Actinopterygii | <i>Nemipterus</i> | <i>furcosus</i> | 4012361 | 50 | 25 | 32 |
| 19 | Crustacea | <i>Scyllarus</i> | <i>demani</i> | 135376 | 55 | 33 | 32 |
| 8 | Crustacea | <i>Actumnus</i> | <i>squamosus</i> | 915 | 54 | 36 | 32 |
| 10 | Phaeophyceae | <i>Padina</i> | sp | 658602 | 56 | 40 | 32 |
| 29 | Actinopterygii | <i>Nemipterus</i> | <i>hexodon</i> | 1421345 | 52 | 21 | 32 |
| 21 | Actinopterygii | <i>Dactylopus</i> | <i>dactylopus</i> | 63493 | 54 | 33 | 32 |
| 7 | Echinoidea | <i>Salmacis</i> | <i>sphaeroides</i> | 342726 | 56 | 38 | 32 |
| 22 | Crustacea | <i>Portunus</i> | <i>tuberculatus</i> | 1226 | 46 | 28 | 32 |
| 14 | Actinopterygii | <i>Fistularia</i> | <i>petimba</i> | 135435 | 44 | 26 | 32 |
| 22 | Gastropoda | <i>Gemmula</i> | sp2 | 7259 | 46 | 28 | 32 |
| 21 | Liliopsida | <i>Halophila</i> | <i>decipiens</i> | 3925942 | 50 | 30 | 32 |
| 8 | Bivalvia | <i>Ctenocardia</i> | <i>virgo</i> cf | 6808 | 54 | 34 | 32 |
| 20 | Echinoidea | <i>Ova</i> | <i>lacunosus</i> | 136339 | 44 | 23 | 31 |
| 8 | Gymnolaemata | <i>Hippothoa</i> | <i>distans</i> | 404 | 55 | 36 | 31 |
| 7 | Actinopterygii | <i>Torquigener</i> | sp1 (gloerfelt-tarp) | 734504 | 57 | 38 | 31 |
| 25 | Actinopterygii | <i>Chaetodermis</i> | <i>penicilligera</i> | 119061 | 59 | 38 | 31 |
| 24 | Actinopterygii | <i>Cynoglossus</i> | sp kopsi group | 58222 | 53 | 28 | 31 |
| 29 | Actinopterygii | <i>Apogon</i> | <i>fasciatus</i> | 223485 | 43 | 24 | 31 |
| 25 | Holothuroidea | <i>Holothuroidea</i> | sp2 | 44967 | 50 | 29 | 31 |
| 33 | Foraminifera | <i>Discobotellina</i> | <i>biperforata</i> | 151281 | 58 | 35 | 31 |
| 10 | Rhodophyceae | <i>Chondrophyucus</i> | sp1 | 29227 | 54 | 38 | 31 |
| 22 | Actinopterygii | <i>Nemipterus</i> | sp juv/unident | 6496 | 47 | 28 | 31 |
| 21 | Actinopterygii | <i>Centrus</i> | <i>scutatus</i> | 19885 | 57 | 35 | 31 |
| 12 | Crustacea | <i>Ebalia</i> | <i>lambriformis</i> | 1021 | 52 | 27 | 31 |
| 2 | Holothuroidea | <i>Stichopus</i> | <i>ocellatus</i> | 2416172 | 49 | 28 | 31 |
| 9 | Asteroidea | <i>Astropecten</i> | <i>granulatus</i> cf | 16683 | 46 | 25 | 31 |
| 19 | Bivalvia | <i>Lomopsis</i> | sp1 | 61039 | 51 | 29 | 31 |
| 12 | Crustacea | <i>Austrolibinia</i> | <i>gracilipes</i> | 1570 | 49 | 26 | 30 |
| 22 | Echinoidea | <i>Chaetodiadema</i> | <i>granulatum</i> | 80329 | 48 | 27 | 30 |
| 29 | Crustacea | <i>Ceratoplax</i> | <i>ciliata</i> | 562 | 42 | 22 | 30 |
| 10 | Crustacea | <i>Penaeus</i> | <i>plebejus</i> | 129674 | 54 | 35 | 30 |
| 25 | Bivalvia | <i>Barbatia</i> | <i>parvillosa</i> cf | 1283 | 49 | 28 | 30 |
| 10 | Liliopsida | <i>Halophila</i> | <i>ovalis</i> | 4093618 | 51 | 32 | 30 |
| 29 | Actinopterygii | <i>Epinephelus</i> | <i>sextfasciatus</i> | 285546 | 48 | 22 | 30 |
| 10 | Liliopsida | <i>Halophila</i> | <i>spinulosa</i> | 13547972 | 53 | 33 | 30 |
| 8 | Rhodophyceae | <i>Dasya</i> | sp1 | 60829 | 55 | 34 | 30 |
| 8 | Chlorophyceae | <i>Udotea</i> | <i>argentea</i> | 785198 | 51 | 34 | 30 |
| 10 | Phaeophyceae | <i>Lobophora</i> | <i>variegata</i> | 14640448 | 54 | 36 | 30 |
| 21 | Rhodophyceae | <i>Osmundaria</i> | <i>fimbriata</i> | 2542368 | 48 | 28 | 30 |
| 21 | Actinopterygii | <i>Nemipteridae</i> | sp juv/unident | 7775 | 52 | 30 | 30 |
| 7 | Actinopterygii | <i>Calliurichthys</i> | <i>ogilbyi</i> | 123272 | 53 | 35 | 30 |
| 31 | Actinopterygii | <i>Trachinocephalus</i> | <i>myops</i> | 1028380 | 53 | 36 | 30 |
| 9 | Bivalvia | <i>Antigona</i> | <i>lamellaris</i> | 23273 | 45 | 25 | 30 |
| 8 | Gastropoda | <i>Xenophora</i> | <i>indica</i> | 25049 | 44 | 27 | 30 |
| 14 | Liliopsida | <i>Halophila</i> | <i>tricostata</i> | 911642 | 45 | 25 | 30 |
| 10 | Gastropoda | <i>Philine</i> | sp1 | 8236 | 54 | 33 | 29 |
| 13 | Gastropoda | <i>Natica</i> | <i>vitellus</i> | 8642 | 53 | 30 | 29 |
| 10 | Bivalvia | <i>Annachlamys</i> | <i>kuhnholtzi</i> | 365468 | 48 | 35 | 29 |
| 25 | Rhodophyceae | <i>Polysiphonia</i> | sp1 | 36529 | 54 | 33 | 29 |
| 20 | Anthozoa | <i>Alertigorgia</i> | <i>orientalis</i> | 33318 | 50 | 27 | 29 |
| 20 | Asteroidea | <i>Astropecten</i> | spp | 76778 | 45 | 26 | 29 |
| 19 | Rhodophyceae | <i>Laurencia</i> | sp2 | 259365 | 50 | 31 | 29 |
| 8 | Crustacea | <i>Scyllarus</i> | <i>martensii</i> | 6856 | 50 | 31 | 29 |
| 24 | Bivalvia | <i>Paphia</i> | <i>undulata</i> cf | 7989 | 45 | 25 | 29 |
| 29 | Bivalvia | <i>Corbula</i> | sp2 | 828447 | 48 | 27 | 29 |
| 6 | Crustacea | <i>Neopalicus</i> | <i>jukesii</i> | 12459 | 47 | 29 | 29 |
| 10 | Bivalvia | <i>Annachlamys</i> | <i>flabellata</i> | 289876 | 51 | 32 | 29 |
| 12 | Crustacea | <i>Oratosquillina</i> | <i>quinquedentata</i> | 62852 | 49 | 26 | 29 |
| 7 | Actinopterygii | <i>Cynoglossus</i> | <i>maccullochi</i> | 32047 | 59 | 35 | 29 |
| 10 | Chlorophyceae | <i>Codium</i> | <i>geppii</i> | 224230 | 52 | 36 | 29 |
| 20 | Actinopterygii | <i>Carangidae</i> | sp juv/unident | 19532 | 38 | 20 | 29 |
| 30 | Gymnolaemata | <i>Schizomavella</i> | spp | 2378 | 39 | 22 | 29 |
| 10 | Actinopterygii | <i>Repomucenus</i> | <i>limiceps</i> | 267345 | 52 | 34 | 29 |

| Group | Class | Genus | Species | Biomass Kg | %Available | %Exposed | %EffortExp |
|-------|----------------|------------------------------|--------------------------|------------|------------|----------|------------|
| 7 | Phaeophyceae | <i>Dictyotales</i> | sp | 433762 | 53 | 35 | 29 |
| 10 | Rhodophyceae | <i>Griffithsia</i> | sp | 10773 | 52 | 33 | 29 |
| 9 | Bivalvia | <i>Corbula</i> | <i>macgillvrayi</i> | 205900 | 47 | 25 | 29 |
| 7 | Crustacea | <i>Leucosia</i> | <i>formosensis</i> | 1341 | 53 | 34 | 28 |
| 7 | Cephalopoda | <i>Sepiidae</i> | spp | 792725 | 49 | 30 | 28 |
| 7 | Crustacea | <i>Portunus</i> | <i>rubromarginatus</i> | 5914213 | 55 | 34 | 28 |
| 10 | Asteroidea | <i>Oreasteridae</i> | sp1 | 2814889 | 56 | 37 | 28 |
| 7 | Crustacea | <i>Sicyonia</i> | <i>rectirostris</i> | 259 | 56 | 34 | 28 |
| 20 | Chlorophyceae | <i>Udotea</i> | <i>glaucescens</i> | 1402555 | 42 | 23 | 28 |
| 11 | Phaeophyceae | <i>Sporochnus</i> | <i>moorei</i> | 2797072 | 53 | 32 | 28 |
| 33 | Polychaeta | <i>Chloeia</i> | <i>flava</i> | 15742 | 49 | 28 | 28 |
| 7 | Chlorophyceae | <i>Cladophora</i> | sp | 39457 | 52 | 33 | 28 |
| 7 | Cephalopoda | <i>Sepiadariidae</i> | sp5 | 17032 | 52 | 33 | 28 |
| 7 | Actinopterygii | <i>Torquigener</i> | cf <i>pallimaculatus</i> | 358774 | 52 | 31 | 28 |
| 21 | Echinoidea | <i>Laganum</i> | <i>depressum</i> | 2276625 | 50 | 30 | 28 |
| 21 | Gymnolaemata | <i>Thalamoporella</i> | spp | 56643 | 53 | 32 | 28 |
| 16 | Gymnolaemata | <i>Retelepralia</i> | <i>mosaica</i> | 62 | 45 | 33 | 28 |
| 10 | Rhodophyceae | <i>Lithophyllum</i> | sp1 | 21086914 | 50 | 33 | 28 |
| 25 | Cephalopoda | <i>Cephalopoda</i> | spp | 750874 | 47 | 27 | 27 |
| 2 | Crustacea | <i>Dromidiopsis</i> | <i>edwardsi</i> | 27212 | 46 | 26 | 27 |
| 2 | Demospongiae | <i>Reniochalina</i> | <i>stalagmitis</i> | 500459 | 41 | 23 | 27 |
| 34 | Actinopterygii | <i>Cynoglossus</i> | sp4 | 466488 | 49 | 31 | 27 |
| 2 | Anthozoa | <i>Trachyphyllia</i> | <i>geoffroyi</i> | 3171803 | 46 | 27 | 27 |
| 10 | Chlorophyceae | <i>Halimeda</i> | sp2 | 477419 | 46 | 30 | 27 |
| 19 | Crustacea | <i>Pagurid</i> | sp17 | 2067 | 47 | 27 | 27 |
| 10 | Gastropoda | <i>Conus</i> | <i>ammiralis</i> | 17677 | 51 | 34 | 27 |
| 12 | Holothuroidea | <i>Holothuroidea</i> | sp22 | 1113121 | 51 | 26 | 27 |
| 10 | Gymnolaemata | <i>Robertsonidra</i> | spp | 12430 | 50 | 33 | 27 |
| 25 | Crustacea | <i>Porcellanid</i> | sp4154 | 693 | 49 | 29 | 27 |
| 28 | Gastropoda | <i>Atys</i> | <i>cylindricus</i> cf | 4963 | 49 | 28 | 27 |
| 7 | Actinopterygii | <i>Sorsogona</i> | <i>tuberculata</i> | 1332608 | 53 | 32 | 27 |
| 8 | Crustacea | <i>Arcania</i> | <i>elongata</i> | 11264 | 47 | 27 | 27 |
| 11 | Rhodophyceae | <i>Heterosiphonia</i> | <i>muelleri</i> | 1083464 | 52 | 31 | 27 |
| 11 | Phaeophyceae | <i>Dictyopteris</i> | sp2 | 1307425 | 52 | 31 | 27 |
| 33 | Gastropoda | <i>Nassarius</i> | <i>conoidalis</i> cf | 2625 | 52 | 29 | 27 |
| 12 | Actinopterygii | <i>Adventor</i> | <i>elongatus</i> | 11470 | 44 | 22 | 26 |
| 2 | Chlorophyceae | <i>Halimeda</i> | <i>borneenses</i> | 10124447 | 45 | 26 | 26 |
| 25 | Actinopterygii | <i>Upeneus</i> | sp juv/unident | 5365 | 48 | 26 | 26 |
| 9 | Crustacea | <i>Dorippe</i> | sp7142-12 | 601019 | 45 | 24 | 26 |
| 29 | Bivalvia | <i>Corbula</i> | <i>fortisulcata</i> | 6462 | 43 | 23 | 26 |
| 1 | Cephalopoda | <i>Sepia</i> | <i>whitleyana</i> | 493757 | 50 | 32 | 26 |
| 11 | Gastropoda | <i>Biplex</i> | <i>pulchellum</i> | 59197 | 47 | 26 | 26 |
| 3 | Actinopterygii | <i>Cynoglossus</i> | <i>ogilbyi</i> | 28505 | 44 | 25 | 26 |
| 25 | Asteroidea | <i>Stellaster</i> | <i>equestris</i> cf | 2055943 | 49 | 29 | 26 |
| 8 | Demospongiae | <i>Mycale (arenochalina)</i> | <i>mirabilis</i> | 401414 | 45 | 31 | 26 |
| 11 | Bivalvia | <i>Spondylus</i> | <i>wrightianus</i> | 103088 | 50 | 30 | 26 |
| 19 | Echinoidea | <i>Peronella</i> | <i>orbicularis</i> cf | 32469 | 50 | 28 | 26 |
| 31 | Gymnolaemata | <i>Orthoscuticella</i> | spp | 26462 | 48 | 30 | 26 |
| 20 | Demospongiae | <i>Disyringa</i> | sp1 | 9021 | 46 | 23 | 26 |
| 30 | Gastropoda | <i>Xenophora</i> | <i>solarioides</i> | 37081 | 47 | 27 | 26 |
| 19 | Actinopterygii | <i>Engyprosopon</i> | <i>grandisquama</i> | 1306624 | 57 | 30 | 26 |
| 20 | Rhodophyceae | <i>Amansia</i> | <i>glomerata</i> | 1902406 | 41 | 21 | 26 |
| 27 | Crustacea | <i>Nursilia</i> | sp nov | 3789 | 50 | 26 | 26 |
| 20 | Echinoidea | <i>Laganidae</i> | sp3 | 190493 | 44 | 24 | 26 |
| 10 | Bivalvia | <i>Chama</i> | spp | 13590 | 50 | 32 | 26 |
| 2 | Crustacea | <i>Portunus</i> | <i>tenuipes</i> | 1911035 | 42 | 22 | 26 |
| 10 | Rhodophyceae | <i>Gracilaria</i> | sp1 | 1475393 | 48 | 29 | 26 |
| 36 | Actinopterygii | <i>Minous</i> | <i>trachycephalus</i> | 649193 | 47 | 26 | 26 |
| 16 | Brachiopoda | <i>Brachiopoda</i> | sp1_MTO | 79799 | 41 | 31 | 25 |
| 27 | Crustacea | <i>Trachypenaeus</i> | <i>granulosus</i> | 424353 | 50 | 25 | 25 |
| 21 | Rhodophyceae | <i>Gracilaria</i> | sp2 | 975404 | 48 | 29 | 25 |
| 1 | Phaeophyceae | <i>Lobophora</i> | sp | 6615675 | 53 | 30 | 25 |
| 10 | Actinopterygii | <i>Erosa</i> | <i>erosa</i> | 175940 | 47 | 32 | 25 |
| 25 | Actinopterygii | <i>Tragulichthys</i> | <i>jaculiferus</i> | 637207 | 47 | 25 | 25 |

| Group | Class | Genus | Species | Biomass Kg | %Available | %Exposed | %EffortExp |
|-------|----------------|------------------------|------------------------|------------|------------|----------|------------|
| 21 | Actinopterygii | <i>Choerodon</i> | <i>cephalotes</i> | 421829 | 46 | 27 | 25 |
| 4 | Actinopterygii | <i>Zebrias</i> | <i>craticula</i> | 206568 | 49 | 30 | 25 |
| 8 | Crustacea | <i>Pilumnus</i> | <i>longicornis</i> | 2472 | 46 | 26 | 25 |
| 7 | Crustacea | <i>Dardanus</i> | <i>callichela var</i> | 29106 | 52 | 31 | 25 |
| 10 | Rhodophyceae | <i>Dasya</i> | sp | 365331 | 49 | 29 | 25 |
| 11 | Bivalvia | <i>Chama</i> | <i>pulchella</i> | 874718 | 46 | 27 | 25 |
| 1 | Phaeophyceae | <i>Dictyota</i> | sp1 | 82767 | 46 | 31 | 25 |
| 25 | Actinopterygii | <i>Upeneus</i> | <i>tragula</i> | 843838 | 47 | 25 | 25 |
| 1 | Crustacea | <i>Allogalathea</i> | <i>elegans</i> | 2905 | 49 | 29 | 25 |
| 31 | Gymnolaemata | <i>Scuticella</i> | <i>plagiostoma</i> | 233332 | 48 | 30 | 25 |
| 36 | Crustacea | <i>Carinosquilla</i> | <i>redacta</i> | 44868 | 41 | 23 | 25 |
| 27 | Actinopterygii | <i>Pseudochromis</i> | <i>quinquedentatus</i> | 1907 | 54 | 26 | 25 |
| 1 | Crustacea | <i>Actaea</i> | <i>jacquelineae</i> | 958 | 46 | 30 | 25 |
| 15 | Crustacea | <i>Phalangipus</i> | <i>filiformis</i> | 30500 | 44 | 23 | 25 |
| 7 | Actinopterygii | <i>Synodus</i> | <i>tectus group</i> | 707843 | 49 | 29 | 25 |
| 6 | Demospongiae | <i>Demospongiae</i> | sp11 | 48060 | 40 | 28 | 25 |
| 25 | Ophiuroidea | <i>Ophiothrix</i> | sp14 | 4806 | 46 | 27 | 25 |
| 1 | Demospongiae | <i>Mycale</i> | sp9 | 1633320 | 47 | 30 | 25 |
| 2 | Anthozoa | <i>Cycloseris</i> | <i>cyclolites</i> | 112329 | 55 | 32 | 24 |
| 34 | Bivalvia | <i>Mimachlamys</i> | <i>gloriosa</i> | 24876 | 44 | 24 | 24 |
| 11 | Crustacea | <i>Myra</i> | <i>mammillaris</i> | 25080 | 46 | 27 | 24 |
| 36 | Demospongiae | <i>Demospongiae</i> | sp89 | 63728 | 50 | 27 | 24 |
| 24 | Actinopterygii | <i>Priacanthus</i> | <i>tayenus</i> | 1576906 | 45 | 19 | 24 |
| 16 | Crustacea | <i>Parapenaopsis</i> | <i>venusta</i> | 10034 | 51 | 32 | 24 |
| | Crustacea | <i>Penaeid unknown</i> | <i>penaeid unknown</i> | 2674 | 44 | 24 | 24 |
| | Gastropoda | <i>Philine</i> | <i>angasi</i> | 5859 | 44 | 24 | 24 |
| | Chondrichthyes | <i>Dasyatis</i> | <i>leylandi</i> | 176702 | 44 | 24 | 24 |
| | Crustacea | <i>Thalamita</i> | <i>hanseni</i> | 54500 | 44 | 24 | 24 |
| | Mollusca | <i>Mollusca</i> | <i>eggs</i> | 18397 | 44 | 24 | 24 |
| | Crustacea | <i>Alpheidae</i> | sp2434 | 164 | 44 | 24 | 24 |
| | Anthozoa | <i>Pteroides</i> | sp1 | 22889 | 44 | 24 | 24 |
| | Anthozoa | <i>Pteroides</i> | sp2 | 9105 | 44 | 24 | 24 |
| | Crustacea | <i>Phalangipus</i> | <i>australiensis</i> | 10355 | 44 | 24 | 24 |
| 20 | Actinopterygii | <i>Choerodon</i> | <i>sugillatum</i> | 525263 | 46 | 24 | 24 |
| 34 | Crustacea | <i>Parthenope</i> | <i>longimanus</i> | 8339 | 49 | 25 | 24 |
| 20 | Demospongiae | <i>Spirastrella</i> | sp3 | 68071 | 41 | 20 | 24 |
| 3 | Crustacea | <i>Lisoporcellana</i> | sp3194 | 354 | 43 | 24 | 24 |
| 3 | Demospongiae | <i>Demospongiae</i> | sp61 | 303087 | 40 | 22 | 24 |
| 7 | Chlorophyceae | <i>Halimeda</i> | <i>cuneata</i> | 5618 | 43 | 30 | 24 |
| 30 | Crustacea | <i>Quollastris</i> | <i>subtilis</i> | 5814 | 36 | 20 | 24 |
| 2 | Bivalvia | <i>Fragum</i> | <i>retusum</i> | 3345 | 47 | 28 | 24 |
| 8 | Gastropoda | <i>Strombus</i> | <i>variabilis</i> | 6886 | 47 | 28 | 24 |
| 23 | Gymnolaemata | <i>Beania</i> | spp | 4544 | 43 | 23 | 24 |
| 1 | Gastropoda | <i>Tudivasum</i> | <i>armigera</i> | 80914 | 44 | 30 | 24 |
| 3 | Bivalvia | <i>Modiolus</i> | sp1 | 2064840 | 39 | 21 | 24 |
| 11 | Asteroidea | <i>Anthenea</i> | sp1_AIM | 72818 | 51 | 30 | 24 |
| 11 | Gymnolaemata | <i>Hiantopora</i> | <i>intermedia cf</i> | 936 | 44 | 30 | 24 |
| 36 | Demospongiae | <i>Ircinia</i> | 2710 | 10672550 | 43 | 23 | 24 |
| 25 | Gastropoda | <i>Nassarius</i> | <i>glans cf</i> | 39749 | 48 | 29 | 24 |
| 6 | Chlorophyceae | <i>Udotea</i> | <i>flabellum</i> | 642280 | 44 | 27 | 24 |
| 11 | Echinoidea | <i>Temnotrema</i> | sp3 | 72568 | 44 | 24 | 24 |
| 4 | Gymnolaemata | <i>Cranosina</i> | <i>coronata</i> | 9 | 46 | 29 | 24 |
| 3 | Bivalvia | <i>Parahytissa</i> | <i>imbricata</i> | 52508 | 42 | 24 | 24 |
| 1 | Rhodophyceae | <i>Laurencia</i> | sp1 | 3004213 | 44 | 24 | 24 |
| 7 | Chlorophyceae | <i>Bornetella</i> | <i>sphaerica</i> | 243558 | 50 | 29 | 24 |
| 2 | Gastropoda | <i>Dolabella</i> | sp1 | 1882244 | 51 | 30 | 24 |
| 19 | Gastropoda | <i>Phos</i> | <i>senticosus</i> | 145869 | 46 | 26 | 24 |
| 8 | Chlorophyceae | <i>Avrainvillea</i> | sp1 | 18392 | 39 | 29 | 24 |
| 11 | Bivalvia | <i>Chlamys</i> | sp2 | 15871 | 46 | 27 | 24 |
| 20 | Crustacea | <i>Carinosquilla</i> | <i>thailandensis</i> | 87298 | 48 | 22 | 24 |
| 16 | Gymnolaemata | <i>Emballotheca</i> | spp | 605916 | 43 | 31 | 24 |
| 20 | Echinoidea | <i>Breynia</i> | <i>desorii</i> | 170066 | 46 | 20 | 24 |
| 10 | Actinopterygii | <i>Parapercis</i> | <i>nebulosa</i> | 705874 | 47 | 29 | 24 |
| 14 | Bivalvia | <i>Fulvia</i> | <i>scalata</i> | 3799 | 40 | 19 | 23 |

| Group | Class | Genus | Species | Biomass Kg | %Available | %Exposed | %EffortExp |
|-------|----------------|--------------------------|---------------------------|------------|------------|----------|------------|
| 17 | Cephalopoda | <i>Sepia</i> | <i>smithi</i> | 664816 | 45 | 26 | 23 |
| 31 | Gymnolaemata | <i>Exochella</i> | <i>conjuncta</i> cf | 2952 | 40 | 28 | 23 |
| 10 | Actinopterygii | <i>Batrachomoeus</i> | <i>dubius/trispinosus</i> | 124764 | 43 | 28 | 23 |
| 35 | Crustacea | <i>Trachypenaeus</i> | <i>fulvus</i> | 2663 | 42 | 26 | 23 |
| 11 | Crustacea | <i>Bathypilumnus</i> | <i>pugilator</i> | 11839 | 46 | 29 | 23 |
| 12 | Bivalvia | <i>Cucullaea</i> | <i>labiata</i> | 238633 | 43 | 21 | 23 |
| 10 | Chlorophyceae | <i>Caulerpa</i> | sp2 | 610672 | 44 | 27 | 23 |
| 20 | Anthozoa | <i>Antipatharia</i> | spp | 22957 | 36 | 17 | 23 |
| 19 | Anthozoa | <i>Heterocyathus</i> | <i>sulcatus</i> cf | 407411 | 46 | 24 | 23 |
| 10 | Echinoidea | <i>Gymnechinus</i> | <i>epistichus</i> | 1300029 | 47 | 27 | 23 |
| 18 | Asteroidea | <i>Metrodora</i> | <i>subulata</i> | 59546 | 45 | 25 | 23 |
| 18 | Actinopterygii | <i>Onigocia</i> | sp juv/unident | 125245 | 44 | 24 | 23 |
| 37 | Demospongiae | <i>Hyrtios</i> | sp6 | 78222 | 38 | 19 | 23 |
| 7 | Crustacea | <i>Thenus</i> | <i>australiensis</i> | 3019359 | 46 | 28 | 23 |
| 1 | Actinopterygii | <i>Paramonacanthus</i> | sp juv/unident | 79035 | 45 | 26 | 23 |
| 1 | Gymnolaemata | <i>Reteporella</i> | spp | 17023 | 41 | 27 | 23 |
| 6 | Actinopterygii | <i>apogon</i> | <i>kiensis</i> | 21415 | 45 | 24 | 23 |
| 12 | Actinopterygii | <i>Repomucenus</i> | <i>sublaevis</i> | 119448 | 44 | 23 | 23 |
| 36 | Holothuroidea | <i>Holothuroidea</i> | spp | 1285178 | 43 | 23 | 23 |
| 16 | Gymnolaemata | <i>Lepralia</i> | <i>elimata</i> | 1214 | 44 | 29 | 23 |
| 1 | Actinopterygii | <i>Grammatobothus</i> | <i>pennatus</i> | 1989097 | 46 | 28 | 23 |
| 2 | Chlorophyceae | <i>Caulerpa</i> | <i>taxifolia</i> | 49177 | 47 | 24 | 23 |
| 17 | Gymnolaemata | <i>Aetea</i> | <i>capillaris</i> | 1456 | 45 | 26 | 23 |
| 36 | Asteroidea | <i>Poraster</i> | <i>superbus</i> | 939166 | 41 | 28 | 23 |
| 11 | Gymnolaemata | <i>Nelliella</i> | spp | 15815 | 45 | 28 | 23 |
| 26 | Asteroidea | <i>Astropecten</i> | sp4_QMS | 11617 | 42 | 22 | 23 |
| 8 | Crustacea | <i>Portunus</i> | <i>granulatus</i> | 21379 | 46 | 26 | 23 |
| 21 | Actinopterygii | <i>Pegasus</i> | <i>volitans</i> | 59795 | 44 | 26 | 23 |
| 4 | Bivalvia | <i>Dosinia</i> | <i>histro</i> cf | 273127 | 43 | 26 | 23 |
| 17 | Cephalopoda | <i>Sepiadariidae</i> | sp2 | 74692 | 44 | 25 | 22 |
| 2 | Crustacea | <i>Thalamita</i> | <i>sima</i> | 49171 | 39 | 23 | 22 |
| 1 | Bivalvia | <i>Chama</i> | sp3 | 182124 | 49 | 26 | 22 |
| 17 | Demospongiae | <i>Ianthella</i> | <i>quadrangulata</i> | 23579428 | 45 | 25 | 22 |
| 1 | Rhodophyceae | <i>Lenormandiopsis</i> | <i>lorentzii</i> | 2877749 | 45 | 26 | 22 |
| 1 | Chlorophyceae | <i>Codium</i> | sp2 | 106881 | 44 | 28 | 22 |
| 34 | Actinopterygii | <i>Pseudomonacanthus</i> | <i>peroni</i> | 110656 | 44 | 26 | 22 |
| 4 | Crustacea | <i>Jonas</i> | <i>luteanus</i> | 49552 | 44 | 25 | 22 |
| 7 | Actinopterygii | <i>Kanekonia</i> | <i>queenslandica</i> | 4114 | 42 | 27 | 22 |
| 4 | Crustacea | <i>Isopoda</i> | sp1 | 10183 | 45 | 27 | 22 |
| 13 | Actinopterygii | <i>Polydactylus</i> | <i>multiradiatus</i> | 418667 | 30 | 20 | 22 |
| 1 | Rhodophyceae | <i>Rhodophyceae</i> | sp3 | 10156570 | 45 | 25 | 22 |
| 1 | Actinopterygii | <i>Pterois</i> | <i>russellii</i> (e form) | 132648 | 44 | 26 | 22 |
| 8 | Crustacea | <i>Sicyonia</i> | <i>lancifer</i> | 80109 | 43 | 26 | 22 |
| 3 | Crustacea | <i>Parthenope</i> | <i>hoplonotus</i> | 5110 | 43 | 21 | 22 |
| 11 | Gastropoda | <i>Gastropoda</i> | <i>eggs</i> | 1359905 | 46 | 28 | 22 |
| 3 | Crustacea | <i>Pilumnus</i> | <i>semilanatus</i> | 5379 | 40 | 22 | 22 |
| 1 | Holothuroidea | <i>Stichopus</i> | <i>horrens</i> | 2145324 | 46 | 26 | 22 |
| 11 | Crustacea | <i>Myra</i> | <i>australis</i> | 138701 | 45 | 24 | 22 |
| 31 | Anthozoa | <i>Junceella</i> | <i>juncea</i> | 64983 | 45 | 30 | 22 |
| 7 | Gastropoda | <i>Volva</i> | <i>volva</i> | 8649 | 46 | 25 | 22 |
| 1 | Chlorophyceae | <i>Ventricaria</i> | <i>ventricosa</i> | 2060 | 36 | 26 | 22 |
| 12 | Crustacea | <i>Clorida</i> | <i>obtusa</i> | 5954 | 45 | 21 | 22 |
| 4 | Anthozoa | <i>Truncatoflabellum</i> | spp | 45894 | 42 | 24 | 22 |
| 23 | Actinopterygii | <i>Rhynchostracion</i> | <i>nasus</i> | 578162 | 45 | 24 | 22 |
| 14 | Bivalvia | <i>Anadara</i> | <i>ferruginea</i> cf | 11718 | 46 | 22 | 22 |
| 31 | Actinopterygii | <i>Upeneus</i> | <i>filifer</i> | 480644 | 45 | 27 | 22 |
| 17 | Echinoidea | <i>Peronella</i> | <i>macroproctes</i> cf | 135607 | 43 | 25 | 22 |
| 2 | Gastropoda | <i>Atys</i> | <i>naucum</i> | 23300 | 40 | 22 | 22 |
| 3 | Demospongiae | <i>Ircinia</i> | spp | 248870 | 37 | 18 | 22 |
| 1 | Actinopterygii | <i>Paramonacanthus</i> | <i>lowei</i> | 565936 | 43 | 27 | 22 |
| 17 | Rhodophyceae | <i>Laurencia</i> | sp4 | 232107 | 43 | 26 | 22 |
| 28 | Echinoidea | <i>Clypeaster</i> | sp3 | 983055 | 53 | 27 | 22 |
| 17 | Crustacea | <i>Hyastenus</i> | <i>sebae</i> | 288 | 43 | 24 | 22 |
| 10 | Phaeophyceae | <i>Distromium</i> | <i>flabellatum</i> | 3445399 | 42 | 27 | 21 |

| Group | Class | Genus | Species | Biomass Kg | %Available | %Exposed | %EffortExp |
|-------|----------------|-----------------------|-------------------------|------------|------------|----------|------------|
| 17 | Rhodophyceae | <i>Laurencia</i> | sp3 | 13655 | 43 | 24 | 21 |
| 26 | Demospongiae | <i>Callyspongia</i> | sp2 | 27739 | 40 | 21 | 21 |
| 25 | Bivalvia | <i>Placamen</i> | sp2 | 119881 | 44 | 23 | 21 |
| 20 | Echinoidea | <i>Peronella</i> | <i>lesueuri</i> | 370761 | 45 | 21 | 21 |
| 18 | Crustacea | <i>Camposcia</i> | <i>retusa</i> | 13044 | 41 | 22 | 21 |
| 1 | Bivalvia | <i>Laternulidae</i> | sp1 | 613938 | 44 | 26 | 21 |
| 1 | Actinopterygii | <i>Pristotis</i> | <i>obtusirostris</i> | 927471 | 43 | 27 | 21 |
| 16 | Actinopterygii | <i>Cottapistus</i> | <i>cottoides</i> | 45746 | 50 | 29 | 21 |
| 4 | Gymnolaemata | <i>Didymozoum</i> | spp | 3120 | 49 | 27 | 21 |
| 16 | Bivalvia | <i>Lima</i> | sp1 | 31065 | 40 | 27 | 21 |
| 17 | Crustacea | <i>Crustacea</i> | spp | 3542 | 43 | 24 | 21 |
| 17 | Anthozoa | <i>Actiniaria</i> | spp | 397342 | 43 | 24 | 21 |
| 1 | Anthozoa | <i>Caryophyllia</i> | spp | 11317 | 42 | 27 | 21 |
| 17 | Crustacea | <i>Metapenaeopsis</i> | <i>rosea</i> | 444889 | 50 | 25 | 21 |
| 1 | Actinopterygii | <i>Eurypegus</i> | <i>draconis</i> | 19336 | 46 | 26 | 21 |
| 16 | Gymnolaemata | <i>Chaperia</i> | spp | 242 | 39 | 27 | 21 |
| 17 | Asteroidea | <i>Goniasteridae</i> | spp | 13864 | 43 | 24 | 21 |
| 1 | Crustacea | <i>Thacanophrys</i> | sp245 | 33062 | 43 | 26 | 21 |
| 17 | Crustacea | <i>Parthenope</i> | <i>harpax</i> | 1416 | 42 | 24 | 21 |
| 23 | Gymnolaemata | <i>Synnotum</i> | spp | 497 | 39 | 22 | 21 |
| 4 | Cephalopoda | <i>Sepiadarium</i> | <i>austrium</i> | 118069 | 43 | 25 | 21 |
| 34 | Actinopterygii | <i>Bothidae</i> | sp juv/unident | 133389 | 42 | 23 | 21 |
| 17 | Bivalvia | <i>Arca</i> | sp1 | 223887 | 43 | 27 | 21 |
| 36 | Demospongiae | <i>Callyspongia</i> | sp6 | 70105 | 43 | 23 | 21 |
| 1 | Cephalopoda | <i>Sepioloidea</i> | <i>lineolata</i> | 177633 | 42 | 26 | 21 |
| 1 | Cephalopoda | <i>Metasepia</i> | <i>pfefferi</i> | 125341 | 44 | 24 | 21 |
| 17 | Cephalopoda | <i>Octopodidae</i> | spp | 1232237 | 42 | 24 | 21 |
| 18 | Gastropoda | <i>Gastropoda</i> | spp | 86018 | 41 | 23 | 21 |
| 31 | Gymnolaemata | <i>Beania</i> | <i>discodermiae</i> cf | 564 | 40 | 25 | 21 |
| 10 | Crustacea | <i>Paguridae</i> | sp213 | 53739 | 42 | 26 | 21 |
| 34 | Actinopterygii | <i>Dactyloptena</i> | <i>papilio</i> | 325477 | 42 | 25 | 21 |
| 6 | Chlorophyceae | <i>Caulerpa</i> | <i>brachypus</i> | 27068 | 39 | 24 | 21 |
| 23 | Demospongiae | <i>Clathria</i> | sp9 | 71609 | 45 | 24 | 21 |
| 4 | Gastropoda | <i>Cymatium</i> | <i>caudatum</i> | 6294 | 41 | 25 | 21 |
| 17 | Crustacea | <i>Petalomera</i> | <i>pulchra</i> | 332 | 42 | 25 | 21 |
| 31 | Gymnolaemata | <i>Arachnopusia</i> | spp | 17312 | 34 | 25 | 21 |
| 17 | Echinoidea | <i>Nudechinus</i> | spp | 9200 | 42 | 25 | 21 |
| 19 | Holothuroidea | <i>Holothuroidea</i> | sp46 | 416848 | 43 | 24 | 21 |
| 8 | Demospongiae | <i>Crella</i> | 1525 | 81406 | 55 | 31 | 21 |
| 6 | Crustacea | <i>Palicoides</i> | <i>whitei</i> | 10059 | 39 | 23 | 21 |
| 17 | Gymnolaemata | <i>Antropora</i> | spp | 645 | 42 | 25 | 21 |
| 18 | Ophiuroidea | <i>Ophioclasma</i> | <i>stellatum</i> | 949536 | 42 | 22 | 21 |
| 17 | Gymnolaemata | <i>Mimosella</i> | <i>verticillata</i> cf | 2138 | 42 | 25 | 21 |
| 24 | Ophiuroidea | <i>Ophiopsila</i> | <i>pantherina</i> | 4629 | 36 | 19 | 21 |
| 37 | Demospongiae | <i>Demospongiae</i> | sp88 | 84681 | 38 | 20 | 21 |
| 20 | Asteroidea | <i>Astropecten</i> | <i>zebra</i> | 12709 | 52 | 26 | 20 |
| 1 | Cephalopoda | <i>Sepia</i> | <i>plangon</i> | 1303519 | 40 | 26 | 20 |
| 16 | Gymnolaemata | <i>Smittina</i> | spp | 1702 | 43 | 24 | 20 |
| 1 | Gymnolaemata | <i>Escharina</i> | <i>pesanseris</i> | 5030 | 43 | 23 | 20 |
| 4 | Ophiuroidea | <i>Ophiacantha</i> | <i>indica</i> cf | 39636 | 44 | 25 | 20 |
| 17 | Anthozoa | <i>Zoanthidae</i> | spp | 5012 | 42 | 25 | 20 |
| 1 | Rhodophyceae | <i>Haloplegma</i> | <i>duperreysi</i> | 3474678 | 44 | 24 | 20 |
| 23 | Demospongiae | <i>Dendrilla</i> | sp4 | 11362 | 37 | 20 | 20 |
| 1 | Chlorophyceae | <i>Microdictyon</i> | sp1 | 690175 | 42 | 23 | 20 |
| 4 | Actinopterygii | <i>Tathicarpus</i> | <i>bulleri</i> | 63577 | 42 | 25 | 20 |
| 16 | Crustacea | <i>Thacanophrys</i> | <i>longispinus</i> | 900 | 39 | 24 | 20 |
| 1 | Rhodophyceae | <i>Hypoglossum</i> | sp1 | 511486 | 43 | 25 | 20 |
| 16 | Gymnolaemata | <i>Crepidacantha</i> | spp | 531 | 39 | 25 | 20 |
| 16 | Gymnolaemata | <i>Calyptotheca</i> | spp | 228473 | 41 | 26 | 20 |
| 20 | Anthozoa | <i>Pteroides</i> | sp3 | 90797 | 42 | 21 | 20 |
| 6 | Demospongiae | <i>Hippospongia</i> | <i>elastica</i> | 727107 | 42 | 22 | 20 |
| 32 | Echinoidea | <i>Echinodiscus</i> | <i>tenuissimus</i> | 116762 | 40 | 25 | 20 |
| 16 | Gymnolaemata | <i>Beania</i> | <i>plurispinosa</i> cf | 1481 | 38 | 25 | 20 |
| 34 | Actinopterygii | <i>Pseudorhombus</i> | <i>dupliciocellatus</i> | 1656810 | 44 | 24 | 20 |

| Group | Class | Genus | Species | Biomass Kg | %Available | %Exposed | %EffortExp |
|-------|----------------|---------------------------|--------------------------|------------|------------|----------|------------|
| 16 | Gymnolaemata | <i>Micropora</i> | <i>variperforata</i> cf | 14843 | 40 | 26 | 20 |
| 17 | Rhodophyceae | <i>Coelarthrum</i> | sp1 | 924225 | 42 | 23 | 20 |
| 32 | Actinopterygii | <i>Engyproson</i> | <i>maldivensis</i> | 444474 | 38 | 25 | 20 |
| 1 | Crustacea | <i>Dardanus</i> | <i>callichela</i> | 66220 | 37 | 25 | 20 |
| 1 | Gastropoda | <i>Chicoreus</i> | sp1 | 533290 | 40 | 25 | 20 |
| 30 | Rhodophyceae | <i>Peyssonnelia</i> | <i>inamoena</i> | 974895 | 38 | 22 | 20 |
| 15 | Gastropoda | <i>Distorsio</i> | <i>reticulata</i> | 57223 | 44 | 22 | 20 |
| 37 | Demospongiae | <i>Hyattella</i> | <i>intestinalis</i> | 454226 | 40 | 22 | 20 |
| 4 | Crustacea | <i>Trachypenaeus</i> | <i>curvirostris</i> | 565850 | 41 | 24 | 20 |
| 14 | Crustacea | <i>Scyllarus</i> | sp3418 | 29264 | 38 | 19 | 20 |
| 3 | Bivalvia | <i>Pteria</i> | <i>coturnix</i> cf | 1806 | 38 | 20 | 20 |
| 11 | Crustacea | <i>Parthenope</i> | sp 67 | 202017 | 43 | 25 | 20 |
| 17 | Crustacea | <i>Achaeus</i> | sp5993 | 2086 | 41 | 25 | 20 |
| 16 | Actinopterygii | <i>Choerodon</i> | <i>venustus</i> | 386846 | 36 | 25 | 20 |
| 1 | Crustacea | <i>Metapenaeopsis</i> | <i>lamellata</i> | 263643 | 39 | 25 | 20 |
| 36 | Demospongiae | <i>Sponge substrate</i> | <i>substrate</i> | 50696 | 42 | 22 | 20 |
| 2 | Chlorophyceae | <i>Halimeda</i> | <i>bikensis</i> | 7008553 | 31 | 19 | 20 |
| 17 | Crustacea | <i>Hyastenus</i> | <i>campbelli</i> | 43855 | 41 | 23 | 20 |
| 10 | Gymnolaemata | <i>Calyptotheca</i> | <i>wasinensis</i> cf | 121815 | 52 | 32 | 20 |
| 1 | Actinopterygii | <i>Antennarius</i> | <i>striatus</i> | 31064 | 44 | 22 | 20 |
| 17 | Bivalvia | <i>Glycymeris</i> | <i>hedleyi</i> | 186408 | 42 | 25 | 20 |
| 34 | Actinopterygii | <i>Lepidotrigla</i> | <i>japonica-like</i> | 1074762 | 43 | 23 | 20 |
| 4 | Actinopterygii | <i>Pseudorhombus</i> | <i>diplospilus</i> | 308042 | 42 | 21 | 20 |
| 18 | Echinoidea | <i>Salmaciella</i> | <i>oligopora</i> | 100584 | 38 | 25 | 20 |
| 17 | Rhodophyceae | <i>Hypnea</i> | sp1 | 136462 | 42 | 23 | 20 |
| 16 | Stenolaemata | <i>Mecynoechia</i> | spp | 2764 | 40 | 23 | 20 |
| 20 | Gastropoda | <i>Cymatium</i> | <i>pfeifferanum</i> | 4305 | 37 | 17 | 20 |
| 1 | Chlorophyceae | <i>Caulerpa</i> | <i>cupressoides</i> | 599194 | 39 | 24 | 20 |
| 7 | Actinopterygii | <i>Orbonymus</i> | <i>rameus</i> | 131532 | 44 | 24 | 19 |
| 1 | Holothuroidea | <i>Holothuria</i> | <i>dofleinii</i> | 957738 | 37 | 24 | 19 |
| 18 | Actinopterygii | <i>Onigocia</i> | sp b | 45271 | 40 | 22 | 19 |
| 17 | Anthozoa | <i>Turbinaria</i> | spp | 8638653 | 42 | 24 | 19 |
| 37 | Gastropoda | <i>Cypraea</i> | <i>walkeri</i> cf | 5844 | 37 | 19 | 19 |
| 37 | Demospongiae | <i>Dysidea</i> | sp10 | 23982 | 36 | 19 | 19 |
| 16 | Calcarea | <i>Calcarea</i> | <i>calcareous</i> sp4 | 41835 | 37 | 20 | 19 |
| 28 | Crustacea | <i>Metapenaeopsis</i> | <i>metapenaeopsis</i> sp | 983880 | 42 | 22 | 19 |
| 16 | Anthozoa | <i>Solenocaulon</i> | sp1 | 244307 | 40 | 22 | 19 |
| 16 | Gymnolaemata | <i>Rhynchozoon</i> | spp | 99667 | 40 | 23 | 19 |
| 23 | Holothuroidea | <i>Pseudocolochirus</i> | <i>violaceus</i> | 2281916 | 36 | 19 | 19 |
| 4 | Liliopsida | <i>Halophila</i> | <i>capricorni</i> | 76915 | 41 | 23 | 19 |
| 18 | Asterioidea | <i>Luidia</i> | <i>maculata</i> | 365271 | 41 | 23 | 19 |
| 16 | Rhodophyceae | <i>Hydrolythion</i> | <i>reinboldii</i> | 9313083 | 38 | 24 | 19 |
| 2 | Rhodophyceae | <i>Peyssonnelia</i> | sp1 | 2379581 | 37 | 22 | 19 |
| 36 | Demospongiae | <i>Demospongiae</i> | sp17 | 18469 | 45 | 22 | 19 |
| 2 | Chlorophyceae | <i>Caulerpa</i> | <i>sertularioides</i> | 265840 | 37 | 19 | 19 |
| 18 | Ophiuroidea | <i>Ophiopsammus</i> | <i>yoldii</i> | 873462 | 41 | 22 | 19 |
| 1 | Cephalopoda | <i>Sepia</i> | <i>papuensis</i> | 363864 | 40 | 23 | 19 |
| 20 | Annelida | <i>Annelida</i> | spp | 5213418 | 42 | 21 | 19 |
| 23 | Animalia | <i>Encrusting</i> | <i>conglomerate</i> | 47582896 | 38 | 21 | 19 |
| 18 | Gastropoda | <i>Fusinus</i> | <i>colus</i> | 463836 | 42 | 24 | 19 |
| 6 | Crustacea | <i>Portunus</i> | <i>argentatus</i> | 470239 | 38 | 23 | 19 |
| 16 | Crustacea | <i>Hyastenus</i> | <i>convexus</i> | 3668 | 40 | 24 | 19 |
| 16 | Gymnolaemata | <i>Vesicularia</i> | <i>papuensis_AIM</i> | 87465 | 40 | 21 | 19 |
| 16 | Actinopterygii | <i>Onigocia</i> | cf <i>macrolepis</i> | 167134 | 33 | 23 | 19 |
| 16 | Gymnolaemata | <i>Pleurocodonellina</i> | spp | 1414 | 39 | 23 | 19 |
| 16 | Holothuroidea | <i>Holothuroidea</i> | sp36 | 4379 | 37 | 23 | 19 |
| 4 | Bivalvia | <i>Circe</i> | sp1 | 93117 | 40 | 22 | 19 |
| 2 | Chlorophyceae | <i>Penicillus</i> | <i>nodulosus</i> | 956607 | 33 | 18 | 19 |
| 15 | Ophiuroidea | <i>Euryalida</i> | <i>fragment</i> | 47945 | 40 | 20 | 19 |
| 18 | Crustacea | <i>Pontocaris</i> | <i>orientalis</i> | 15667 | 41 | 21 | 19 |
| 4 | Actinopterygii | <i>Apogon</i> | <i>timorensis</i> | 123542 | 38 | 23 | 19 |
| 17 | Gymnolaemata | <i>Plesiocleidochasma</i> | spp | 62133 | 42 | 22 | 19 |
| 17 | Chlorophyceae | <i>Halimeda</i> | <i>gracilis</i> | 5839218 | 36 | 23 | 19 |
| 16 | Gymnolaemata | <i>Figularia</i> | <i>clithridiata</i> cf | 1135 | 33 | 23 | 19 |

| Group | Class | Genus | Species | Biomass Kg | %Available | %Exposed | %EffortExp |
|-------|----------------|--------------------------|------------------------------|------------|------------|----------|------------|
| 29 | Crustacea | <i>Iphiculus</i> | <i>spongiosus</i> | 364 | 43 | 18 | 18 |
| 16 | Crustacea | <i>Thacanophrys</i> | sp879 | 336 | 39 | 22 | 18 |
| 16 | Gymnolaemata | <i>Trypostega</i> | spp | 1350 | 38 | 23 | 18 |
| 23 | Asteroidea | <i>Pentaceraster</i> | <i>gracilis</i> | 2811190 | 40 | 20 | 18 |
| 16 | Anthozoa | <i>Dichotella</i> | sp1 | 72514 | 38 | 22 | 18 |
| 2 | Ophiuroidea | <i>Ophiomaza</i> | <i>cacaotica</i> cf | 11435 | 37 | 20 | 18 |
| 4 | Bivalvia | <i>Cardita</i> | sp1 | 160513 | 39 | 23 | 18 |
| 6 | Chlorophyceae | <i>Phyllocladion</i> | sp1 | 47831 | 38 | 21 | 18 |
| 4 | Echinoidea | <i>Temnopleuridae</i> | sp2_QMS | 31430 | 36 | 23 | 18 |
| 4 | Crustacea | <i>Izanami (matuta)</i> | <i>inermis</i> | 238633 | 39 | 23 | 18 |
| 30 | Demospongiae | <i>Hyattella</i> | <i>intestinalis (form b)</i> | 579612 | 38 | 21 | 18 |
| 16 | Gymnolaemata | <i>Beania</i> | <i>regularis</i> | 763 | 38 | 22 | 18 |
| 25 | Crustacea | <i>Gonodactylaceus</i> | <i>graphurus</i> | 6851 | 49 | 26 | 18 |
| 2 | Actinopterygii | <i>Richardsonichthys</i> | <i>leucogaster</i> | 46959 | 37 | 22 | 18 |
| 34 | Gymnolaemata | <i>Cribralaria</i> | spp | 4312 | 42 | 22 | 18 |
| 6 | Gymnolaemata | <i>Teuchopora</i> | <i>verrucosa</i> cf | 1197 | 39 | 21 | 18 |
| 16 | Gymnolaemata | <i>Smittipora</i> | <i>abyssicola</i> cf | 2036 | 37 | 23 | 18 |
| 17 | Crustacea | <i>Micippa</i> | <i>philyra</i> | 155538 | 39 | 21 | 18 |
| 8 | Gastropoda | <i>Xenophora</i> | <i>cerea</i> cf | 289919 | 30 | 21 | 18 |
| 16 | Echinoidea | <i>Temnotrema</i> | <i>bothryoides</i> | 41067 | 38 | 22 | 18 |
| 4 | Crustacea | <i>Takedana</i> | <i>eriphoides</i> | 3374 | 33 | 22 | 18 |
| 37 | Crustacea | <i>Gaillardellus</i> | <i>rueppelli</i> | 5494 | 35 | 18 | 18 |
| 5 | Stenolaemata | <i>Nevianipora</i> | spp | 3235 | 40 | 23 | 18 |
| 16 | Demospongiae | <i>Hyattella</i> | sp2 | 408228 | 38 | 22 | 18 |
| 23 | Demospongiae | <i>Pseudoceratina</i> | sp6 | 189002 | 40 | 22 | 18 |
| 16 | Gymnolaemata | <i>Celleporina</i> | spp | 5556 | 38 | 23 | 18 |
| 13 | Crustacea | <i>Pagurid</i> | sp2358-1 | 15945 | 44 | 20 | 18 |
| 17 | Echinoidea | <i>Nudechinus</i> | sp4_MTO | 133160 | 38 | 22 | 18 |
| 16 | Asteroidea | <i>Euretaster</i> | <i>insignis</i> | 205115 | 40 | 21 | 18 |
| 15 | Crustacea | <i>Arcania</i> | <i>gracilis</i> | 14190 | 39 | 19 | 18 |
| 10 | Bivalvia | <i>Plicatula</i> | <i>chinensis</i> cf | 3083202 | 47 | 29 | 18 |
| 18 | Gastropoda | <i>Chicoreus</i> | <i>banksii</i> cf | 52142 | 37 | 22 | 18 |
| 5 | Ophiuroidea | <i>Ophiuroidea</i> | spp | 12185 | 38 | 19 | 18 |
| 23 | Gymnolaemata | <i>Nolella</i> | spp | 1536 | 39 | 19 | 18 |
| 23 | Octocorallia | <i>Octocorallia</i> | spp | 71346 | 34 | 18 | 18 |
| 16 | Gymnolaemata | <i>Parasmittina</i> | spp | 142379 | 38 | 21 | 18 |
| 37 | Demospongiae | <i>Fascaplysinopsis</i> | sp1 | 367349 | 35 | 18 | 18 |
| 16 | Stenolaemata | <i>Mesonea</i> | <i>radians</i> | 80 | 37 | 21 | 18 |
| 15 | Demospongiae | <i>Raspailia</i> | sp2 | 648941 | 38 | 19 | 18 |
| 18 | Actinopterygii | <i>Halicampus</i> | <i>grayi</i> | 8694 | 39 | 21 | 18 |
| 4 | Actinopterygii | <i>Hippocampus</i> | <i>queenslandicus</i> | 9042 | 37 | 21 | 17 |
| 20 | Actinopterygii | <i>Pseudorhombus</i> | <i>argus</i> | 353532 | 38 | 15 | 17 |
| 4 | Actinopterygii | <i>Samaris</i> | <i>cristatus</i> | 151891 | 43 | 23 | 17 |
| 23 | Asteroidea | <i>Goniodiscaster</i> | <i>rugosus</i> cf | 90526 | 41 | 20 | 17 |
| 10 | Actinopterygii | <i>Lethrinus</i> | <i>genivittatus</i> | 6198005 | 45 | 24 | 17 |
| 17 | Anthozoa | <i>Sphenopus</i> | <i>marsupialis</i> | 923474 | 48 | 29 | 17 |
| 16 | Gymnolaemata | <i>Macropora</i> | spp | 13357 | 34 | 22 | 17 |
| 32 | Gymnolaemata | <i>Savignyella</i> | spp | 211 | 37 | 21 | 17 |
| 24 | Actinopterygii | <i>Elates</i> | <i>ransonnetii</i> | 431203 | 30 | 12 | 17 |
| 17 | Phaeophyceae | <i>Dictyota</i> | sp2 | 150709 | 33 | 18 | 17 |
| 34 | Gymnolaemata | <i>Exostesia</i> | <i>didomatia</i> | 348205 | 43 | 22 | 17 |
| 20 | Crustacea | <i>Lupocyclus</i> | <i>rotundatus</i> | 73747 | 44 | 21 | 17 |
| 16 | Gymnolaemata | <i>Pleurocodonellina</i> | <i>laciniosa</i> cf | 16498 | 35 | 22 | 17 |
| 36 | Actinopterygii | <i>Lagocephalus</i> | <i>sceleratus</i> | 210666 | 44 | 22 | 17 |
| 16 | Gymnolaemata | <i>Didymosellidae</i> | spp | 173000 | 35 | 22 | 17 |
| 16 | Gymnolaemata | <i>Conopeum</i> | spp | 550 | 37 | 21 | 17 |
| 16 | Gymnolaemata | <i>Mucropetraliella</i> | <i>serrata</i> cf | 167605 | 38 | 22 | 17 |
| 5 | Anthozoa | <i>Solenocaulon</i> | sp2 | 3573 | 37 | 18 | 17 |
| 17 | Crustacea | <i>Parthenope</i> | <i>longispinus</i> | 12376 | 38 | 21 | 17 |
| 5 | Crustacea | <i>Oreophorus</i> | <i>reticulatus</i> | 89789 | 37 | 18 | 17 |
| 5 | Gymnolaemata | <i>Conescharellina</i> | spp | 667 | 41 | 22 | 17 |
| 16 | Gymnolaemata | <i>Arthropoma</i> | spp | 215 | 35 | 21 | 17 |
| 37 | Gastropoda | <i>Ceratosoma</i> | <i>tenue</i> | 15808 | 36 | 18 | 17 |
| 37 | Calcarea | <i>Calcarea</i> | <i>calcareous</i> sp5 | 28284 | 37 | 21 | 17 |

| Group | Class | Genus | Species | Biomass Kg | %Available | %Exposed | %EffortExp |
|-------|----------------|-------------------------|------------------------|------------|------------|----------|------------|
| 18 | Chlorophyceae | <i>Halimeda</i> | <i>discoidea</i> | 70817 | 36 | 21 | 17 |
| 16 | Gymnolaemata | <i>Calloporina</i> | <i>sigillata</i> | 8060 | 32 | 22 | 17 |
| 4 | Crustacea | <i>Penaeus</i> | <i>longistylus</i> | 1997680 | 38 | 20 | 17 |
| 23 | Echinoidea | <i>Salmacis</i> | <i>belli</i> | 1045645 | 37 | 20 | 17 |
| 3 | Gymnolaemata | <i>Biflustra</i> | <i>savartii</i> | 2006 | 36 | 18 | 17 |
| 5 | Actinopterygii | <i>Rogadius</i> | <i>patriciae</i> | 557252 | 40 | 21 | 17 |
| 3 | Rhodophyceae | <i>Cryptonemia</i> | sp | 38912 | 34 | 16 | 17 |
| 16 | Gymnolaemata | <i>Smittoidea</i> | <i>incucula</i> cf | 481 | 37 | 20 | 17 |
| 36 | Actinopterygii | <i>Apogon</i> | <i>truncatus</i> | 736274 | 42 | 20 | 17 |
| 6 | Gastropoda | <i>Murex</i> | <i>tenuirostrum</i> cf | 648731 | 42 | 20 | 17 |
| 23 | Gymnolaemata | <i>Celleporaria</i> | sp1_QMS | 213092 | 36 | 20 | 17 |
| 16 | Phaeophyceae | <i>Sargassum</i> | sp | 1025790 | 35 | 21 | 17 |
| 23 | Gymnolaemata | <i>Fenestrulina</i> | spp | 37498 | 40 | 21 | 17 |
| 16 | Gymnolaemata | <i>Cellaria</i> | spp | 42280 | 39 | 21 | 17 |
| 31 | Holothuroidea | <i>Holothuroidea</i> | sp44 | 38221 | 37 | 19 | 17 |
| 4 | Gymnolaemata | <i>Nellia</i> | <i>tenella</i> cf | 24071 | 40 | 20 | 17 |
| 24 | Bivalvia | <i>Pitar</i> | sp2 | 7904 | 41 | 18 | 17 |
| 16 | Gymnolaemata | <i>Lacernidae</i> | sp2 | 380 | 33 | 21 | 17 |
| 37 | Demospongiae | <i>Tethya</i> | sp2 | 15694 | 32 | 17 | 16 |
| 1 | Gymnolaemata | <i>Cosciniopsis</i> | spp | 621 | 32 | 20 | 16 |
| 37 | Demospongiae | <i>Demospongiae</i> | <i>conglomerate</i> | 442636 | 34 | 18 | 16 |
| 16 | Gymnolaemata | <i>Elzerina</i> | <i>blainvillii</i> cf | 824 | 30 | 21 | 16 |
| 17 | Ophiuroidea | <i>Ophiotrix</i> | sp6 | 2696 | 36 | 20 | 16 |
| 16 | Gymnolaemata | <i>Schizomavella</i> | <i>australis</i> cf | 9036 | 37 | 20 | 16 |
| 13 | Bivalvia | <i>Solen</i> | <i>siphons</i> only | 69535 | 49 | 23 | 16 |
| 6 | Actinopterygii | <i>Parapercis</i> | <i>snyderi</i> | 4966 | 31 | 20 | 16 |
| 5 | Actinopterygii | <i>Apogon</i> | sp juv/unident | 11812 | 36 | 17 | 16 |
| 23 | Holothuroidea | <i>Cercodermas</i> | <i>anceps</i> | 95366 | 33 | 19 | 16 |
| 17 | Crustacea | <i>Diogenidae</i> | sp2 | 69702 | 35 | 20 | 16 |
| 5 | Actinopterygii | <i>Choerodon</i> | sp juv/unident | 2959 | 36 | 17 | 16 |
| 17 | Gymnolaemata | <i>Adeonella</i> | <i>lichenoides</i> cf | 84065 | 40 | 23 | 16 |
| 37 | Demospongiae | <i>Demospongiae</i> | sp14 | 15430 | 37 | 18 | 16 |
| 2 | Anthozoa | <i>Scolymia</i> | spp | 14597 | 34 | 19 | 16 |
| 23 | Actinopterygii | <i>Liocranium</i> | <i>praepositum</i> | 81364 | 37 | 20 | 16 |
| 18 | Echinoidea | <i>Temnopleuridae</i> | sp5 | 41136 | 38 | 18 | 16 |
| 32 | Gymnolaemata | <i>Amastigia</i> | <i>rudis</i> | 3429 | 34 | 17 | 16 |
| 30 | Demospongiae | <i>Dysidea</i> | sp5 | 90011 | 32 | 17 | 16 |
| 37 | Demospongiae | <i>Acanthella</i> | <i>cavernosa</i> | 37239 | 35 | 19 | 16 |
| 18 | Ophiuroidea | <i>Ophiarachnella</i> | <i>infernalis</i> cf | 35459 | 37 | 20 | 16 |
| 4 | Crustacea | <i>Myrine</i> | <i>kesslerii</i> | 1228 | 39 | 20 | 16 |
| 15 | Echinoidea | <i>Lovenia</i> | <i>elongata</i> | 92701 | 41 | 19 | 16 |
| 31 | Actinaria | <i>Anemone</i> | sp9 | 6537 | 39 | 19 | 16 |
| 21 | Actinopterygii | <i>Sillago</i> | <i>ingenuua</i> | 400298 | 48 | 24 | 16 |
| 3 | Gastropoda | <i>Scutus</i> | <i>unguis</i> | 12865 | 33 | 19 | 16 |
| 16 | Asteroidea | <i>Ophidiasteridae</i> | sp1 | 12687 | 34 | 19 | 16 |
| 4 | Gymnolaemata | <i>Hippopetraliella</i> | <i>magna</i> cf | 10537 | 31 | 20 | 16 |
| 17 | Gymnolaemata | <i>Triphylozoon</i> | spp | 150801 | 34 | 19 | 15 |
| 16 | Asteroidea | <i>Iconaster</i> | <i>longimanus</i> | 17227 | 33 | 19 | 15 |
| 23 | Cephalopoda | <i>Photololligo</i> | <i>chinensis</i> | 350906 | 37 | 19 | 15 |
| 16 | Gymnolaemata | <i>Phonicosia</i> | <i>circinata</i> | 91 | 34 | 20 | 15 |
| 16 | Gymnolaemata | <i>Tubulipora</i> | spp | 707 | 36 | 19 | 15 |
| 16 | Gymnolaemata | <i>Schizomavella</i> | <i>triqueta</i> cf | 1490 | 34 | 19 | 15 |
| 6 | Crustacea | <i>Leucosia</i> | <i>magna</i> | 13372 | 36 | 17 | 15 |
| 6 | Demospongiae | <i>Demospongiae</i> | sp13 | 302059 | 31 | 20 | 15 |
| 18 | Gymnolaemata | <i>Steginoporella</i> | spp | 13187 | 33 | 19 | 15 |
| 24 | Actinopterygii | <i>Arnoglossus</i> | <i>waiti</i> | 2352 | 37 | 17 | 15 |
| 5 | Actinopterygii | <i>Diagramma</i> | <i>pictum labiosum</i> | 185953 | 35 | 16 | 15 |
| 5 | Anthozoa | <i>Nephtyigorgia</i> | sp1 | 7191 | 35 | 17 | 15 |
| 32 | Crustacea | <i>Actumnus</i> | <i>setifer</i> | 1499 | 32 | 19 | 15 |
| 23 | Gymnolaemata | <i>Microporella</i> | spp | 1529 | 33 | 19 | 15 |
| 16 | Polychaeta | <i>Polychaete</i> | spp | 6371 | 34 | 17 | 15 |
| 5 | Demospongiae | <i>Demospongiae</i> | <i>fragment</i> | 2417 | 34 | 18 | 15 |
| 23 | Ascidiacea | <i>Ascidacea</i> | spp | 6019123 | 32 | 18 | 15 |
| 4 | Echinoidea | <i>Pseudoboletia</i> | <i>indiana</i> | 45457 | 43 | 24 | 15 |

| Group | Class | Genus | Species | Biomass Kg | %Available | %Exposed | %EffortExp |
|-------|----------------|----------------------------|----------------------------|------------|------------|----------|------------|
| 16 | Actinopterygii | <i>Abalistes</i> | <i>stellatus</i> | 766691 | 35 | 19 | 15 |
| 12 | Crustacea | <i>Urnalana</i> | <i>whitei</i> | 41726 | 47 | 22 | 15 |
| 12 | Holothuroidea | <i>Holothuroidea</i> | sp43 | 70289 | 32 | 19 | 15 |
| 28 | Gastropoda | <i>Atys</i> | sp1 | 32478 | 42 | 17 | 15 |
| 4 | Gymnolaemata | <i>Retiflustra</i> | spp | 33182 | 36 | 19 | 15 |
| 31 | Chlorophyceae | <i>Microdictyon</i> | <i>umbilicatum</i> | 1285617 | 31 | 19 | 15 |
| 6 | Crustacea | <i>Parthenope</i> | <i>turriger</i> | 2190 | 27 | 15 | 15 |
| 16 | Gymnolaemata | <i>Scrupocellaria</i> | spp | 12955 | 36 | 18 | 15 |
| 20 | Gymnolaemata | <i>Tetraplaria</i> | <i>ventricosa</i> cf | 9058 | 36 | 15 | 15 |
| 16 | Gymnolaemata | <i>Porina</i> | <i>vertebralis</i> cf | 1154 | 34 | 18 | 15 |
| 32 | Actinopterygii | <i>Apogon</i> | <i>9(dg)</i> | 62289 | 33 | 16 | 15 |
| 16 | Ophiuroidea | <i>Euryale</i> | <i>asperum</i> | 905776 | 36 | 19 | 15 |
| 2 | Holothuroidea | <i>Actinopyga</i> | <i>spinea</i> cf | 5107122 | 29 | 16 | 14 |
| 13 | Actinopterygii | <i>Apogon</i> | <i>cavitiensis</i> | 7972 | 47 | 22 | 14 |
| 23 | Gymnolaemata | <i>Cyclostomata</i> | spp | 466 | 33 | 19 | 14 |
| 30 | Demospongiae | <i>Dendroceratid</i> | sp1 | 86107 | 32 | 17 | 14 |
| 20 | Anthozoa | <i>Studeriotis</i> | sp2 | 11794 | 41 | 15 | 14 |
| 23 | Crustacea | <i>Charybdis</i> | <i>jaubertensis</i> | 76639 | 31 | 15 | 14 |
| 30 | Demospongiae | <i>Niphates</i> | sp17 | 306985 | 33 | 16 | 14 |
| 26 | Demospongiae | <i>Dysidea</i> | sp3 | 50439 | 28 | 14 | 14 |
| 16 | Gymnolaemata | <i>Adeonellopsis</i> | <i>pentapora</i> | 7400 | 34 | 18 | 14 |
| 16 | Anthozoa | <i>Dichotella</i> | <i>gemmacea</i> | 21485 | 35 | 18 | 14 |
| 16 | Gymnolaemata | <i>Amathia</i> | spp | 668802 | 35 | 17 | 14 |
| 32 | Gymnolaemata | <i>Filicrisia</i> | <i>geniculata</i> | 959 | 32 | 18 | 14 |
| 23 | Bivalvia | <i>Malleus</i> | <i>albus</i> | 311540 | 31 | 17 | 14 |
| 23 | Crustacea | <i>Actaea</i> | <i>Tuberculosa</i> | 6454 | 28 | 18 | 14 |
| 5 | Gastropoda | <i>Haustellum</i> | <i>tweedianum</i> | 12376 | 35 | 18 | 14 |
| 15 | Bivalvia | <i>Nemocardium</i> | <i>bechei</i> | 14205 | 37 | 16 | 14 |
| 5 | Gastropoda | <i>Latirus</i> | <i>paetelianus</i> cf | 21199 | 35 | 16 | 14 |
| 16 | Anthozoa | <i>Umbellulifera</i> | sp1 | 775140 | 32 | 18 | 14 |
| 23 | Demospongiae | <i>Callyspongia</i> | sp23 | 87841 | 39 | 17 | 14 |
| 16 | Echinoidea | <i>Temnopleurus</i> | <i>alexandri</i> | 57525 | 31 | 18 | 14 |
| 5 | Asteroidea | <i>Anseropoda</i> | <i>rosacae</i> cf | 34571 | 33 | 16 | 14 |
| 16 | Bivalvia | <i>Lima</i> | <i>vulgaris</i> | 21760 | 30 | 18 | 14 |
| 35 | Actinopterygii | <i>Rogadius</i> | <i>pristiger</i> | 447881 | 34 | 14 | 14 |
| 37 | Demospongiae | <i>Dendrilla</i> | sp5 | 72702 | 32 | 14 | 14 |
| 34 | Actinopterygii | <i>Nemipterus</i> | <i>theodorei</i> | 5326939 | 35 | 17 | 14 |
| 16 | Gymnolaemata | <i>Metropieriella</i> | spp | 6097 | 33 | 18 | 14 |
| 5 | Gastropoda | <i>Chicoreus</i> | spp | 49916 | 32 | 17 | 14 |
| 34 | Crustacea | <i>Myra</i> | <i>eudactyla</i> | 5119 | 42 | 17 | 14 |
| 3 | Demospongiae | <i>Callyspongia</i> | <i>schultzi</i> | 451419 | 31 | 16 | 14 |
| 5 | Bivalvia | <i>Liochonca</i> | <i>polita</i> | 11024 | 37 | 16 | 14 |
| 32 | Actinopterygii | <i>Fistularia</i> | <i>commersoni</i> | 8270 | 31 | 15 | 14 |
| 23 | Holothuroidea | <i>Holothuroidea</i> | sp38 | 68431 | 30 | 18 | 14 |
| 5 | Gymnolaemata | <i>Bugula</i> | <i>robusta</i> cf | 2346 | 33 | 17 | 14 |
| 5 | Gymnolaemata | <i>Bugula</i> | spp | 2368 | 34 | 18 | 14 |
| 14 | Crustacea | <i>Portunus</i> | <i>spinipes</i> | 5017 | 35 | 12 | 13 |
| 37 | Demospongiae | <i>Clathria (thalsias)</i> | <i>vulpina</i> | 1011817 | 34 | 17 | 13 |
| 2 | Actinopterygii | <i>Paramonacanthus</i> | <i>oblongus</i> | 139092 | 41 | 20 | 13 |
| 30 | Crustacea | <i>Carinosquilla</i> | <i>australiensis</i> | 66990 | 28 | 13 | 13 |
| 26 | Cyanophyceae | <i>Lynngbya</i> | sp | 50986 | 21 | 12 | 13 |
| 16 | Gymnolaemata | <i>Tetraplaria</i> | <i>immersa</i> | 30440 | 29 | 17 | 13 |
| 23 | Actinopterygii | <i>Apogon</i> | cf <i>fuscocomaculatus</i> | 196097 | 32 | 16 | 13 |
| 5 | Crustacea | <i>Carinosquilla</i> | <i>carita</i> | 10419 | 38 | 17 | 13 |
| 5 | Actinopterygii | <i>Engyprosopon</i> | sp juv/unident | 14226 | 34 | 17 | 13 |
| 16 | Gymnolaemata | <i>Phidoloporidae</i> | sp1 | 10087 | 28 | 17 | 13 |
| 23 | Gymnolaemata | <i>Puellina</i> | spp | 274 | 30 | 17 | 13 |
| 23 | Gymnolaemata | <i>Hippopodina</i> | <i>feegeensis</i> cf | 1957 | 32 | 17 | 13 |
| 37 | Demospongiae | <i>Demospongiae</i> | sp6 | 873739 | 30 | 15 | 13 |
| 16 | Asteroidea | <i>Tamaria</i> | sp3 | 22911 | 30 | 17 | 13 |
| 6 | Actinopterygii | <i>Choerodon</i> | <i>frenatus</i> | 96061 | 37 | 16 | 13 |
| 23 | Anthozoa | <i>Mopsella</i> | sp1 | 81629 | 32 | 17 | 13 |
| 32 | Gymnolaemata | <i>Parmularia</i> | spp | 2514 | 30 | 17 | 13 |
| 18 | Crinoidea | <i>Crinoidea</i> | spp | 2425469 | 32 | 16 | 13 |

| Group | Class | Genus | Species | Biomass Kg | %Available | %Exposed | %EffortExp |
|-------|----------------|-------------------------|-----------------------|------------|------------|----------|------------|
| 31 | Actinopterygii | <i>Lujanus</i> | <i>adelii</i> | 1042450 | 33 | 21 | 13 |
| 16 | Gymnolaemata | <i>Catenicella</i> | spp | 44158 | 34 | 16 | 13 |
| 32 | Chlorophyceae | <i>Struvea</i> | <i>elegans</i> | 25785 | 21 | 18 | 13 |
| 5 | Echinoidea | <i>Asthenosoma</i> | sp1 | 746377 | 29 | 14 | 13 |
| 37 | Gymnolaemata | <i>Canda</i> | spp | 27116 | 33 | 16 | 13 |
| 5 | Gymnolaemata | <i>Celleporidae</i> | spp | 1453 | 33 | 15 | 13 |
| 37 | Gastropoda | <i>Chicoreus</i> | <i>terrillus</i> cf | 15996 | 31 | 15 | 13 |
| 32 | Actinopterygii | <i>Engyprosopon</i> | <i>latifrons</i> | 13430 | 29 | 15 | 13 |
| 16 | Gymnolaemata | <i>Hippaliosina</i> | spp | 59823 | 25 | 16 | 13 |
| 23 | Gymnolaemata | <i>Bicrisia</i> | spp | 39 | 30 | 14 | 13 |
| 23 | Gymnolaemata | <i>Crisia</i> | <i>elongata</i> cf | 175749 | 32 | 16 | 13 |
| 23 | Actinopterygii | <i>Apogon</i> | <i>brevicaudatus</i> | 125557 | 28 | 14 | 12 |
| 16 | Crustacea | <i>Parthenope</i> | sp32091 | 1191 | 25 | 16 | 12 |
| 6 | Actinopterygii | <i>Goby</i> | sp juv/unident | 1042 | 34 | 15 | 12 |
| 23 | Gymnolaemata | <i>Caberea</i> | spp | 15510 | 30 | 16 | 12 |
| 23 | Gymnolaemata | <i>Celleporaria</i> | spp | 15622360 | 31 | 16 | 12 |
| 32 | Actinopterygii | <i>Dactyloptena</i> | <i>orientalis</i> | 168574 | 29 | 15 | 12 |
| 15 | Crustacea | <i>Pandalidae</i> | sp916 | 11205 | 38 | 17 | 12 |
| 2 | Chlorophyceae | <i>Halimeda</i> | <i>gigas</i> | 3224417 | 29 | 14 | 12 |
| 25 | Asteroidea | <i>Tamaria</i> cf | sp3 | 66687 | 43 | 20 | 12 |
| 16 | Gymnolaemata | <i>Bugula</i> | <i>dentata</i> cf | 212133 | 29 | 16 | 12 |
| 32 | Actinopterygii | <i>Apogon</i> | <i>septemstriatus</i> | 47319 | 31 | 14 | 12 |
| 3 | Echinoidea | <i>Prionocidaris</i> | <i>bispinosa</i> | 210039 | 29 | 14 | 12 |
| 2 | Chlorophyceae | <i>Halimeda</i> | <i>opuntia</i> | 269000 | 25 | 15 | 12 |
| 13 | Actinopterygii | <i>Siganus</i> | <i>canaliculatus</i> | 377618 | 42 | 19 | 12 |
| 15 | Gymnolaemata | <i>Schizomavella</i> | <i>inclusa</i> cf | 3672 | 33 | 15 | 12 |
| 23 | Gymnolaemata | <i>Margaretta</i> | spp | 43670 | 30 | 16 | 12 |
| 23 | Gymnolaemata | <i>Thornleya</i> | spp | 32344 | 30 | 15 | 12 |
| 23 | Ophiuroidea | <i>Placophiothrix</i> | sp2 | 3343 | 29 | 15 | 11 |
| 28 | Anthozoa | <i>diaseris</i> | <i>distorta</i> cf | 1117 | 37 | 13 | 11 |
| 3 | Bivalvia | <i>Arca</i> | <i>avellana_MTQ</i> | 325791 | 29 | 15 | 11 |
| 3 | Demospongiae | <i>Dendrilla</i> | sp6 | 243595 | 29 | 14 | 11 |
| 2 | Chlorophyceae | <i>Caulerpa</i> | <i>serrulata</i> | 346047 | 25 | 13 | 11 |
| 5 | Gymnolaemata | <i>Codonellina</i> | <i>montferrandii</i> | 42 | 34 | 14 | 11 |
| 32 | Gymnolaemata | <i>Chaperiopsis</i> | spp | 49 | 25 | 15 | 11 |
| 37 | Demospongiae | <i>Demospongiae</i> | sp53 | 442819 | 31 | 12 | 11 |
| 31 | Anthozoa | <i>Subergorgia</i> | <i>suberosa</i> | 14020 | 32 | 16 | 11 |
| 37 | Demospongiae | <i>Chondrilla</i> | sp1 | 17714 | 29 | 13 | 11 |
| 18 | Actinopterygii | <i>Pentapodus</i> | <i>paradiseus</i> | 2615371 | 34 | 16 | 11 |
| 23 | Holothuroidea | <i>Holothuroidea</i> | sp30 | 1110532 | 27 | 15 | 11 |
| 32 | Anthozoa | <i>Acanthogorgia</i> | sp1 | 10489 | 27 | 13 | 11 |
| 23 | Gymnolaemata | <i>Celleporaria</i> | sp1_AIM | 548232 | 26 | 14 | 11 |
| 13 | Crustacea | <i>Eucrate</i> | <i>affinis</i> | 2137 | 48 | 18 | 11 |
| 16 | Actinopterygii | <i>Pentapodus</i> | <i>nagasakiensis</i> | 1132057 | 23 | 15 | 11 |
| 6 | Crustacea | <i>Naxoides</i> | <i>taurus</i> | 3086 | 26 | 13 | 11 |
| 32 | Actinopterygii | <i>Dendrochirus</i> | <i>brachypterus</i> | 49521 | 27 | 13 | 11 |
| 16 | Gymnolaemata | <i>Escharoides</i> | <i>longirostris</i> | 15371 | 27 | 14 | 11 |
| 32 | Gymnolaemata | <i>Cigclisula</i> | spp | 2170 | 26 | 14 | 11 |
| 6 | Crustacea | <i>Lupocyclus</i> | <i>tugelae</i> | 22309 | 30 | 12 | 11 |
| 37 | Ophiuroidea | <i>Ophiopeza</i> | <i>spinosa</i> cf | 347 | 26 | 12 | 10 |
| 2 | Chlorophyceae | <i>Udotea</i> | <i>orientalis</i> | 842312 | 34 | 16 | 10 |
| 23 | Gymnolaemata | <i>Catenicella</i> | sp1_CMR | 46744 | 34 | 14 | 10 |
| 37 | Demospongiae | <i>Fascaplysinopsis</i> | sp3 | 380560 | 39 | 12 | 10 |
| 15 | Crustacea | <i>Carid</i> | sp4931 | 714 | 32 | 13 | 10 |
| 38 | Gymnolaemata | <i>Amathia</i> | <i>crispa</i> | 22713 | 27 | 14 | 10 |
| 23 | Demospongiae | <i>Callyspongia</i> | sp26 | 128191 | 25 | 14 | 10 |
| 5 | Gymnolaemata | <i>Hippopetraliella</i> | <i>concinna</i> | 6873 | 34 | 14 | 10 |
| 28 | Demospongiae | <i>Gelliodes</i> | sp1 | 74197 | 31 | 11 | 10 |
| 20 | Actinopterygii | <i>Upeneus</i> | <i>luzonius</i> | 584420 | 36 | 15 | 10 |
| 15 | Crustacea | <i>Quollastris</i> | <i>gonypetes</i> | 21257 | 31 | 12 | 10 |
| 23 | Hydrozoa | <i>Hydroida</i> | spp | 338440 | 26 | 13 | 10 |
| 23 | Gymnolaemata | <i>Turbicellepora</i> | <i>laevis</i> | 648863 | 25 | 13 | 10 |
| 26 | Crustacea | <i>Thalamita</i> | <i>parvidens</i> | 112316 | 20 | 6 | 10 |
| 18 | Anthozoa | <i>Dendronephthya</i> | spp | 1302022 | 29 | 13 | 10 |

| Group | Class | Genus | Species | Biomass Kg | %Available | %Exposed | %EffortExp |
|-------|----------------|---------------------------|----------------------|------------|------------|----------|------------|
| 5 | Crustacea | <i>Diogenidae</i> | sp379 | 318 | 30 | 13 | 9 |
| 32 | Crustacea | <i>Paguridae</i> | sp444 | 3476 | 22 | 12 | 9 |
| 6 | Crustacea | <i>Solenocera</i> | <i>pectinata</i> | 14069 | 29 | 11 | 9 |
| 13 | Bivalvia | <i>Solen</i> | sp3 | 35340 | 45 | 17 | 9 |
| 37 | Demospongiae | <i>Dysidea</i> | <i>arenaria</i> | 267675 | 26 | 10 | 9 |
| 5 | Actinopterygii | <i>Siphamia</i> | <i>versicolor</i> | 14154 | 27 | 12 | 9 |
| 23 | Gymnolaemata | <i>Celleporaria</i> | sp2_QMS | 87816 | 28 | 12 | 9 |
| 6 | Crustacea | <i>Oncinopus</i> | <i>aranea</i> | 8497 | 23 | 12 | 9 |
| 15 | Demospongiae | <i>Spirastrella</i> | sp2 | 528299 | 35 | 14 | 9 |
| 12 | Bivalvia | <i>Globivenus</i> | <i>embrithes</i> cf | 113931 | 42 | 15 | 9 |
| 16 | Gymnolaemata | <i>Stylopoma</i> | spp | 13328 | 24 | 12 | 9 |
| 3 | Anthozoa | <i>Euplexaura</i> | sp6 | 483859 | 36 | 15 | 9 |
| 24 | Actinopterygii | <i>Sirembo</i> | <i>imberbis</i> | 91767 | 34 | 9 | 8 |
| 31 | Gastropoda | <i>Bolma</i> | <i>aureola</i> | 48007 | 24 | 12 | 8 |
| 3 | Crustacea | <i>Hyastenus</i> | <i>elatus</i> | 18772 | 33 | 13 | 8 |
| 23 | Gymnolaemata | <i>Hippomenella</i> | <i>avicularis</i> | 67 | 27 | 12 | 8 |
| 26 | Demospongiae | <i>Tethya</i> | sp3 | 17612 | 28 | 11 | 8 |
| 3 | Gymnolaemata | <i>Micropora</i> | <i>angusta</i> cf | 1459 | 24 | 11 | 8 |
| 24 | Actinopterygii | <i>Lepidotrigla</i> | <i>calodactyla</i> | 873992 | 25 | 10 | 8 |
| 23 | Gymnolaemata | <i>Steginoporella</i> | <i>magnilabris</i> | 43117 | 20 | 11 | 8 |
| 35 | Cephalopoda | <i>Photololligo</i> | sp1 | 126860 | 32 | 14 | 8 |
| 32 | Chlorophyceae | <i>Caulerpa</i> | <i>racemosa</i> | 485706 | 25 | 10 | 8 |
| 26 | Bivalvia | <i>Fulvia</i> | <i>undatopicta</i> | 14593 | 24 | 10 | 8 |
| 23 | Demospongiae | <i>Demospongiae</i> | sp27 | 12702 | 26 | 11 | 8 |
| 31 | Gymnolaemata | <i>Telopora</i> | spp | 442 | 28 | 14 | 8 |
| 31 | Gymnolaemata | <i>Crassimarginatella</i> | spp | 222 | 27 | 14 | 8 |
| 23 | Gymnolaemata | <i>Euthyrisella</i> | <i>obtecta</i> | 191941 | 24 | 11 | 7 |
| 18 | Actinopterygii | <i>Parupeneus</i> | <i>heptacanthus</i> | 331277 | 23 | 10 | 7 |
| 23 | Asteroidea | <i>Goniasteridae</i> | sp5 | 4161 | 19 | 9 | 7 |
| 20 | Actinopterygii | <i>Lufjanus</i> | <i>vitta</i> | 316853 | 37 | 13 | 7 |
| 24 | Actinopterygii | <i>Paramonacanthus</i> | <i>filicauda</i> | 8764207 | 39 | 11 | 7 |
| 23 | Demospongiae | <i>Demospongiae</i> | sp26 | 22270 | 21 | 9 | 7 |
| 3 | Crustacea | <i>Austrolabidia</i> | <i>gracilipes</i> | 12992 | 33 | 12 | 7 |
| 3 | Demospongiae | <i>Oceanapia</i> | <i>tubes only</i> | 3664 | 33 | 13 | 7 |
| 17 | Anthozoa | <i>Iciligorgia</i> | sp1 | 129051 | 31 | 13 | 7 |
| 23 | Anthozoa | <i>Melithaea</i> | sp2 | 61500 | 22 | 10 | 7 |
| 15 | Demospongiae | <i>Demospongiae</i> | sp16 | 43858 | 34 | 12 | 7 |
| 3 | Bivalvia | <i>Arca</i> | <i>navicularis</i> | 7242 | 22 | 9 | 7 |
| 32 | Crustacea | <i>Naxoides</i> | sp53287 | 2151 | 20 | 9 | 7 |
| 32 | Actinopterygii | <i>Apogon</i> | <i>capricornis</i> | 73308 | 21 | 9 | 7 |
| 12 | Actinopterygii | <i>Choerodon</i> | <i>monostigma</i> | 285266 | 36 | 9 | 7 |
| 16 | Anthozoa | <i>Junceella</i> | sp2 | 137591 | 28 | 12 | 7 |
| 15 | Actinopterygii | <i>Upeneus</i> | <i>moluccensis</i> | 337152 | 25 | 7 | 6 |
| 16 | Crustacea | <i>Barnacle</i> | sp1 | 5009088 | 23 | 12 | 6 |
| 37 | Cephalopoda | <i>Loligo</i> | sp1 | 87486 | 30 | 11 | 6 |
| 2 | Actinopterygii | <i>Oxycheilinus</i> | <i>bimaculatus</i> | 48838 | 19 | 8 | 6 |
| 23 | Gymnolaemata | <i>Adenifera</i> | <i>armata</i> | 196265 | 19 | 9 | 6 |
| 26 | Gastropoda | <i>Terebellum</i> | <i>terebellum</i> | 635 | 31 | 6 | 6 |
| 23 | Gymnolaemata | <i>Sinupetraliella</i> | spp | 3960 | 30 | 9 | 6 |
| 15 | Actinopterygii | <i>Parapriacanthus</i> | <i>ransonneti</i> | 210816 | 23 | 8 | 5 |
| 23 | Calcarea | <i>Clathrina</i> | sp1 | 24817 | 19 | 8 | 5 |
| 23 | Demospongiae | <i>Demospongiae</i> | sp10 | 184966 | 18 | 8 | 5 |
| 28 | Anthozoa | <i>Heteropsammia</i> | <i>cochlea</i> | 22620 | 30 | 8 | 5 |
| 23 | Anthozoa | <i>Mopsella</i> | sp2 | 26395 | 24 | 9 | 5 |
| 15 | Demospongiae | <i>Demospongiae</i> | sp146 | 6870 | 31 | 9 | 5 |
| 28 | Crustacea | <i>Calappa</i> | sp 1984 | 16292 | 33 | 6 | 5 |
| 15 | Crustacea | <i>Arcania</i> | <i>heptacantha</i> | 962 | 23 | 5 | 5 |
| 15 | Ophiuroidea | <i>Ophionereis</i> | <i>semoni</i> cf | 7324 | 30 | 8 | 4 |
| 23 | Crustacea | <i>Thalamita</i> | <i>intermedia</i> | 3456 | 22 | 8 | 4 |
| 37 | Demospongiae | <i>Coelocarteria</i> | <i>singaporensis</i> | 110035 | 11 | 4 | 4 |
| 23 | Anthozoa | <i>Echinogorgia</i> | sp5 | 11065 | 26 | 8 | 4 |
| 37 | Demospongiae | <i>Demospongiae</i> | sp109 | 119911 | 25 | 6 | 4 |
| 15 | Crustacea | <i>Pilumnus</i> | <i>spinicarpus</i> | 1620 | 26 | 7 | 4 |
| 15 | Crustacea | <i>Solenocera</i> | <i>choprai</i> | 124686 | 26 | 5 | 4 |

| Group | Class | Genus | Species | Biomass Kg | %Available | %Exposed | %EffortExp |
|-------|----------------|-----------------------|------------------------|------------|------------|----------|------------|
| 17 | Crustacea | <i>Thacanophrys</i> | sp165 | 885 | 25 | 6 | 3 |
| 18 | Ophiuroidea | <i>Ophiarachnella</i> | <i>paucigranula</i> cf | 15532 | 18 | 5 | 3 |
| 3 | Actinopterygii | <i>Centrogenys</i> | <i>vaigiensis</i> | 20426 | 23 | 5 | 3 |
| 37 | Demospongiae | <i>Oceanapia</i> | sp21 | 5236461 | 25 | 5 | 3 |
| 3 | Anthozoa | <i>Carijoa</i> | sp1 | 78340 | 25 | 5 | 3 |
| 37 | Demospongiae | <i>Cinachyrella</i> | sp1 | 3327419 | 25 | 5 | 3 |
| 23 | Anthozoa | <i>Echinogorgia</i> | sp3 | 110904 | 18 | 5 | 3 |
| 3 | Actinopterygii | <i>Inegocia</i> | <i>harrisii</i> | 217420 | 22 | 5 | 3 |
| 32 | Actinopterygii | <i>Crossorhombus</i> | <i>howensis</i> | 76179 | 22 | 4 | 3 |
| 37 | Demospongiae | <i>Cinachyrella</i> | <i>australiensis</i> | 125583 | 20 | 5 | 3 |
| 18 | Actinopterygii | <i>Canthigaster</i> | <i>rivulata</i> | 31856 | 12 | 4 | 3 |
| 2 | Chlorophyceae | <i>Dictyosphaeria</i> | <i>cavernosa</i> | 1430663 | 21 | 2 | 2 |
| 14 | Crustacea | <i>Cloridina</i> | <i>chlorida</i> | 374 | 29 | 3 | 2 |
| 30 | Echinoidea | <i>Mespilia</i> | <i>globulus</i> | 22836 | 12 | 3 | 2 |
| 3 | Crustacea | <i>Metapenaeopsis</i> | <i>novaeguineae</i> | 16882 | 9 | 2 | 2 |



AUSTRALIAN INSTITUTE
OF MARINE SCIENCE
Australian Institute of
Marine Science
PMB 3, Townsville MC
TOWNSVILLE, Qld.
4810
Australia



Marine & Atmospheric
Research
Mathematics &
Information Sciences
233 Middle Street
CLEVELAND, Qld.
4163 Australia



Queensland
Department of Primary
Industries
Northern Fisheries
Centre
Tingara Street
CAIRNS, Qld. 4870
Australia



Queensland Museum
Queensland Government

Queensland Museum
SOUTH BRISBANE,
Qld. 4101
Australia
Museum of Tropical
Queensland
TOWNSVILLE, Qld.
4810